

The

Meteorological Magazine

January 1990

Steady states in a turbulent atmosphere
Remotely sensed data for wave forecasting



DUPLICATE JOURNALS

National Meteorological Library
FitzRoy Road, Exeter, Devon. EX1 3PB

HMSO

Met.O.992 Vol. 119 No. 1410



3 8078 0010 2437 3

The Meteorological Magazine

January 1990
Vol. 119 No. 1410

551.513.1:551.58

Steady states in a turbulent atmosphere*

A.A. White

Meteorological Office, Bracknell

Summary

The roles of conceptual models and thought experiments in meteorological dynamics are described for the non-theorist. A survey of steady-state solutions of the equations of fluid motion indicates the value of such solutions in attempts to understand weather and climate anomaly patterns as well as long-term average fields.

1. Introduction

The attainment of a physically consistent understanding of atmospheric dynamics is one of the main aims of meteorology. In addition to being a natural scientific goal, it is clearly relevant to the improvement of forecasting methods. This article describes how a knowledge of possible steady flow states can contribute to the desired understanding of motion on the synoptic scale and larger.

Conceptual models are basic to the understanding of any physical system. Section 2 considers briefly the nature of conceptual models in dynamical meteorology, noting that they may be coarsely divided into steady-state and time-dependent types; an historical perspective proves helpful. Steady flow states are discussed from a theoretical standpoint in sections 3 and 4, some observational results are presented in section 5, and conclusions follow in section 6.

2. Understanding atmospheric dynamics

Since the atmosphere is widely agreed to obey the laws of classical physics, its behaviour is already 'understood' in a very restricted sense. But the atmosphere presents such a wide range of dynamical phenomena, on various space and time scales, that a useful understanding must deal with each phenomenon and its relationship to the others.

2.1 Conceptual models and thought experiments

Conceptual models consist of the notions we have about the phenomena which occur in the atmosphere. They are the building blocks of our understanding of atmospheric behaviour. They are based on observational experience, on a general knowledge of physics, and on results of controlled experiments. The controlled experiments may be actual laboratory experiments (see, for example, Hide 1988), or numerical experiments, or — as will be emphasized here — they may be *thought experiments*: theoretical analyses of the behaviour of an idealized atmosphere under precisely defined conditions. (Narrower definitions are perhaps more usual. Here it is convenient to consider as thought experiments even those theoretical analyses which involve lengthy and detailed mathematics.)

Conceptual models should be flexible structures, for new observations or controlled experiments may reveal inadequacies which suggest their revision (or indeed rejection). Hoskins (1983) discusses further the importance of evolving conceptual models and their relationship with observations and various experimental results.

2.2 Steady-state and time-dependent aspects of atmospheric behaviour

The atmospheric phenomena listed in Table I are divided into possible quasi-steady and time-dependent categories. Such a subdivision depends on tacit choices of a discriminating time scale τ (say) with respect to

* Based on a colloquium given at the Meteorological Office on 22 February 1989.

Table I. A possible division of selected atmospheric phenomena into quasi-steady and time-dependent categories (see text for discussion of the arbitrariness of this division)

Quasi-steady	Time-dependent
Climatological averages	Day-to-day weather changes
Climate anomalies	'Low frequency variability'
Blocking and other weather anomalies lasting up to several weeks	Quasi-biennial oscillation El Niño/Southern Oscillation

which quasi-steadiness or time-dependence is to be judged. The categorization of Table I is thus not unique — the same phenomenon may be viewed as quasi-steady or time-dependent according to the choice of τ .

For example, the blocking phenomenon (see Shutts 1987a) may be considered as quasi-steady in relation to an advective time scale L/U , where L and U are synoptic space and velocity scales in the horizontal; note that $L = 1000\text{ km}$ and $U = 10\text{ m s}^{-1}$ give $L/U \approx 1$ day. But since blocking lasts for only a few weeks, at most, it might also be considered as a natural variability on that time scale. This duality may be recognized to some extent in many atmospheric phenomena.

A steady-state emphasis suggests conceptual models based on steady solutions of the governing equations, while a time-dependent emphasis suggests models based on initial-value problems. The thought experiments in the two cases are thus essentially different. An initial-value problem asks what happens if chosen field patterns are set up at an initial time $t = 0$. A steady-state problem seeks the field patterns for which *nothing* happens when $t > 0$ — the initial state persists.

Since most phenomena have elements of both steadiness and time dependence, conceptual models which emphasize one aspect are likely to give useful (if incomplete) pictures. Putting the different models together can lead to a balanced understanding of the real phenomena.

2.3 Ancient and modern views of the atmosphere's general circulation

The working and interplay of steady-state and time-dependent models may be further elucidated by considering the history of general circulation theory up to about 1970. Some milestones are indicated in Table II. Early theories — up to about 1900 — stressed steady-state aspects, attempting to explain the observed time-averaged circulation directly in terms of the time-averaged distribution of diabatic heating and cooling. A typical example is the circulation pattern proposed by Ferrel (1856) and shown in Fig. 1. The pioneering meteorologists of the day were well aware of the variability of atmospheric flow, especially outside the tropics, but they considered that it did not play a

Table II. Some milestones in general circulation theory (for detailed references see Lorenz 1967)

Date	Scientist	Summary of contribution
1686, 1735	Hadley	Solar heating drives a thermally direct symmetric circulation; zonal component of Coriolis force.
1856	Ferrel	Thermally indirect circulations possible; meridional component of Coriolis force.
1900, 1902	Bigelow	Mid-latitude cyclone/anticyclone systems carry large poleward heat fluxes.
1921	Defant	Mid-latitude motion may be regarded as large-scale turbulence.
1926	Jeffreys	Cyclone/anticyclone systems carry important meridional fluxes of angular momentum as well as heat.
1947	Charney	} Instability of baroclinic westerly currents demonstrated.
1949	Eady	

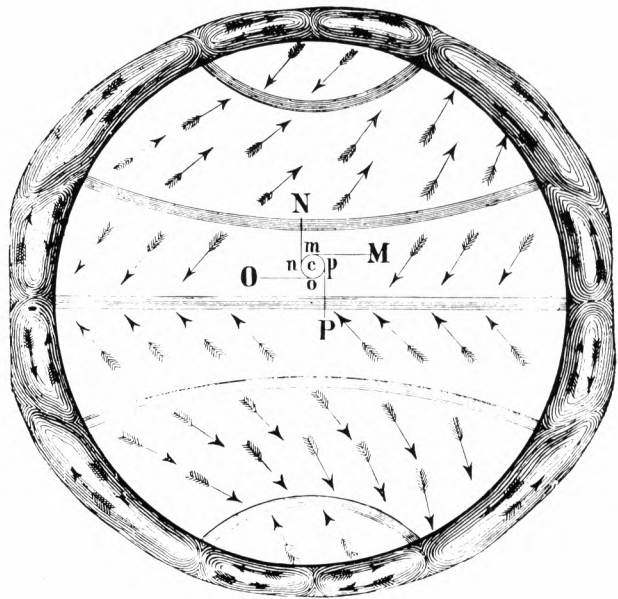


Figure 1. The atmosphere's general circulation according to Ferrel (1856). Arrows indicate the proposed time averaged flow. (Letters M, m, etc. relate to Ferrel's analysis of the forces to which moving air parcels are subject.)

significant part in determining the time-averaged state of the atmosphere. This was a reasonable view to adopt until the need for a more complex picture became clear.

At the turn of the twentieth century it began to be appreciated that the transient cyclones and anticyclones of the extratropics play a key role in the regional heat and momentum budgets of the atmosphere, and hence that the effects of such time-dependent phenomena cannot be omitted from a reliable conceptual model of the time-averaged circulation. The self-contained steady-state models of the eighteenth and nineteenth century thus gave place to steady-state models in which the effects of transient motion played a conspicuous part.

Interest in time-dependent models of transient motion consequently increased, and their study was given added impetus in the late 1940s by Charney's and Eady's instability analyses — *thought experiments* which showed that a baroclinic westerly current could be unstable to wave-like perturbations (Charney 1947, Eady 1949). Theories of transient eddy parametrization (Green 1970) and geostrophic turbulence (Charney 1971) marked the continuation of this trend.

Scientific understanding of atmospheric behaviour undoubtedly increased as a result of the emphasis on time-dependent phenomena which the twentieth century brought. However, it has been widely recognized in recent years that steady-state conceptual models can give useful insight into other atmospheric phenomena besides the long-term average general circulation. Blocked circulation types, other weather anomaly patterns, and climate anomaly patterns are the most promising candidates. The thought experiments which underlie the relevant steady-state models are considered in sections 3 and 4.

Two caveats should be noted about the brief account of general circulation theory given in this section. Table II represents, of course, only a very abridged and selective history; Lorenz (1967) and Pearce (1985) give thorough surveys. Also, though the emphasis in theoretical studies during the 1950s and 1960s was mainly on time-dependent conceptual models and thought experiments, much important work on steady-state models of various phenomena was done too. See, for example, Charney and Eliassen (1949) and Smagorinsky (1953).

3. Steady flow states

The non-divergent barotropic vorticity equation (BVE) is well known as a good qualitative description of atmospheric motion at upper tropospheric levels, and it provides a convenient vehicle for a discussion of steady flow states. Attention is limited to solutions of the complete non-linear equation, so that no restriction to small amplitude disturbances is necessary.

With a vorticity forcing term F the BVE reads

$$\left(\frac{\partial}{\partial t} + \mathbf{v} \cdot \nabla\right)q = F. \quad (1)$$

The horizontal relative velocity \mathbf{v} and absolute vorticity q are defined in terms of a streamfunction ψ as

$$\begin{aligned} \mathbf{v} &= \mathbf{k} \times \nabla\psi, \\ q &= \nabla^2\psi + f. \end{aligned} \quad (2)$$

Here \mathbf{k} is unit vector in the local vertical, \times indicates the vector product, ∇ is the horizontal gradient vector operator and ∇^2 is the corresponding Laplacian operator; f is the Coriolis parameter $2\Omega\sin\phi$ (ϕ = latitude, Ω = earth's rotation rate).

Equation (1) governs the time evolution of $\nabla^2\psi$ (and hence of ψ) in terms of the advection of absolute vorticity and the forcing F . Forced solutions satisfy equation (1) with $F \neq 0$, while free solutions require $F = 0$. Steady solutions obey $\partial/\partial t = 0$, and thus represent flow patterns which are stationary relative to the rotating earth. (A wider definition of steadiness — which would complicate the discussion — would require only that the flow pattern be stationary relative to some uniformly rotating coordinate frame and not necessarily the earth's.)

3.1 Steady free flows

When $F = \partial/\partial t = 0$, equation (1) reduces to

$$\mathbf{v} \cdot \nabla q = \mathbf{k} \cdot (\nabla\psi \times \nabla q) = 0. \quad (3)$$

The horizontal flow \mathbf{v} is everywhere parallel to the contours of constant absolute vorticity q , or, in other words, the contours of constant q are everywhere parallel to the streamlines.

Geostrophically balanced zonal flows obviously satisfy equation (3), but a very wide range of more complicated solutions exists. This fact is of great meteorological importance. Equation (3) is obeyed if there is a functional relation between q and ψ :

$$q = \nabla^2\psi + f = S(\psi). \quad (4)$$

The function $S(\psi)$ is known as the signature of the free flow. Any reasonable function may be chosen, but equation (4) is most easily solved for ψ when S is linear in ψ , and naturally this case has received the most attention.

3.1.1 Stationary Rossby waves

Suppose that $S(\psi) = -\mu\psi$, where μ is some constant. Then equation (4) can be written as

$$\nabla^2\psi + \mu\psi = -2\Omega\sin\phi. \quad (5)$$

The eigenfunctions of the horizontal Laplacian operator ∇^2 are obviously relevant to the solution of equation (5). On a sphere, they are the surface harmonics $P_n^m(\sin\phi)\cos(m\lambda + \epsilon)$ where λ = longitude, ϵ is an arbitrary phase factor and the integers m and n are the rank and

degree of the associated Legendre polynomial P_n^m . The choice $\mu = n(n+1)/a^2$, where 'a' is the radius of the sphere, yields a solution of equation (5) consisting of a simple 'solid rotation' zonal flow and a surface spherical harmonic:

$$\psi = -a^2\omega\sin\phi + AP_n^m(\sin\phi)\cos(m\lambda+\epsilon), \tag{6}$$

where

$$\omega = \frac{2\Omega}{(n+2)(n-1)}$$

If $m \neq 0$, the spherical harmonic part of equation (6) represents the spatial structure of a Rossby-Haurwitz wave (or Rossby wave, for short). Its amplitude A is arbitrary. The zonal flow included in the solution is simply that solid rotation which brings the Rossby wave to rest relative to the earth. (The singular case $n=1$ is well understood but will not be discussed further.)

Various extensions of the solution to equation (6) may be made (see Ertel (1943), Craig (1945) and Neamtan (1946); equation (6) is Ertel's 'specific solution'.) For example, the single Rossby wave in equation (6) may be replaced by any linear combination of waves having the same degree (or total wavenumber)

n ; so different zonal wavenumbers $m (\leq n)$ may be present. Zonal flows having P_n^0 streamfunction structure are also permitted.

Quite complicated steady, free solutions of the BVE thus exist. Fig. 2 shows the hemispheric streamfunction field of a solution composed of a solid rotation zonal flow and Rossby waves of degree $n=6$. The signature $q=S(\psi)$ is shown in Fig. 4(a). An infinity of related solutions may be obtained by changing the amplitudes of the constituent Rossby waves; each member of the family has a signature having the same slope $dS/d\psi$.

Similar solutions of the three-dimensional quasi-geostrophic equations (QGEs) are readily constructed (Kuo 1959, Mitchell and Derome 1983, White 1986). The general functional relationship is now

$$Q = S(\psi, z)$$

in the rest frame of the wave, where z is the vertical coordinate and Q the quasi-geostrophic potential vorticity. An interesting example is the neutral, equivalent barotropic mode which is a finite amplitude, long-wave solution of Charney's baroclinic instability problem (see Held *et al.* 1985).

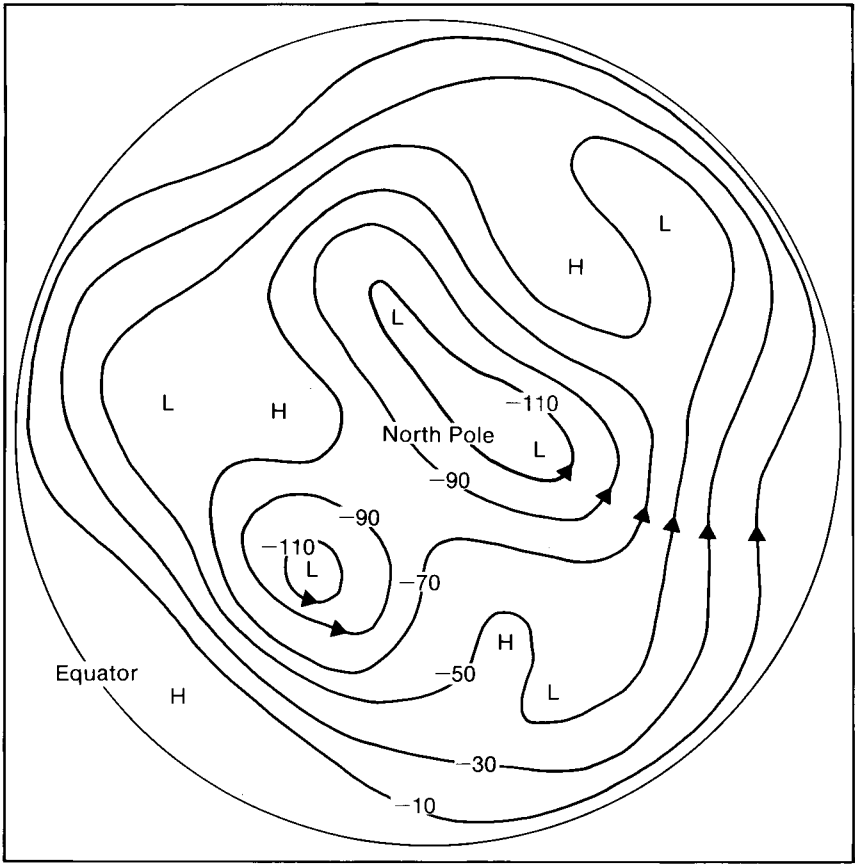


Figure 2. Streamfunction pattern of a multiple Rossby wave solution of the barotropic vorticity equation on a hemisphere. (Distance from north pole is proportional to co-latitude.) The solution is composed of a solid rotation zonal flow and spherical harmonics having $n=6$ and $m=1, 3, 5$. Arrows indicate direction of flow. Contour interval is 20 in units of $10^{-2} \times \Omega a^2 / 28$, where 'a' is the earth's radius; this unit corresponds to a geopotential height difference of about 1 dam at latitude $45^\circ N$ (assuming geostrophic balance). In the same units the amplitudes of the constituent Rossby waves are 15, 25 and 6 for $m=1, 3$ and 5; the phases of the $m=1$ and $m=5$ waves relative to that of the $m=3$ wave are $-\pi/4$ and π .

3.1.2 Modons

The Rossby waves presented in the previous section are non-localized, global solutions of the BVE. Global solutions whose spatial variation is essentially localized also exist, including those often referred to as *modons*. Modons consist of interior and exterior regions in which the function $S(\psi)$ takes different forms; continuity conditions are applied at the boundary separating the two regions. In the simplest cases (see Stern 1975 and McWilliams 1980) plane geometry is assumed, the functions $S(\psi)$ are linear, the boundary is circular and the interior streamfunction has dipole form. The flow in the exterior is predominantly zonal. A typical streamfunction field, taken from Butchart *et al.* (1989), is shown in Fig. 3, and the $S(\psi)$ signature — two straight lines — is illustrated in Fig. 4(b).

The amplitude of a modon is not arbitrary but is related in a complicated way to the radius of the boundary and to various other parameters of the system. Certain conditions have to be obeyed by the far-field zonal flow; see, for example, Haines and Marshall (1987). Nevertheless, modons represent a very wide class of possible solutions of the BVE and related equations. Various similar solutions, and some important modifications, have been analyzed in spherical geometry by Verkley (1984, 1987); see also Tribbia (1984).

3.2 Steady forced flows

The free flows discussed in section 3.1 might appear to be meteorologically inapposite precisely because they are free — the forcing F vanishes everywhere. To underpin conceptual models of quasi-steady flows in the real atmosphere it is helpful also to consider steady, forced solutions of the BVE:

$$\mathbf{v} \cdot \nabla q = \mathbf{v} \cdot \nabla (\nabla^2 \psi + 2\Omega \sin \phi) = F. \tag{7}$$

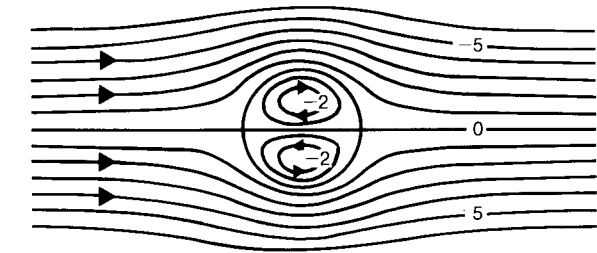
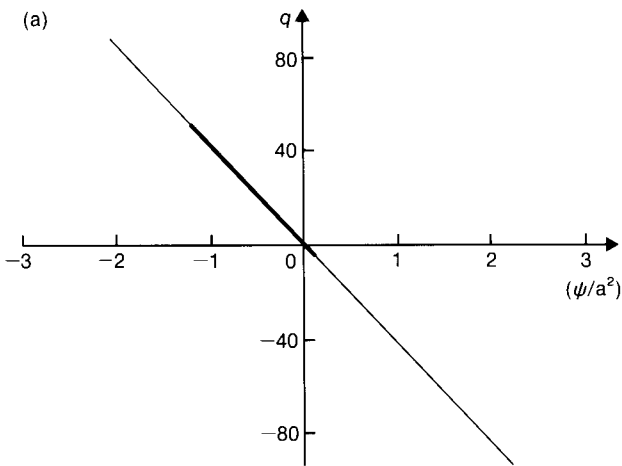


Figure 3. Streamfunction pattern of an equivalent barotropic modon in westerly flow. Units are $10^7 \text{ m}^2 \text{ s}^{-1}$; arrows indicate direction of flow. From Butchart *et al.* (1989).

3.2.1 Exact solutions

As is well known, any reasonable streamfunction field ψ will be a solution of equation (7) if the forcing F takes an appropriate form: to find F , simply substitute the desired ψ into equation (7) (using equation (2))! Reversing the procedure is generally much more difficult, but it is straightforward if F has certain special properties — indeed, families of solutions of the BVE and of the QGEs may be obtained with wave amplitude as parameter (Derome 1984, Shutts 1987a). The important case in which $F = \mathbf{v} \cdot \nabla h$ (where h represents orography) can clearly be dealt with, but the problem is generally not susceptible to analytical solution when F depends on ψ in such a way that the energetics are non-trivial.

3.2.2 Nearly free flows

In reality, the forcing F is the residual of terms representing various processes, each with its own spatial variation or dependence on ψ . For example, if ψ is a time-averaged streamfunction, F will represent transient eddy vorticity flux convergences as well as frictional dissipation (see, for example, Shutts (1983)). If these processes were in balance everywhere then F would

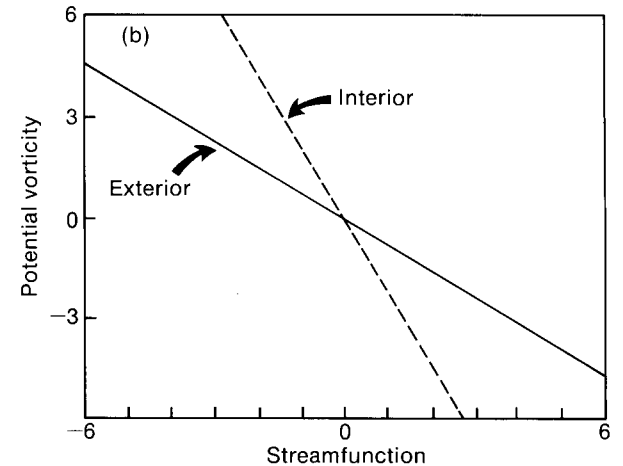


Figure 4. (a) The $q = S(\psi)$ signature (see equations (2) and (4)) of the Rossby wave solution shown in Fig. 2 (bold line), and the remainder of the line (thin) which contains the signatures of all members of the same family of solutions — see text. Both q and ψ/a^2 are plotted in units of $\Omega/28$. (b) The signature of the equivalent barotropic modon shown in Fig. 3. Potential vorticity is here defined as the vorticity relative to the Coriolis parameter on the axis of the flow, plus a term (linear in the streamfunction) which represents the equivalent barotropic character of the flow. Units are $10^7 \text{ m}^2 \text{ s}^{-1}$ for streamfunction and $9 \times 10^{-6} \text{ s}^{-1}$ for potential vorticity.

vanish and ψ would be a steady free state; the possibility of analogous states being attained in baroclinic models has been discussed by Mitchell and Derome (1983), Shutts (1987b) and Marshall and So (1989). More generally, systems which are close to a free state, but do not necessarily attain it, may be treated by regarding the time-averaged flow as free at zero order in some suitable parameter and examining the modifications required at first order by the residual forcing F . Thus, with δ as the (small) parameter, and

$$\mathbf{v} = \mathbf{v}_0 + \delta \mathbf{v}_1 + \delta^2 \mathbf{v}_2 + \dots,$$

$$q = q_0 + \delta q_1 + \delta^2 q_2 + \dots,$$

$$F = \delta F_1,$$

equation (7) becomes

$$\mathbf{v}_0 \cdot \nabla q_0 = 0 \quad \text{at zero order}$$

$$\text{and} \quad \mathbf{v}_0 \cdot \nabla q_1 + \mathbf{v}_1 \cdot \nabla q_0 = F_1 \quad \text{at first order.}$$

The deviation from free flow is sufficiently small in many real systems to enable useful and detailed models to be constructed in this way. An important aspect of the analysis is that a solvability condition arises which constrains the signature ($q_0 = S_0(\psi_0)$) of the zero-order free flow in terms of parameters describing the residual forcing.

This 'nearly free' analysis, which is currently the subject of much study, has been used in oceanographical or meteorological contexts by Niiler (1966), Rhines and Young (1982), Pierrehumbert and Malguzzi (1984), Marshall and Nurser (1986) and others.

4. Discussion

It is important to make clear how the solutions surveyed in section 3 guide the development of conceptual models of quasi-steady flow patterns in the atmosphere. All the solutions are global in the sense that they are defined in an entire geometric region (such as the surface of a sphere). This is so even in the case of modons, although most of their spatial variation is localized. The main significance of such global steady states is not that they could conceivably occur in the real atmosphere, rather they should be regarded as mathematical embodiments of the physical principle that time evolution may be very slow in regions in which the fields adopt certain patterns. In a way, it is a bonus that simple global solutions such as those described in section 3 can be constructed.

In order to illustrate this fundamental point further, let us consider the stationary Rossby waves of section 3.1.1. Only a special sub-set of streamfunction fields — albeit an infinite one — can be expressed solely in terms of spherical harmonics having the same degree (and a

solid rotation component). Arbitrary initial conditions applied to the BVE must therefore be expected to evolve through the advection terms in equation (1), with transfer of energy (and error) between different spatial scales. The message of the steady global solutions is that the evolution may be much slower than the formal advection time L/U would suggest, and that it will be particularly slow in regions where the flow approaches ideal stationary Rossby wave form.

Various other aspects or extensions of the solutions are of interest and will be briefly discussed.

4.1 Accessibility

That states similar to the idealized solutions are accessible from reasonable initial conditions has been demonstrated in many cases by numerical integrations of the BVE or QGEs. See, for example, Shutts (1983), Mitchell and Derome (1983), Hou and Farrell (1986) and Haines and Marshall (1987).

4.2 Stability

General theoretical criteria are usually not helpful in attempts to demonstrate the stability of non-zonal flows to perturbation. Furthermore, the question of the stability of time-averaged flows is beset by problems of interpretation (see Andrews (1984) and references therein). However, the numerical integrations just cited in section 4.1 indicate the effective stability of many steady flow states — although some cases remain to be investigated. Instability on a fairly short time-scale has been demonstrated for some modon-like structures, but others are far more resilient to perturbation (Verkley 1988). Rossby waves become unstable when certain critical amplitudes are exceeded (Baines 1976).

4.3 Variational principles

Important connections, which can only be hinted at here, have been demonstrated between steady, free flows and extremal principles (such as enstrophy minimization at constant energy). See Stern (1975), Bretherton and Haidvogel (1975), Young (1987) and Verkley (1988).

4.4 Steady solutions of the hydrostatic primitive equations

As has been noted, the solutions of the BVE described in section 3 have many counterparts in the QGEs. Except for zonal flows in geostrophic balance, however, very few steady, free solutions of the nonlinear hydrostatic primitive equations (HPEs) are known. (The HPEs form the basis of most modern weather prediction and climate simulation models and are perhaps the most important approximate dynamical formulation used in meteorology.) Zhang *et al.* (1986) describe solutions corresponding to Rossby waves which were derived by applying an iterative numerical method to the HPEs.

In some respects the existence of steady HPE solutions is a side issue, since the known steady solutions

of the BVE and QGEs indicate that *slowly-evolving* states exist in flow governed by the HPEs. The BVE and QGEs are, after all, good approximations to the HPEs for motion on the synoptic scale.

Nevertheless, it is useful in data analysis to be able to define the problem in the HPEs, even if its mathematical solution is generally difficult, for the extent to which real flows approach steady, free states may then be studied. A way of doing this was pointed out to the author by Dr D.G. Andrews in 1985, and an application to atmospheric data will be described in the next section. The analytical details will not be given here. The key result is that a steady, free state of the HPEs yields a functional relationship between Ertel's potential vorticity, P , on any surface of constant potential temperature, θ , and the streamfunction Ψ of the quantity $\mathbf{v} \partial p / \partial \theta$ on the same surface. Here \mathbf{v} is the horizontal flow, p = pressure and P is given by

$$P = -(f + \zeta_{\theta}) \frac{\partial \theta}{\partial p}$$

in which ζ_{θ} is the relative vorticity evaluated on a potential temperature surface. (See Hoskins *et al.* (1985) for a full account of the properties and usefulness of P .) Thus

$$P = S(\Psi, \theta)$$

(where S is the signature) in steady, free flow governed by the HPEs.

The approach to such a state in a real flow may be gauged by plotting against each other the values of P and Ψ obtained from a chosen potential temperature surface. Such 'scatter diagrams' indicate the extent of deviation from a functional relation, and hence allow the departure of the flow from steady, free form to be appraised; for an ideal free, steady flow the scatter diagram of course gives the signature (at the chosen value of θ). Read *et al.* (1986) describe the use and interpretation of similar diagrams within the confines of quasi-geostrophic dynamics.

5. An observational study

Fig. 5(a) shows the fields of Ertel potential vorticity P and the streamfunction Ψ computed from 1985/86 winter (December, January, February) mean fields interpolated to the 330 K potential temperature surface. (This surface is in the troposphere in low latitudes, crosses the tropopause in middle latitudes and remains in the stratosphere in high latitudes.) Initialized ECMWF data formed the basis for the calculations, which were carried out by Dr N. Butchart.

The contours of Ertel potential vorticity tend to be concentrated in high latitudes, and the contours of streamfunction in lower latitudes. This behaviour is to be expected given the inverse role of $\partial p / \partial \theta$ in the two fields (see section 4.4) and the increased static stability in the stratosphere. Nevertheless, the contours of the two

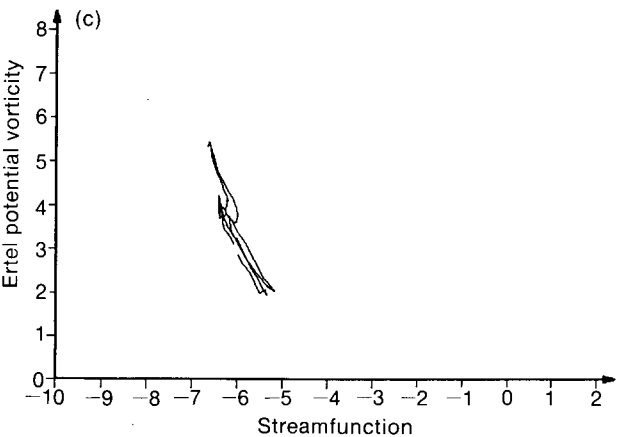
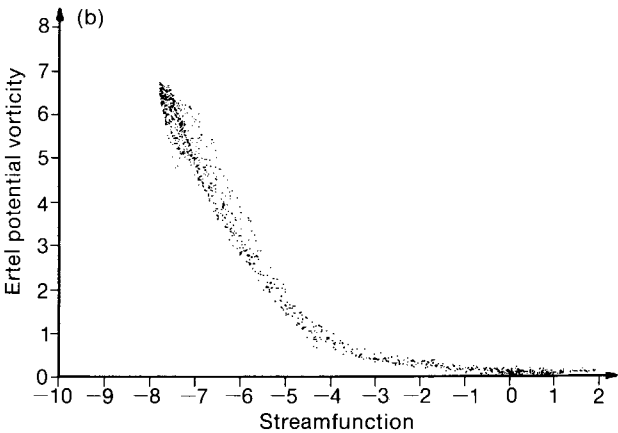
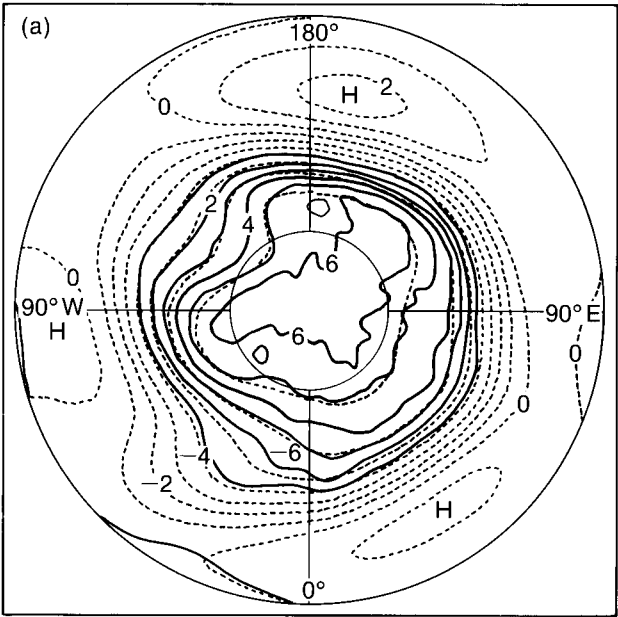


Figure 5. (a) Northern hemisphere fields of Ertel potential vorticity P (full lines) and streamfunction Ψ (broken lines) on the 330 K potential temperature surface, computed from mean initialized ECMWF data for winter 1985/86. Units $10^{-6} \text{ m}^2 \text{ s}^{-1} \text{ K kg}^{-1}$ for P , $10^{-10} \text{ N K}^{-1} \text{ s}^{-1}$ for Ψ . (b) Scatter diagrams composed of P and Ψ values from all northern hemisphere data grid-points. (c) 'Zonal transect' consisting of P and Ψ values from all data grid-points lying along latitude 40°N . Values from adjacent longitudes have been joined by straight lines.

fields clearly tend to run parallel to one another. The closeness to a functional relationship between P and Ψ is brought out by the scatter diagrams shown in Figs 5(b) and 5(c): Fig. 5(b) contains the P and Ψ values from all data grid-points in the northern hemisphere, while Fig. 5(c) shows the values only from points lying on latitude 40° N. (Zonal transects such as Fig. 5(c) reveal the extent to which hemispheric plots such as Fig. 5(b) reflect merely the latitude variations of the Coriolis parameter and the zonal mean static stability.)

Some departure from free form is, of course, inevitable in real flows. There is also some slight uncertainty in the interpretation of the results shown in Fig. 5 since the plotted quantities are calculated from the seasonal mean flow and pressure fields (rather than being the actual seasonal means of P and Ψ). However, the typical results shown in Fig. 5 strongly suggest that free, steady states constitute good zero-order models of the seasonal mean flow; Fig. 5(c) is a particularly reliable indicator. This is precisely the position which quasi-geostrophic theory is now equipped to exploit (see section 3.2).

6. Conclusions

Approximate forms of the equations governing atmospheric motion possess a wide variety of large amplitude, steady solutions. The essence of these solutions is the ability of the flow to adopt patterns in which a vorticity (or potential vorticity) field is nearly similar in form to a streamfunction field. Evidence of such configurations in seasonal mean data has been presented. Butchart *et al.* (1989) find similar behaviour in 5-day mean fields in a blocking episode: they offer persuasive evidence of the characteristics of the modon solutions of the barotropic vorticity equation which were noted here in section 3.2. It remains to be seen whether other anomaly patterns approach steady, free states and whether their signatures will afford useful characterizations.

Although the atmosphere is obviously a time-varying system, a full understanding of its behaviour should take into account its ability to settle into slowly varying states (usually with transient motion superimposed). In other words, conceptual models should be based on the results of searches for steady states as well as on the results of initial value problems. By their very nature, slowly varying states will contribute disproportionately to long-term average statistics.

Time variability and quasi-steadiness reflect different possible conditions of (potential) vorticity advection. At the extreme of maximum time-variability, the advection is comparable in magnitude with the product of a typical horizontal velocity U and a typical vorticity gradient; time variation occurs on the advective time scale L/U (L being a typical horizontal length scale) and energy and error are transferred between different scales of motion. At the opposite extreme the advection vanishes (although the fields may have complicated form) and

there is no time variation or transfer of properties between different scales. Evolution on time scales greater than L/U should therefore be an expected property of large-scale atmospheric flow, whether or not it is regarded as a form of turbulence. Perhaps a slowly varying substructure should be considered as an intrinsic part of the turbulence.

References

- Andrews, D.G., 1984: On the stability of forced non-zonal flows. *Q J R Meteorol Soc*, **110**, 657–662.
- Baines, P.G., 1976: The stability of planetary waves on a sphere. *J Fluid Mech*, **73**, 193–213.
- Bretherton, F.P. and Haidvogel, D.B., 1976: Two-dimensional turbulence above topography. *J Fluid Mech*, **78**, 129–154.
- Butchart, N., Haines, K. and Marshall, J.C., (1989): A theoretical and diagnostic study of solitary waves and atmospheric blocking. *J Atmos Sci*, **46**. To appear.
- Charney, J.G., 1947: The dynamics of long waves in a baroclinic westerly current. *J Meteorol*, **4**, 135–162.
- , 1971: Geostrophic turbulence. *J Atmos Sci*, **28**, 1087–1095.
- Charney, J.G. and Eliassen, A., 1949: A numerical method for predicting the perturbations on the middle latitude westerlies. *Tellus*, **1**, No. 2, 38–54.
- Craig, R.A., 1945: A solution of the nonlinear vorticity equation for atmospheric motion. *J Meteorol*, **2**, 175–178.
- Derome, J., 1984: On quasi-geostrophic, finite amplitude disturbances forced by topography and diabatic heating. *Tellus*, **36A**, 313–319.
- Eady, E.T., 1949: Long waves and cyclone waves. *Tellus*, **1**, No. 3, 33–52.
- Ertel, H., 1943: Über stationäre oszillatorische Luftströmungen auf der rotierenden Erde. *Meteorol Z*, **60**, 332–334.
- Ferrel, W., 1856: An essay on the winds and the currents of the oceans. Reprinted (1882) in *Popular essays on the movements of the atmosphere*, Prof. papers Signal Service (Washington), **12**, 7–19.
- Green, J.S.A., 1970: Transfer properties of the large-scale eddies and the general circulation of the atmosphere. *Q J R Meteorol Soc*, **96**, 157–185.
- Haines, K. and Marshall, J., 1987: Eddy-forced coherent structures as a prototype of atmospheric blocking. *Q J R Meteorol Soc*, **113**, 681–704.
- Held, I.M., Panetta, R.L. and Pierrehumbert, R.T., 1985: Stationary external Rossby waves in vertical shear. *J Atmos Sci*, **42**, 865–883.
- Hide, R., 1988: Studies of geostrophic turbulence, chaos and other non-linear phenomena in rotating fluids: the role of combined laboratory and numerical experiments. *Meteorol Mag*, **117**, 33–34.
- Hoskins, B.J., 1983: Dynamical processes in the atmosphere and the use of models. *Q J R Meteorol Soc*, **109**, 1–21.
- Hoskins, B.J., McIntyre, M.E. and Robertson, A.W., 1985: On the use and significance of isentropic potential vorticity maps. *Q J R Meteorol Soc*, **111**, 877–946.
- Hou, A.Y. and Farrell, B.F., 1986: Excitation of nearly steady finite-amplitude barotropic waves. *J Atmos Sci*, **43**, 720–728.
- Kuo, H.L., 1959: Finite-amplitude three-dimensional harmonic waves on the spherical earth. *J Meteorol*, **16**, 524–534.
- Lorenz, E.N., 1967: The nature and theory of the general circulation of the atmosphere. Geneva, WMO No. 218, TP. 115.
- McWilliams, J.C., 1980: An application of equivalent modons to atmospheric blocking. *Dyn Atmos Oceans*, **5**, 43–66.
- Marshall, J.C. and Nurser, G., 1986: Steady, free circulation in a stratified quasi-geostrophic ocean. *J Phys Oceanogr*, **16**, 1799–1813.
- Marshall, J.C. and So, D.W.K., (1989): Thermal equilibration of planetary waves. Submitted to *J Atmos Sci*.
- Mitchell, H.L. and Derome, J., 1983: Blocking-like solutions of the potential vorticity equation: their stability at equilibrium and growth at resonance. *J Atmos Sci*, **40**, 2522–2536.
- Neamtan, S.M., 1946: The motion of harmonic waves in the atmosphere. *J Meteorol*, **3**, 53–56.
- Niiler, P.P., 1966: On the theory of wind-driven ocean circulation. *Deep Sea Res*, **13**, 597–606.
- Pearce, R.P., 1985: The global atmospheric circulation and weather forecasting. In *Recent advances in meteorology and physical oceanography*. Royal Meteorological Society.

- Pierrehumbert, R.T. and Malguzzi, P., 1984: Forced coherent structures and local multiple equilibria in a barotropic atmosphere. *J Atmos Sci*, **41**, 246–257.
- Read, P.L., Rhines, P.B. and White, A.A., 1986: Geostrophic scatter diagrams and potential vorticity dynamics. *J Atmos Sci*, **43**, 3226–3240.
- Rhines, P.B. and Young, W.R., 1982: Homogenization of potential vorticity in planetary gyres. *J Fluid Mech*, **122**, 347–367.
- Shutts, G.J., 1983: The propagation of eddies in diffuent jet-streams: eddy vorticity forcing of 'blocking' flow fields. *Q J R Meteorol Soc*, **109**, 737–761.
- , 1987a: Persistent anomalous circulation and blocking. *Meteorol Mag*, **116**, 116–124.
- , 1987b: Some comments on the concept of thermal forcing. *Q J R Meteorol Soc*, **113**, 1387–1394.
- Smagorinsky, J., 1953: The dynamical influence of large-scale heat sources and sinks on the quasi-stationary mean motions of the atmosphere. *Q J R Meteorol Soc*, **79**, 342–366.
- Stern, M.E., 1975: Minimal properties of planetary eddies. *J Mar Res*, **33**, 1–13.
- Tribbia, J.J., 1984: Modons in spherical geometry. *Geophys Astrophys Fluid Dyn*, **30**, 131–168.
- Verkley, W.T.M., 1984: The construction of barotropic modons on a sphere. *J Atmos Sci*, **41**, 2492–2504.
- , 1987: Stationary barotropic modons in westerly background flows. *J Atmos Sci*, **44**, 2383–2398.
- , 1988: On atmospheric blocking and the theory of modons. (Ph D thesis, University of Amsterdam.)
- White, A.A., 1986: Finite amplitude, steady Rossby waves and mean flows: analytical illustrations of the Charney-Drazin non-acceleration theorem. *Q J R Meteorol Soc*, **112**, 749–773.
- Young, W.R. 1987: Selective decay of enstrophy and the excitation of barotropic waves in a channel. *J Atmos Sci*, **44**, 2804–2812.
- Zhang, X., Zeng, Q. and Bao, N. 1986: Nonlinear baroclinic Haurwitz waves. *Adv Atmos Sci*, **3**, 330–340.

551.466.3:551.501.7

Remotely sensed data for wave forecasting

R.A. Stratton

Meteorological Office, Bracknell

Summary

Measurements of wave height and wind speed will be available, after the launch, from the altimeter on ERS-1. The effects of assimilating such data in a global wave model have been investigated using altimeter measurements from SEASAT and GEOSAT. The assimilation improves agreement between the model and the altimeter wave-heights, and it is still evident in a 5-day forecast. These results provide encouragement for the future use of altimeter data.

1. Introduction

ERS-1, the first European Remote Sensing satellite (Duchossois 1983), is scheduled to be launched in 1990. The satellite will carry a radar altimeter, and a wind scatterometer. The instrument of use to wave modellers and forecasters is the altimeter, which is capable of measuring surface wind speed and significant wave height, every second, over a footprint of several square kilometres directly below the satellite. The wind scatterometer also measures surface wind speed and direction over the sea surface, to one side of the satellite track. The data from the altimeter and the wind scatterometer are expected to be available to users within 3 hours of measurement, making it possible to use such data in operational weather and wave forecasting. In this paper the assessment of radar altimeter data only is discussed

At present the Meteorological Office runs two operational wave models: a global version, and a European version covering the North Sea, the Baltic and the Mediterranean. Both models are driven by wind fields from the lowest level of the corresponding numerical weather prediction (NWP) model (Bell and Dickinson 1987).

The Meteorological Office's wave models specify the energy density, $E(f, \theta)$, at each model grid-point where f is the frequency and θ the direction. Wave energy is related to the total surface height variance. The basic physics used for wave growth and dissipation is an improved version of that described by Golding (1983). An extra term has been added to improve the wave model spectrum in situations where the model wind direction turns quickly. A correction term has been added to the advection scheme to ensure that energy moves on great circles.

Actual wave observations are not used to initialize either of the wave models in the present operational suite. Instead the wave forecast is preceded by a wave hindcast to provide an initial wave field. The wave hindcast is a 12-hour wave model run using winds from the NWP assimilation. The hindcast run starts from the wave field at the end of the preceding hindcast. This provides a better initial wave field for the next wave forecast than a wave field obtained from the previous forecast.

To fully initialize a global wave model requires full wave spectral measurements and wind measurements

distributed evenly over the world's oceans. A wave spectrum can consist of either a full two-dimensional spectrum of the energy density in each frequency and direction, or a one-dimensional spectrum where only the energy in each frequency is known. If the full wave spectral information is not available, integrated parameters, e.g. wave height and wave period, could be used instead. The problems with using integrated data are mentioned in section 2.

At present wave spectral information is scarce and not generally available. Some buoys, and new instruments deployed on satellites and aircraft, can measure spectral information, but it is not always easy to interpret the satellite return signals in such a way as to generate the original full two-dimensional wave spectrum in an unambiguous fashion.

Up to now the only sources of wave data have been buoys, ocean weather ships, oil platforms and ships of passage. The ship observations (while the most numerous) are normally visual estimates, and therefore are not regarded as accurate and reliable enough for use in verification or initialization of wave model forecasts. Fig. 1 shows the location of the buoys, ocean weather ships and oil platforms reporting regularly (usually every hour) wave height, wind speed and wave period.

The oil platforms are located in the North Sea. Apart from three weather ships across the Atlantic, the rest of the stations are located within a few hundred kilometres of the coast. There is virtually no data in the southern hemisphere. The lack of data and the concentration of what there is along the coasts do not provide a good coverage of the world's oceans. Data assimilation into the global wave model using the present data would not be worthwhile.

In recent years several new techniques for measuring waves have been developed. These have led to the use of high frequency radar to measure wave heights near to the coast, and radar altimeters to measure wave height and surface wind speed over the open ocean. In 1978 the satellite SEASAT was launched with a radar altimeter, wind scatterometer and synthetic aperture radar on board. The satellite operated for 3 months before failing, providing a large amount of data, the full potential of which has only recently been exploited for wave modelling. In 1985, GEOSAT, a USA naval satellite with a radar altimeter was launched, and is still functioning. Fig. 2 shows the satellite ground track for GEOSAT for a period of 24 hours. The coverage of the oceans is far better than shown in Fig. 1 and makes wave data assimilation appear worth investigating ready for

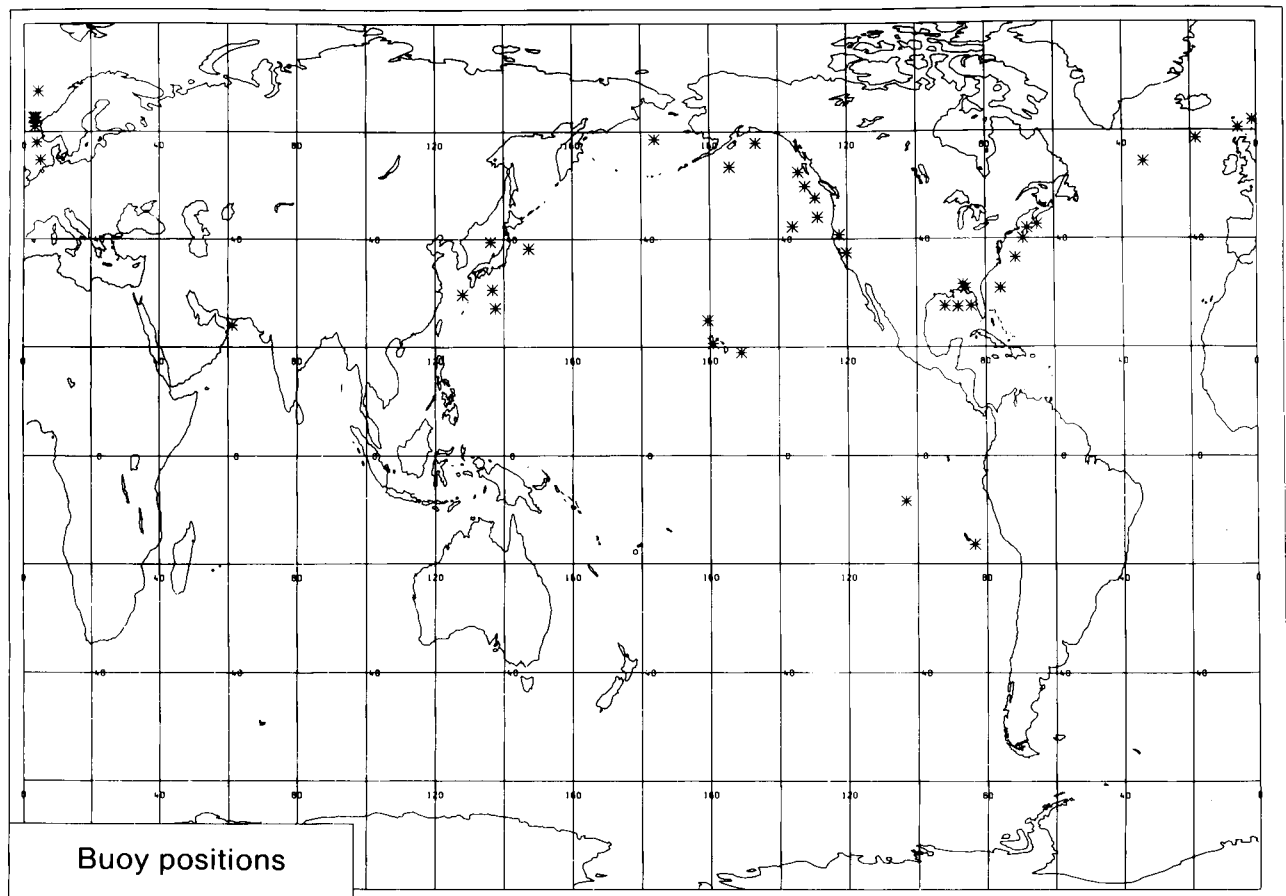


Figure 1. The location of buoys, oil platforms and ocean weather ships reporting wave heights used regularly in operational verification of the Meteorological Office's global wave model. Each station is plotted as an asterisk.

the launch of ERS-1. ERS-1 is expected to have similar global coverage in a 24-hour period to that shown in Fig. 2.

To develop an assimilation scheme for the wave data from ERS-1, it is necessary to use satellite data from the past. The data from GEOSAT has recently become available and has been used in addition to SEASAT data to develop a wave data assimilation scheme for the Meteorological Office's global wave model. The results of wave data assimilation using SEASAT and GEOSAT data are described in section 3.

2. Using remotely sensed data in a wave model

The most useful form of wave measurements for assimilation would be two-dimensional wave spectral data, but this is not available, so integrated parameters such as significant wave height must be used instead. Significant wave height, H_s , is given by

$$H_s = 4 \sqrt{E_{TOT}}$$

where E_{TOT} , the wave energy as calculated by the model, is in units of m^2 and

$$E_{TOT} = \int E(f, \theta) d\theta df$$

the integral of the energy density (in units of $m^2 s rad^{-1}$) over direction, θ , and frequency, f .

It is not a simple matter to turn a measurement of H_s into an energy density spectrum which can be used to adjust the model value. A scheme to retrieve an energy density spectrum from a wave height measurement, making use of a co-located wind speed measurement, has been described by Thomas (1988). A modified version of this scheme has been applied to retrieving an energy spectrum for assimilation into the global wave model (Francis and Stratton 1990). The assimilation scheme used is a successive correction scheme, i.e. it makes use of the observations at their datum time, and spreads the influence of the observation over neighbouring grid-points. Observations are assimilated every hour into the global wave model.

The accuracy and spatial representativeness of an observation need to be considered in order to make good use of any data in an assimilation scheme. The altimeter algorithms determine the wave height and wind speed by measuring the return signal received by the satellite when it sends out a pulse of microwave energy down to the ocean below. The pulse emitted by the radar altimeter has a rectangular shape which is distorted by the uneven sea surface. Energy reflected by the wave-peaks returns to the altimeter sooner than

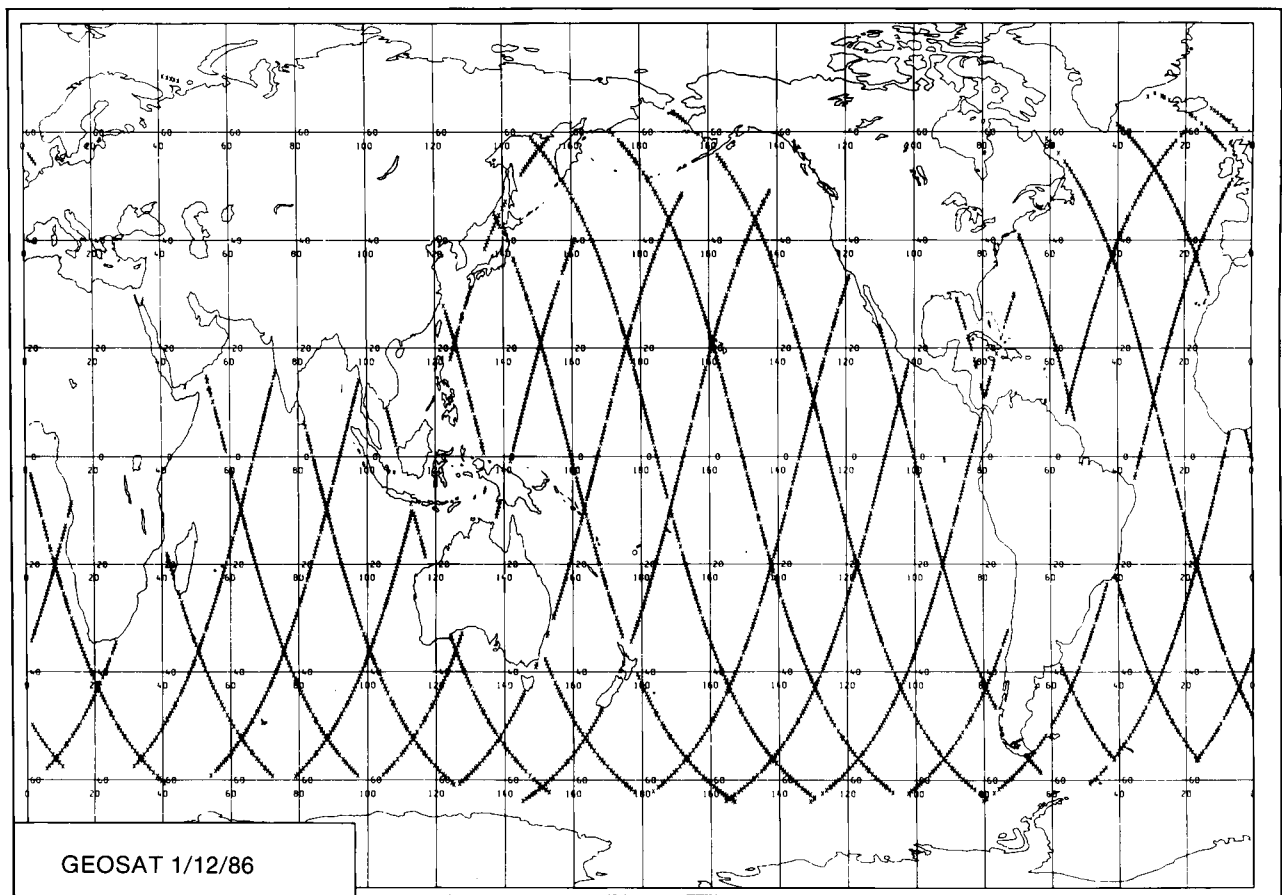


Figure 2. The coverage of quality controlled and averaged GEOSAT altimeter measurements for 24 hours (1 December 1986).

energy reflected from the troughs, leading to a sloped return pulse. The algorithm for wave height uses the slope of the return pulse to calculate the wave height. The wave height algorithm has been compared with buoy measurements up to wave heights of 6 metres, with good agreement (Fedor and Brown 1982, for SEASAT data, and Dobson *et al.* 1987 for GEOSAT data). The altimeter accuracy is usually specified as $\pm 10\%$ or ± 0.5 m whichever is the larger for wave height measurements. Most buoys measure to ± 0.5 m.

The wind speed algorithm depends on the backscatter cross-section. There are several different algorithms in existence but they are inaccurate at high wind speeds where the incident microwave energy is scattered more widely by the rough sea surface; hence the energy scattered back to the altimeter is very small, and small differences in the backscatter can produce large differences in the retrieved wind speed. The altimeter accuracy is specified as $\pm 2 \text{ m s}^{-1}$ for wind speeds up to 18 m s^{-1} . Buoys usually measure to $\pm 1 \text{ m s}^{-1}$ or $\pm 10\%$.

The altimeters operated so far have produced measurements at intervals of about 1 second in time and between 5 and 10 km in distance. The resolution of the present global wave model is approximately 150 kilometres. The SEASAT and GEOSAT altimeter measurements are averaged over 20 seconds to create observations of spatial resolution approximately equal to that of the wave model. As part of the averaging process the altimeter data are quality controlled to remove measurements over ice, close to coasts or significantly different from adjacent values.

3. Wave data assimilation experiments

Until the mid 1980s very little work had been done on developing assimilation schemes for wave models. Since then the ideas put forward by Thomas (1988) have been applied in different ways by several other groups to data assimilation using SEASAT altimeter data (Janssen *et al.* 1989, Esteva 1988 and Hasselmann *et al.* 1988).

So far two different sources of satellite altimeter data have been used in wave data assimilation experiments at the Meteorological Office. The first experiments used data from SEASAT for a period of 6 days starting on 15 September 1978. The second set of experiments used GEOSAT data for 31 days in 1986 starting on 11 November.

3.1 SEASAT data assimilation

A detailed account of the SEASAT assimilation experiments is given in Francis and Stratton (1990) and will not be repeated here. The main objective of the SEASAT work was to show that altimeter data could be successfully assimilated into a wave model, and that improvement of the wave field and the following forecast would result. This was achieved by first running the global wave model for the 6 days in September 1978, without assimilation, to produce a control run. The resulting wave heights were then compared with the

averaged altimeter values. The run was then repeated, assimilating wave data for 24 hours, followed by a further 5 days running without assimilation (experiment 1), in order to assess the impact of the added data. Finally the assimilation was continued for the full 6 days (experiment 2), to see if the wave field required a 'warm up' period to adjust fully to the assimilated data.

Fig. 3 shows the main results of the three runs in the form of a time-series plot of daily mean and root-mean-square differences, for the altimeter minus the model wave heights. The 24-hour assimilation (experiment 1) reduced the mean wave height difference, for the whole globe, between the altimeter data and the wave model from 0.8 m to 0.3 m. The difference relaxed back towards 0.8 m over the following 5 days. This implies that corrections to the initial wave field may have an impact on the following wave forecast even at the end of 5 days. Continuous assimilation (experiment 2) resulted in the wave heights moving closer to the altimeter values. By 19 September the bias was almost zero. Continuous assimilation did not result in a significant further reduction of the root-mean-square difference after the initial fall on 15 September. This suggests that the root-mean-square difference has reached a lower limit imposed by the errors contributed by the model and its driving winds.

Comparison of the model wave heights from the control run, with the altimeter values for the whole globe, gave a mean difference of -0.8 m (model minus altimeter value), and a standard deviation of 1.0 m. The corresponding wind speed differences were a mean scalar difference of -0.4 m s^{-1} and a standard deviation of 3.0 m s^{-1} . This is consistent with the suggestion that the underestimation in wave height is caused by the model winds being too low. The SEASAT altimeter wave heights used in the experiments were calculated using an algorithm which has been shown (Fedor and Brown 1982) to overestimate wave height by 0.5 m for wave heights above 2 m. Hence the altimeter wave heights may be too high, so that the underestimation of the model waves relative to the altimeter values may be too large.

3.2 GEOSAT data assimilation

The GEOSAT data provided an opportunity to investigate the results of assimilating altimeter data into a wave model during the northern hemisphere winter. In 1986 there were far more buoy reports available than in 1978 and so it was possible to use the buoy data as an independent means of checking the results of the assimilation.

The global wave model was run for 31 days starting on 11 November 1986 to provide a control run, and the resulting wave heights were compared with the averaged altimeter wave heights for the last 27 days. The 31-day GEOSAT run was repeated, this time assimilating altimeter data into the wave model, and the results for the last 27 days were compared with those of the control

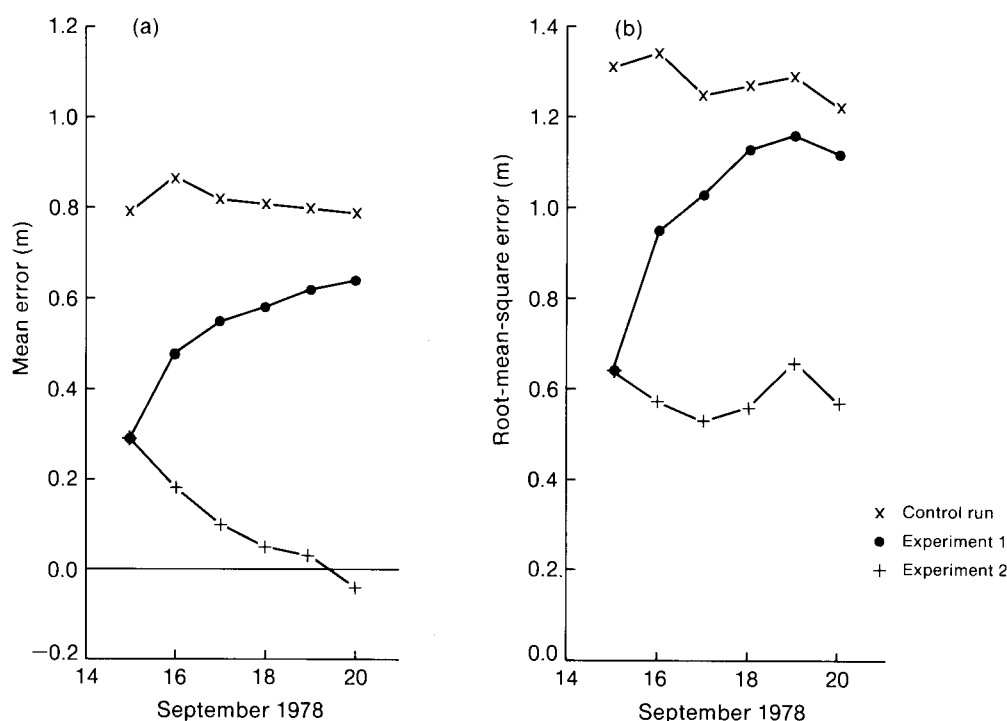


Figure 3. The SEASAT control run and experiments 1 and 2 wave height (observed–model) errors; (a) mean and (b) root-mean-square values.

run. The first 4 days were omitted from the comparison to allow the model to adjust to the assimilated data. Table I gives the results of the comparison of the model wind speeds and wave heights against the averaged altimeter values, broken down into latitude bands for both the control and assimilation runs. The model wind speeds are biased lower than the altimeter values for the whole globe with model wind speeds being higher than the measured values in the northern hemisphere between 20° and 60°N. The largest number of winds greater than 15 m s⁻¹ are observed by the altimeter in this region. In the northern hemisphere the NWP analysis of deep depressions with strong surface winds is likely to be better than in the southern hemisphere because of the greater number of observations, hence the model

prediction of high waves will be better in the northern hemisphere.

The wave height differences for the latitude bands show the effect of the bias in wind speeds, the model wave heights being lower than the altimeter in the south and higher in the north. In the assimilation run, the overall bias is modified so that model values are higher than altimeter values in all areas. The assimilation of wave data reduces the spread of differences, as found in the SEASAT work, but this time as the GEOSAT retrieval algorithm gives unbiased wave heights, the mean difference is not substantially changed. In fact the mean difference changes from an underestimation for the low waves (0–3 m) to an overestimation. This may indicate that the wave model does not dissipate swell

Table I. Wave height and wind speed difference statistics for the GEOSAT control and assimilation runs 00 UTC on 15 November 1986 to 00 UTC on 12 December 1986. Differences are model minus altimeter average.

Latitude range (°)	Wind speed (m s ⁻¹)			Wave height (m)				
	Number	Mean	s.d.	Number	Control Mean	Control s.d.	Assimilation Mean	Assimilation s.d.
40–60 N	6 745	1.1	3.7	7 210	0.6	1.0	0.2	0.6
20–40 N	11 399	0.5	2.5	11 415	0.2	0.6	0.2	0.4
0–20 N	15 639	–0.3	2.5	15 663	0.1	0.6	0.2	0.4
20–0 S	15 902	–0.5	2.0	15 916	–0.1	0.4	0.2	0.3
40–20 S	19 282	–0.5	2.3	19 297	–0.3	0.6	0.1	0.3
60–40 S	25 969	–0.3	3.0	26 002	–0.4	0.9	0.1	0.5
All	98 551	–0.2	2.7	99 321	–0.1	0.8	0.1	0.4

energy quickly enough, or that the assimilation process is spreading energy into the wrong directions.

The results from latitudes 20°–60°N have been studied further by comparing the differences between the model and altimeter with those found between the model and buoy or ocean weather ship reports. Table II gives the wind speed difference statistics broken down into several wind speed ranges. At low wind speeds both the altimeter and the buoy values are lower than the model. Whereas buoys measure wind speeds at heights between 6 m and 10 m above mean sea level, ocean weather ships measure values at 19.5 m, and the altimeter algorithm is valid for winds at 19.5 m. Since model wind speeds are at a nominal height of 20 m, it is not surprising that the buoy values are lower than those of the model. Comparison of the model wind speeds

with the altimeter values shows that altimeter algorithm also underestimates the wind speeds below 15 m s⁻¹. At winds greater than 15 m s⁻¹ the wave heights can exceed 5 m. Measurements of high wind speeds by buoys with anemometer heights of only 6 m may be affected by such high waves. At higher wind speeds, as mentioned in section 2, the algorithm is no longer reliable. The scatter in the differences increases with wind speed for both buoys and altimeter measurements. These results show that altimeter wind speeds must be used with some caution, particularly at high wind speeds. However, in view of their co-location with the altimeter wave-height measurements, the wind speeds remain an acceptable source of data for the assimilation scheme.

The wave-height difference statistics are given in Table III (model minus altimeter) and Table IV (model

Table II. Wind speed difference statistics for the GEOSAT control run 00 UTC on 15 November 1986 to 00 UTC on 12 December 1986. Values given are for model minus altimeter and model minus buoy/weather ship for latitudes 20°–60°N.

Wind-speed range (m s ⁻¹)	Model–altimeter (m s ⁻¹)			Model–buoy/ship (m s ⁻¹)		
	Number	Mean	s.d.	Number	Mean	s.d.
0–10	13 198	0.5	2.5	6230	0.8	2.4
10–15	4 414	1.6	3.6	2115	1.0	3.0
> 15	532	–0.7	4.8	1053	–0.1	3.5
All	18 144	0.7	3.0	9398	0.7	2.7

Table III. Wave height difference statistics for GEOSAT data 00 UTC on 15 November 1986 to 00 UTC on 12 December 1986. Values are for model minus altimeter. Latitude band 20°–60°N.

Wave-height range (m)	Control (m)			Assimilation (m)	
	Number	Mean	s.d.	Mean	s.d.
0–3	11 679	0.3	0.6	0.2	0.4
3–6	6 069	0.5	1.0	0.2	0.6
> 6	877	0.8	1.3	0.1	0.8
All	18 625	0.4	0.8	0.2	0.5

Table IV. Wave height difference statistics for buoys and weather ships, 00 UTC on 15 November 1986 to 00 UTC on 12 December 1986. Values are for model minus observation.

Wave-height range (m)	Control (m)			Assimilation (m)	
	Number	Mean	s.d.	Mean	s.d.
0–3	5163	0.2	0.7	0.2	0.6
3–6	2997	0.2	1.0	0.1	0.9
> 6	1183	0.4	1.6	–0.1	1.5
All	9343	0.2	1.0	0.1	0.9

minus buoy/ocean weather ship). The results show that the model overestimates wave heights when compared with both altimeter and buoy values. This overestimation is consistent with the overestimation of wind speeds found in Table II. The differences increase with wave height. The assimilation process, as might be expected, reduces the difference between the altimeter and model values, to 0.2 m for 0–6 m waves and to 0.1 m for waves greater than 6 m. The assimilation scheme has a greater impact on the higher waves which are mainly due to the local wind. The buoy statistics are also improved particularly at high wave heights (> 6 m), changing the model bias from an overprediction to underprediction

relative to the buoy/ship measurements. This may indicate a difference in the calibration of the altimeter and the buoy/ship measurements. The process whereby the assimilation scheme adjusts the model at the buoy locations is indirect, as satellite overpasses are relatively few. The improvement in agreement between the model and the buoy values comes mainly from energy propagated outwards from corrections made to the model along the satellite track.

Figs 4(a) and 4(b) show time-series of wind speeds and wave heights for 5 days in December at the ocean weather station Lima. The wind time-series, Fig. 4(a), shows an error in timing between the model and the

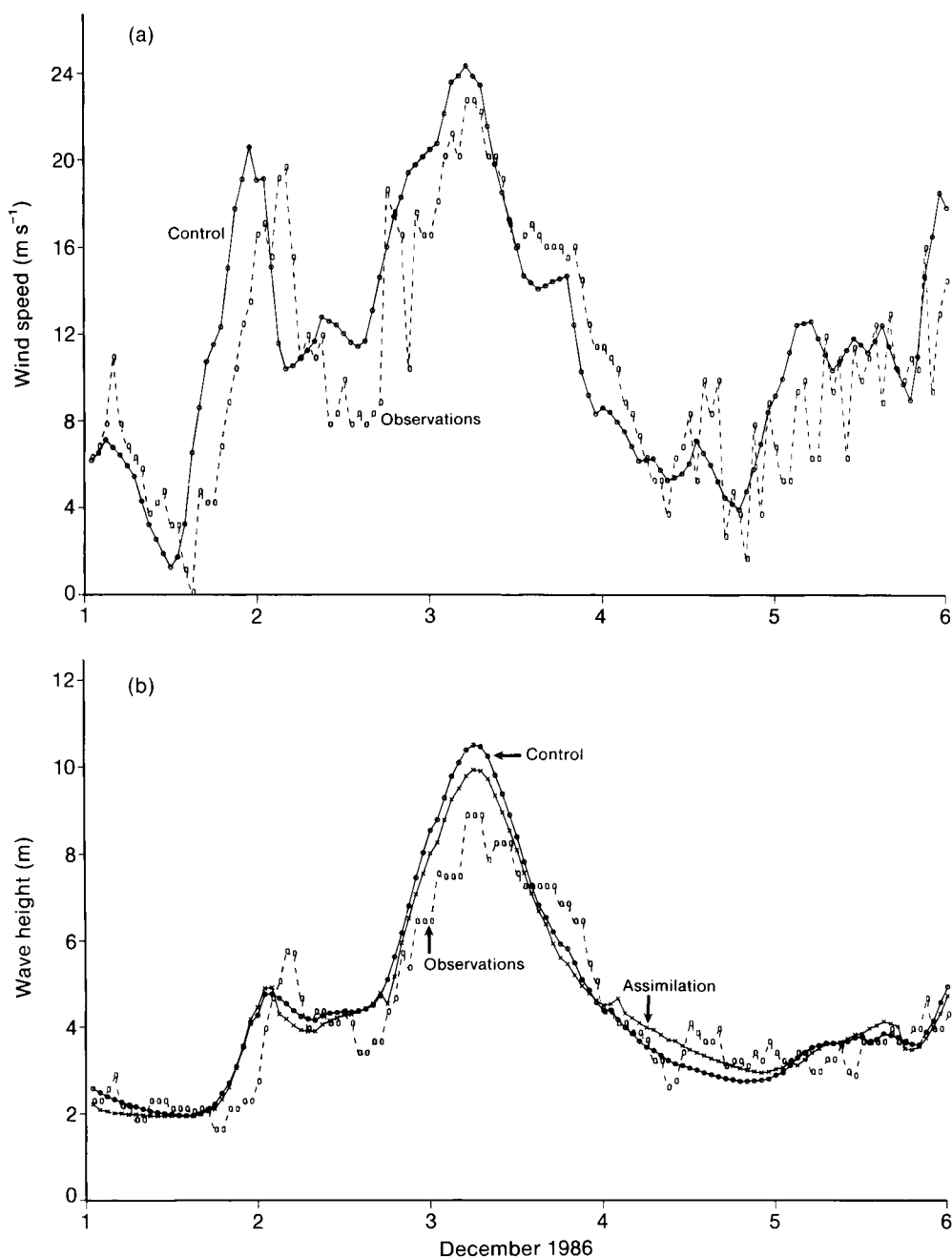


Figure 4. Time-series for ocean weather ship Lima (57° N, 20° W) for 5 days in December 1986 for (a) wind speed and (b) wave height. All values are plotted hourly.

4. Conclusions

and the altimeter. The results of the assimilation persist for at least 5 days and may improve the operational global wave model 5-day forecasts. The largest improvements are found in the southern hemisphere where the driving winds are not so well analysed due to the lack of observations in the atmospheric assimilation.

After the launch of the ERS-1 scatterometer, wind data will be used in the atmospheric assimilation scheme and therefore the quality of the surface winds should improve in the southern hemisphere.

The GEOSAT study has shown that the global wave model agrees well with the altimeter measurements of wave height before assimilation. Assimilation of the altimeter data reduces the differences between the altimeter and the wave model, but individual time-series show that the altimeter corrections do not always agree with the buoy or ship observations. This study has also shown that in a northern hemisphere winter month the use of altimeter data in assimilation does improve the overall agreement between the model and independent reports from buoys or ocean weather ships.

So far no work has been done on assimilating data into a shallow-water wave model like the Meteorological Office's European wave model. Before assimilating data into such a model it will be necessary to develop a

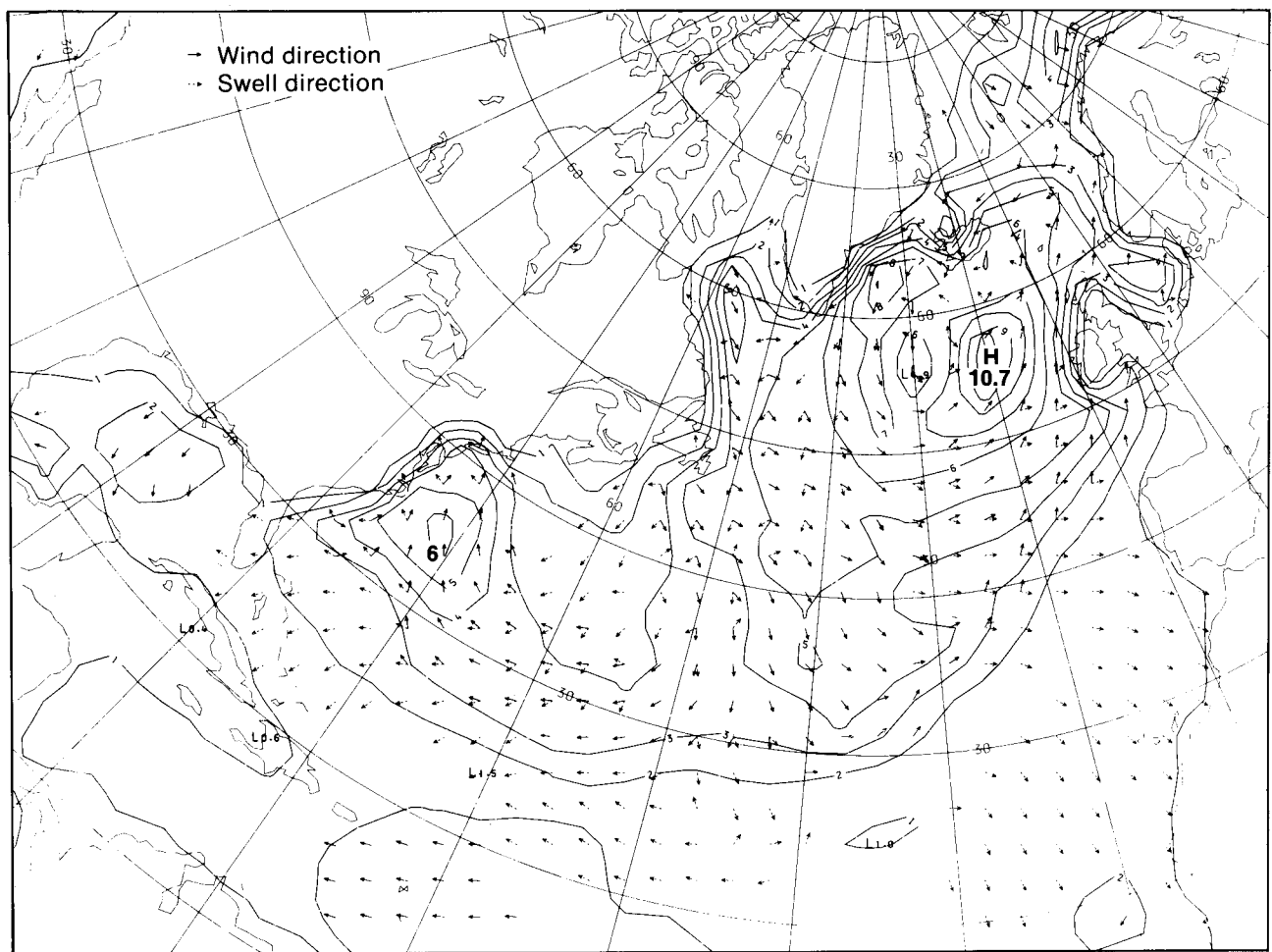


Figure 5. Wave height (m) isopleth chart for the North Atlantic 06 UTC on 3 December 1986 from the control run.

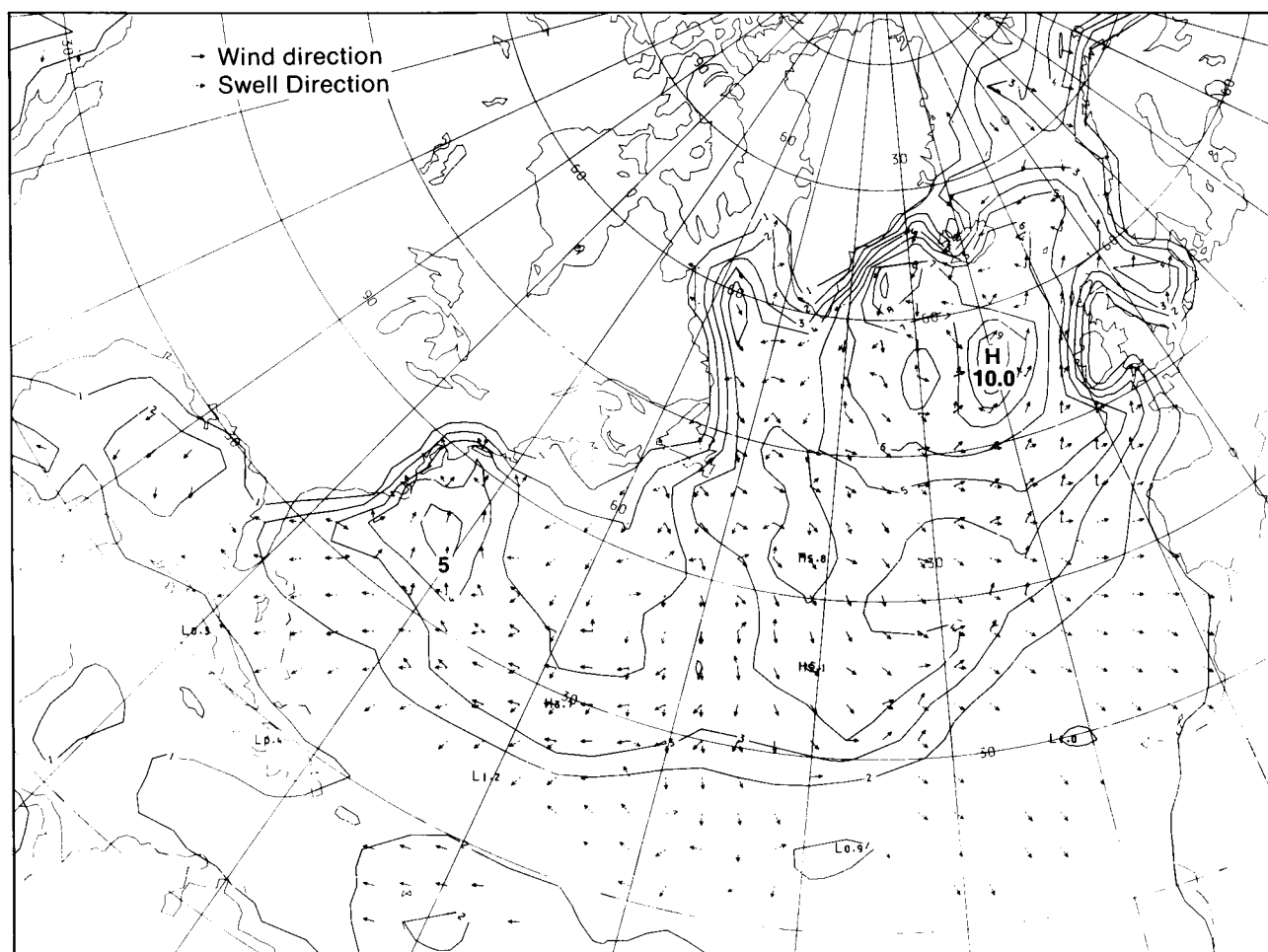


Figure 6. As Fig. 5 but from a run assimilating GEOSAT data.

method to spread the influence of an observation over an area of sea with varying depth.

If spectral wave data becomes available in the future it should be relatively simple to extend the existing wave assimilation scheme. Two-dimensional wave spectra can be used directly in the assimilation process. These developments are possibilities for the future, in the meantime we may look forward to making use of the wind and wave data from ERS-1.

Acknowledgements

The assistance of K. Rider throughout this work is gratefully acknowledged.

References

- Bell, R.S. and Dickinson, A., 1987: The Meteorological Office operational numerical weather prediction system. *Sci Pap, Meteorol Off*, No. 41.
- Dobson, E., Monaldo, F., Goldhirsch, J. and Wilkerson, J., 1987: Validation of GEOSAT altimeter derived wind speeds and significant wave heights using buoy data. Baltimore, Maryland, Johns Hopkins University, Applied Physics Laboratory, *Tech Dig*, 8, No. 2, 222-234.
- Duchossois, G., 1983: The first European remote sensing satellite (ERS-1): Overall description, potential applications and users. European Space Agency (ESA) SP-205, 25-36.
- Esteve, D.C., 1988: Evaluation of preliminary experiments assimilating SEASAT significant wave heights into a spectral wave model. *J Geophys Res*, 93, 14099-14105.
- Fedor, L.S. and Brown, G.S., 1982: Wave height and wind speed measurements from the SEASAT radar altimeter. *J Geophys Res*, 87, 3254-3260.
- Francis, P.E. and Stratton, R.A., (1990): Some experiments to investigate the assimilation of SEASAT altimeter wave height data into a global wave model. (Submitted to *Q J R Meteorol Soc*.)
- Golding, B., 1983: A wave prediction system for real-time sea state forecasting. *Q J R Meteorol Soc*, 109, 393-416.
- Hasselmann, K., Hasselmann, S., Bauer, E., Bruning, C., Lehner, S., Graber, H. and Lionello, P., 1988: Development of a satellite SAR image spectra and altimeter wave height data assimilation system for ERS-1. Max Planck Institute for Meteorology, report No. 19, European Space Agency contract report, contract No. 6875/87 HGE I(SC).
- Janssen, P.A.E.M., Lionello, P., Reistad, M. and Hollingsworth, A., 1989: Hindcast and data assimilation studies with the WAM model during the SEASAT period. *J Geophys Res*, 94, 973-993.
- Thomas, J.P., 1988: Retrieval of energy spectra from measured data for assimilation into a wave model. *Q J R Meteorol Soc*, 114, 781-800.

Award

The Rank Prize Fund Award for Opto-electronics, 1989

In 1972, in accordance with the wishes of the late Lord Rank, a fund was set up for prizes to be awarded to researchers making significant advances in opto-electronics.

Prizes from this fund have been awarded to a group of workers responsible for the design and use of the Pressure Modulator Radiometer (PMR) for investigating the temperature of atmospheres and the concentration of gaseous components. The group consists of Drs F.W. Taylor, G.D. Peskett and C.D. Rodgers of the Department of Atmospheric, Oceanic and Planetary Physics, Clarendon Laboratory, Oxford and Dr J.T. Houghton, formerly at Oxford, but now Director-General of the Meteorological Office.

The PMR is a device which enables the outgoing radiation (often very weak) from different gases in a planetary atmosphere, and from different levels, to be measured. Radiation which is easily absorbed can only escape from the upper layers of an emitting gas, while radiation which is only slightly absorbed can travel upwards from lower layers. The radiation observed depends upon the temperature and concentration profiles of the gas — if one is known then the other can be estimated from the observations. The absorption depends upon the precise wavelength of observation, so in principle a few narrow spectral bands at carefully selected wavelengths could be used to measure radiation from a chosen range of layers of an atmosphere. The penalty is that the radiation in individual narrow wavebands is very small.

This problem can be overcome by observing the strength of the upwelling radiation alternately through a cell containing the gas of interest and through an empty

one a combination which acts like a filter with numerous spectral slits. The general level of the atmosphere from which the radiation is emitted is determined by the cell gas pressure. The disadvantage is the difficulty of maintaining stable optical balance of the two cells. In the PMR, only one cell is used, the gas pressure being modulated sinusoidally by a piston in a connecting cylinder and the amplitude of the difference signal at that frequency is related to the radiation from levels above those observed with an unmodulated cell. A further benefit is that the piston frequency can be made to indicate the cell gas pressure, allowing calibration remotely. An adaptation of the PMR utilizing the 'Stirling cycle' is also used to cool the radiation detectors to low temperatures to increase their sensitivity.

PMRs designed and built at the Clarendon Laboratory and by the Meteorological Office have been flown on several earth satellites. Observations of CO₂, with its constant known mixing ratio, enable the temperature profile to be deduced. Observations of the radiation from other trace gases (the oxides of nitrogen, for instance) can then be used to deduce their concentrations. A PMR was also flown on the Pioneer Venus satellite to observe the temperature structure of the atmosphere of Venus from observations of CO₂ radiation.

The prize-giving took place at the Royal Society's meeting rooms on 26 September 1989. After a welcoming address by Sir John Davis, CVO, who is the chairman of the Trustees of the Rank Prize Funds, the awards were made by Sir George Porter (President of the Royal Society). Dr Taylor responded on behalf of the four prize winners.

On the same occasion, Dr J.L. Monteith, well known for his work on meteorological aspects of plant physiology (especially evapotranspiration), was awarded one of the Rank prizes for Nutrition, for his elucidation of the physical principles determining crop growth.



The photograph shows from left to right — Dr C.D. Rodgers, Sir George Porter, Dr F.W. Taylor, Sir John Davis, Dr J.T. Houghton and Dr G.D. Peskett.

Workshop report

Workshop on Numerical Products from Bracknell, Meteorological Office College, Shinfield Park, Reading 26–28 June 1989

A Workshop on Numerical Products from Bracknell was held at the Meteorological Office College, Shinfield Park from 26 to 28 June 1989 and was attended by some 44 delegates from 32 countries, including many forecasters and numerical modellers. The principal aim of the workshop was to describe and illustrate the range of specialized products that are derived from the Meteorological Office operational numerical weather prediction global and regional models for use by the forecasters, which could have direct application and uses in other Meteorological Services. Presentations were made to the workshop by Meteorological Office staff mostly from the Central Forecasting Office (CFO), and the Forecasting Products and Forecasting Research Branches. A brochure was prepared with the help of the Graphics Office and Editing Section containing abstracts of the presentations along with illustrations of most of the specialized products available.

The workshop was chaired jointly by Dr P. Ryder, Deputy Director (Forecasting), and Mr R. Morris, Assistant Director (Central Forecasting) who, as head of the Bracknell Regional Specialized Meteorological Centre (RSMC) for WMO, was also responsible for the organization of the workshop.

The workshop was formally opened by Dr J.T. Houghton, the Director-General of the Meteorological Office, who welcomed the delegates and pointed out the importance of the basic WMO philosophy of free exchange of data and products between Member States. No amount of sophisticated modelling or more powerful computer hardware can replace observations, and so all Members have their part to play in the process.

Following a wide-ranging and interesting review by A. Gadd of the history of the development of numerical weather prediction (NWP), there were two talks on data assimilation. Firstly, A. Lorenc described the system of four-dimensional data assimilation used in the current operational models, and then M. Stubbs described some of the techniques used by forecasters to add value to the NWP analysis, largely through skilful interpretation of satellite imagery. C. Hall showed some results from the process of monitoring the observations used by the NWP models; in particular it was shown how systematic errors could be identified in the data, which were then used to correct the data before processing. The first day was concluded with a talk from A. Woodroffe who described how forecasters in the CFO evaluate and interpret the NWP products in formulating their guidance to dependent forecasters and others.

On the following morning, the delegates were given a tour of the Richardson Wing of the Meteorological

Office Headquarters, which contains the operational forecasting, telecommunications and computing centres. After lunch, the workshop reassembled to hear about developments in telecommunications from P. Sowden, who described new methods being devised to handle the increasing volume of data, including the use of communication channels on Meteosat for broadcast to Africa. This was followed by a talk from R. Morris, who demonstrated the capability of the global model to simulate the development of tropical storms and to predict the movement of these storms with some skill over 5 days ahead. An important part of the forecasting process was the fine tuning of the analysis by forecasters in the CFO, making use of local tropical cyclone advisories and satellite imagery. It was noted that the CFO had issued advisories twice daily to Member States in the South Pacific throughout the 1988/89 season. K. Pollard described the range of products that are derived from the NWP model output to help the forecaster with preparation of significant weather charts for civil aviation. Most of the weather elements that are required can now be derived directly from the model output, leaving the forecaster with the task of fine tuning the final product. Several airlines are now making more direct use of the forecast winds by having headwind components calculated for specific routes, for example.

P. Francis spoke about the Meteorological Office wave and storm surge models, the wave model using the NWP model predictions of surface wind to calculate the wave heights and periods, and also the spectrum of energy levels. The storm surge model is used principally to predict tidal levels around the UK continental shelf, but the model can be applied wherever coastal areas are prone to tidal flooding. Finally, M. Cullen outlined the specification of the new unified model which will become operational on the supercomputer in 1990. The new global model will have a grid length only slightly greater than the current regional model and will therefore be able to simulate smaller-scale features such as tropical cyclones more realistically than hitherto.

There were two open forums chaired by H. Lyne in which the delegates were invited to comment on products that are available to Member States. Feedback on the usefulness of the products was regarded as essential, and it was important to know whether national requirements would be satisfied by the new products being developed at Bracknell.

It was concluded that the workshop had achieved its prime objective of creating a greater awareness of the range and quality of NWP products available at Bracknell RSMC. In turn, the delegates were conscious of the importance of timely and accurate observations without which numerical modelling would be of little value.

B.K. Lloyd

Radar photographs — 8 November 1989 at 0600 and 1200 UTC

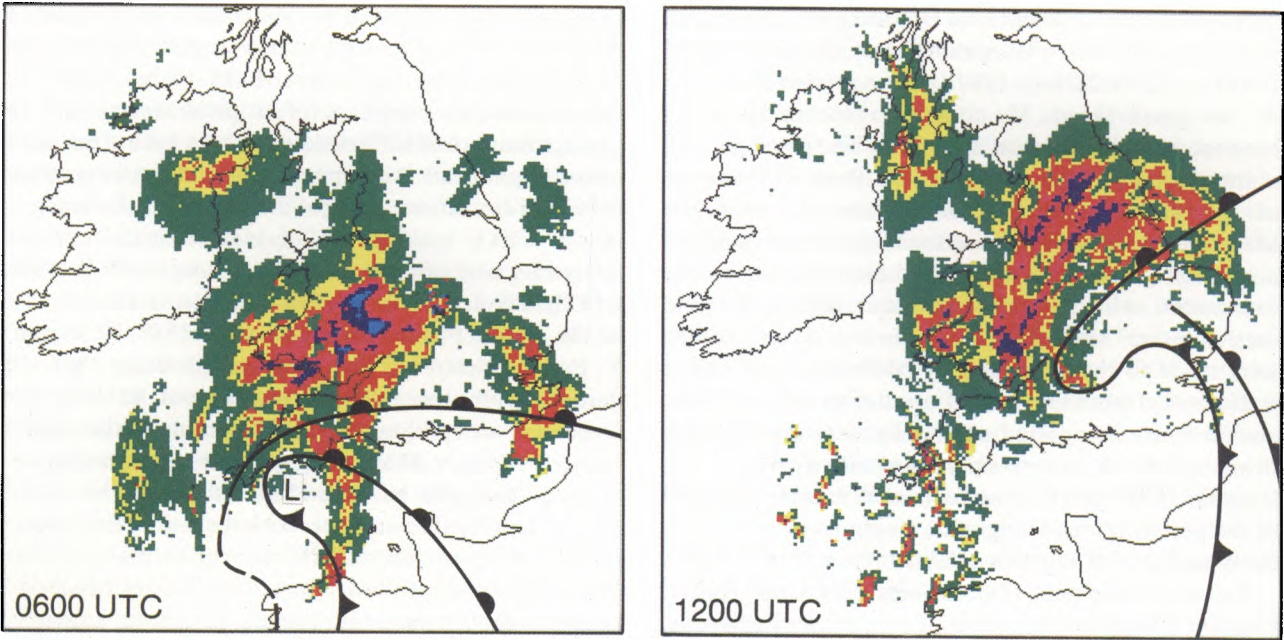


Figure 1. Radar pictures for 0600 and 1200 UTC on 8 November 1989. Increasing rainfall rates are represented by the colour sequence: green, yellow, red, magenta, blue and cyan. Frontal locations are superimposed, dashed where uncertain.

The major feature in the pictures is a broad band of rain to the north of and curving around the western flank of an intense deepening low. Sequential replay of images indicated that the precipitation pattern as a whole moved with the low, although individual precipitation elements within its western flank turned cyclonically and quickly decayed. The rain-bands over south-east England and the English Channel at 0600 UTC moved quickly north-eastwards and by 1200 UTC convection was occurring over south-west England (Fig. 1).

The surface frontal analysis is particularly interesting. Detailed analysis of temperature and dew-point (Fig. 2) suggests the double structure shown. The strongest thermal gradient is associated with the northern warm front, which is related to the major rain area and is bent back around the low centre, where there is a small warm core. There is no evidence of occlusion. By 1200 UTC, it was difficult to locate two cold fronts.

The overall distribution of precipitation and surface weather was similar to that of several other intense depressions, including the storm of October 1987. In each case a bent back warm front* could be analysed which was very active in terms of thermal contrast and precipitation with very low temperatures observed in the area of heavy rain to the north. Behind the low (usually

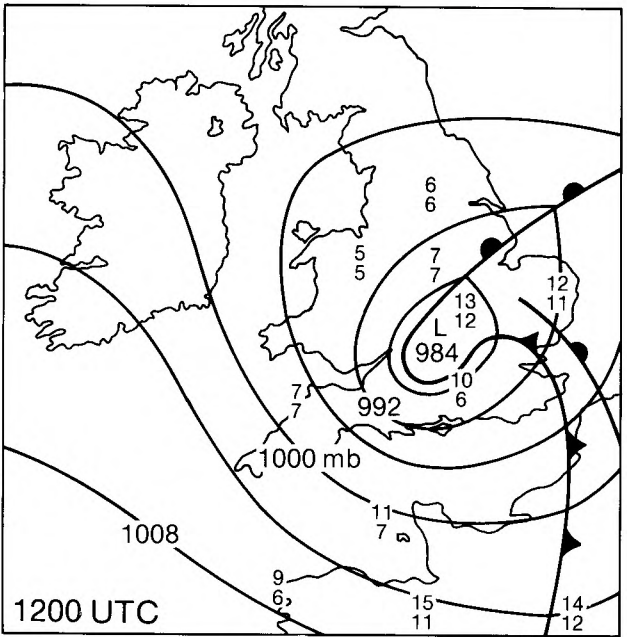


Figure 2. Surface analysis at 1200 UTC on 8 November 1989. Temperatures (°C) (upper) and dew-points (lower) are shown for selected observing stations.

on the western flank), precipitation decayed rapidly. Strongest winds within each cyclonic system lay within and just ahead of the region of precipitation decay.

G.A. Monk

* Shapiro, M.A. (1989) The mesoscale structure of extratropical marine cyclones. IAMAP 1989. Abstracts, Vol. 2.

GUIDE TO AUTHORS

Content

Articles on all aspects of meteorology are welcomed, particularly those which describe results of research in applied meteorology or the development of practical forecasting techniques.

Preparation and submission of articles

Articles, which must be in English, should be typed, double-spaced with wide margins, on one side only of A4-size paper. Tables, references and figure captions should be typed separately. Spelling should conform to the preferred spelling in the *Concise Oxford Dictionary* (latest edition). Articles prepared on floppy disk (Compucorp or IBM-compatible) can be labour-saving, but only a print-out should be submitted in the first instance.

References should be made using the Harvard system (author/date) and full details should be given at the end of the text. If a document is unpublished, details must be given of the library where it may be seen. Documents which are not available to enquirers must not be referred to, except by 'personal communication'.

Tables should be numbered consecutively using roman numerals and provided with headings.

Mathematical notation should be written with extreme care. Particular care should be taken to differentiate between Greek letters and Roman letters for which they could be mistaken. Double subscripts and superscripts should be avoided, as they are difficult to typeset and read. Notation should be kept as simple as possible. Guidance is given in BS 1991: Part 1: 1976, and *Quantities, Units and Symbols* published by the Royal Society. SI units, or units approved by the World Meteorological Organization, should be used.

Articles for publication and all other communications for the Editor should be addressed to: The Director-General, Meteorological Office, London Road, Bracknell, Berkshire RG12 2SZ and marked 'For Meteorological Magazine'.

Illustrations

Diagrams must be drawn clearly, preferably in ink, and should not contain any unnecessary or irrelevant details. Explanatory text should not appear on the diagram itself but in the caption. Captions should be typed on a separate sheet of paper and should, as far as possible, explain the meanings of the diagrams without the reader having to refer to the text. The sequential numbering should correspond with the sequential referrals in the text.

Sharp monochrome photographs on glossy paper are preferred; colour prints are acceptable but the use of colour is at the Editor's discretion.

Copyright

Authors should identify the holder of the copyright for their work when they first submit contributions.

Free copies

Three free copies of the magazine (one for a book review) are provided for authors of articles published in it. Separate offprints for each article are not provided.

Editor: B.R. May
Editorial Board: R.J. Allam, R. Kershaw, W.H. Moores, P.R.S. Salter

Vol. 119
No. 1410

Contents

	Page
Steady states in a turbulent atmosphere. A.A. White	1
Remotely sensed data for wave forecasting. R.A. Stratton	9
Award	
The Rank Prize Fund Award for Opto-electronics, 1989	18
Workshop report	
Workshop on Numerical Products from Bracknell, Meteorological Office College, Shinfield Park, Reading, 26–28 June 1989	19
Radar photographs — 8 November 1989 at 0600 and 1200 UTC	
G.A. Monk	20

Contributions: It is requested that all communications to the Editor and books for review be addressed to the Director-General, Meteorological Office, London Road, Bracknell, Berkshire RG12 2SZ, and marked 'For *Meteorological Magazine*'. Contributors are asked to comply with the guidelines given in the *Guide to authors* which appears on the inside back cover. The responsibility for facts and opinions expressed in the signed articles and letters published in *Meteorological Magazine* rests with their respective authors. Authors wishing to retain copyright for themselves or for their sponsors should inform the Editor when submitting contributions which will otherwise become UK Crown copyright by right of first publication.

Subscriptions: Annual subscription £30.00 including postage; individual copies £2.70 including postage. Applications for postal subscriptions should be made to HMSO, PO Box 276, London SW8 5DT; subscription enquiries 01–873 8499.

Back numbers: Full-size reprints of Vols 1–75 (1866–1940) are available from Johnson Reprint Co. Ltd, 24–28 Oval Road, London NW1 7DX. Complete volumes of *Meteorological Magazine* commencing with volume 54 are available on microfilm from University Microfilms International, 18 Bedford Row, London WC1R 4EJ. Information on microfiche issues is available from Kraus Microfiche, Rte 100, Milwood, NY 10546, USA.

ISBN 0 11 728661 3 ISSN 0026–1149

© Crown copyright 1990. First published 1990

The Meteorological Magazine

February 1990

Heavy snowfall event
Exeter temperatures



DUPLICATE JOURNALS

National Meteorological Library

FitzRoy Road, Exeter, Devon. EX1 3PB

HMSO

Met.O.992 Vol. 119 No. 1411



3 8078 0010 2441 5

The Meteorological Magazine

February 1990
Vol. 119 No. 1411

551.578.45:551.553.11:551.547.5:551.513.2(420+261.26)

Persistent coastal convergence in a heavy snowfall event on the south-east coast of England

W.S. Pike

19 Inholmes Common, Woodlands St. Mary, Newbury, Berkshire RG16 7SX

Summary

A detailed investigation of the heavy coastal snowfall during the period 11–13 January 1987 is presented, accompanied by an explanation of the sequence of events.

1. Introduction

General insurance losses associated with severe weather and heavy snowfalls in south-east England during January 1987 have been assessed at £285 million. Taking account of inflation, this is the third-largest figure for natural disasters affecting all of the United Kingdom since 1975, ranking only after the £2000 million (approximately) for the Great Storm of October 1987 and the arctic conditions during the winter of 1981–82 (which cost near £327 million) in terms of total losses sustained by the main UK insurance companies (Jackson 1988).

Small-scale (i.e. large area coverage) synoptic charts plus NOAA-9 and NOAA-10 AVHRR satellite pictures have already been published to illustrate accounts of the bitterly cold polar continental outbreak over the period 10–15 January 1987, when both extremely low 1000–500 mb thickness values and daytime temperatures were recorded on the 12th (Mortimore 1987, Brugge 1987, Webb 1987).

The heavy but localized snowfalls during this period near coasts bordering the southern North Sea and the English Channel have been well-described by (chronologically) Bacon (1987), Selfe (1987), Van den Berg (1987), Monk (1987), Kain (1988) and Lumb (1988,

1989). Three of these authors mention coastal convergence between over-land and over-sea airflows as being a significant cause of the localized snowfalls.

This paper aims to pursue their ideas, using analyses of satellite and surface observations, and present larger-scale synoptic charts drawn at 6-hourly intervals to illustrate mesoscale features. Concern has been expressed regarding the adequacy of synoptic charts with isobars drawn at 4 mb intervals in mesoscale analysis; in this work isobars at smaller intervals are used which reveal more clearly important features present in the surface synoptic situation during this period.

Fig. 1 locates most of the places referred to in the text.

2. The Synoptic situation

The general situation was, at first, dominated by a powerful anticyclone which reached its maximum central pressure over the Central Norwegian Massif during the evening of the 11th, 1055.0 mb (corrected to mean sea level) being recorded at Bråtå (61° 54'N, 7° 52'E, alt. 710 m) at 18 UTC. Thereafter, pressure fell steadily over the United Kingdom as a depression began to develop and move eastwards over France during the 13th.

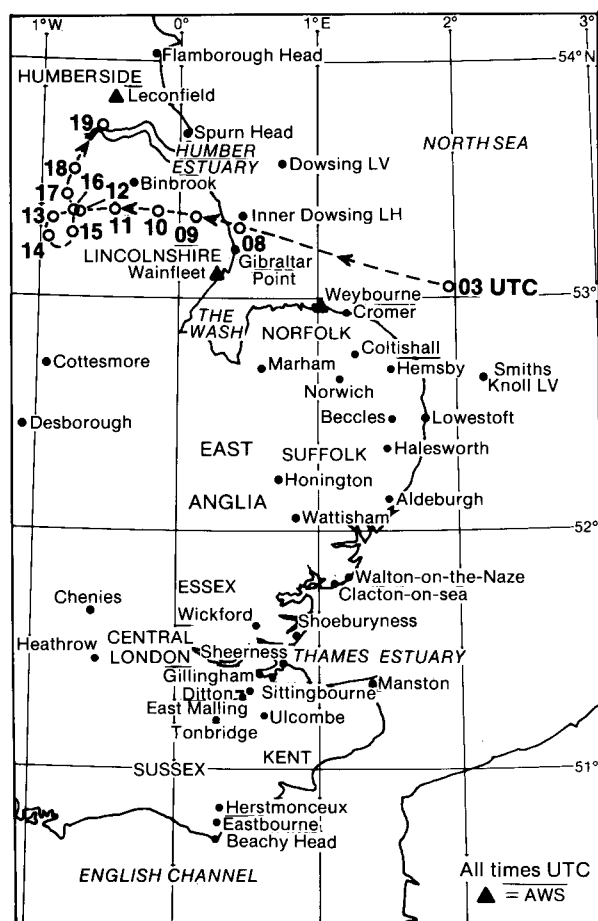


Figure 1. Location of most of the places referred to in the text. Also shown is the track of a small disturbance on 12 January 1987, numbers are times (UTC).

However, during the first evening of this cold outbreak on 10 January, surface wind reports from The Netherlands and East Anglia indicated that a trough was beginning to form where increasingly cold polar continental air was advecting from the east over the relatively warm southern North Sea. This trough is not readily apparent in surface charts drawn at 4 or 5 mb intervals as, for example, in Brugge (1987). Fig. 2(a) suggests that by 03 UTC on the 11th, this trough was well developed; a sequence of these large-scale synoptic charts (Figs 3(a)–3(h)) underlines its persistence, which spanned some 66 hours, until late on the 13th. The marine trough appears to have been thermally maintained from the surface, and independent of the movement overhead of minor ‘cold airmass’ troughs, such as that shown crossing East Anglia from the north-east later on the 11th in Figs 3(a)–3(c).

Therefore, this offshore trough may be regarded as a quasi-stationary wintertime marine feature associated with relatively warm water, in its formation similar to the summertime thermal depression (or, more familiar heat low) which develops, often over the warmest ground inland.

Troughing over the sea has an important effect, particularly in this instance along the east Suffolk–Essex coastline (and also on 12 January 1987 off southern Cornwall), through backing the pressure gradient precisely where the onshore wind could make a smaller angle with that coastline than would otherwise have occurred in a straightforward easterly airflow.

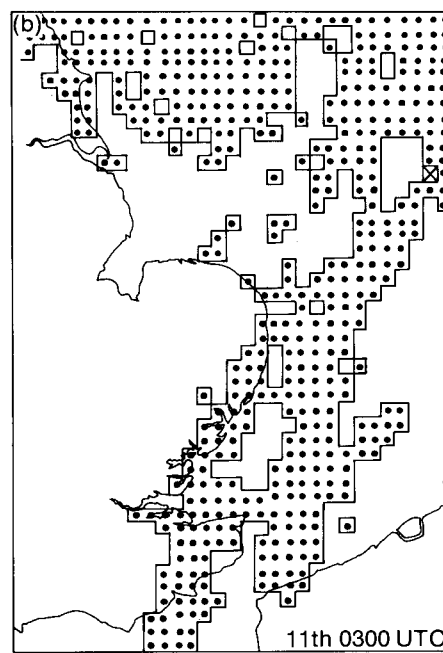
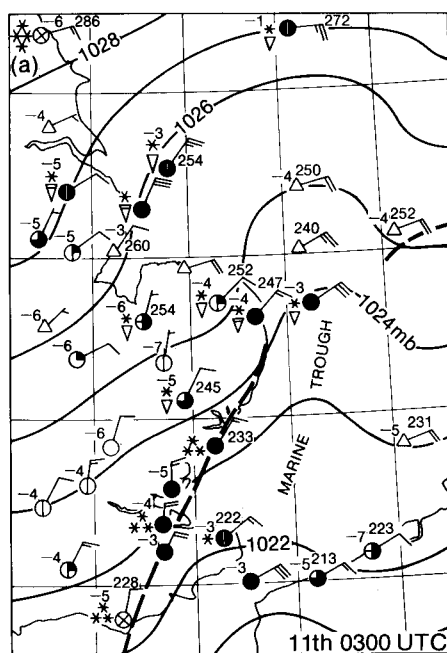


Figure 2. Situation at 03 UTC on 11 January 1987; (a) surface observations (usual symbols with triangles denoting automatic weather stations), isobars (thin continuous lines), air-mass trough (thick continuous line), convergence lines/coastal fronts (dashed lines), (b) areally averaged (for 10 km × 10 km squares) Meteosat cloud-top temperatures, open above -20 °C or no cloud, dotted -20 °C to -30 °C, hatched -30 °C to -40 °C, solid below -40 °C.

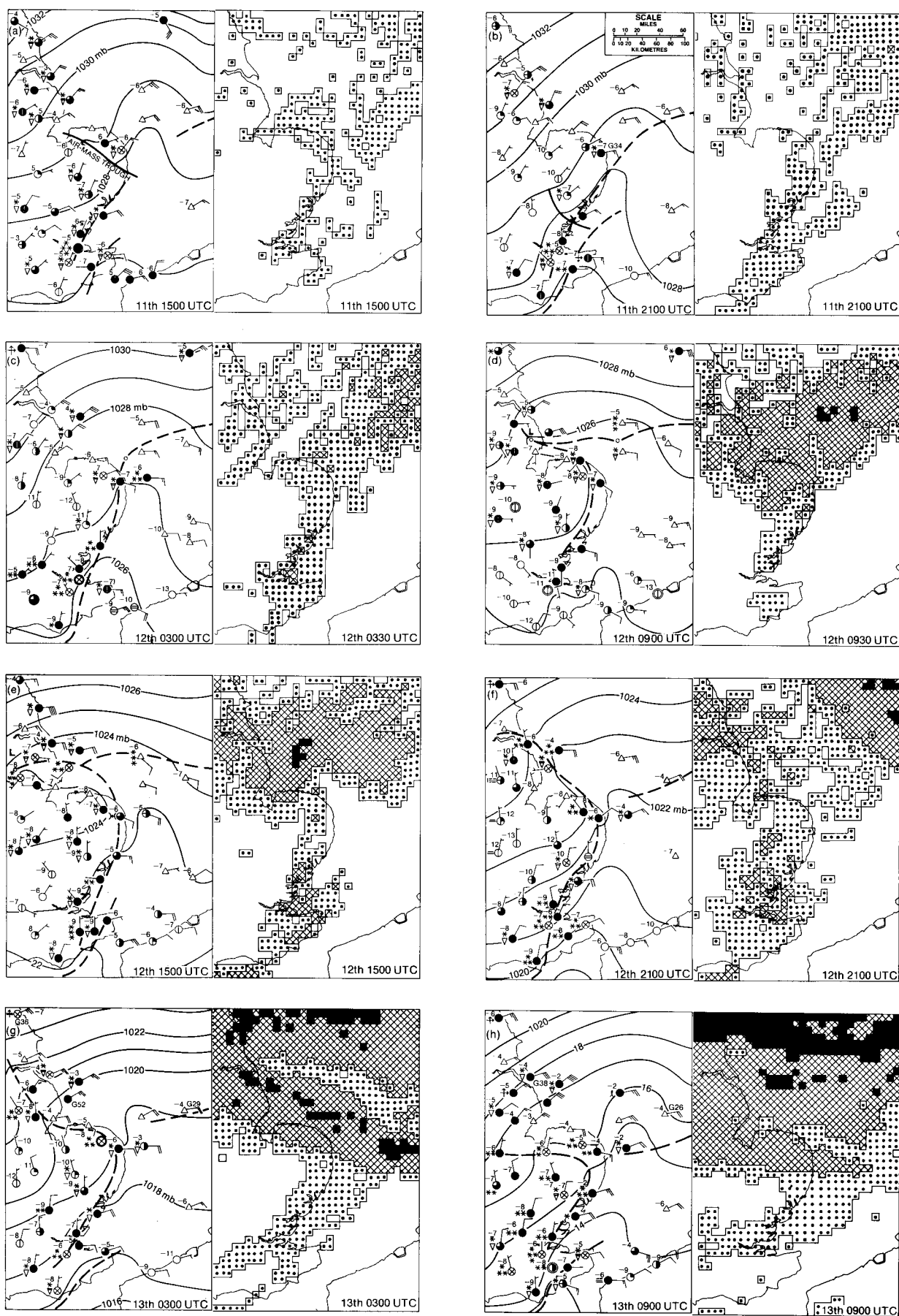


Figure 3. As Fig. 2, but for the sequence of times shown.

3. Coastal frictional convergence

Coastal zones are particularly subject to frictional convergence of low-level airflow, due to roughness difference between the land and sea surfaces. Excluding thermodynamic effects, frictional convergence in itself leads to sometimes-pronounced upward air motion, which has been found to have a maximum when an appreciable (i.e. stronger than moderate) onshore wind makes a shallow angle (between 14° and 25° clockwise) with the coastline (Bergeron 1949, Roeloffzen *et al.* 1986).

The effects of these conditions were greatest along the east Suffolk–Essex coastline early in the cold outbreak period when the gradient wind was stronger (Fig. 2(a)), probably leading to the continuous moderate snow that was being reported by 03 UTC on the 11th, not only from Walton-on-the-Naze and Sheerness, but also from Herstmonceux, indicating that the cloud and precipitation had extended downwind (between 020–035°/25–30 kn at the 800 mb level) towards the Beachy Head area of Sussex. Fig. 2(b) confirms that a belt of colder-topped (higher) cloud stretched south-south-westwards from Lowestoft at this time. Also, allowing for a slight existing cover, snow depths measured at 09 UTC on the 11th (Fig. 4) verify that the heaviest overnight falls occurred just downwind of the east Suffolk–Essex coast in north-west Kent (e.g. Ulcombe 18, Keycol 15 and Wigmore 13 cm).

However, continued development of the offshore trough slackened the pressure gradient locally near the

East Anglian coast where, as a result, onshore winds over much of 11–13 January 1987 were only moderate (see Figs 3(a)–3(h)). Van den Berg (1987) describes how thermodynamic effects in the boundary layer (i.e. due to temperature and stability differences) become more important than differential surface friction in coastal frontogenesis as the onshore winds moderate.

4. The quasi-orographic effect of cold air stagnating over East Anglia

As they had done locally the previous night, temperatures fell more widely to –10 °C in East Anglia by 21 UTC on 11 January 1987, particularly since winds had fallen to light, and strong radiational cooling was occurring beneath clearing skies. Lower temperatures still were recorded over snow-covered ground, a minimum of –14.8 °C was recorded at Marham, with a grass minimum of –22.2 °C. While clear skies persist, a stagnating pool of cold, stable air is likely to form inland (see Roach and Brownscombe 1984).

Fig. 3 also shows Meteosat infra-red imagery interpretations which may be taken as closely comparable in terms of time and area covered with the surface charts. They indicate that, although some cells moved through the pattern, there was remarkable persistence of clear skies inland while a band of cloud parallel to the coastline appeared to be stationary near the East Anglian coast (especially where east Suffolk and Essex border the North Sea). Whether cloud penetrated well inland on the 12th at 21 UTC is uncertain because the

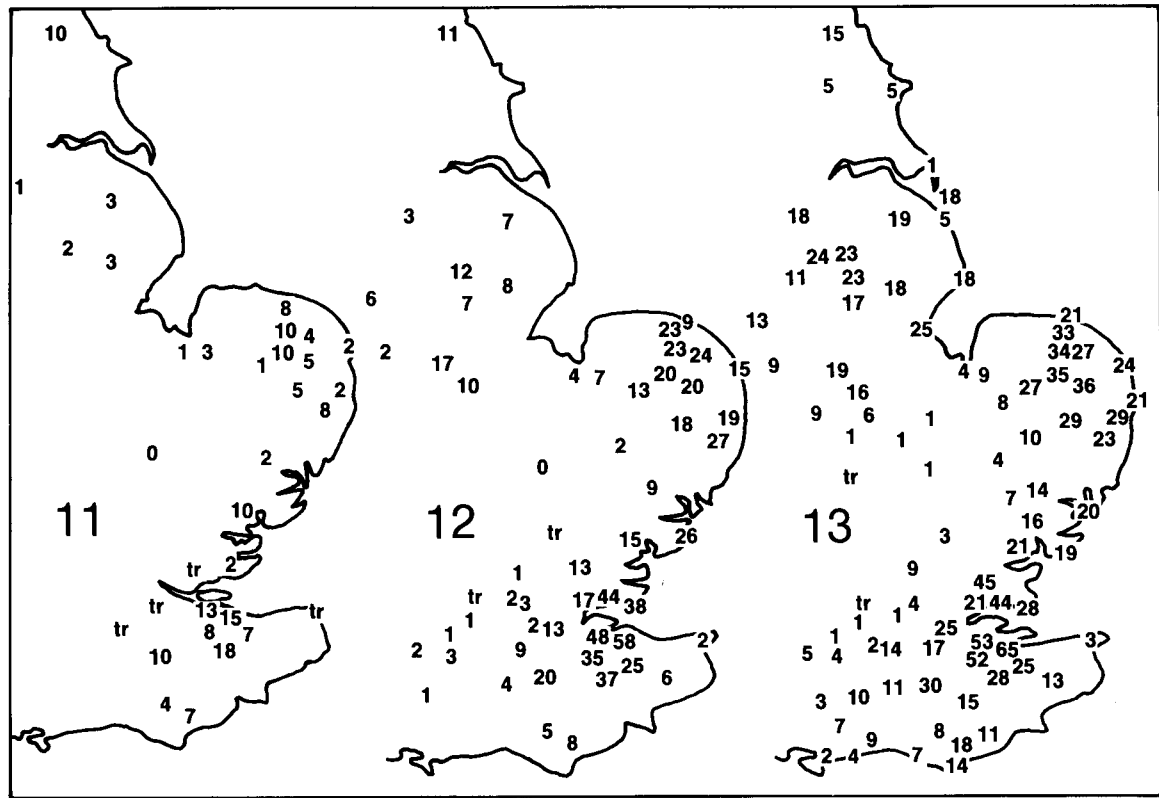


Figure 4. Snow depths (cm) measured at 09 UTC on the dates shown (11, 12, 13) January 1987.

infra-red radiometer might have been registering very low ground temperatures, below -20°C at that time. Bacon (1987) produced an unconfirmed thermograph trace from Desborough, Northamptonshire, where the air temperature (in a sheltered, upland valley exposure) hovered close to 0°F (-18°C) between 1930 and 2045 UTC. Also, that evening, a grass minimum (over snow) of -24.6°C was recorded at Cottesmore.

When investigating enhanced precipitation occurring just inland from the Dutch coast overnight on 17–18 November 1977, Oerlemans (1980) reasoned that while radiation formed a stable layer over land, instability had prevailed over the warmer North Sea. From reported surface wind variations, pronounced low-level convergence had occurred along the coast. While these conditions persisted, and the stable air inland remained undisturbed, a quasi-orographic effect was diagnosed, whereby a hill of stationary air forced uplift of onshore winds over otherwise flat country. Called ‘The θ -hill effect’, it was shown (by radar study) to have formed a relatively narrow belt of enhanced cloud and precipitation parallel to the coastline along a low-level convergence line which had remained quasi-stationary just inland from the coast.

Fig. 5 shows a remarkable series of observations from Coltishall and Hemsby in Norfolk on 12 January, with just 22 km between the stations. Wind directions were in almost-complete opposition between 06 and 18 UTC, with light land-breeze north-westerlies at Coltishall (indicative of the undisturbed air inland) while a moderate onshore east-south-easterly wind persisted at Hemsby, suggesting maintenance of a quasi-stationary convergence line between these two stations over more-or-less flat land, an unusually balanced situation aided by extremely cold air (see section 7) advecting over the sea to Hemsby. During the period 06–18 UTC on the 12th, thermal contrast was quite small, dry-bulb maxima being -5.6°C (despite the sunshine and only isolated passing showers moving in from the sea) at Hemsby, and -6.4°C (beneath cloud and in almost-continuous snow) at Coltishall.

The observational evidence suggests that a quasi-orographic hill of cold surface air remained undisturbed over East Anglia during the 12th, and persisted in the south of the region for a total of approximately 48 hours until the evening of the 13th (when both upper-cloud cover and surface wind increased). Fig. 3 and the averaged Meteosat data (which indicates cloud persistence/development areas) in Fig. 6 confirm the general maintenance of cloud, closely correlating with the East Anglian coastline.

5. Land-breezes

The land-breeze has become a well-known factor in the generation of lake-effect snowstorms in the vicinity of Lake Michigan, USA, and such events have been intensively studied since 1977. Lake Michigan is about 130 kilometres wide and, although not quite as far as the

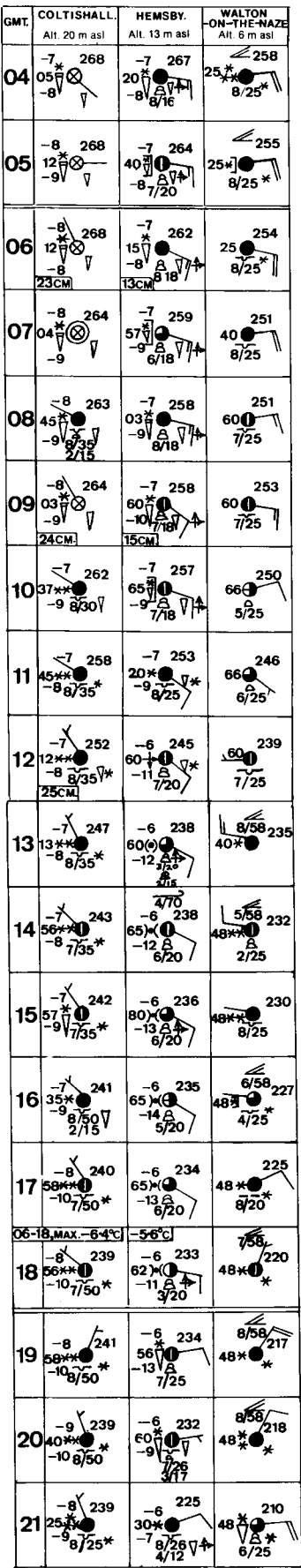


Figure 5. Hourly surface observations from Coltishall, Hemsby and Walton-on-the-Naze for the times shown on 12 January 1987.

distance from East Anglia to the Dutch coast, presents approximately the same fetch of warmer water to a cold easterly airflow as does the southern North Sea between East Kent and continental Europe at the Dutch–Belgian border. Arctic outbreaks are relatively common in the mid-western USA in January, therefore at least some of the American studies might have relevance to events in south-east England over the period 11–13 January 1987.

Two cases of snowfall on the western shores of Lake Michigan have similar aspects, and are discussed in Ballentine (1982), as is the role of the land-breeze in producing a nearly stationary band of precipitation (the snow band) parallel to the western shoreline. Both Ballentine (1982) and Schoenberger (1984) mention that the radar studies of Passarelli and Braham (1981) had demonstrated: (a) a vital role played by the land-breeze in forming cloud and precipitation bands parallel to the shoreline, and (b) these bands sometimes consisted of discrete cores of heavier precipitation embedded within the more uniform precipitation band, the intense cores or cells tending to move in a direction parallel to the axis of the belt, resulting in very little movement of the band

itself. Schoenberger (1984) defined the land-breeze as a ‘shallow density current’ and described the land-breeze cold front (when it pushed out over the water) as the line separating radiationally cooled over-land air from the warmer over-sea air.

What may be interpreted as a discrete line of isolated colder (higher) topped convective cells appeared from the Essex coast to north-west Kent by 0330 UTC on 12 January 1987 as in Fig. 3(c), indicating probable land-breeze involvement. These cells first appeared at 02 UTC over the Thames Estuary on the Meteosat infra-red imagery, where cloud tops had previously been lower.

Surface observations from Walton-on-the-Naze coast-guard station (Figs 5 and 7) trace three probable land-breeze events there over the period 11–12 January 1987, each accompanied by outbreaks of snow associated with oscillations overhead of the coastal convergence line, and each featuring a temporary offshore wind from between north and west in direction. Interaction with a minor cold air-mass trough which was moving south-westwards (Figs 3(a) and 3(b)) appears responsible for

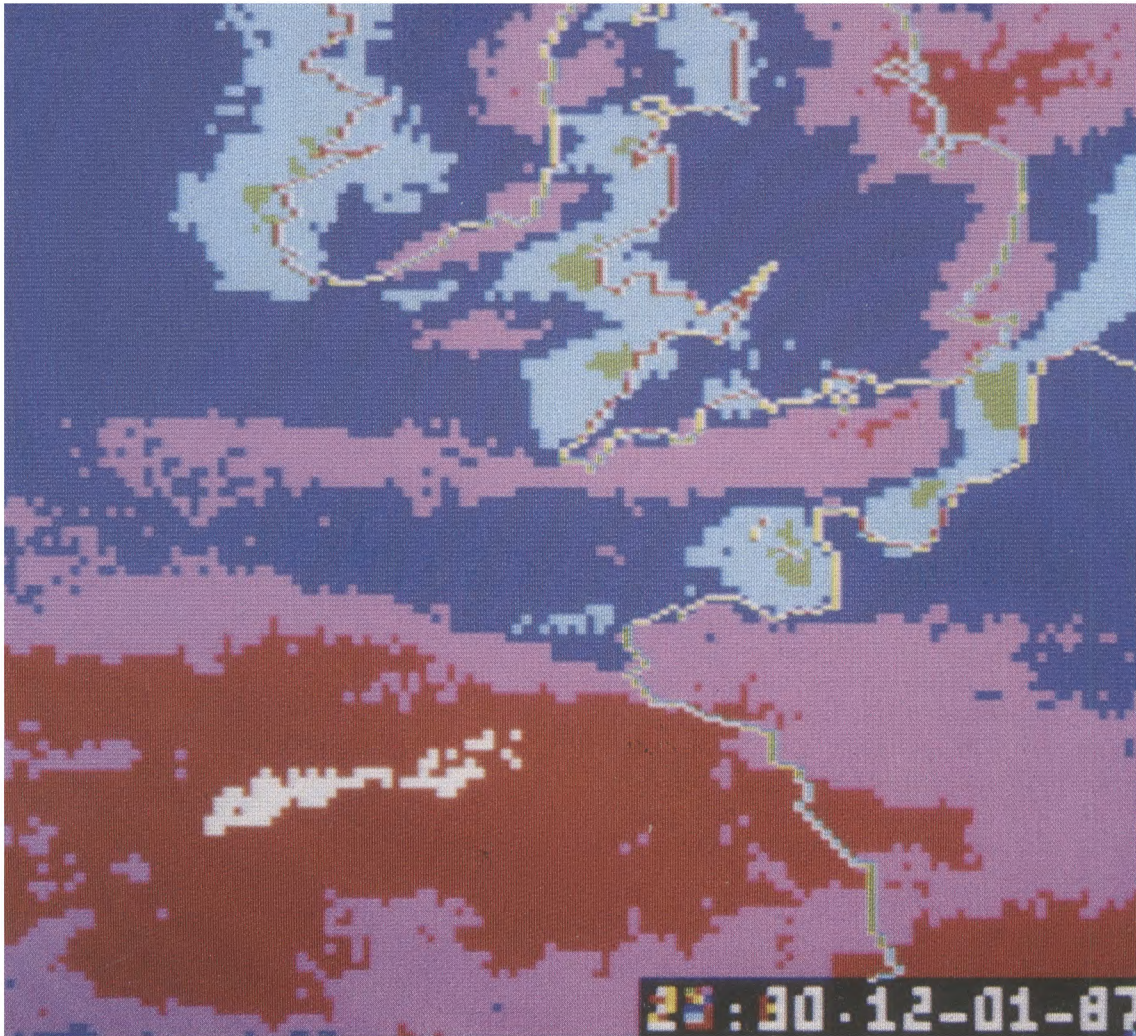


Figure 6. Cloud-top temperatures from Meteosat averaged infra-red imagery averaged over $10\text{ km} \times 10\text{ km}$ squares for the period from 10 to 21 UTC on 12 January 1987.

the period of particularly heavy snow around 18–19 UTC on the 11th, but the renewed continuous snowfall between 01 and 04 UTC on the 12th appears to have been related purely to a land-breeze-induced oscillation of the coastal convergence line. Temperatures are not recorded at Walton, but nearby at Shoeburyness the thermograph trace clearly indicated temporary 2-hour

duration dips of 2 °C and 1 °C which, although not all that great considering the snowfall, were probably associated with these two respective oscillations. Off south-east Essex, the sea froze on 12 January 1987 in places from Shoeburyness to Westcliffe, and Brugge (1987) has mentioned that ice floes were seen half a mile out to sea, which is very shallow off Southend. But a

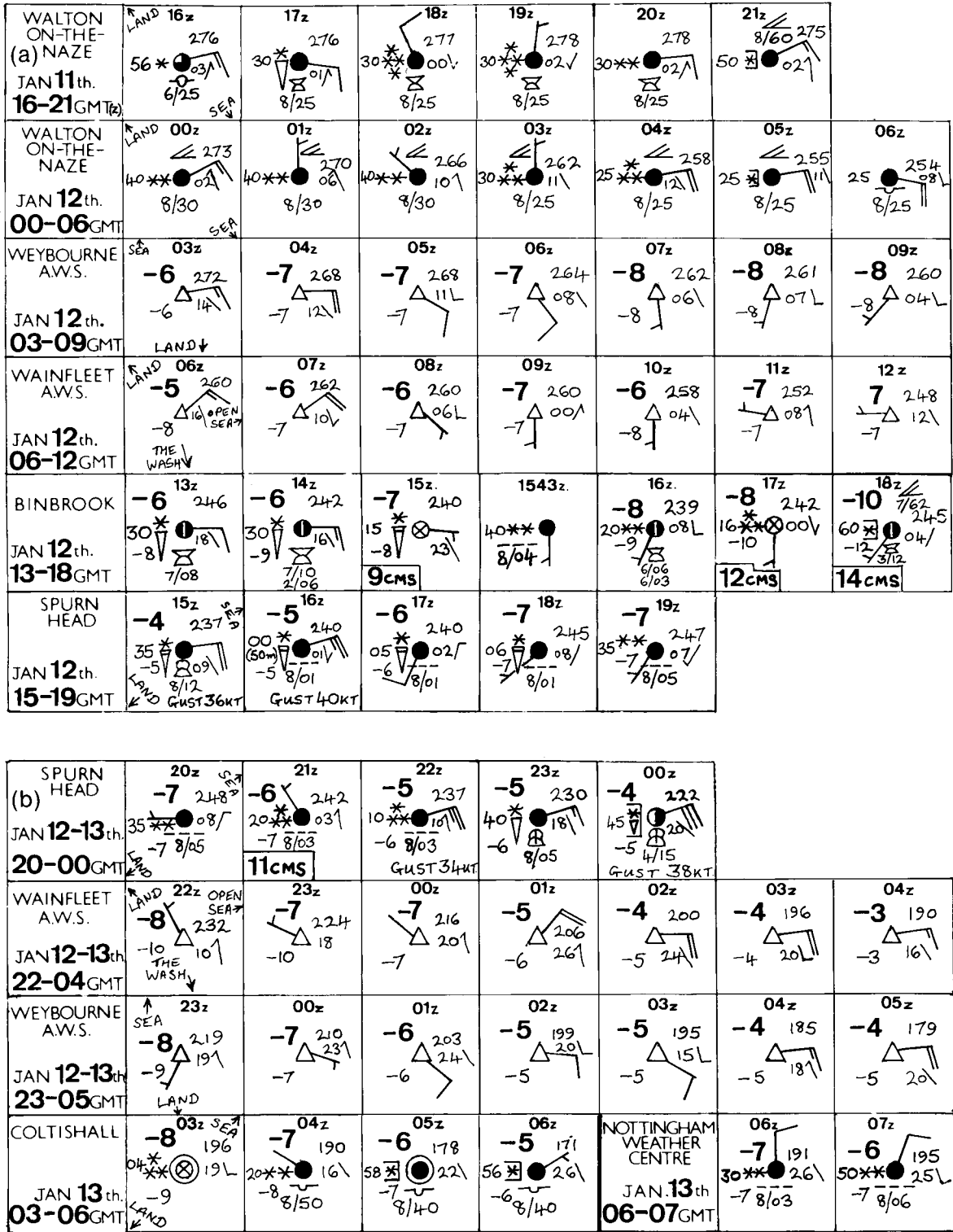


Figure 7. Further sequences of surface observations to illustrate passages of (a) the land-breeze cold front, and (b) the warm coastal front from 11 to 13 January 1987.

particular reason for ice formation here (suggested by isotherms of maximum temperature over the adjacent land in Fig. 8 and Bacon (1987), also by the reported surface wind directions) was that this area of Essex appeared to be beneath the main outflow of cold surface air where it was draining from over East Anglia as a land-breeze. From 09 to 18 UTC on the 12th, very cold maximum air temperatures of -9°C were recorded on the coast at Southend and Shoeburyness. Observations from Walton-on-the-Naze (Fig. 5) clearly indicate that this land-breeze over Essex pushed the coastal convergence line there out to sea for a 4-hour period between 12 and 16 UTC on the 12th; however, this movement may have been aided by the development occurring further north.

6. A mesoscale circulation

As deeper cold air began to arrive, to the north-east of Norfolk a small circulation began to form in the developing marine trough from approximately 03 UTC on the 12th. Continuity of this disturbance's centre is given in Fig. 1, as it moved initially west-north-westwards over the sea towards Gibraltar Point, developing as an eddy vortex, (a) on the boundary (convergence) line propagating downwind westwards from the Dutch Wadden islands and (b) between fast flowing air over the sea to the north and slow moving air which was stagnating over East Anglia.

Interestingly, surface observations (Fig. 7) showed a *veering* of surface winds, where steady addition of the land-breeze to the synoptic scale east-north-easterlies occurs, at first on the Norfolk coast (between 04 and 07 UTC at Weybourne) then later in south Lincolnshire (gradually between 07 and 11 UTC at Wainfleet).

Fig. 3 shows the mesoscale centre tracking over-land into Lincolnshire by 09 UTC on the 12th, thereafter retarding and turning soon after midday to drift north-north-eastwards towards the Humber, where it lost its identity some 16 hours after first forming, having produced 15–20 cm of snow in its immediate vicinity (Fig. 4(c)). Associated with this centre and its change of track, the coastal convergence lines combined to move north-eastward over Lincolnshire as a land-breeze cold front, having developed a 2°C thermal contrast (Fig. 3(e) and the detailed sequential observations in Fig. 7), passing through Binbrook close on 1530 UTC and reaching Spurn Head, some 25 km distant, about an hour later, although passage of the small depression nearby may have hastened this movement.

7. Extremely low 1000–500 mb thickness values

It should be emphasized that the heavy coastal snowfalls over the period 11–13 January 1987 occurred in association with extremely low 1000–500 mb thickness values for Britain. The height of 497 geopotential decametres (dam) recorded at Hemsby on the 12th at 12 UTC exactly equalled the previous lowest UK measurement, coincidentally also at Hemsby at 12 UTC

on 1 February 1956. However, on that previous occasion, the coldest air moved southwards to the east of Britain, so therefore, there is every likelihood that 12 January 1987 saw extreme low values throughout southern England, and later also in South Wales as this particular cold pool untypically moved westwards (see Fig. 8 inset), albeit warming slightly with time.

During the early evening of 12 January, thickness values were probably near 495–496 dam overhead areas immediately south-west of The Wash, where clear calm conditions and a fresh snow cover together combined to produce the coldest surface temperatures seen in England since the 1981/82 winter, and caused the θ -hill effect to persist over East Anglia.

8. Discussion of the snowfalls

For forecasters based in the United Kingdom, early indications of coastal convergence, initially forming in the boundary layer and aligned east-north-east to west-south-west near the north Dutch Wadden islands, were given by observations from West Terschelling Lighthouse (see Fig. 8 and sketch map in Groenland, 1987), where the surface wind veered to a direction south of easterly (indicating addition of the land-breeze) accompanied by continuous snow from 18 UTC on 10 January 1987. When unusually cold polar continental air is advecting from the east, similar coastal snowfall may well begin to affect south-east England 3–6 hours hence. Van den Berg (1987) cites the Wadden Islands coastal front as having had a known history of producing large amounts of snow especially on Terschelling (e.g. over 40 cm in January 1985, and 50 cm in the early-February 1956 outbreak).

Groenland (1987) reported that, during a 60-hour accumulation period from 10–13 January 1987, 22 cm had fallen at Buren (Ameland) and 50 cm at Hoorn (Central Terschelling) by 06 UTC on the 13th, when a maximum of 56 cm was measured on West Terschelling. There was negligible snowfall at Groningen and further south in Friesland.

Van den Berg (personal communication) related that, typically, snow depths tend to increase rapidly from east to west over the Dutch Waddens, with only very limited penetration southwards over the mainland. He noticed that, this particular 10–13 Jan. 1987 event formed a persistent line of heavy snow showers on the boundary between clear air over land and showery air over the sea, which he describes as 'The North Sea Lake Effect'.

Snowfalls were particularly spectacular around the Thames Estuary during the early hours and again over late afternoon-evening of 11 January. Thirty-three centimetres of snow (including a fresh 20 cm since the 09 UTC observation) was measured at 2130 UTC in Wigmere, near Gillingham, with snow still falling heavily. Just 10 km to the east at Keycol, 11 cm had fallen between 16 and 19 UTC; with a further 15 cm by 22 UTC, which can be interpreted as continuous and often heavy snow falling at a rate of up to 5 cm hr^{-1} (a

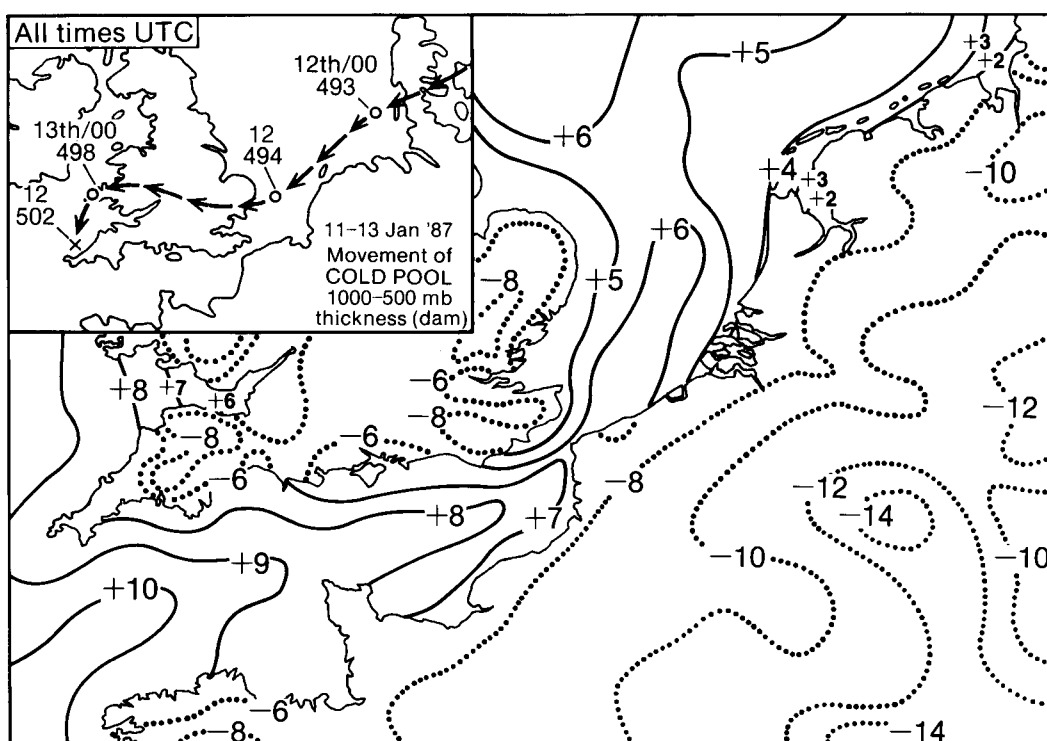


Figure 8. The 5-day mean sea surface temperature (°C) chart for 11–15 January 1987. The dotted lines over land are isotherms of maximum daytime temperatures (°C) on 12 January. Inset shows continuity of the movement of the centre of the 1000–500 mb cold pool, with central value.

rate only exceeded in north-east Norfolk around 02 to 04 UTC on the 12th). Therefore, it was hardly surprising that British Rail were unable to keep its routes through north Kent operating, since a traction system depending on good ‘ground-contact’ with the conductor-rail for electrification is perhaps the most vulnerable of all to heavy snow accumulating in very cold conditions.

It has been remarked that such heavy accumulations as occurred had not been adequately predicted (Prichard 1988), although for the most part Monk (1987) has successfully defended the UK mesoscale forecast model’s precipitation distribution simulation, on a chart presented for 09 UTC on 13 January 1987. However, this was after the event, and snowfall amounts in north and east Norfolk were generally underestimated by a factor of 3, and the heaviest falls in north-west Kent by a factor of 2.

Observations of water equivalents of the overnight snowfalls (that were made early on the 12th at Keycol, Wigmore, and Leigh-on-Sea, Essex) indicate the new, powdery, dry snow, 35–45 cm deep, yielded only between 28 and 32 mm; which suggests that one source of model error was probably the assumption of a 1:10 ratio between rainfall and snow depth, which could well have been nearer 1:12 in the unusually cold conditions. At Braemar, Thompson (1963) showed 1:12 to be the most frequently-found ratio in water equivalents of snow when the air temperature fell into the -5°C to -8°C range (as experienced in south-east England).

Prichard (1988) also observed that the Thames Estuary snowfalls had been inadequately represented on radar displays from the Chenies (London) radar.

Relevant Hemsby ascents and hourly Meteosat infra-red data (Fig. 3) indicate that the heavy snow falling on the 11th in areas bordering the Thames Estuary, emanated from a cloud band lying parallel to the Essex–east Suffolk coast with tops below 12 000 ft (i.e. tops warmer than -30°C did not exceed the 650 mb/3.5 km level until 02 UTC on the 12th). Assuming Chenies to be 70 km from this precipitating cloud band, the radar beam would be elevated about 900 m high at this range. Therefore, it would not see the lowest portion of cloud (or beneath, in the boundary layer) where the largest snowflakes would almost certainly be concentrated.

Although a new radar has been commissioned near Lincoln recently, an installation located east of London in Kent or Essex may well be an answer to underestimation of precipitation in easterly airstreams, especially in extremely cold winter weather when dryness of falling snow may well combine again with modest vertical development of cloud to exacerbate the problem.

The shallowness of coastal snow-producing cloud-systems in Sweden has been remarked upon by Bergeron (1949), who investigated two snowfalls which built up over about a week in two successive Januarys over flat land of the Stockholm peninsula. Both cases produced 35–40 cm of snow falling in a belt parallel to the shoreline, approximately 15–20 km wide, with its axis (and maximum falls) situated approximately 20 km from the outlying islands of eastern Sweden. Bergeron believed these events to have been partly caused by frictional convergence and lifting within an onshore wind, and partly by the sudden increase of vertical

mixing at the coastline. The apparently stratiform cloud systems responsible for the snowfalls were, in reality, low and untypical, dwarflike, cumulonimbus clouds fused into a more-or-less continuous cloud deck, forming within the lowest unstable layer at the coastline.

Roeloffzen *et al.* (1986) confirmed theoretically that the effects of differential friction alone (given a strong onshore wind over a fairly flat coastline) produced maximum upward motion, in the order of 400–500 m vertically over some 25 km from the coast, when the geostrophic wind made a small ($\approx 20^\circ$ clockwise) angle with the coastline, and least upward motion when near perpendicular to it.

Figs 3 and 4 indicate that the areas of greatest snow depth by 13 January 1987 followed an approximate shape of the East Anglian coast, if this were moved 20–30 km south-south-westwards. Snowfall charts in Bacon (1987) and Lumb (1988) confirm this idea. Historically, Bosart *et al.* (1972) originally linked the physical coastal configuration with convergence line or frontal orientation in USA Eastern Seaboard case studies, and Draghici's Black Sea coastal frontogenesis study (1984) confirmed this hypothesis.

The author had to make a return journey to London (from Newbury) on the 12th, and concluded that the climate of London was similar to Calgary (if only for a day). There was an unfamiliar absence of thawing snow where normally, underground sources of heat should have at least some effect. Along the M4 motorway, snow became apparent on the landscape from the vicinity of Heathrow Airport eastwards. In the West End of London, traffic wardens were nowhere to be seen, probably due to the extreme cold, and road markings in Piccadilly area (double yellow lines etc.) had been obscured by 3 cm of snow. A 15-minute walk early that evening to the car produced severely-chapped lips.

Skies had remained almost clear during the day in London, and there is a theoretical diurnal minimum in coastal convergence activity towards midday as thermal contrast between land and sea diminishes temporarily, due to solar heating of the ground. Apart from near the small centre over Lincolnshire, there did appear to be a temporary abatement of snowfall elsewhere in south-east England between 10 and 14 UTC on the 12th. Skies cleared almost completely over north-west Kent (Fig. 9) from about 06 UTC, with an observer at East Malling noting the cloud returning around 1330, snowfall recommencing at 1410 UTC and continuing thereafter.

Water equivalent and snowfall maxima occurred in the Gillingham–Sittingbourne–Southend area. Before drifting in strengthening winds occurred, an average depth of 65 cm had built up by 09 UTC at Keycol, and 61 cm was measured in Wigmore at 1515 UTC (both in north-west Kent) on the 13th. However, on the Essex and east Suffolk coast, several reported snow depths were less on the 13th than on the 12th at 09 UTC (e.g. at Shoeburyness, Clacton, and at Halesworth), with observers noting that the snow had become more

compact. Reductions here and at other locations near the sea were most probably due to stronger winds causing drifting, and ablation by salt particles.

Illustrating the dry, powdery nature of the snow cover, a helicopter pilot, cautiously attempting a landing into wind at Wickford, Essex, at 1335 UTC on the 13th, was so disorientated by the machine's downwash which caused all external references to be lost in rotor-blown snow (estimated to have been 45 cm deep), that the helicopter was inadvertently flown through a hedge before coming to rest in an adjacent field. Although the aircraft suffered substantial damage, fortunately no one was hurt — from *Department of Transport Air Accident Investigation Branch Bulletin*, March 1987.

To demonstrate how closely the convergence zone had been associated with the east Suffolk–Essex coast since the 11th, Fig. 4(c) shows that places 40 km to the north-west and to the south-east (notably Stansted and Manston, each with 3 cm) were only reporting a thin cover at 09 UTC on 13 January 1987; Cambridge Botanical Gardens reporting no snow at all until then, when 1 cm was recorded. Meanwhile, there was turmoil around the Thames Estuary, where the Isle of Sheppey had become cut off and supplies were brought in either by sea, by helicopter, or by the Army on skis. Over the week 11–17 January 1987, Kent's newly-opened Radio Invicta Helpline received a record 23 000 telephone calls from motorists and householders requesting aid or advice in conditions described as the worst in living memory by the automobile associations — from *IBA Yearbook*, 1988.

9. The coastal front moves inland during 13 January 1987

At 21 UTC on the 12th, a light south-easterly wind at Leconfield AWS (just north of the Humber in Fig. 3(f)) indicates that this was the northernmost extent of the land-breeze cold front which, from observations, did not reach the outer Dowsing Light Vessel.

After halting, this land breeze front began to return south-westwards as a warm coastal front, whose passage was typically marked by a surface wind increase and veer (to a more easterly point) with a dry-bulb temperature rise over 1–2 hours of at least 1°C hr^{-1} . The coastal frontal passage may also be regarded as terminating the θ -hill effect. The front arrived (Fig. 7 shows sequential observations) dramatically at Spurn Head by 22 UTC, with gusts to 34 kn; reaching Weybourne and Binbrook by 00 UTC on the 13th; Wainfleet by 01 UTC; Scampton in Lincolnshire by 04 UTC; Coltishall between 05 and 06 UTC; and Nottingham Weather Centre (the farthest inland frontal passage was still recognizable) between 06 and 07 UTC; then through Marham and Cottesmore by 09 UTC; Shoeburyness by 12 UTC; and Wattisham, also East Malling by 13 UTC.



Photograph courtesy of Mrs E. Taylor



Photograph courtesy of Mr W. Tribe

Figure 9. Snowfall on 12 January at (a) 0930 UTC near Sittingbourne, and (b) 1100 UTC near Maidstone.

The remarkable reluctance of the coastal front to finally detach itself from the Essex coastline appears to be directly due to an absence of the cloud cover which had overwhelmed the θ -hill effect much earlier further north, where in Norfolk and Lincolnshire, thick upper- and medium-level cloud was spreading over rapidly from the east at 03 UTC on the 13th (Fig. 3(g)).

10. General summary and conclusions

The location of snowfall maxima over south-east English coastal areas from Lincolnshire to north-west Kent over 11–13 January 1987 resembles those in the Swedish events investigated by Bergeron (1949); the snowfall on Terschelling in the north Dutch Wadden islands over the same days and also on 1–2 February 1956 (Van den Berg 1987); plus exhibiting distinct similarities to some lake-effect snowstorms seen on the western shores of Lake Michigan in the mid-west of the USA (see Passarelli and Braham 1981, Ballentine 1982).

As with the 1956 case in the northern Netherlands' islands, heavy coastal snowfalls were associated with extremely low 1000–500 mb thickness values arriving. The reading of 497 dam at Hemsby on 12 January 1987 at 12 UTC exactly equals the previous lowest UK record, and probably has a return period near 30 years. Given these unusual conditions, where exceptionally cold and quite unstable air flows over relatively warm waters, heavy snow showers may be expected to develop along the boundary line between clear air over cold land and showery air over the sea.

Around the Thames Estuary heavy snowfalls accumulated over 11–13 January 1987 because of coastal convergence of over-sea and over-land airflows persisting along one such boundary line near the east Suffolk–Essex coastline, and closely associated with it. Maximum falls were in excess of 60 cm (2 feet) deep in north-west Kent.

The coastal convergence here was brought about and enhanced by:

(a) Differential surface friction — rapid development and remarkable persistence (for over 60 hours) of an offshore marine trough over the relatively warm North Sea around East Anglia, with this trough providing a vital backing to north-easterly of the pressure gradient at the coast of Essex and east Suffolk in particular, where the geostrophic wind continued to make a shallow (15–30° clockwise) angle with the shore. With at least moderate wind force, these are conditions suitable for differential surface friction to produce maximum uplift of the onshore breeze just inland from the coast.

b) Thermodynamic effects — development of a mesoscale disturbance (like an eddy vortex) forming in the marine trough after 03 UTC on the 12th effectively slackened the pressure gradient over East Anglia, where a quasi-orographic hill of cold surface air stagnated inland, allowing land-breezes to develop near the coast.

Thermal contrast developing across the probably pre-existing frictional convergence line oscillates it either seaward as a land-breeze cold front or inland as a warm coastal front. Where the opposing forces balanced, the coastal convergence line lay quasi-stationary over north-east Norfolk between 06 and 18 UTC on the 12th.

A large surface temperature gradient (e.g. from Fig. 8, as existed on the 12th between the East Anglian Heights and the southern North Sea, resulted in land-breeze-induced oscillations of the coastal convergence lines/ fronts which persisted near these large surface-temperature gradients, producing large amounts of snow in their immediate vicinity and just downwind.

While skies remained clear inland, the quasi-orographic θ -hill effect persisted over East Anglia, and

perhaps this was the single most important factor in maintaining convergence near the east Suffolk–Essex coastline for some 66 hours, resulting in the heaviest snowfalls (65 cm) being reported immediately downwind in north-west Kent.

The land-breeze cold front reached to a maximum distance of 50 km out to sea north-east of The Wash at 15 UTC on 12 January 1987 (probably aided by movement of the small eddy-vortex, at that time over eastern England). The feature then halted, and returned westwards during the 13th as a warm coastal front, still being just recognizable as passing over Nottingham Weather Centre (Fig. 7) between 06 and 07 UTC, some 100 km inland.

Following Leslie's remarks (1988) on the closure of Binbrook concerning the limitations of synoptic automatic weather stations (SAWS), it may be concluded from Figs 3 and 7 that while the SAWS at Leconfield, Weybourne and Wainfleet give good additional records of surface pressure, temperature, wind speed and direction; they can at present offer no acceptable substitute for the human observation of snowfall.

The SAWS observations of surface winds veering rather than backing as the land-breeze takes over from the gradient wind (see section 6) could be an interesting area for future research.

Acknowledgements

To Meteorological Office staff: at Bracknell, particular thanks to the Nowcasting and Satellite Applications Branch (G.A. Monk) for supplying Meteosat data, also to the Advisory Services Branch for AWS data from Weybourne; and to the Library and Archives staff (particularly M. Wood) for their friendly help.

Extra observations from outstations came from J. Leslie (Binbrook), B. Morris (Manston), L. Gurney (Hemsby) and J. Davies (Frinton-on-Sea coastguard for Walton). Copies of autographic records were kindly supplied by M. Wickenden (East Mallings) and S. Cardy (Shoeburyness), and correspondence came from R.J. Prichard and C.R. Burlton at LWC, Holborn.

Special thanks also to Dr Van den Berg for correspondence and kindly sending a copy of his Ph. D thesis on *Coastal Frontogenesis in The Netherlands* (now available in National Meteorological Library, Bracknell). Thanks to J. Webb of the Tornado and Storm Research Organization (TORRO) for the extra snow depths, to J.D. Bacon (Anglia TV, Norwich) for sending his paper on the snowfalls in East Anglia, to F.E. Lumb (Camberley) for prompting verification of the Marine Trough and to A. Sampson (Sheringham High School) for bringing the existence of Weybourne AWS to the author's attention. Also to Drs Meaden and Briscoe for supply of addresses of observers in Climatological Observers Link (COL).

In gratitude to the amateur observers, many being COL or TORRO members, who have sent observations and photographs (N. Brooks, R. Selfe, B. Smith, E. and N. Taylor, E. and W. Tribe, and D. Venuti) to help the author build up a more complete picture of the south-east coastal snowfalls on 11–13 January 1987.

Figures are by the author, based on information supplied by the Meteorological Office as detailed above. Extra snow depths, authenticated as far as possible, have been added by the author to Fig. 4, through COL and TORRO data supply.

References

- Bacon, J.D., 1987: Heavy snowfall in East Anglia, January 1987. Norwich, Anglia Television, Weather Department.
- Ballentine, R.J., 1982: Numerical simulation of land-breeze-induced snowbands along the western shore of Lake Michigan. *Mon Weather Rev*, **110**, 1544–1553.
- Bergeron, T., 1949: The coastal orographic maxima of precipitation in autumn and winter. *Tellus*, **1**, No. 3, 15–32.
- Bosart, L.F., Vaudo, C.J. and Helsdon, J.H. Jnr, 1972: Coastal frontogenesis. *J Appl Meteorol*, **11**, 1236–1258.
- Brugge, R., 1987: Low daytime temperatures over England and Wales on 12 January 1987. *Weather*, **42**, 146–152.
- Draghici, I.F., 1984: Black Sea coastal frontogenesis. In *Proceedings of Nowcasting II Symposium*, Norrköping, Sweden, 3–7 September 1984. ESA SP-208.
- Groenland, R., 1987: Kustfront overzicht Januari: sneeuw op de Wadden. *Weerspiegel*, **14**, 140–143, 148.
- Jackson, G., 1988: Insurance aspects of the great storm. *Proceedings of the Royal Meteorological Society Discussion Meeting*, 7 May 1988, University of Reading.
- Kain, D.G., 1988: Ice accretion — English Channel, 12–13 January 1987. *Mar Obs*, **58**, 13.
- Leslie, J.G., 1988: Closure of Meteorological Office at Royal Air Force Binbrook. *Meteorol Mag*, **117**, 318–319.
- Lumb, F.E., 1988: Snow depths on 12 January 1987. Letter to *Weather*, **43**, 31.
- , 1989: Snow depths on 12 January 1987: further comments. Letter to *Weather*, **44**, 34–35.
- Monk, G.A., 1987: Topographically related convection over the British Isles. *Satellite and Radar Imagery Interpretation*. Workshop Preprint Vol., 20–24 July 1987, Shinfield Park. Bracknell, Meteorological Office.
- Mortimore, K.O., 1987: Weather summary: January 1987. *J Meteorol UK*, **12**, 139–143.
- Oerlemans, J., 1980: A case study of a subsynoptic disturbance in a polar outbreak. *Q J R Meteorol Soc*, **106**, 313–325.
- Passarelli, R.E., Jnr and Braham, R.R., Jnr, 1981: The role of the winter land-breeze in the formation of Great Lake snow storms. *Bull Am Meteorol Soc*, **62**, 482–491.
- Prichard, R.J., 1988: Return periods. Letter to *Weather*, **43**, 57.
- Roach, W.T. and Brownscombe, J.L., 1984: Possible causes of the extreme cold during winter 1981–82. *Weather*, **39**, 362–372.
- Roeloffzen, J.C., Van den Berg, W.D. and Oerlemans, J., 1986: Frictional convergence at coastlines. *Tellus*, **38A**, 397–411.
- Schoenberger, L.M., 1984: Doppler Radar Observation of a land-breeze cold front. *Mon Weather Rev*, **112**, 2455–2464.
- Selfe, R.W., 1987: The snowfalls of 11th–14th January 1987 in south-east Essex. *J Meteorol UK*, **12**, 125–126.
- Thompson, A.B., 1963: Water yield from snow. *Meteorol Mag*, **92**, 332–335.
- Van den Berg, W., 1987: Coastal frontogenesis in The Netherlands: observations and modelling. Ph.D. thesis, University of Utrecht.
- Webb, J.D.C., 1987: The cold spell and snowfalls of January 1987. *J Meteorol UK*, **12**, 229–233.

Exeter temperatures: monthly means from 1782 to 1839, and from 1985 to 1988

R.F.M. Hay

Burnham Market, Norfolk

Summary

A table of monthly mean temperatures representative of the vicinity of Exeter has been derived for the period from 1782 to 1839, linking with and completing the tables previously derived for 1840 to 1984.

1. Introduction

In an earlier paper (Hay 1985) monthly mean temperatures (MMTs) representative of the vicinity of Exeter for 1840 to 1984 were presented, based mainly on records kept at the Devon and Exeter Institution (DEI) and by the Revd Thomas Heberden (HEB) of Exeter Cathedral, and to a lesser extent, at several other stations in the neighbourhood. In this paper a description is given of the extension of the record back to 1782 and forward to 1988 (see Table I).

2. Derivation of the additional MMTs

The Heberden* records (undated) as available from 1782–1855 give monthly mean values of temperature for 0800 and 1400 clock time. The DEI record begun in 1817 similarly includes daily temperatures, taken at the fixed hours 0800, 1400 and 2200 clock time from 1817 to 1829, and daily maximum and minimum temperatures from 1830 onwards.

MMTs for DEI had not been computed in the original records, so these were next obtained from the daily values for 0800, 1400 and 2200. The following procedure was used to ensure that MMTs derived for the years before 1830 for HEB and DEI data, using only the fixed hourly data available, should be comparable with MMTs as obtained from mean monthly (MM) maximum and minimum temperatures for the later years.

The *Observatories' Year Book* for 1900 includes values of MMTs for Falmouth Observatory for each fixed hour 0000 to 2400, meaned for the 30-year period 1871–1900, together with MM maximum and minimum temperatures for the same period. (Falmouth was used as being the nearest station to Exeter where hourly data are available, and since both stations lie adjacent to the English Channel). Mean monthly ranges of temperature defined as (MM maximum–MM minimum) were then obtained over similar periods for Falmouth and Exeter for each month, and monthly ratios (MM range

Exeter/MM range Falmouth) were derived. These ratios for each month were then used to multiply the MM differences of each Falmouth mean hourly temperature (0, 1, 2.... to 24 hours) from the appropriate 24-hourly means for Falmouth to obtain derived Exeter MM differences to be expected at each hour (0–24 hours) from the appropriate 24-hour means for each month. The Exeter MM differences, derived here for 0800, 1400 and 2200 hours alone, were then used to obtain corrections to be applied to the MMTs derived from $(T_{0800} + T_{1400} + T_{2200})/3$ to derive the MMTs to be found from MM maxima and minima if these had been available. The same procedure was also applied to the Heberden records available from 0800 and 1400 hours.

The Heberden record between 1782 (when it was begun) and 1817 when the DEI temperature series begins, is unfortunately not supported by any other record, except for a record from Earnshill, Somerset (see Table II) which is complete between September 1798 and December 1804 inclusive. However when MMTs had been determined for Earnshill (EAR) from this record, and mean differences (EAR–HEB) between MMTs obtained over the 6 complete years available, it was decided not to use Earnshill to modify the Heberden data in deriving Exeter MMTs. Earnshill MMTs meaned for the period 1799–1804 were found to be higher than Exeter from March to November, the differences reaching up to 2.0–2.2 °C in June and July. They were slightly below Exeter MMT values from December to February. An additional consideration against the use of the Earnshill data here was that, as a result of a visit to Earnshill House, it became evident that, while the house lay in an open rural situation, the present owner was unable to give any details regarding the site (or sites) used, or details of instruments and times of observations, apart from the meagre information already available in the records themselves.

* A note written in volume I of the Weather Records of the Revd Thomas Heberden gives details of his places of residence, and states that he was Canon Residentiary of Exeter Cathedral from 1788 until his death in 1843. While no other details are given relating to the position where his observations were made, it can reasonably be inferred therefore that his residence was very near to the Cathedral and his observations of temperatures etc. were made at a location not very far from the position where the DEI installed their thermometers in 1817. The differences between individual observations suffice to suggest the sites were not identical but at least their heights above mean sea level were similar and their distance apart quite small.

Table 1. Monthly mean and yearly temperatures (°C) for Exeter, 1782–1839 and 1985–1988

	Jan.	Feb.	Mar.	Apr.	May	June	July	Aug.	Sept.	Oct.	Nov.	Dec.	Year
1782	—	—	—	—	—	—	—	—	—	—	—	5	—
1783	6	—	—	—	—	—	—	—	—	11	—	6	—
1784	1	(1)	—	—	—	—	—	—	—	—	—	—	—
1785	(7)	2	2	10	12	17	17	15	15	11	8	5	(10.1)
1786	7	6	3	11	11	17	16	17	—	—	—	—	—
1787	—	—	—	—	—	—	16	17	15	11	6	6	—
1788	—	—	—	—	—	—	15.9	16.5	14.4	10.8	6.3	0.0	—
1789	3.6	6.2	(2.1)	8.9	11.7	13.0	15.0	16.1	12.9	9.0	5.2	6.8	9.2
1790	5.7	7.2	6.9	(6.0)	11.5	14.1	15.1	16.2	13.1	11.2	7.1	6.4	10.0
1791	6.3	5.5	6.6	10.8	10.7	15.1	15.0	16.3	14.9	9.8	6.9	3.2	10.1
1792	5.2	6.0	6.6	10.5	10.8	14.0	15.4	17.2	12.6	9.6	8.2	6.9	10.3
1793	4.6	6.4	5.6	7.2	11.1	13.4	18.4	16.2	12.9	12.1	7.6	6.4	10.2
1794	2.4	[8.3]	8.6	10.8	11.4	16.0	18.6	15.4	12.9	10.9	8.7	5.4	(10.8)
1795	−1.9	3.4	5.4	8.9	11.9	12.9	14.3	16.2	16.4	[12.8]	5.7	(9.1)	(9.6)
1796	[8.6]	5.6	4.6	9.9	11.4	14.8	15.7	16.0	14.9	9.2	5.6	1.3	(9.8)
1797	4.9	5.2	5.3	7.5	11.1	(12.3)	15.4	15.2	13.0	8.7	7.7	6.6	9.4
1798	5.2	5.0	6.1	10.5	12.5	17.2	16.5	17.1	14.1	11.2	5.4	2.7	10.3
1799	3.7	5.1	4.4	6.0	10.5	14.8	15.9	14.9	12.9	8.7	7.3	1.5	8.8
1800	4.8	4.0	5.1	10.1	11.9	13.6	18.5	(18.7)	(15.9)	11.2	6.8	5.7	10.5
1801	6.6	5.3	7.9	8.8	11.8	15.3	16.9	18.5	(16.4)	12.2	6.8	4.7	10.9
1802	2.8	5.3	6.1	(10.8)	12.2	15.3	14.6	18.2	14.6	11.4	6.7	5.4	10.3
1803	2.3	4.7	7.1	9.1	10.9	14.2	(19.2)	(18.0)	13.0	10.7	6.3	6.5	10.2
1804	(8.1)	5.1	5.9	7.3	13.1	17.1	16.8	17.1	15.7	11.5	8.2	3.3	10.8
1805	2.9	5.0	6.6	8.0	10.5	13.3	16.7	17.4	15.7	9.5	7.0	5.4	9.8
1806	5.9	6.1	6.0	7.4	13.1	15.9	17.9	16.9	14.3	11.8	[9.2]	(9.1)	(11.1)
1807	4.3	6.1	3.6	8.3	12.8	13.7	17.7	18.0	13.0	12.6	4.7	4.3	9.9
1808	4.0	4.2	4.1	6.6	14.0	15.0	18.6	17.7	14.0	9.0	8.2	4.2	10.0
1809	4.6	7.8	6.6	5.8	12.8	14.6	16.8	15.7	14.1	11.3	5.6	5.5	10.1
1810	3.7	5.3	6.9	9.4	10.5	15.8	16.5	15.7	14.9	11.2	6.2	6.4	10.2
1811	1.8	6.6	8.1	9.4	13.2	14.8	17.4	16.3	14.9	13.4	8.4	5.3	10.8
1812	3.7	6.7	4.7	7.5	12.0	13.9	16.1	16.0	14.5	10.8	7.1	2.5	9.6
1813	3.2	6.0	7.4	8.3	12.1	14.0	15.4	16.8	13.7	10.2	6.5	4.1	9.8
1814	−0.7	3.2	3.5	10.0	10.3	13.3	16.5	16.1	14.3	8.8	6.5	6.5	9.0
1815	1.2	7.8	8.7	8.8	12.9	14.5	16.4	16.4	14.3	10.6	4.6	3.8	10.0
1816	3.4	3.8	4.6	7.4	10.4	12.5	12.9	13.5	12.9	10.7	5.0	4.0	8.4
1817	5.7	7.9	6.8	8.2	9.5	14.7	14.2	14.6	14.1	7.3	10.4	4.4	9.8
1818	5.6	4.3	6.2	8.2	12.4	17.5	18.9	16.7	13.9	13.1	11.2	4.4	11.0
1819	6.1	5.9	7.4	9.6	12.3	13.6	17.3	18.1	14.7	10.2	5.9	3.6	10.4
1820	1.2	3.7	5.3	9.9	11.8	14.5	16.2	15.9	13.1	9.5	6.3	5.3	9.4
1821	4.7	3.1	7.1	9.8	10.2	12.8	15.4	17.3	15.8	11.4	10.1	7.6	10.4
1822	5.8	7.0	9.1	9.1	13.6	17.7	16.2	15.9	13.7	11.5	9.2	2.8	11.0
1823	1.1	5.1	6.1	7.9	12.9	13.1	14.6	15.6	13.5	9.9	7.3	6.2	9.4
1824	4.6	6.1	5.8	7.7	11.3	13.8	16.7	16.5	14.9	10.7	9.2	6.9	10.3
1825	4.9	5.6	6.5	10.5	12.6	14.7	18.6	17.3	16.6	12.1	6.8	6.3	11.0
1826	3.1	7.8	7.1	10.2	12.6	18.1	18.9	18.0	15.3	12.8	6.1	7.7	11.5
1827	3.7	1.8	7.5	9.7	12.3	14.3	17.6	15.8	14.6	11.8	9.2	8.4	10.6
1828	6.8	6.6	7.9	9.2	12.9	15.8	16.6	15.3	15.4	11.2	9.3	9.2	11.3
1829	1.4	6.3	5.2	7.4	13.6	14.6	15.7	15.1	11.9	10.2	5.7	1.9	9.1
1830	0.2	3.0	8.5	9.6	12.4	13.4	16.6	14.9	12.5	11.5	8.2	3.2	9.5
1831	3.1	6.1	7.7	9.6	12.1	15.5	16.8	17.6	14.2	13.2	7.6	6.8	10.9
1832	4.6	4.2	6.4	8.4	11.7	14.8	16.6	16.3	13.3	10.6	7.5	6.5	10.1
1833	3.2	6.8	3.7	8.4	14.0	14.2	16.3	14.7	12.2	11.1	7.9	8.1	10.1
1834	8.1	6.2	7.8	8.5	13.5	14.6	16.7	16.3	14.5	11.3	6.5	6.1	10.8
1835	4.8	6.7	6.4	8.8	11.7	15.4	17.7	17.2	13.9	9.5	7.7	3.2	10.3
1836	5.1	3.3	6.5	7.6	11.4	15.0	16.3	16.2	12.6	9.2	6.7	5.3	9.6
1837	3.6	6.5	2.6	4.8	10.6	15.5	17.8	16.2	13.9	11.5	6.9	5.9	9.7
1838	0.3	2.2	6.4	7.2	11.7	14.2	16.3	16.6	13.6	11.2	6.2	5.4	9.3
1839	4.5	5.6	5.8	7.2	11.1	15.1	15.8	15.4	13.4	9.9	7.7	6.0	9.8
1985	1.4	4.3	5.7	9.1	11.6	13.9	16.6	15.3	14.5	11.6	5.3	8.1	9.8
1986	5.7	0.3	6.3	6.2	11.1	15.3	16.4	13.9	11.9	11.9	8.7	7.8	9.6
1987	2.1	5.2	5.7	10.0	11.1	13.8	16.6	16.7	14.9	10.9	7.9	7.1	10.2
1988	7.0	5.7	7.7	8.6	12.2	15.5	15.1	15.5	14.1	11.9	7.3	8.8	10.8

Brackets () = value doubtful, [] = value derived (see text).

Italic figures are used for years 1782–1816 when HEB was the only station available for Exeter. For the years 1817–1839, HEB and DEI (and Shapter) values were available.

Returning to the original Heberden record, it begins with an interrupted series of monthly data made at Bridestowe, North Devon between December 1782 and October 1786, and this is followed by a few monthly observations made at Whimble, near Exeter until January 1788. In May 1788, Heberden began the series of MMTs at Exeter near the Cathedral, which continued without a break until 1843.

For the derivation of a reliable homogeneous series of MMTs for the location of Exeter from 1789 onwards, the Heberden record was virtually the only one available until 1817, the year when the DEI series was started—the Earnshill records for 1798–1804 have already been considered. Both records are nearly complete between 1817 and 1839, the period covered in this paper. Another

record has also been published by Shapter (see Table III and references) covering the period 1824–53. However when a comparison was made between Shapter’s figures and the DEI data, it became evident that Shapter had taken his data direct from the DEI data. The former’s data were therefore not used in deriving the Exeter series presented here, except in some instances when DEI data were doubtful or not available, and in most of these cases the individual MMTs derived were then based upon Heberden and Shapter instead.

While deriving all the MMTs, values of the differences (HEB–DEI) were also noted and classified according as to whether they lay within the limits of 0.0–0.4, 0.5–0.9, or $\geq 1.0^{\circ}\text{C}$. In the end it was only found necessary to make use of this grouping when considering

Table II. Stations used for analysis of Exeter temperatures

Station	Latitude	Longitude	Height (feet) (metres)		Period of observations
Exeter, Devon and Exeter Institution (DEI)	50° 43'N	03° 32'W	155	47	1817–43
Bridestowe, Devon	50° 41'N	04° 06'W	520	158	1782–86
Whimble, Devon	50° 46'N	03° 21'W	165	50	1787–88
Earnshill House, Somerset	51° 00'N	02° 52'W	66	20	1798–1804

Table III. Corrections used to reduce original observations made at fixed hours to their equivalent values of monthly mean temperature (MMT) related to $(T_{\min} + T_{\max})/2 (^{\circ}\text{C})$

Station	Fixed hours	Jan.	Feb.	Mar.	Apr.	May	June	July	Aug.	Sept.	Oct.	Nov.	Dec.
Exeter, Heberden record	0800 and 1400	−0.2	−0.1	−0.5	−0.9	−1.2	−1.2	−1.2	−1.1	−0.9	−0.6	−0.3	−0.3
Exeter, DEI record	0800, 1400 and 2200	−0.1	0.0	−0.1	−0.2	−0.3	−0.3	−0.1	−0.2	−0.2	−0.1	−0.1	−0.1
Shapter table	Daily max and min from 1824	0.1	−0.1	−0.2	−0.4	−0.9	−1.1	−0.9	−0.7	−0.4	−0.2	0.1	0.2
Bridestowe, early years of Hederden record	0800 and 1400	0.3	0.2	−0.5	−1.3	−2.0	−2.0	−1.7	−1.3	−1.1	−0.6	0.0	0.3

The above corrections include those for site effect (see correction C in Hay (1985)), fixed hourly values and for height a.m.s.l. In the case of Exeter DEI, correction C is not included here but was applied to the figures used in Table I before their inclusion in the table.

the reliability of a number of doubtful cases of MMTs, some when $(\text{HEB}-\text{DEI}) \geq 1.0^\circ\text{C}$, which were found through the period 1789–1839. In dealing with these months, the doubtful values as first derived were compared with the long period (LP) monthly extremes, highest or lowest, as appropriate, for Exeter, Oxford and Central England (CE). In most cases, doubtful values derived from $(\text{DEI}+\text{HEB})/2$ arose because, when checked against the LP extremes, highest or lowest, for Exeter DEI as already derived for 1840–1984 in Hay (1985), these doubtful cases were found to be equal to or outside the LP limits. It remained to devise a stricter routine in this work, as follows. Firstly, all cases in which the MMT lay beyond the LP extremes and up to 1.1°C (i.e. just inside the LP extremes) were noted. A decision on whether the high (or low) value of each doubtful MMT was correct (or nearly so) was then made possible in almost every doubtful case by applying this same procedure to the known MMTs for the same months for Oxford (from 1815 onwards) and for CE for the whole period from 1789. Where the DEI value of an MMT still remained doubtful, then the temperature anomalies (TAs) for DEI, HEB, Oxford and CE (with respect to the appropriate LP monthly averages) were derived and an inspection of their geographical distribution with respect to each other was sufficient to resolve the difficulty. For a ‘hard core’ of four cases ‘derived MMTs’ were found by making use of the data shown in Table IV. This table yields derived MMTs falling within the LP extreme MMT values in three cases, while it suggests February 1794 probably represents another extreme (mild) month. These derived values have therefore been included in Table I, as being the best available, to make it complete for the whole period.

3. Comparisons with Manley’s Central England Series

Support for the accuracy of the figures in Table I using Manley’s data for CE (1974) has been obtained as follows. Differences through 10-year periods 1810–191860–69 between monthly 10-yearly means of $(\text{CE}-\text{Exeter})$ were first extracted. This was done to ensure that no serious inhomogeneity existed between Exeter MMTs as derived for months for 1840 onwards in Hay (1985), and those for 1839 and earlier years as shown here in Table I. Any abrupt change in Exeter MMT through the years around 1840 should be shown by this comparison with the corresponding MMTs for CE. In fact the differences in MMTs for $(\text{CE}-\text{Exeter})$ between the means for 1830–39 and for 1840–49 amounted to $+0.5^\circ\text{C}$ in winter (December, January, February) and -0.2°C in summer (June, July, August) respectively. The largest differences for individual months were similarly $+0.9^\circ\text{C}$ in December and -0.3°C in July. (For the 30-year periods 1810–39 and 1840–69 the differences were similarly 0.0°C in winter and -0.6°C in summer.) Similarly the differences $(\text{CE}-\text{Exeter})$ over the 30-year (or 40-year) periods 1811–40, 1841–70, 1871–1900, 1901–40 and 1941–70 were respectively -1.3 , -1.3 , -1.2 , -1.4 and -1.4°C in winter, and -0.7 , 0.0 , -0.3 , -0.4 and -0.3°C respectively in summer.

The variances of the two sets of differences of annual mean temperatures $(\text{CE}-\text{Exeter})$ for the periods 1789–1839 and 1941–1973 were computed and found to be 0.0728 and 0.04 respectively, giving a variance ratio (F) of 1.82. Reference to the relevant tables show that for degrees of freedom 50 and 32 and assuming that, prior to calculating them, it was not known which period showed the greater variance, then the significance

Table IV. Monthly mean temperatures ($^\circ\text{C}$) — derivation of doubtful cases

	Exeter Heberden initial reduced value	Exeter extremes 1840– 1980	Exeter means 1841– 1980	CE means 1851– 1950	Differences (CE–Exeter) in months shown	Differences (CE–Exeter) for LP means	CE MMT for month shown	Derived* MMT for Heberden	† Col. 8 –Col. 2
	1	2	3	4	5	6	7	8	9
1794 Feb.	9.0	8.3	5.2	4.1	–1.8	–1.1	7.2	8.3	0.0
1795 Oct.	14.0	13.7	10.7	9.6	–2.3	–1.1	11.7	12.8	–0.9
1796 Jan.	9.2	9.0	5.0	3.7	–1.9	–1.3	7.3	8.6	–0.4
1806 Nov.	10.4	9.9	7.4	6.0	–2.6	–1.4	7.8	9.2	–0.7

* For each month (Derived Heberden) = $(\text{CE}-\text{Exeter})$ i.e. (col. 7–col. 6).

† Values in col. 9 show the differences in each case between ‘Derived Heberden’ and the long period (LP) extreme. Feb. 1794 probably represents an extreme (mild) month, the other three months falling up to approximately 1°C below the appropriate extreme values.

level was low (around 10%) and hence it is probable these two variances are not significantly different. This result can be regarded as satisfactory, together with the fact that the overall mean differences (CE—Exeter) between mean annual temperatures were found to be -1.0°C during 1789–1939 and -0.8°C for 1941–1973 respectively.

The general conclusion drawn from the comparisons described above suggests that the MMTs, as derived here, for 1782–1839 for Exeter, while being virtually independent from CE, are in fact broadly in agreement with MMTs as given in Manley's long-period series. Besides providing a new 200 years MMT series for the Exeter area, these figures also afford a useful back-up for Manley's results through the period here considered.

Acknowledgement

Valuable assistance given by D. Griffith, Senior Meteorological Officer, Exeter Airport, in making

available temperature records for the Airport from 1942 to date as needed, is gratefully acknowledged.

References and bibliography

- Devon and Exeter Institution: Meteorological observations kept in observation books at the Devon and Exeter Institution in Exeter, 1817–1975.
- Earnshill House, The meteorological records kept by the Combe family in 1799–1804, deposited with the Public Record Office, Taunton.
- Hay, R.F.M., 1985: Exeter temperatures: monthly means from 1840 to 1984. *Meteorol Mag*, **114**, 332–343.
- Heberden, T.: Weather record of the Revd Thomas Heberden 1785–1855. (Original manuscript available in the Devon Record Office, Central Library, Exeter.)
- HMSO, 1949: Industrial experimentation, fourth edition.
- Knox-Shaw, H. and Balk, J., 1932: Radcliffe observations, 55.
- Manley, G., 1974: Central England temperatures: monthly means 1659 to 1973. *Q J R Meteorol Soc*, **100**, 389–405.
- Shapter, T., 1862: The climate of the south of Devon, second edition. London, John Churchill.

Notes and news

American Society for Testing and Materials (ASTM) symposium on Mapping and Geographic Information Systems, San Francisco, California, 21–22 June 1990

This symposium is sponsored by the ASTM Standards Writing Committee D-18 on Soil and Rock. The Committee D-18 is one of 134 ASTM technical standards writing committees, and ASTM (organized in 1898) is one of the largest voluntary standards developments systems in the world.

The purpose of the symposium is to bring together an interdisciplinary, international group of engineers and scientists to:

- Provide a forum to exchange experiences related to the needs and methods for Geographic Information Systems (GIS), maps, and remote sensing, and the potential for standardization of some elements of each.
- Learn from both successful and unsuccessful case histories.
- Promote technology transfer between the various disciplines and countries represented.
- Provide an education resource for those attendees who may be considering using, for the first time, the three elements that make up an overall land information system.

More information is available from the symposium chairman:

Ivan Johnson
7474 Upham Court
Arvada
Colorado 80003, USA
Tel: 303-425-5610.

Reviews

Weather sensitivity and services in Scotland, edited by S.J. Harrison and K. Smith. 180 mm \times 257 mm, pp. viii+180, *illus.* Edinburgh, Scottish Academic Press, 1989. Price £25.00.

This book is the outcome of a conference which was jointly organized by the Meteorological Office and the Climatic Hazards Unit of the University of Stirling. It was held in February 1988 and was attended by about 150 delegates associated with a wide range of weather-sensitive activities.

The objectives of the conference, and therefore this volume, were to demonstrate the role of weather and climate information in the management of weather-sensitive activities and to encourage interaction between the providers and users of such information. This is a laudable aim and any small step in facilitating this is to be welcomed.

Four main areas are covered: advances in observing and forecasting the weather; transport; agriculture, water and wind resources; industrial applications. Some contributions expand on their topic at some length, while others are short and sometimes superficial. Indeed, individual contributions vary in length from 18 pages to little more than 3 pages. A contribution by Professor Keith Smith serves as a good introduction to the volume. He explores weather variability and its social and economic effects and, quite reasonably, argues that the drive towards greater efficiency leads to a greater vulnerability to weather extremes.

In the first of the four sections which follow, the papers by Collier and Golding give useful overviews of the topics: the use of radar and satellite data in forecasting; numerical weather prediction. Much of the material can be found in earlier papers by these authors,

but these contributions are put together in a way which non-specialists will find palatable. It will be interesting to look back at the predictions, for numerical forecasting in the 1990s, made by Golding at the end of this article.

I found none of the articles in the section (on transport) particularly inspiring, but they serve the purpose of highlighting the needs of road and rail transport, and the attempts to cater for these needs by the Meteorological Office.

The third section contains three articles: one each on agriculture, water resource management and the wind-turbine industry. Callander points to the 'minimal' exploitation of weather services by the Scottish agricultural community, even more so since the demise of the Agricultural Meteorology Unit in Edinburgh in 1981. He holds out the hope that the provision of information from the eventual extension of the weather radar network (long a bone of contention with the broader meteorological community in Scotland) will provide real benefits to agriculture. The article by Sargent focuses on the expected benefits from radar in terms of flood forecasting, and Elliot and Barton bemoan the paucity of wind data appropriate for the wind-power industry.

The final section contains seven articles under the general title 'industrial applications'. Some of the contributions are very short and serve little purpose, but the enormous potential for better use of meteorological information is brought out — for instance, losses due to weather-related stoppages in the construction industry are estimated at £400m. The article by Steel on weather sensitivity in the gas industry is the longest, and in my opinion the best, contribution to this section. It presents demand-forecasting models used by the industry, expressing general satisfaction with presently available weather information.

This book will not have a large market, but forms a useful addition to a library alongside such texts as Maunders' *The uncertainty business*. It would be improved by the addition of even a short index.

K.J. Weston

A short course in cloud physics, third edition, by R.R. Rogers and M.K. Yau. 151 mm × 228 mm, pp. xiv+293, illus. Oxford, New York, Beijing, Frankfurt, São Paulo, Sydney, Tokyo, Toronto, Pergamon Press, 1989. Price £15.00, US\$27.00 (paperback), £30.00, US\$54.00 (hardback).

This book is the third edition of a book by the first author originally published in 1976. It is one of a series on Natural Philosophy which includes a few other titles of interest to meteorologists.

Lecture notes from a graduate course for physical meteorology students form the basis of the book, but it will also be suitable for undergraduates with a good knowledge of physics and mathematics. No previous knowledge of meteorology is assumed. Familiarity with

differential equations is essential although the derivation of many equations is omitted. Prof. Rogers is experienced in the interpretation of cloud observations, especially the use of radar data, while this revised edition has also benefitted from the cloud modelling expertise of Dr Yau.

The book is intended to provide a basic understanding of cloud processes and it includes the necessary general meteorology to achieve this, for example, thermodynamics and stability. The treatment is brief but comprehensive. The treatment of most topics is not as deep as in the books by Pruppacher and Klett or Mason and, although therefore the book may not appeal to the cloud physics specialist, it is ideal for the more general meteorologist or for those who are concerned with the applications of cloud physics.

The first four chapters discuss the thermodynamics of dry and moist air, buoyancy and convection. They include a good description of thermodynamic diagrams and of the different instabilities in atmospheric flows. A new, and up to date, chapter on the observed properties of clouds begins a series of chapters which include most of the topics which come under the heading of cloud physics, cloud droplet and ice crystal growth, precipitation processes, severe storms and weather radar. Weather modification receives a rather cursory discussion which would have benefitted from more examples. Cloud electrification and lightning are not mentioned. The book ends with a chapter on numerical cloud-models which has been substantially rewritten and provides a clear discussion of the limitations of different types of model and of the scientific advances which have come about through the use of models, especially the dynamical interactions leading to the maintenance of severe storms.

Apart from the major changes mentioned above, the text has been revised in many places to include recent developments such as advances in the understanding of entrainment processes. It is a pity that SI units are not universally adopted in this edition; the application of empirical formulae often causes difficulties when different units are used.

The author has included in this edition, as in earlier editions, a number of examples for the student to work through. These are well thought out, reinforcing, and in several cases extending, the material. The answers, where provided, should be easily understood. Comprehensive and up-to-date references are provided and several of these are identified as providing fuller details in areas which are treated briefly. The book is well illustrated with carefully chosen and well reproduced diagrams; the use of colour for the radar images might have improved the attractiveness of the book but their absence does not affect the clarity of the argument.

The earlier editions of this book have been successful. The present edition is a significant improvement and is recommended to those who wish, or need, to know something of the complex processes which are too often

dismissed by statements such as 'the air is forced to rise, as it does so it cools and water condenses to form rain'.

P.R. Jonas

Spacious skies, by R. Scorer and A. Verkaik. 222 mm × 288 mm, pp. 192, *illus.* Newton Abbot, London, David and Charles, 1989. Price £20.00.

Richard Scorer has long been regarded as a foremost authority on cloud physics, and uses cloud photography to illustrate his theories. This book could be looked upon as a supplement to his excellent *Clouds of the World*, published in 1972, by adding many well produced satellite pictures and comprehensive notes on their details. In addition, the many photographs of cumulus-type clouds by Arjen Verkaik greatly add to those used by Dr Scorer in his earlier work. Arjen Verkaik became fascinated as a boy by the ever-changing skies and from this began to collect many cloud photographs. This led to a desire to understand the physical processes at work and, encouraged by his wife, he delved even deeper into the subject. Fortunately, their common interest drew the two authors together in 1984 and resulted in the planning of this book.

The object of the book is to show how rewarding 'sky-watching' can be, and so help the reader to understand what clouds and their changes can tell us, using 'discerning eyes and tinted vision'. By photographing clouds and taking time-sequence series, the changes can be studied at leisure and the physical processes thus deduced.

The second and seventh chapters are devoted to satellite pictures. In chapter 2 there are many fine illustrations of the effect of land features on the overall cloud pattern. Many of the finer details could be overlooked had our attention not been drawn to them by Richard Scorer. The effects caused by Jan Mayen island are strikingly illustrated and he asserts that (para 3.1.a) 'It is undoubtedly the most interesting oceanic island in the World for the variety of patterns it generates'. Chapter 7 gives details of satellite orbits and the filters used to differentiate various cloud and dust or haze features. More striking satellite pictures show frontal cyclonic and anticyclonic cloud systems with comments, at times, almost poetical at the beauty so exhibited.

Chapter 3 discusses in a general way the convective processes, frontal clouds and variations in ALTO and ICE clouds. The illustrations are well chosen and adequate notes are given for each. Chapters 4–6 deal with cumulus-type clouds and related phenomena such as tornadoes etc. as seen by the camera of Arjen Verkaik. The wide experience of Richard Scorer can be detected in the text, and numerous explanatory diagrams are reproduced from his *Clouds of the World*. There are many sequence pictures to explain the thinking behind the deductions made. The discussion on cumulonimbus is interesting with its development from

a single cell to multiple cells. The term 'dryline storm' is introduced and illustrated — a phenomenon not known in western Europe. The pictures in these three chapters, covering about half the book, and Haboob effects in chapter 13, are practically all taken in Canada and are the work of Arjen Verkaik.

A useful appendix is given on the physical nature of clouds and allied phenomena; the Index is comprehensive. There are few errors and the quality of the text and illustrations are good. Many of the pages are unnumbered, which hinders cross reference and the fifth picture referred to in para 6.30.e in the series does not appear.

As an experienced and enthusiastic cloud watcher and photographer myself, I can recommend this book as a must for all meteorological libraries, for students of cloud physics and to those dedicated cloud watchers who wish to delve more deeply into the subject.

R.K. Pilsbury

Books received

The listing of books under this heading does not preclude a review in the Meteorological Magazine at a later date.

Weather radar and the water industry, by the British Hydrological Society (Wallingford, Oxfordshire, Institute of Hydrology, 1989) summarizes the proceedings of a seminar held at the Institute of Hydrology on 6 April 1989. It contains eight papers on the various aspects of the subject by authors from a cross-section of viewpoints.

Turning up the heat, by F. Pearce (London, Glasgow, Toronto, Sydney, Auckland, Paladin, 1989) is a wide-ranging survey of the pollutants that have caused concern about global warming. Ways of rethinking the approaches to the subject are presented.

Our drowning world, second edition, by A. Milne (Bridport, Dorset, Prism Press, 1989) contains explanations for the author's belief that nearly two thirds of the earth's surface will be flooded by polar ice-cap water — the result of human activity.

Earth's changing climate, by A. Milne (Bridport, Dorset, Prism Press, 1989) explores the importance of extra-terrestrial influences on the earth's weather patterns. It is a companion book to *Our drowning world*.

Atlas of the surface heat balance of the continents, by D. Henning (Berlin, Stuttgart, Gebrüder Borntraeger, 1989) presents detailed analyses of mean multi-period values of many varied fluxes and parameters. A discussion of the three methods of data treatment used, an explanation of the main features of the maps, and tabulated area averages are included.

Satellite photograph — 23 November 1989 at 0824 UTC

Figs 1 and 2 illustrate the pattern of convective cloud near southern Britain as polar air flowed south and west over warm seas. Over the North Sea, tops of the convection probably approached 700 mb. However, further west the convection was limited by a marked subsidence inversion at 850 mb caused by an anticyclone which had recently developed near Ireland.

The NOAA-10 visible image (Fig. 1) indicates cellular cumulus cloud over the North Sea, but elsewhere the cloud top has a mostly stratiform appearance. Two cloud bands are noteworthy — a gradually widening band, within which a narrow line of cumulus tops (labelled A) is to be observed along the English Channel, and a similar but less well defined band (B) west of the Bristol Channel.

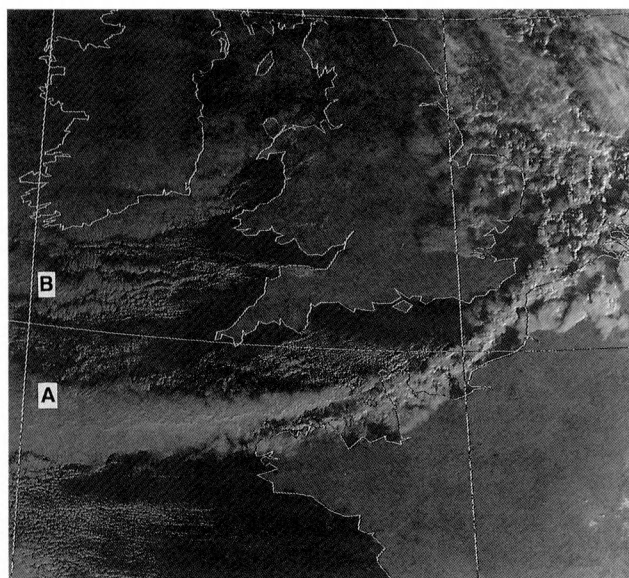


Figure 1. NOAA-10 visible image for 0824 UTC on 23 November 1989. The isobaric pattern at 1200 UTC is superimposed.

Sequences of Meteosat and NOAA images showed the bands persisted with little lateral movement for more than 2 days. During the subsequent long anticyclonic easterly period of weather, the English Channel band occurred on all but 2 of the next 18 days, although its position varied between the French and British coasts depending on the exact wind direction, and probably the strength of the land-breeze circulation. Further evidence of the persistence of the bands was obtained by calculating the mean brightness of sequences of Meteosat visible images that were 'normalized' (i.e. brightness corrected according to sun angle). The result for 23 November is shown in Fig. 2. Streamlines drawn directly from surface wind analyses derived from UK mesoscale-model data (Fig. 3) indicate marked convergence

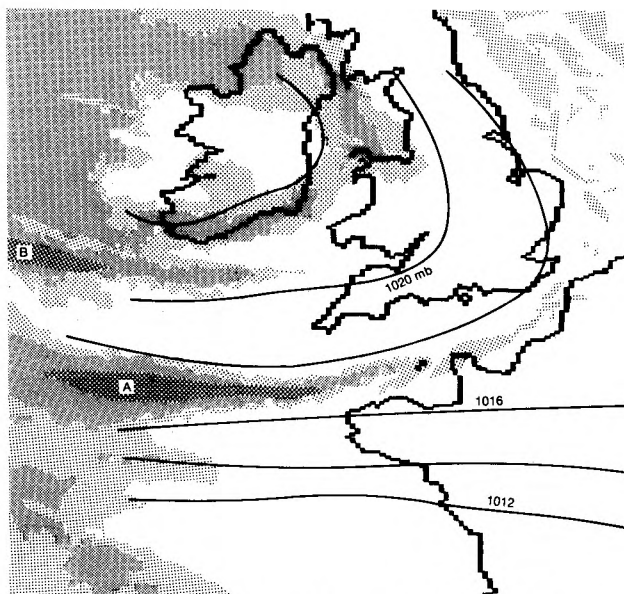


Figure 2. Average visible brightness during hours of strong daylight — 0930–1430 UTC inclusive — at intervals of 30 minutes.

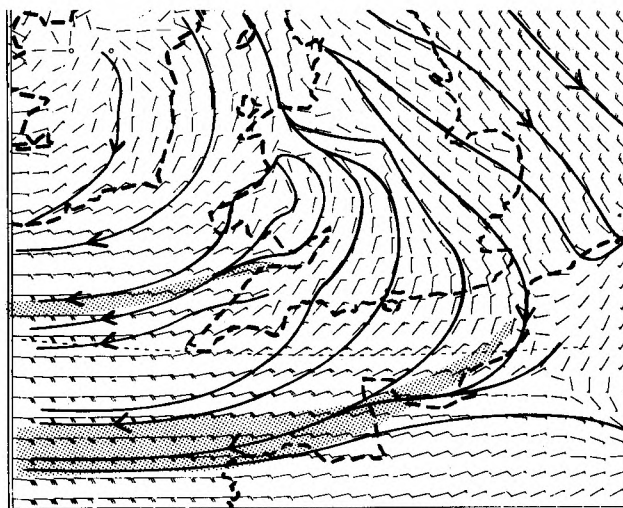


Figure 3. Streamlines of surface winds valid at 1200 UTC, drawn on a 12-hour forecast from the UK mesoscale model. The cloud bands associated with the convergence are shown hatched.

co-located with the cloud band in the English Channel, and weak convergence in the Bristol Channel. Due to the limited depth of the convection, precipitation beneath the bands was generally patchy and light. However, when instability is deep, convergence around the coast of southern Britain can lead to localized extreme accumulations of precipitation as described in Pike*, and another imminent issue.

G.A. Monk

* Pike, W.S.; Persistent coastal convergence in a heavy snowfall event on the south-east coast of England. *Meteorol Mag*, 119, 1990, 21–32.

GUIDE TO AUTHORS

Content

Articles on all aspects of meteorology are welcomed, particularly those which describe results of research in applied meteorology or the development of practical forecasting techniques.

Preparation and submission of articles

Articles, which must be in English, should be typed, double-spaced with wide margins, on one side only of A4-size paper. Tables, references and figure captions should be typed separately. Spelling should conform to the preferred spelling in the *Concise Oxford Dictionary* (latest edition). Articles prepared on floppy disk (Compucorp or IBM-compatible) can be labour-saving, but only a print-out should be submitted in the first instance.

References should be made using the Harvard system (author/date) and full details should be given at the end of the text. If a document is unpublished, details must be given of the library where it may be seen. Documents which are not available to enquirers must not be referred to, except by 'personal communication'.

Tables should be numbered consecutively using roman numerals and provided with headings.

Mathematical notation should be written with extreme care. Particular care should be taken to differentiate between Greek letters and Roman letters for which they could be mistaken. Double subscripts and superscripts should be avoided, as they are difficult to typeset and read. Notation should be kept as simple as possible. Guidance is given in BS 1991: Part 1: 1976, and *Quantities, Units and Symbols* published by the Royal Society. SI units, or units approved by the World Meteorological Organization, should be used.

Articles for publication and all other communications for the Editor should be addressed to: The Director-General, Meteorological Office, London Road, Bracknell, Berkshire RG12 2SZ and marked 'For Meteorological Magazine'.

Illustrations

Diagrams must be drawn clearly, preferably in ink, and should not contain any unnecessary of irrelevant details. Explanatory text should not appear on the diagram itself but in the caption. Captions should be typed on a separate sheet of paper and should, as far as possible, explain the meanings of the diagrams without the reader having to refer to the text. The sequential numbering should correspond with the sequential referrals in the text.

Sharp monochrome photographs on glossy paper are preferred; colour prints are acceptable but the use of colour is at the Editor's discretion.

Copyright

Authors should identify the holder of the copyright for their work when they first submit contributions.

Free copies

Three free copies of the magazine (one for a book review) are provided for authors of articles published in it. Separate offprints for each article are not provided.

Editor: B.R. May
Editorial Board: R.J. Allam, R. Kershaw, W.H. Moores, P.R.S. Salter

Contents

	Page
Persistent coastal convergence in a heavy snowfall event on the south-east coast of England. W.S. Pike	21
Exeter temperatures: monthly means from 1782 to 1839, and from 1985 to 1988. R.F.M. Hay	33
Notes and news	
American Society for Testing and Materials (ASTM) symposium on Mapping and Geographic Information Systems, San Francisco, California, 21-22 June 1990	37
Reviews	
Weather sensitivity and services in Scotland. S.J. Harrison and K. Smith (editors). K.J. Weston	37
A short course in cloud physics, third edition. R.R. Rogers and M.K. Yau. P.R. Jonas	38
Spacious skies. R. Scorer and A. Verkaik. R.K. Pilsbury	39
Books received	39
Satellite photograph — 23 November 1989 at 0824 UTC G.A. Monk	40

Contributions: It is requested that all communications to the Editor and books for review be addressed to the Director-General, Meteorological Office, London Road, Bracknell, Berkshire RG12 2SZ, and marked 'For *Meteorological Magazine*'. Contributors are asked to comply with the guidelines given in the *Guide to authors* which appears on the inside back cover. The responsibility for facts and opinions expressed in the signed articles and letters published in *Meteorological Magazine* rests with their respective authors. Authors wishing to retain copyright for themselves or for their sponsors should inform the Editor when submitting contributions which will otherwise become UK Crown copyright by right of first publication.

Subscriptions: Annual subscription £30.00 including postage; individual copies £2.70 including postage. Applications for postal subscriptions should be made to HMSO, PO Box 276, London SW8 5DT; subscription enquiries 01-873 8499.

Back numbers: Full-size reprints of Vols 1-75 (1866-1940) are available from Johnson Reprint Co. Ltd, 24-28 Oval Road, London NW1 7DX. Complete volumes of *Meteorological Magazine* commencing with volume 54 are available on microfilm from University Microfilms International, 18 Bedford Row, London WC1R 4EJ. Information on microfiche issues is available from Kraus Microfiche, Rte 100, Milwood, NY 10546, USA.

ISBN 0 11 728662 1 ISSN 0026-1149

© Crown copyright 1990. First published 1990

The

Meteorological Magazine

March 1990

Mesoscale heavy snowfall
Measuring ozone for 64 years



DUPLICATE JOURNALS

National Meteorological Library
FitzRoy Road, Exeter, Devon. EX1 3PB

HMSO

Met.O.992 Vol. 119 No. 1412



3 8078 0010 2445 6

The Meteorological Magazine

March 1990
Vol. 119 No. 1412

551.578.45:551.515.42(410)

A heavy snowfall within a mesoscale convergence zone

R.M. Sanderson

Meteorological Office, Royal Air Force High Wycombe

B.W. Golding and M.J. Bader

Meteorological Office, Bracknell

Summary

The localized heavy snowfall over central southern England on the night of 18/19 March 1987 is investigated using mesoscale-model output and satellite and radar imagery. Factual and conjectural reasoning is employed to propose a conceptual model of the event.

1. Introduction

On the night of 18/19 March 1987, heavy snow — up to 30 cm in places — fell in a narrow band from Gwent in Wales to west Hampshire (Fig. 1). It caused considerable disruption to power supplies and road traffic. Satellite and radar images showed that the snow surprisingly fell a few hundred kilometres east of an initially conspicuous, well-developed comma cloud that moved south-east in a decaying state across Cornwall, and did not fall from cloud that developed, as is more usual, along the tail of the comma.

This case-study shows how images from satellites and radar, together with diagnostics from the mesoscale and fine-mesh models may be used to alert the forecaster to this type of development and to help understand the main physical and dynamical processes at work.

2. Synoptic discussion

A deep, mature vortex was located over the northern North Sea under the cloud spiral, V, shown in the first of a sequence of NOAA-9 satellite infra-red images (Fig. 2(a)) at 0415 UTC on 18 March. Cold, unstable north-westerly winds (depicted by the cumuliform clouds on the image) prevailed over the north-east

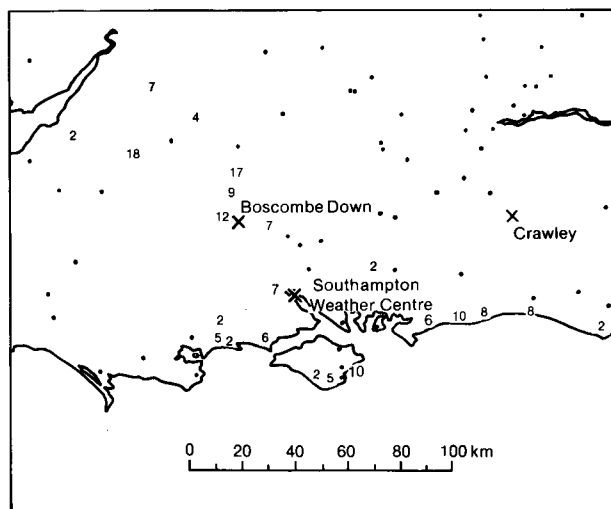
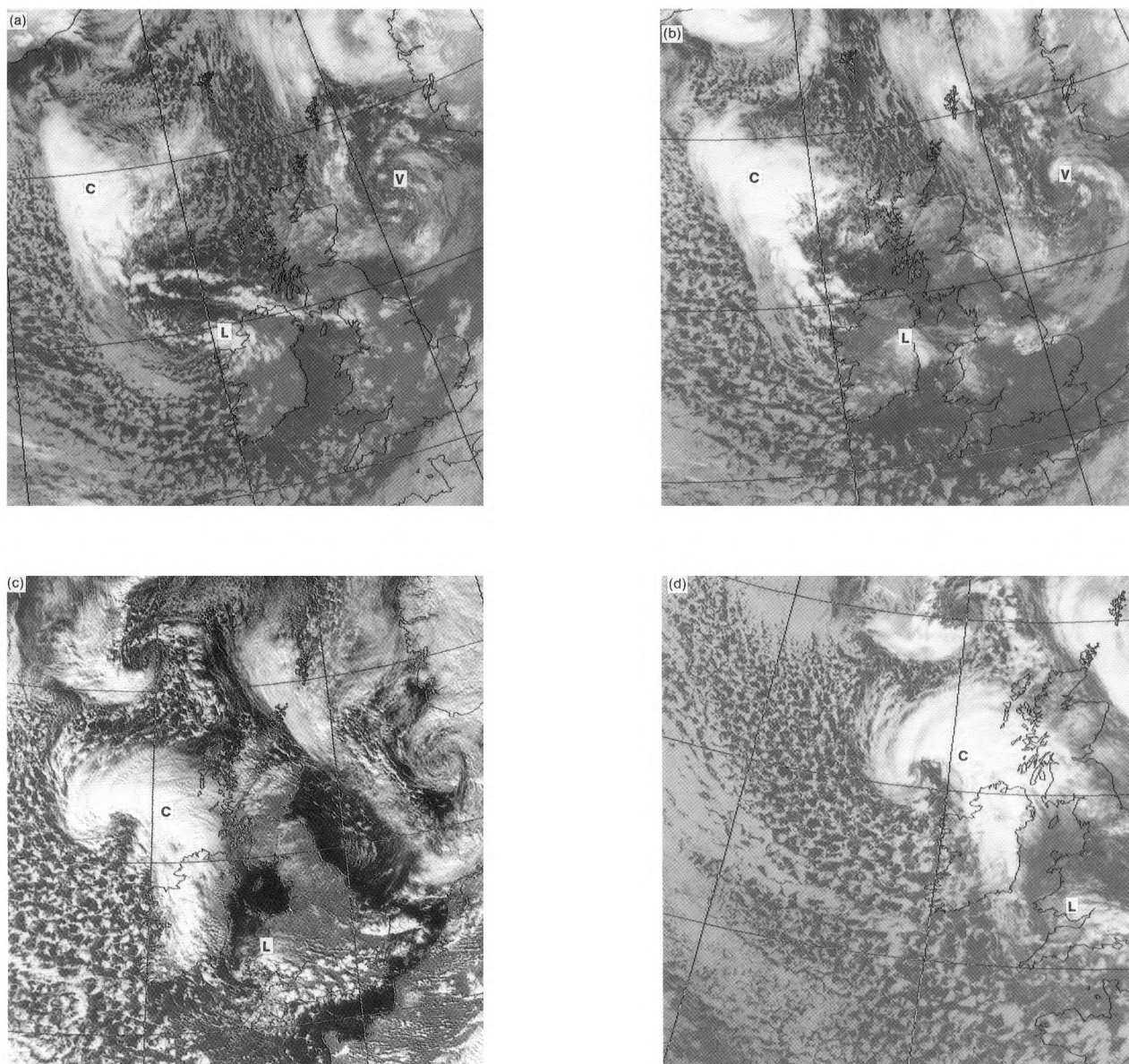


Figure 1. Snow depths (cm) over southern England at 0900 UTC on 19 March 1987 (dots are places with no snow). Southampton Weather Centre and Boscombe Down are stations whose weather sequence is shown in Fig. 8, and a Crawley radiosonde ascent is shown in Fig. 10.



Photographs by courtesy of University of Dundee

Figure 2. NOAA satellite infra-red images at (a) 0415, (b) 0820, (c) 1409, and (d) 1551 UTC on 18 March 1987, showing a mature vortex, V, over the northern North Sea, an area of cloud, C, that developed into a comma and an area of enhanced convection, L. C and L moved south-eastwards.

Atlantic and the United Kingdom on the western flank of V. Embedded in this airstream was an area of very cold cloud, C, situated between Iceland and Northern Ireland while a small vortex of enhanced convection, L, was evident downstream near north-west Ireland. C and L moved south-eastwards at 35–40 kn, C still to the west of the Hebrides, and L over eastern Ireland by 0820 UTC (Fig. 2(b)) although L was less prominent having crossed colder land. The visible image (not shown) reveals that C was bright and lumpy, i.e. deep and convective. By 1409 UTC (Fig. 2(c)), C had developed into a comma, with its ‘tail’ — interpreted as a belt of ascending air frequently giving precipitation — extending across Ireland. Meanwhile, L had moved into

Wales and contained fresh convective cells formed topographically and by diurnal heating of the land. The curvature of the clouds still indicated the presence of a small vortex over South Wales. Both systems continued moving south-eastwards, the tail of C extending to south-west England by 1551 UTC (Fig. 2(d)). L was over the Severn Estuary having decelerated to about 20 kn and still showing signs of a vortex. The speed of the centre of C was now about 35 kn; at this velocity it would be close to south-west England by midnight, with its tail lying a little further east.

C was situated in a diffluent region just ahead of a well-defined upper trough (Fig. 3(a)) and was collocated with a large area of ascent shown in the fine-mesh

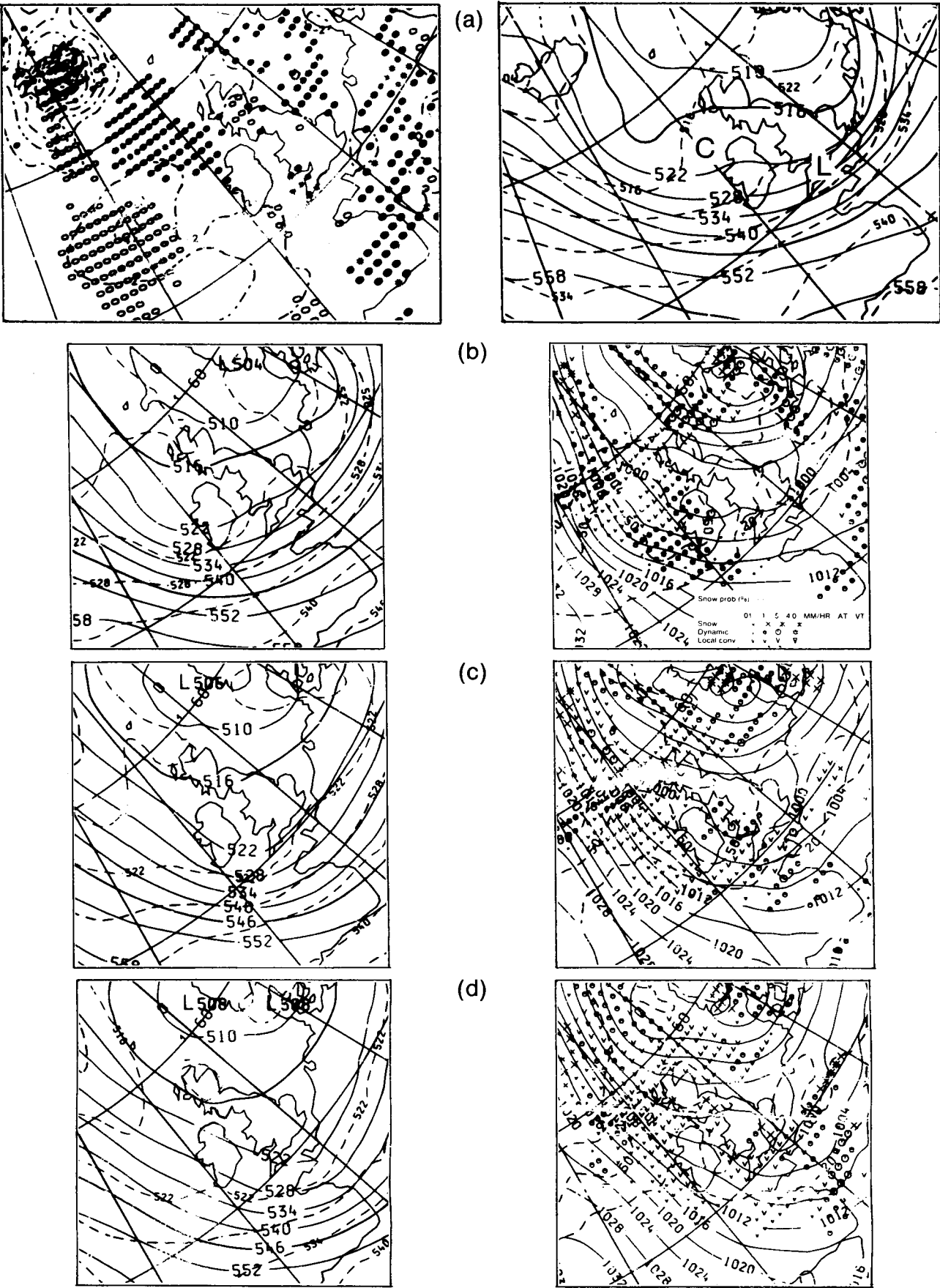


Figure 3. Fine-mesh model output on 18 March 1987 (a) analysis for 1200 UTC (open symbols — descending, closed symbols — ascending, dash-dot line — thermal advection cooling between 850 and 500 mb), C and L as in Fig. 2, (b) forecast for 1800 UTC, (c) forecast for 0001 UTC on 19 March, and (d) forecast for 0600 UTC on 19 March.

model's analysis. (It is worth noting that without satellite images, the scale and structure of C would not have been determined until it had moved into Ireland.) Another smaller region of ascent was situated over the south-west of the United Kingdom and was collocated with L. In the absence of any warm air advection, both regions of ascent resulted from advection of positive vorticity (PVA).

The fine-mesh model forecast the upper trough to move south-eastwards at about 40 kn (Figs 3(b)–3(d)) taking the surface trough and any 'dynamical' precipitation south-eastwards from Ireland across southern England to northern France during the night. Indeed, snow was forecast at two grid-points over southern England at 0600 UTC on the 19th, close to the surface trough and east of the extrapolated position of the comma system. The analysis over the British Isles for 1800 UTC shows that the centre of the circulation associated with the comma approached north-west Ireland (Fig. 4) but there was also a surface trough with significant falls of pressure ahead of it which had moved south-eastwards to central southern England and which was associated with L.

The following sections showed how the fine-mesh model's forecast of precipitation may be fine-tuned using satellite and radar images together with mesoscale model guidance so that the areas most prone to mesoscale areas of precipitation — which in this case may be persistent (because of the light upper winds) and may fall as snow — can be identified and the dynamical processes explained.

3. Mesoscale-model forecast

Fig. 5 shows the dynamic and convective precipitation predicted by the mesoscale model for 2100, 0000 and 0300 UTC using a re-run of the 1800 UTC operational run with the comma reinitialized 250 km further west, to north-west Ireland. The precipitation patterns were almost identical to the original operational run, hinting that the comma system itself was not a primary factor in the development of the snow event. At 2100 UTC, an area of rain and snow was forecast to extend from the Bristol Channel northwards through Wales, curving round towards Northern Ireland. This pattern conformed with the shape of the comma (Figs 2(c) and 2(d)) and was forecast to move south-eastwards, being a natural

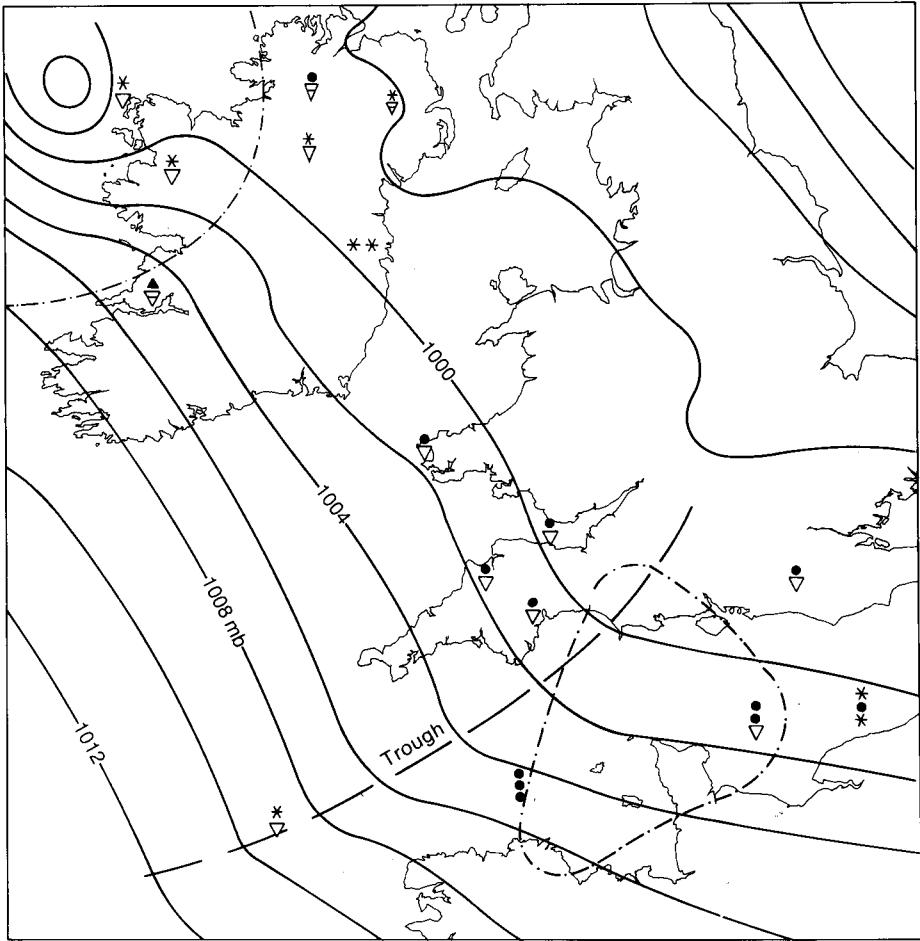


Figure 4. Mean-sea-level pressure analysis for 1800 UTC on 18 March, showing a developing trough over southern England and the circulation associated with the comma cloud approaching north-west Ireland. Places reporting significant present weather are shown, using conventional symbols. The areas enclosed by the dot-dash lines are where pressure is falling by $\geq 1 \text{ mb } 3\text{h}^{-1}$.

evolution of existing features. However, over central southern England, to the east of the comma tail, the model developed a separate area of rain and snow, perhaps related to the earlier decelerating vortex L. This precipitation was forecast to move slowly east, turning increasingly to snow (Figs 5(b) and 5(c)). Shower symbols were present within the areas of dynamic rain,

suggesting release of potential instability. Showers were also forecast, especially over the sea and the windward coasts.

To what extent did the features on the satellite and radar images support the mesoscale-model guidance in the forecast period?

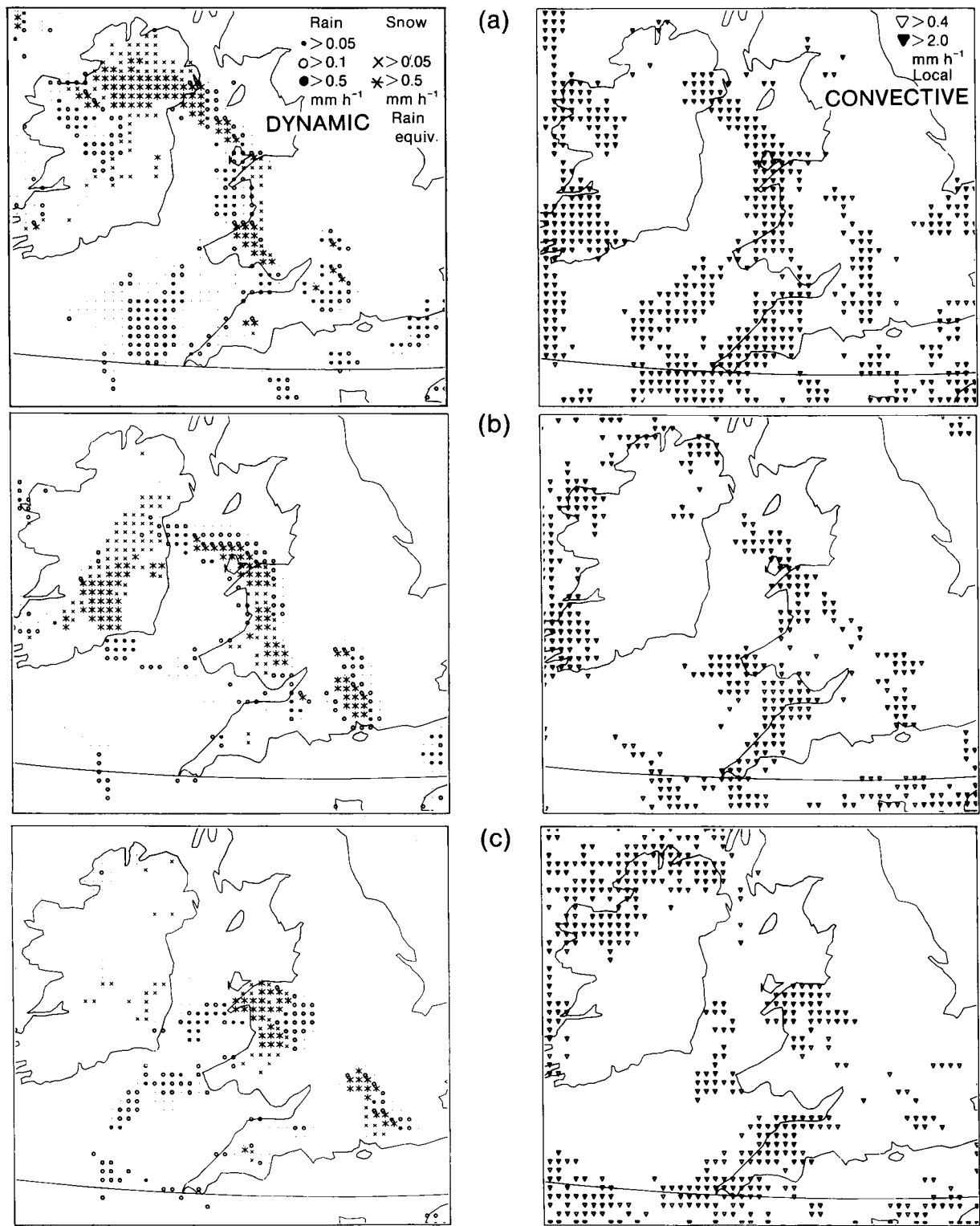


Figure 5. Mesoscale-model forecasts of precipitation, based on a data time of 1800 UTC on 18 March 1987 for (a) 2100 UTC on 18 March, (b) 0001 UTC on 19 March, and (c) 0300 UTC on 19 March. See key for explanation of symbols.

4. Comparison between mesoscale-model forecast with satellite and radar images

False colour satellite images from Meteosat were used to follow the evolution more closely near the United Kingdom during the evening of the 18th. At 1900 UTC (Fig. 6(a)) the tail of the comma cloud extended south-east from western Ireland towards South Wales, while relatively warm convective cloud tops (with a sharp northern temperature gradient) associated with L in Fig. 2 covered the southern United Kingdom. After 1900 UTC the cloud tops in the tail warmed, but a new area of cloud grew just east of the tail over central southern England (Fig. 6(b)), shown more clearly by observations from the UK weather radar network (Figs 7(a) and 7(b)). Precipitation from the tail fell in a band over south-west England and west Wales while the new cloud area was associated with another band of precipitation orientated in the same direction to the east. This pattern supported the mesoscale-model forecast (Fig. 5(a)) except that the model developed the new band a little too far east.

By 0130 UTC on 19 March (Fig. 6(c)) the depth and area of cloud over central southern England had grown considerably and produced the heaviest precipitation (Fig. 7(c)) which fell on or just to the west of the surface trough shown on Fig. 4. Other features of interest were the sharp south-western edge of the precipitation band (not an idiosyncrasy of the radar data) and the vortex-

shaped echo over south-west England associated with the south-eastward moving comma. The mesoscale-model forecast over central southern England for midnight (Fig. 5(b)) compared favourably with the observed pattern except that the forecast precipitation band was orientated more north-south. The band lasted until early on the 19th (Figs 6(d) and 7(d)) as predicted by the mesoscale model.

Examination of the higher resolution radar data from Chenies, to the north-west of London, shows that the band of precipitation consisted of heavy showers which were effectively stationary for periods exceeding one hour, accounting for considerable accumulation of snow in some parts. Fig. 8 shows the hourly observations from Boscombe Down and Southampton Weather Centre, both situated within the band, where continuous snow, often moderate or heavy, was reported between about 0000 and 0500 UTC. Further details about the distribution of the snowfall are given in Pike (1989).

The mesoscale model has captured the development and persistence of the band sufficiently well for a conceptual model of the principal airflows to be deduced from appropriate diagnostics.

5. Conceptual model

Several factors, combining to produce the snow event, now assist in the construction of a conceptual model. They fall into 'factual' and 'conjectural' categories.

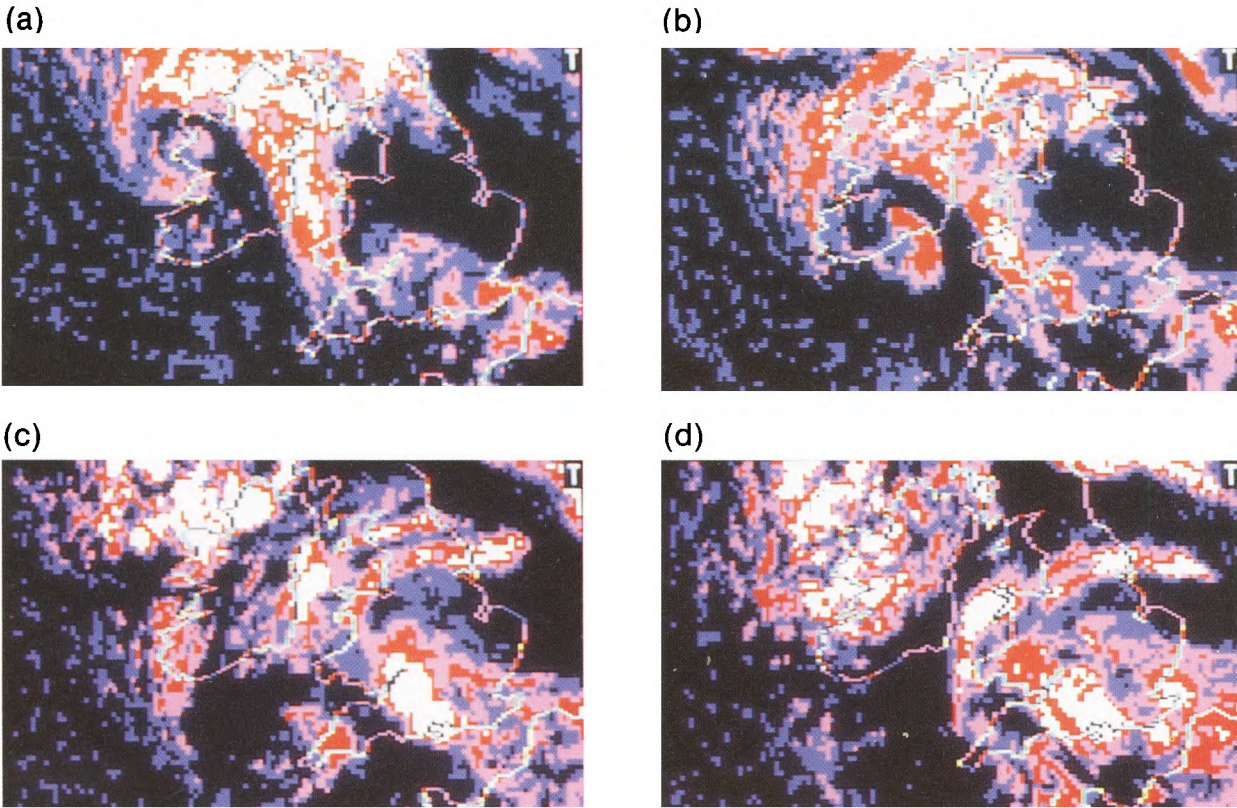


Figure 6. False colour Meteosat infra-red images showing the south-eastward movement and warming of the cloud associated with the comma, centred initially west of Ireland, and the growth of the cloud east of the comma tail over central southern England for (a) 1900 UTC on 18 March 1987, (b) 2200 UTC on 18 March, (c) 0130 UTC on 19 March, and (d) 0400 UTC 19 March. White denotes coldest tops ($< -40^{\circ}\text{C}$). The other colours are interpreted as follows: dark red, $< -30^{\circ}\text{C}$; pink, $< -20^{\circ}\text{C}$; dark blue, $< -10^{\circ}\text{C}$; black, $> -10^{\circ}\text{C}$.

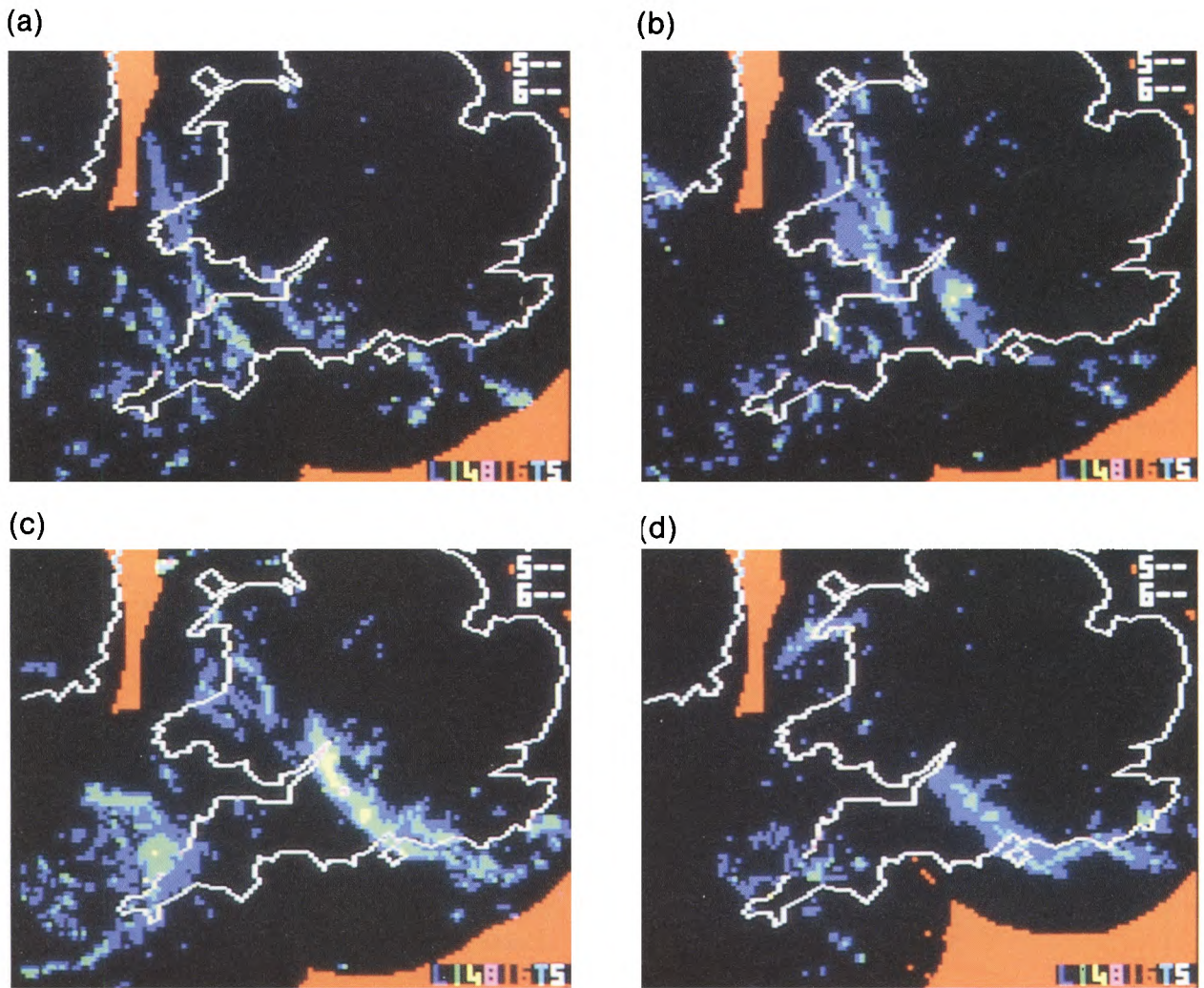


Figure 7. Precipitation shown by the UK weather radar network at (a) 1900 UTC on 18 March, (b) 2200 UTC on 18 March, (c) 0100 UTC on 19 March, and (d) 0400 UTC on 19 March. Equivalent rainfall rates are as follows: dark blue, $< 1 \text{ mm h}^{-1}$; green, $1\text{--}4 \text{ mm h}^{-1}$; yellow, $> 4 \text{ mm h}^{-1}$.

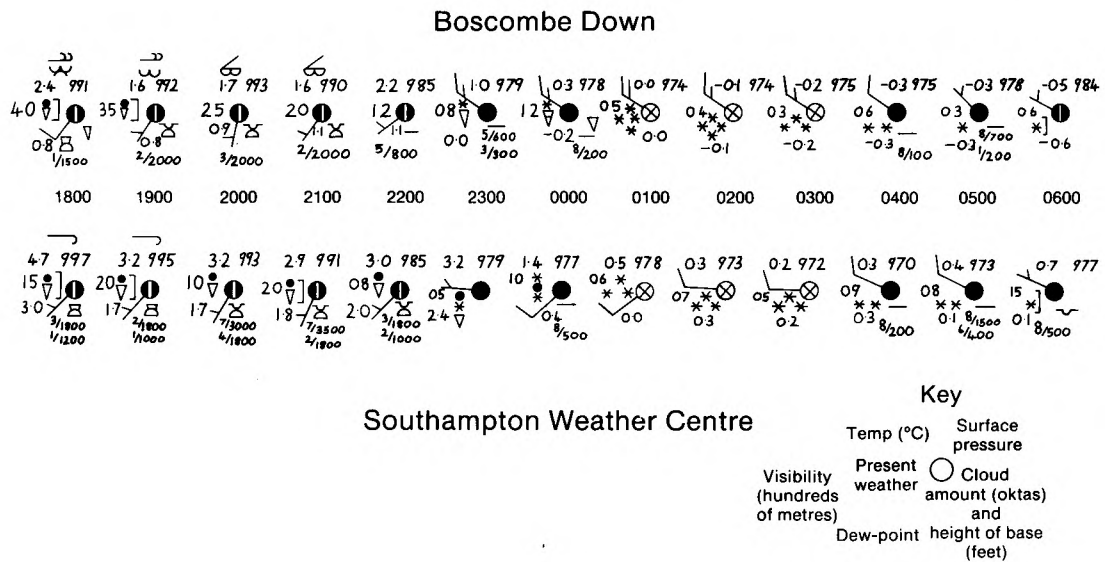


Figure 8. Hourly (UTC) surface weather observations, using conventional symbols, during night of 18/19 March 1987 at Boscombe Down and Southampton Weather Centre, whose locations are shown in Fig. 1. See key for explanation.

5.1 Factual information

- (a) The limits of the snow band were well defined from the imagery and the observational network (see Figs 1 and 7).
- (b) The western edge was sharp, suggesting significant undercutting of cold air from the west.
- (c) Strong westerly winds on the southern flank of the comma system extended across the snow area during the event and moved away southwards, as shown by the sequence of observations at Boscombe Down in Fig. 8. (Southampton Weather Centre is more sheltered.)
- (d) An upper trough crossed the south-west peninsula at about 40 kn (Fig. 9) and a little slower over the snow area. It was ill-defined further north. Its axis lay over southern England at 0400 UTC, when the snow was dying out in the north-west of the band, and from Cherbourg to Brest at 0600 UTC, when the snow had ceased over central southern England (Fig. 8).

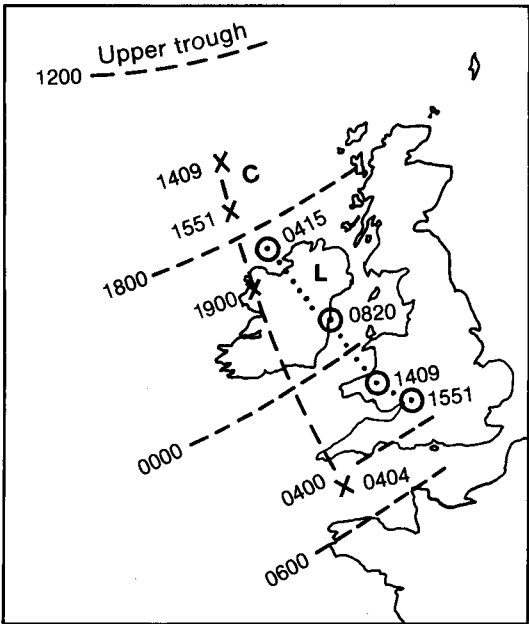


Figure 9. Tracks of cloud systems C and L (shown in Fig. 2) and upper trough axis, from 1200 UTC on 18 March to 0600 UTC on 19 March 1987.

- (e) Winds below 600 mb at Crawley became easterly at midnight on the 19th (Fig. 10). There was no easterly component before or after this time. The easterly wind was supported by wind profiles derived from the mesoscale model from spot locations within and just east of the snow area.
- (f) A cross-section from south-west England to the Thames Estuary (Fig. 11(a)), derived from the mesoscale-model forecast, reveals a tongue of high wet-bulb potential temperature (WBPT) over the eastern portion at about 600 m above the surface. The dynamical precipitation shown in Fig. 5 was forecast to be close to the western edge of this tongue.

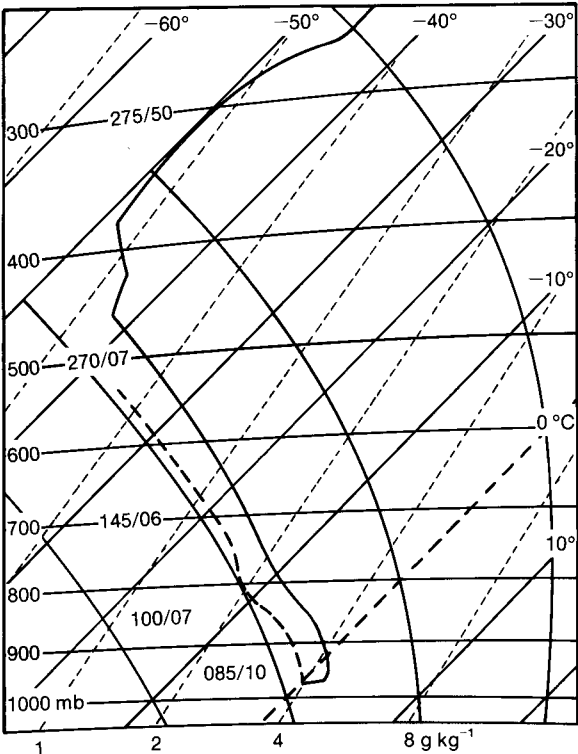


Figure 10. Radiosonde sounding at Crawley (see Fig. 1) at 0001 UTC on 19 March 1987.

- (g) The ascent at Crawley for midnight on 19 March (Fig. 10) showed potential instability. Since the higher WBPT layer was centred at 600 m, only about 200 m (20 mb) of lifting would have sufficed to release this instability.
- (h) Fig. 12 shows an isentropic analysis of air on the 7 °C surface (i.e. representing the warm tongue) relative to a 'system' speed of 300° 12 kn. This system speed was chosen from the model's forecast of the 700 mb wind on the western edge of the area of high WBPT over southern England during the early stages of the precipitation event. This corresponds to the velocity of the precipitation band. The relative flow chart for 2100 UTC (Fig. 12(a)) shows a circulation centre and zone of convergence just east of the Bristol Channel. To the east, the weak ascent is probably sufficient (see (g)) to release the potential instability. Later on, at midnight and 0300 UTC (Figs 12(b) and 12(c)), there is more rapid ascent up the steepest slope of the potential temperature surfaces; it is associated with the main area of precipitation in Figs 5(b) and 5(c).

5.2 Conjectural factors

- (a) A 'cold dome' of WBPT, where the precipitation fell (see Fig. 11(b)), was probably due to heat being extracted from the air by melting snow.
- (b) A cross-section of the winds (Fig. 13) at 2100 and midnight UTC shows the westerly winds advecting air of low WBPT towards the slower-moving warm tongue and creating a convergence zone over central

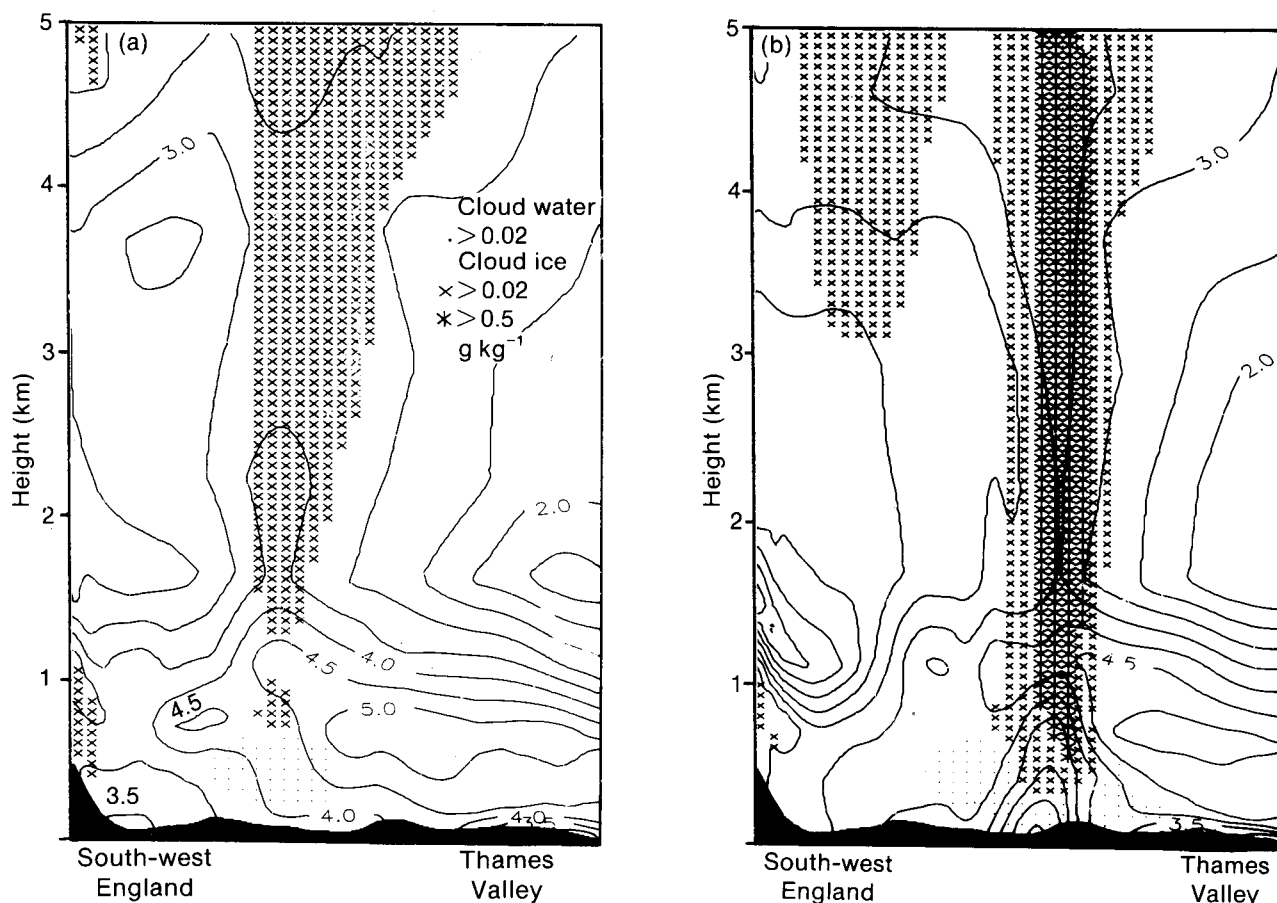


Figure 11. Cross-section of wet-bulb potential temperature ($^{\circ}\text{C}$) and cloud at (a) 2100 UTC on 18 March, and (b) 0001 UTC on 19 March 1987 (from the mesoscale-model forecast at 1800 UTC). Note the warm tongue of air in the bottom right-hand corner and the cold dome becoming established near the ground at 0001 UTC due probably to latent heat being extracted from the air as the snow melts. Symbols are explained in the key.

southern England. Any undercutting of the potentially unstable flow by the cooler westerlies on the southern side of the comma system may have produced enough lifting to release the instability, the effect becoming self-perpetuating due to the generation of the 'cold dome', thus contributing towards the persistence of the snowfall.

(c) Although the air mass was equally inherently unstable over much of southern England and the layer of high WBPT extended over the whole of south-east England, it is significant that the area covered by the snow was very limited. The main factors occurring over the snow area and not further east were the undercutting westerlies and probably a PVA maximum ahead of the upper trough. Furthermore, the snow ceased when the south-eastward moving upper trough axis crossed the area and, almost coincidentally, the undercutting westerlies were transferred to the south, as the comma system moved away.

Using the imagery from Meteosat and the radar network and the isentropic analysis from the mesoscale model, a conceptual model has been constructed (Fig. 14).

Fig. 14(a) shows principal airflows at 2200 UTC. With the southern end of the old comma tail then decaying, the westerlies near the surface extended into central southern England, undercutting a new warm conveyor belt formed as the easterly flow rose along the inclined 7°C potential temperature surface (Fig. 12). By 0130 UTC (Fig. 14(b)), the old comma tail had decayed over much of England and Wales, but the new ascending warm conveyor belt overriding the colder air was now well established over central southern England.

These ideas are supported by the features on the NOAA-9 satellite picture for 0404 UTC on 19 March (Fig. 15). It shows the old comma between south-west England and Brest and the ascending (cloudy) warm conveyor belt over central southern England, with its well-marked western edge.

The ascending warm conveyor belt is well analysed by the fine-mesh model at midnight on the 19th showing the tongue of high 850 mb WBPT extending from northern France into southern England (Fig. 16(a)) and air ascending within it (Fig. 16(b)) containing low and medium cloud (Fig. 16(c)). These patterns suggest that the warm conveyor belt constituted part of a larger scale dynamical circulation even though a mesoscale explan-

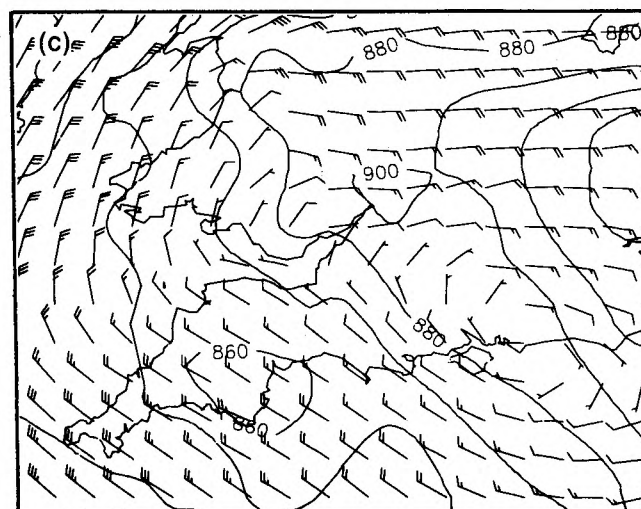
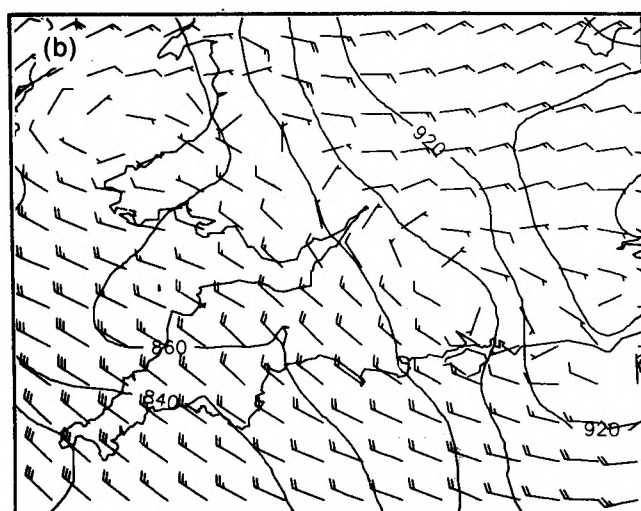
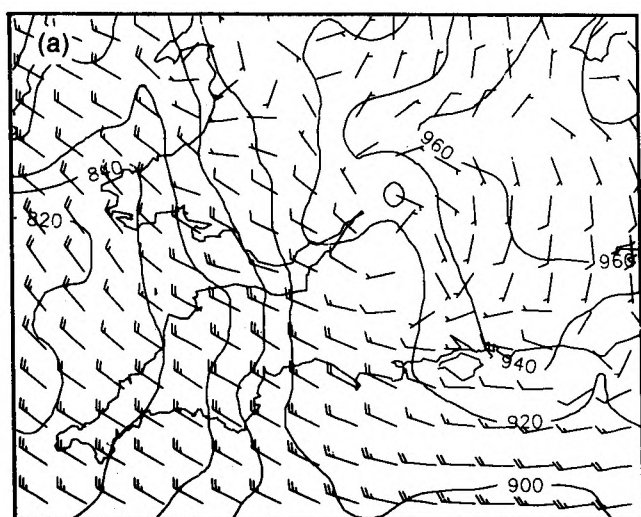


Figure 12. Relative-flow, isentropic analysis (from the mesoscale-model forecasts) along the 7 °C potential temperature surface (mb) at (a) 2100 UTC on 18 March 1987, (b) 0001 UTC on 19 March 1987, and (c) 0300 UTC on 19 March 1987. Compare with the precipitation forecast at the same times shown in Fig. 5.

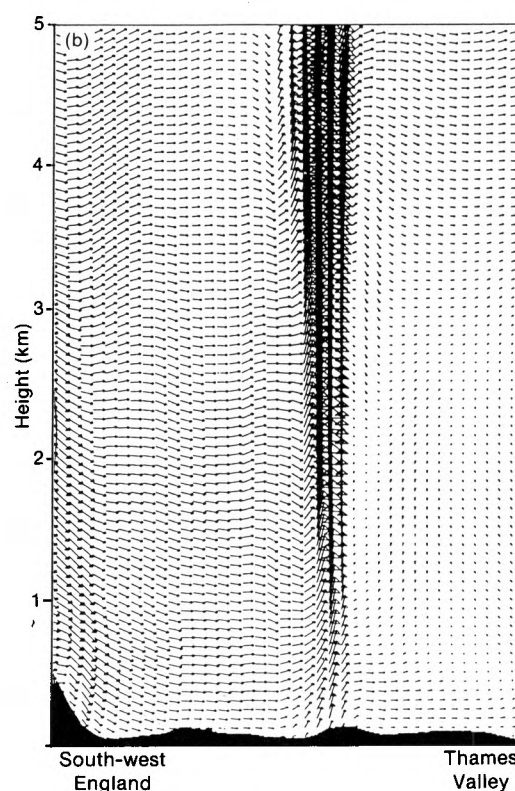
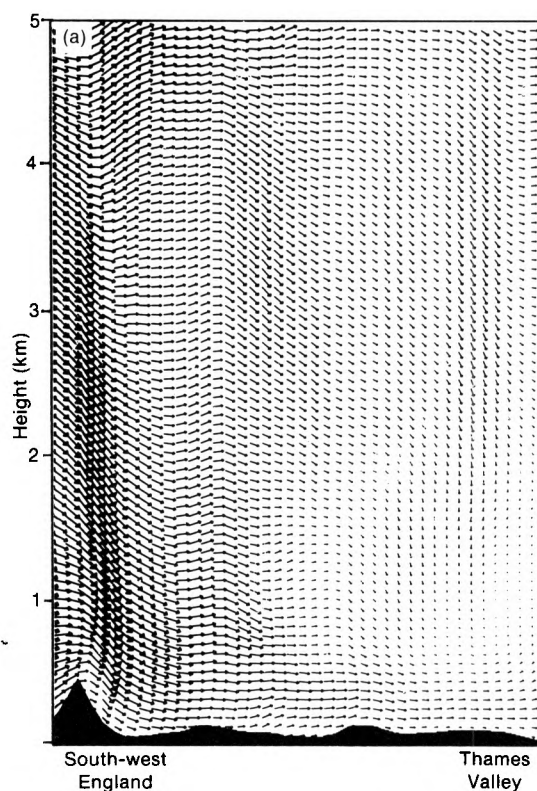


Figure 13. Cross-section of winds from the mesoscale-model forecast along the same line as shown in Fig. 11 at (a) 2100 UTC on 18 March 1987, and (b) 0001 UTC on 19 March 1987.

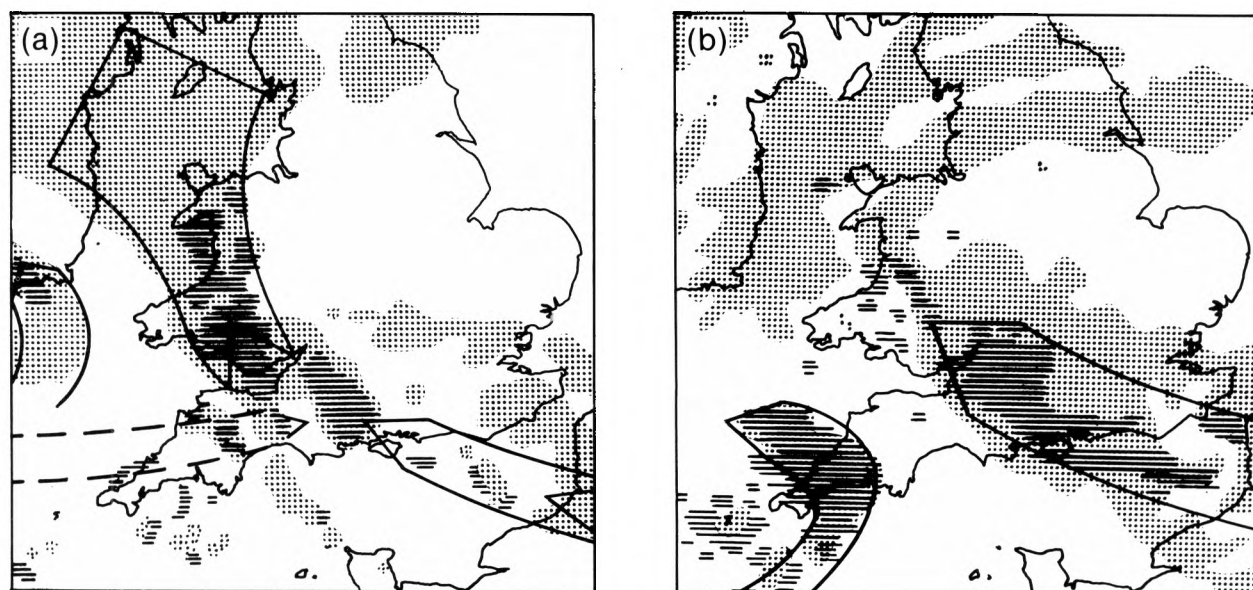
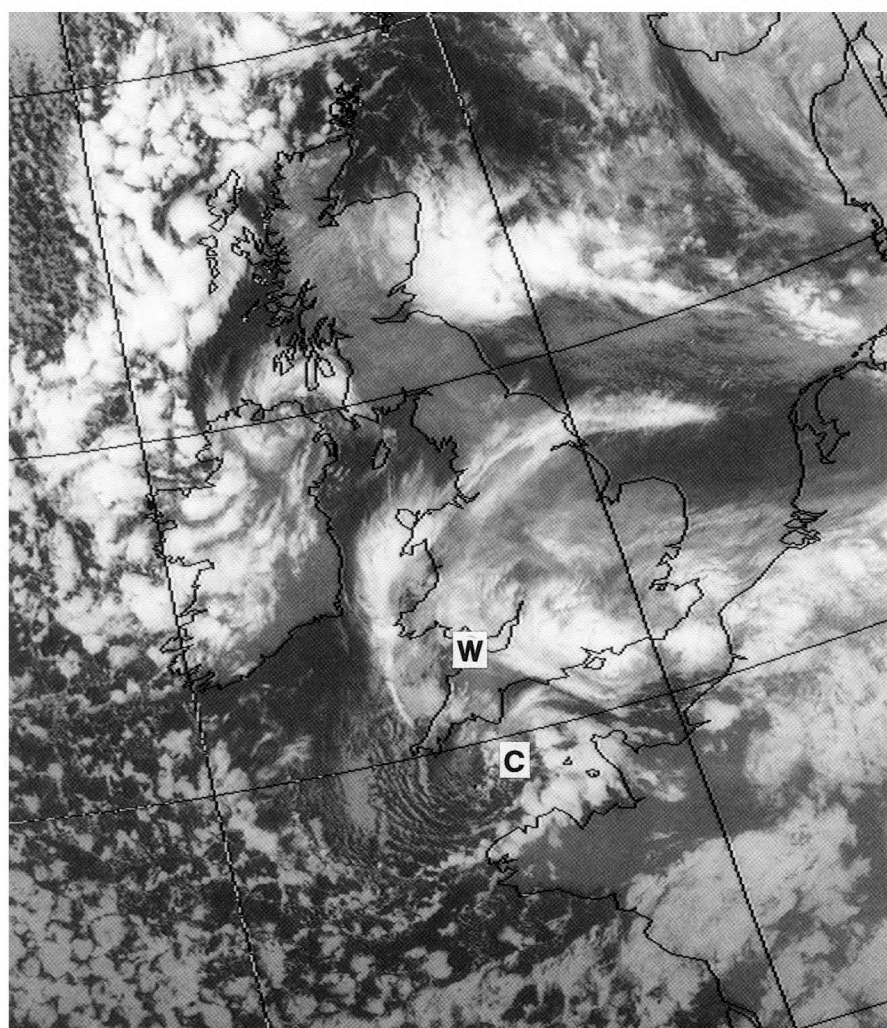


Figure 14. Conceptual model of principal airflows at (a) 2200 UTC on 18 March 1987, and (b) 0130 UTC on 19 March 1987. Cloud tops $< -20^{\circ}\text{C}$ stippled, precipitation, as detected by the radar network, striated.



Photograph by courtesy of University of Dundee

Figure 15. NOAA-9 satellite infra-red image at 0404 UTC on 19 March 1987, showing the comma cloud, C, between south-west England and Brest, and the sharp western edge, W, of the cloud over central southern England.

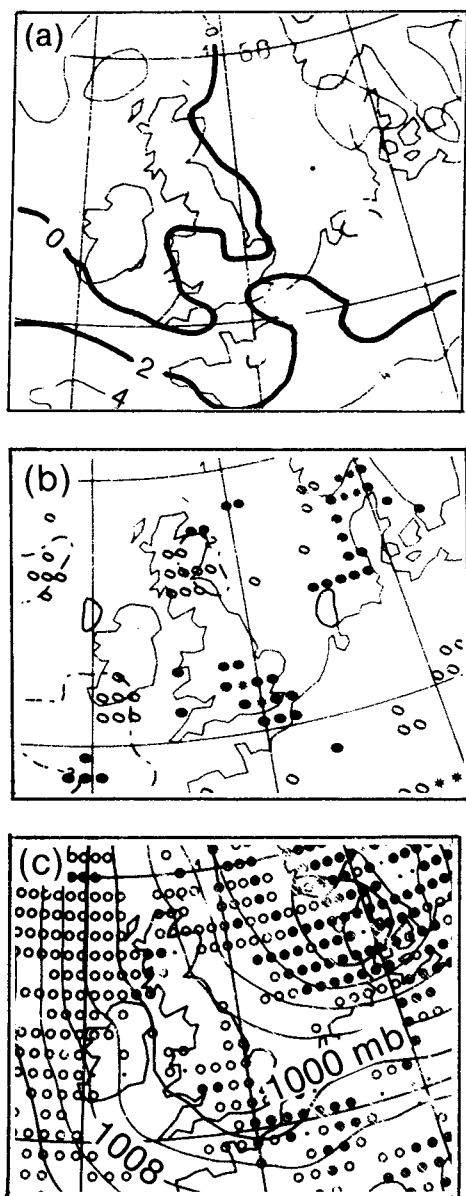


Figure 16. Fine-mesh model analysis at 0001 UTC on 19 March 1987 of (a) 850 mb wet-bulb potential temperature ($^{\circ}\text{C}$), (b) vertical velocity and thermal advection (symbols as in Fig. 3(a)), and (c) medium cloud (open circles), low cloud (dots) and mean-sea-level pressure at 4 mb intervals.

ation might seem attractive on the basis of the area and duration of precipitation.

6. Conclusion

This case shows how forecasts from the mesoscale model and frequent monitoring of the satellite and radar images can enable the forecaster to justify playing down the likely impact of an initially conspicuous feature (the comma) in favour of a probable new important mesoscale development (i.e. the band of heavy snow) that does not conform with conventional ideas (i.e. the development of precipitation along an existing comma tail). It also showed how the diagnostics from the mesoscale model, supported by those from the fine-mesh model, can enhance the understanding of the main physical and dynamical processes at work.

The eventual arrival of faster Information Technology Systems such as the Outstation Display System (ODS), AUTOSAT 2 and the weather information system and network (WIS/WIN) will provide outstation forecasters with more imagery and a wider range of model diagnostics such as isentropic analysis (related to the speed of a specific system) to help with their diagnosis and prognosis.

Acknowledgements

The authors wish to thank M.V. Young for helpful discussions and L. Rowley for processing the model products.

Reference

- Pike, W.S., 1989: The heavy localised snowfall over central southern England overnight 18th–19th March 1987. *J Meteorol UK*, **14**, 76–82.

Correction

Meteorological Magazine, December 1989, p. 265, Summary. Mr R.A. Murray has pointed out that the winter of 1988/89 was not particularly dry. The author's intention was to stress the exceptional combination of mildness and dryness.

Sixty-four years of regular ozone measurements

E.L. Simmons

23, The Brackens, Crowthorne, Berkshire RG11 6TB

Summary

A brief account is given of the development of the Dobson ozone spectrophotometer which has been used for over 60 years to make world-wide measurements of atmospheric ozone amounts. These observations define the normal behaviour of ozone against which recent reductions – the Antarctic ozone hole – can be compared.

1. Introduction

Regular daily ozone measurements have been made since the year 1926, but while one instrument type has dominated the measurements for nearly the whole of this period, the reasons for making the measurements have changed over the years. Researchers today concerned with the long-term changes in the atmospheric ozone column, would be very interested in the whole of this extensive data set, but nobody at the time imagined our present day interests, and only the data from Arosa in Switzerland have been retained and corrected to form as nearly as possible a consistent data set. It must be recognized, though, that early data are likely to contain systematic errors which are difficult to estimate.

In 1879 Cornu suggested that the sharp ultraviolet cut-off in the solar spectrum might be due to ozone, and in the following year Hartley measured the absorption band which bears his name. Visible light in the incoming solar spectrum is much more intense than ultraviolet, so scattered light is always a problem in measuring ozone, but in 1920 Fabry and Buisson used a double photographic spectrograph and obtained a value 0.3 cm of pure ozone at standard temperature and pressure (i.e. 300 milli atm. cm) for the equivalent vertical ozone column. This is the sort of value to be expected in early summer when they made their measurements.

In 1921 Lindemann (later Lord Cherwell) suggested a way of determining the density of the upper atmosphere from the visible brightness, speed and height of meteor trails. The results showed densities orders of magnitude greater than expected in an isothermal atmosphere at the temperatures recently measured in the lower stratosphere. Lindemann saw that absorption of solar radiation by ozone could account for the rise in temperature with height he had to postulate. It was also known that the lower stratosphere was colder over a surface anticyclone than over a surface 'low'. This led to the speculation that these surface features might be caused by variations in the ozone column. This was the motivation for the first regular ozone measurements (Dobson 1966).

2. Theory of ozone-column measurements

The basic theory of differential absorption is the same for all ozone-column measurements. It is reproduced

here with specific reference to the notation used for the Dobson spectrophotometer so that the significance of improvements can be seen. The slit widths used by Dobson were such that all light within the pass-band can be assumed to have the same absorption coefficient, so Beer's law can be used in the form

$$\log_{10} (I_{\lambda}/I_{\lambda'}) = \log_{10} (I_{0\lambda}/I_{0\lambda'}) - \mu x(\alpha - \alpha') - m(\beta - \beta') - \sec Z(\delta - \delta')$$

where x is the ozone-column amount; I_{λ} , $I_{\lambda'}$ are the measured intensities, and $I_{0\lambda}$, $I_{0\lambda'}$ the intensities outside the atmosphere; α , α' the absorption coefficients; β , β' the Rayleigh scattering coefficients; δ , δ' the aerosol scattering functions, all at wavelengths λ , λ' ; μ is the secant of the zenith solar angle at the height of the ozone layer, m the Bemporad air-mass function and Z the solar zenith angle at the surface (where most of the aerosol scattering is assumed to arise). The last three parameters can be calculated from the station coordinates and the time and date. Putting

$$A = (\alpha - \alpha'), B = (\beta - \beta'), N = -\log_{10} (I_{\lambda}/I_{\lambda'}), \text{ and}$$

$$N_0 = -\log_{10} (I_{0\lambda}/I_{0\lambda'}),$$

$$\text{then } x = \{N - N_0 - Bm - (\delta - \delta') \sec Z\} / \mu A. \quad (1)$$

Equation (1) can be rearranged to be

$$N/\mu - Bm/\mu = Ax + N_0/\mu$$

so that N_0 can be evaluated by means of a Langley plot, i.e. a plot of $N/\mu - Bm/\mu$ against $1/\mu$ under conditions where x can be assumed constant and the aerosol scattering negligible.

If two wavelengths designated A and D are used, equation (1) becomes

$$x = (N_A - N_{0A} - N_D + N_{0D}) / \mu(A_A - A_D) - (B_A - B_D)m / \mu(A_A - A_D).$$

With the wavelengths designated A and D by Dobson, the second term amounts to 9 milli atm. cm for a station at mean sea level. The B -terms vary as λ^{-4} , the δ -terms vary significantly less rapidly, and except in unusual conditions can safely be assumed negligible.

3. Apparatus developed by Dobson

G.M.B. Dobson designed the first ozone spectrograph for routine use. To keep the apparatus simple he used a single Féry prism which combines a prism and a concave mirror in a single piece of quartz. Thus there is only one air-dielectric interface, though it is traversed twice, and this minimizes the amount of scattered light. Further reduction in visible light was achieved by a filter comprising a fused silica cell filled with chlorine, bromine and (it transpired) chlorine bromide. After some time spent refining the process of developing the photographic plates and measuring their density, reproducible results were obtained. It was found that there were significant day-to-day variations correlated with surface pressure variations and (surprisingly at the time) an annual variation with a maximum in spring.

In 1926, five more photographic spectrographs were made by Dobson and sent to Valentia (Ireland), Lerwick (Shetland), Arosa (Switzerland), Abiska (Sweden) and

Lindenberg (Germany). The plates were sent back to Oxford for processing. If any practical use was going to be made of ozone measurements for weather forecasting, the delay caused by posting and batch processing the plates was unacceptable. The hope that ozone measurements could help weather forecasts took a long time to die, and total ozone column measurements were made at Lerwick and some mainland stations during the 1939–45 war with the results radioed to Oxford in cipher. This was the incentive for the design of the first photoelectric spectrophotometer.

Dobson built his first photo-electric spectrophotometer in 1926. It was in regular use until his death in 1976, and its optical design was reproduced in the first commercial instrument designated No. 2 built by R. & J. Beck in 1930. This instrument, shown in Fig. 1, was loaned to the Meteorological Office around 1960 and later donated by Professor Dobson's widow. It is still in daily use, formerly at the Office's experimental site at Beaufort Park, near Bracknell, and since autumn 1989 at Camborne, where it is less subject to disturbance by atmospheric pollution. It is a double spectrophotometer with quartz prisms as the dispersing element (Fig. 2). Light passing through the two wavelength selecting slits S_2 and S_3 is recombined by the second optical train

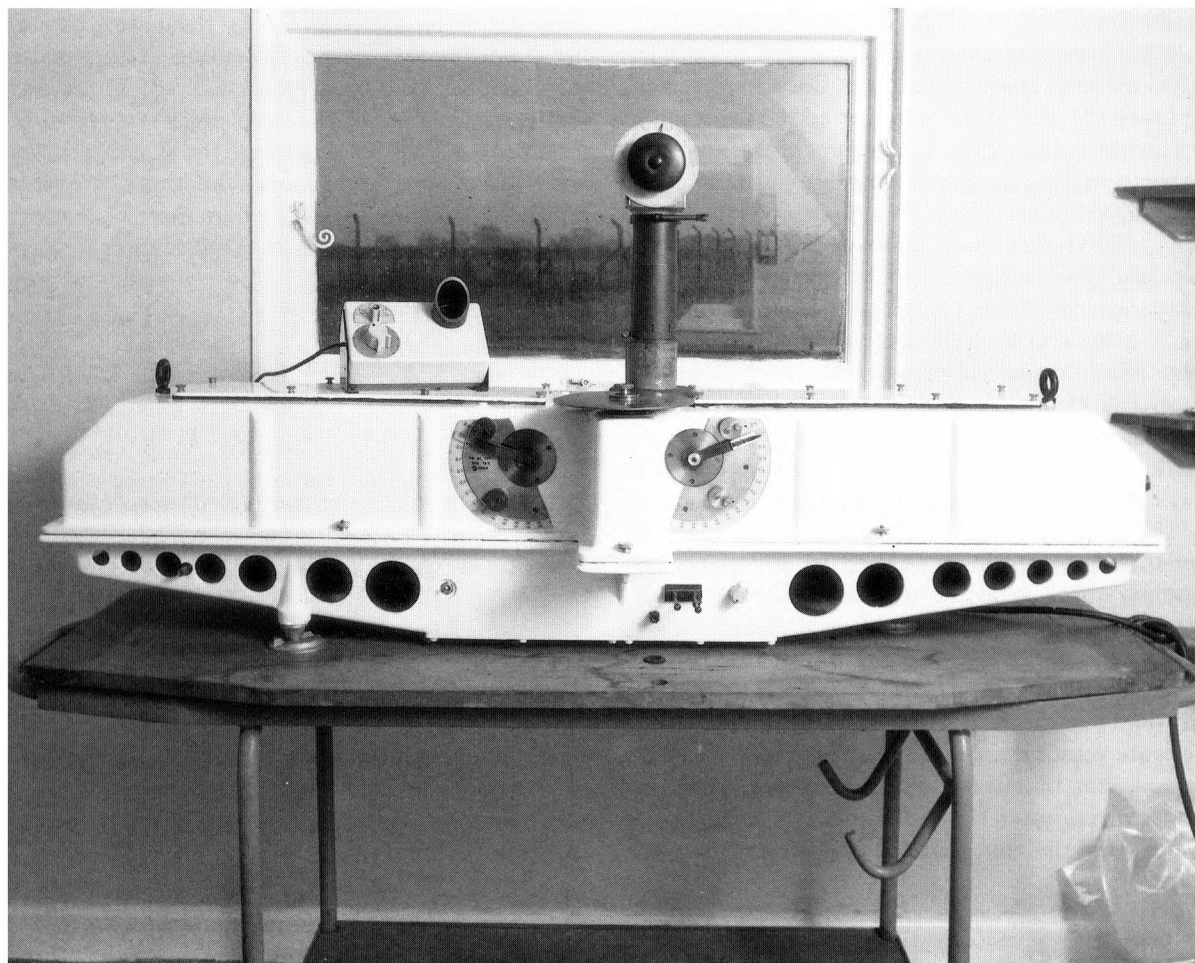


Figure 1. View of the Dobson ozone spectrophotometer.

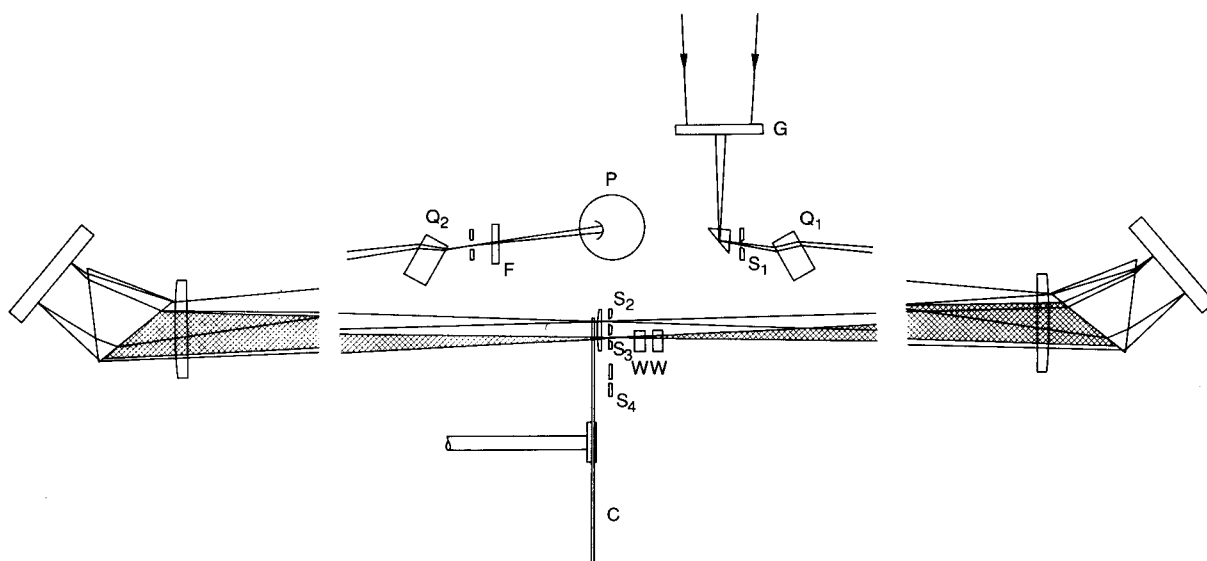


Figure 2. Optical system of the Dobson ozone spectrophotometer. C is the rotating chopper disc which exposes S_2 and S_3 alternately; F is the glass ultraviolet filter; G is the ground quartz plate used for normal direct Sun measurements; P is the photomultiplier; Q_1 and Q_2 are the quartz plates which are tilted to select the required wavelength pairs; S_1 is the input slit, which is curved concave upwards; S_2 and S_3 are the wavelength determining slits; S_4 is now only used in conjunction with an auxiliary lamp during wedge calibration; Ws are the two optical wedges.

which is a mirror image of the first. Light at wavelength λ' passing through S_3 is attenuated by a pair of optical wedges moving in opposition and actuated by a dial. A rotating disc chopper allows light from first one slit then the other to reach the detector. The operator rotates the dial until the two detector currents are equal, when there is no alternating-current component in the amplifier output, and notes the dial reading R . The dial needs to be calibrated to relate the reading to the value of N in the above theory. For the accuracy demanded today, the wedges need to be re-calibrated about every 4 years.

The first detectors used were sodium photocells. It was not until 1945 that they were replaced by photomultipliers, and this made it possible to use a wider range of wavelengths. Dobson (1957) designated four wavelength pairs and it was soon appreciated that using two pairs had the advantage noted in the theory above. Earlier observations were derived from measurements made on the C-wavelength pair only, and are subject to greater errors due to aerosol scattering. If the input slit is illuminated by a source with a continuous spectrum the instrument will assign to the source a certain N -value for each wavelength. This value drifts slowly and it has become customary to perform standard lamp-tests every month and to adjust the R - N tables to keep the lamp N -value constant. A second lamp is kept at each station which is used once a year. Earlier filament lamps lacked stability and were prone to premature failure. Quartz-halogen lamps introduced in the mid 1960s were a great improvement. A system using separate current and potential leads and a stabilized direct-current supply introduced by Dr W.D. Komhyr of NOAA was a further improvement. Used like this the two lamps normally agree well,

implying it is the instrument which drifts. If standard lamps are exchanged between instruments, this might seem to be a method for transferring the additive constant N_0 . In practice, making observations of the Sun with two instruments side-by-side yields results which differ slightly from those obtained by exchanging lamps, and for results of the highest accuracy there is no alternative to side-by-side comparison.

Dobson found conditions at Oxford unsatisfactory for producing Langley plots to determine N_0 . He took his instrument to Arosa on a number of occasions, and after the international comparison of Dobson instruments at Belsk in 1974 it was resolved that the instrument No. 83 which had been calibrated at Mauna Loa (Hawaii) under conditions of low turbidity and small ozone variability should become the world standard. The calibration of most instruments is now traceable directly or indirectly to this instrument.

Dobson received a grant of £50 from the Royal Society to build No. 1, the instrument he himself made. R. & J. Beck charged £500 for No. 2, and a batch of instruments, made for the International Geophysical Year in 1957, were offered at a special price of £385. A recent batch of Dobson instruments are believed to have cost in the region of £35 000 each. This alone provides a strong incentive to find an alternative.

4. Other instruments

The USSR has made extensive use of filter instruments, the M83 patented in 1964 and the later improvement, the M124 patented in 1981. These have very much wider wavelength acceptance and therefore suffer from progressive hardening of the radiation as the ozone amount and/or path length increase. They also use only

one wavelength pair, and cannot secure the same freedom from errors caused by turbidity which can be obtained by using two wavelength pairs. An instrument based on narrow-band interference filters (each filter comprising two filters in cascade) was described by Basher and Matthews (1977), but suffered from long-term drift of the filters. The remaining contender is the Brewer instrument (Brewer 1973). This is a single-grating instrument which depends on recent advances in grating manufacturing techniques, together with absorption filters to remove long-wavelength radiation, to achieve an acceptable freedom from scattered light. It has five wavelength-selecting slits which are exposed in turn by a rotating chopper. One wavelength is chosen for the measurement of sulphur dioxide, and this makes it possible to correct the ozone readings on the occasions when this gas has accumulated under an inversion. The photomultiplier is used in a photon counting mode, so that after a common amplifier and discriminator the pulses are gated into five separate counters. There are thus no optical wedges, but a correction is needed at the higher count-rates for the finite dead-time of the counters. The digital form of the output lends itself readily to interfacing with a microcomputer which can be programmed to print out the ozone values directly. It

is smaller, lighter and less expensive than the Dobson instrument, but there were a number of problems with the earlier manufactured versions, and it is possible that it is these which have led to a reluctance to accept it as the internationally recognized standard.

5. The changing interest in ozone measurements

The motivation for early measurements lay in the relationship between ozone production and stratospheric circulation. Ozone was observed to have an annual variation with a maximum amount in spring and a minimum in autumn, as shown in the record for Bracknell for the period 1969–85 (see Fig. 3). Following the work of Götz (1953) it was possible to obtain vertical profiles of ozone from measurements with an ozone spectrophotometer directed at the clear zenith sky, extending through sunrise or sunset. These vertical profiles were obtained in much greater detail when Brewer invented the first chemical ozone sondes (Brewer and Milford 1960). Chapman (1930) had given a theory of the photochemical production of ozone in a pure oxygen/nitrogen atmosphere, which for a long time seemed adequate, and the picture that ozone is generated at around the 10 mb level and transported to

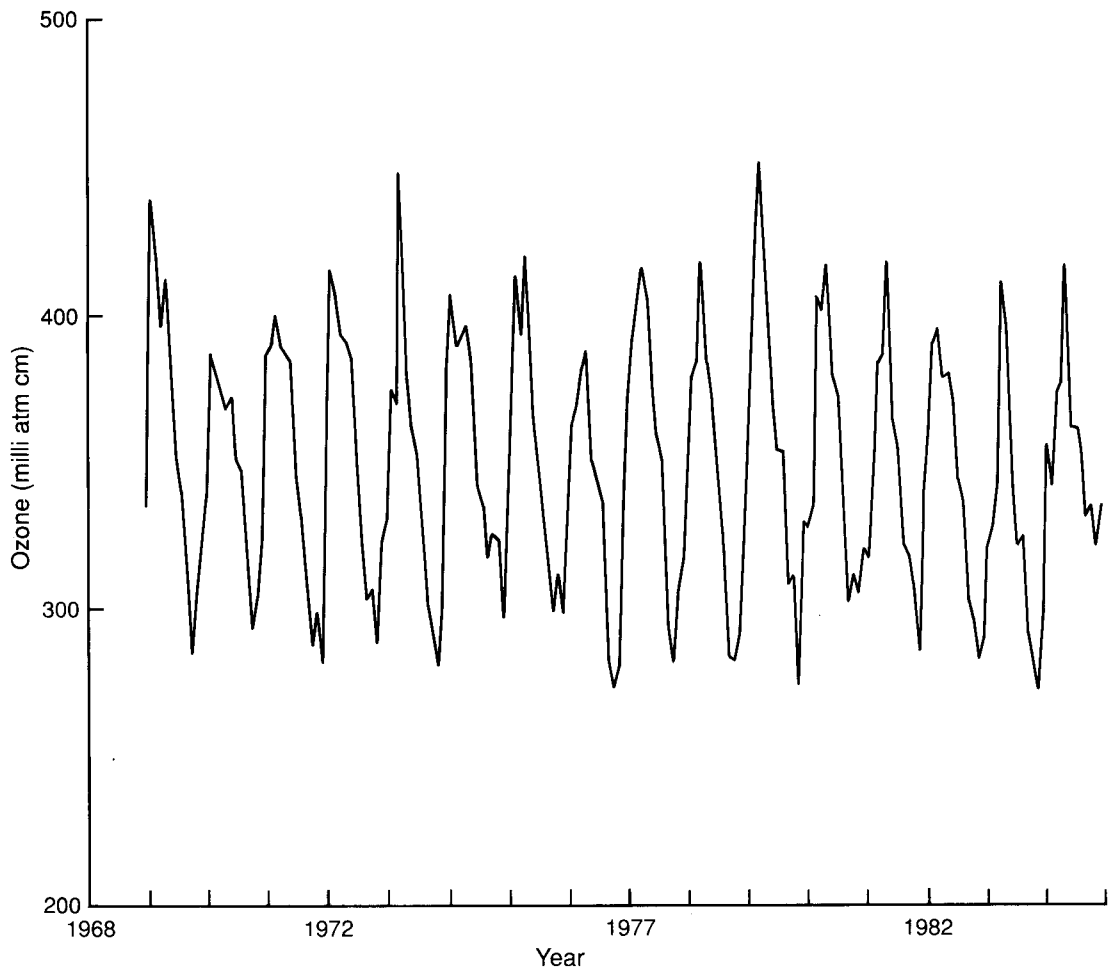


Figure 3. Monthly mean ozone column for Bracknell showing the annual cycle with a marked interannual variability.

lower levels and higher latitudes almost as an inert tracer is still valid, but in the late 1960s it began to be suspected that there were additional photochemical reactions at work in the lower stratosphere resulting in a destruction of ozone at rates greater than could be explained by the Chapman theory. Destruction by odd nitrogen species (NO and NO₂) odd hydrogen (OH and HO₂) and odd chlorine (Cl and ClO) were recognized as being important, and it was seen that the transport of chlorofluorocarbon species into the stratosphere would represent a threat to the ozone layer, which was now seen to be important in shielding the surface from short-wavelength ultraviolet radiation.

Attempts to confirm the importance of odd nitrogen species were made using calculations of the deposition of odd nitrogen in the stratosphere by nuclear weapon testing (Goldsmith *et al.* 1973), solar proton events, and the more extended deposition of oxides of nitrogen produced by the action of energetic particles in the upper atmosphere during the 11-year sunspot cycle. All these involved statistical analysis of as many observations as possible on the global scale. None proved really conclusive.

Detection of the effect of a slow build up of chlorine was expected to be even more difficult, even though statistical analysis of the total ozone column records suggested that it should be possible to detect a rate of change of about 1% per decade in a decade. It was expected that if the effect of ozone destruction were seen anywhere it would be in tropical latitudes, where insolation is greater and ozone variability less, and at high altitudes around 35–40 km. It was therefore a

complete surprise that the first indication of a significant destruction of ozone by chlorine was seen in the records of one station, Halley Bay in Antarctica. Subsequent intensive studies showed that the ozone destruction was almost total in the lower stratosphere and that it was associated with the almost total isolation of the air in the southern polar vortex and the very low temperatures existing there at the end of the polar night.

The conditions prevailing in Antarctica in the Austral spring are not to be found elsewhere, but they illustrate the fact that there may yet be processes about which we are not yet aware and there is no substitute for continued monitoring of the total atmospheric ozone column with the greatest accuracy that can be achieved.

References

- Basher, R.E. and Matthews, W.A., 1977: Problems in the use of interference filters for the spectrophotometric measurement of atmospheric ozone. *J Appl Meteorol*, **16**, 795–802.
- Brewer, A.W., 1973: A replacement for the Dobson spectrophotometer? *Pure Appl Geophys*, **106–108**, 919–927.
- Brewer, A.W. and Milford, J.R., 1960: The Oxford Kew ozone sonde. *Proc R Soc*, **256**, 470–495.
- Chapman, S., 1930: A theory of upper-atmosphere ozone. *Memoirs III No. 26*. London, Royal Meteorological Society.
- Dobson, G.M.B., 1957: Adjustment and calibration of ozone spectrophotometer. ICSU, Spec Comm, Ann. IGY 1957–58, **5**, Pt I, 90–114.
- Dobson, G.M.B., 1966: Forty years' research on atmospheric ozone. Oxford, Clarendon Laboratory, Atmospheric Physics Memorandum No. 66.1.
- Goldsmith, P., Tuck, A.F., Foot, J.S., Simmons, E.L. and Newson, R.L., 1973: Nitrogen oxides, nuclear weapons testing, Concorde and stratospheric ozone. *Nature*, **244**, 545–551.
- Götz, F.W., 1953: Vertical distribution of ozone. UGGI Ass Met Proc Verb Bruxelles.

Notes and news

The hundredth meeting of the Meteorological Committee

This is the record of a speech made by Dr John Houghton at the dinner following the 100th meeting of the Meteorological Committee on 16 October 1989.

I thought it would be interesting on this occasion of the 100th meeting of the Meteorological Committee to give some brief history of the Committee and its work and to present a few highlights gleaned from my perusal of the Committee's minutes over the years.

The Committee has had three manifestations during the last 122 years. Its first meeting was on 3 January 1867 at Burlington House, London; it was then a committee of the Royal Society and was chaired by the President. It met about once a fortnight and the £10 000 per annum budget of the Meteorological Office was under its control. Meetings on this regular basis continued for 10 years until 1877 in which year the Committee was renamed the Meteorological Council. The major difference between the Council and the Committee was that the members of the Council were

paid for their work. Since they met once a fortnight and since they were in executive control of the Meteorological Office they felt that it was only reasonable that they should be paid for their services. Meetings of the Council continued until 1905 when, under the new Director of the Meteorological Office, Dr Napier Shaw (later Sir Napier Shaw), some different arrangements for the Committee were established.

The first meeting of the new Committee was on 20 May 1905 with the Director, Dr Napier Shaw, in the Chair. The Committee consisted of two members appointed by the Royal Society, the Hydrographer of the Navy, a representative of the Board of Trade, a representative of the Board of Agriculture and Fisheries, and a representative of the Treasury. They met four times per year and they were still in executive control of the finances of the Meteorological Office whose budget by then had risen to £19 000 per year. All cheques had to be signed by the Director and countersigned by a member of the Committee.

At the 97th Meeting of that manifestation of the Committee, on 15 October 1919, it was reported that the Meteorological Office was to come under the auspices of the Air Ministry. The Meteorological Committee remained much the same except that it was now chaired not by the Director but by the Controller General Civil Aviation. Amongst the representatives around the table were now two from the Air Ministry, one from the War Office and one from the Admiralty replacing the Hydrographer of the Navy in addition to those who were there before. The 114th meeting of the Committee was in 1922 when the Under Secretary of State for Air took over the chairmanship of the Committee from the Controller General Civil Aviation. At the 160th meeting on 4 July 1939, the last before the Second World War, there was an important discussion about the research work of the Office which resulted in the setting up of the Meteorological Research Committee. No more meetings occurred until the 161st meeting on 3 October 1946 when the Committee, still under the chairmanship of the Under Secretary for State for Air, was widened in its representation by even more government departments. During the years following the war the Committee met less frequently. At the 169th meeting on 15 June 1954 new television weather forecast presentations were described in which Meteorological Office personnel were taking part for the first time.

The year 1956 was an important year for the Office: in that year the move of the Office to Bracknell was agreed and approval for the purchase of the first Meteorological Office computer — the Ferranti 'Mercury', was given. Also in that year the last meeting of that second manifestation of the Committee occurred on the 18th October. At that meeting Mr Christopher Soames, the Secretary of State for Air, explained from the chair that the report of the Brabazon Committee had been received. This Committee had addressed the place of the Meteorological Office in government; it suggested a new structure for the Office and also a new structure for the Meteorological Committee. During that meeting Sir David Brunt said that he agreed that the Meteorological Committee as it was then constituted did not perform any useful purpose but he considered there was a need for an independent advisory body as a guarantee that the meteorological requirements of other important users were not subordinated to those of aviation.

So the third manifestation of the Meteorological Committee came into being. Its first meeting was on 17 October 1957 in the Historic Room 13, at the Air Ministry in Whitehall Gardens. It was a much smaller committee. Lord Hurcomb was in the chair, Sir Austin Anderson represented shipping, Sir David Brunt and Sir Charles Normand represented the scientific community and Colonel Stockford Sackville represented agriculture. Also present were Sir Graham Sutton, the Director-General of the Meteorological Office, Sir Folliot Sandford a Deputy Under Secretary from the Ministry of Defence, and Mr Crotch who was the Secretary. One

of the matters discussed on that occasion concerned charges for forecasts. A recommendation of the Select Committee on Estimates was that a fee should be paid for forecasts supplied to the BBC and independent television companies proportionate to the fees paid by them for news items. The Committee's comment was that it was difficult to do this because the BBC and the TV companies do not pay fees for news items!

The 7th meeting of this new Committee was just 30 years ago in 1959 when Sir Graham Sutton was invited to speculate aloud about future developments in the Meteorological Office. Sir Graham said that he had recently embarked upon a new series of studies with his staff which he hoped would lead to an increasing use of electronic computers to relieve the human element of much of the present necessary drudgery. Development, he thought, would take about 5 years and might not be fully implemented for a decade, but he foresaw the time when the data flowing into the communications centre on punched tape could be directed immediately to an electronic computer which processed the observations to produce, on the face of a cathode-ray-tube, maps of the existing pressure distribution and also forecasts of the distribution of pressure up to 12 hours and perhaps even further ahead. This turned out to be an accurate forecast (even if somewhat optimistic on time-scale) of the development of numerical weather prediction in the Office. At the 9th meeting of the Committee in 1960, soon after the first artificial satellites were launched, a report was presented about the formation of the High Atmosphere Research Branch of the Office which was set up to respond to the new opportunities of satellite observations; 21 extra staff were taken on to form this new branch.

I became involved with the Committee around 1977 in my capacity as Chairman of the Meteorological Research Committee. I was interested to read the minutes of the 58th meeting in November 1977 when the Earl of Halsbury was in the chair — it is a special delight that he is able to be with us this evening. Dr Birks from BP and myself were the only other members of the Committee present on that occasion. Dr Mason, later of course Sir John Mason, Mr J.H. Nelson DUS(Air), Mr George Corby the Director of Services, Dr Ken Stewart the Director of Research, and Mr Colin Hughes the Secretary of the Office (who it is also good to have with us this evening) were also present. It was at that meeting that Sir John Mason put forward his view of the future development of the Office. He made two particular emphases which between them have increasingly dominated the work of the Office through the 1980s. First he addressed the development of commercial services saying that every effort should be made to expand and improve the Office's specialized services to industry, the Public Service and Commerce, thereby making a maximum contribution to the national economy. He pointed out that the Office had already become more commercially minded and cost-conscious;

it had increased its revenue from £2m in 1969–70 to an estimated £8.8m for the year 1977 an increase from 21% to 30% of gross expenditure. Of that £8.8m, £6.8m came from civil aviation and about £600 000 from the offshore industry. I was interested to read that at that meeting I commented on the Office's commercial activities saying that I believed that their expansion would be good for the Office and for the country because it would lead to greater benefit being realized from the work done by the Meteorological Office. The problem I saw was how this could be done without more freedom from the restrictions which inevitably accompany Civil Service activities. Not bad, I thought for a view from my Oxford ivory tower.

Sir John Mason's second point of emphasis at that meeting was the environment and the possible effects of man's activities on weather and climate which he predicted was likely to become of increasing political and economic importance. The Office should therefore give increased attention to understanding the physical basis of climate and to developing models to simulate and, perhaps, eventually predict climate changes both natural and man-made. This would almost certainly necessitate greater attention to the interaction between the oceans and the atmosphere and the development of joint atmosphere/ocean models.

As we moved into the 1980s the Committee itself became more involved with the Office's commercial activities. The Committee itself became larger, more customers were invited to join the committee and the interaction between the Office and the Committee has been an effective and useful way for the Office keeping in touch with its customers. Now as the Meteorological Office becomes an Executive Agency we enter a new era. There will be more freedom of action and more opportunities to serve the community in professional and commercial ways. I am sure that the Meteorological Committee will continue to provide, more than ever, valuable advice and guidance to the Office's Chief Executive.

No one would have predicted a hundred meetings ago the scale of the revolution which has been brought about by computers and by satellite observations. Nor would anyone have predicted the success of these tools and the scientific advances associated with them in improving the accuracy and the range of forecasts, and their availability to all sections of the community. If we project ourselves to the 200th meeting of this Committee we could, perhaps, imagine that meeting reflecting on the forecasts of climate made by the Office 50 years before. We can also, perhaps, rather dimly imagine them reflecting on the enormous increase in the development of technology and in the development of meteorological science and applications which had occurred during the first half of the twenty-first century. But, however they view those years I am sure they will be exciting and that future managers of the Meteorological Office will continue to look back with pleasure and appreciation at

the advice, stimulation and gentle steer given by Meteorological Committee.

First All Africa International Symposium on Lightning, Harare, Zimbabwe, 30 April–4 May 1990

The symposium, which is being organized by the Zimbabwe Institution of Engineers (and co-sponsored by the UK Institution of Electrical Engineers), has already attracted more than 20 world-wide speakers.

The main objectives of the symposium are the encouragement of research, the exchange of information and investigations, recommendations and decisions on the possible establishment of a communications network to facilitate the exchange and dissemination of new knowledge and practices.

The topics to be covered will include structural protection, surge suppression, earthing, personnel and livestock protection, regulations, standards, codes of practice, techniques, equipment and industrial trends. It should be of particular interest to engineers, physicists and meteorologists, and over 200 international delegates are anticipated. Also, there will be technical visits to places of appropriate interest in and around Harare.

The Director-General of the Standards Association of Zimbabwe has described the forthcoming symposium as 'one of the most important technical meetings ever to be held in this country'.

Please contact the Editor, Meteorological Magazine has further details, or write direct to:

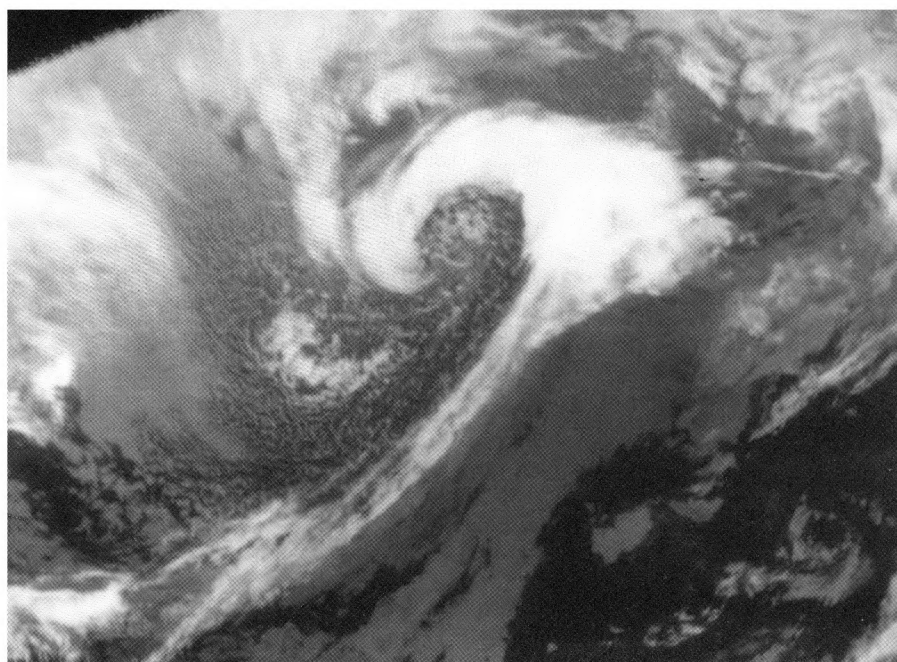
The Secretary
Symposium Organizing Committee
P.O.Box 1921
Harare, Zimbabwe
Africa.

British Hydrological Society

Allan Lambert, Special Projects Manager for Dwr Cymru (Welsh Water), is the new President of the British Hydrological Society for the next 2 years. The Society was formed in 1983 and now has over 600 members including a number of meteorologists with a special interest in hydrology. C. Collier, head of the Meteorological Office's Nowcasting and Satellite Applications Branch, is a member of the main committee. The Society aims to promote interest and scholarship in both the scientific and applied aspects of hydrology, and to foster the involvement of its members in international activities.

National and regional meetings are held on a wide range of hydrological topics, and a regular newsletter called *Circulation* is distributed to all members. If you are interested in knowing more about the Society and its activities contact C Collier, Room 140f, Meteorological Office, London Road, Bracknell, RG12 2SZ.

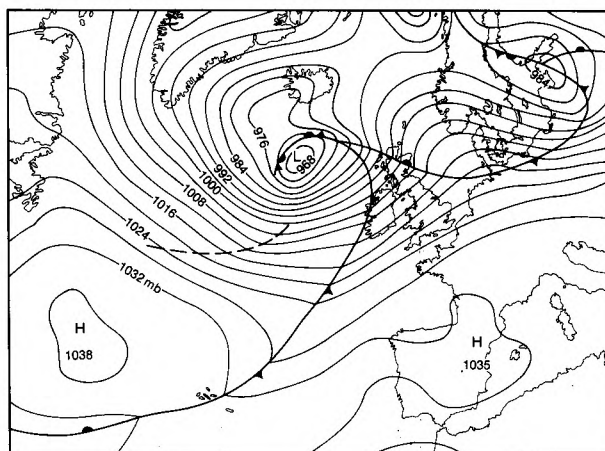
Satellite photograph — 16 January 1990 at 1200 UTC



This Meteosat infra-red image has been reprojected on to a polar-stereographic projection. The accompanying surface chart is on the same projection and covers the same area as the image. Note that the north-west corner of the image is missing; this is because this portion of the earth cannot be seen by Meteosat. Note also that the resolution of the basic satellite data is rather poor near this corner.

The main feature of interest is the cloud associated with the depression centred south of Iceland. The cold front and occlusion are readily apparent, although a rather amorphous cloud mass associated with the development and movement of the depression is more identifiable than anything particularly associated with the warm front. Indeed, at 0600 UTC the warm front had not been analysed as being connected to the cold front of the depression near the Baltic — instead, it had been trailed round into the Gulf of Genoa. There is some evidence on the image of a feature with this alignment, but it is an upper-level, frontolytic feature and not worthy of inclusion on the surface analysis. Similarly, there is evidence of a vortex in the western Mediterranean, but this again is an upper feature well documented on the 250 mb analysis (not shown).

Another feature of note is the area of enhanced convection south-west of the main depression, associated with a surface trough. The enhanced convection is also ahead of an upper trough, but neither the surface nor upper trough can separately explain the shape of the



area of enhanced convection. The following day, this feature became merged with the cloud associated with the occlusion, but at the time of this image they are quite distinct.

The image was reprojected using the Autosat-2 computer system which is at present under development in a number of Branches of the Meteorological Office. It will be used to process digital data from geostationary and polar-orbiter satellites, and promulgate them in appropriate projections to forecasters in the Central Forecasting Office, Bracknell, and also outstations and media customers.

R.W. Lunn

GUIDE TO AUTHORS

Content

Articles on all aspects of meteorology are welcomed, particularly those which describe results of research in applied meteorology or the development of practical forecasting techniques.

Preparation and submission of articles

Articles, which must be in English, should be typed, double-spaced with wide margins, on one side only of A4-size paper. Tables, references and figure captions should be typed separately. Spelling should conform to the preferred spelling in the *Concise Oxford Dictionary* (latest edition). Articles prepared on floppy disk (Compucorp or IBM-compatible) can be labour-saving, but only a print-out should be submitted in the first instance.

References should be made using the Harvard system (author/date) and full details should be given at the end of the text. If a document is unpublished, details must be given of the library where it may be seen. Documents which are not available to enquirers must not be referred to, except by 'personal communication'.

Tables should be numbered consecutively using roman numerals and provided with headings.

Mathematical notation should be written with extreme care. Particular care should be taken to differentiate between Greek letters and Roman letters for which they could be mistaken. Double subscripts and superscripts should be avoided, as they are difficult to typeset and read. Notation should be kept as simple as possible. Guidance is given in BS 1991: Part 1: 1976, and *Quantities, Units and Symbols* published by the Royal Society. SI units, or units approved by the World Meteorological Organization, should be used.

Articles for publication and all other communications for the Editor should be addressed to: The Director-General, Meteorological Office, London Road, Bracknell, Berkshire RG12 2SZ and marked 'For Meteorological Magazine'.

Illustrations

Diagrams must be drawn clearly, preferably in ink, and should not contain any unnecessary or irrelevant details. Explanatory text should not appear on the diagram itself but in the caption. Captions should be typed on a separate sheet of paper and should, as far as possible, explain the meanings of the diagrams without the reader having to refer to the text. The sequential numbering should correspond with the sequential referrals in the text.

Sharp monochrome photographs on glossy paper are preferred; colour prints are acceptable but the use of colour is at the Editor's discretion.

Copyright

Authors should identify the holder of the copyright for their work when they first submit contributions.

Free copies

Three free copies of the magazine (one for a book review) are provided for authors of articles published in it. Separate offprints for each article are not provided.

March 1990

Editor: B.R. May

Vol. 119

Editorial Board: R.J. Allam, R. Kershaw, W.H. Moores, P.R.S. Salter

No. 1412

Contents

	Page
A heavy snowfall within a mesoscale convergence zone.	
R.M. Sanderson, B.W. Golding and M.J. Bader	41
Correction.	52
Sixty-four years of regular ozone measurements. E.L. Simmons	53
Notes and news	
The hundredth meeting of the Meteorological Committee	57
First All African International Symposium on Lightning, Harare, Zimbabwe, 30 April–4 May 1990	59
British Hydrological Society	59
Satellite photograph — 16 January 1990 at 1200 UTC R.W. Lunnon	60

Contributions: It is requested that all communications to the Editor and books for review be addressed to the Director-General, Meteorological Office, London Road, Bracknell, Berkshire RG12 2SZ, and marked 'For *Meteorological Magazine*'. Contributors are asked to comply with the guidelines given in the *Guide to authors* which appears on the inside back cover. The responsibility for facts and opinions expressed in the signed articles and letters published in *Meteorological Magazine* rests with their respective authors.

Subscriptions: Annual subscription £30.00 including postage; individual copies £2.70 including postage. Applications for postal subscriptions should be made to HMSO, PO Box 276, London SW8 5DT; subscription enquiries 01–873 8499.

Back numbers: Full-size reprints of Vols 1–75 (1866–1940) are available from Johnson Reprint Co. Ltd, 24–28 Oval Road, London NW1 7DX. Complete volumes of *Meteorological Magazine* commencing with volume 54 are available on microfilm from University Microfilms International, 18 Bedford Row, London WC1R 4EJ. Information on microfiche issues is available from Kraus Microfiche, Rte 100, Milwood, NY 10546, USA.

ISBN 0 11 728663 X

ISSN 0026–1149

© Crown copyright 1990. First published 1990

The

DUPLICATE

Meteorological Magazine

April 1990

Variations in Indian south-west monsoon
Rainfall patterns in north-east England
The spring of 1989



DUPLICATE JOURNALS

National Meteorological Library
FitzRoy Road, Exeter, Devon. EX1 3PB

HMSO

HMSO Met.O.992 Vol. 119 No. 1413



National Meteorological Library & Archive
London Road, Bracknell, Berkshire, RG12 2SZ U.K.
TEL: 01344 85 4838/9 GTN: 1443 4838/9
Docfax : 01344 85 4840

This publication must be returned or renewed by the last date shown below.
Renewal depends on reservations. Extended loans must be authorised by the
Librarian. Publications should NOT be passed to other readers.

--	--	--



3 8078 0003 9806 7

The Meteorological Magazine

April 1990
Vol. 119 No. 1413

551.553.21:551.589.1(54)

Variations in the onset of the Indian south-west monsoon and summer circulation anomalies

I. Subbaramayya, S. Vivekananda Babu and C.V. Naidu

Department of Meteorology and Oceanography, Andhra University, Waltair, India

Summary

Anomaly circulations in April and May over India associated with the late onset of the summer monsoon at eight locations in India have been obtained by using correlation techniques. Regression equations using significantly correlated winds in April and May have been developed to forecast the dates of onset at the eight locations. Onset forecasts for the central parts of the country appear to be reasonably good.

1. Introduction

The mean dates of the onset of the south-west monsoon over India, and their variability, trends and periodicities were studied by Subbaramayya *et al.* (1984, 1987, 1988). The circulation changes preceding the onset of the monsoon were examined by Maung Tun Yin (1949), Sircar and Patil (1962), Ramamurthi and Keshavamurthy (1964), Pant (1964), Wright (1967), de la Mothe (1968), Ananthakrishnan (1970) and Kuettner and Unninayar (1981). The important changes found over India are (a) westward displacement of an upper trough in the subtropical westerlies from 90° E to 75° E, (b) northward displacement of the subtropical anticyclone over the Arabian Sea, and (c) establishment of an anticyclone over Tibet and an easterly jet over peninsular India. It is also suggested that, if the above circulation changes occur early or late, accordingly there would be changes in the onset of the monsoon.

Investigations have been made of the correlations of some meteorological parameters spread widely over the globe in April and May with the seasonal monsoon rainfall in attempts to forecast the monsoon rainfall using highly correlated antecedent factors. Similarly, attempts were made (Kung and Sharif 1981) to forecast

the date of the onset over the Kerala State coast in the extreme south-west of peninsular India. No satisfactory study of the circulation anomalies in April and May with the onset in different parts of the country have been made so far. The authors have therefore studied the correlations of the onset dates with the winds in April and May at different levels at eight locations. From this the anomaly circulations associated with delayed monsoons were obtained. Regression equations to forecast the onset dates using significantly correlated wind parameters were also obtained.

2. Data and analysis

The eight locations selected were Trivandrum, Madras, Visakhapatnam, Bombay, Nagpur, Calcutta, Lucknow and New Delhi, the locations of which are shown in Fig. 1. The monthly mean winds in April and May at 700, 500 and 300 mb at these locations for the period 1959–88 were obtained from *Monthly climatic data for Indian stations* published by the India Meteorological Department.

Onset dates at these eight locations for the period were obtained from estimates of the position of the

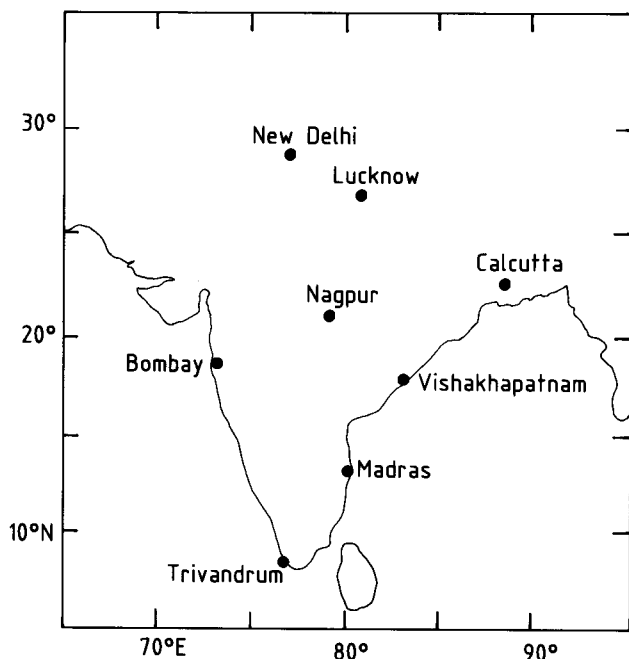


Figure 1. Locations mentioned in the text.

northern limit of the monsoon prepared each day during the period of the advance of the monsoon, following the procedure described by Subbaramayya and Bhanu Kumar (1978). The onset dates are reckoned from 1 May, thus an onset date of 5 June is taken as day 36.

Correlations between the onset dates at each location and the zonal and meridional winds at the above three levels at all eight locations were evaluated. To obtain the anomaly circulations related to the delayed monsoon at any location, the standard deviations of both zonal and meridional components of winds at the eight locations were first multiplied by the respective correlation coefficients. These values were then vectorially combined and the results were plotted and streamlines drawn at each level. Anomaly winds were plotted by the standard shaft and barb method.

The nature of the anomaly patterns relative to the mean circulations were studied. Keeping the consistency of the anomaly patterns in view, the wind parameters with the highest correlations were chosen to develop regression equations for forecasting the onset date at each location. However, the correlations at Lucknow

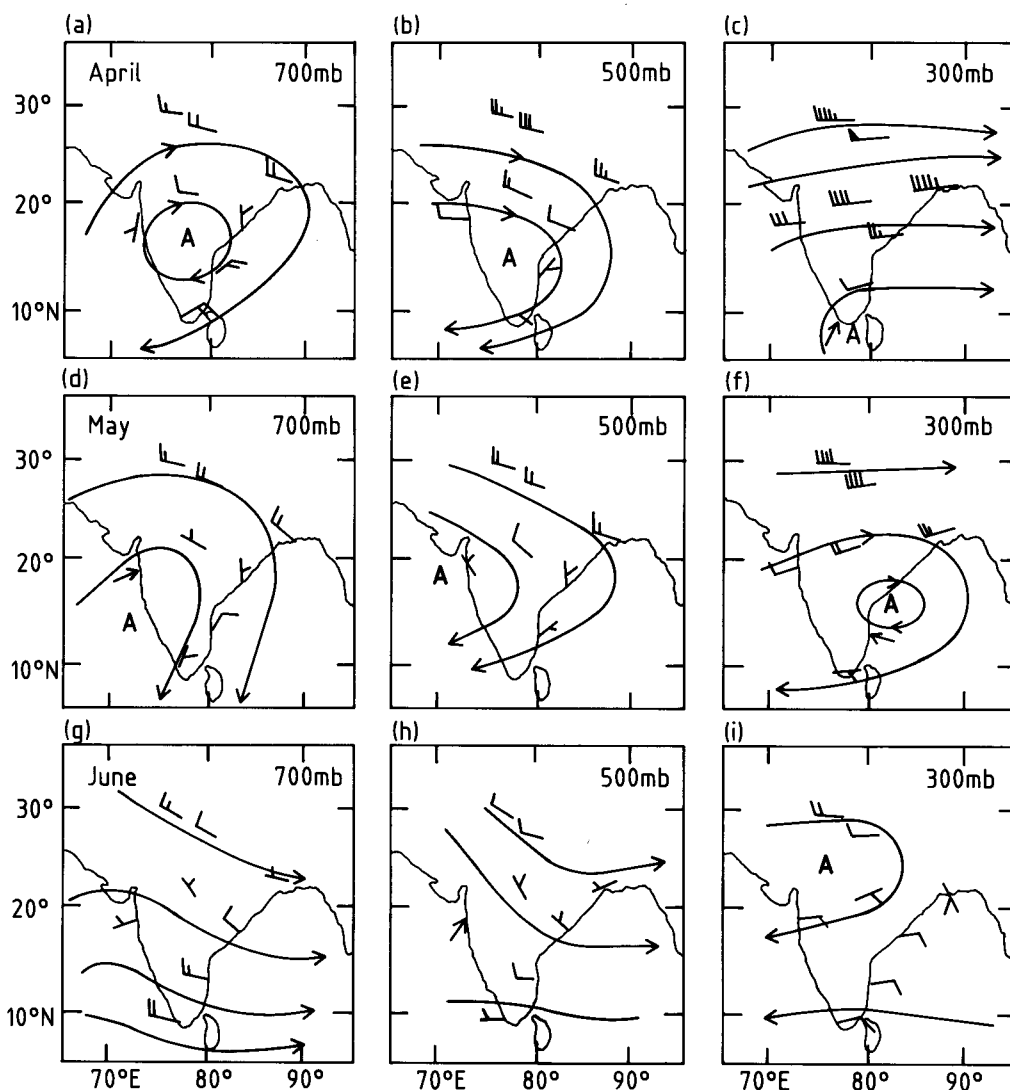


Figure 2. Mean winds and streamlines at 700, 500 and 300 mb over India for April, May and June for the period 1959–88.

were not considered when developing regression equations because the wind data in some years were missing. However, the available winds were also plotted to examine the consistency of the anomaly circulations. The significance of the regressions were examined by the Student's *t*-test.

3. Results and discussion

3.1 Mean circulations in April, May and June

The mean circulations over India at different levels in April, May and June are shown in Fig. 2. In April at 700 mb there are west-north-westerlies over northern India and north-easterlies over the north peninsula with an anticyclone in between. At 500 mb there are strong westerlies over northern India but the north-easterlies over the south of the peninsula are weak. The subtropical ridge in between is situated at relatively low latitudes. At 300 mb the westerlies over northern India are stronger than at lower levels and have extended to the north peninsula. The subtropical ridge is thus situated more to the south at this level. While at 500 mb the subtropical anticyclonic cell is over the west Arabian Sea and the peninsula, at 300 mb it is over the south of the Bay of Bengal. The above features indicate a general northward decrease of temperature throughout the troposphere and relatively higher temperatures in the south Bay of Bengal than over the south Arabian Sea in the upper troposphere.

In May the circulation features are essentially similar to those in April but the winds are relatively weaker and the axis of the subtropical ridge is more nearly vertical. This indicates that the meridional temperature gradient in the more southerly latitudes has weakened considerably. However, temperatures east of the peninsula are higher than those to the west.

In June there are strong westerlies over the south of the peninsula in the lower troposphere whose strength decreases with height, while easterlies prevail in the upper troposphere. Over northern India there are westerlies throughout the troposphere and they are relatively strong in the upper troposphere. The subtropical ridge is situated over northern India. These features indicate a reverse temperature gradient over southern and central India. The zonal wind shear in the lower troposphere shows considerable cyclonic vorticity over southern and central India and anticyclonic vorticity over northern India. In the upper troposphere over the entire region there is anticyclonic vorticity.

3.2 Circulation anomalies associated with the delayed monsoon at different locations

Trivandrum. The circulation anomalies in April and May associated with the delayed monsoon at Trivandrum, evaluated by the procedure described in section 2, are shown in Fig. 3(a). In April there is (a)

cyclonic anomaly over the north-east of the peninsula and the adjoining north-west Bay of Bengal throughout the troposphere, and (b) north-easterly anomaly over north India in the middle and upper troposphere. This means that the normal westerlies over north India are more meridional and the anticyclonic circulation over eastern India and the west Bay of Bengal is weaker.

In May there is a significant anticyclonic anomaly over the south-west of the peninsula and the south-east Arabian Sea in the lower and middle tropospheres and a cyclonic anomaly in the middle and upper tropospheres over north-west India and anomalous westerlies in the upper troposphere in the extreme south. It is interesting to note that in the extreme south the easterlies are stronger in the lower troposphere and weaker in the upper troposphere than is the normal in May. Also, the anomalous circulation in the upper troposphere over the north-west Bay of Bengal and the adjoining land area shifts to north-west India by May.

Madras. The anomalous circulations related to the late onset at Madras are shown in Fig. 3(b). In April there is cyclonic circulation in the lower troposphere over the north-west Bay of Bengal and the adjoining parts of eastern India. In the middle and upper troposphere there are north-easterlies over north India and easterlies over the peninsula. These anomalous circulations are similar to those associated with the delayed monsoon at Trivandrum. In May also there is a significant anticyclonic anomaly in the lower and middle troposphere over the south-west of the peninsula and the east Arabian Sea as in the case of Trivandrum, but there is no cyclonic anomaly in the higher levels over north-west India.

Bombay. The anomalous circulations associated with delayed monsoons at Bombay are shown in Fig. 3(c). In April there is anticyclonic circulation throughout the troposphere over the west peninsula and it is particularly pronounced in the middle troposphere. The anomaly winds in May show an anticyclonic circulation across the centre of the peninsula in the lower troposphere and cyclonic circulation in the middle and upper troposphere over north-west India.

Visakhapatnam. The anomaly circulations (Fig. 3(d)) show anticyclonic circulation in the lower troposphere which shifts westward with height. Northerly anomaly over central India is strong, particularly in the upper troposphere. In May there is a ridge extending from the south-west peninsula to north-east India in the lower troposphere. There is a trough over north-west India which is quite pronounced in the middle and upper troposphere.

Nagpur. The anomaly circulations are shown in Fig. 3(e). In April there is a strong anticyclonic circulation over the central west peninsula in the lower

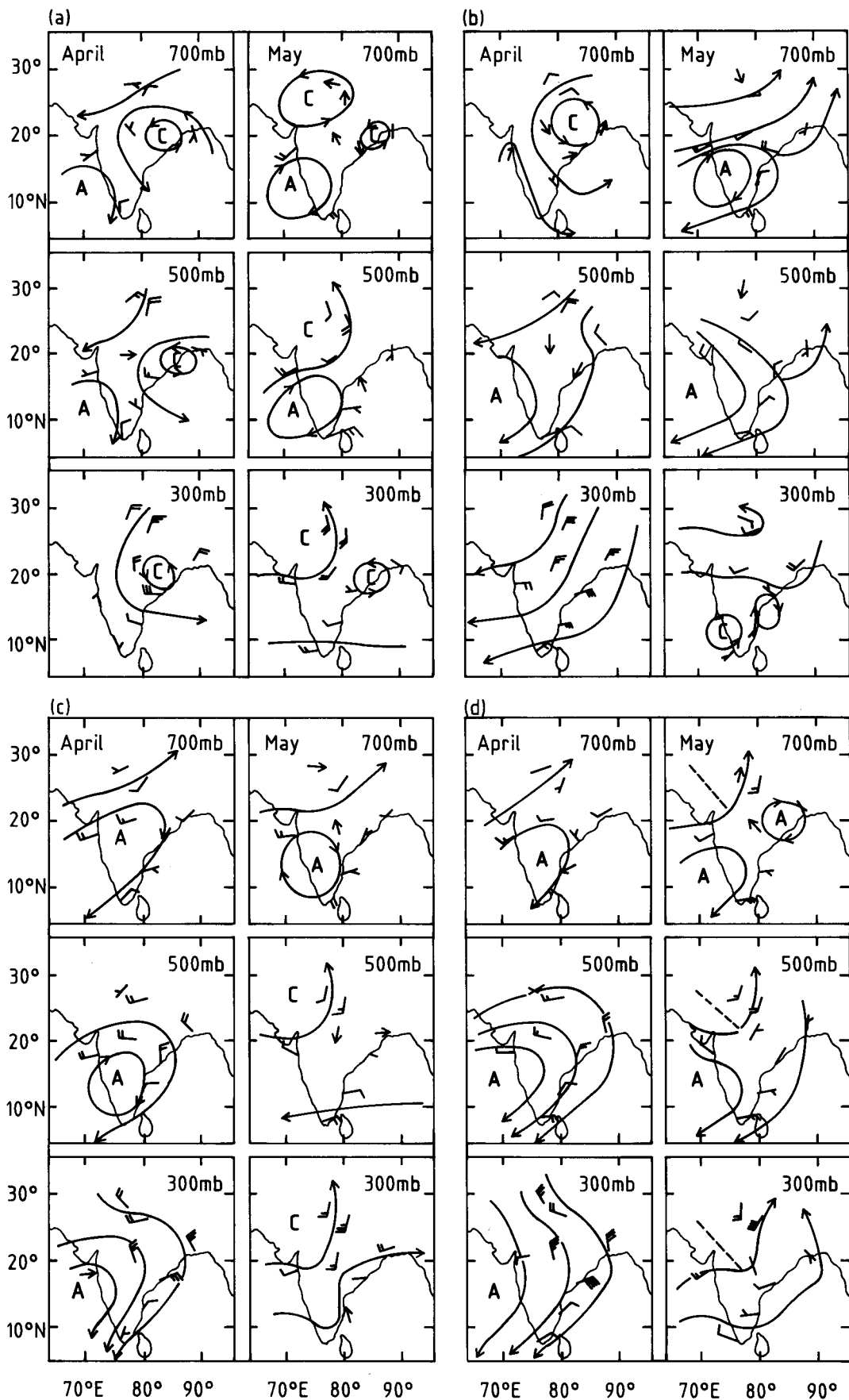


Figure 3. Anomaly circulations associated with the delayed monsoon at (a) Trivandrum, (b) Madras, (c) Bombay, (d) Visakhapatnam, (e) Nagpur, (f) Calcutta, (g) Lucknow and (h) New Delhi.

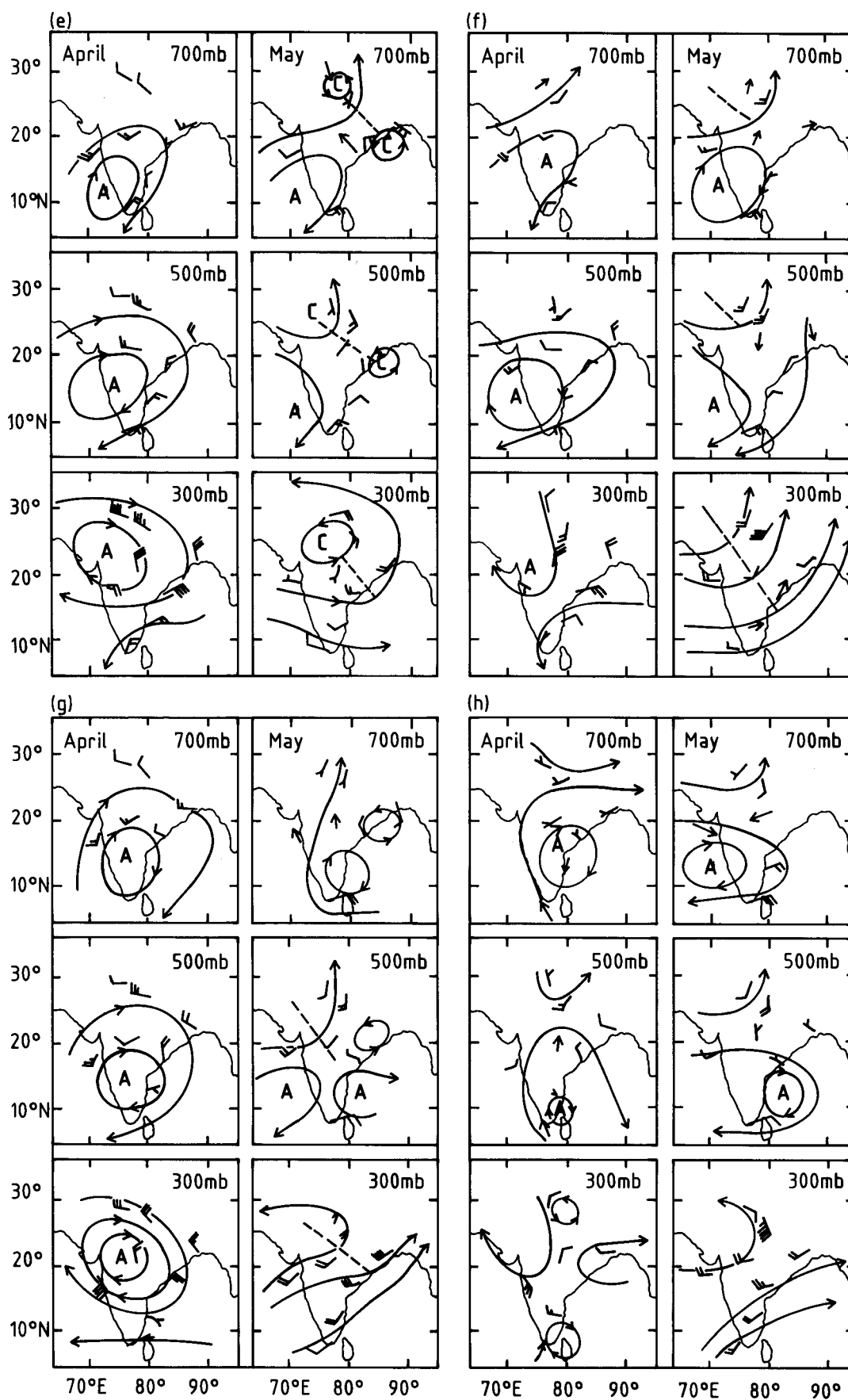


Figure 3. continued.

troposphere which extends into the upper troposphere but gradually shifts to the north with height. This indicates a meridional temperature gradient (increasing northwards) anomaly over western India. In May there is an anticyclonic circulation in the lower and middle troposphere over the west peninsula, and a significant cyclonic circulation over north-west India with a trough extending throughout the troposphere to the north Bay of Bengal.

Calcutta. The anomaly circulations in April (Fig. 3(f)) indicate anticyclonic circulation over west central peninsula in the lower and middle troposphere and a ridge in the upper troposphere over north-west India. In May the anticyclonic anomaly in the lower troposphere over west central peninsula persists and there is a trough over north-west India at all levels.

Lucknow. The anomaly circulations are shown in Fig. 3(g). In April there is a strong anticyclonic circulation, tilting northward with height, in the lower troposphere over the south of the peninsula. This anomaly feature is similar to that associated with the delayed monsoon at Nagpur. In May there is a trough over north-west India extending into central India in the middle and upper troposphere, and a ridge in the middle troposphere across the south of the peninsula. Also, there is a pronounced westerly anomaly in the upper troposphere across central India.

New Delhi. In April the correlations are small and the anomaly circulations show a weak anticyclonic circulation over the peninsula (Fig. 3(h)). In May the correlations are relatively high and significant. There is a ridge in the lower and middle troposphere across peninsular India and a strong cyclonic flow is present in the upper troposphere over north-west India.

3.3 Regression equations for forecasting the onset date of the monsoon

Wind parameters with good forecast values are selected as mentioned in section 2, and regression equations are developed to forecast the onset-date at each location. Two regression equations are obtained for each location, one involving the important wind component at the location itself and the other involving two significant wind parameters over the whole country. The first one is to enable the meteorologist at the location itself to prepare the forecast using data collected by them while the second one is to prepare a better forecast. At the locations where the onset generally takes place in May only one set of equations using April winds is developed, but at the other locations where the onset normally occurs after the first week of June, two sets of equations, one with April winds and the other with May winds, have been developed. The forecasting equations thus developed are given in the Appendix. Multiple correlations, standard deviations of the errors and the level of significance of the regressions are also noted.

All the regression equations are highly significant except some at Madras and Visakhapatnam. Those equations that are significant at the 1% level or more are indicated by asterisks. Some of the prognostic equations for the onset at Bombay, Calcutta and Lucknow have multiple correlations of 0.6 or more and these locations lie in the core-area of the Indian summer monsoon.

The standard deviation of the errors of estimates of these more significant equations is less than one week — this is still a large value. Nevertheless the equations would be useful in forecasting large deviations from the normal with good reliability in the absence of more accurate methods.

These equations have been used to produce onset forecasts for the year 1989 which are shown in Table I

Table I. Actual and forecast dates of onset of the monsoon in 1989

Location	Forecast dates				Actual dates
	April winds Eq. 1	Eq. 2	May winds Eq. 1	Eq. 2	
Trivandrum	13 May	8 May	—	—	20 May
Madras	5 June	5 June	—	—	5 June
Bombay	9 June	14 June	3 June	5 June	7 June
Visakhapatnam	9 June	12 June	—	10 June	8 June
Nagpur	13 June	11 June	—	12 June	12 June
Calcutta	9 June	8 June	9 June	10 June	12 June
Lucknow	4 July	3 July	—	25 June	23 June
New Delhi	—	—	—	5 July	13 July

along with the actual dates of onset. The dates forecast by the different equations are nearly the same at most of the locations except at Trivandrum and also in the case of one equation each at Bombay and Lucknow. Comparison of the forecast dates with the actual dates show large deviations at Trivandrum, Lucknow and New Delhi. However, the onset forecast at Lucknow with May winds gave a better result. Thus, the forecasts on the whole are reasonably good.

4. Conclusions

The onset dates are significantly correlated with winds in the pre-monsoon season at some locations. They reveal systematic anomaly circulations associated with delayed monsoon. These anomaly circulations related to the onset at different locations in general are:

- (a) anticyclonic circulation over the west central peninsula in the lower troposphere,
- (b) cyclonic circulation over north-west India in the upper troposphere, and
- (c) westerlies over north India.

However, they differ in detail with the onset at different places.

The forecasts based on the present equations in 1989 are found to be reasonably good, particularly in the central parts of the country covering a large area.

References

- Ananthakrishnan, R., 1970; The seasonal march of surface pressure gradients across India and the south-west monsoon. *Curr Sci*, **39**, 248–251.
- de la Mothe, P.D., 1968; Middle-latitude wavelength variations at 500 mb. *Meteorol Mag*, **97**, 333–339.
- Kuettner, J.P. and Unninayar, M.S., 1981; The near-equatorial jet south of India and its role in the onset of the monsoon. In Proceedings of the International Conference on early results of FGGE and large scale aspects of its monsoon experiments, Tallahassee, Florida, 12–17 January 1981. Geneva, ICSU/WMO.
- Kung, E.C. and Sharif, T.A., 1981; Long-range multi-regression forecasting of the Indian summer monsoon onset and rainfall with antecedent upper air pattern and sea surface temperature. In Proceedings of the International Conference on early results of FGGE and large scale aspects of its monsoon experiments, Tallahassee, Florida, 12–17 January 1981. Geneva, ICSU/WMO.
- Maung Tun Yin, 1949; A synoptic-aerologic study of the onset of the summer monsoon over India and Burma. *J Meteorol*, **6**, 393–400.
- Pant, P.S., 1964; Onset of monsoon over India. *Ind J Meteorol and Geophys*, **15**, 375–380.
- Ramamurthi, K.M. and Keshavamurthy, R.N., 1964; Synoptic oscillations of Arabian anticyclones in the transition season. *Ind J Meteorol and Geophys*, **15**, 227–234.
- Sircar, N.C.R. and Patil, C.D., 1962; A study of high level wind tendency during premonsoon months in relation to time of onset of southwest monsoon in India. *Ind J Meteorol and Geophys*, **13**, 468–471.
- Subbaramayya, I. and Bhanu Kumar, O.S.R.U., 1978; The onset and the northern limit of the south-west monsoon over India. *Meteorol Mag*, **107**, 37–48.
- Subbaramaya, I., Bhanu Kumar, O.S.R.U. and Vivekanandababu, S., 1987; Variations in the onset of the summer monsoon over India. *Meteorol Mag*, **116**, 309–317.
- Subbaramayya, I., Babu, S.V. and Rao, S.S., 1984; Onset of the summer monsoon over India and its variability. *Meteorol Mag*, **113**, 127–135.

Subbaramayya, I., Vivekananda Babu, S. and Naidu, C.V., 1988; A note on the normal dates of onset of summer monsoon over south peninsular India. *Meteorol Mag*, **117**, 371–377.

Wright, P.B., 1967; Changes in 200 mb circulation patterns related to the development of the Indian south-west monsoon. *Meteorol Mag*, **96**, 302–315.

Appendix

In the following equations the zonal and meridional winds (m s^{-1}) are represented by u and v , respectively. The locations and levels of the winds are indicated by adding the appropriate location abbreviation and the pressure level as suffixes. The abbreviations used are BMB=Bombay, CAL=Calcutta, LKN=Lucknow, MDS=Madras, NDH=New Delhi, NGP=Nagpur, TRV=Trivandrum and VSK=Visakhapatnam. The multiple correlations (CC) of the equations, standard deviations of errors of estimates (SDE) and the level of significance (SIG) of the regressions are shown below each equation. Equations that are significant at the 1% level or more are indicated by asterisks.

Trivandrum (April winds)

- (1) Onset = $8.4 - 3.03v_{TRV700}$
CC = 0.42; SDE = 8.9 days; SIG = 5%
- *(2) Onset = $-0.9 - 3.69v_{TRV700} + 1.54u_{VSK500}$
CC = 0.57; SDE = 8.1 days; SIG = 1%

Madras (April winds)

- (1) Onset = $34.3 - 0.56u_{MDS300}$
CC = 0.28; SDE = 8.3 days; not significant at 10% level
- (2) Onset = $34.0 - 0.39u_{MDS300} - 0.73v_{CAL300}$
CC = 0.4; SDE = 7.9 days; SIG = 5%

Bombay (April winds)

- (1) Onset = $29.5 + 1.78u_{BMB500}$
CC = 0.46; SDE = 7.3 days; SIG = 2%
- *(2) Onset = $23.2 + 1.81u_{BMB500} - 1.78u_{TRV500}$
CC = 0.6; SDE = 6.6 days; SIG = 0.1%

Bombay (May winds)

- *(3) Onset = $35.6 + 3.09u_{BMB700}$
CC = 0.56; SDE = 6.7 days; SIG = 1%
- *(4) Onset = $35.4 + 2.15u_{BMB700} - 0.67u_{TRV700}$
CC = 0.58; SDE = 6.6 days; SIG = 1%

Visakhapatnam (April winds)

- (1) Onset = $37.5 - 1.16v_{VSK500}$
CC = 0.33; SDE = 6.7 days; SIG = 10%
- (2) Onset = $34.4 - 0.42v_{VSK500} - 1.25u_{TRV500}$
CC = 0.41; SDE = 6.4 days; SIG = 5%

Visakhapatnam (May winds)

- *(3) Onset = $41.5 - 1.07u_{TRV700} + 0.95v_{NDH500}$
CC = 0.54; SDE = 6.0 days; SIG = 1%

New Delhi (May winds)

- * (1) $\text{Onset} = 57.6 + 1.21u_{VSK300} - 1.25u_{TRV700}$
CC = 0.56; SDE = 7.5 days; SIG = 1%

Nagpur (April winds)

- (1) $\text{Onset} = 43.0 - 0.88v_{NGP300}$
CC = 0.45; SDE = 7.4 days; SIG = 2%
* (2) $\text{Onset} = 35.2 + 2.33v_{BMB700} - 1.16v_{VSK500}$
CC = 0.62; SDE = 6.5 days; SIG = 0.1%

Nagpur (May winds)

- (3) $\text{Onset} = 54.0 - 1.02u_{TRV700} - 0.59u_{NDH300}$
CC = 0.43; SDE = 7.5 days; SIG = 5%

Calcutta (April winds)

- (1) $\text{Onset} = 34.2 - 1.55v_{CAL500}$
CC = 0.4; SDE = 6.4 days; SIG = 5%
* (2) $\text{Onset} = 31.1 + 1.50v_{BMB700} - 1.27v_{CAL500}$
CC = 0.52; SDE = 6.0 days; SIG = 1%

Calcutta (May winds)

- * (3) $\text{Onset} = 36.1 - 1.48u_{TRV700}$
CC = 0.62; SDE = 5.5 days; SIG = 0.1%
* (4) $\text{Onset} = 39.5 - 1.51u_{TRV700} + 0.92v_{NDH500}$
CC = 0.69; SDE = 5.1 days; SIG = 0.1%

Lucknow (April winds)

- (1) $\text{Onset} = 31.5 + 1.75u_{LKN500}$
CC = 0.48; SDE = 7.7 days; SIG = 5%
* (2) $\text{Onset} = 25.9 + 2.0v_{BMB700} + 1.9u_{CAL500}$
CC = 0.64; SDE = 6.6 days; SIG = 0.1%

Lucknow (May winds)

- * (3) $\text{Onset} = 54.4 + 1.08u_{VSK300} + 0.60v_{LKN500}$
CC = 0.58; SDE = 7.5 days; SIG = 1%

551.577.21(428)

Modelling long-term rainfall patterns in north-east England

D. Wheeler

Sunderland, United Kingdom

Summary

Mean annual and monthly rainfalls from 133 gauges in north-east England have been used to study the variation of rainfall with height and location in this area.

1. Introduction

Rainfall is one of most important climatological elements. Despite a traditional reliance on rain-gauge data it must not be forgotten that they provide only point sample data from a geographically continuous population. The underlying character of that population can only be established by statistical inferential methods that model and generalize its behaviour, often in relation to other variables of which the three spatial dimensions of height and location (defined by Cartesian coordinates) are, arguably, the most important. This paper examines the utility of such models insofar as they are able to reproduce and, by inference, 'explain' the geography of rainfall. It takes as its point of departure the mean annual and monthly rainfalls from a sample of 133 gauges distributed over north-east England. Regression, and trend-surface methods are studied and their results used to identify underlying order and pattern in rainfall information.

Past efforts have been directed towards relating mean annual rainfall to altitude and to the spatial variables of

latitude and longitude. Rodda (1962) used regression analysis of annual rainfall over 2 years to produce '...an objective method for assessment of areal rainfall amounts...', in this case based on 19 sites in mid-Wales. Unwin (1969) used trend-surface analysis to study systematic geographical variation in mean annual rainfall in the Snowdonia district. His study employed data from 47 stations and concluded with a multiple regression model based on altitude as well as the two spatial dimensions. Chuan and Lockwood's (1974) study covered much of Lancashire and Yorkshire and examined monthly, as well as annual, relationships between rainfall and altitude. The authors used data from 260 stations and studied also the effects of exposure and distance from the Pennine ridge.

The present paper takes a broadly similar approach and attempts to respond also to the prompting of Bleasdale and Chan (1972) who stressed the need for more detailed regional studies of rainfall patterns. It also complements the synoptic-based climatological

studies such as those undertaken in the region by Jackson (1969) and elsewhere by, for example, Barry (1963).

The region comprises the 3300 km² of land which was administered by the Northumbrian Water Authority and which includes the counties of Durham, Northumberland, Tyne and Wear and parts of Cleveland and Cumbria. This region is not a mere administrative device but has strong claims to a geographical identity. Its boundaries are major hydrological divides of, by English standards, notable elevation; the Pennines to the west, the Cheviots to the north and the North Yorkshire Moors to the south (Fig. 1). Of equal geographic significance is the North Sea, forming the eastern limit of the region and comprising the coldest stretch of water along the British coast. The effect of the Pennines is especially noteworthy. In north-east England they achieve their greatest and most continuous heights and create a degree of climatic distinctiveness through the shelter they afford from the dominant westerlies. Manley (1935), for one, has been at pains to emphasize the integrity of the region's climate. The physiography of the region is helpfully uncomplicated, and consists of a Tertiary erosion surface tilting from west to east (Trotter 1929) and is disrupted only by the valleys of the region's three major rivers, the Tyne, Wear and Tees. The abrupt and irregular relief that characterizes so much of upland Britain is largely absent and so too, by inference, is the correspondingly complex geography of rainfall that, in these latitudes, is so often closely governed by height.

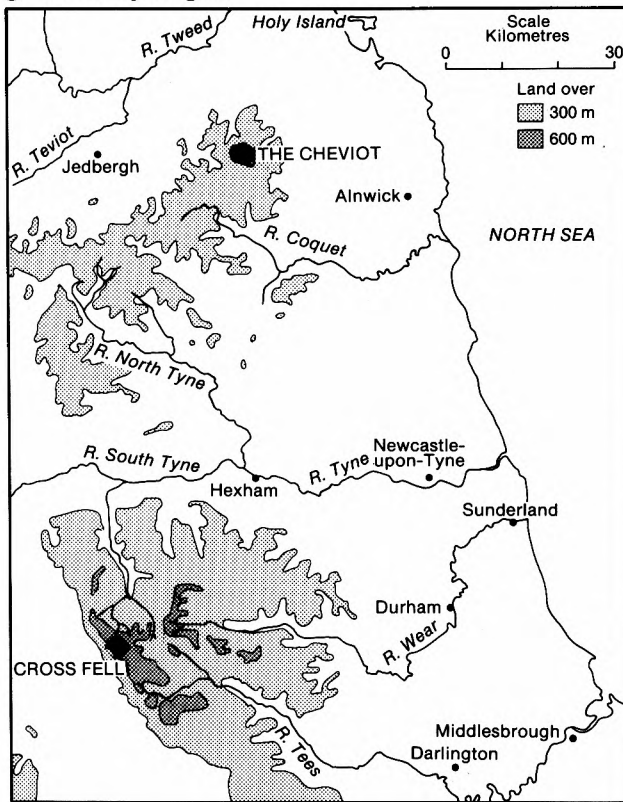


Figure 1. Relief map of north-east England showing principal rivers.

Because of the importance of altitude in the following analysis, the sample was stratified within 50 m altitudinal bands. Only at high level, and because of lack of stations, did this requirement have to be relaxed. The bias that might otherwise have resulted from the abundance of low-level stations was avoided and the skewness of the statistical distribution of station altitude was only +0.156.

2. Variation of rainfall with altitude

2.1 Annual rainfall

The geography of the region's rainfall is shown in Fig. 2. Visual comparison alone with Fig. 1 suggests a degree of correspondence between rainfall and altitude. Such an association has been appreciated for many years (Salter 1918). Table I summarizes the relationship between mean annual rainfall and altitude in the region and sets it against that for the adjacent Yorkshire area (Chuan and Lockwood 1974). The two show similar regression parameters and equally strong correlations between rainfall and altitude. Similar correlations were also found in Snowdonia (Unwin 1969) and in mid-Wales (Rodda 1962). Table I also gives the regression model for national data (Bleasdale and Chan 1972). In comparison with the latter, the north-east region has a lower intercept term and regression coefficient; expressed otherwise, both mean-sea-level rainfall and its rate of increase with altitude are significantly below the

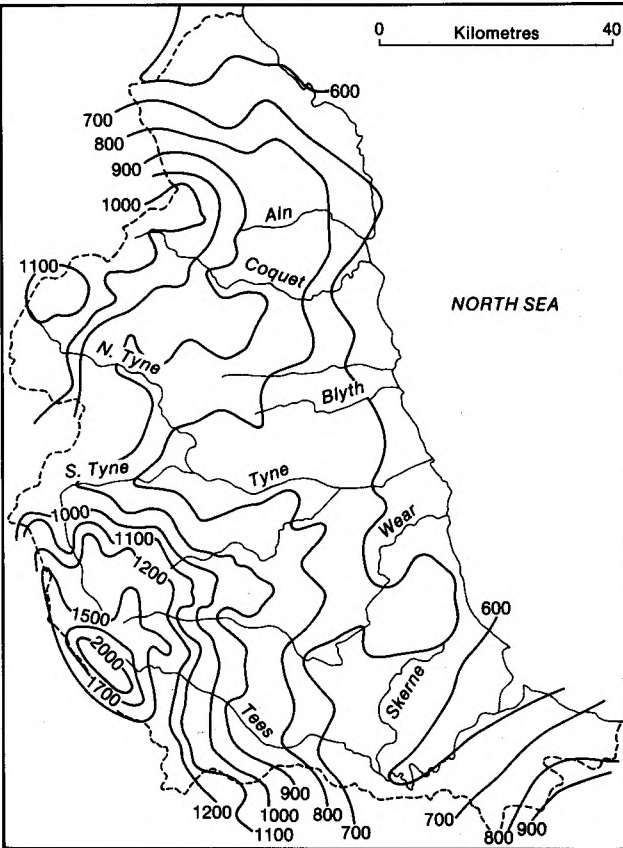


Figure 2. Isohyets of mean annual rainfall (mm) over north-east England.

national average and are an expression of the shelter from the rain-bearing westerlies.

2.2 Monthly rainfall

Variations between mean monthly rainfall–altitude associations have not received the wide attention given to annual data. Nevertheless the level of inter-monthly variation in average rainfall is in the order of 100 per cent and is matched by equally important variations in the relationships between rainfall and height. Regression and correlation coefficients are at a maximum in winter but a minimum in summer (Table II and Fig. 3). This result confirms Chuan and Lockwood’s findings for the Yorkshire region and suggests it to be more than a local phenomenon. No published data exist to permit comparison with other regions of Britain. The nearest attempt at a corresponding exercise was that by Bleasdale and Chan (1972) who merely observed that winter (November to February) showed an ‘intensification’ of the rainfall–altitude correlation.

It should be emphasized that the similarity between monthly regression and correlation coefficient trends cannot be dismissed on statistical grounds and that the two parameters measure different aspects of the same bivariate population. This is important because it means that, for example, winter rainfall is not only more closely correlated with altitude but the rate at which it

Table I. Regression models of mean annual rainfall (*Y*) against elevation (*X*) for the United Kingdom and some of its regions. Coefficients of explanation (*r*²) and correlation (*r*) are also given. Heights are in metres AMSL and rainfall in millimetres.

Region	Regression equation	<i>r</i> ² (<i>r</i>)
North-east England	<i>Y</i> = 552.07 + 1.776 <i>X</i>	0.76 (0.87)
Yorkshire	<i>Y</i> = 564.27 + 2.024 <i>X</i>	0.71 (0.84)
Mid-Wales*	<i>Y</i> = 868.2 + 1.667 <i>X</i>	0.71 (0.84)
United Kingdom	<i>Y</i> = 714.0 + 2.42 <i>X</i>	n/a

* Equation originally expressed in imperial units.

Table II. Correlation and regression analyses for mean monthly rainfall, *Y* (mm), and altitude, *X* (metres AMSL), in north-east England. In all cases the associations are significant at the 0.01 probability level.

Month	<i>r</i> ² (<i>r</i>)	Regression equation	Standard error of estimate of <i>Y</i> (mm)
January	0.79 (0.89)	<i>Y</i> = 44.59+0.188 <i>X</i>	15.46
February	0.82 (0.90)	<i>Y</i> = 35.77+0.163 <i>X</i>	12.18
March	0.79 (0.89)	<i>Y</i> = 27.39+0.134 <i>X</i>	10.79
April	0.77 (0.88)	<i>Y</i> = 30.38+0.127 <i>X</i>	10.98
May	0.68 (0.82)	<i>Y</i> = 42.43+0.104 <i>X</i>	11.32
June	0.62 (0.79)	<i>Y</i> = 41.73+0.086 <i>X</i>	10.25
July	0.47 (0.69)	<i>Y</i> = 54.35+0.094 <i>X</i>	15.57
August	0.62 (0.79)	<i>Y</i> = 67.19+0.145 <i>X</i>	17.71
September	0.73 (0.85)	<i>Y</i> = 46.94+0.160 <i>X</i>	15.44
October	0.76 (0.87)	<i>Y</i> = 39.48+0.178 <i>X</i>	15.79
November	0.77 (0.88)	<i>Y</i> = 53.35+0.191 <i>X</i>	16.18
December	0.75 (0.86)	<i>Y</i> = 36.97+0.205 <i>X</i>	18.76

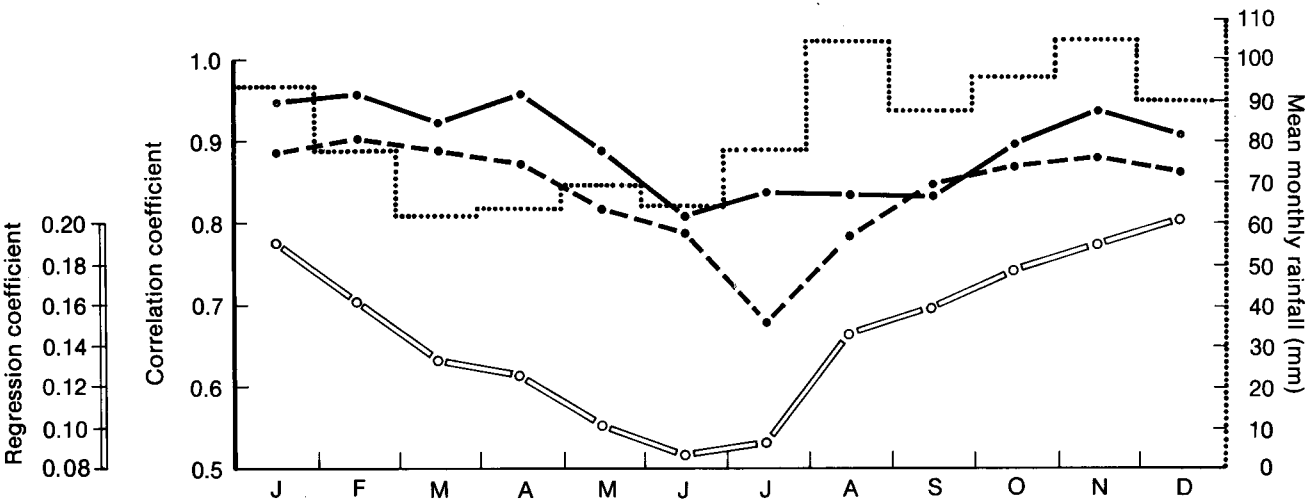


Figure 3. Graph showing variations throughout the year in regression coefficients (hollow line) and correlation coefficients (dashed line) between altitude and mean monthly rainfall in north-east England. Chuan and Lockwood’s (1974) correlation coefficients for the nearby Yorkshire region are also shown (solid line). Mean monthly rainfalls in north-east England are shown by means of the superimposed bar graph.

increases with height is also more marked. On the other hand summer rainfall is less well correlated with altitude and simultaneously rises less quickly with elevation. Hence conclusions drawn from annual data may disguise important monthly and seasonal variations even in climates normally regarded as having a well distributed rainfall regime.

3. Spatial patterns of rainfall

Trend surface analysis allowed the geographical character of annual and monthly mean rainfall to be studied. The methodology is well described in King (1967) and need not be reviewed here other than to add that the use of a ‘buffer’ zone of points around but beyond the limit of study was impossible in the absence of rainfall data from the North Sea.

The spatial dimensions were defined in Ordnance Survey (OS) grid references to give ‘eastings’ (X coordinate) and ‘northings’ (Z coordinate). The linear trend surface model is given by

Y = a + bX + cZ

where Y is mean rainfall and a, b, and c the constants.

Using the linear surface (Table III) the degree of variance explanation of rainfall is less than that obtained by a simple regression model based on altitude. On an annual basis the respective coefficients of explanation (*r*²) are 0.76 and 0.65. However the quadratic and cubic models allow more flexibility in the fitted surface by using polynomial instead of linear expressions of the relationship between rainfall and location (Figs 4 to 6). The quadratic surface is described thus;

Y = a + bX + cZ + dX² + eXZ + fZ²

and the cubic surface is given by;

Y = a + bX + cZ + dX² + eXZ + fZ² + gX³ + hX²Z + iXZ² + jZ³.

With these expressions the degree of variance explanation is significantly improved from that obtained using the rainfall–altitude regression models (Table III). At the same time the pattern of greater winter, but decreased summer, degrees of variance explanation persist in the quadratic model. To paraphrase the findings, winter rainfall has a more clearly defined spatial pattern than does that of summer. Comparison with Unwin’s (1969) work is difficult as the latter was carried out using ‘equivalent (sea level) precipitation estimates’ rather than the raw data. Given that Unwin had standardized his rainfall data prior to trend-surface analysis the results in Table III can only be seen as favourable. The quadratic and cubic surfaces in particular fall only little short of the efficiency of Unwin’s models. This finding also suggests the difficulty

Table III. Trend surface analysis data for mean monthly and annual rainfall in north-east England. SEE is the standard error of estimate of rainfall (mm) and *r*² is the coefficient of explanation. In all cases the surfaces are significant at the 0.01 level.

Month	Linear		Quadratic		Cubic	
	<i>r</i> ²	SEE	<i>r</i> ²	SEE	<i>r</i> ²	SEE
January	0.66	19.45	0.80	15.08	0.82	13.24
February	0.67	16.37	0.78	13.47	0.82	11.44
March	0.67	13.59	0.80	10.61	0.84	8.98
April	0.67	13.10	0.81	10.06	0.83	8.70
May	0.63	12.14	0.75	10.06	0.79	8.62
June	0.56	11.28	0.72	9.13	0.77	7.69
July	0.55	14.43	0.76	10.73	0.80	8.92
August	0.61	18.13	0.75	14.69	0.78	12.75
September	0.69	16.48	0.81	12.30	0.85	10.73
October	0.65	18.96	0.82	13.72	0.85	11.72
November	0.61	21.30	0.76	16.81	0.80	14.36
December	0.67	21.40	0.84	14.97	0.86	13.02
Annual	0.65	188.4	0.80	145.3	0.82	126.8

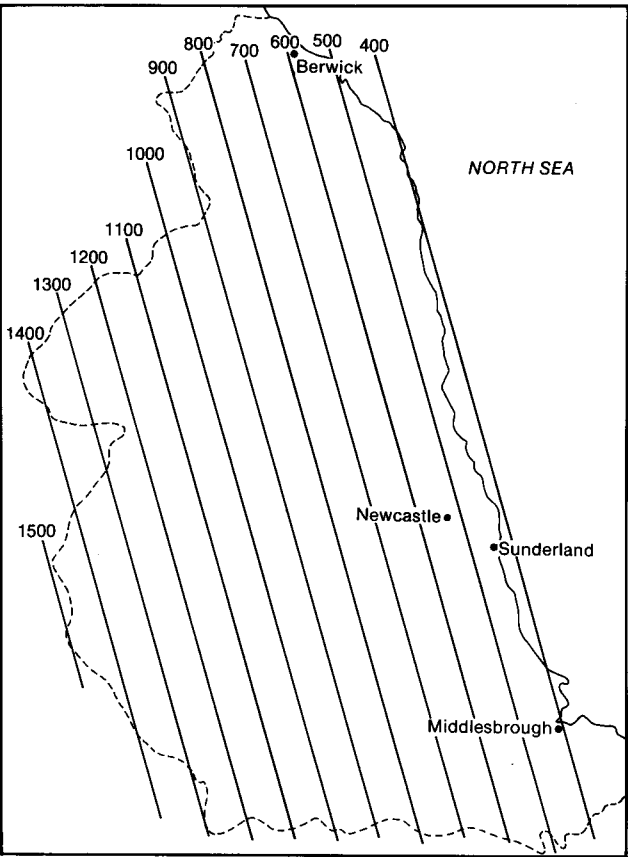


Figure 4. Linear trend surface for mean annual rainfall (mm) in north-east England.

of modelling the complex geography of local rainfall in an area such as Snowdonia a point which Unwin himself emphasized.

4. Multiple regression models of rainfall

In the present study both northings (with *r* = +0.22) and eastings (with *r* = −0.69) are significantly correlated

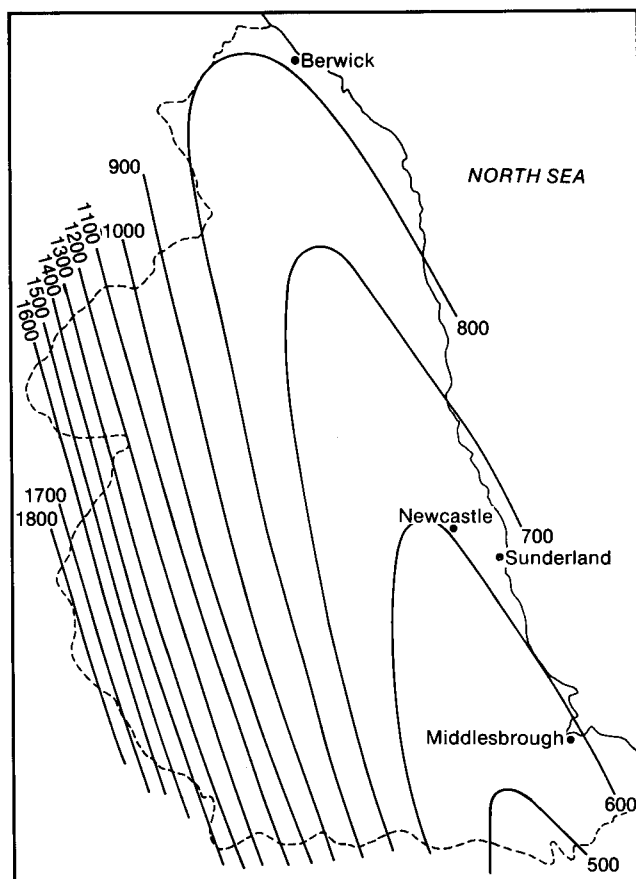


Figure 5. Quadratic trend surface of mean annual rainfall (mm) in north-east England.

with altitude, i.e. altitude increases both northwards and westwards. In order to unravel the intercorrelations between the three variables the trend surface and regression approaches can be combined to employ altitude and the two spatial dimensions. In the linear case the method is one of straightforward multiple regression. In the higher-order polynomial quadratic and cubic treatments of the spatial coordinates the regression equation becomes a polynomial expression combined with a linear altitudinal component. The r^2 values of these models were, for all monthly and the annual data, above 0.83. While such a high order of variance explanation gives confidence in spatial interpolation between known points, they are less helpful when attempting to reveal the underlying trends from the inherently variable picture which nature presents to us. Attention is concentrated initially, therefore, on the simplest model

$$Y = a + bU + cX + dZ \quad (1)$$

where Y is mean monthly or annual rainfall, U is the altitude, and a , b , c and d are constants or partial regression coefficients. The annual pattern of rainfall predicted from this model is shown in Fig. 7 and can be compared with the isohyets in Fig. 2. The pattern of positive and negative residuals shows a degree of spatial autocorrelation in which the model underestimates the

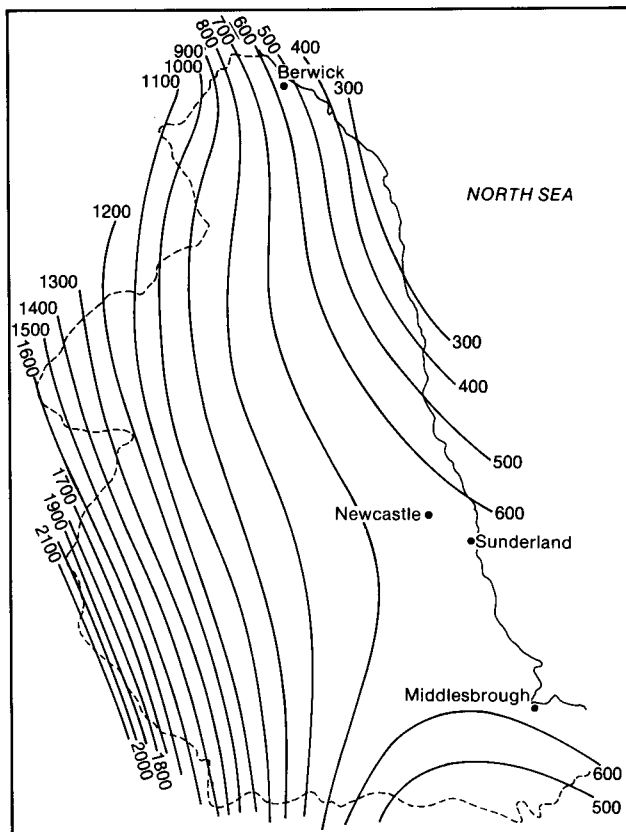


Figure 6. Cubic trend surface of mean annual rainfall (mm) in north-east England.

rainfall in eastern districts generally and also on the highest ground of the Pennines in the far west of the region. No additional variable could be found to significantly reduce the degree of residual autocorrelation, indeed the very high coefficients of explanation associated with this model (Table IV) forcefully suggest that such a variable may not exist.

More usefully, the partial regression coefficients and beta weights gave a measure of the variables' independent contributions to rainfall; a contribution that again varies through the year (Table IV). It might be anticipated that the inclusion of altitude would render the spatial dimensions of marginal importance. Such, interestingly, was not the case. All the partial coefficients for altitude and eastings (longitude), and most for northings (latitude), are significant at the 0.05 level.

The partial regression coefficients for altitude are, as expected, smaller than their zero-order counterparts. The latter, however, measure the net regional effect of altitude on rainfall irrespective of other variables such as location, while the former measure the rate of rainfall change with height but with the locational element 'fixed' or 'controlled' but not removed. This change notwithstanding, the annual rhythm is again encountered with its now characteristic winter maximum and summer minimum.

The partial regression coefficients for eastings (which because of the geography of the high ground is all but

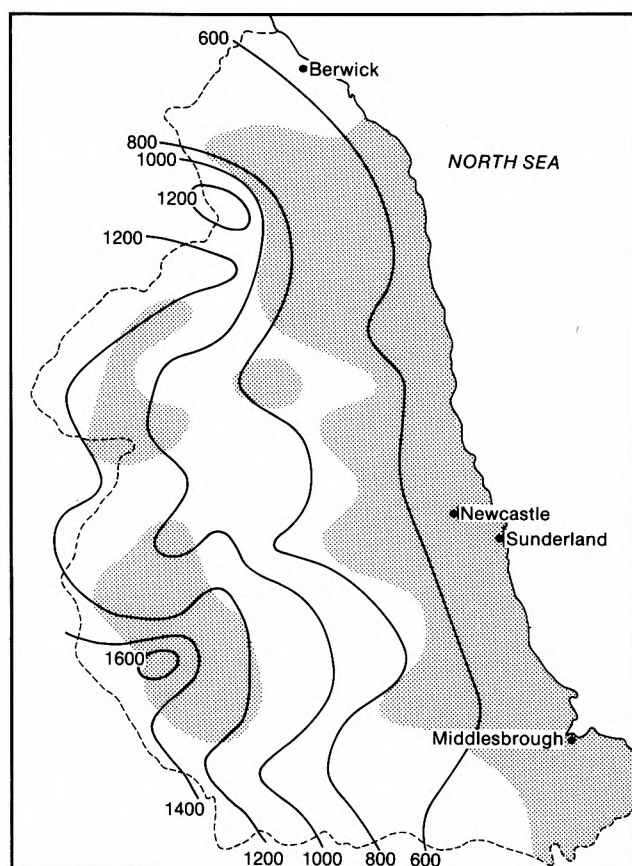


Figure 7. Map of modelled annual rainfall (mm) in north-east England based on a multiple regression model using height, eastings and northings as the independent variables. The stippled areas are those of positive residuals — clear areas are negative.

identical with distance from the Pennine watershed) are also significant. In this case it is altitude and longitude that are ‘controlled’ yet rainfall continues to decline eastwards along imaginary lines of constant elevation (and at rates indicated by the coefficients themselves). The effect is secondary to the altitudinal control, but is nonetheless important. Chuan and Lockwood (1974) also examined the effect of distance from the Pennine divide in Yorkshire, and found a corresponding relationship, but they did not examine its monthly character which here again shows variation with a more rapid eastwards decline in rainfall during the autumn and winter, but a less marked tendency during the spring and summer. In Unwin’s (1969) Snowdonia study eastings, in contrast, played no significant role in the rainfall model.

No less intriguing is the pattern of rainfall change northwards. Again it is subordinate to altitude, but statistically significant in all but 3 months (May, June and September). The partial coefficients show the degree of rainfall change along imaginary longitudinal lines of fixed altitude. The magnitude of this effect again varies between the months. In summer it is positive, i.e. the rainfall tends to increase northwards, but at other times of the year it is negative, the rainfall tending to decrease northwards. The net effect is to obscure the

importance of this dimension in the annual model where the partial coefficient is not significant. It can thus be demonstrated that the statistical and, by inference, climatological roles of the two spatial dimensions and altitude are independently exercised and to degrees that differ through the year.

Finally, turning back to the issue of modelling which seeks to reproduce reality and not necessarily simplify it, mention can be made of the most efficient of the models under study. These are the trend surface quadratic and cubic expressions containing an additional linear term for altitude. In respect of degrees of variance explanation these are unquestionably the most efficient, as Table IV demonstrates, and might well be the preferred tool of the hydrologist concerned more with extending rainfall records across areas of interest rather than with climatological investigation. They persist also in showing a less ordered scheme of rainfall in summer compared with that of winter, though the detailed rhythms are less clear. But such is the very character of these models that these underlying trends, so persuasively distilled in the simple models, are obscured in the variability that they permit. From this point of view climatologists might argue that the models are less useful having forsaken simplification for reproduction and inevitable complication.

5. The climatology of the region’s rainfall

The above findings reaffirm the importance of altitude as a control on rainfall, but the degree of control was shown to vary. The summer minimum reflects the activity of convectionally driven rainfall which, by its very nature, is spatially random and less influenced by altitude than the winter cyclonic rainfall with its large-scale vertical motions, particularly within the humid warm sectors, over the Pennines. At the same time there is also a significant, and independent, locational element. Rainfall can be seen to decrease eastwards, even when the effect of altitude is ‘controlled’. The average annual effect is a 490.66 mm decrease for every 100 km eastwards (100 km is the co-ordinate unit used in the models). The partial regression coefficient represents the rainfall change per unit distance, and here quantifies the rate of rainfall decrease eastwards; the loss of moisture through precipitation not being made up by evaporation or transpiration gains from the surface — it is, in fact, an acknowledgement of the ‘rain shadow’ effect isolated from the altitudinal influence. It appears, once again to be less well marked during the summer months. The influence varies between a 61 mm per 100 km decrease in December to only 23 mm per 100 km decrease in June. Northings or latitude, also exercise an independent influence. In August this reaches a peak of 18.68 mm per 100 km northwards increase, declining to a 29.4 mm per 100 km northwards decrease in December. Rainfall is known (Sawyer 1956) to decrease away from cyclonic centres. Given that depressions generally adopt eastward routes to the north of Britain in summer, but

Table IV. Partial regression coefficients used to predict mean annual and monthly rainfall (mm) in north-east England. The predictor variables are Ordnance Survey eastings and northings (expressed in units of 100 km) and station altitude (m). Multiple regression equation (1) was used to derive these monthly and annual models. Only those coefficients marked (*) are not significant at the 0.05 level. The three columns of r^2 values are for the (a) linear (equation 1), (b) spatial quadratic plus linear altitude, and (c) spatial cubic plus linear altitude models. Figures in parentheses beneath the partial regression coefficients are their respective beta weights (measures of their relative importance).

Month	Partial regression coefficients			r^2		
	Easting	Northing	Altitude	(a)	(b)	(c)
January	−48.53 (−0.29)	−14.08 (−0.12)	0.1398 (0.66)	0.82	0.91	0.92
February	−31.54 (−0.22)	−19.18 (−0.20)	0.1271 (0.70)	0.84	0.90	0.92
March	−30.12 (−0.26)	−17.99 (−0.23)	0.0999 (0.66)	0.83	0.91	0.92
April	−35.34 (−0.31)	−15.05 (−0.20)	0.0891 (0.62)	0.86	0.90	0.92
May	−32.43 (−0.33)	5.55* (0.08)	0.0777 (0.61)	0.76	0.87	0.91
June	−23.32 (−0.28)	4.33* (0.08)	0.0676 (0.62)	0.70	0.84	0.86
July	−37.35 (−0.35)	14.21 (0.20)	0.0664 (0.49)	0.63	0.83	0.90
August	−41.00 (−0.29)	18.68 (0.19)	0.1163 (0.63)	0.75	0.87	0.91
September	−61.44 (−0.42)	−10.37* (−0.11)	0.1012 (0.54)	0.79	0.90	0.92
October	−49.78 (−0.31)	−14.32 (−0.13)	0.1283 (0.63)	0.79	0.92	0.93
November	−35.92 (−0.21)	−11.42 (−0.10)	0.1545 (0.71)	0.79	0.89	0.91
December	−61.25 (−0.33)	−29.41 (−0.24)	0.1389 (0.59)	0.79	0.92	0.93
Annual	−490.66 (−0.31)	−87.67* (−0.08)	1.3066 (0.64)	0.79	0.90	0.92

shift southwards in winter, then the form of annual rhythm shown for the latitudinal effect would follow as a matter of course.

6. Conclusion

The results demonstrate clearly that, in this case at least, order in rainfall regimes and distributions can be both recognized and quantified to the advantage of hydrologists and climatologists. Spatial (trend-surface) models of quadratic and cubic form are preferred to regression models using spot heights, but the most efficient methods combine all three dimensions, height, latitude and longitude. It has also been shown that monthly models might be preferred to annual models when detailed reconstruction interpretations are sought.

References

Barry, R.G., 1963: Aspects of the synoptic climatology of central south England. *Meteorol Mag*, **92**, 300–308.

Bleasdale, A. and Chan, Y.K., 1972: Orographic influences on the distribution of precipitation. *In* Distribution of precipitation in mountainous areas. Geilo Symposium, Norway, 31 July–5 August 1972. Geneva, WMO, No. WMO.326.

Chuan, G.K. and Lockwood, J.G., 1974: An assessment of topographical controls on the distribution of rainfall in the central Pennines. *Meteorol Mag*, **103**, 275–287.

Jackson, I.J., 1969: Pressure types and precipitation over north-east England. University of Newcastle. Dept. of Geography, Research Series No. 5.

King, C.A.M., 1967: An introduction to trend surface analysis. University of Nottingham, Dept. of Geography, Bulletin of quantitative data for geographers, No. 12.

Manley, G., 1935: Some notes on the climate of north-east England. *QJR Meteorol Soc*, **61**, 405–410.

Rodda, J.C., 1962: An objective method for assessment of areal rainfall amounts. *Weather*, **17**, 54–59.

Salter, M. de C.S., 1918: The relation of rainfall to configuration. *In* British Rainfall 1918. London, British Rainfall Organization.

Sawyer, J.S., 1956: Rainfall of depressions which pass eastward over or near the British Isles. *Prof Note, Meteorol Off*, No. 118.

Trotter, F.M., 1929: The Tertiary uplift and resultant drainage of the Alston block and adjacent areas. *Proc Yorkshire Geol Soc*, **21**, 161–180.

Unwin, D.J., 1969: The areal extension of rainfall records: an alternative model. *J Hydrol*, **7**, 404–414.

The spring of 1989 in the United Kingdom

G.P. Northcott

Meteorological Office, Bracknell

Summary

Spring was a season of some contrasts with a very cool April in most places, but a warm March and May; a very wet March over central and western areas of Scotland, and a very wet April in central England, then followed by a very dry May, exceptionally so in southern England, with record-breaking sunshine amounts.

1. The spring as a whole

Mean temperatures were below the seasonal normal in Northern Ireland and western parts of Scotland, but above normal everywhere else in the United Kingdom, ranging from 1.5 °C above normal in places in Kent and East Sussex to 0.4 °C below normal at Isle of Rhum, Western Isles.

Spring rainfall amounts were above normal over most of the United Kingdom although some eastern areas had well below average rainfall; however, the 153% of normal at Fort Augustus, Highland Region in the west contrasted somewhat with about 60% of normal around Newcastle upon Tyne in the east.

Spring sunshine amounts were about normal everywhere in the United Kingdom varying from around 90% in a few western areas to over 130% in the north Midlands.

Information about temperature, rainfall and sunshine during March–May 1989 is given in Fig. 1 and Table I.

2. The individual months

March. Mean monthly temperatures were generally above normal, ranging from near normal in the north and west of Scotland to more than 2.5 °C above normal

just to the north of London. Much of East Anglia and south-east England had a very warm day on the 6th, one of the warmest early March days this century, with highest temperatures of 16 to 18 °C. On the 31st London Weather Centre measured 19.9 °C, the highest March temperature there for 21 years.

Monthly rainfall amounts were above normal in most parts of the United Kingdom with more than two and a half times the normal rainfall at Glasgow, Strathclyde Region. In contrast some eastern coastal areas of England and Scotland were rather dry and Newcastle upon Tyne had less than a third of its normal rainfall.

Sunshine amounts were generally above normal in Scotland, Northern Ireland and northern England but below normal in southern areas. The brightest area was eastern Scotland and north-east England with more than 120% of normal while south-west England and South Wales were generally rather dull with less than 80% of average sunshine.

The month started somewhat cool and windy but bright, then became unsettled and generally milder, with rain, persistent and heavy at times, and brighter showery interludes. Between the 20th and 23rd wintry conditions

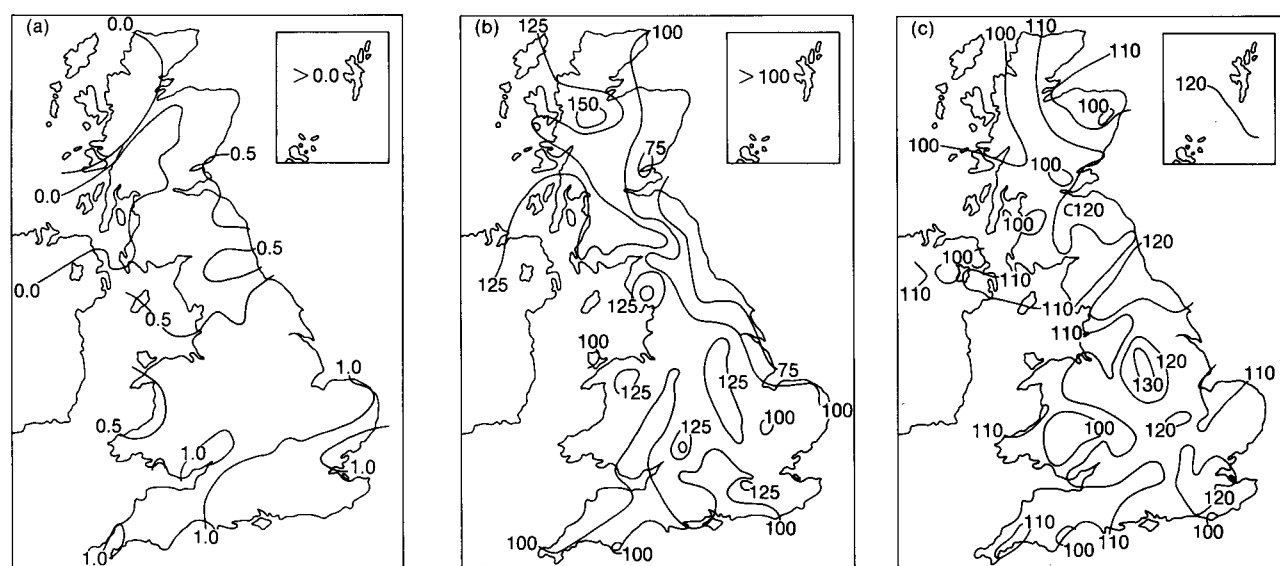


Figure 1. Values of (a) mean temperature difference (°C), (b) rainfall percentage and (c) sunshine percentage for spring, 1989 (March–May) relative to 1951–80 averages.

Table I. District values for the period March–May 1989, relative to 1951–80 averages

District	Mean temperature (°C)	Rain-days	Rainfall	Sunshine
	Difference from average		Percentage of average	
Northern Scotland	0.0	+2	108	104
Eastern Scotland	+0.3	0	98	113
Eastern and north-east England	+0.6	0	93	114
East Anglia	+0.9	0	106	110
Midland counties	+0.9	0	112	111
South-east and central southern England	+1.3	0	108	110
Western Scotland	−0.1	+2	111	105
North-west England and North Wales	+0.6	+1	120	109
South-west England and South Wales	+0.9	0	102	105
Northern Ireland	−0.1	+2	125	103
Scotland	+0.1	+1	110	107
England and Wales	+0.8	0	107	110

Highest maximum: 29.4 °C in south-east and central southern England in May.
Lowest minimum: −7.9 °C in western Scotland in March.

with snow and sleet and some hail pushed southwards from Scotland, temporarily reaching as far south as east Kent. After the 23rd the rest of the month became gradually more settled as the high pressure over the near Continent became established.

April. Mean monthly temperatures were below normal nearly everywhere in the United Kingdom, the main exception being Lerwick, Shetland with 0.2 °C above normal; at Exeter, Devon the mean temperature was nearly 2 °C below normal. At Oxford the mean monthly temperature was 1.3 °C below the normal; only 1903 and 1972 were lower in 109 years of records. Broom's Barn, Suffolk reported that the afternoon temperature of 5.2 °C on the 24th was the lowest maximum recorded in the last 10 days of April since the station opened in 1963. The temperature of 15.1 °C at Hampstead, Greater London on the 1st was the lowest April maximum there since 1972. Halesowen, West Midlands reported the lowest maximum since 1978 and the lowest night minimum since 1968.

Monthly rainfall totals were above normal in most places in England, Wales and Northern Ireland, but in many parts of Scotland amounts were below normal, as little as 40% at Kinlochewe, Highland Region. In contrast, Wyton, Cambridgeshire had more than 250% of normal. Wingerworth, Derbyshire reported the wettest April for 20 years. Hampstead, Greater London had the wettest April since 1983 and Coventry School (Bablake), Warwickshire the wettest since 1920.

Sunshine amounts were below average nearly everywhere, the exceptions being parts of central southern England, south-west England and southern and western Wales where sunshine was slightly above average, ranging from about 70% of normal in south-east England to 109% of normal at Plymouth, Devon and Aberporth, Dyfed.

April was generally cool and unsettled, with rain or showers at times. Snow occurred in many places in the

first week, especially on the 5th with some reports of blizzard conditions over higher ground. On the 7th a golfer was struck by lightning at Southampton and badly burned. A mean wind of 49 kn was recorded at Milford Haven, Dyfed on the 11th, with a new record gust for April of 84 kn, while Aberporth recorded a gust of 78 kn, the highest April gust there for over 50 years. The strong winds brought chaos to the roads, and battered ships in the Irish Sea, blew down trees and caused structural damage to buildings throughout Wales. Thousands of homes in Devon and Cornwall and south-west and central Wales were without power after falling trees brought down overhead power cables. On the 13th Halstead, Essex had a violent thunderstorm with heavy rain and hail between 1830 and 2015 and local flooding; hail lay to a depth of 5 cm for a while.

May. Monthly mean temperatures were above normal in all areas, ranging from just above normal in parts of western Scotland to more than 3 °C above normal in the London area. The overall mean temperature of 14.4 °C and the maximum of 19.7 °C at Hampstead, Greater London were the highest for May since records began there in 1909; at Oxford the mean temperature was the highest since May 1952. On the 21st the temperature at Kinlochewe, Highland Region reached 27.4 °C and at Cape Wrath, Highland Region a maximum of 24.4 °C was recorded, the highest May value in a record that goes back to 1940. On the 24th the temperature at Wyton reached 28.4 °C, the hottest May day at the station since records began in 1954. The mean temperature at Newtown Linford, Leicestershire was the highest for May at the station for 25 years. It was the warmest May recorded at North Wyke, Devon since the record began in 1960.

Rainfall was well below average except in some north-eastern parts of Scotland where it was nearer normal, reaching 104% at Lerwick, Shetland. Parts of eastern and southern England were particularly dry although

local thundery outbreaks produced variable amounts of rain; for example Farnborough, Hampshire received 117% of its May average, while London Weather Centre, 50 km away had only 2%. Central London had its driest May for about 300 years and over England and Wales as a whole it was the driest May since 1896. Many places in the south and east had less than 10 mm of rain and a number of places in Kent including Manston and Ulcombe had less than 1 mm and Faversham and Herne Bay were among several places reporting nil rainfall. Ryhope, Co. Durham and Letheringham, Suffolk also reported nil rainfall. Worthing, East Sussex and Durham had the driest May since records started there in 1902 and 1886, respectively. At Oxford, about 95% of the month's rain fell during a thunderstorm on the 24th. On the same day 63 mm fell at Mickleham, Surrey and 60 mm at South Farnborough, Hampshire.

Monthly sunshine amounts were above normal over the whole of United Kingdom, reaching 163% of the average in central London, but only just above normal, 102%, at Benbecula, Western Isles. Some places measured record amounts of sunshine, with most places

south of a line from south Devon to north Norfolk measuring in excess of 300 hours; the last time such a large area of the United Kingdom experienced sunshine totals of over 300 hours in May was probably 1909. Oxford reported the highest May sunshine amount (301 hours) in 110 years of record.

The month was warm, dry and sunny generally. However, thunderstorms developed over East Anglia on the 11th and 12th and north-west England and North Wales on the 19th when a flash flood at Halifax, West Yorkshire caused considerable damage. On the 20th and 21st there were thundery showers in the south-west; on the 22nd thunderstorms developed over southern England and moved north-westwards. On the 23rd and 24th widespread thunderstorms brought floods to central and southern England, the Midlands and northern areas. On the 24th Easthampstead, Berkshire recorded hailstones up to 23 mm in diameter. A marked dust devil was reported at Hurst Green near Oxted, Surrey during the afternoon of the 9th. It lifted garden furniture and raised a child's metal slide 4 m into the air and carried it nearly 12 m.

Review

The human impact of climate uncertainty, by W.J. Maunder. 154 mm × 233 mm, pp. xxv+170, *illus.* London, New York, Routledge, 1989. Price £10.95 (paperback), £25.00 (hardback).

The author introduced the field of economic climatology to the scientific community in *The value of weather* (1970) and to the business community in *The uncertainty business* (1986). In the current volume he presents a broad view to the non-specialist of the role of weather and climate information in economic, social and political decision making.

The author presents the simple, infancy state of this topic as it exists and a proposed future in which the variable nature of the atmosphere must be acknowledged as an integral part of resource management. As an important component of the Earth's resources the atmosphere must be monitored carefully, its interaction with other components investigated and the value of weather/climate information assessed. The need for this work and progress so far forms the main theme of this book. There are 11 chapters, many examples mostly from New Zealand or the USA and extensive, up-to-date bibliographies.

The first two chapters examine the conflicting views of those who see economic climatology as 'non

scientific', hence inherently undesirable and of little use, and those who regard it as beneficial and essential in a world of increasing population, pressure on resources and sensitivity to weather variations. An historical review of the development of climatology from static description to an evolving and interactive component of decision making is discussed.

Chapters III to V form a crucial foundation for subsequent chapters. Firstly the components of the atmospheric resource and the concept of limitation or adaptive responses to specific changes in this resource are outlined. The international institutional framework for atmospheric matters is considered. Current climate-change issues such as greenhouse warming are reviewed briefly and used to illustrate political implications of climate change. These are then set within the decision-making framework. Dissemination of climate/weather information from the scientist to the decision maker is critically evaluated and the value of this information as opposed to weather sensitivity itself is stressed. Facilities for monitoring and forecasting weather/climate are introduced and a severe criticism raised that the research in this area is not yet being matched adequately by that in application and sensitivity analysis.

A chapter on climate impacts and sensitivities is very general although it has useful forward references to

examples in later chapters. It is stressed that the meteorologist must express sensitivities in a usable form.

Probably one of the most interesting and important topics is that of commodity-weighting weather data with respect to its economic influence for decision making. Weather anomalies are assessed in terms of the spatial distribution of the anomaly relative to that of commodity production and the contribution of the commodity to the national economy. This is illustrated well with examples from New Zealand and the USA.

Chapters VIII and IX illustrate the role of weather information in management and planning in agriculture, electricity production, manufacturing, retail trade, construction and transport. Each section is in itself a fairly cursory overview of the specific topic but are illustrated by many examples from around the world.

This theme is built up on in chapter X. Here the author suggests the current and future role of weather information in production forecasting and assessment

by use of commodity weighted weather/climate information in explanatory or empirical models.

The book is concluded in chapter XI (which is confusingly numbered IX) with a look to the future of this topic. It begins with an imaginative futuristic agenda for a day in the life of a weather administrator in 1994. It is envisaged that, within a decade, meteorologists must be making significant contributions to economic and political decisions.

The whole book is packed with exciting examples. A thorough, although sometimes repetitive, case is presented for increased effort to treat the atmosphere as a valuable resource to incorporate weather/climate information in political and economic decision-making. It is an interesting and challenging introductory text for non-specialists in this field, but any specialist in the many contributory disciplines may be disappointed by the depth of discussion in their particular field.

M.F. Mylne

Satellite photographs — 24 January 1990 at 1515 UTC and 25 January 1990 at 0330 and 1325 UTC

The photographs in Figs 1 to 3 were taken at approximately 12-hour intervals during cyclogenesis of the storm that caused extensive wind damage and loss of life over southern Britain on 25 January 1990. The locations of the superimposed synoptic features are based on evidence derived from imagery and conventional surface data (interpolated where necessary using data from main synoptic hours).

The cloud pattern on the visible image (Fig. 1) suggests two distinct frontal zones — 'F' associated with the main jet stream, and 'P' being a secondary frontal zone forming in the cold air mass. The overall cloud area, encompassing cloud associated with both fronts, constitutes a 'cloud head' characteristic of impending explosive cyclogenesis and generation of hurricane force winds*.

During subsequent cyclogenesis (Figs 2 and 3) the wave on front 'F' gradually sharpens, but the part of the front 'P' behind the low accelerates around the right flank of the low

so as to leave a core of warm air near its centre. This also occurred during development of the October storm of 1987† and in each of the intense depressions that crossed southern and central Britain during the stormy period of January and February 1990. The most active front (in terms of thermal contrast) was always the 'bent-back' warm front (not an occlusion) around the left flank of the low, and the strongest winds (stippled area in Fig. 4) always occurred at and behind the secondary cold front 'P' in an area bounded by the bent-back front.

The frontal analyses shown here are consistent with thermal fields derived from the UK fine-mesh model. The warm core and bent-back front are clearly evident in the 850 mb wet-bulb potential temperature field shown in Fig. 4.

G.A. Monk

* Botger, H., Eckhardt, M. and Katargiannakis, U.; Forecasting extratropical storms with hurricane intensity using satellite information. *J Appl Meteorol*, 14, 1975, 1259–1265.

† Monk, G.A. and Bader, M.J.; Satellite images showing the development of the storm of 15–16 October 1987. *Weather*, 43, 1988, 130–135.

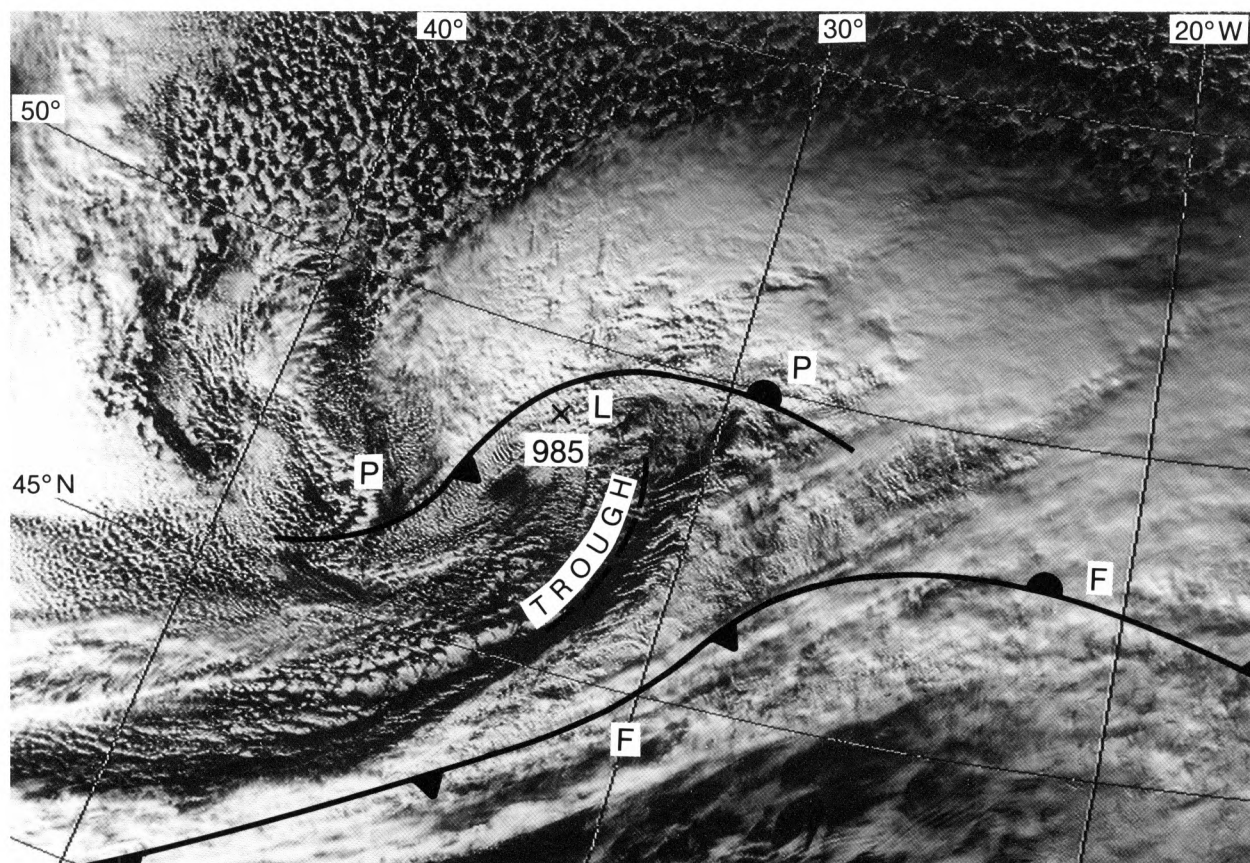


Figure 1. NOAA-11 visible image at 1515 UTC on 24 January 1990 with fronts and surface low superimposed.

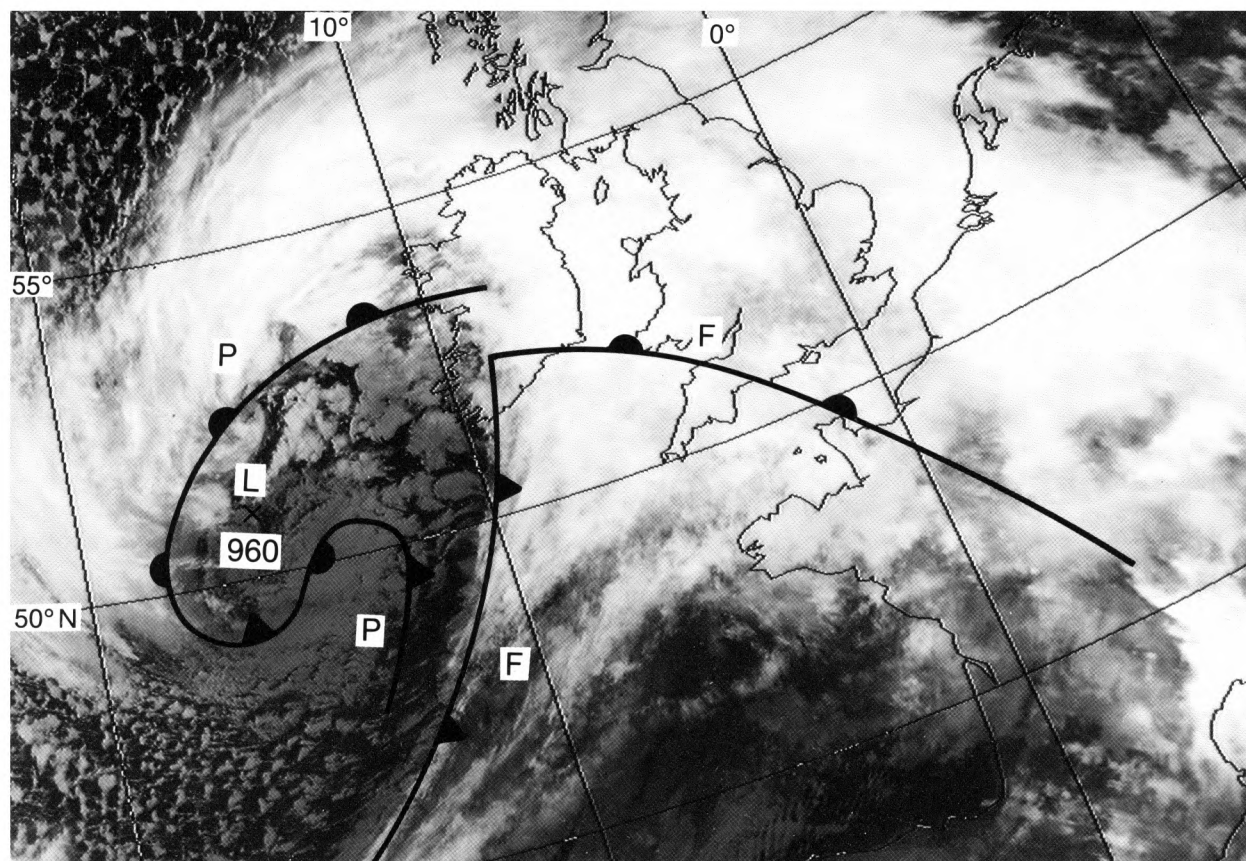
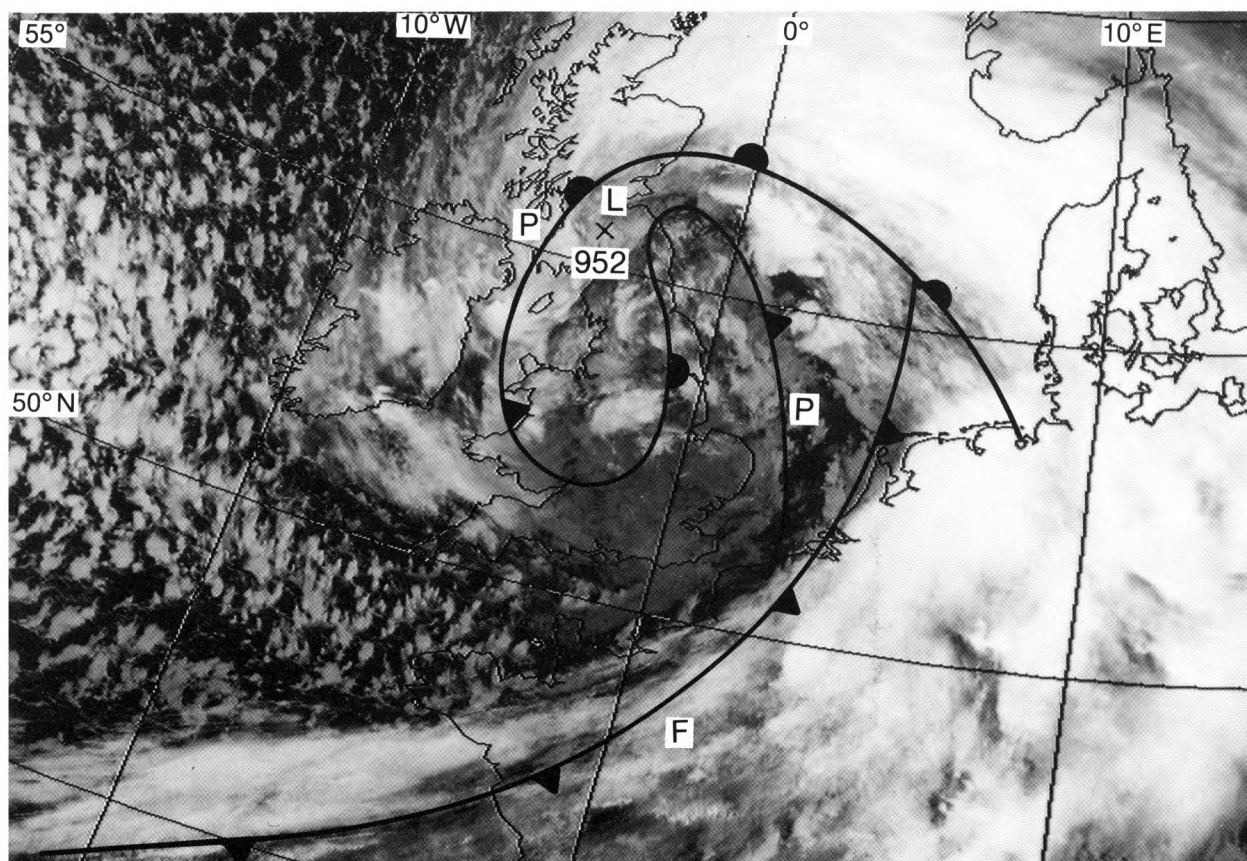


Figure 2. NOAA-11 infra-red image at 0330 UTC on 25 January 1990 with fronts and surface low superimposed.



Photographs by courtesy of University of Dundee

Figure 3. NOAA-11 infra-red image at 1325 UTC on 25 January 1990 with fronts superimposed.

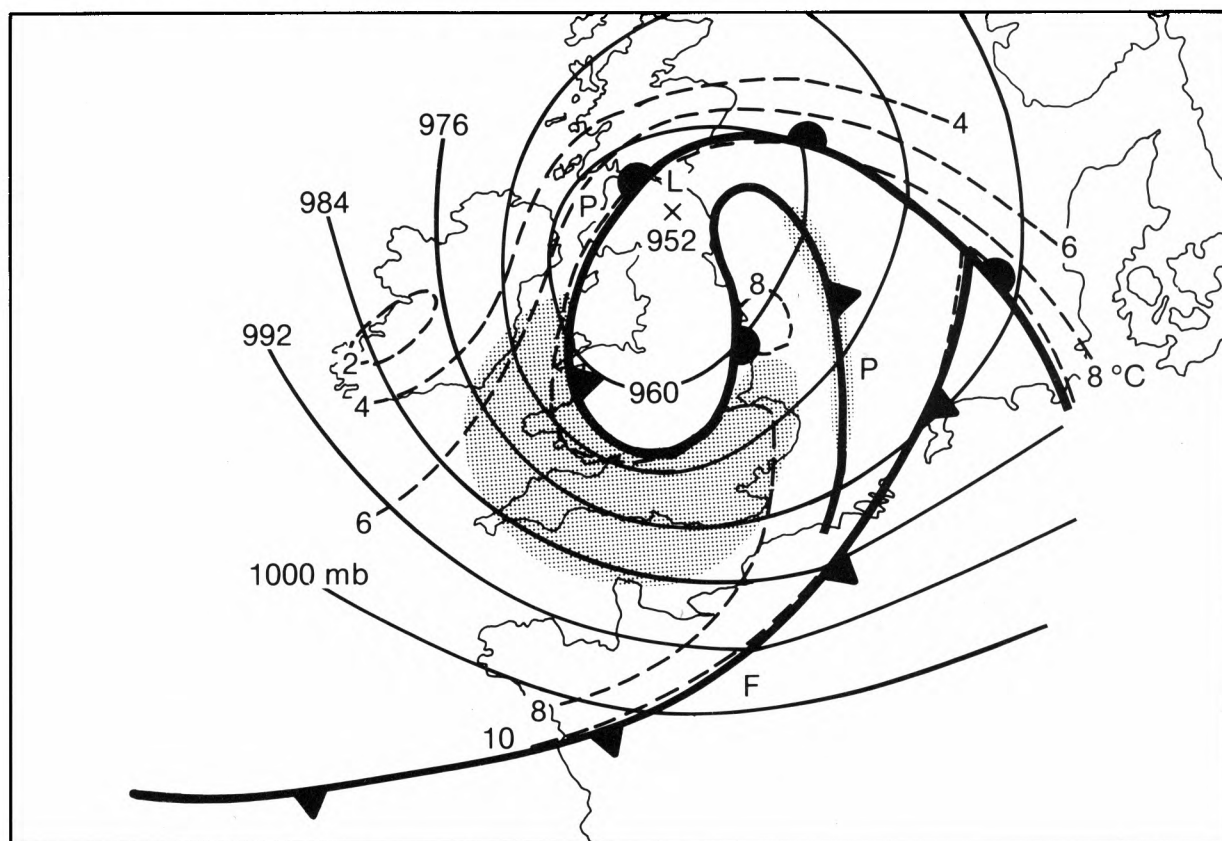


Figure 4. Surface isobars, isopleths of 850 mb wet-bulb potential temperature (°C) (dashed lines — from the 1200 UTC analysis of the fine-mesh model) and the region of strongest winds (stippled area) at 1300 UTC.

GUIDE TO AUTHORS

Content

Articles on all aspects of meteorology are welcomed, particularly those which describe results of research in applied meteorology or the development of practical forecasting techniques.

Preparation and submission of articles

Articles, which must be in English, should be typed, double-spaced with wide margins, on one side only of A4-size paper. Tables, references and figure captions should be typed separately. Spelling should conform to the preferred spelling in the *Concise Oxford Dictionary* (latest edition). Articles prepared on floppy disk (Compucorp or IBM-compatible) can be labour-saving, but only a print-out should be submitted in the first instance.

References should be made using the Harvard system (author/date) and full details should be given at the end of the text. If a document is unpublished, details must be given of the library where it may be seen. Documents which are not available to enquirers must not be referred to, except by 'personal communication'.

Tables should be numbered consecutively using roman numerals and provided with headings.

Mathematical notation should be written with extreme care. Particular care should be taken to differentiate between Greek letters and Roman letters for which they could be mistaken. Double subscripts and superscripts should be avoided, as they are difficult to typeset and read. Notation should be kept as simple as possible. Guidance is given in BS 1991: Part 1: 1976, and *Quantities, Units and Symbols* published by the Royal Society. SI units, or units approved by the World Meteorological Organization, should be used.

Articles for publication and all other communications for the Editor should be addressed to: The Chief Executive, Meteorological Office, London Road, Bracknell, Berkshire RG12 2SZ and marked 'For Meteorological Magazine'.

Illustrations

Diagrams must be drawn clearly, preferably in ink, and should not contain any unnecessary or irrelevant details. Explanatory text should not appear on the diagram itself but in the caption. Captions should be typed on a separate sheet of paper and should, as far as possible, explain the meanings of the diagrams without the reader having to refer to the text. The sequential numbering should correspond with the sequential referrals in the text.

Sharp monochrome photographs on glossy paper are preferred; colour prints are acceptable but the use of colour is at the Editor's discretion.

Copyright

Authors should identify the holder of the copyright for their work when they first submit contributions.

Free copies

Three free copies of the magazine (one for a book review) are provided for authors of articles published in it. Separate offprints for each article are not provided.

April 1990

Editor: B.R. May

Vol. 119

Editorial Board: R.J. Allam, R. Kershaw, W.H. Moores, P.R.S. Salter

No. 1413

Contents

	Page
Variation in the onset of the Indian south-west monsoon and summer circulation anomalies. I. Subbaramayya, S. Vivekananda Babu and C.V. Naidu	61
Modelling long-term rainfall patterns in north-east England. D. Wheeler	68
The spring of 1989 in the United Kingdom. G.P. Northcott	75
Review	
The human impact of climate uncertainty. W.J. Maunder. <i>M.F. Mylne.</i>	77
Satellite photographs — 24 January 1990 at 1515 UTC and 25 January 1990 at 0330 and 1325 UTC. G.A. Monk	78

Contributions: It is requested that all communications to the Editor and books for review be addressed to the Chief Executive, Meteorological Office, London Road, Bracknell, Berkshire RG12 2SZ, and marked 'For *Meteorological Magazine*'. Contributors are asked to comply with the guidelines given in the *Guide to authors* which appears on the inside back cover. The responsibility for facts and opinions expressed in the signed articles and letters published in *Meteorological Magazine* rests with their respective authors.

Subscriptions: Annual subscription £30.00 including postage; individual copies £2.70 including postage. Applications for postal subscriptions should be made to HMSO, PO Box 276, London SW8 5DT; subscription enquiries 071-873 8499.

Back numbers: Full-size reprints of Vols 1-75 (1866-1940) are available from Johnson Reprint Co. Ltd, 24-28 Oval Road, London NW1 7DX. Complete volumes of *Meteorological Magazine* commencing with volume 54 are available on microfilm from University Microfilms International, 18 Bedford Row, London WC1R 4EJ. Information on microfiche issues is available from Kraus Microfiche, Rte 100, Milwood, NY 10546, USA.

ISBN 0 11 728664 8

ISSN 0026-1149

© Crown copyright 1990. First published 1990

The Meteorological Magazine

May 1990

Met. Office mesoscale model
Radar study of snowfall in Cornwall



DUPLICATE JOURNALS

National Meteorological Library
FitzRoy Road, Exeter, Devon. EX1 3PB

HMSO

Met.O.992 Vol. 119 No. 1414



3 8078 0010 2480 3

The Meteorological Magazine

May 1990
Vol. 119 No. 1414

551.509.313:551.509.5(41)

The Meteorological Office mesoscale model

B.W. Golding

Meteorological Office, Bracknell

Summary

A description is given of the Meteorological Office's mesoscale (15 km grid-spacing) forecasting model. Results of verification of model (objective) forecasts against human (subjective) forecasts for a selection of weather elements are given.

1. Introduction

Numerical weather prediction models in current operational use give valuable guidance to forecasters on the broad-scale atmospheric structure. In the Meteorological Office a grid-length of about 150 km is used in a global prediction model and half that in a regional model covering the North Atlantic and Europe. However, even this latter model cannot represent the topographic differences between parts of the United Kingdom which are important for short-period forecasting. A mesoscale numerical forecast model with very fine resolution has been developed to tackle this problem with the aim of providing guidance to forecasters on the local variations of weather in the period up to a day ahead. This model is closely tied to the regional model through its boundary conditions so it must be seen as a sophisticated tool for adding detail to the predictions of the coarser models. In particular it will not be able to correct timing errors in systems that pass through the boundaries. On the other hand, in slow moving situations the topographically induced effects should be well forecast and should be of considerable help to the local forecaster. It is widely recognized that model predictions of mesoscale systems that are not forced by topography will be difficult. However, the errors will often be in timing or location so that the products may still provide useful guidance on many occasions. It may also be that much of the mesoscale variation in weather from larger-scale systems is actually induced by topographic variations, perhaps through the surface

temperature or moisture. In these cases the added detail will be of considerable value provided that the regional model has correctly predicted the large-scale evolution. Any anticipated errors in the large-scale timing or development will have to be taken into account when interpreting the mesoscale guidance. The remaining sections will describe the model formulation, the methods currently used for preparing the initial data, and some recent results. The model formulation is described more fully in Golding (1989).

2. The forecast model as at January 1990

2.1 Spatial resolution and coverage

The model presently has a 15 km grid-length and covers the British Isles and near Continent except for Shetland (see Fig. 1). With this resolution a reasonably faithful representation of the orography can be given, and the coastline, indicated by the zero height contour in Fig. 1, has a realistic shape. Nevertheless, individual peaks and valleys less than 30 km across cannot be represented. Their effects must be added to the model guidance by forecasters familiar with the small-scale climatology of each district.

2.2 Dynamics

The basic dynamical equations used by the model have been described for a dry atmosphere in Tapp and White (1976) and Carpenter (1979). The vertical

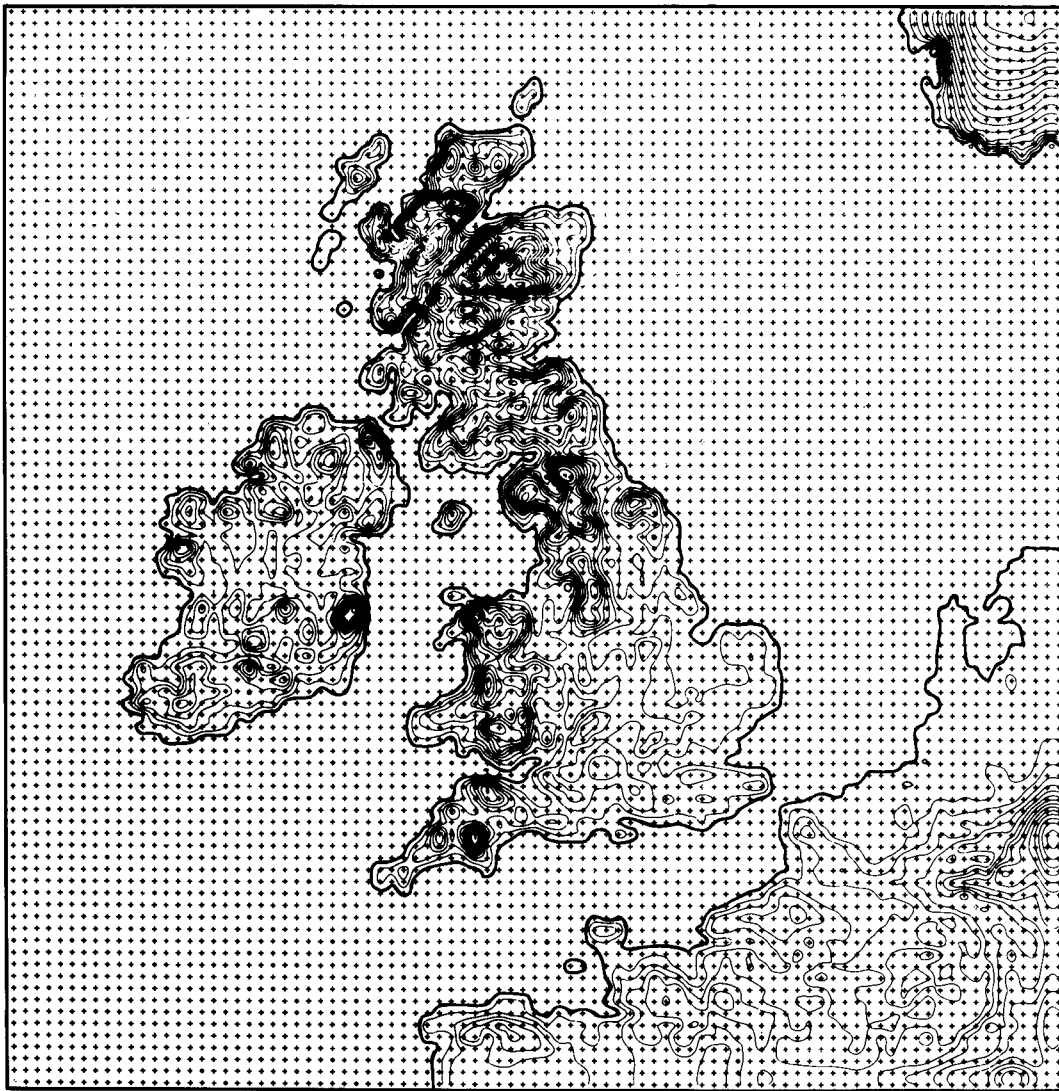


Figure 1. Model domain and orography. The grid points have a 15 km spacing and the contour interval is 50 m. The bold contour is at zero height and indicates the model coastline.

coordinate is height above the land surface. Thus, model surfaces follow the orography as shown in Fig. 2 for the current version with 16 levels. The lowest level is at 10 m and the spacing increases linearly from 110 m to 1510 m at the top. The highest level is at 12 010 m which is normally in the stratosphere. This arrangement gives five levels in the lowest kilometre and an almost constant spacing of 60 mb from there up to the tropopause.

The model is non-hydrostatic and compressible and so has prognostic equations for the vertical velocity and Exner pressure variable $\pi = (p/p_0)^{R/c_p}$ where R is the universal gas constant, c_p the specific heat at constant pressure and p_0 a reference pressure. It uses thermodynamic variables which are conserved in the processes of condensation and evaporation. The potential temperature and Exner variable are split into a basic state and deviation. Source terms represent contributions from the sub-grid-scale parametrizations for deep convection, radiation, precipitation and diffusion. The method of

solution is a semi-implicit one in which the terms supporting sound waves in the basic state are separated and solved implicitly.

2.3 Radiation

The short-wave radiation budget is computed at two levels, the ground, and the highest cloud top if below 5 km. The transmission is obtained by applying, multiplicatively, transmission coefficients for Rayleigh scattering, water vapour absorption, aerosol scattering and cloud. Each is a function of bulk atmospheric quantities. The expression for cloud transmission was fitted to computations obtained using the model of Slingo and Shrecker (1982). At cloud top, absorption is parameterized as a function of solar zenith angle only, and is constrained not to exceed the long-wave cooling in the same layer.

The long-wave scheme uses a modified form of the scheme developed by Roach and Slingo (1979). The upward and downward fluxes of radiation are computed

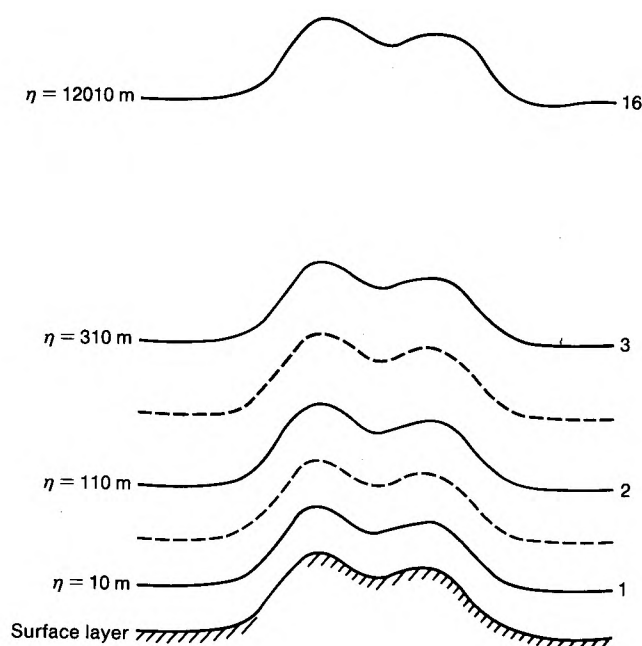


Figure 2. Vertical structure of the model. The vertical coordinate is height above ground (η) and there are 16 levels from 10 to 12 010 m. Wind pressure, temperature, humidity and cloud are specified at the main levels indicated by solid lines. Vertical velocity and turbulent kinetic energy are specified at intermediate levels (dashed lines).

for each model level in five wavelength bands. The transmission functions are represented as products of functions for water vapour, carbon dioxide and cloud, the latter being weighted linearly by the maximum cloud fraction in the slab.

2.4 Surface exchanges

The surface heat balance consists of four components; the net radiation, the ground heat flux and the atmospheric sensible and latent heat fluxes (Fig. 3). The net radiation consists of the net long-wave flux, described in section 2.3, and the absorbed part of the solar radiation. The short-wave albedo is set to 0.18 over land surfaces except where snow is present.

The ground heat flux is obtained from the diffusion equation applied to the layer represented by the surface temperature T_* and the soil temperature T_s . The fluxes of heat, moisture and momentum into the atmosphere are computed using drag-law expressions with transfer coefficients computed from Monin–Obukhov similarity theory as a function of roughness length and Richardson number. Over Britain, roughness lengths were obtained from the drag-coefficient map of Smith and Carson (1977). Other land areas use a roughness length of 10 cm. Over the sea the wind-speed dependent formula of Charnock (1955) is used. The roughness length for heat and moisture is one fifth that for momentum and is not permitted to exceed 0.1 m.

In the flux of moisture, the surface humidity is unknown so it is eliminated using the concept of a surface resistance to evaporation after Monteith (1964). The resistance is set to zero over the sea or when dew is

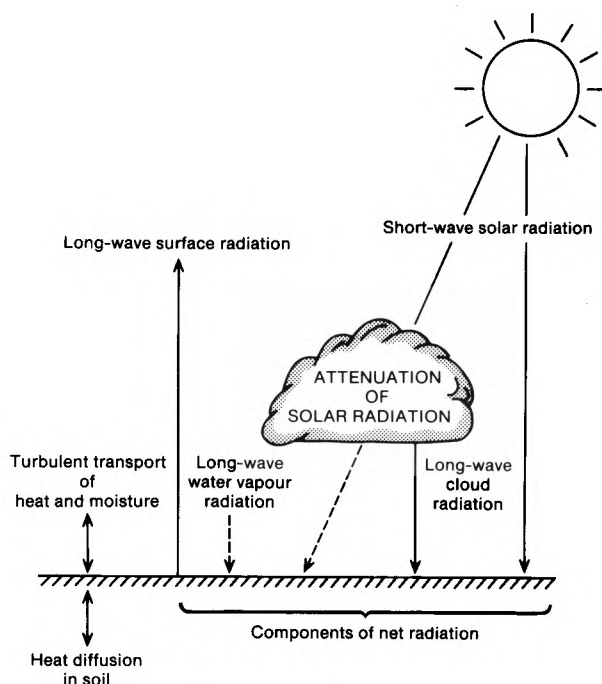


Figure 3. Schematic diagram of the processes involved in the surface heat balance of the model.

being deposited, and to 500 s m^{-1} elsewhere at night. Otherwise the resistance is computed from weekly estimates of soil moisture deficit extracted from the MORECS system (Thompson *et al.* 1981). Where moisture or snow is lying on the surface, a value of 50 s m^{-1} is used.

In order to avoid instability in the surface temperature T_* , the surface heat equation is integrated implicitly using the first term of a Taylor series expansion as an estimate of the sensitivity of each of the fluxes to variations in T_* .

2.5 Turbulent mixing

Vertical mixing is parametrized using a $1\frac{1}{2}$ -order closure scheme based on Yamada and Mellor (1979) as adapted by Smith (1984a, 1984b). In this scheme a formal expansion of the equations in mean and turbulent quantities is truncated after the second order. In the resulting set of equations, only the time rate of change (E) of turbulent kinetic energy (TKE) is retained, the equations for the other second-order quantities being reduced to diagnostic relations. The equation for E then contains four terms, representing generation of turbulence by shear, changes due to buoyancy (including latent heat release), turbulent transport of TKE and dissipation.

Manipulation of the second-order equations leads to flux gradient relationships with the mixing coefficients given by complex expressions involving E , buoyancy, shear and a diagnosed mixing length. The numerical solution for the turbulent fluxes is performed implicitly for all variables including the turbulent kinetic energy itself.

2.6 Grid-scale cloud and precipitation

In the advective and diffusive processes, the model uses variables which are conserved through changes of state. However, for the parametrization of radiation and precipitation, it is necessary to distinguish between vapour, water cloud, and ice cloud. Rain water is assumed to fall immediately and is not carried in the model. Snow is assumed to be indistinguishable from ice cloud. The diagnosis is performed using the mean and turbulent parts of the temperature and humidity distributions to define a probability distribution of unsaturated and saturated states within the grid volume. The distribution used has a top-hat shape. The proportion of saturated states is then the fractional cloud cover, and the excess water in them is the cloud water content.

The expression for the variance of the distribution contains two terms: the first represents turbulent variability while the second has been added to allow for non-turbulent variations which are assumed to become greater as the depth of the grid box increases. The phase of the cloud depends on whether the ambient temperature is above or below a critical temperature. The critical temperature is $-15\text{ }^{\circ}\text{C}$ unless snow is already present in which case it is $0\text{ }^{\circ}\text{C}$. The critical humidity for cloud formation is saturation over water unless snow is already present when it is saturation over ice. The effect of this formulation is shown in Fig. 4 where supercooled water cloud can deepen until it reaches the $-15\text{ }^{\circ}\text{C}$ level when it glaciates fully down to $0\text{ }^{\circ}\text{C}$.

The precipitation processes are modelled quite differently for ice cloud and liquid water cloud. Ice (or snow) is assumed to fall at a speed that is weakly dependent on mixing ratio (Heymsfield 1977) (approximately 1 m s^{-1} for dense cloud).

No snow will fall out of a cloudless layer with such a formulation so it effectively prevents snow falling

through dry layers. In order to avoid this when high vertical resolution is used, a realistic evaporation is calculated over the depth of the layer and this overrides the calculation of fall-out from a layer when this would be smaller.

Below the freezing level, snow falls to the ground within a timestep. Both evaporation and melting are based on Rutledge and Hobbs (1983). Melting is computed as a function of precipitation rate and wet-bulb temperature.

Rain is formed from liquid water cloud by two processes, local production, and accretion on rain falling through the layer (Fig. 5). At the surface, the precipitation is defined as snow if the majority is snow or if the snow rate is greater than 0.2 mm h^{-1} (water equivalent).

2.7 Deep convection

The deep convection scheme was based originally on that of Fritsch and Chappell (1980). It retains their concept of diagnosing instability and then assuming that the resulting convection will last for many model timesteps. In the scheme here, convection lasts for one hour and is advected across the grid with the ambient wind at the middle level. Instability is diagnosed by lifting model layers to the next layer, where grid-scale vertical motion is upward, and then testing whether they are upwardly buoyant. If so, the parcel is lifted, with entrainment, until it is no longer buoyant. The parcel is detrained at this level with a small value of supersaturation, and with the parcel horizontal velocity. The mass flux in the updraught is related to the depth of cloud.

Instability is tested every 15 minutes so it is possible to have up to four such clouds in a grid square at one time. Precipitation is computed from the parcel supersaturation when it reaches cloud top if the cloud-top temperature is colder than $-5\text{ }^{\circ}\text{C}$. Some condensate is detrained into

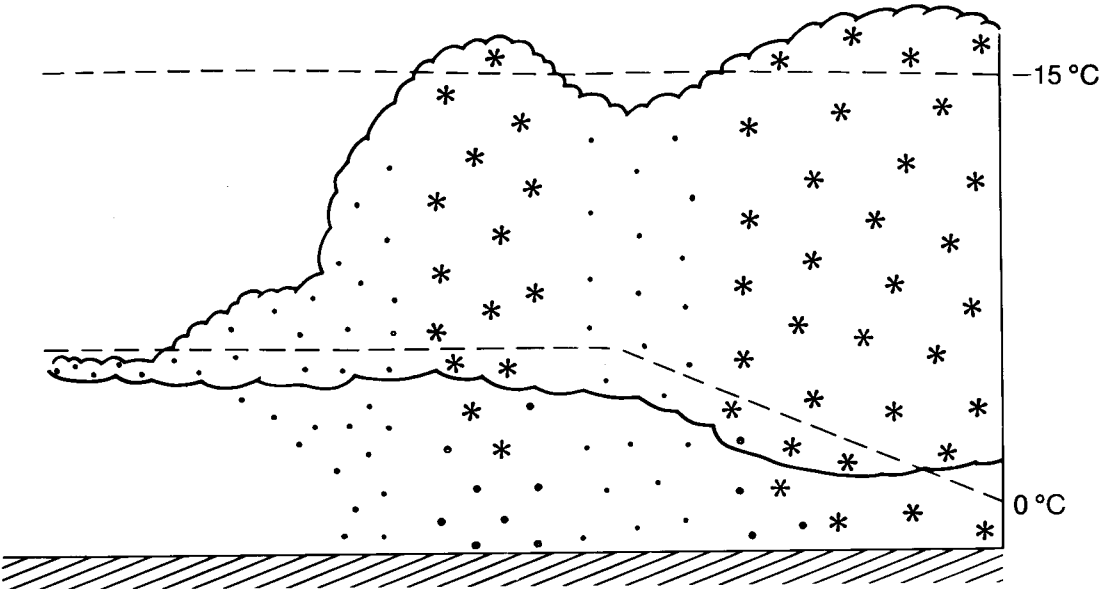


Figure 4. Schematic diagram of the representation of snow and rain in the precipitation scheme.

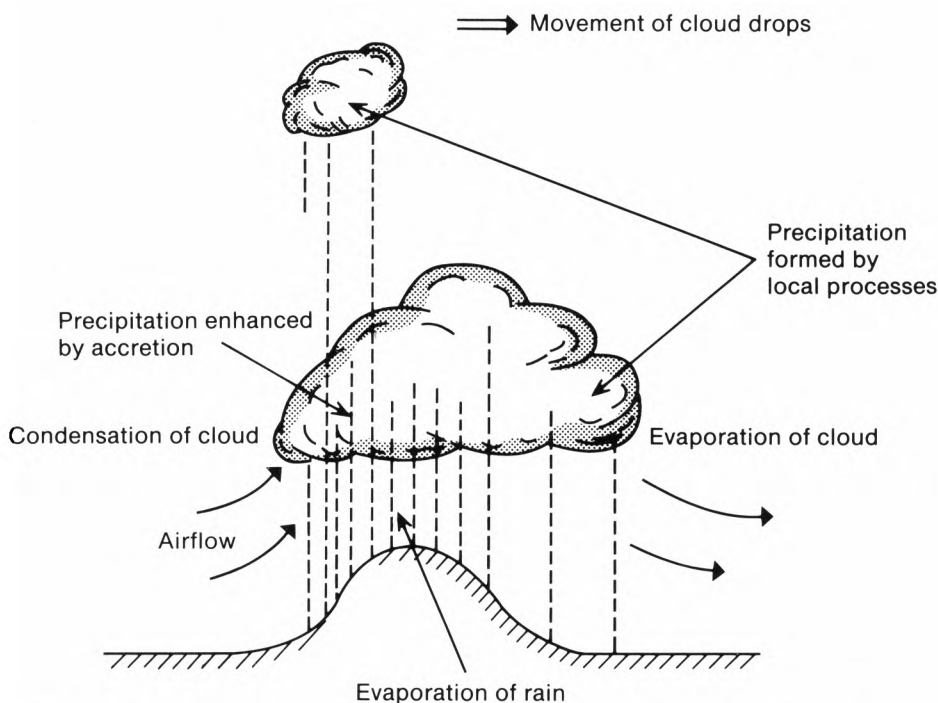


Figure 5. Schematic diagram of the processes involved in the liquid water precipitation scheme.

the anvil and some is evaporated in the downdraught to keep it saturated at cloud levels and 80% saturated below cloud. A cloud-top temperature-dependent efficiency factor is also applied, further reducing the precipitation from clouds with tops warmer than about -15°C . In order to convert the precipitate into a rain rate it is necessary to diagnose a rain area. This is related to the depth of cloud and the shear between base and top. The downdraught mass flux is related to the mass of air lying beneath the cloud that is available for evaporative cooling, and to the rain rate.

If the temperature of the downdraught exceeds the ambient temperature at 10 m, it is assumed not to reach the ground and the effects of the outflow are ignored. At cloud base it has the ambient potential temperature and humidity and these are modified by evaporation as the air descends. The resulting modified air is detrained in the model's lowest layer.

The most important effect of the convection on the grid-scale flow occurs through the subsidence required to compensate for the convective-scale updraught and downdraught. This is modelled by a source term in the pressure equation. Since the model is non-hydrostatic, it responds with grid-scale vertical accelerations to redistribute the mass.

2.8 Aerosol

An estimate is made of the cloud condensation nucleus (CCN) concentration assuming no sources and sinks within the grid. A single concentration representative of the boundary layer is used and is advected with the 1010 m wind. Boundary values are fixed at 50 cm^{-3} on sea boundaries and 300 cm^{-3} on land boundaries. At present the CCN concentration does not influence the

model evolution but is used in diagnosing visibility for output.

2.9 Boundary conditions

There are five boundaries to the mesoscale model, the four lateral boundaries and the top. Values from the fine-mesh model are used on each of them. The upper boundary is also adjusted so as to give a mass flux which compensates for any drift in the mean pressure at 5 km away from that prescribed from the fine-mesh model. The fine-mesh values are extracted at 3-hour intervals, interpolated in time and space and adjusted for the different orography. Pressures are recomputed from the interpolated surface pressure and potential temperature profile. Land surface and sea surface temperatures are interpolated separately.

3. Initialization

The representation of the initial state of the atmosphere is of critical importance to the quality of forecast that can be expected from the model. As with large-scale models, the constraints of near-geostrophy must be satisfied if a stable forecast evolution is to be obtained. However, a short-range forecast model must also be correctly initialized with cloud if the temperature and precipitation are to be realistically forecast. Indeed, the atmosphere 'remembers' much of its initial state over a 12-hour period on many occasions and this contributes to the accuracy of subjective forecasts based on modified extrapolation procedures.

Three sources of data are currently used to initialize each forecast. They are an interpolation of the latest fine-mesh forecast, a 3-hour mesoscale forecast, and observations. A cycle of 3-hour forecasts is maintained

throughout the day permitting a continuous passing forward of mesoscale forecast data where observations are not available. The interpolation of fine-mesh model fields is an important part of the mix since it is by this means that information about the synoptic-scale structure is obtained. This is the only way that upper-air observations reach the analysis as their resolution is too low to justify the effort of incorporating them directly on to the 15 km grid. The resolution of local-area TIROS operational vertical sounder retrievals is much better than radiosondes, but these lack detail in the vertical structure. Interpolation of the fine-mesh fields is a complex process since the models use different map-projections and a different vertical coordinate as well as the mesoscale model having finer resolution. In addition the specification of orography is quite different. For these reasons, interpolated data are not normally used in the boundary layer. Here the latest mesoscale forecast is used if available. It is also used as first guess for the moisture field and is filtered to give short-wavelength detail in all fields which is added to the smooth interpolated fields. This is justified on the assumption that such detail is often related to the detailed orography in the model. This combination of data from the two forecast models forms a 'hybrid' which is used as the first guess for the analysis procedure.

The initialization scheme can be run in two modes: interactive or objective. In the objective mode, the initialization uses surface reports of pressure, wind, rainfall, cloud cover, cloud base and 8-groups (cloud type/base groups), visibility, state of ground, snow depth, temperature and dew-point. These are obtained from reports in SYNOP, SHIP, LIGHT VESSEL, METAR, DRIBU, NCM and SREW codes. If a quality-controlled radar image and a calibrated Meteosat cloud-top temperature image are available for the analysis time, they will also be used. In the interactive mode, analysts can override either the observations or the analysis of any variable. They can also choose to use off-time images, a raw radar image or to recalibrate the Meteosat image. They can compare the vertical structure of the initialization against radiosonde ascents and modify accordingly. Finally, they have sferics reports available for guidance in the rainfall analysis.

Many of the observed variables are of little value in the model initialization in isolation. However, in combination with others, they are used to adjust other model fields in a consistent manner. This is particularly important for the humidity structure which has probably the most important control over mesoscale development.

The initialization procedure starts with the main dynamical fields of pressure, wind and potential temperature. First, the surface pressure is analysed from a first-guess interpolated fine-mesh field. This is followed by an analysis of wind components. Prior to this, however, the mesoscale forecast first guess is averaged with geostrophic winds based on the pressure

analysis. This is particularly useful over the sea and where a sharp trough has been introduced in the pressure analysis. Following the wind analysis, pressure, wind and potential-temperature increments are computed for all levels from the adjustments made to the surface pressure and wind fields. The surface-wind adjustments are applied with decreasing weight up to 1010 m. The pressure adjustments are used to compute geostrophic wind and hydrostatic potential-temperature increments which are applied with decreasing weight up to 8010 m and shifted upstream with a 1:100 slope. The upstream direction is a mean for the whole domain. Below 1010 m the geostrophic wind adjustments have reduced weight.

The moisture distribution is then computed starting with an analysis of surface rainfall. Where available, this uses the radar image as first guess. Surface present weather and precipitation accumulations (SREWs) are used to estimate rates at observing stations. These are analysed assuming a small radius of influence within radar range, but a broader influence elsewhere. In the interactive mode, the analyst can use the satellite image and sferics reports to assist in finalizing this analysis. The overall cloud cover is analysed next. If available, the Meteosat cloud-top temperature image is used to compute a first guess assuming that all tops colder than 10 °C below predicted surface temperature must be cloud. After analysis of the surface reports, the satellite image is adjusted in areas of partial cloud to allow for the transmission of surface infra-red emission to the satellite. The adjusted image is then used to derive a cloud-top distribution (if an image is not available, the mesoscale-forecast cloud top is used). The forecast cloud base is then adjusted to ensure that it is at least 200 m below cloud top, and is then used as first guess for an analysis of cloud-base observations. If the cloud-base analysis conflicts with cloud top, one or the other is adjusted. Below 8000 ft (2438 m) the base is assumed correct and above 8000 ft the top is preferred. Using the analysed (and checked) cloud cover, base and top as constraints, a cloud-cover analysis is then performed for every model level. This is done by first interpreting the observed 8-groups in the light of the first guess interpolated to each observation position, to give a profile of cloud-cover values at model levels. These are then analysed a level at a time. At this point the analyst may select to view profiles of temperature and cloud fraction at several locations to ensure that they are realistic and consistent (e.g. boundary-layer cloud does not extend above the boundary-layer inversion). If locations are selected for which radiosonde ascents are available, these are displayed as a guide. Modification can be made to either or both profiles, and applied to an area delineated on the map by the analyst.

The final set of analyses relate to surface conditions. They are the visibility, surface wetness or snow depth (frozen deposits are treated as negative, liquid ones as positive with state of ground reports of dry, moist, flooded and frost interpreted quantitatively), surface

temperature and dew-point. The humidity mixing ratio is calculated at screen level and then assumed constant up to 20 m. This, together with the visibility analysis, is used to estimate a cloud condensation nucleus distribution for the boundary layer.

The humidity is set at each level to be consistent with the analysed cloud cover using a simplified form of the relation in the forecast model. The cloud liquid/ice mixing ratio is then initialized with empirical profiles for different analysed rain rates. These are then adjusted interactively to give the analysed rate when the model precipitation equations are applied. The surface temperature analysis is used to adjust soil temperatures. Then temperature profiles are adjusted from screen-level upwards to spread the influence of surface observations and to ensure that there is no convective instability except within analysed cloud where it must be consistent with the model turbulence equations. While this is done, the deviation of the mean temperature from that in the first guess is minimized so as to avoid unbalancing the model. Finally, the vertical velocities required to replace cloud which is precipitating are calculated and the divergence fields adjusted accordingly.

The impact of the interactive technique has been tested in several case-studies (Wright and Golding 1989) and has been found to be greatest when there is little large-scale control of the evolution. A notable example was a case from Project Haar (Findlater *et al.* 1989) in which the objective analysis misrepresented the coverage of fog over the North Sea. In the forecast this resulted in premature clearance of the fog (Fig. 6(a)). Interactive modification of the initial fog distribution produced a much improved forecast (Fig. 6(b)) in which the fog was retained over a much larger area (in reality it did not lift to stratus around the coast and did not penetrate so far in land).

4. The operational trial

4.1 General aspects

A weekly trial of the forecast system in the first part of 1984 was followed by an operational trial from October 1984–January 1985 in which a single 12-hour forecast was run each day from 06 UTC. The results were sufficiently encouraging for a second extended trial to be started in April 1985. Meanwhile, the efficiency of the forecast was improved so that it now takes about 1 minute per hour of forecast time. Major improvements have been: the turbulence scheme using conservative variables in June 1985; the revised ice-phase precipitation scheme in September 1985; the system for carrying information forward from one forecast to the next in November 1985; the cloud-top radiation budget in May 1986 and the snowmelt formulation in December 1986. Since March 1987 a range of products has been disseminated by digital facsimile to a small number of local forecast stations for assessment there. During August 1988 the Central Forecasting Office (CFO)

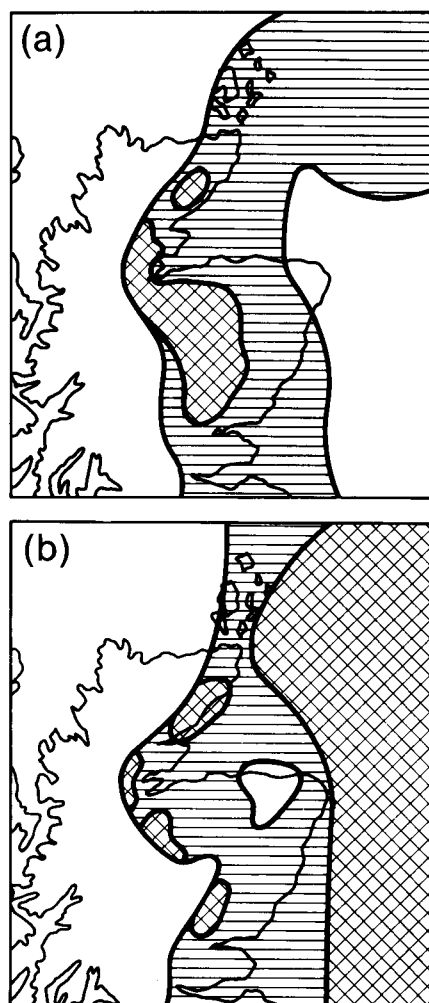


Figure 6. Nine-hour forecasts from 06 UTC on 29 April 1984 in a fog situation. (a) Initial conditions from the objective analysis, and (b) initial conditions modified via interactive VDU taking account of satellite imagery. Low cloud is shown by horizontal shading, and fog by hatching.

began routine use of the interactive mesoscale initialization scheme to introduce radar and satellite imagery into the forecasts. In October 1989 the model domain was enlarged to include the North Sea, the multi-level long-wave radiation scheme was incorporated, and the cloud-top temperature dependence of shower precipitation was introduced.

The objective assessment of this trial has been carried out at all observing stations for most observed variables and permits great flexibility in the comparisons that can be made. It has been supplemented by various subjective assessment techniques including comparison with the local area forecast for Bracknell, with temperatures forecast by Weather Centres for gas boards, and with cloud and visibility predictions at the local stations receiving model products.

In general, the synoptic-scale evolution predicted by the mesoscale model differs little from the fine-mesh model — as intended. It does not generally improve on timing and development errors and does not consistently forecast mesoscale dynamical developments such as rain

bands with accuracy. One difference that has been noted is a tendency to speed up cold fronts — thus exacerbating a tendency for the fine-mesh model to be too fast in this respect. At its present stage of development it should therefore be seen as a detailed diagnostic tool which enables the effects of topographic variation to be taken into account and, by using more sophisticated physical parametrizations, enables the variables required by forecast users to be predicted directly.

A general assessment of the usefulness of the forecasts can be obtained by analysing references to the products in the Synoptic Reviews (SRs) issued by CFO. Due to time of availability, comments appear in Part 2 or 3 of the review and frequently are used to support forecasts already disseminated in Part 1. References are also made to advise those stations receiving mesoscale products of aspects to be disregarded, and to advise other stations of useful features of the forecast. In Table I references are analysed into three categories for each weather element. The first category contains references where CFO are communicating useful model guidance. The second contains references to features which are considered unlikely but that should be noted for caution. The third category is of features to be ignored. The period of analysis is October–November 1989 during which 73 forecasts were referenced.

Consistent with subjective impressions the wind is very reliable, but it is not often an important element in central guidance. The temperature is referred to most often, usually in comparison with Model Output Statistics (MOS) hence the large number of entries in the caution column. Precipitation is most often referred to in support of an enlargement of a fine-mesh rain area or to introduce an area of showers missed by the fine mesh. Cloud and fog are recognized to be unreliable. However, in the anticyclonic spell in November 1989, both were referenced repeatedly.

Table I. Analysis of model references in synoptic reviews, October–November 1989

Element	Number of references		
	Guidance	Caution	Ignore
Cloud	19	3	5
Temperature	32	15	2
Wind	10	1	0
Precipitation	12	2	4
Fog	11	7	3

4.2 Specific aspects

4.2.1 Temperature

With the first model level at 10 m, screen-level temperature has to be diagnosed from the predicted ground- and first-level values. At present a linear interpolation in height is used when an inversion is

present and the average of the two taken otherwise. This procedure produces good results provided the cloud is reasonably correct. Errors in cloud have most effect at night in winter and in the day in summer. Fig. 7 shows percentages of maximum and minimum temperature forecasts within given tolerances of observations for each month since autumn 1985. All observing stations in the British Isles are included. The results depend on the weather type: mild, cloudy weather producing better statistics than clear weather in both summer and winter.

November and December statistics indicate that the warm bias in night-time temperatures had been removed in the latest version of the model. In November, the 12 UTC run had a mean error between $\pm 0.2^{\circ}\text{C}$ at all forecast times. The 00 UTC run had an increasing negative error reaching -0.6°C by dawn which corrected itself after sunrise. This was much smaller in December and was probably related to the cloud deficit in the early part of the forecast (see below). Also in November, taking minimum temperatures for 18–06 UTC, air frost occurred in 14.7% of observations and was forecast in 15.8% with a hit rate of 70% and a false-alarm rate of 35%.

The geographical distribution of large errors in January 1989 is shown in Figs 8(a) and 8(b) showing that many of the errors in Fig. 7 are occurring at highland or coastal locations, unrepresentative of the surrounding area.

The mesoscale model predictions are significantly better than those obtained directly from the fine-mesh model. By statistically relating fine-mesh predictions to observations at 32 specific sites, MOS predictions score about 5% more cases within 2°C than the mesoscale model. The model, however, does better in unseasonable weather.

A comparison with subjective forecasts issued to the gas boards is shown in Table II. The predictions are from 15-hour forecasts of the model. The subjective forecasts are issued at 1530 LST for 3 a.m. but rather earlier for 3 p.m. giving the model a slight advantage in the latter prediction. The results are similar at most locations but reflect the difficulty of interpolating between land and sea points at Cardiff and possibly Southampton, and the effect of the urban setting of London Weather Centre.

4.2.2 Wind

Wind speed and direction predictions are generally considered to be good although light winds tend to be overpredicted. In November 1989, observed winds below 6 kn were predicted with a significant positive mean error of about 3 kn, an r.m.s. error of 4–5 kn and r.m.s. direction errors of $40\text{--}50^{\circ}$. Observed winds of 6–16 kn had a zero mean error, an r.m.s. error of 4 kn and r.m.s. direction errors of about 30° . Observed winds of 16–27 kn had a small negative mean error, an r.m.s. error of 6 kn and r.m.s. direction errors of $20\text{--}25^{\circ}$. Above this speed, the sample is small and is dominated

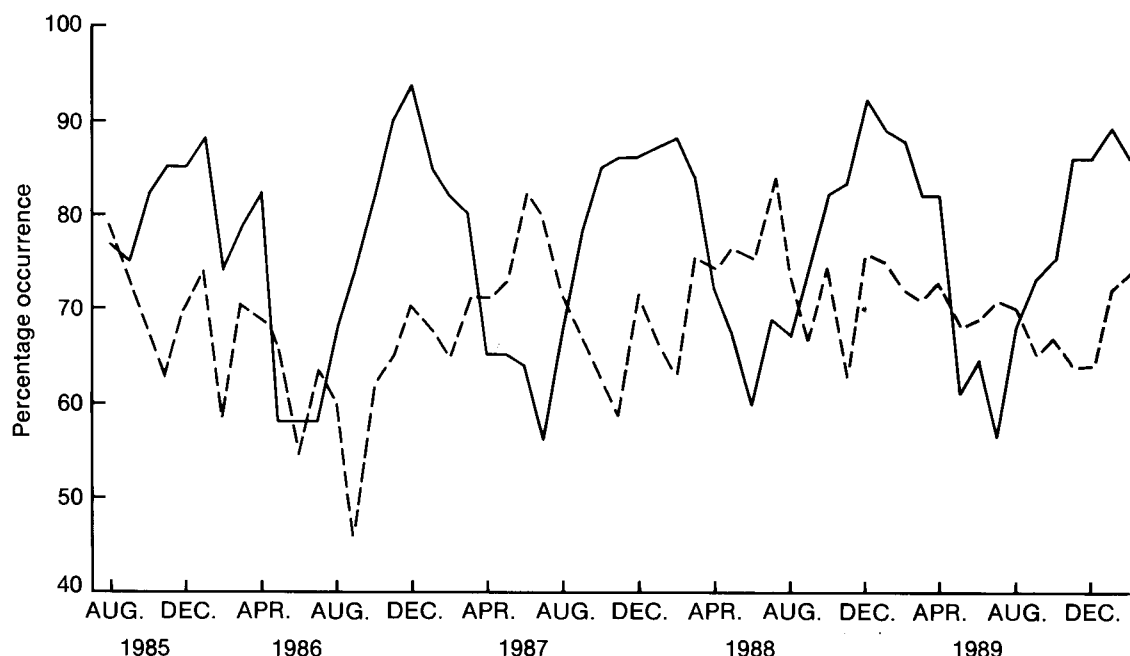


Figure 7. Percentages of predicted maximum (continuous line) and minimum (dashed line) temperatures within 2 °C of observed values for a sample of stations in the British Isles for 1985–90.

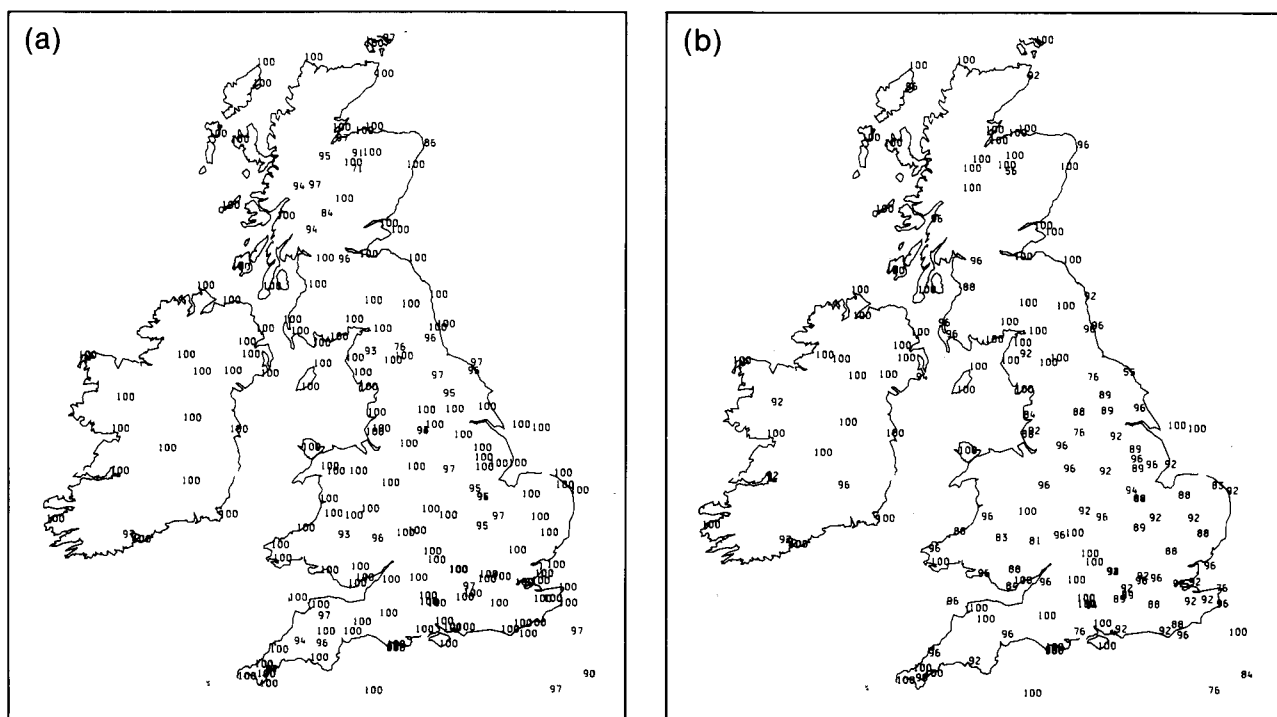


Figure 8. Maps of percentages of forecast screen temperatures within 4 °C of observed values in January 1989. (a) 15-hour forecasts for 15 UTC, and (b) 18-hour forecasts for 06 UTC.

by unrepresentative locations such as Cairn Gorm and Great Dun Fell. At all observed speeds, the statistics are affected by large positive speed errors at some inland stations in the Republic of Ireland and at some valley locations in Scotland; and large negative speed errors at Cairn Gorm, Great Dun Fell and Cape Wrath. The geographical distribution of errors in January 1989 is shown in Fig. 9. Most inland stations have an r.m.s.

vector error of less than 5 kn. The fine-mesh forecasts, adjusted for altitude, show worse direction errors at low speeds, and worse speed errors at high speeds.

Comparisons of model with subjective forecasts have been carried out at Manchester and Glasgow for 9-hour forecasts. The forecasters extracted model predictions from charts and recorded their own predictions based on terminal aerodrome forecasts (TAFs) for their own

$$\pm 4^{\circ}\text{C} = 8^{\circ}\text{C}?$$

Table II. Percentage of subjective and mesoscale forecasts of 03/15 UTC temperature within 2° of observed in 1989

Station	03 UTC		15 UTC	
	Forecaster	Mesoscale	Forecaster	Mesoscale
Glasgow	73	83	80	79
London	88	75	79	85
Southampton	83	86	83	81
Cardiff	84	76	87	82
Nottingham	—	—	81	81

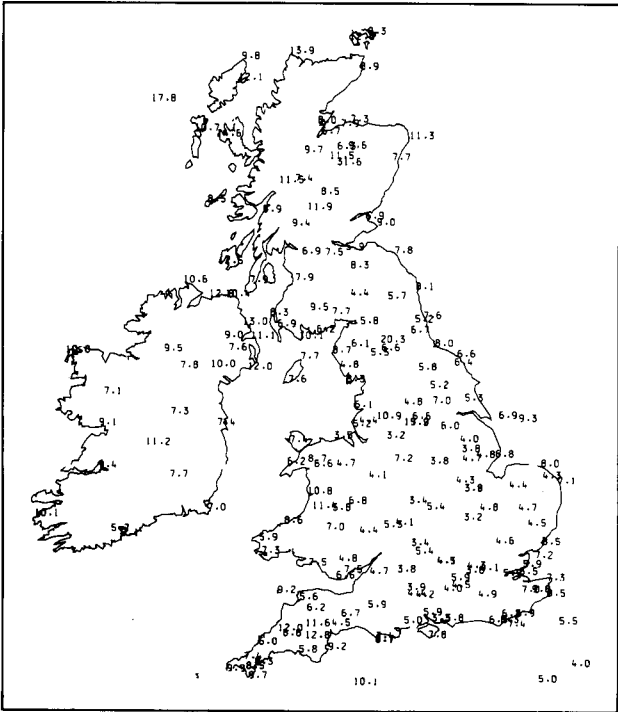


Figure 9. Map of root-mean-square vector wind errors (kn) in 15-hour predictions for 15 UTC in January 1989.

and a remote airport. Cases with observed wind speed below 5 kn were omitted from the direction comparison. The results are shown in Table III.

An example of a wind forecast is shown in Fig. 10. The observations are for 15 UTC on 25 January 1990 at the height of a storm which caused extensive damage. At this time the area of strongest winds covered much of south and central England and was characterized by inland wind speeds of about 40 kn. Exposed locations,

particularly on Salisbury Plain and near the coast were experiencing 50 kn. The forecast was initialized at midnight and successfully predicted the general level of the strong winds, though not the more extreme observations. Note the reduced strength (35 kn) in much of the Home Counties as a result of the higher roughness lengths used in the model there.

4.2.3 Cloud

Since the latest version of the model was introduced in October 1989, there has been a marked reduction in cloud after initialization which gradually recovers over 6–9 hours. The reason for this is not yet known. The underprediction is particularly noticeable below 2000 ft (610 m).

Cloud is characterized by both cover and height in the observations, so it is difficult to devise a verification scheme which adequately measures the overall skill. For this reason, the accuracy of predicting a series of user-related thresholds is tested. For instance, one series of tests measures the skill in predicting 3 oktas or more of cloud with a base below 1000 ft (305 m), 2000 ft (610 m) or 6000 ft (1829 m). For each test, four measures of skill are tabulated — the frequency with which it was forecast (which may be compared with the actual frequency); the percentage of actual occurrences that were correctly forecast (the hit rate); the percentage of forecasts of the event which were wrong (the false-alarm rate), and the Hansen and Kuiper skill score, defined as the percentage of occurrences correctly forecast less the percentage of non-occurrences wrongly forecast.

In November 1989 there were 3 oktas or more of cloud with a base below 6000 ft (1829 m) in about 60% of observations. In general, the model forecasts achieved a 60–70% hit rate and 20–30% false-alarm rate. About

Table III. Assessment of model/forecaster predictions of wind for 09/21 UTC in 1989

Station	Speed errors (kn)		Direction errors (deg)	
	Mean	r.m.s.	Mean	r.m.s.
Glasgow	0.3/1.0	4.1/3.9	10/0	36/31
Aberdeen	2.2/1.3	4.6/4.4	5/1	30/33
Manchester	0.1/0.7	3.3/3.7	7/5	29/27
Blackpool	1.2/0.7	4.4/3.6	6/5	31/32

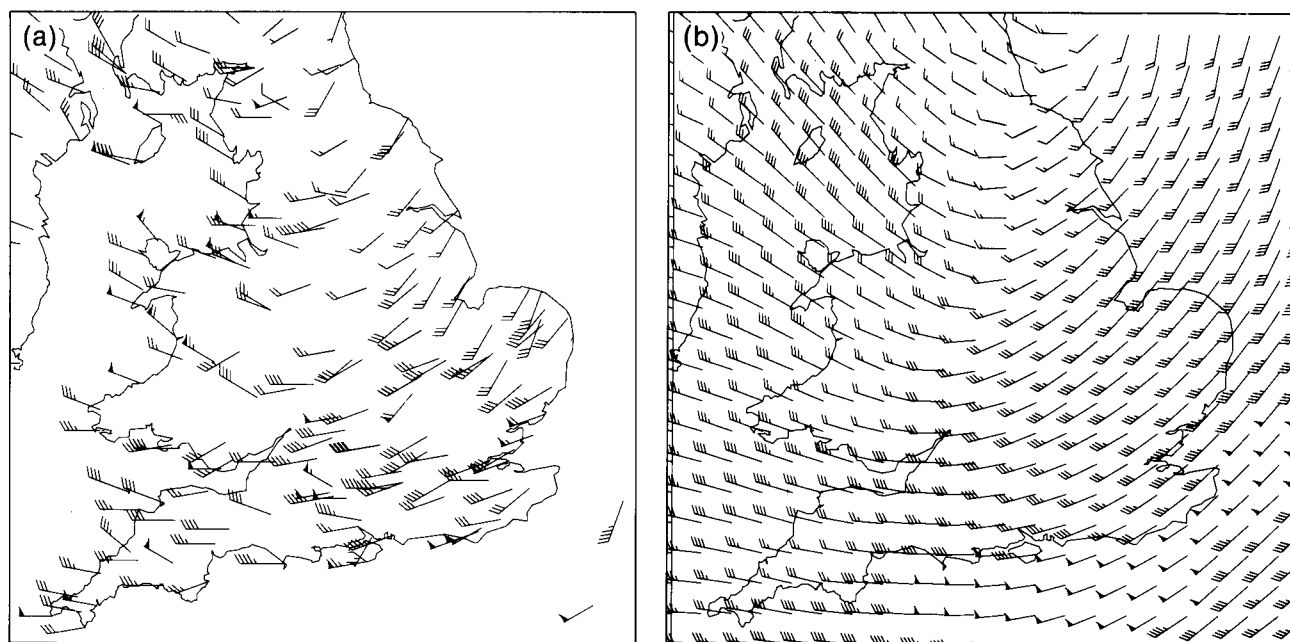


Figure 10. Mean winds (conventional symbols) at 15 UTC on 25 January 1990. (a) Observed, and (b) 15-hour forecast.

45% of observations met a 5 oktas threshold. For these the model achieved the same hit rate with a false-alarm rate of 30–40%. For lower height-thresholds, the hit rate reduced and the false-alarm rate increased. The statistics are very variable geographically and are not obviously related to topography.

Table IV shows comparative results for model/forecaster predictions of significant cloud below 1000 ft at several stations during 1989. The forecasters extracted the model predictions from charts and recorded their own forecasts based on TAFs, local area forecasts, etc. Note the geographical bias in the stations represented here.

The potential usefulness of the model in forecasting cloud base can be gauged from the comparisons with observations in Fig. 11. They show the evolution of the cloud base at Leuchars through the period 24–27 May 1987. To facilitate comparison, the observations have

been moved to the nearest model level and these have been plotted at a nearby representative height (i.e. 500, 1000, 2000, 3000 ft). Apart from the forecast from 12 UTC on 24 January which lowered the base too early, they would all have given useful guidance to a forecaster.

An example of a forecast of cloud distribution is shown in Fig. 12. During early January 1987, the British Isles were affected by an extremely cold air mass which formed over the USSR and moved westwards across Europe. The cold air with temperatures below -20°C over Europe developed convective cloud as it moved over the warmer sea (temperature $8\text{--}10^{\circ}\text{C}$) which led to heavy snowfall over windward coasts. The cloud pattern is well picked out in the infra-red image (Fig. 12(a)) from the NOAA-9 satellite on the morning of the 12th. In particular the cloud crosses the Lizard and Land's End peninsulas in Cornwall and considerable snow was

Table IV. Skill scores for 3 oktas or more cloud below 1000 ft in 1989 — model/forecaster. See text for definition of terms.

Station	Times assessed (UTC)	Occasions observed	Occasions forecast	Hit rate	False-alarm rate	Skill score
Glasgow	09/21	43	39/45	35/51	62/51	30/47
Aberdeen	09/21	57	48/74	40/63	52/51	35/55
Manchester	09/21	36	34/51	31/58	68/59	26/52
Blackpool	09/21	54	21/59	9/48	76/56	6/41
Lyneham	09/12/15	148	82/164	28/64	49/42	23/55
Brize Norton	09/12/15	127	74/118	31/53	46/43	27/46
Wattisham	09/15	23	10/28	30/78	30/36	29/73
Marham	09/15	41	39/48	46/66	51/44	40/59
Honington	09/15	71	33/82	30/68	36/41	27/60
Coningsby	09/15	56	30/56	23/46	57/54	20/41

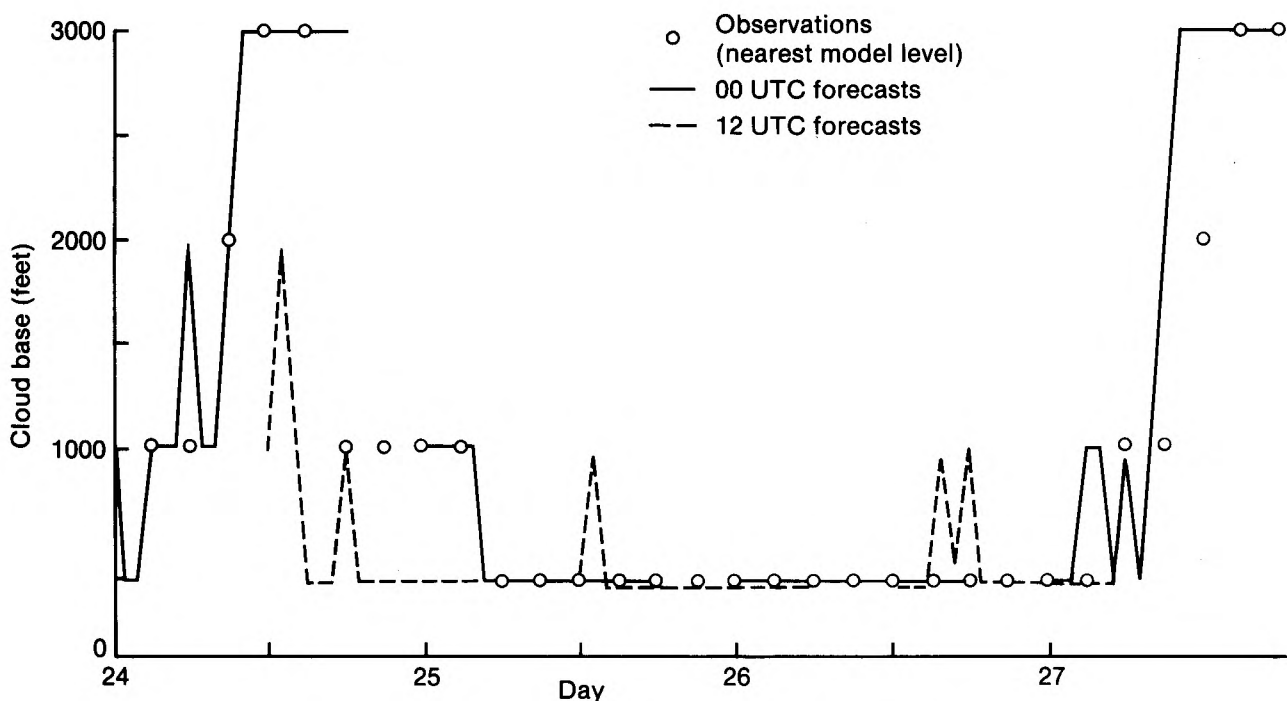


Figure 11. Forecast cloud base at Leuchars from T+1 to T+18 for 24–27 January 1987, compared with observations.

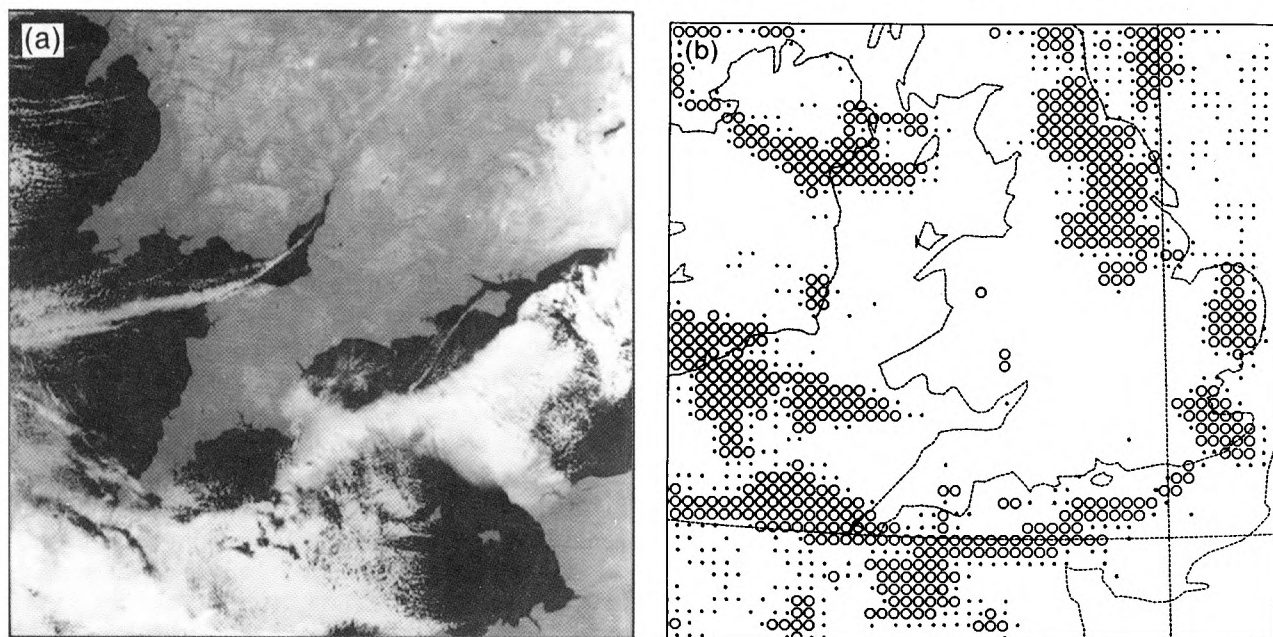


Figure 12. Cloud distribution at about 03 UTC for 12 January 1987. (a) NOAA-9 infra-red image at 0410 UTC, and (b) 9-hour forecast of total cloud cover. In (b) dots represent 4–7.5 oktas and open circles represent 7.5–8 oktas.

deposited in this area. The model’s 9-hour low-cloud prediction (Fig. 12(b)) accurately portrays this cloud distribution and realistic snow amounts were forecast.

4.2.4 Visibility

In diagnosing visibility from model results, it is recognized that it may fall substantially before the humidity reaches saturation, even locally. Thus the criterion for cloud formation can be used for fog but not for mist or haze. It is also recognized that the relationship between visibility and water content

depends on the cleanliness of the air. The visibility is therefore calculated from three quantities; the 10 m relative humidity and liquid water content, and the boundary-layer CCN concentration.

By its nature, fog is a local phenomenon often developing in hollows and along water courses at a scale of 1 km or less. Such patchiness is clearly impossible to predict with a 15 km resolution model. Although generally unreliable, model forecasts have provided useful guidance on several occasions when other techniques were uncertain. When using the results, it

must always be remembered that the model cannot, at present, distinguish between shallow fog, deep fog and stratus below 200 ft, and is attempting to give a forecast representative of a 15 km square.

Statistics for November 1989 show that the performance of the 00 UTC forecast was far better than that from 12 UTC. The 00 UTC forecast increased its fog coverage to about twice that observed by dawn and retained that level through the day for 200 m fog, but reduced it to the correct frequency for thinner fog and mist. The 12 UTC forecast cleared most of the observed fog very quickly and then gradually developed it again. By 06 UTC it had nearly four times the observed frequency of 200 m fog. For afternoon forecasts from the 00 UTC run, the hit rate was near 50% for the 200 m, 1 km, and 5 km thresholds. However, the false-alarm rate decreased from 75% for 200 m fog to below 50% for 5 km. The

overprediction in the afternoon was due to too wide a distribution and fog was actually underpredicted in south-east England. Very few false alarms were forecast for this area. Details of the visibility prediction during 11–22 November 1989 are shown for Wattisham in Fig. 13. The overall trends are well captured by the model indicating that it is responding to forcing and initial conditions in a realistic manner. However, the forecasts show more variability than the observations, especially between fog and mist, suggesting that a more sophisticated parametrization of the growth of fog droplets may be needed.

Results from several airfield stations are shown in Table V for the accuracy of predictions of aviation fog during the day. The results are heavily weighted towards performance in the anticyclonic spell in November/December when the model predictions scored more hits

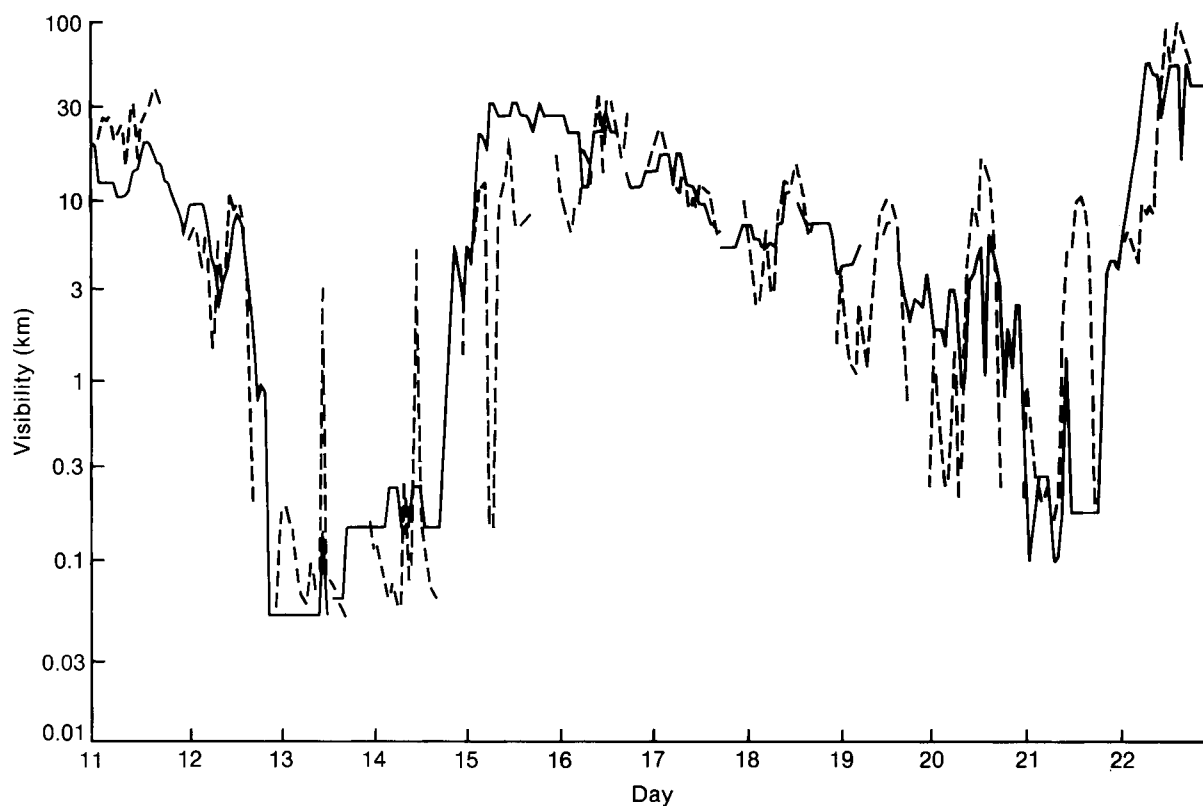


Figure 13. Observations (continuous line) and forecasts from 00 UTC (dashed line) of visibility at Wattisham, 11–22 November 1989.

Table V. Skill scores (model/forecaster) for daytime visibility below 1 km in 1989. See text for definition of terms.

Station	Times assessed (UTC)	Occasions observed	Occasions forecast	Hit rate	False-alarm rate	Skill score
Lyneham	09/12/15	29	37/14	38/31	70/36	35/30
Brize Norton	09/12/15	16	45/12	75/56	73/25	71/56
Wattisham	09/15	10	13/4	70/40	54/0	67/40
Marham	09/15	13	20/11	54/46	65/45	50/45
Honington	09/15	19	34/12	58/47	68/25	53/47
Coningsby	09/15	16	33/13	50/63	76/23	45/62

than the forecaster at most stations, especially in the afternoon (15 UTC).

Fig. 14 shows an example of a fog forecast from July 1986. The difficulty of verification is well illustrated by the small number of stations which actually lie within the forecast fog area. The erroneous sea fog is due to saturation of cold air flowing off the land. The

mechanism is similar to sea smoke but is occurring on too large a scale in the model.

4.2.5 Precipitation

The precipitation pattern usually follows that of the fine-mesh model, though with rather more light rain and showers. However, the finer resolution permits a better representation of orographic enhancement and rain shadow. A comparison between forecast 12-hour accumulations and observations for the month of January 1989 is shown in Figs 15(a) and 15(b). The general pattern is in good agreement, especially in Scotland where extremely large values were recorded. Fine-mesh model accumulations for the same period were less than half of the recorded totals.

The model's main deficiency is in the excessive prediction of small amounts of rain, especially as showers. The latter error is much improved since the introduction of the new version of the model. However, there is some evidence of an increase in the forecasting of spurious heavy showers. Results for December still indicate very light rain being predicted about twice as often as it occurs at night with a much smaller overprediction in the day. The fine-mesh model predicts about half as much very light rain as occurs in the day and 70–75% at night. However, for moderate and heavier rain both models overpredict at night and underpredict during the day.

During the period of snow threat in December 1989, the performance of the mesoscale model was generally encouraging and its usefulness was referred to in several SRs. The overall statistics, however, show about ten

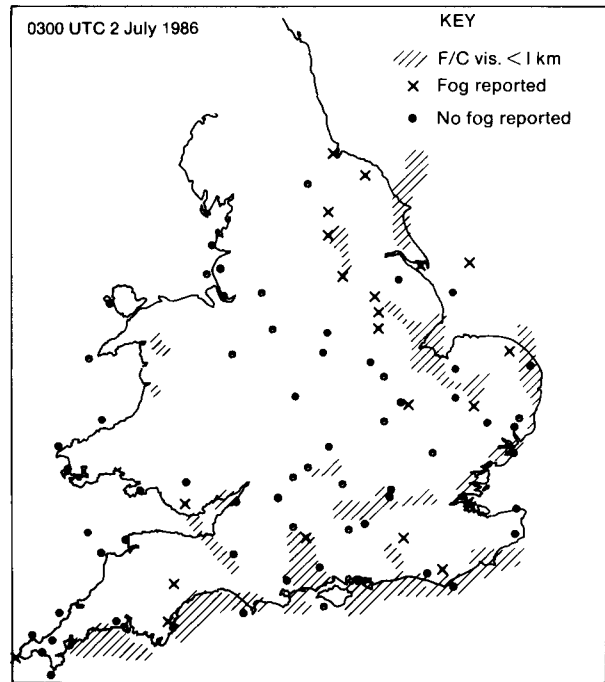


Figure 14. Comparison of observed fog areas 02–04 UTC with 9-hour forecast for 03 UTC on 2 July 1986.

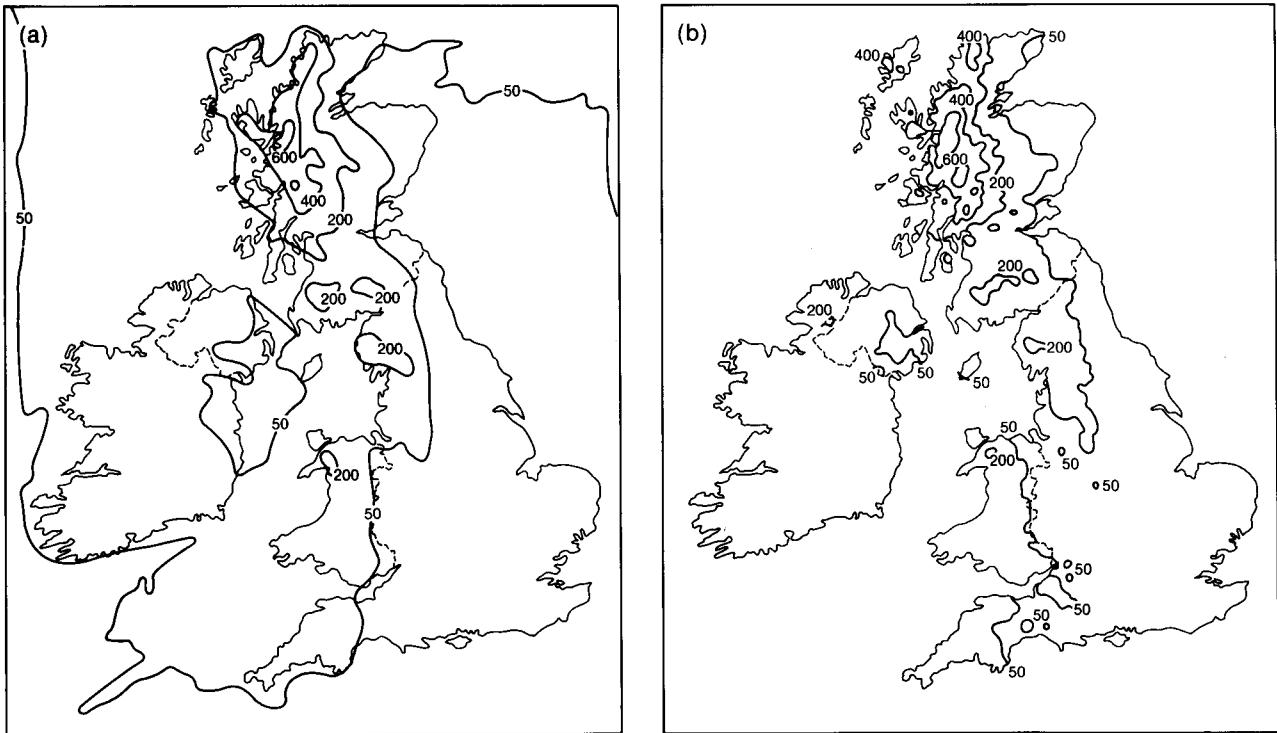


Figure 15. Rainfall totals (mm) for January 1989. (a) Sum of totals from the first 12 hours of each forecast, and (b) actual totals from the climatological rain-gauge network.

times as many occasions of snow predicted as observed and hit rates mostly in the range 20–40%. Applying the criterion to fine-mesh data that snow will occur if the freezing level is below 1000 ft gave prediction rates much closer to reality but a zero hit rate.

Forecasts of precipitation distribution are difficult to verify in a way that reflects their usefulness, especially in showery situations. A successful forecast of showers is therefore presented to illustrate the model’s potential. On 24 May 1989 extensive thunderstorms affected much of England. The radar network recorded the development as shown in Fig. 16. At 11 UTC the area of rain in the Midlands remained from a mesoscale convective

system (MCS) which moved north from France (Fig. 16(a)). This was not captured by the model (Fig. 16(c)). However, the new development to the south-west of London was well predicted in both time and location (Fig. 16(d)). The predicted showers over London were a little premature, and those over Wales and the north-west rather too extensive. As the afternoon progressed, the new showers spread towards London and south-west along a convergence line; and then also extended north-west from London, linking with the MCS in the north Midlands. This was well predicted by the model, though perhaps with the rain spreading rather too far east by this time.

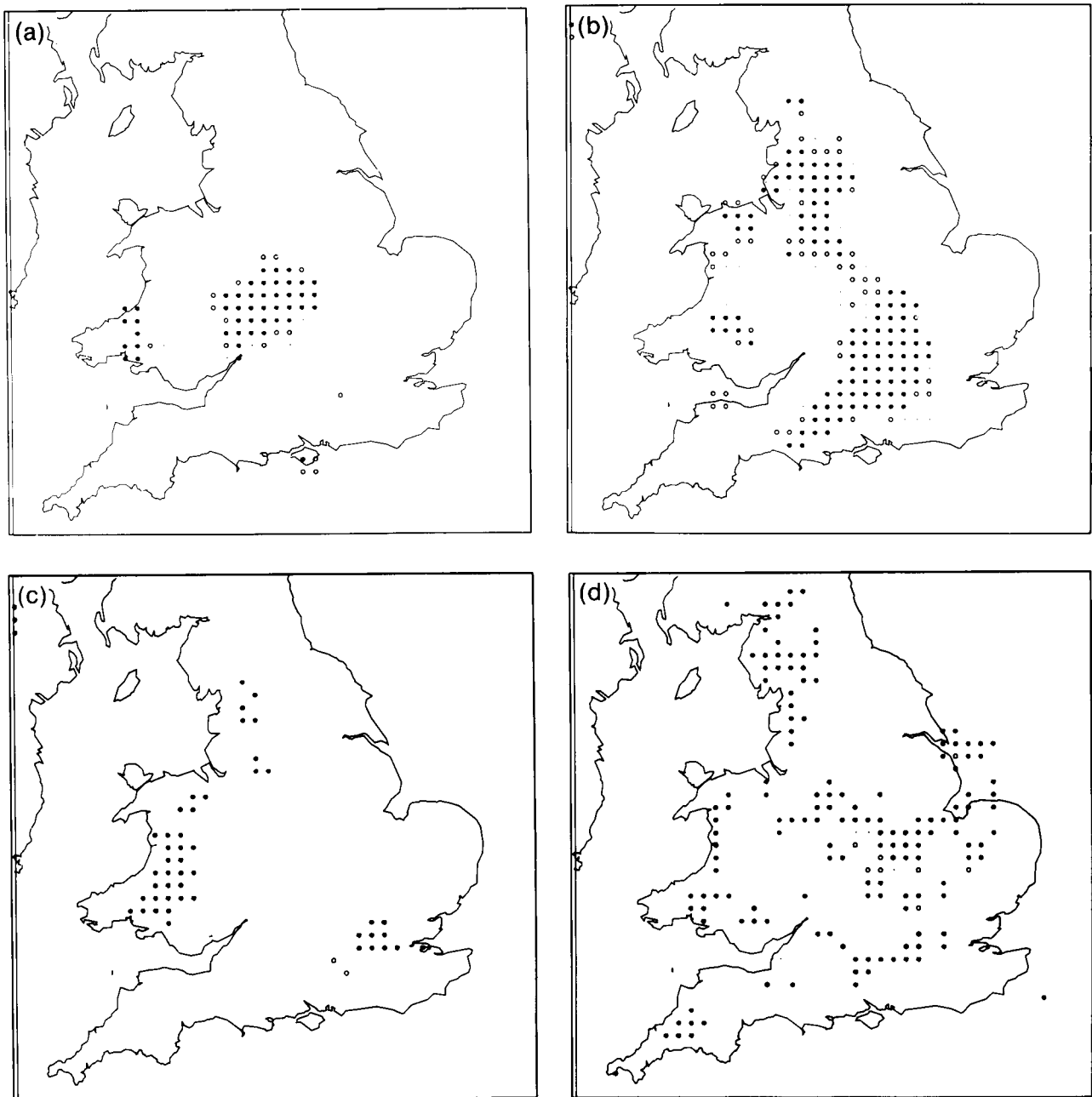


Figure 16. Distribution and development of showers and thunderstorms on 24 May 1989. (a) Radar observation at 11 UTC when the first showers developed south-west of London, (b) radar observation at 15 UTC, (c) 11-hour forecast for 11 UTC, and (d) 15-hour forecast for 15 UTC. Rainfall intensities are shown (in ascending order) by small dots, open circles and large dots.

5. Future Developments

Later this year, the mesoscale model will be transferred to the new Cray YMP supercomputer along with the operational forecast suite. The increased power will be used to increase the number of levels to meet requirements for low-cloud precision and to raise the top of the model to 15 km. A multi-level short-wave radiation scheme will also be implemented. Later, an improved advection scheme will be implemented, allowing a lower level of computational diffusion, which should also benefit the cloud forecasts. Improvements in data will come primarily from increased use of products from AUTOSAT-2, the Meteorological Office's satellite imagery processor. Dissemination of products will be improved by running the mesoscale forecast before the fine mesh, and by extensions to the GRAFNET facsimile network, resulting in quicker and more widespread availability of the model products.

References

- Carpenter, K.M., 1979: An experimental forecast using a non-hydrostatic mesoscale model. *Q J R Meteorol Soc*, **105**, 629–655.
- Charnock, H., 1955: Wind stress on a water surface. *Q J R Meteorol Soc*, **81**, 639–640.
- Findlater, J., Roach, W.T. and McHugh, B.C., 1989: The haar of north-east Scotland. *Q J R Meteorol Soc*, **115**, 581–608.
- Fritsch, J.M. and Chappell, C.F., 1980: Numerical prediction of convectively driven mesoscale pressure systems. Part I: Convective parameterization. *J Atmos Sci*, **37**, 1722–1733.
- Golding, B.W., 1989: The Meteorological Office experimental mesoscale numerical weather prediction system: July 1989. (Unpublished, copy available in National Meteorological Library, Bracknell.)
- Heymsfield, A.J., 1977: Precipitation development in stratiform ice clouds: a microphysical and dynamical study. *J Atmos Sci*, **34**, 367–381.
- Monteith, J.L., 1964: Evaporation and environment. *Symp Soc Exp Biol*, **19**, 205–234.
- Roach, W.T. and Slingo, A., 1979: A high resolution infrared radiative transfer scheme to study the interaction of radiation with cloud. *Q J R Meteorol Soc*, **105**, 603–614.
- Rutledge, S.A. and Hobbs, P.V., 1983: The mesoscale and microscale structure and organization of clouds and precipitation in midlatitude cyclones. VIII: A model for the “seeder-feeder” process in warm frontal rainbands. *J Atmos Sci*, **40**, 1185–1206.
- Slingo, A. and Schrecker, H.M., 1982: On the shortwave radiative properties of stratiform water clouds. *Q J R Meteorol Soc*, **108**, 407–426.
- Smith, F.B. and Carson, D.J., 1977: Some thoughts on the specification of the boundary layer relevant to numerical modelling. *Boundary Layer Meteorol*, **12**, 307–330.
- Smith, R.N.B., 1984a: The representation of boundary layer turbulence in the mesoscale model. Part I — The scheme without changes of state. (Unpublished, copy available in National Meteorological Library, Bracknell.)
- , 1984b: The representation of boundary layer turbulence in the mesoscale model. Part II — The scheme with changes of state. (Unpublished, copy available in National Meteorological Library, Bracknell.)
- Tapp, M.C. and White, P.W., 1976: A non-hydrostatic mesoscale model. *Q J R Meteorol Soc*, **102**, 277–296.
- Thompson, N., Barrie, I.A. and Ayles, M., 1981: The Meteorological Office Rainfall and Evaporation Calculation System MORECS (July 1981). *Hydrol Memo, Meteorol Off*, No. 45.
- Wright, B.J. and Golding, B.W., 1989: The impact of the interactive mesoscale initialisation. (Unpublished, copy available in National Meteorological Library, Bracknell.)
- Yamada, T. and Mellor, G.L., 1979: A numerical simulation of BOMEX data using a turbulence closure model coupled with ensemble cloud relations. *Q J R Meteorol Soc*, **105**, 915–944.

Radar study of the snowfall in south-west Cornwall on 12 January 1987

W.S. Pike

19 Inholmes Common, Woodlands St. Mary, Newbury, Berkshire RG16 7SX

Summary

A heavy snowfall affecting south-west Cornwall during January 1987 is analysed using surface observations, Camborne 2 km radar data, and AVHRR satellite pictures to determine its causes, geographical extent and temporal limits.

1. Introduction

The general synoptic situation featuring extremely cold air advecting from the east during 12 January 1987 is shown in Fig. 1. Transfer westwards of convective cloud formed in cold air along a major convergence line over the relatively warm English Channel is shown in two AVHRR infra-red satellite pictures taken at 0410 and 0829 UTC on 12 January (Fig. 2). Note that the Lizard Peninsula is cloud-covered in the latter picture.

Lumb (1988) has described heavy snowfall affecting only the south-west of Cornwall, and an interesting report of 'pack snow' causing slight to moderate icing on the m.v. *Shell Explorer*, which was sailing through the snowfall in the English Channel off the Lizard that day, has been documented by Kain (1988) and Pike (1990a). It was deduced that these snowfalls had come within the 70 km range of Camborne's fine-mesh (i.e. 2 km \times 2 km) radar coverage and that a study of radar images of

precipitation at suitable intervals should be rewarding. These images are shown in Fig. 3 and are selected from a sequence originally recorded at 15-minute intervals.

2. Snowfall interpretation

Four Camborne hourly radar scans from 0300 to 0600 UTC on the 12th (Figs 3(a) to 3(d)) show bands of cold-frontal precipitation moving away south-westwards. Ignoring stationary ground-clutter returns from the hills around Camborne (Hensbarrow Down etc.) stippled areas represent slight snow (averaged over 2 km \times 2 km squares) falling with equivalent rainfall rates of less than 0.5 mm hr⁻¹. Black areas represent areas of at least moderate snow with equivalent rainfall rates of 0.5 mm hr⁻¹ or more. Isolated cells first appear east of the Lizard at 0600 UTC and thereafter continue to develop and move westwards at about 12–15 kn during

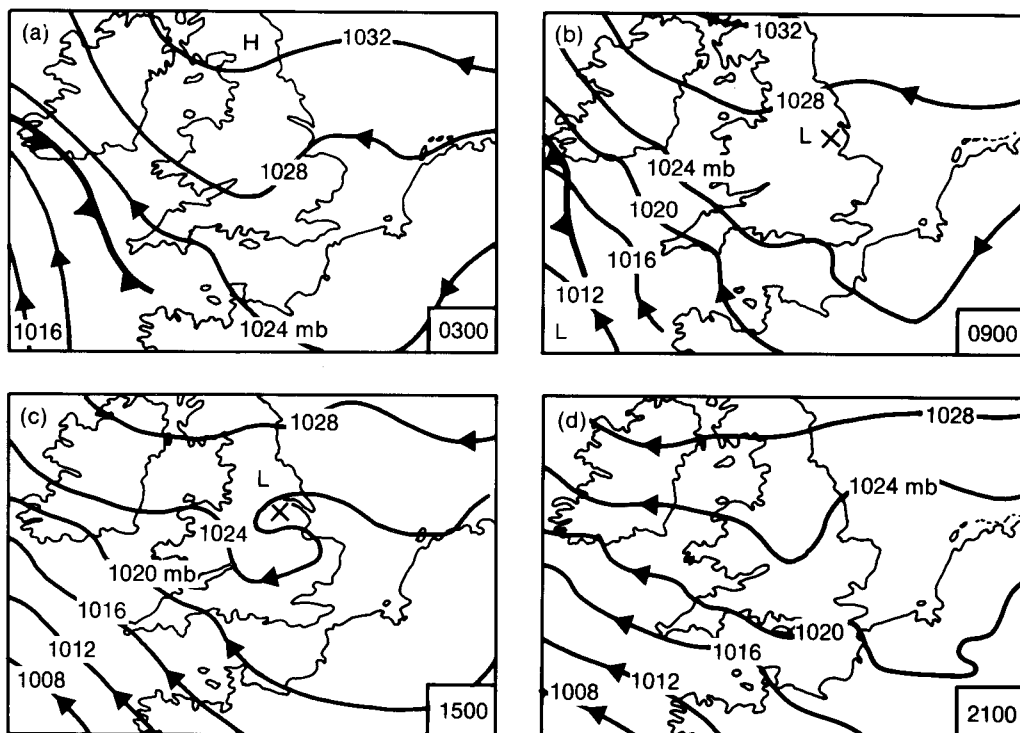


Figure 1. Surface synoptic charts for 0300, 0900, 1500 and 2100 UTC on 12 January 1987.



Photographs by courtesy of University of Dundee

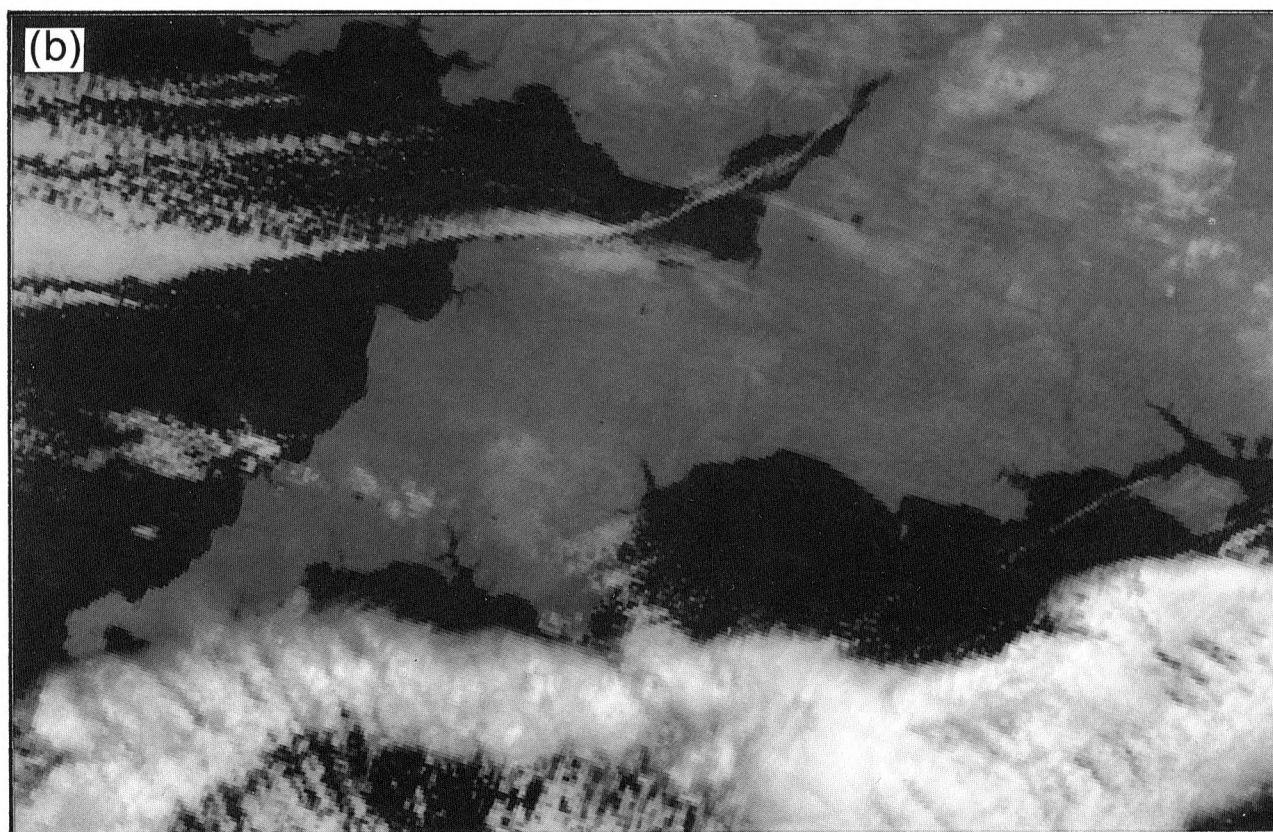


Figure 2. NOAA AVHRR infra-red satellite pictures for (a) 0410 UTC and (b) 0829 UTC on 12 January 1987.

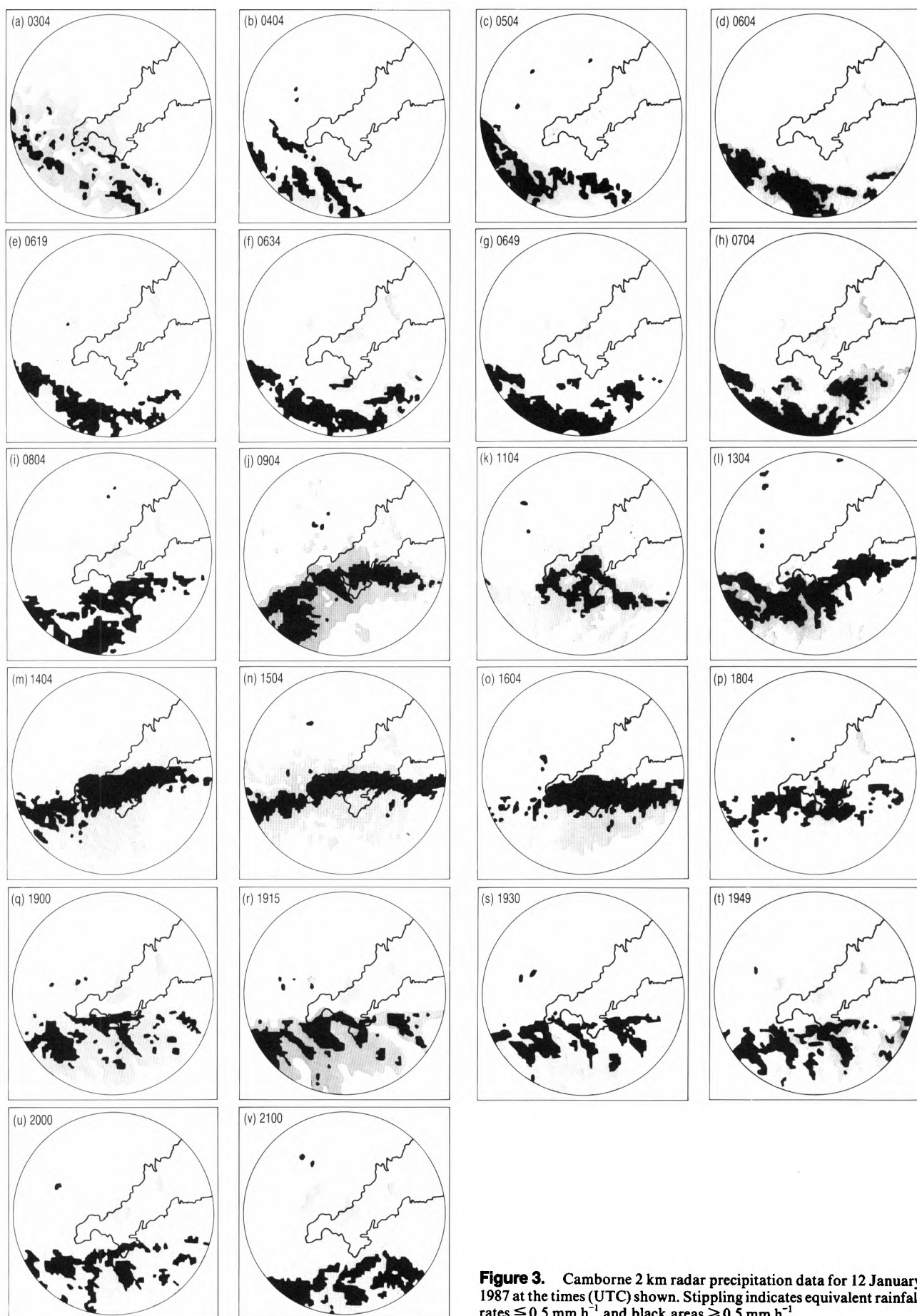


Figure 3. Camborne 2 km radar precipitation data for 12 January 1987 at the times (UTC) shown. Stippling indicates equivalent rainfall rates $\leq 0.5 \text{ mm h}^{-1}$ and black areas $\geq 0.5 \text{ mm h}^{-1}$.

the next hour (Figs 3(e) to 3(h)). Further cells of precipitation merge together into a more or less continuous belt as they develop over the sea to the south-east, and snow begins to fall over the Lizard Peninsula between 0700 and 0800 UTC as this belt moves north-westwards. By 0900 UTC the snow belt covers much of south-west Cornwall, the precipitation zone never being more than 50 km wide, with the heavier snow area occupying up to half of this width. Fig. 2(b) for 0829 UTC gives the distinct impression that a series of convective cells were being built up primarily by the strong south-east to east-south-easterly over-water flow as it met lighter north-easterly to east-north-easterly low-level land-breezes along the length of a major convergence line which by now had propagated westwards along the English Channel from Sussex to west Cornwall.

As 'tracers' of the land-breeze, shallow 'plumes' of convective cloud are revealed by the NOAA AVHRR infra-red satellite pictures (Fig. 2) to be streaming downwind from promontories (especially The Needles on the Isle of Wight — see Fig. 2(a)) and also from the Wye Gorge, as a well-developed land-breeze drains down from the Forest of Dean over the warmer water of the Severn Estuary and the Bristol Channel.

East to west orientation of the precipitation belt axis appears to have closely correlated with a median position for the English Channel coastal convergence during this period (0900–2100 UTC on 12 January 1987), along or close to a line from Falmouth to Penzance at the boundary between the two (over land and over sea) low-level airflows.

Figs 3(j) to 3(n) show the behaviour and movement of the precipitation belt during daylight hours on the 12th. Probably the belt is genuinely narrow in the extreme south-east where cells are developing over the sea, but this might be due to a range- or masking-factor associated with the radar itself. A few breaks do appear at about 1100 UTC (Fig. 3(k)) but the precipitation remains continuous and more or less stationary during the day, although the heavier cells do tend to merge and the band moves a little further north during the afternoon. When breaks did appear in the morning, individual cells could be traced moving along the band through the pattern of general slight snow, as had been suspected earlier over the Thames Estuary (Pike 1990b) and after Passarelli and Braham (1981). The signature of land-breeze involvement may well be the sharp landward edge of precipitation (as in Fig. 3(l)) in comparison with the ragged seaward edge where irregular uplift is taking place.

The snow belt reaches its most northerly point over St. Austell Bay towards 1400 UTC (Fig. 3(m)), when perhaps the diurnal effects of land-breezes were weakest, before beginning to edge southward again. The 1504 UTC image introduces a narrow band of heavier snow 10–20 km wide, which is a feature of the following 3 hours as the belt continues to move southwards (Figs 3(n) to 3(p)) exhibiting a notably straight and sharp northern edge from 1800 to 2000 UTC indicating a strengthening land-breeze involvement. The black echelon-shaped precipitation areas appear to be a typical signature of convergent airflows being active in their formation. They move quite rapidly, at maybe



© Crown copyright. Photograph by courtesy of Photographic Dept., RNAS Culdrose

Figure 4. Car buried under extensive snow drift at RNAS Culdrose, near Helston, Cornwall on 12 January 1987.

25–35 kn, from east to west between 1900 and 2000 UTC and would seem to be particularly worthy of note. The snow finally clears the Lizard peninsula at around 2100 UTC having given substantial dry snowfall over the past 14 hours, there being a particularly sharp northern edge to the snow-affected areas.

Fig. 4 shows drifts to car-top height at the Royal Naval Air Station at Culdrose following snowfalls of 20–30 cm experienced during the 12th. On the Isles of Scilly, Tresco Botanical Gardens lost 70% of its trees and shrubs (many of which were subtropical species) during this brief period of extreme cold. Staff arrived on Monday 12 January in almost continuous heavy snow showers which left 9 inches (23 cm) lying by the end of the day when temperatures had fallen to -8.0°C .

It should be noted that these heavy snowfalls in the south-west occurred immediately prior to record low 1000–500 mb thickness values arriving from the east. Readings of 500 dam at Larkhill (at 1200 UTC on the 12th) and 502 dam (at Camborne and Valentia by 0000 UTC on the 13th) appear to be the lowest values recorded there since regular upper-air soundings began over 50 years ago.

3. Conclusions

Fig. 5 demonstrates the close relationship between Camborne radar returns and the snow depths measured in south-west Cornwall on the 12th. When integrated over 6-hour periods (0900–1500 and 1500–2100 UTC) the Camborne 2 km data gives a very good indication of

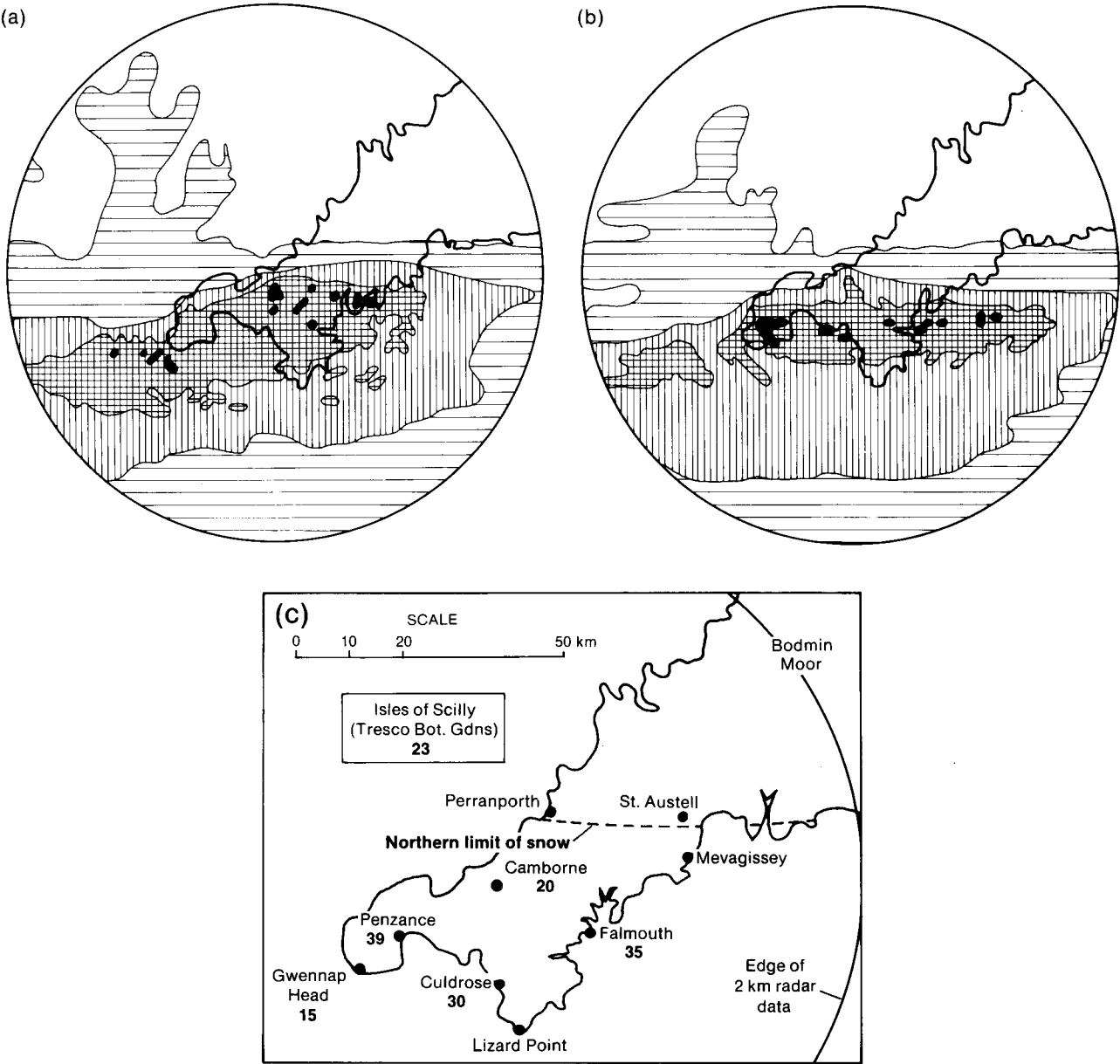


Figure 5. Integrated Camborne $2 \text{ km} \times 2 \text{ km}$ radar precipitation data for the 6-hour periods (a) 0900–1500 UTC and (b) 1500–2100 UTC on 12 January 1987 related to (c) snowfall (cm) reported to have occurred during 12 January 1987. In (a) and (b) integrated rates of equivalent rainfall are indicated by horizontal shading ($< 1.0 \text{ mm h}^{-1}$), vertical shading ($1.0\text{--}2.9 \text{ mm h}^{-1}$), hatching ($3.0\text{--}4.9 \text{ mm h}^{-1}$) and black ($\geq 5.0 \text{ mm h}^{-1}$).

average snowfall intensity experienced over these particular time spans. The hatched areas clearly indicate those regions in which at least moderate snowfall predominated, taking the form of heaviest accumulations affecting a 25 km wide belt whose axis lay from approximately Falmouth (where 35 cm fell) to Penzance (39 cm).

Acknowledgements

To Meteorological Office staff at Bracknell, particularly to Geoff Monk of the Nowcasting and Satellite Applications Branch for supplying the Camborne 2 km radar data and integrations. Also to Commander P.L. Stubbs, RN, for kindly sending observations and photographs from RNAS Culdrose, and to J. Webb of 'TORRO' for additional snow depth observations.

References

- Kain, D.G., 1988; Ice accretion; English Channel. *Mar Obs*, 58, 13.
Lumb, F.E., 1988; Letter to *Weather*, 43, 31.
Passarelli R.E. Jr. and Braham, R.R. Jr, 1981; The role of the winter land breeze in the formation of Great Lake snowstorms. *Bull Am Meteorol Soc*, 62, 482–491.
Pike, W.S., 1990a; Land-breezes, snowfalls, and cold air convergence near coastlines in southern Britain. *Mar Obs*, 60, 26–32.
—; 1990b; Persistent coastal convergence in a heavy snowfall event on the south-east coast of England. *Meteorol Mag*, 119, 21–32.

Notes and news

Hydrologists meet to study precipitation measurement problems

(Note based on a news release from the WMO Press Office)

The summer of 1989 serves as a reminder that a deficiency of rainfall, especially like that over England and Wales, causes many hardships to the public and industry.

If anything, small rainfalls require more careful measurement than large ones if their benefits are to be maximized. But there is still a requirement for research into the attainable accuracy measurement of all rainfalls at points or their estimation over areas, both over land and sea.

The WMO has been involved in the study of methods of precipitation measurement for more than 30 years. With its Members, it has conducted many trials and tests of different instruments and methods in different parts of the world, but a number of problems remain.

The International Workshop on Precipitation Measurement, which was held in St Moritz, Switzerland, from 4 to 7 December 1989 addressed these precipitation-measurement problems and broader ones concerning the interaction between climate and the global water cycle. The Workshop was jointly organized by the WMO, the International Association of Hydrological Sciences (IAHS) and the Swiss Federal Institute of Technology (ETH).

At present the 160 000 rain-gauges (about 4000 in the United Kingdom alone) distributed over the land area of the globe, along with weather radars (8 in the United Kingdom) and satellite observations go a long way towards providing adequate meteorological information about rainfall over populated regions. However, they do not yet provide the accurate values of precipitation falling at a particular place on the earth's surface or over specific river catchments.

Water is as essential to our existence as the very air we breathe. Without rain, snow and other forms of precipitation to water the soil, raise the rivers and recharge the reservoirs, the economy and society of the planet would soon stop. But man is also affected by too much rain — floods are among the most serious disasters. More accurate information on this phenomenon is needed by hydrologists and all those concerned with water availability in the face of a changing climate.

The can-type precipitation gauge, in common use, has certain inherent deficiencies. Because most countries have developed their own gauges, each with its own characteristics, comparisons of precipitation amount across international boundaries may be difficult. Accurate assessments of global precipitation are also very difficult because there are virtually no measurements made over the oceans. Such information must be inferred from ground-based radar and satellite observations, which themselves rely on conventional rain-gauge measurements for calibration.

The Workshop studied these problems by bringing together experts in determining precipitation by various means, to promote improvements and to hasten the move towards truly homogeneous measurements. It directed attention to the research needed, especially in the World Climate Programme and Global Energy and Water Cycle Experiment (GEWEX) which is being planned as the major international effort in the study of the climate for the latter half of the 1990s.

New Meteorological Office buildings at Bracknell

For some years it has been acknowledged that the amount of accommodation space available to staff at Bracknell has been inadequate. As a consequence, the use of new buildings giving increased space, has commenced.

Three new office blocks adjacent to the main Headquarters building have been acquired, and two of these are to be named the Johnson and Sutton Buildings after past Heads of the Office (see below). The Sutton Building is already occupied by the Commercial Section of the Office; the Johnson Building will soon be occupied by staff responsible for data provision and consultancy. The third building will house the staff who will be at the forefront of the United Kingdom's research into climate change and it is felt that the name 'Climate Research Centre' will be a sufficiently clear identification of this building and its purpose.

The use of a further building, to replace the premises currently used at Eastern Road to house the Archives, has also been negotiated. These new premises for the Archives will be known as the Scott Building.

The list of 'named' parts of the Office includes: the FitzRoy, Napier Shaw, Dines and Richardson Wings of the Main Building, the Experimental Site at Beaufort Park, Easthampstead, and the Simpson Building at Western Road, Bracknell (which houses the stores and test facilities).

Listed below are short notes about the meteorologists who are commemorated in this way. Those who were in charge of the Office are collectively referred to as 'Heads' — in reality the name of this position has changed several times.

Vice-Admiral R. FitzRoy, FRS, 1805–1865. Head 1855–65.

In his earlier days Fitzroy captained HMS *Beagle*, with Charles Darwin on board as naturalist, and at one stage was the Governor of New Zealand. While at the Board of Trade, which was responsible for Meteorological Services at that time, he introduced storm warnings and the issue of daily forecasts to the Press.

R.H. Scott, MA, FRS, 1833–1916. Head 1867–1900.

Scott was responsible for the setting-up of the first official weather observing stations in the United Kingdom, to provide data for forecasting and climate studies. He was also interested in the meteorology of the oceans. During the period 1874–1900 he was secretary to the International Meteorological Committee.

Sir William Napier Shaw, D.Sc, FRS, 1854–1945. Head 1900–20.

Shaw initiated the systematic study of atmospheric processes, which laid the foundations for scientific weather forecasting. He had a particular interest in upper-air studies, and was president of the International Meteorological Committee from 1907 to 1923.

Sir George Simpson, KCB, CBE, D.Sc, LL D, FRS, 1878–1965. Head 1920–38.

As a younger man, Simpson was a pioneer of Antarctic meteorology. He supervised the integration of the Meteorological Office into the Air Ministry in the early 1920s. After retirement he returned to the Office to take charge of the Observatories, where he specialized in studies of the electrical charging in thunderstorms.

Sir Nelson Johnson, KCB, D.Sc, ARCS, 1892–1954. Head 1938–53.

Johnson's early days were spent in studies of atmospheric diffusion and temperature variations close to the ground. Later, as head of the Office, he was responsible for the installation of stations for making upper-air soundings and sferics measurements. He was the last president of the International Meteorological

Organization and the first of its replacement — the World Meteorological Organization.

Sir Graham Sutton, CBE, FRS, 1903–77. Head 1953–65.

Sutton was notable for promoting the exchange of ideas between the research and services sides of the Office, and the development of services to non-aviation customers. During his tenure, the Office acquired its first electronic computer.

W.H. Dines, FRS, 1855–1927.

After a 4-year apprenticeship in steam-locomotive design and building, and 3 years studying mathematics at Cambridge, Dines turned his attention to the measurement of meteorological variables. He designed a pressure-tube anemometer and a tilting-siphon rain-gauge, both of which are still in use to this day.

L.F. Richardson, D.Sc, FRS, 1881–1953.

Richardson's meteorological work showed a rare combination of theoretical and experimental ability. His studies of atmospheric turbulence are commemorated in the Richardson number. His pioneering work on numerical weather prediction was ahead of its time, there being neither adequate observations of the atmosphere nor computers available for his methods to be exploited.

Rear-Admiral Sir Francis Beaufort, FRS, 1774–1857.

Beaufort is mainly known for introducing two systems for describing aspects of weather which do not rely upon a knowledge of English. These are his Scale of Wind Force in which wind speeds are described by numbers, and a Notation of Weather using letters.

Books received

The listing of books under this heading does not preclude a review in the Meteorological Magazine at a later date.

Global climate change, by S.F. Singer (New York, Paragon House, 1989) divides the problems into inadvertent human intervention, purposeful human intervention and outside human intervention. The common themes relating to human survival are investigated.

Meteorology and World War II, Parts I and II, edited by B.D. Giles (Royal Meteorological Society, 1987, 1989) contain descriptions of the various meteorological endeavours of the period by many people who were there. The two volumes are the products of two conferences held at the University of Birmingham in 1986 and 1988.

Satellite and radar photographs — 25 March 1990 at 0900 and 1500 UTC

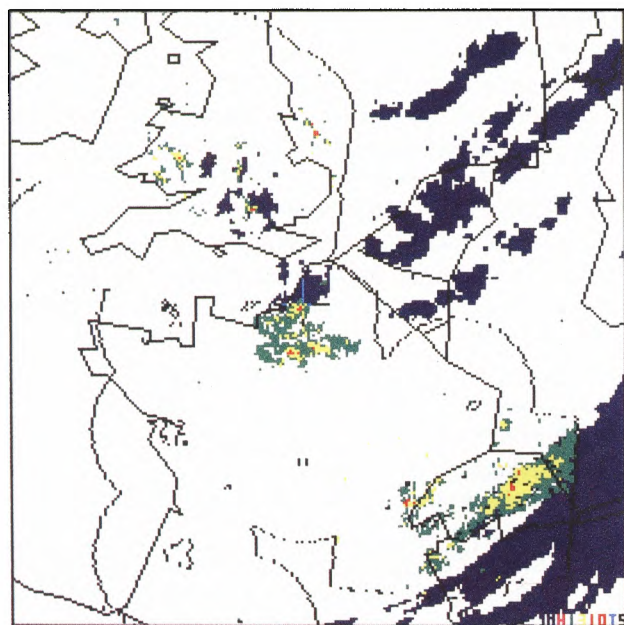


Figure 1. COST 73 (Co-operation in Science and Technology project 73) satellite and radar picture at 0900 UTC on 25 March 1990. Dark blue represents cloud tops colder than -15°C . Green, yellow, red and light blue represent progressively increasing rainfall rates. Coastlines, national boundaries and the limits of radar coverage are shown in black.

The Meteosat satellite and radar photographs shown in Figs 1 and 2 illustrate the intensification of showers due to daytime heating in a cold northerly airstream. Cloud colder than -15°C is shown (in dark blue) except at pixels where precipitation is also occurring, when the radar-derived rainfall intensity is shown. At the present time radar information is restricted to the British Isles, France and Switzerland.

At 0900 UTC (Fig. 1) the leading edge of the cold airmass was located over Switzerland, marked by a cold front and related band of cloud and precipitation. Within the cold air, cloud and showers were chiefly restricted to a trough extending from Denmark to southern Britain and northern France. Convection was enhanced by daytime heating, identified at 1500 UTC (Fig. 2) by a considerable increase in the area and intensity of showers. Synoptic observations indicated that hail and thunder occurred within some of the showers near the trough. Elsewhere showers were generally less heavy and over western France and western and northern Britain showers were either absent or very light due to the influence of a large area of high pressure (see Fig. 3).

G.A. Monk

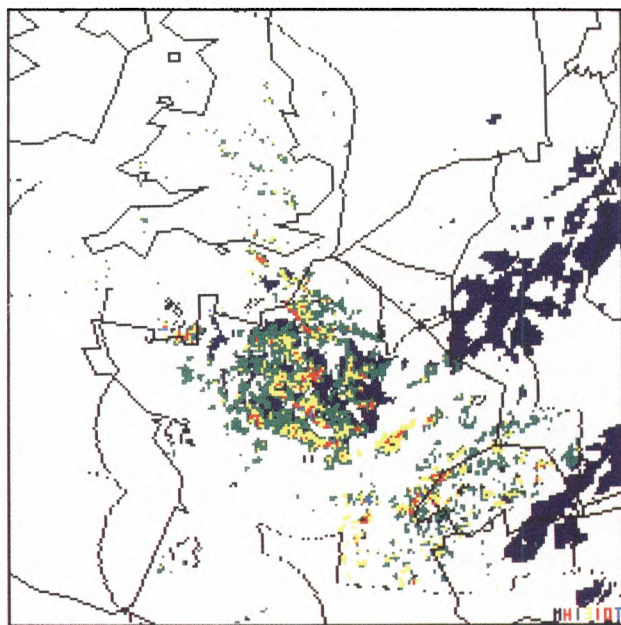


Figure 2. As Fig. 1 but for 1500 UTC on 25 March 1990.

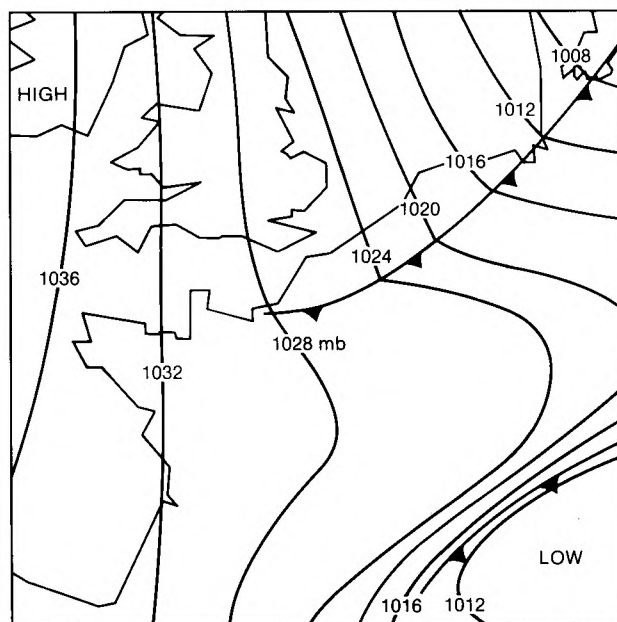


Figure 3. Surface analysis at 1200 UTC on 25 March 1990.

GUIDE TO AUTHORS

Content

Articles on all aspects of meteorology are welcomed, particularly those which describe results of research in applied meteorology or the development of practical forecasting techniques.

Preparation and submission of articles

Articles, which must be in English, should be typed, double-spaced with wide margins, on one side only of A4-size paper. Tables, references and figure captions should be typed separately. Spelling should conform to the preferred spelling in the *Concise Oxford Dictionary* (latest edition). Articles prepared on floppy disk (Compucorp or IBM-compatible) can be labour-saving, but only a print-out should be submitted in the first instance.

References should be made using the Harvard system (author/date) and full details should be given at the end of the text. If a document is unpublished, details must be given of the library where it may be seen. Documents which are not available to enquirers must not be referred to, except by 'personal communication'.

Tables should be numbered consecutively using roman numerals and provided with headings.

Mathematical notation should be written with extreme care. Particular care should be taken to differentiate between Greek letters and Roman letters for which they could be mistaken. Double subscripts and superscripts should be avoided, as they are difficult to typeset and read. Notation should be kept as simple as possible. Guidance is given in BS 1991: Part 1: 1976, and *Quantities, Units and Symbols* published by the Royal Society. SI units, or units approved by the World Meteorological Organization, should be used.

Articles for publication and all other communications for the Editor should be addressed to: The Chief Executive, Meteorological Office, London Road, Bracknell, Berkshire RG12 2SZ and marked 'For Meteorological Magazine'.

Illustrations

Diagrams must be drawn clearly, preferably in ink, and should not contain any unnecessary or irrelevant details. Explanatory text should not appear on the diagram itself but in the caption. Captions should be typed on a separate sheet of paper and should, as far as possible, explain the meanings of the diagrams without the reader having to refer to the text. The sequential numbering should correspond with the sequential referrals in the text.

Sharp monochrome photographs on glossy paper are preferred; colour prints are acceptable but the use of colour is at the Editor's discretion.

Copyright

Authors should identify the holder of the copyright for their work when they first submit contributions.

Free copies

Three free copies of the magazine (one for a book review) are provided for authors of articles published in it. Separate offprints for each article are not provided.

May 1990

Editor: B.R. May

Vol. 119

Editorial Board: R.J. Allam, R. Kershaw, W.H. Moores, P.R.S. Salter

No. 1414

Contents

	Page
The Meteorological Office mesoscale model. B.W. Golding	81
Radar study of the snowfall in south-west Cornwall on 12 January 1987. W.S. Pike	97
Notes and news	
Hydrologists meet to study precipitation measurement problems	102
New Meteorological Office buildings at Bracknell	102
Books received	103
Satellite and radar photographs — 25 March 1990 at 0900 and 1500 UTC G.A. Monk	104

Contributions: It is requested that all communications to the Editor and books for review be addressed to the Chief Executive, Meteorological Office, London Road, Bracknell, Berkshire RG12 2SZ, and marked 'For *Meteorological Magazine*'. Contributors are asked to comply with the guidelines given in the *Guide to authors* which appears on the inside back cover. The responsibility for facts and opinions expressed in the signed articles and letters published in *Meteorological Magazine* rests with their respective authors.

Subscriptions: Annual subscription £30.00 including postage; individual copies £2.70 including postage. Applications for postal subscriptions should be made to HMSO, PO Box 276, London SW8 5DT; subscription enquiries 071-873 8499.

Back numbers: Full-size reprints of Vols 1-75 (1866-1940) are available from Johnson Reprint Co. Ltd, 24-28 Oval Road, London NW1 7DX. Complete volumes of *Meteorological Magazine* commencing with volume 54 are available on microfilm from University Microfilms International, 18 Bedford Row, London WC1R 4EJ. Information on microfiche issues is available from Kraus Microfiche, Rte 100, Milwood, NY 10546, USA.

ISBN 0 11 728665 6

ISSN 0026-1149

© Crown copyright 1990. First published 1990

The Meteorological Magazine

June 1990

Sea-breeze at Darwin
Links between convection and waves
Surface wind gusts using radar



DUPLICATE JOURNALS

National Meteorological Library
FitzRoy Road, Exeter, Devon. EX1 3PB

HMSO

Met.O.992 Vol. 119 No. 1415



3 8078 0010 2476 1

The Meteorological Magazine

June 1990
Vol. 119 No. 1415

551.553.11(948)

The sea-breeze at Darwin: a climatology

L.M. Lloyd

Australian Bureau of Meteorology

Summary

The characteristics of the diurnal cycle of the sea-breeze at Darwin are examined and compared for different times of the year, with the aid of tables and diagrams depicting the frequency, time of onset and decline, direction, strength, and sense of rotation. The relationships between the evolution of the sea-breeze, and the diurnal and seasonal variation of the boundary layer in the Darwin region are discussed.

1. Introduction

The sea-breeze is a thermally driven circulation (Atkinson 1981) dependent on land-sea temperature differences which vary diurnally, according to the diurnal changes in land temperature, and seasonally, according to the seasonal changes of sea surface temperatures (SSTs) and land temperatures. The purpose of this study is to develop a climatology of the sea-breeze at Darwin, and to suggest some reasons for its behaviour.

Darwin is situated on the central northern coastline of Australia ($12^{\circ} 26'S$, $130^{\circ} 52'E$) (see Fig. 1). North-westerly monsoon flow prevails during the summer months (December–February) whilst south-easterly trades of continental origin predominate for the rest of the year. There are many inlets and indentations in the shoreline around Darwin but it runs roughly from a south-west to a north-east direction. Consequently, the north-west is the most favourable, though not exclusive, direction from which the sea-breeze develops.

2. Selection of data

The data used for this study were obtained directly from Bureau of Meteorology Dines anemograph charts for Darwin Airport and cover the 5-year period 1980–84 inclusive. The aerodrome where the meteorological readings are taken is 28.7 m above sea level and approximately 5 km from the sea-shore.

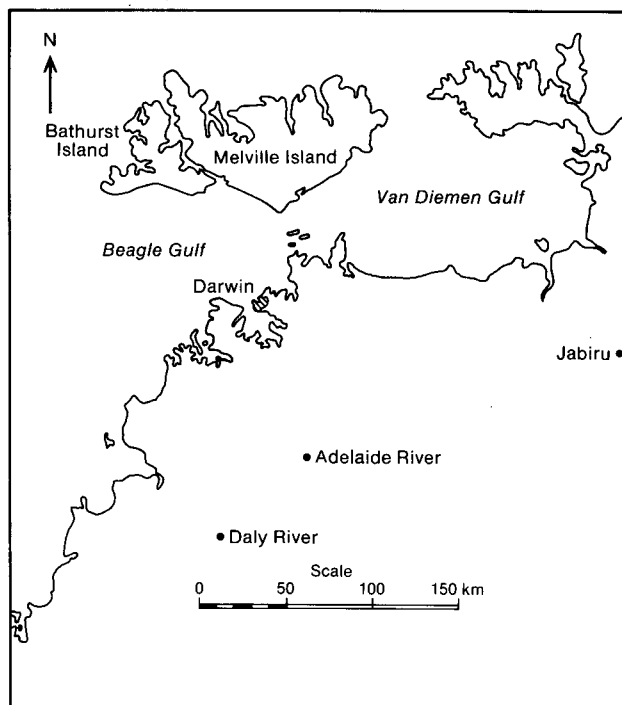


Figure 1. The area around Darwin showing places mentioned in the text.

3. Onset, duration and decline

A clear-cut start and finish to the sea-breeze is sometimes difficult to determine, especially during the wet season months of November–February inclusive, when there is an almost continuous north-westerly airflow over Darwin. This made it necessary to examine the daily anemograph charts and subjectively allocate times for the onset and cessation of the sea-breeze. In many cases, the duration time could only be determined when the wind speed fell to zero or the wind direction changed so that it could no longer be called a sea-breeze.

The onset time of the sea-breeze varies greatly from month to month and even day to day, especially during the dry season. This marked variation can be seen by examining Table I. As the wet season draws to a close, the almost continuous westerly airflow starts to break down — sea-breezes become easy to distinguish due to the abrupt change in wind direction and have a very distinct onset time.

The month of March can be seen as a transition period between the westerly and south-easterly regimes. The figures in Table I show that March has a bi-modal distribution of onset times. The major peak between 0900–0959* is probably the result of the downward mixing of the westerly gradient wind as the boundary layer heats up. The second peak between 1300–1359 would indicate the percentages of ‘true’ sea-breezes or those formed with an opposing gradient wind.

As the dry season becomes established and the south-easterly trades strengthen, the onset of the sea-breeze becomes later, being most frequent around 1230 in April and 1630 in July. During August there is a re-emergence of the bi-modal onset pattern — the trade winds sometimes weaken and occasionally give way to westerlies. Gradient winds with westerly components become more frequent through September and October due to the development of an inland synoptic-scale heat low.

The 0900–0959 onset maxima may be due to downward mixing of westerly gradients, or in times of light gradient winds may be a true early sea-breeze induced by the large land–sea temperature contrast during these months (see Figs 2 and 3(b)). The maxima between the hours 1300–1359 is evidently a common time of onset with opposing (easterly component) gradient winds.

Table II shows the percentage frequency of the duration of sea-breezes. It can be seen that between September and March inclusive, the majority of sea-breezes last in excess of 8 hours, whilst from November to February inclusive, north-westerly winds blow almost continuously. The life of the sea-breeze is abruptly shortened during the dry season. In April, only 17% of them last for 8 hours or more; in May the majority have a life span of less than 5 hours, while in June and July most have a life span of less than 6 hours.

An appreciation of inland temperatures and their likely effects on the development of sea-breezes can be obtained by considering the inland stations Jabiru Airport (12° 40’S, 132° 54’E) or Daly River (13° 41’S, 130° 38’E) which are over 50 km from the coast compared with Darwin which is 5 km inland.

Fig. 2 shows the average seasonal SST–land temperature difference using composite maximum temperatures from Jabiru Airport and Daly River. A minimum SST–land temperature difference of around 3.5 °C occurs in June, and a maximum difference of around 9 °C occurs during September and October.

Figs 3(a) and 3(b) show the average diurnal land–sea temperature contrasts that can be expected during the periods of minima (June) and maxima (September) respectively. The shaded area above the SST line gives an indication of the thermal energy available to drive the sea-breeze. The average daily period during which this thermal energy is available is from 1200 to 1800 (6 hours) in June and 0900–1930 (10½ hours) in September.

Table I. Percentage frequency of onset times of the sea-breeze at Darwin Airport

Month	Time of onset								
	0900– 0959	1000– 1059	1100– 1159	1200– 1259	1300– 1359	1400– 1459	1500– 1559	1600– 1659	1700– 1759
Mar.	33	9	7	6	19	10	8	6	2
Apr.	4	5	15	20	11	14	10	16	5
May	2	1	7	6	10	16	18	22	19
June	5	3	2	7	19	17	18	20	10
July	3	5	5	10	12	14	19	23	9
Aug.	14	7	11	18	14	16	15	4	1
Sept.	27	13	12	12	18	12	3	3	0
Oct.	40	13	18	11	5	7	4	2	0
Nov.–Feb.	Almost continuous north-westerly flow								

* All times referred to in this paper are local time.

Taking into account the inertia of the sea-breeze circulation, these periods relate reasonably well to the data given in Tables I–III.

Table III shows that the vast majority of sea-breezes dissipate between 1800 and 2200 during the months of April–September. In fact the most frequent time of

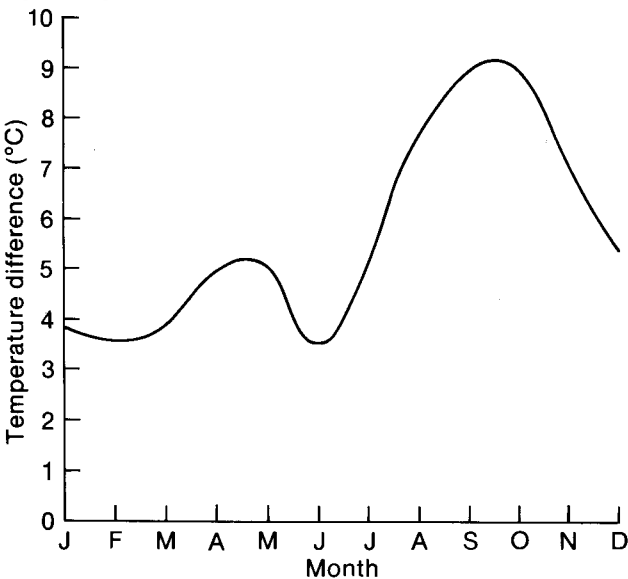


Figure 2. Variation of the diurnal maximum land–sea temperature difference in the Darwin region based on monthly values of average daily maximum temperature (composite of Jabiru and Daly River). (Australian Bureau of Meteorology 1988).

Table II. Percentage frequency of the duration of the sea-breeze to the nearest whole hour at Darwin Airport

Month	Duration (hours)							
	1	2	3	4	5	6	7	≥8
Mar.	Over 50% exceed 8 hours							
Apr.	2	7	10	17	11	19	16	17
May	5	16	19	19	13	9	11	7
June	5	13	12	17	19	13	8	12
July	2	11	17	10	18	14	12	16
Aug.	0	0	3	8	15	17	13	45
Sept.–Oct.	Over 50% exceed 8 hours							
Nov.–Feb.	Almost continuous north-westerly flow							

dissipation in May and June is between 1900 and 1959, which is 1–1½ hours after sunset, and 1–2 hours after the average inland temperature has fallen below the SST.

Sea-breezes that continue to blow after 2200 do so with the assistance of the gradient wind. The direct influence of the westerly monsoons can be seen by the

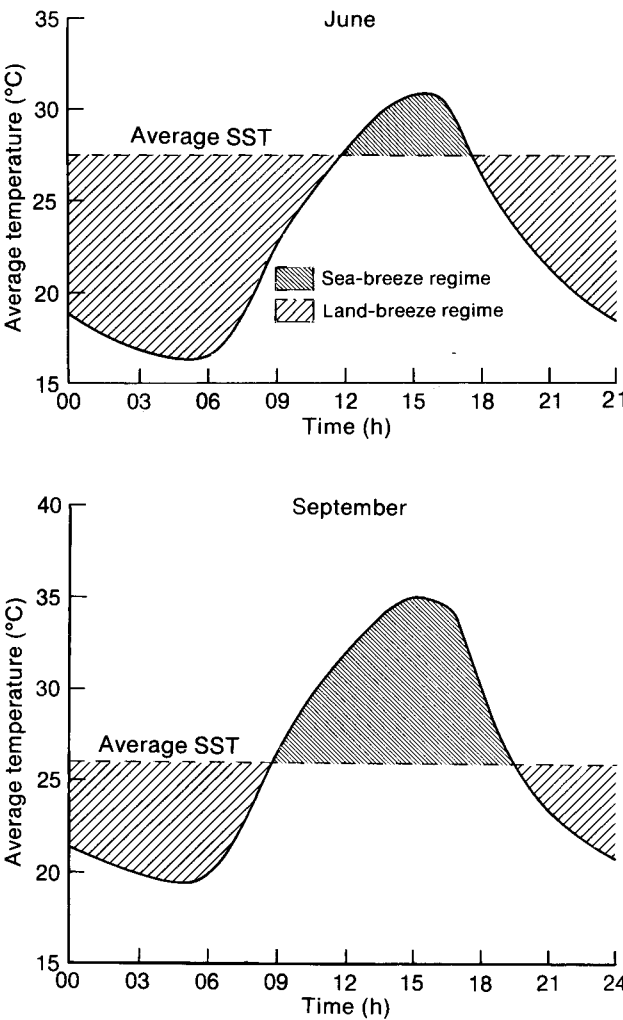


Figure 3. Average diurnal temperatures (as Fig. 2) and the average sea surface temperature off Darwin for the months indicated.

Table III. Percentage frequency of the decline times of the sea-breeze at Darwin Airport

Month	Time of decline						
	1600–1659	1700–1759	1800–1859	1900–1959	2000–2059	2100–2159	After 2159
Mar.	Over 50% continued after 2159						
Apr.	8	6	20	30	24	6	7
May	1	0	29	45	10	11	3
June	0	0	14	43	27	12	5
July	0	0	15	33	26	12	16
Aug.	0	0	10	29	18	14	29
Sept.–Oct.	Over 50% continued after 2159						
Nov.–Feb.	Almost continuous north-westerly flow						

substantial increase in the percentage of onshore breezes which continue after 2200 during August, until they become an almost continuous occurrence from November to February, making it impossible to distinguish the sea-breeze from the predominant westerly airflow.

4. Direction

It is well known that the direction of the sea-breeze is influenced by local topography, the strength and direction of the gradient-level wind, and Coriolis force (Atkinson 1981). In sunny conditions with light offshore gradient winds (usually less than 5 m s^{-1}), and as a direct response to the horizontal temperature gradient caused by the unequal heating of the land and sea surfaces, the sea-breeze initially tends to blow perpendicular to the coastline. The data shown in Table IV confirms this, with the most frequent initial direction being from the north-west. However, under the influence of strong east to north-east gradient winds, the sea-breeze also frequently develops in the north to north-east sector.

The dominance of the west to north-westerly monsoon during the months of November–March inclusive, makes it difficult to distinguish the sea-breeze circulation from the general westerly airflow. Fig. 4 shows the mean speed and direction of the surface wind at Darwin Airport during these months. In November, the south-easterly trades can still be seen to influence the surface wind in the morning between 1000 and 1100, while from December to March, and apart from the occasional interruption, they blow almost continuously from the north-west sector.

Table IV. Percentage frequency of the initial direction from which the sea-breeze develops at Darwin Airport

Month	Initial direction of the sea-breeze			
	W	NW	N	NE
Apr.	22	39	11	28
May	12	32	24	32
June	14	47	18	21
July	7	41	34	18
Aug.	7	46	20	27
Sept.	7	41	33	19
Oct.	18	46	25	11
Nov.–Mar.	See Fig. 4			

The direction of the sea-breeze during the months April–October inclusive does not remain as constant as that depicted in Fig. 4, frequently veering after onset before backing several hours later.

Neumann (1977) found that the rate of local turning was primarily due to three effects:

- the Coriolis force,
- the cross product of the horizontal mesoscale pressure gradient (approximately equivalent to the diurnal heating/cooling of the land relative to the sea) and the velocity of the sea-breeze, and
- the cross product of the horizontal large-scale pressure gradient (assumed not to be affected by the diurnal heating) and the velocity of the sea-breeze.

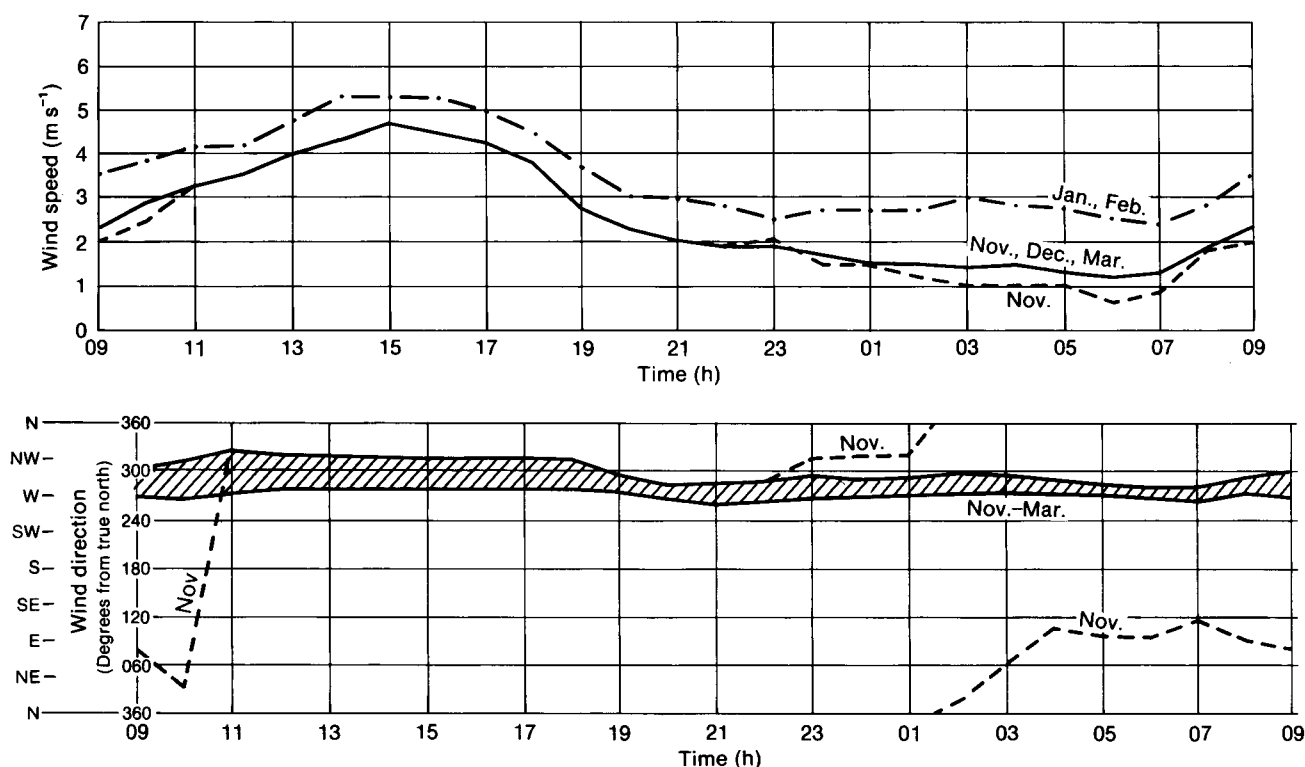


Figure 4. Mean speed and direction of the surface wind at Darwin Airport in a 24-hour period for the months from November to March inclusive.

- Thus the rate of turning is governed by:
- (a) the diurnal variation of the temperature over the land,
 - (b) the horizontal pressure gradient, and
 - (c) the strength of the sea-breeze.

Table V shows that during the months of April–October inclusive, only 37% of the sea-breezes held a steady direction during their life cycle and that of these, 86% originated in the north-east sector.

The synoptic-scale horizontal pressure gradient over Darwin is markedly higher for north to north-east sea-breezes and these seldom rotate during their life cycle. A clearer understanding of the turning of the sea-breeze can be obtained if those sea-breezes that developed in the north to north-east sector are excluded.

Mean hourly wind vectors were determined for days when the sea-breeze developed in the north-west quadrant during May and June, and September alone, and plotted on polar diagrams. The resulting hodographs are shown in Figs 5(a) and 5(b) and show the rotation of the sea-breeze during a 24-hour period, from which it is apparent that the pattern of diurnal rotation of the sea-breeze varies with the time of the year.

In both hodographs, the sea-breeze first veers toward the north soon after developing then backs a few hours later. During the middle of the year (Fig. 5 (a)) the sea-breeze continues to back (even though the wind speed is low) until either a land-breeze is established or the south-easterly trades resume their flow. Later in the year, around September when the south-easterly trades are weaker (Fig. 5(b)), the sea-breeze often becomes west-north-westerly and, although weak, can persist until the early hours of the morning.

Table VI shows some directional characteristics of the Darwin sea-breeze during each month between April and October. The majority of sea-breezes during May and June veer only and do not back before dissipating. During the month of August the mean life-span of the sea-breeze increases significantly (see Table II) and, correspondingly, the number of sea-breezes which back after first veering also increases.

Veering also occurs consistently about 2 hours after the sea-breeze reaches the Airport, irrespective of the actual time of onset. The backing of the sea-breeze on the other hand, takes place at a more definite time of the day, usually between 1720 and 1816.

Table V. Percentage of sea-breezes with a steady direction (to within ± 10 degrees) during their diurnal cycle

	Apr.	May	June	July	Aug.	Sept.	Oct.	All months
Percentage of all sea-breezes	42	59	42	44	34	31	17	37
Percentage of sea-breezes in N-NE sector	70	93	86	86	96	89	69	86

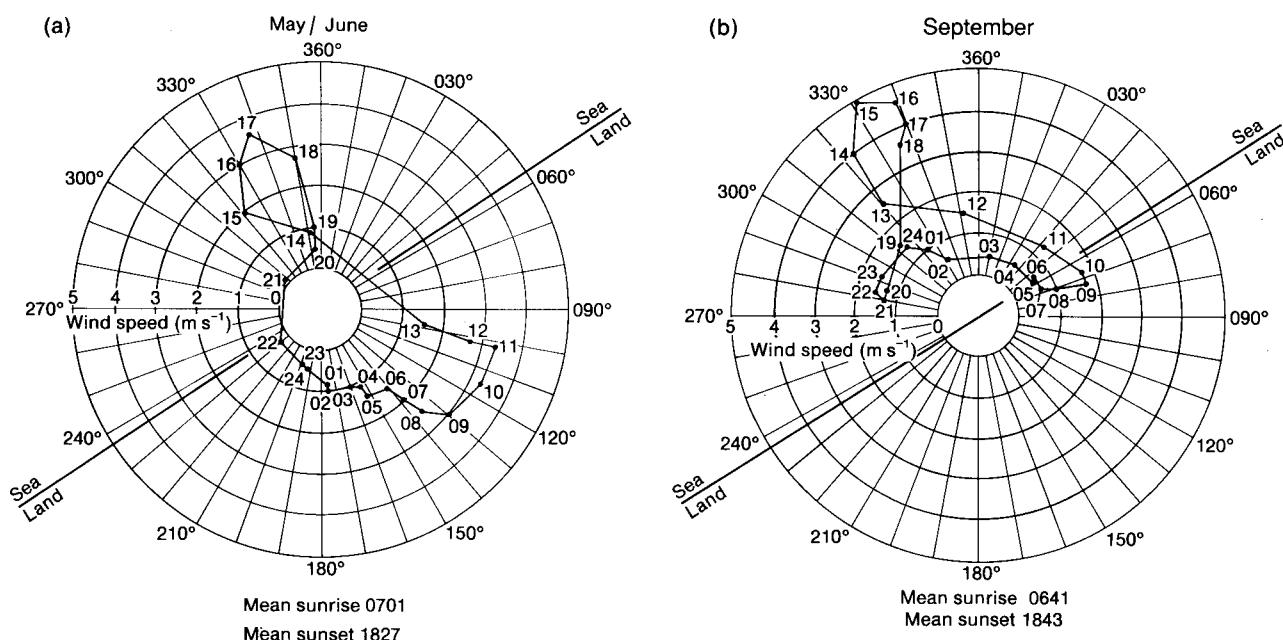


Figure 5. Plotted mean hourly wind vectors for west to north-north-west sea-breeze days at Darwin during (a) May–June, and (b) September. After McCaffery (1966).

Table VI. Percentage frequency and turning time of the sea-breeze at Darwin Airport (excluding sea-breezes that developed in the N-NE sector). VT = average length of time elapsed after development before the sea-breeze veers (hours: minutes), V = average time of day the sea-breeze starts to veer, B = average time of day the sea-breeze starts to back, Nil = doesn't back or veer.

Month	Veers only	Veers/ backs	Backs only	Nil	VT	V	B
Apr.	39	15	29	18	2:04	1508	1737
May	60	14	16	9	1:58	1608	1745
June	71	14	6	9	1:53	1615	1720
July	49	16	23	11	1:47	1612	1747
Aug.	42	26	27	2	2:03	1534	1809
Sept.	39	26	30	5	2:20	1504	1744
Oct.	11	39	44	6	2:36	1406	1816

Coriolis considerations, first incorporated by Haurwitz (1947), dictate that in the southern hemisphere, a sea-breeze should rotate anticlockwise during its life cycle. However, the Coriolis term diminishes greatly in equatorial regions and is a negligible quantity at Darwin's latitude. Notwithstanding this fact, Figs 5(a) and 5(b) show an overall net anticlockwise rotation of Darwin's sea-breeze over a 24-hour cycle. Kusuda and Abe (1989) have pointed out that meteorological effects other than Coriolis force should be taken into account when considering the rotation of the sea-breezes, and have indicated that horizontal advection over time can have a determining effect.

The continued backing of the sea-breeze after sunset is aided by the cool evenings experienced in inland regions during the middle of the dry season. Minimum temperatures reach their lowest during July and conditions become favourable for the development of a land-breeze at night. This in turn effects the behaviour and rotation of the evening breeze, and is one of the distinguishing features between the May/June and September hodographs.

The unusual phenomenon of the sea-breeze veering after initial development is probably due to the close proximity of two large islands, Bathurst and Melville, whose southern coasts are approximately 70 km to the north of Darwin (see Fig. 1). Kimble *et al.* (1946) observed sea-breeze circulations extending 80 km inland and 80 km out to sea in the tropics. This is consistent with observations of visible satellite imagery at Darwin where the sea-breeze front is commonly seen of the order of 80 km inland. Clarke (1989) has shown that a still distinguishable sea-breeze could be found 315 km inland. Given this range of penetration, the initial veering of the sea-breeze in Darwin could be caused by a complex interaction of two distinct sea-breeze cells: a small one set up by the islands, and a second much larger cell generated by the land mass on which Darwin lies.

5. Strength

Walsh (1974) showed that the strength of the sea-breeze is directly related to the amount of thermal

energy available to drive the sea-breeze mechanism (numerically depicted by the land-sea temperature contrast). Although the model that Walsh used proved unsuitable for use in Darwin on a daily basis (Lloyd 1988), the strength of the sea-breeze can be shown to be seasonally dependent.

Figs 6 and 7 show the mean speed and gustiness of sea-breezes developing in May/June and September respectively. These are further divided into two groups, (a) those developing in the north-west quadrant, and (b) those developing in the north to north-east sector. Fig. 4 shows the mean speed as well as the direction of the

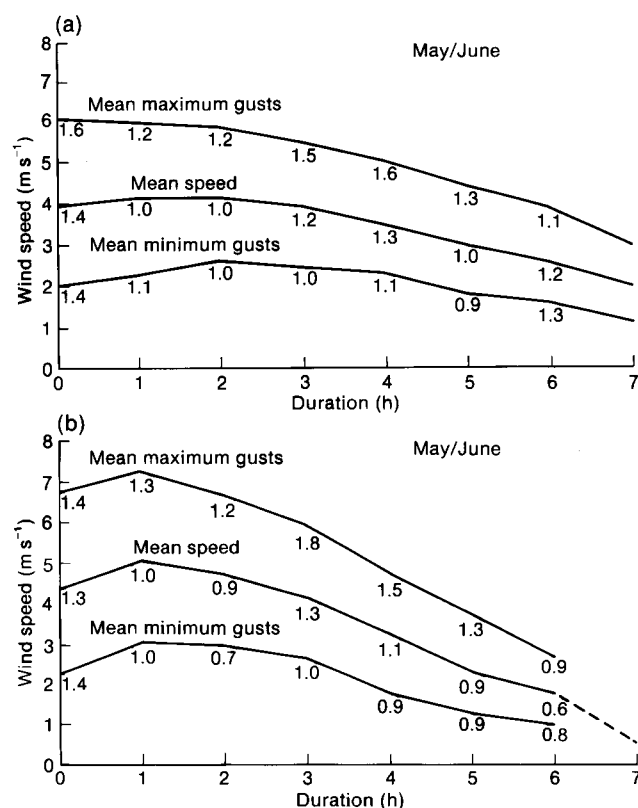


Figure 6. Mean speed and gustiness of sea-breezes developing in (a) the north-west quadrant, and (b) the north to north-east sector during May-June. The numbers below each line are the standard deviations.

surface wind recorded at Darwin Airport during the months of November–March inclusive. The graphs of Figs 6 and 7 represent average speeds; an indication of the variation is presented by listing one standard deviation (SD) for each hour of duration.

Sea-breeze strengths under three classifications are now discussed.

5.1 North-westerly sea-breezes

Sea-breezes developing during the latter part of the dry season are on average 2 m s^{-1} stronger than those developing early in the season (compare Figs 6 and 7). The strength of the sea-breeze is dependent on the amount of thermal energy available to drive the sea-breeze mechanism. Fig. 3 shows that the average period during which this thermal energy is available varies from 6 hours in June to $10\frac{1}{2}$ hours in September. Fig. 6(a) shows that those developing in the north-west quadrant during May/June have a mean speed soon after onset of around 4 m s^{-1} (SD 1.4 m s^{-1}) for 2–3 hours before gradually easing off. In September (Fig. 7(a)), sea-breezes attain a mean speed soon after onset of around 4.7 m s^{-1} (SD 1.6 m s^{-1}), they then increase to around 6 m s^{-1} after the first hour, remain steady for the next hour and then gradually ease off. Gustiness is greatest at onset, ranging from 2.0 – 6.1 m s^{-1} in May/June and 2.3 – 7.6 m s^{-1} in September.

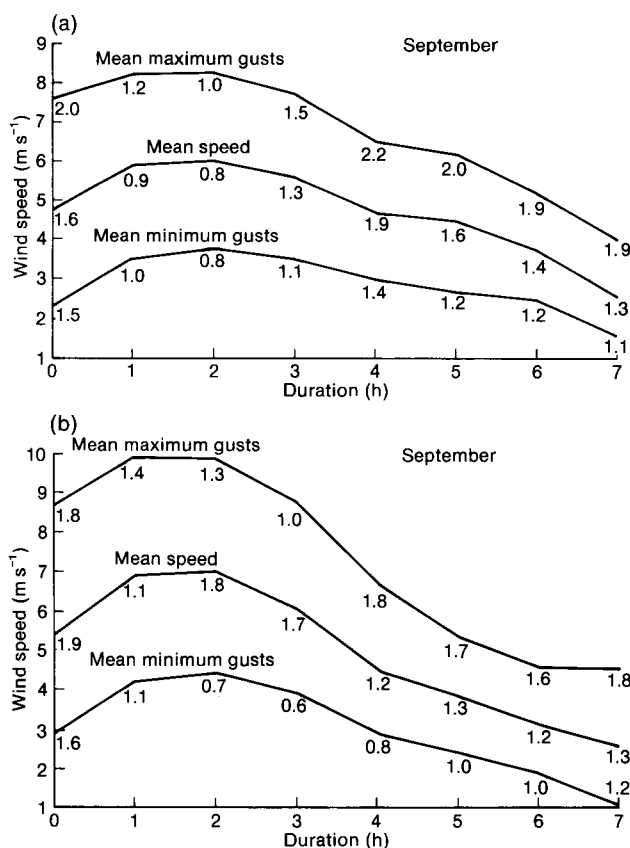


Figure 7. As Fig. 6 but for September.

5.2 North to north-easterly sea-breezes

While sea-breezes are generally stronger during the latter half of the dry season, they also are strongest when they develop in the north to north-east sector. For example, Fig. 6(b) shows that sea-breezes developing in this sector during May/June have a mean speed soon after onset of around 4.4 m s^{-1} (SD 1.3 m s^{-1}). The speed then increases to around 5 m s^{-1} after the first hour and then steadily decreases to less than 2 m s^{-1} during the next 5 hours. In September (Fig. 7(b)), mean speeds soon after onset are around 5.4 m s^{-1} (SD 1.9 m s^{-1}). The mean speed increases to around 7 m s^{-1} after the first hour, then rapidly decreases to around 2.5 m s^{-1} during the next 5 hours. Gustiness is greatest during the first 2 hours after onset for May/June, ranging from 2.3 – 6.7 m s^{-1} , and for the first 3 hours for September, ranging from 2.9 – 8.6 m s^{-1} at onset.

5.3 Wet-season breezes

Onshore breezes in the wet season, or more specifically the months November–March inclusive, usually remain north-westerly throughout the day. They attain their maximum strength of around 5 m s^{-1} between the hours of 1400 and 1600, then steadily decline to reach a minimum between the hours of 0600 and 0700 (see Fig. 4).

Daily wind speeds can be highly variable during the wet season, being strongly influenced by the monsoonal flow and local thunderstorm activity. For example, during a strong monsoonal flow, average surface winds speeds of 8 – 10 m s^{-1} can be sustained for a period of 2–3 days. Wind gusts, generated from inland thunderstorms that move over Darwin, greatly influence the wind speed. This is reflected in the large increase of the standard deviation of the average wind speed from 1.5 m s^{-1} when there is no storm activity, to 7.6 m s^{-1} with storm activity.

6. Conclusion

This study has described the diurnal and seasonal variations of the sea-breezes at Darwin. The different characteristics of the sea-breeze can be grouped into three broad periods: (a) the months from April to July (early to mid dry season), when the land–sea temperature contrast is at a minimum and the south-east trades are at a maximum, (b) August–October (late dry season), when the land–sea temperature contrast reaches a maximum and the south-east trades are losing their influence, and (c) November–March (main wet season) when there is a predominantly north-westerly air flow interspersed with occasional monsoon disturbances.

Acknowledgements

The author would like to thank I.J. Butterworth for his help with the original manuscript, and R. Falls for his help with the revised version.

References

- Atkinson, B.W., 1981: Meso-scale atmospheric circulations. London, Academic Press.
- Australian Bureau of Meteorology, 1988: Climatic averages. Melbourne, AGPS.
- Clarke, R.H., 1989: Sea-breezes and waves: the 'Kalgoorlie sea-breeze' and the 'Goondiwindi breeze'. *Aust Meteorol Mag*, **37**, 99–107.
- Haurwitz, B., 1947: Comments on the sea-breeze circulation. *J Meteorol*, **4**, 1–8.
- Kimble, G.T.H. and Collaborators, 1946: Tropical land and sea breezes. *Bull Am Meteorol Soc*, **27**, 99–113.
- Kusuda, M. and Abe, N., 1989: The contribution of horizontal advection to the diurnal variation of the wind direction of land-sea breezes: Theory and observations. *J Meteorol Soc Jpn*, **67**, 177–185.
- Lloyd, L.M., 1988: The sea-breeze at Darwin Airport: a forecasting aid. (Unpublished copy available in the Australian Bureau of Meteorology.)
- McCaffery, W.D.S., 1966: On sea-breeze forecasting techniques. (Unpublished, copy available in the National Meteorological Library, Bracknell.)
- Neumann, J., 1977: On the rotation of the direction of sea and land breezes. *J Atmos Sci*, **34**, 1913–1917.
- Walsh, J.E., 1974: Sea breeze theory and applications. *J Atmos Sci*, **31**, 2012–2026.

551.558.1:532.59:797.5

Links between convection and waves

T.A.M. Bradbury

94 The Beagles, Cashes Green, Stroud, Gloucestershire

Summary

Observations from gliders and powered aircraft show that in conditions of vertical wind shear there is an interaction between thermal updraughts in the convective boundary layer and wave flow in the stable layer above. Numerical models in two and three dimensions have shown that there can be a feedback between the two types of motion.

1. Introduction

Waves were first observed from gliders in 1933. A theoretical treatment of waves was given by Scorer (1949). For many years waves and thermals were treated as separate phenomena. It was assumed that thermals in the convective boundary layer inhibited the development of waves in the stable atmosphere above. Lee waves were believed to develop towards evening when thermals had died out, and decay during the heat of the day when convection had made the lower atmosphere turbulent.

Before the end of the 1960s pilots had observed that waves could persist even above the tops of large convective clouds. More recently it has been noted that the development of convection within the boundary layer can stimulate the formation of waves higher up. Studies suggest that once these waves have been set off they affect the growth and distribution of cumulus underneath. This is a review of some observations and numerical studies.

2. Early accounts of waves above convective layers

One of the first suggestions that cumuliform clouds could produce gravity waves came from Newton (1960) who wrote that the updraught in cumulonimbus (Cb)

clouds could obstruct the horizontal flow of air, and so produce internal gravity waves.

An early observation of waves above cumulus appeared in an article by Bradbury (1963). On this occasion the cumulus tops were limited by a stable layer and winds increased with height while remaining constant in direction.

Waves formed by thermals rising into an inversion were described by Townsend (1966, 1968). He pointed out that vertical shear was important for the development of these waves.

The occurrence of waves aligned parallel to cloud streets was reported by Jaeckisch (1968). A glider had encountered lift in clear air above cloud streets. This lift extended far above the tops of shallow cumulus. The important factor on this occasion was a marked directional shear of wind above the cumulus. At cloud level the wind direction was parallel to the alignment of the cloud streets but above them the direction was approximately at right angles. The lines of cloud appeared to be acting as small ridges stimulating waves in the flow aloft. The wave lift, which was not marked by cloud, lay parallel to the cloud streets (Fig. 1). Since then a number of glider pilots have observed that similar

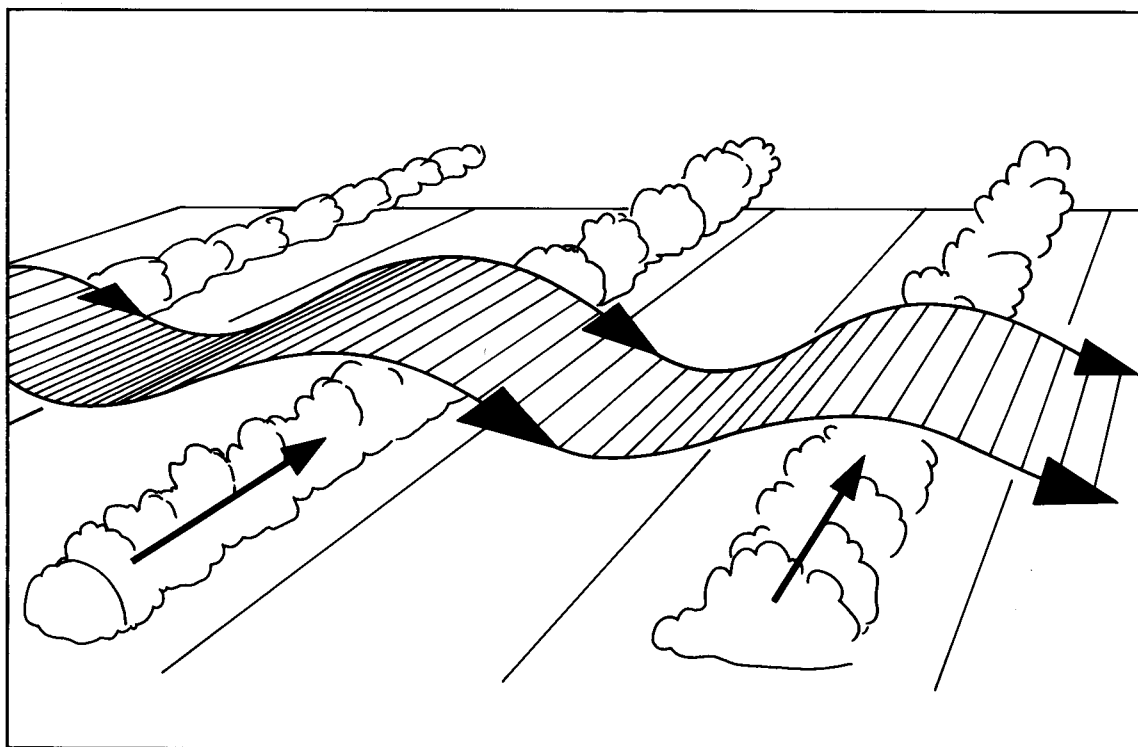


Figure 1. A three-dimensional sketch of waves above cumulus streets when the upper wind direction is at right angles to the wind in the convective layer.

waves can occur, even though the change of wind direction is much less than a right angle.

Cloud streets are not essential for the formation of such waves. Kuettner (1972) reported that waves had also been observed over individual cumulus clouds growing in a vertical wind shear.

3. Observations by glider pilots

3.1 Waves in shear conditions

Reports from glider pilots showed that individual clouds remained vertical while growing but began to tilt in the direction of shear when the updraught ceased. However, fresh thermals often produced new cells on the upshear side (Fig. 2). Such clouds produced transient wave-lift on the windward side. Glider pilots found rising air not only over the top of the cloud but also on the upshear side. This wave-like lift sometimes extended down below the condensation level. A number of pilots who halted their climbs to avoid entering cloud were subsequently able to ascend further in clear air just outside the cumulus. Some pilots found that if they remained circling in clear air just upwind of the cloud a new cell would soon envelop them.

This is different from what is observed in no shear conditions. Then, while the air inside a growing cumulus is moving upward, the edge of the cloud is more often a region of descent. This is usually the case when the cloud contains the kind of vortex-ring circulation proposed by Woodward (1959) and reported in cumulus clouds by Blythe *et al.* (1988).

3.2 Waves above cumulus congestus

Glider pilots have climbed in wave lift above the tops of very large cumulus. Such flights seem to be possible when the glider starts its climb:

- (a) before the cumulus has grown large, or
- (b) when the convection is temporarily suppressed.

In the first case gliders start by soaring hill-slopes before either thermals or waves have developed. On some days the development of cumulus seems to stimulate waves, and sailplanes are then able to climb in clear air up the windward face of large cumulus. Once at height they can remain in wave lift even if the clouds grow large enough to produce showers.

In the second case the passage of a heavy shower may cause a temporary halt to convection. During this lull, wave flow can descend to low levels and gliders are then able to climb up above the tops of further convective clouds. Heights in excess of 5 km have been reached when the shower clouds were large enough to produce a thunderstorm within 100 km.

3.3 Transverse waves over cloud streets

It is easy to visualize how parallel waves may form when the wind aloft blows across streets of cumulus. It is harder to see why transverse waves should be found when the wind direction aloft remains parallel to the streets. However, wave bars can be found on satellite pictures even when the flow is parallel to the alignment of the hills. For example, wave bars aligned north-north-west to south-south-east can form over Bantry Bay in Ireland when the west-south-westerly wind is

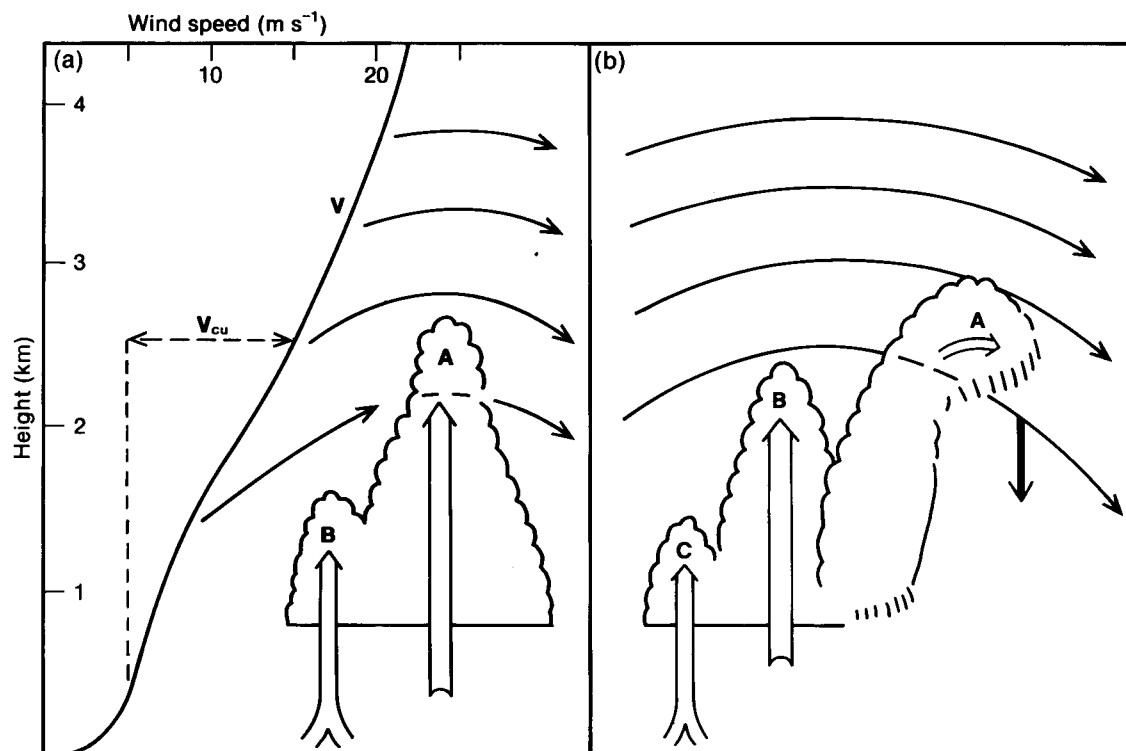


Figure 2. Waves over an isolated cumulus growing through a vertical wind shear. Individual thermals are labelled A, B and C. (a) shows an early stage with thermals at A and B, (b) shows the original cloud tilting and decaying when thermal A has ceased but a fresh thermal forming at C on the upshear side of the cloud. The variation of wind speed with height is shown on the left-hand side of (a), V_{cu} is the velocity of the cloud top relative to its base.

parallel to the peninsulas there. Evidently the preferred alignment of these waves is across the wind and it does not matter whether the starting impulse comes from a series of peninsulas sticking out into the flow or a long ridge at right angles to it.

Observations by pilots suggest that such transverse waves are common above cloud streets. They occur when the tops of cumulus are restricted by a stable layer and the wind speed increases with height while maintaining a constant direction. Fig. 3 shows a simplified version of the pattern. When the air aloft is too dry for lenticular clouds to develop, the position of wave crests is generally marked by a thickening in the lines of cumulus and a rise in the level of cloud tops. A description of these waves encountered by glider pilots over the United Kingdom appeared in an article by Bradbury (1984).

The conditions for transverse waves are also favourable for the development of orographic waves, and many of the transverse waves observed over the United Kingdom do seem to be initiated by hills. However, these waves are not rigidly controlled by the shape and alignment of major ridges. The unstable air often extends so far above the mountain tops that there seems to be no direct link between the underlying topography and the wave pattern aloft. It seems that the first wave is stimulated by stronger convection over the mountains. If the wave energy is trapped below a zone of very strong upper winds a regular pattern of wave bars can extend downstream with little regard for the underlying topography. The tendency for regular waves to extend

across an area of irregular mountains has been mentioned by Scorer and Verkaik (1989).

3.4 The mobility of transverse waves

Most purely orographic waves usually appear long before convection begins and remain anchored to some feature of the topography for long periods.

Pilots' observations show that on days of deep convection the waves did not develop until cumulus clouds had formed. Waves which depend on the growth of convective clouds are not very stable and pilots find them less reliable than purely orographic waves. An example of a moving wave above cloud streets was reported by Purnell (1977). He encountered a cloudless transverse wave above cumulus streets whose tops were about 2400 m. The wave lift reached 4300 m near Basingstoke, at least 150 km downwind of the Welsh mountains. The region of lift appeared to be drifting slowly downwind so it seems that this wave was not anchored to any topographical feature.

Absence of visible wave bars can make it difficult to confirm the presence of such waves on satellite pictures. Even when wave clouds do appear there is nothing to show if they are stationary or moving.

4. Satellite pictures of transverse waves over cloud streets

Figs 4–6 illustrate the cloud patterns seen when transverse waves formed above cloud streets. Figs 4 and 5 are of Scotland when a north-westerly flow covered the country. Cumulus streets formed as soon as the air

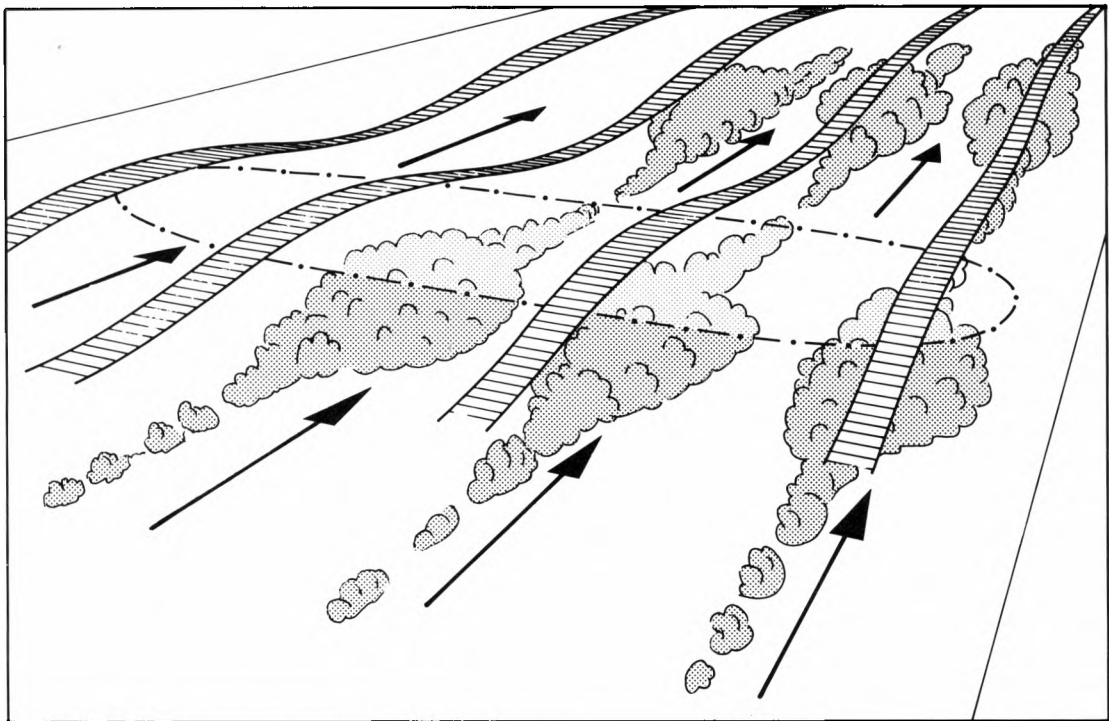
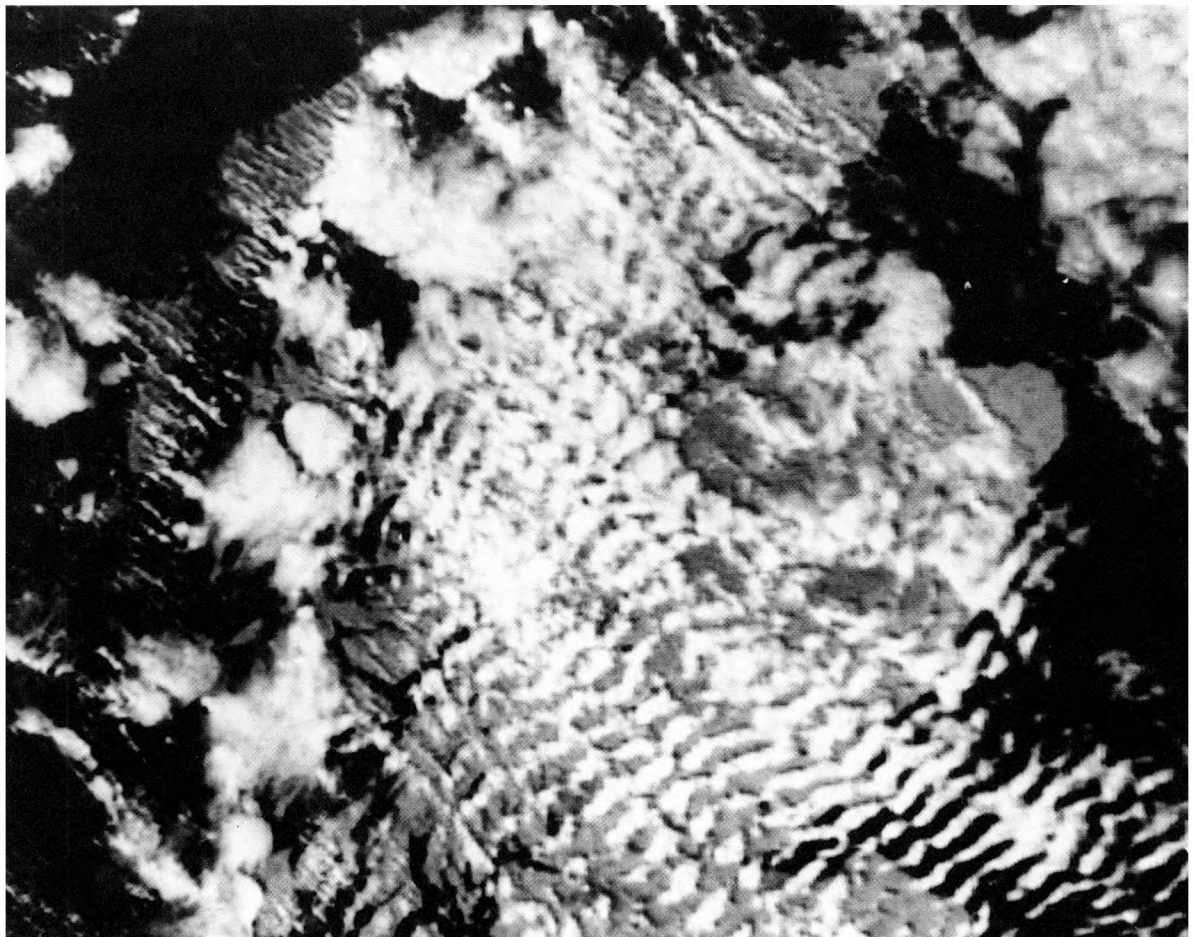
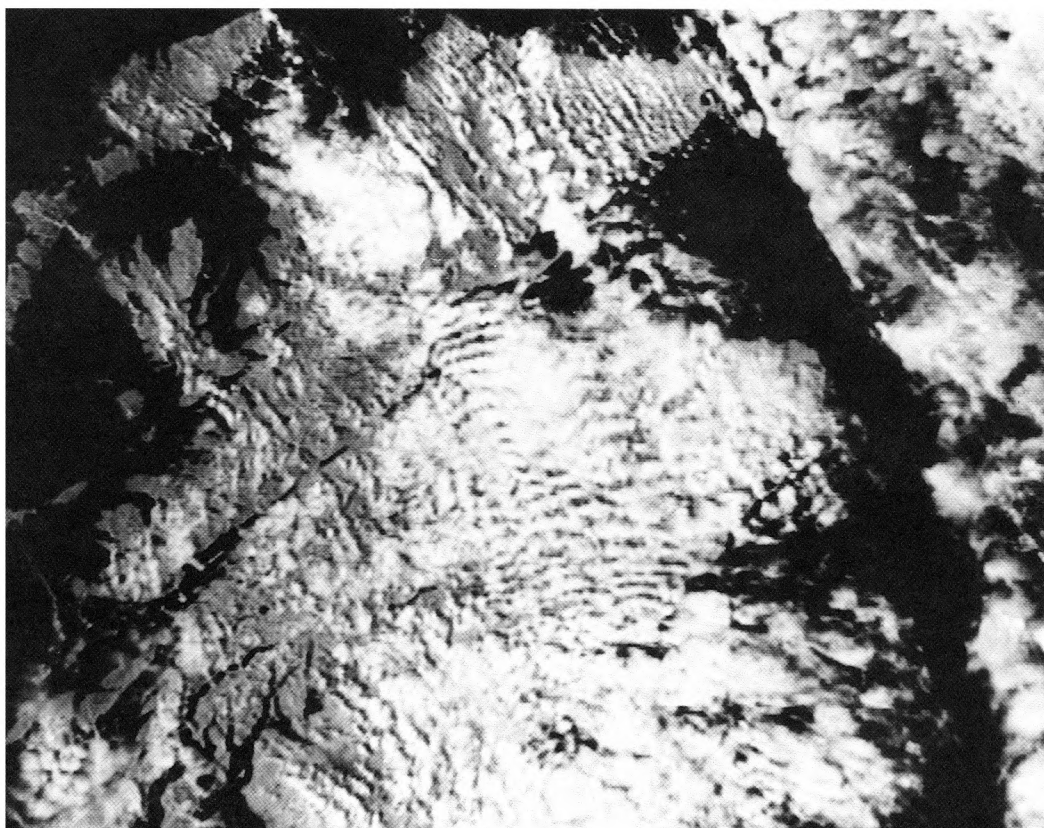


Figure 3. A three-dimensional sketch of waves with lines of peaks and troughs at right angles to lines of cumulus. The region within the dash-dot line shows where lenticular cloud may occur if the air aloft has sufficient moisture.



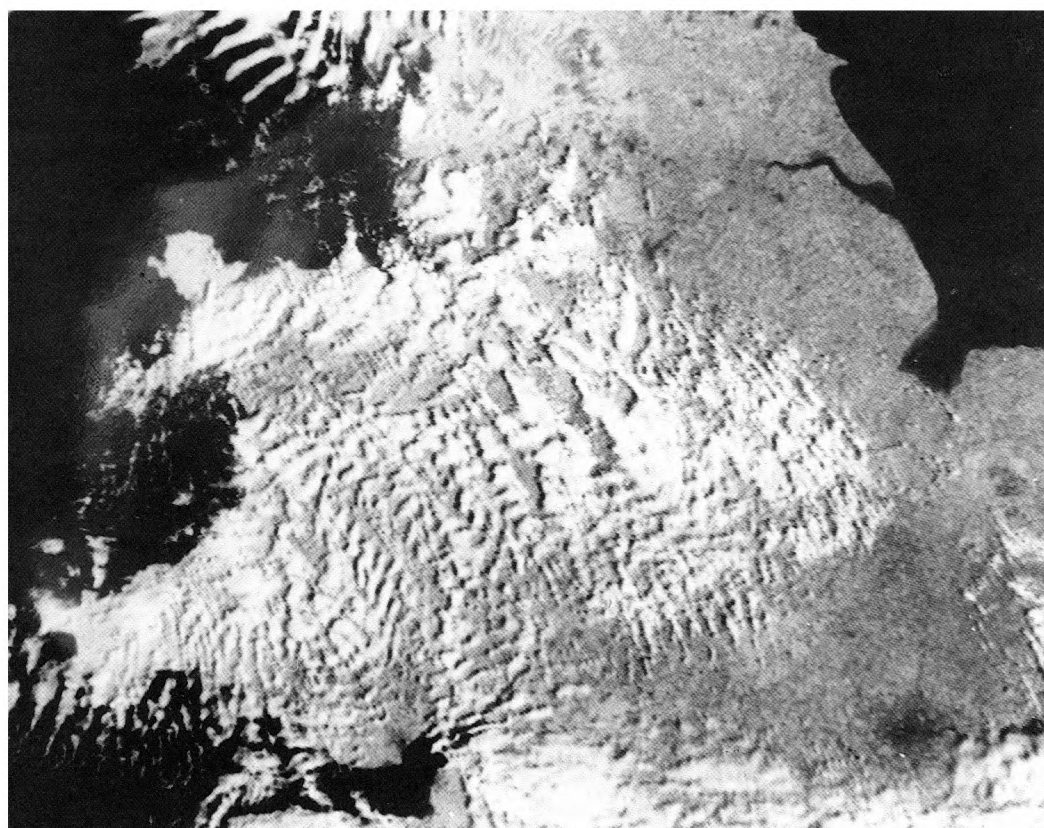
VHRR picture by courtesy of University of Dundee

Figure 4. Cloud streets and transverse waves over Scotland 1538 UTC 21 August 1980.



VHRR picture by courtesy of University of Dundee

Figure 5. Cloud streets and transverse waves over Scotland 1515 UTC 23 August 1980.



VHRR picture by courtesy of University of Dundee

Figure 6. Cloud streets and transverse waves over Wales and the Midlands of England 0838 UTC 21 August 1980.

reached land and transverse wave bars developed over the mountains. It seems evident that most, if not all, the visible waves were due to the mountains. However, in several places streets can be seen to persist under the wave clouds. This indicates that the helical circulation associated with cumulus streets was too deep to be disrupted by passage over the mountains. Where wave motion fails to produce transverse bars of cloud, the streets develop thicker patches in phase with the wave. This can be seen downwind of Cape Wrath.

Fig. 6 shows the pattern over Wales and the Midlands. Here the wave bars are neither so regular nor so prominent as over Scotland but there are several regions where transverse waves can be seen across lines of cumulus. In the region south-east of Birmingham there are transverse bands which do not seem to have any close association with the alignment of mountain ranges upstream. Over level ground the cloud streets sometimes appear to extend further downwind than the wave bars.

5. Importance of vertical wind shear

A growing cumulus can rise almost vertically even if it encounters a strong shear of wind. Kuettner *et al.* (1987) found a difference in velocity of $8\text{--}10\text{ m s}^{-1}$ between the interior of an active cumulus and the free air surrounding it. Although some of the environmental air may be entrained into the cloud, much of the flow is deflected over the top thus producing a vertical motion in the clear air above.

Lemone (1989) showed that strong shear tends to inhibit the growth of the weaker members of a field of cumulus but enables stronger ones to grow very much larger than they would in an atmosphere without shear. The shear increased both the horizontal dimensions and the life-time of the cumulus and suggested that the size to which a cumulus can grow may be a function of the shear. This effect could be attributed to wave development aloft, a theory also supported by Balaji and Clark (1988).

6. Exploration by powered aircraft

Although sailplanes are useful for detecting very small vertical motions they cannot make a thorough exploration of these waves. Powered aircraft are necessary to carry out a proper survey of wave-thermal interaction. Such a survey was carried out over Nebraska, USA, in a region 250–450 km east of the Rocky Mountains and reported by Kuettner *et al.* (1987).

Flights were made above long streets of cumulus when the wind direction changed by as much as 75 degrees between the cumulus level and the stable flow above. A vertical wind shear in excess of $3\text{ m s}^{-1}\text{ km}^{-1}$ was observed. A surprising discovery by these flights was the vertical extent of waves. Wave oscillations were found to extend above 9 km (the height limit of

the aircraft used). Vertical motions were in the range $1\text{--}3\text{ m s}^{-1}$ and the horizontal wavelengths varied between 5 and 15 km.

7. Numerical models

Although mathematical models of large-scale weather systems have existed for over 40 years it is only in the last 10 years that features as small as individual thermals could be resolved successfully. An early account by Mason and Sykes (1982) described a numerical model of horizontal roll vortices. This model also produced gravity waves which were very sensitive to the orientation of the rolls.

Some years later Clark *et al.* (1986) published the results from a two-dimensional model. This was used to investigate the developments when the upper winds blew across cumulus streets. The model results agreed well with observations made by aircraft and reported by Kuettner *et al.* (1987).

This line of research was extended by Balaji and Clark (1988) who showed that gravity waves could be formed in the stable layer aloft by excitation from convective eddies in the planetary boundary layer. Once formed these waves began to modulate the convection; in some circumstances very much larger cumulus could be produced after the waves had formed.

Although a rather different line was followed by Bretherton and Smoliarkiewicz (1989), their model also showed that a growing cumulus could produce a circulation in the environment which appeared to be due to spreading gravity waves.

Two dimensions are inadequate to describe developments in and above a field of cumulus so a three-dimensional model was developed by Hauf and Clark (1989). The changes produced by the extra dimension were:

- (a) The long lines of cumulus used in the two-dimensional model were replaced by individual clouds scattered over the whole area.
- (b) There was competition between longitudinal rolls forming cloud streets along the shear and transverse gravity waves aligned at right angles to these streets.
- (c) The gravity waves tended to destroy the cloud streets but there still remained weak elements aligned along the shear. The pattern has been described as having a 'varicose-like' structure. Fig. 6 shows such a pattern over the Midlands of England.

8. Stages of development shown by numerical models

The numerical models showed the following sequence of events as convective eddies and waves interact:

- (a) Surface heating sets off thermals which rise to the top of the convective layer and deform the interface producing undulations which act like hills to the flow above. Initially the size and spacing of these undulations depends on the characteristics of the

boundary layer. Typically the wavelength of these undulations is about twice the depth of the convective layer.

(b) Gravity waves are set off by the flow of air across these undulations. The waves propagate upwards at $4\text{--}5\text{ m s}^{-1}$ and can reach the tropopause in less than an hour. However, it may take several hours for a quasi-steady state to develop throughout the troposphere. If the high-level winds are very strong the waves may be trapped below the tropopause and propagate long distances downstream. If they are not trapped, some wave energy may extend into the stratosphere. The horizontal wavelength shows wide variations but typically averages 9 km.

(c) Internal gravity waves then start to influence the growing thermals in the convective boundary layer. Convection is enhanced in regions beneath upward wave flow and inhibited where the waves impart a downward motion. As a result, new convective cells grow on the upshear side of the clouds. Any clouds which find themselves beneath the descending current are suppressed and presently disappear. Since the gravity waves usually have a wavelength greater than the initial spacing between cumuli, the waves slowly alter the size of eddies in the boundary layer. The distance between thermals in the boundary layer eventually adjusts to fit the length of the gravity waves aloft.

(d) If the convective layer is deep some cumulus may grow very much larger while others are totally suppressed.

The sequence is shown schematically in Fig. 7 which indicates vertical motions at several levels. Convective up- and downdraughts start at A. At B smoother wave flow starts in the stable layer at and above 2 km. At point C the feedback from waves aloft starts to dominate the eddies in the convective layer. The cumuli grow larger and are spaced further apart.

9. Effects of variations in shear and depth of instability

The cumulus clouds tend to grow on the upwind side and decay on the downwind side under the influence of the waves above. If the convective layer is shallow the movement of waves aloft is likely to reduce the life of individual thermals rising from the ground and clouds remain small. With a deeper convective layer a few of the cumuli grow large because they happen to be in phase with the wave lift above. Once a cumulus exceeds a certain size the favoured cloud continues to grow at the expense of smaller clouds all round. Continued growth then influences the gravity waves above and a positive feedback is established.

If there is no vertical shear the thermals produce hardly any gravity waves in the stable layer. The waves which do occur tend to move outward along the interface (like ripples on a pond) without propagating upwards.

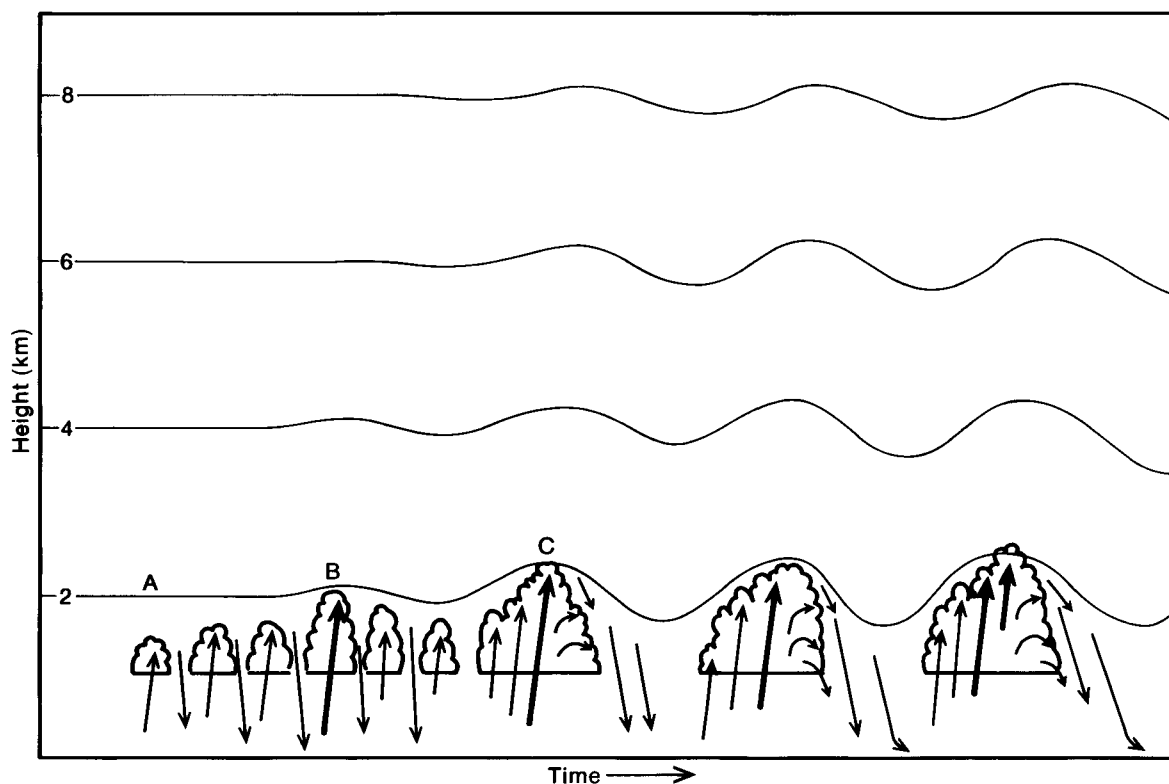


Figure 7. Height-time diagram showing schematically the development of thermals in the convective layer at A followed by upward propagating waves in the stable layer at B. The spacing of convective eddies becomes dominated by wave flow aloft beyond C.

10. Waves from the tops of cumulonimbi

There are reports of rare occasions when the tops of a vigorous Cb cloud over the USA penetrated the tropopause and set off a train of waves which moved away horizontally. These waves later initiated a further outbreak of convective storms far downwind of the original cloud (Uccellini 1975, Stobie *et al.* 1983).

Small amplitude waves occasionally produce a pattern in the anvil of cirrus blown off the top of a Cb.

An example is shown in Figs 8 and 9. The pictures show the anvil cirrus streaming from the top of a maritime Cb over the Indian Ocean south of the island of Gan in the Maldives. The tops of Cb extended up to an easterly jet stream with velocities exceeding 100 kn at levels between 200 and 150 mb. One Cb set off this wave pattern in the cirrus. It was visible for several minutes before lower cloud obscured the view.



Figure 8. Waves in anvil cirrus downwind of a maritime cumulonimbus (Cb) over the Indian Ocean just south of Gan. The tops of a distant Cb had penetrated the equatorial easterly jet where wind speeds exceeded 100 kn.



Figure 9. Westward extension of the same train of waves as that shown in Fig. 8.

11. Conclusions

In an atmosphere with a vertical wind shear the development of thermals in the convective boundary layer can produce obstructions to the horizontal flow. These obstructions act like temporary hills and set off gravity waves in the stable layer. Such waves have been observed to propagate to heights in excess of 9 km and may penetrate the lower stratosphere. Some time after these gravity waves have developed aloft they begin to influence the location of convective updraughts from the surface. Thermals are stimulated beneath regions where wave flow is ascending but are suppressed where wave flow is descending. Thus the location and size of cumulus clouds is modified by the waves. On days of deep convection this effect may result in some cumuli becoming very much larger.

If the depth of convection is limited by a stable layer and cloud streets occur, the waves form parallel to the streets when the winds aloft blow across them. If there is no change in wind direction with height, transverse waves may form at right angles to the cloud streets. Although such waves are influenced by topography they can form even when strong convection extends far above any mountain summits. Then the initial stimulus to wave flow is provided by stronger thermals over the mountains rather than direct coupling between the terrain and the stable air immediately above.

References

- Balaji, V. and Clark, T.L., 1988: Scale selection in locally forced convective fields and the initiation of deep cumulus. *J Atmos Sci*, **45**, 3188–3211.
- Blythe, A.M., Cooper, W.A. and Jensen, J.B., 1988: A study of the source of entrained air in Montana cumuli. *J Atmos Sci*, **45**, 3944–3964.
- Bradbury, T.A.M., 1963: Glider observations of lee waves in and above a field of cumulus cloud. *Meteorol Mag*, **92**, 156–161.
- Bradbury, T.A.M., 1984: Wave soaring over the British Isles. *Sailplane and Gliding*, **35**, 166–169.
- Bretherton, C.S. and Smoliarkiewicz, P., 1989: Gravity waves, compensating subsidence and detrainment around cumulus clouds. *J Atmos Sci*, **46**, 740–759.
- Clark, T.L., Hauf, T. and Kuettner, J.P., 1986: Convectively forced internal gravity waves: Results from two-dimensional numerical experiments. *Q J R Meteorol Soc*, **112**, 899–925.
- Hauf, T. and Clark, T.L., 1989: Three-dimensional numerical experiments on convectively forced internal gravity waves. *Q J R Meteorol Soc*, **115**, 309–333.
- Jaekisch, H., 1968: Waveflow above convection streets. OSTIV Publication X.
- Kuettner, J.P., 1972: Thermal wave soaring. *Swiss Aero Revue*, 394–396.
- Kuettner, J.P., Hildebrand, P.A. and Clark, T.L., 1987: Convection waves: Observations of gravity wave systems over convectively active boundary layers. *Q J R Meteorol Soc*, **113**, 445–467.
- Lemone, M.A., 1989: The influence of vertical wind shear on the diameter of cumulus clouds in CCOPE. *Mon Weather Rev*, **117**, 1480–1491.
- Mason, P.J. and Sykes, R.I., 1982: A two-dimensional numerical study of horizontal roll vortices in an inversion capped planetary boundary layer. *Q J R Meteorol Soc*, **108**, 801–823.
- Newton, C.W., 1960: Hydrodynamic interactions with ambient wind field as a factor in cumulus development. In (Anderson, C.E. (ed.)) *Cumulus dynamics*. New York, Pergamon Press.
- Purnell, A., 1977: Wave at 14000 over Basingstoke. *Sailplane and Gliding*, **28**, 194–197.
- Scorer, R.S., 1949: Theory of waves in the lee of mountains. *Q J R Meteorol Soc*, **75**, 41–56.
- Scorer, R.S. and Verkaik, A., 1989: *Spacious skies*. Newton Abbot, England, David & Charles.
- Stobie, J.G., Einaudi, F. and Uccellini, L.W., 1983: A case study of gravity waves-convective storms interaction: 9 May 1979. *J Atmos Sci*, **40**, 2804–2830.
- Townsend, A.A., 1966: Internal waves produced by a shear layer. *J Fluid Mech*, **24**, 307–319.
- , 1968: Excitation of internal waves in a stably-stratified atmosphere with considerable wind-shear. *J Fluid Mech*, **32**, 145–171.
- Uccellini, L.W., 1975: A case study of apparent gravity-wave initiation of severe convective storms. *Mon Weather Rev*, **103**, 497–513.
- Woodward, B., 1959: The motion in and around thermals. *Q J R Meteorol Soc*, **85**, 144–151.

Real-time analysis of surface wind gusts using radar data: 25th January 1990

R.M. Blackall, R. Brown and C.G. Collier
Meteorological Office, Bracknell

Summary

Methods of estimating gust strengths near showers using radar derived velocities are explained, and possible future operational uses discussed.

1. Introduction

During Thursday 25 January 1990 a deep depression moved rapidly across the British Isles causing widespread damage, disruption to transport and interruption to electricity supplies over southern England and Wales. Forty-seven people are reported to have been killed by falling trees, masonry and scaffolding, in car accidents, and by drowning at sea. The total damage cost is expected to be well over a billion pounds.

Winds gusting to over 85 kn at ground level were recorded, comparable with the severe storm of October 1987. However damage was more severe and the death toll higher than in 1987 as the high winds occurred during the daytime when many people were out of doors, and over a greater area. The Meteorological Office forecasted the event very well, the first indication of an unusually low pressure system being issued 5 days in advance. Warnings of a severe storm were broadcast at midnight on Wednesday night.

Although the widespread destruction caused by the event was not fully reported until around midday on 25 January, the decision was taken during the morning to carry out the real-time analysis of the winds using radar data, employing the research and development versions of the operational Meteorological Office FRONTIERS system now known as Merlin (Browning and Carpenter 1984). The two systems were operated in parallel throughout the day, and the wind analyses and their implications for future operational systems are reported here.

2. Background

Since the early 1950s radar has been used to study the motion of small precipitation areas (see, for example, Ligda and Mayhew 1954, Tatehira *et al.* 1976, Parsons and Hobbs 1983). Unfortunately the movement of radar echoes may be related to the wind velocity at various levels in the atmosphere, and therefore care must be taken in associating echo movement with wind velocity at particular heights.

Bond *et al.* (1981) described a study of the speed of travel of shallow showers during the 1979 Fastnet Yacht Race and other occasions of strong winds. They found that such measurements gave a good indication of the

peak surface gusts at exposed coastal locations (see section 6). In discussing the possible operational utility of such measurements, they concluded that radar images with a spatial sampling interval of at least 5 km and a temporal resolution of at least 5 minutes are needed to give reliable velocities from showers which are restricted to a well-mixed boundary layer (≤ 3 km deep). For comparison it should be noted that 100 kn is approximately equal to 3.1 km min^{-1} . Thus it was likely that an objective cell-tracking procedure was needed. This was confirmed by Monk *et al.* (1987), who also found that an operationally useful indication of the speed and direction of movement of two cyclonic vortices was provided by radar echoes.

In this paper an analysis procedure implemented in real time is discussed. In spite of the restrictions imposed by the availability of radar data only every 15 minutes, it has been possible to derive meaningful analyses which were generated within about 20 minutes of the nominal observation time.

3. Synoptic situation on 25 January 1990

An Atlantic depression underwent dramatic, well forecast, deepening early in the morning and moved north-east over Ireland and southern Scotland with a central pressure of about 955 mb and with a shallow trough extending southwards to the rear of the surface cold front. Radar composite images at 0930 and 1000 UTC on 25 January 1990 are shown in Figs 1(a) and 1(b). The position of the front is indicated in Fig. 1(a) as the three areas of heavy precipitation over south-east and central England. Winds increased as the trough, marked by the precipitation over Wales and Cornwall, approached. Behind this trough winds eased somewhat in the south. A rapid rise of pressure behind the trough over Ireland caused a tightening of the gradient in the north where the strongest winds were from north of west.

4. FRONTIERS velocity analysis facilities

The FRONTIERS precipitation nowcasting system allows the forecaster to derive the velocity of features in

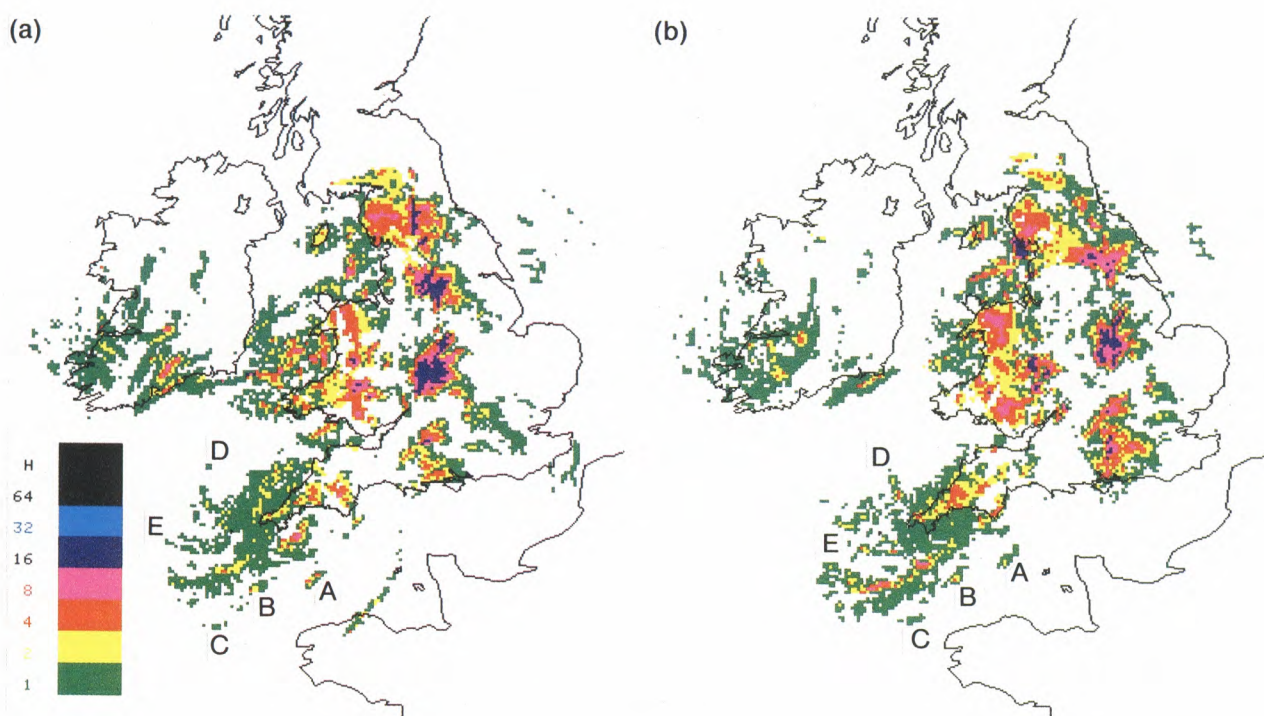


Figure 1. Radar composite images at (a) 0930 and (b) 1000 UTC on 25 January 1990. Each data square is 5 km × 5 km and different colours represent instantaneous rainfall rates (mm h⁻¹) as shown on the colour code given on the left of the images. Cells used to derive echo motion are labelled with the letters A-E on each image.

the radar (or satellite) imagery. At present the methods are only semi-automated and the forecaster interacts with the system through visual display units (VDUs) equipped with touch-sensitive screens. The imagery is presented in colour on a main monitor and control menus appear on alphanumeric VDUs. Radar data are available at 15-minute intervals but forecasts are only produced from data at half-hourly intervals.

Two methods are available for determining velocities, Touch Same Feature (TSF) being the quicker method. The forecaster is invited to touch the same feature in the current and T-30 mins radar pictures and the system computes the velocity from the displacement. The 30-minute interval is a compromise between the need for a significant displacement relative to the 5 km resolution of the radar data and the need to be able to identify the same feature. It is very difficult to use if the target is evolving or other potential targets are nearby.

The preferred method is known as Lagrangian Replay (LR). The forecaster sets up a replay sequence of radar pictures, typically 1-2 hours duration, and touches the same feature on the first and last picture of the sequence. From these touch points the system computes a velocity as for TSF. The entire sequence is then replayed at several frames per second with the computed velocity being subtracted. If the chosen feature remains stationary then its velocity must equal that which is being subtracted. If it is not quite stationary, it can be made so using a joystick attached to the system and the velocity is recomputed. This method is generally more accurate than TSF, especially for low velocities. On this occasion

the two methods yielded similar velocities because large displacements occurred over a half-hour period.

5. Echo-velocity measurement and analysis

The velocity vectors shown in Fig. 2 were obtained using the development version of the FRONTIERS system, known as Merlin, which is located in the Nowcasting and Satellite Applications Branch of the Meteorological Office. A speculative measurement made around 1020 UTC gave a velocity of 85 kn for a discrete echo over the English Channel which, bearing in mind the results of Bond *et al.* (1981), indicated the likelihood of severe gusts. Therefore it was decided to operate Merlin in real time to evaluate the number of cell velocities which might be obtained operationally and to compare the measured velocities with observed gusts. Real-time measurements commenced at 1130 UTC and terminated at 1500 UTC. The number of velocities obtained was probably more than would be obtained during operational use of the current FRONTIERS system because the rest of the rainfall analysis normally carried out on FRONTIERS was omitted. Thus about 9 minutes was devoted to echo velocity determination per 30-minute cycle, compared with about 5 minutes available operationally. However the FRONTIERS' software runs more slowly on Merlin because the computer is shared with many other users.

The targets used to find the vectors were ideally small, well defined and long-lasting echoes. The showers ahead of the trough in the English Channel, and to rear, north of the Scillies were easy to follow. Farther north and east

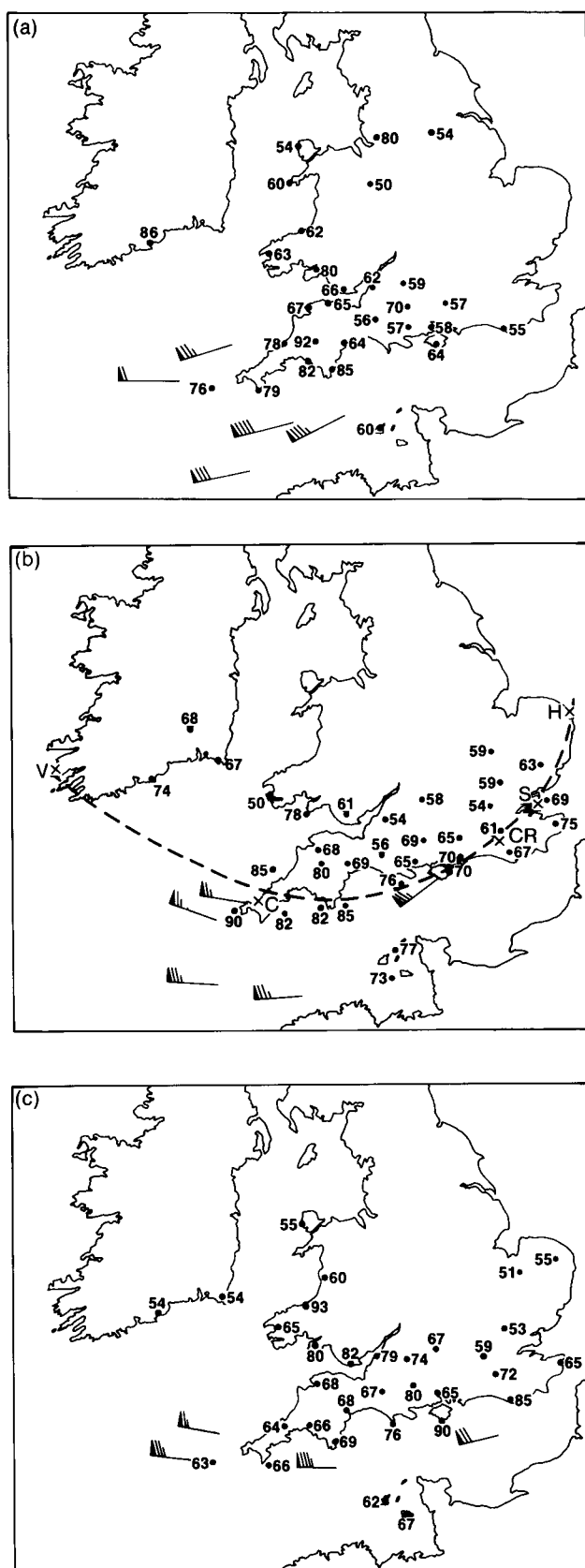


Figure 2. Anemometer measured gust speeds over 50 kn shown as numbers at (a) 1000 UTC, (b) 1200 UTC and (c) 1400 UTC on 25 January 1990. Wind arrows show radar echo speeds derived in real time. In Fig. 2(b) the streamline from Valentia (V) in the west to Hemsby (H) in the east is shown, passing through Camborne (C), Crawley (CR) and Shoeburyness (S) (see Fig. 4).

individual echoes were less discernible and so the analysis concentrated upon the south. The larger areas of precipitation evident in Figs 1(a) and 1(b) were not used because they would be likely to give velocities characteristic of the trough or front which would not necessarily be that of the wind at the top of the boundary layer. Cells lettered A–E in Figs 1(a) and 1(b) were chosen to determine wind speeds, and comparison of their positions in the two figures gives dramatic indication of their movement in only 30 minutes.

Almost all the vectors were obtained using LR because it normally avoids confusion over exactly which feature is being tracked. However, occasionally time was wasted because totally unrealistic velocities were obtained, e.g. $315^\circ/08$ kn around Lands End at 1400 UTC. This was the consequence of a stroboscopic effect which can occur with fast moving discrete cells. For example if shower lines are 20 km apart and move 20 km in 15 minutes then little movement would be seen during a replay as one cell was replaced by the next cell upwind.

The results of the analysis at 1000, 1200 and 1400 UTC are shown in Fig. 2. Because the real-time analysis began after gusts of over 60 kn were widespread across the south, it was decided to analyse the 1000 UTC data retrospectively, although the 85 kn vector west of the Channel Islands was obtained in real time. The gusts reported on the synoptic hour are shown as numbers and the echo-derived velocities as wind shafts, with one full feather representing 10 kn. The east-north-east progression of the largest gust is apparent from Fig. 2. The key feature of Fig. 2 is that the echo velocities and largest gusts are of comparable magnitude, as found by Bond *et al.* (1981). However the spatial distribution of the echo velocities does not appear to be particularly illuminating. For example, the gusts of up to 90 kn on the west coast of Cornwall at 1200 UTC are not reflected in comparable upwind velocities (Fig. 2(b)), although comparable velocities were obtained to the south at 1000 UTC (Fig. 2(a)). It was not possible to measure velocities over south-east England and East Anglia in the afternoon, due to power failures at the Wardon Hill and Chenies radars. Therefore it is not possible to determine whether a maximum in echo velocity tracked east-north-east as did the maximum in gust magnitude.

6. Depth of convection

In the study of Bond *et al.* (1981) the agreement between the speed of the showers and the magnitude of the gusts was attributed to the shallow nature of the convection. Thus the echo speed was unambiguously characteristic of the wind speed one or two kilometres above the surface, which could plausibly be brought unmodified to the surface by downdraughts. In addition, the shallow nature of the convection prevented vigorous downdraughts developing which, upon reaching the surface, might have diverged and generated gusts greatly in excess of the shower velocity.

The FRONTIERS system allows the operator to

extract quickly the mean and minimum temperature within a designated area from the Meteosat infra-red data. On this occasion only the 1400 UTC satellite data were received into the Merlin system in real time. Then the convective cells which were tracked in the western English Channel were found to have tops at -31°C , and are very close to the positions identified as a source of atmospherics (lightning). Study of the FRONTIERS archived data showed that earlier the coldest cloud tops being tracked were about -18°C . Both these values fit well with inversions apparent on the midday ascent from Camborne at around 630 mb and 450 mb as in Fig. 3. Therefore most of the targets used had tops around 3000 m at first, rising to more than 6000 m later.

Since the convection was not particularly shallow, the justification for equating the speed of the showers to the maximum gusts is the absence of shear above 850 mb as indicated by Fig. 3. To confirm that this was a general feature, a cross-section of wind speeds is shown at Fig. 4. The horizontal axis is the nearly circular arc as sketched in Fig. 2(b). This is very nearly a streamline and runs from Valentia (V) in south-west Ireland, through Camborne (C) in Cornwall, and through Crawley (CR) and Hemsby (H) in the south-east of England. Unfortunately neither Larkhill nor Shoeburyness were able to launch balloons successfully around midday, but Hemsby had to launch an extra flight 45 minutes after the first. Allowing 110 km displacement for this delay,

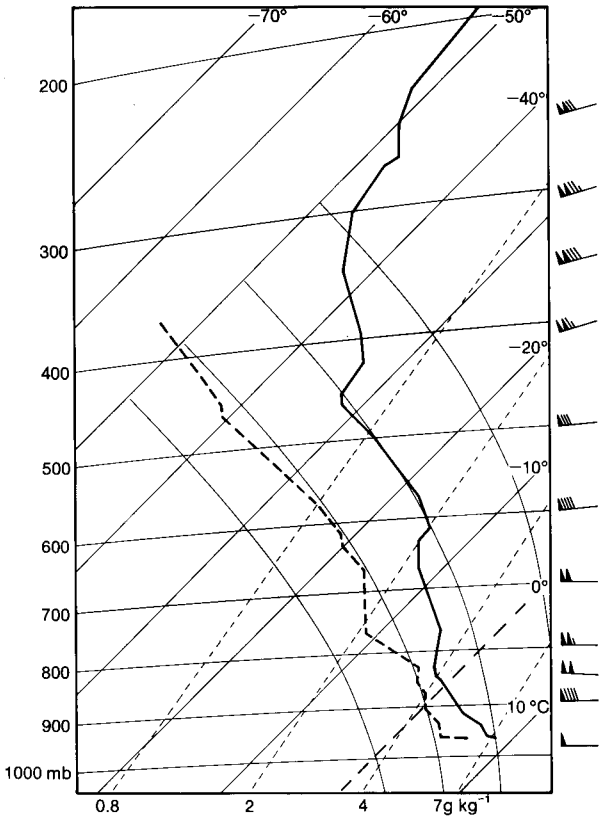


Figure 3. Radiosonde sounding at Camborne in south-west England at 1100 UTC on 25 January 1990. Winds are also shown, traditionally.

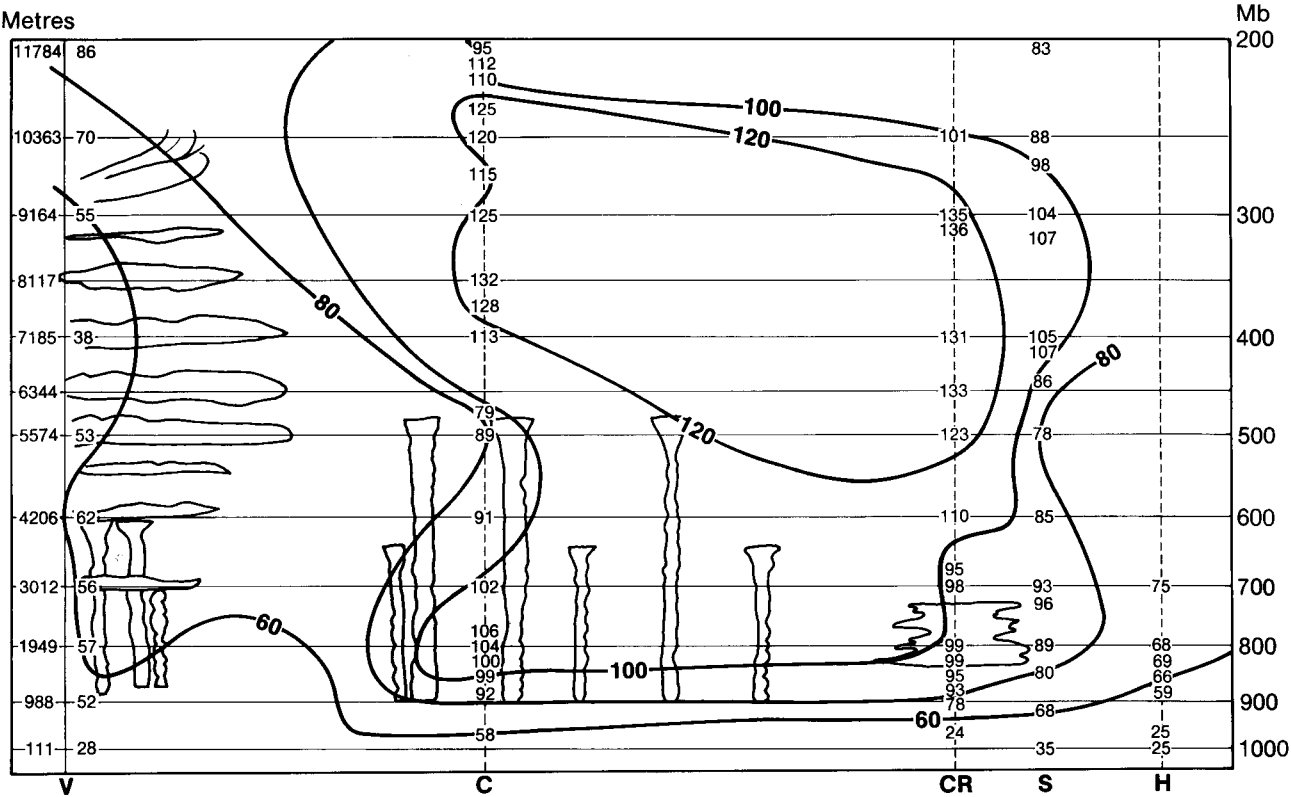


Figure 4. Vertical cross-section at 1200 UTC on 25 January 1990 of the wind speed (kn) approximately along a streamline between Valentia and Hemsby (see Fig. 2(b)). Also shown, schematically, are the extents of the observed clouds.

winds have been included for a location near Shoeburyness.

The cross-section confirms the very strong shear in the boundary layer and the insignificant shear above 850 mb. Thus even if the speed of the echoes is governed by the wind speed at some level between 850 and 600 mb, this should still be a good guide to the wind speed lower down. In fact, for reasons that are not clear, the modal speed of the echoes, which is around 75 kn, is less than the wind above the sheared region, which is around 100 kn.

7. Implications for future operational use

The analysis of winds described in this paper was carried out in real time in parallel with the operation of FRONTIERS in the Central Forecasting Office. The question arises as to whether or not such a dedicated procedure can be combined with the routine analysis of the radar and satellite data embodied in normal FRONTIERS operation.

Clearly the surface winds were the 'problem of the day' as the precipitation was not exceptional, yet precipitation analyses are still required continuously. Therefore it may be that either FRONTIERS must be further automated to allow the forecaster to concentrate on particular problems of severe weather if the need arises, or in such circumstances parallel operation of two (or more) workstations as envisaged by Browning and Golding (1984) must be undertaken. The use of a research system might be appropriate when such severe weather is expected, particularly as the case described in this paper suggests that it might be possible to link the location of the showers to occurrences of falling trees and therefore increased risk of damage and even death.

Constraints on forecaster availability exist at present, and undoubtedly this will be the situation in the future.

Hence the multiple workstation approach may not be practical, except for situations in which tasks are very different; for example one workstation for numerical model initialization and another for imagery interpretation. There is scope, however, to develop a future generation of FRONTIERS systems with a capability to operate automatically, producing routine products whilst allowing the forecaster to function in a separate mode, which may be to cope with emergencies or to deal with specific difficult analysis problems. Of particular interest might be the possibility of determining radar echo height and absence of wind shear from three-dimensional reflectivity and Doppler data which may become available in the future generation of operational radars in the United Kingdom. These data, used with numerical model output, offer intriguing possibilities. The need to consider these alternatives is highlighted by the analysis reported here.

References

- Bond, J.E., Browning, K.A. and Collier, C.G., 1981: Estimates of surface gust speeds using radar observations of showers. *Meteorol Mag*, **110**, 29–40.
- Browning, K.A. and Carpenter, K.M., 1984: FRONTIERS five years on. *Meteorol Mag*, **113**, 282–288.
- Browning, K.A. and Golding, B.W., 1984: Mesoscale forecasting in the Meteorological Office: the way ahead? *Meteorol Mag*, **113**, 302–313.
- Ligda, M.G.H. and Mayhew, W.A., 1954: On the relationship between the velocities of small precipitation areas and geostrophic winds. *J Meteorol*, **11**, 421–423.
- Monk, G.A., Browning, K.A. and Jonas, P.R., 1987: Forecasting application of radar-derived precipitation echo velocities in the vicinity of polar lows. *Tellus*, **39A**, 426–433.
- Parsons, D.B. and Hobbs, P.V., 1983: The mesoscale and microscale structure and organization of clouds and precipitation in midlatitude cyclones. XI: Comparisons between observational and theoretical aspects of rainbands. *J Atmos Sci*, **40**, 2377–2397.
- Tatehira, R., Sato, H. and Makino, Y., 1976: Short-term forecasting of digitized echo pattern. *J Meteorol Res Jpn*, **28**, 61–70.

Notes and news

Old views on climate change

The following are extracts from an address which would be topical even today; the speaker and the date are revealed at the end.

'There are, I believe, few persons who have noticed, and who can recollect, the state of the climate of England half a Century ago, who will not be found to agree in opinion that considerable changes have taken place in it; and that our Winters are now generally warmer than they were at that period. My own habits and pursuits, from a very early period of my life to the present time, have led me to expose myself much to the weather in all seasons of the year, and under all circumstances; and no doubt whatever remains in my mind but that our Winters are generally a good deal less severe than formerly, our Springs more cold and ungenial, our Summers, and particularly the latter parts of them, as warm at least as they formerly were, and our Autumns considerably warmer; and I think that I can point out some physical causes and adduce some rather strong facts, in support of these opinions.

Within the last fifty years very extensive tracts of ground, which were previously covered with trees, have been cleared, and much waste land has been enclosed and cultivated; and by means of trenches and ditches and other improvements in agriculture and covered drains, the water which falls from the clouds, and that which arises in excess out of the ground, has been more rapidly and more efficiently carried off than at previous periods. The quantity of water which our rivers contain and carry to the sea in Summer and Autumn, is in consequence, as I have witnessed in many instances, greatly diminished; and upon the estate where I was born, and which I now possess, my title deeds, and the form of the ground, prove a mill to have stood, in the reign of Queen Elizabeth, and probably at a good deal later period, in a situation to which sufficient water to turn a mill-wheel one day in a month cannot now be obtained in the latter part of the Summer and Autumn. Under these circumstances the ground must necessarily become much more dry in the end of May than it could have been previously to its having been enclosed and drained and cultivated; and it must consequently absorb and retain much more of the warm Summer rain (for but little usually flows off) than it did in an uncultivated state; and as water in cooling is known to give out much heat to surrounding bodies, much warmth must be communicated to the ground, and this cannot fail to affect the temperature of the following Autumn. The warm Autumnal rains, in conjunction with those of the Summer, must necessarily operate powerfully upon the temperature of the succeeding Winter; and,

consistently with this hypothesis, I have observed that during the last forty years, when the weather of the Summer and Autumn has been very wet, the succeeding Winter has been in the climate of this vicinity generally mild. And that when north-east winds have prevailed after such wet seasons the weather in the Winter has been cold and cloudy, but without severe frost, probably in part owing to the ground upon the opposite shores of the Continent being in a state similar to that on this side the Channel.

Supposing the ground to contain less water in the commencement of Winter on account of the operation of the drains above-mentioned, as it almost always will, and generally must do, more of the water afforded by dissolving snows, and the cold rains of Winter, will be necessarily absorbed by it; and in the end of February, however dry the ground may have been at the Winter solstice, it will almost always be found saturated with water derived from those unfavourable sources; and as the influence of the sun is as powerful on the last day of February, as on the 15th of October, and as it is almost wholly the high temperature of the ground in the latter period, which occasions the different temperature of the air in those opposite seasons, I think it can scarcely be doubted that if the soil have been rendered more cold by having absorbed a larger portion of water at very near the freezing temperature, the weather of the Spring must be, to some extent, injuriously affected. But whether it be owing to the preceding, or other causes, I feel most perfectly confident that the weather in the Spring has been considerably less favourable to the blossoms of Fruit Trees, and to vegetation generally, during the last thirty years, than it was in the preceding period of the same duration; and I shall in conclusion adduce one fact, the evidence of which I think cannot easily be controverted. The Herefordshire farmers formerly calculated upon having a full crop of acorns upon the oaks, which grew dispersed over their farms, once in three years; but a good crop of acorns is now a thing of rare occurrence, upon the value of which the farmer has almost wholly ceased to calculate, even upon those farms which contain extensive groves of Oaks. The trees nevertheless blossom annually very freely, but no fruit is produced. Many causes may be assigned for the diminished produce of Orchards, and of Fruit Trees generally; but the blossoms of the Oak must be now as capable of bearing cold as they were half a century ago, and their failing to produce acorns can only be attributed to the agency of some external cause; and I am wholly unable to conjecture any such cause except the above-mentioned.'

The address entitled 'Upon the supposed changes in the Climate of England' was given on 5 May 1829 to the Royal Society by its President, Thomas Andrew Knight.

Review

Turning up the heat, by F. Pearce. 129 mm × 197 mm, pp. 230, *illus.* London, Glasgow, Toronto, Sydney, Auckland, Paladin Books, 1989. Price £4.99.

The late 1980s were marked by a tremendous rise in public awareness of 'green affairs'. Concern was directed on the one hand towards issues that affected our own back yards — toxic and nuclear waste disposal, food quality — and on the other towards global issues; in particular, human interference with the chemical composition of the atmosphere — the greenhouse effect and the ozone hole. None of these issues look likely to disappear in the near future, and it is hoped that the decade of the 1990s will be marked by positive action to reduce these threats. However, public concern must be matched by public knowledge. To succeed, pressure for change requires a sound basis of scientific understanding. There is therefore a very real need for a literature that will describe, in terms understandable to the intelligent lay-person, the chemical, physical and biological processes which, coming together, have the capacity to constitute environmental threat.

Turning up the heat is a contribution to the non-specialist literature on the greenhouse effect, advertising itself as 'The First Handbook to the Greenhouse Age'. The subject matter ranges widely from the straightforward consideration of the principles underlying the greenhouse effect, through matters as diverse as the death of the dinosaurs and the political debate surrounding the Montreal Protocol. A book with such diverse themes requires a strong structure, and yet the material in one chapter seldom bears any clear link to what has gone before, and what follows.

The book opens with a discussion of the ozone hole (what it is, how it was discovered) and the Montreal Protocol. Chapter 2 looks at the origins of the Earth, and spends some considerable time describing the evolution of the scientific debate that surrounds the Gaia hypothesis. This is followed by two chapters covering (too superficially) desertification, the green revolution, deforestation and other related (?) issues. Then it's back to hard science, with a chapter on cloud formation, the role of algae and dimethyl sulphide. Finally, in chapters 6 and 7, we come to radiative mechanisms which underlie the greenhouse effect, the role of the oceans, feedbacks, and the potential impacts — what climatologists would generally regard as the nuts and bolts of the whole issue. Chapter 8 looks at El Niño Southern Oscillation, and chapter 9 at the causes of Ice Ages, Milankovitch cycles and the role of the deep ocean circulation. Chapter 10 examines the sources of non-CO₂ greenhouse gases, chapter 11 rising sea levels, chapter 12 increasing global populations and chapter 13 possible ways to defuse the greenhouse effect.

As can be seen from the preceding paragraph, my

major criticism of this book is its lack of organization. In general, the material is up-to-date and presented in terms possible for the lay-person to understand without dodging the issues or being condescending. There is some tendency to oversimplify, most obvious in the early and, in part, superfluous chapters on African agriculture and the Amazonian rain forests. The author is clearly well-read and well-informed, although not as much as he would perhaps like us to believe — I was interested to read that Alayne Street-Perrot has undergone a sex change. All in all, however, if I was looking for a book to inform my teenage children or my next-door neighbour on the greenhouse effect, this is one that I would be happy to hand over.

J.P. Palutikof

Books received

The listing of books under this heading does not preclude a review in the Meteorological Magazine at a later date.

Operational analysis and prediction of ocean wind waves, by M.L. Khandekar (New York, Berlin, Springer-Verlag, 1989) is an attempt to compile the present state of knowledge of the topic. It aims to satisfy the need for a ready reference on the various techniques and their uses.

Carbon dioxide and global change: earth in transition, by S.B. Idso (Tempe, Arizona, IBR Press, 1989) contains an analysis and review of the many potential consequences of the rising carbon dioxide content of the earth's atmosphere. Included also are 100 pages of references to publications on the many interrelated aspects of the subject.

Noctilucent clouds, by M. Gadsden and W. Schröder (Berlin, Heidelberg, New York, London, Paris, Tokyo, Hong Kong, Springer-Verlag, 1989) includes what is known about noctilucent clouds, drawn from many separate sources. It is aimed at a wide variety of readers.

Weather radar networking, edited by C.G. Collier and M. Chapuis (Dordrecht, Boston, London, Kluwer Academic Publishers, 1990) gives an account of the lectures presented at a COST 73 Project seminar in Brussels on 5–8 September 1989. Almost 60 papers are included on the many aspects of the theory and application of the subject.

Impact models to assess regional acidification, edited by J. Kämäri (Dordrecht, Boston, London, Kluwer Academic Publishers, 1990) divides the subject into terrestrial and aquatic effects, and model reliability and utility. Also included is a chapter on future directions for research.

Satellite photograph — 21 April 1990 at 1445 UTC

The NOAA-11 visible photograph shown in Fig. 1, showing the central and eastern Atlantic, has been reproduced from a picture received on a facsimile machine. The picture shows several frontal zones, each seen by clearly defined bands of cloud. Comparison with the corresponding infra-red image (not shown) indicates that, except near Spain (lower right), almost all the cloud is at low levels.

Apart from the front labelled 'W', all the surface fronts can be located using cloud information — either along the narrow cloud bands ('C' and 'I'), or along the axis of the bright (thickest) cloud ('E'). Front 'I' is associated with a depression which is centred between Iceland and Greenland. South of Iceland, the front is marked by a rope cloud — a narrow filament of cloud

associated with low-level line convection. It is unusual to see rope clouds so far north since, near depressions, most middle-latitude fronts are covered by middle/upper-level cloud.

Fronts 'C' and 'E' have become slow moving within a region of high pressure (Fig. 2). Fronts tend to become weak near anticyclones, but as this image shows they may persist as distinct cloud features.

In the cloud-free zone off the coast of south-east Greenland, there is a narrow gap separating a region of thin ice (out to sea) and thick ice (near the coast). Nearer Iceland, a chain of cloud vortices indicates that there is considerable small-scale detail which is not indicated on the synoptic-scale chart shown in Fig. 2.

G.A. Monk



Figure 1. NOAA-11 visible image on 21 April 1990 at 1445 UTC. Frontal positions have been superimposed. South of Iceland, front 'I' is marked by arrows.

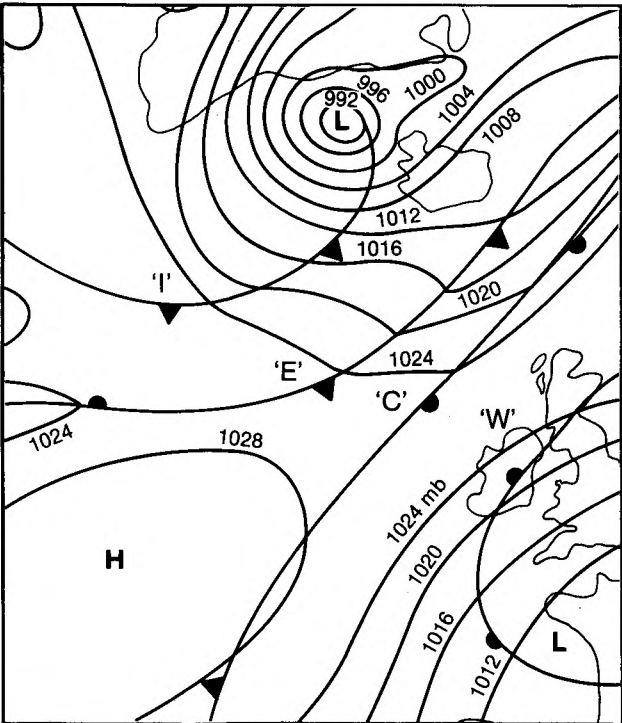


Figure 2. Surface analysis on 21 April 1990 at 1200 UTC.

GUIDE TO AUTHORS

Content

Articles on all aspects of meteorology are welcomed, particularly those which describe results of research in applied meteorology or the development of practical forecasting techniques.

Preparation and submission of articles

Articles, which must be in English, should be typed, double-spaced with wide margins, on one side only of A4-size paper. Tables, references and figure captions should be typed separately. Spelling should conform to the preferred spelling in the *Concise Oxford Dictionary* (latest edition). Articles prepared on floppy disk (Compucorp or IBM-compatible) can be labour-saving, but only a print-out should be submitted in the first instance.

References should be made using the Harvard system (author/date) and full details should be given at the end of the text. If a document is unpublished, details must be given of the library where it may be seen. Documents which are not available to enquirers must not be referred to, except by 'personal communication'.

Tables should be numbered consecutively using roman numerals and provided with headings.

Mathematical notation should be written with extreme care. Particular care should be taken to differentiate between Greek letters and Roman letters for which they could be mistaken. Double subscripts and superscripts should be avoided, as they are difficult to typeset and read. Notation should be kept as simple as possible. Guidance is given in BS 1991: Part 1: 1976, and *Quantities, Units and Symbols* published by the Royal Society. SI units, or units approved by the World Meteorological Organization, should be used.

Articles for publication and all other communications for the Editor should be addressed to: The Chief Executive, Meteorological Office, London Road, Bracknell, Berkshire RG12 2SZ and marked 'For Meteorological Magazine'.

Illustrations

Diagrams must be drawn clearly, preferably in ink, and should not contain any unnecessary or irrelevant details. Explanatory text should not appear on the diagram itself but in the caption. Captions should be typed on a separate sheet of paper and should, as far as possible, explain the meanings of the diagrams without the reader having to refer to the text. The sequential numbering should correspond with the sequential referrals in the text.

Sharp monochrome photographs on glossy paper are preferred; colour prints are acceptable but the use of colour is at the Editor's discretion.

Copyright

Authors should identify the holder of the copyright for their work when they first submit contributions.

Free copies

Three free copies of the magazine (one for a book review) are provided for authors of articles published in it. Separate offprints for each article are not provided.

June 1990

Editor: B.R. May

Editorial Board: R.J. Allam, R. Kershaw, W.H. Moores, P.R.S. Salter

Vol. 119

No. 1415

Contents

	Page
The sea-breeze at Darwin: a climatology. L.M. Lloyd	105
Links between convection and waves. T.A.M. Bradbury	112
Real-time analysis of surface wind gusts using radar data. R.M. Blackall, R. Brown and C.G. Collier	121
Notes and news	
Old views on climate change	126
Review	
Turning up the heat. F. Pearce. J.P. Palutikof	127
Books received	127
Satellite photograph — 21 April 1990 at 1445 UTC G.A. Monk	128

Contributions: It is requested that all communications to the Editor and books for review be addressed to the Chief Executive, Meteorological Office, London Road, Bracknell, Berkshire RG12 2SZ, and marked 'For *Meteorological Magazine*'. Contributors are asked to comply with the guidelines given in the *Guide to authors* which appears on the inside back cover. The responsibility for facts and opinions expressed in the signed articles and letters published in *Meteorological Magazine* rests with their respective authors.

Subscriptions: Annual subscription £30.00 including postage; individual copies £2.70 including postage. Applications for postal subscriptions should be made to HMSO, PO Box 276, London SW8 5DT; subscription enquiries 071-873 8499.

Back numbers: Full-size reprints of Vols 1-75 (1866-1940) are available from Johnson Reprint Co. Ltd, 24-28 Oval Road, London NW1 7DX. Complete volumes of *Meteorological Magazine* commencing with volume 54 are available on microfilm from University Microfilms International, 18 Bedford Row, London WC1R 4EJ. Information on microfiche issues is available from Kraus Microfiche, Rte 100, Milwood, NY 10546, USA.

ISBN 0 11 728666 4

ISSN 0026-1149

© Crown copyright 1990. First published 1990

The Meteorological Magazine

July 1990

Forecasting the storm of 8 November 1989
UK/WMO Voluntary Co-operation Programme
The summer of 1989



DUPLICATE JOURNALS

National Meteorological Library
FitzRoy Road, Exeter, Devon. EX1 3PB

HMSO

Met.O.992 Vol. 119 No. 1416



3 8078 0010 2472 0

The Meteorological Magazine

July 1990
Vol. 119 No. 1416

551.509.313:551.509.5:551.515.1(420)

Forecasting the storm of 8 November 1989 — a success for the man-machine mix

A. Woodroffe

Meteorological Office, Bracknell

Summary

A description is given of the beneficial influence of forecasters' expertise in modifying guidance provided by the Meteorological Office's numerical weather prediction models for a storm over southern England on 8 November 1989.

1. Introduction

The Meteorological Office produces numerical weather predictions using two forecast models — a global coarse-mesh model with a horizontal grid spacing of about 150 km, and a fine-mesh model covering the North Atlantic and north-west Europe with a 75 km grid spacing. Both models use 15 levels in the vertical.

Most forecasters have developed considerable respect for the overall quality of the guidance provided by these models. In the case of short-period forecasts up to 36 hours, it is relatively rare these days for the models to get the evolution totally wrong; the forecaster is mainly concerned with fine-tuning the guidance and interpreting it to meet customer needs. The models have proved particularly good at handling major cyclogenetic events, resulting in a significant improvement in the accuracy and timeliness of gale warnings from the Central Forecasting Office (CFO) over the last decade.

Despite these advances, there have been some notable failures, in particular the case of the so-called 'Great Storm' of 15–16 October 1987 (Woodroffe 1988, Gadd and Morris 1988). It is important, therefore, that the forecaster should not become complacent when assessing the model output. Another example of poor model guidance occurred more recently on 8 November 1989 in a situation which, though much less severe, presented certain forecasting problems resembling those associated with the Great Storm. On this occasion, the forecasters

in CFO made important changes to the model output, thereby effecting a significant improvement in the quality of the guidance. The main purpose of this paper is to discuss the reasoning behind those changes, since some of the factors may serve as a warning signal to forecasters in similar situations in the future.

2. Synoptic developments

On 8 November 1989 a vigorous depression moved north-eastwards over southern Britain, bringing a broad band of moderate/heavy rain across England and Wales and very strong winds in its circulation. Many stations in southern England and East Anglia reported gusts exceeding 50 kn, with 75 kn being recorded at Portland Bill and 60 kn at London Weather Centre (at the time the highest wind speed recorded in London since the Great Storm). The development of the depression (labelled Low 'U') is portrayed in Fig. 1 which shows the CFO mean-sea-level pressure (MSLP) and the 500 mb height analyses at 12-hourly intervals, commencing at 0000 UTC on 7 November 1989. At that initial time the low was just a shallow wave over the central North Atlantic near 42° N, 34° W (though due to a lack of ship data, its exact position and depth were both uncertain). During the next 36 hours the centre deepened substantially as it moved east-north-eastwards ahead of the sharpening upper trough.

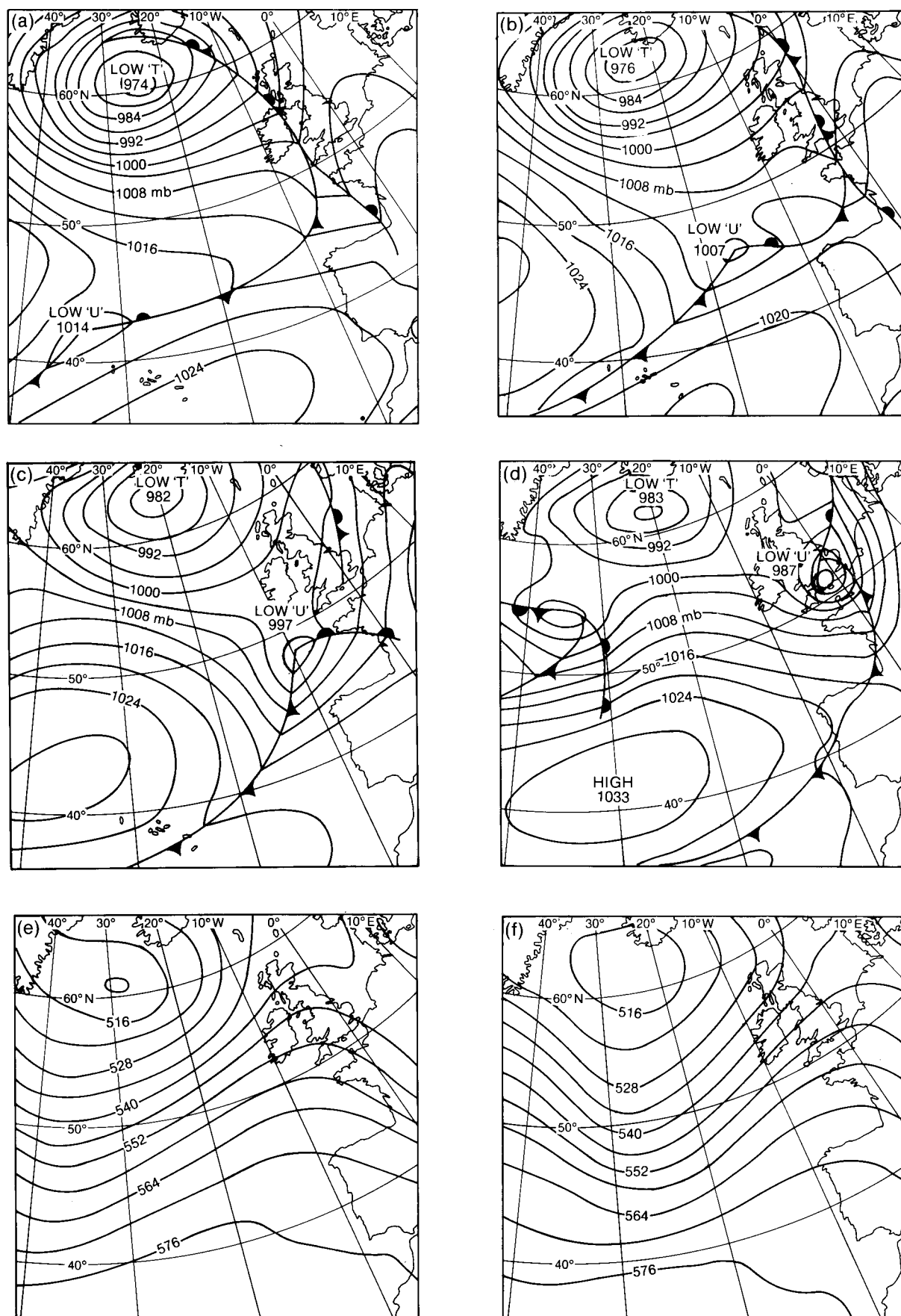


Figure 1. MSL pressure analyses for (a) 0000 UTC on 7 November 1989, (b) 1200 UTC on 7 November 1989, (c) 0000 UTC on 8 November 1989 and (d) 1200 UTC on 8 November 1989. (e) to (h) are 500 mb analyses (heights in dam) for the same times as (a) to (d).

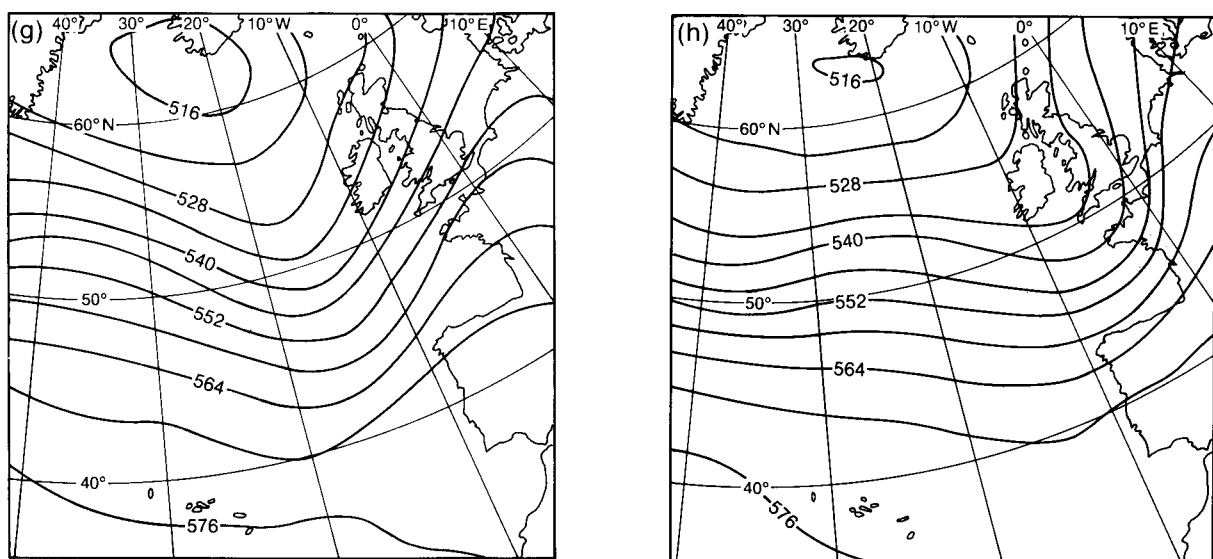


Figure 1. Continued.

The track of the low and its central pressure are plotted in Fig. 2. Although the rate of deepening appears rather erratic, this is likely to be a reflection of the uncertainty in the analysed depth at various stages. The steady curving of the track to the left in the latter stages of deepening was a critical factor in determining the extent of the strong winds over southern Britain. However, at no time was the rate of deepening exceptional, the largest pressure falls being of the order of 8–9 mb per 3 hours over south-west England on the morning of the 8th. As so often happens, the very strong winds were mainly a consequence of the marked pressure rises which developed behind the centre, in association with the confluent forward portion of the upper trough.

An additional complication underlying the analysis was the suggestion of a complex structure with a shallow wave running ahead of the main centre. For example, the analysis for 0600 UTC on 7 November 1989 (not

shown) indicated two distinct waves based on ship observations and CFO's interpretation of the satellite imagery. Detailed analysis of observations to the south of Ireland on the evening of 7 November also revealed signs of a forward centre. Whilst any such double structure was of relatively little significance for the weather over the United Kingdom, it may have had an impact on the performance of the model, as will be discussed later.

3. Medium-range forecasts

Medium-range guidance from both the coarse-mesh model and from the numerical model run by the European Centre for Medium-range Weather Forecasts (ECMWF) generally failed to capture the vigorous nature of the development, as is evident from the MSLP forecasts reproduced in Fig. 3. These charts are all valid at 1200 UTC on 8 November 1989 (when the low was an active feature of 984 mb centred just north-west of

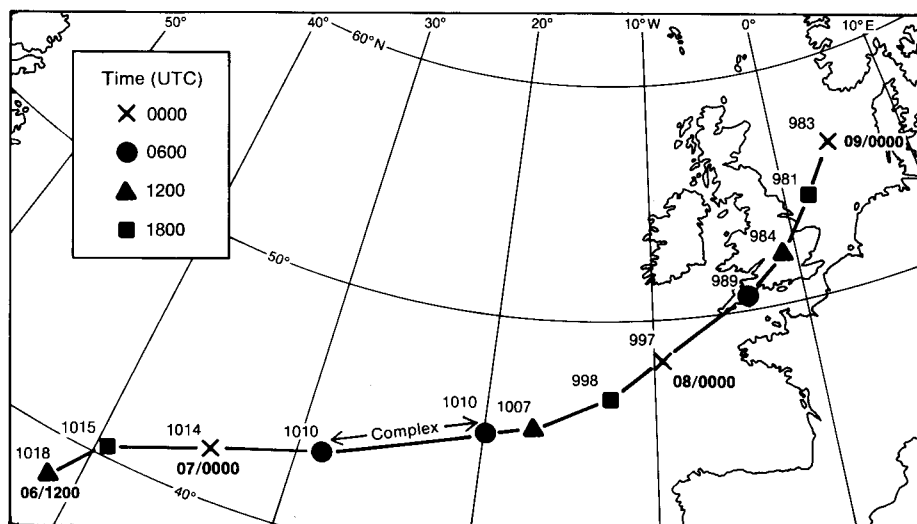


Figure 2. Track and central pressure (mb) of the low from 1200 UTC on 6 November to 0000 UTC on 9 November 1989.

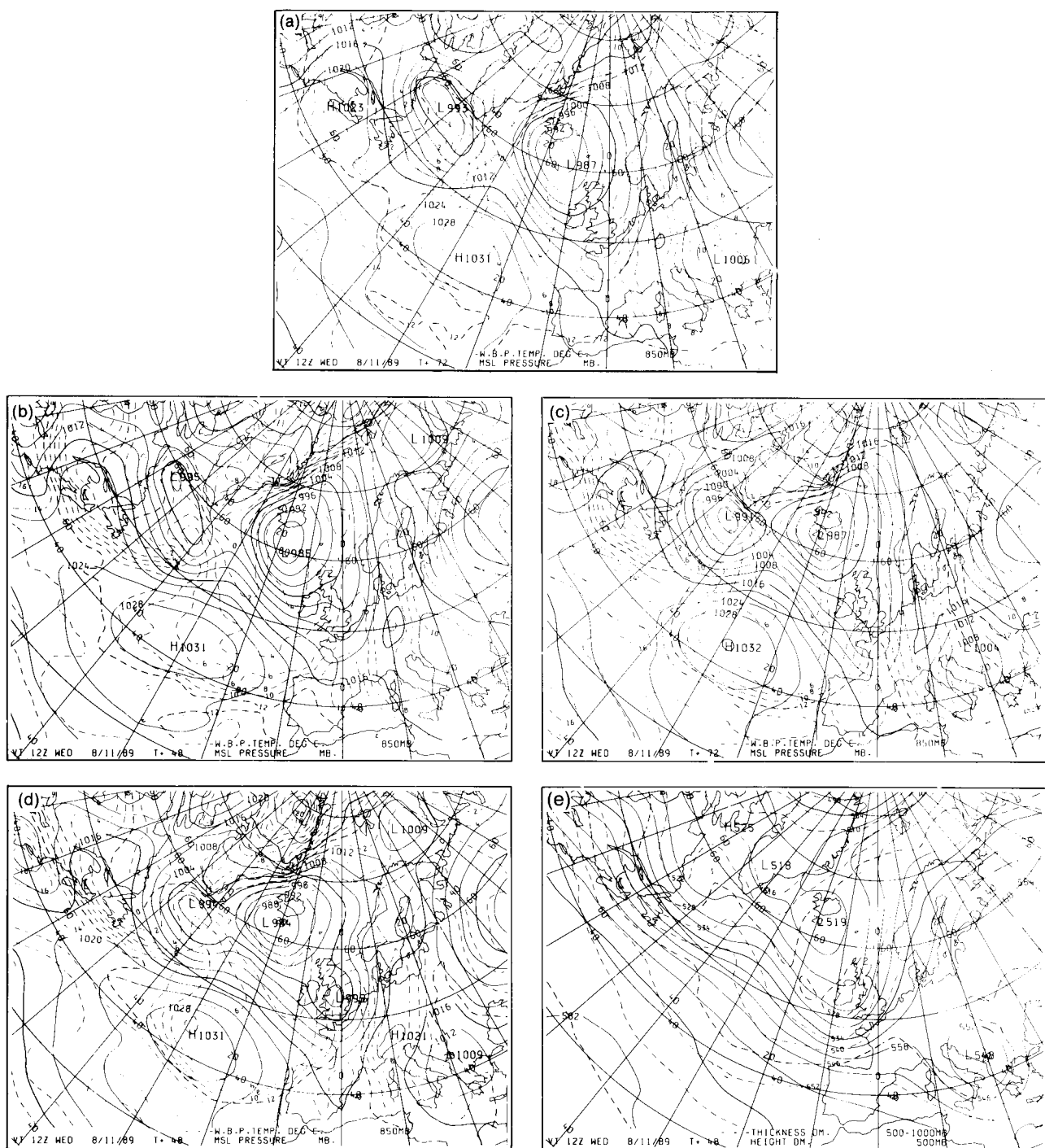


Figure 3. Continuous lines show (a) coarse-mesh 72-hour MSL pressure forecast, (b) coarse-mesh 48-hour MSL pressure forecast, (c) ECMWF 72-hour MSL pressure forecast, (d) ECMWF 48-hour MSL pressure forecast, and (e) coarse-mesh 48-hour 500 mb forecast (heights in dam) all valid for 1200 UTC on 8 November 1989.

London) and typify the guidance received from the models over the preceding days. The 72-hour forecasts from both models produced just a weak trough over the United Kingdom, bearing no resemblance to the features which actually developed.

The 48-hour forecast from the coarse-mesh model (Fig. 3(b)) was almost identical to its 72-hour forecast (Fig. 3(a)); such consistency might normally be expected to bolster confidence in the products. On this occasion the forecasters were far from happy! The featureless

nature of the MSLP patterns seemed odd in relation to the substantial troughing generated at 500 mb (Fig. 3(e)), leading to a feeling that there could be much more to this system than the coarse-mesh MSLP fields implied. This suspicion was reinforced by the ECMWF 48-hour MSLP forecast (Fig. 3(d)) which did indicate a more substantial depression over the United Kingdom. Even so, the centre was still too shallow (error ≈ 11 mb) and the strength of the gradients significantly underestimated.

At least some of the differences between the coarse-mesh and ECMWF 48-hour forecasts might be explained by the fact that the ECMWF model started from an analysis with a more pronounced thermal ridge over the incipient wave (the maximum difference in thickness being 3 dam). It is certainly true that the coarse-mesh 48-hour thickness forecast was about 10 dam too low over south-east England, but part of this error was probably a result of the lack of development rather than a cause. Errors in the corresponding ECMWF thickness forecast were generally very small. Further investigations were undertaken to try and determine how critical a factor the initial analysis was; these results are discussed in section 6.

4. Short-range guidance

It was always recognized by the forecasters in CFO that, irrespective of any deficiencies in the analysis, the bland appearance of the medium-range prognoses from the model might be partly attributable to the smoothing effect of the coarse grid. Small-scale or intense systems cannot be resolved properly by this grid and the forecasters had to wait for the short-period fine-mesh forecasts to throw further light on the likely developments.

The fine-mesh run starting from 1200 UTC on 6 November 1989 provided the first reliable indications from the 15-level model of the eventual vigour and track of the low centre. In particular, it will be seen that the 36-hour MSLP forecast (Fig. 4) compares well with the analysis in Fig. 1(c). The 48-hour forecast from the same run (produced for back-up purposes and not generally disseminated) placed the low centre over Hampshire with a reasonably vigorous circulation, and central pressure about 996 mb. It was at this stage that the

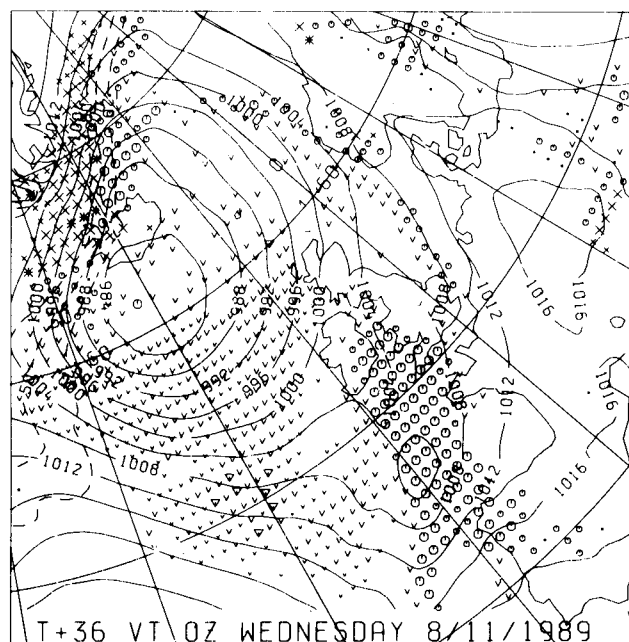


Figure 4. Fine-mesh 36-hour MSL pressure forecast valid for 0000 UTC on 8 November 1989, the various symbols showing areas of precipitation.

first firm warnings were given of the likely developmental nature of the low, the synoptic review issued at 2245 UTC on the 6th indicating that the low was likely to deepen substantially as it engaged the cold air over the Atlantic and that it could turn a little more to the left as a result. Emphasis was also placed on the likelihood of heavy rain, in view of the high dew-points (16 °C) in the warm air.

Following the above comments, the results of the next fine-mesh run based on data for 0000 UTC on 7 November 1989 came as a considerable shock. The model showed a reversion to the weak non-developmental pattern favoured by earlier coarse-mesh runs, as can be seen from the 24- and 36-hour forecasts in Figs 5(a) and 5(b) respectively. At the same time, there appeared to be significant defects in the fine-mesh analysis (even when allowance was made for the uncertainties engendered by a lack of data in the crucial area). In particular, the 1000–500 mb thickness analysis (Fig. 6(a)) failed to show the warm bulge over the wave which one would normally expect with the large well-developed plume of cloud evident on satellite imagery (Fig. 7(a)).

In view of these perceived analysis deficiencies — the forecast sharpening of the upper trough, and previous fine-mesh and ECMWF guidance — it was decided to opt for a much more developmental scenario. The CFO 24-hour MSLP forecast for 0000 UTC on 8 November 1989 (Fig. 5(c)) continued the idea of the wave developing into a vigorous centre as it moved over the south-west approaches, pressure levels being adjusted to be about 12 mb lower than the fine-mesh values (Fig. 5(a)). The corresponding coarse-mesh run started from a rather better analysis of the 1000–500 mb thickness pattern near the wave (Fig. 6) with the help of additional artificial or ‘bogus’ observations derived from the forecaster’s interpretation of the imagery. Although it still failed to develop a discrete centre on its 24-hour forecast (Fig. 5(d)), the marked troughing produced to the south-west of the British Isles encouraged the forecasters, since it was not totally inconsistent with the idea of a deeper centre if allowance was made for the inherent smoothing associated with the coarser grid.

Consideration of the upper-air patterns and satellite imagery provided further support for this cyclogenetic theme. At 0000 UTC on 7 November 1989 the wave was located just ahead of a flat and slightly confluent upper-air trough (Fig. 8) which was also associated with a broad region of strong baroclinicity. Similar patterns have accompanied some notable occasions of marked cyclogenesis (Young 1989), in particular the ‘Great Storm’ of October 1987 and the ‘Burns’ Day’ storm of 25 January 1990 (McCallum 1990). Satellite imagery (Fig. 7(a)) also showed a region of enhanced convection (C) in the cold air slowly approaching the baroclinic cloud plume, suggesting increasing positive vorticity advection over the wave which could help trigger further development. Later images (Fig. 7(b)) revealed the start

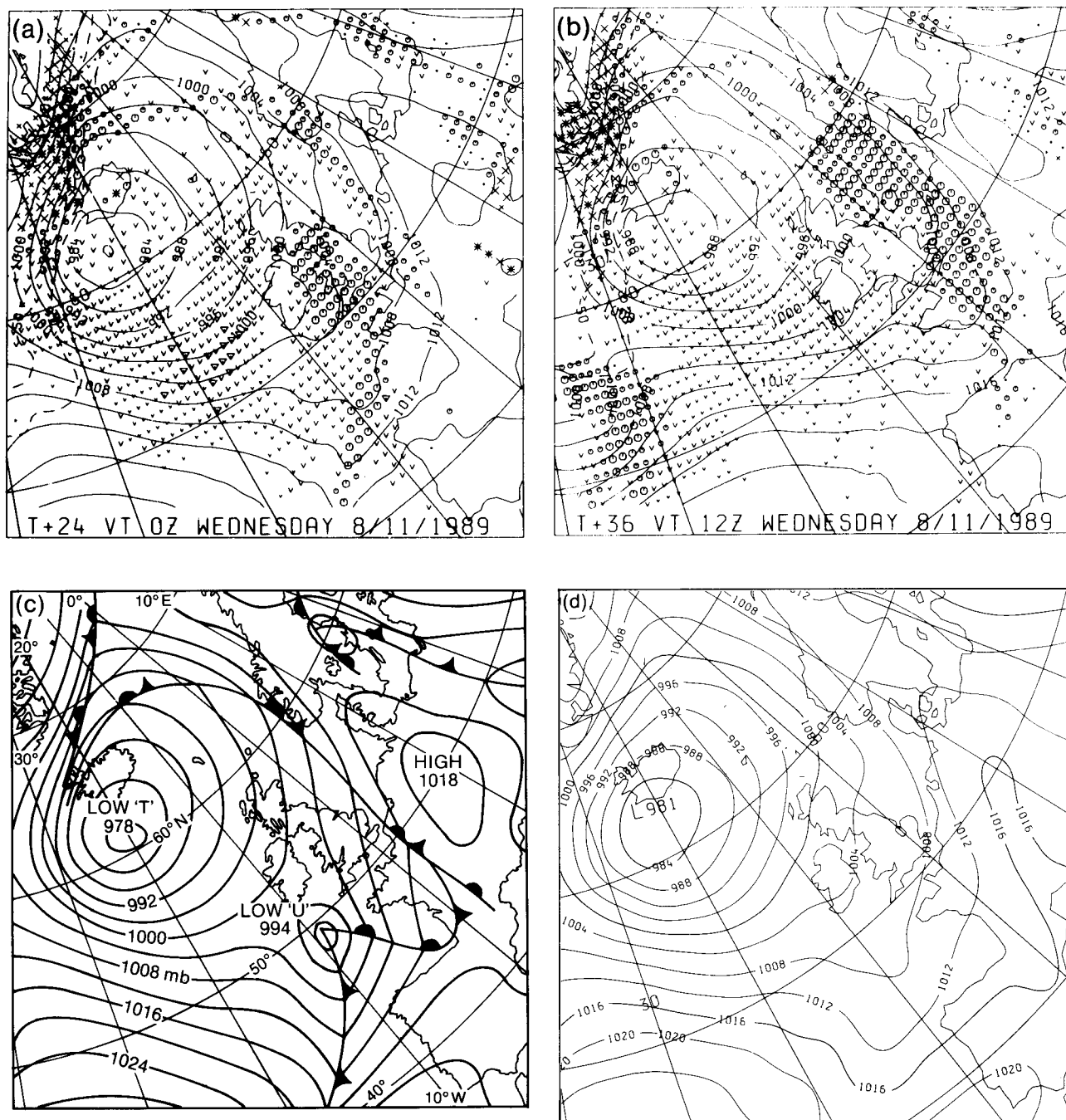


Figure 5. (a) Fine-mesh 24-hour MSL pressure forecast valid for 0000 UTC on 8 November 1989, (b) fine-mesh 36-hour MSL pressure forecast valid for 1200 UTC on 8 November 1989 (the various symbols showing areas of precipitation), (c) CFO 24-hour MSL pressure forecast valid for 0000 UTC on 8 November 1989, and (d) coarse-mesh 24-hour MSL pressure forecast valid for 0000 UTC on 8 November 1989.

of an extrusion of middle level cloud (E) on the poleward side of the plume. Such a feature is also indicative of major cyclogenesis (Young 1989).

In spite of this evidence, not all forecasters were convinced that the low was going to become a major system and considerable debate took place during the 7th over the likely developments. The evolution was, of course, crucially dependent on how well the wave phased in with the amplifying upper trough which had moved eastwards from Canada during the preceding 4–5 days. The variability in the numerical guidance no doubt reflected both the sensitivity of the development

to this ‘phase-lock’ between the upper trough and surface centre, and the uncertainties in the analysis.

The next two runs of the fine-mesh model (based on data for 0600 and 1200 UTC on 7 November 1989) both showed more vigorous development of the low, lending further support to the line taken by CFO. However, as can be seen from Fig. 9(a), the forecast track of the centre lay across the extreme south-east of England, thereby restricting the strong winds to the English Channel and south-east coasts, raising some forecasting problems similar to those associated with the Great Storm.

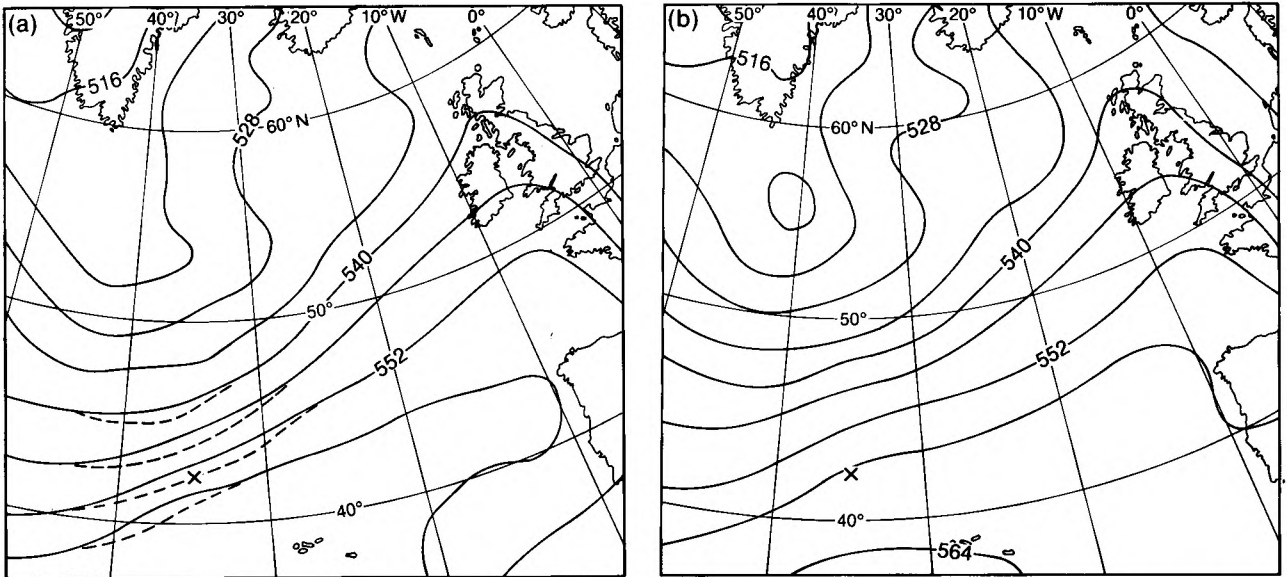


Figure 6. (a) Coarse-mesh thickness (dam) analysis (continuous line) with fine-mesh differences (dashed lines) at 0000 UTC on 7 November 1989, and (b) CFO 1000–500 mb thickness (dam) analysis for 0000 UTC on 7 November 1989. X marks the position of the wave tip.

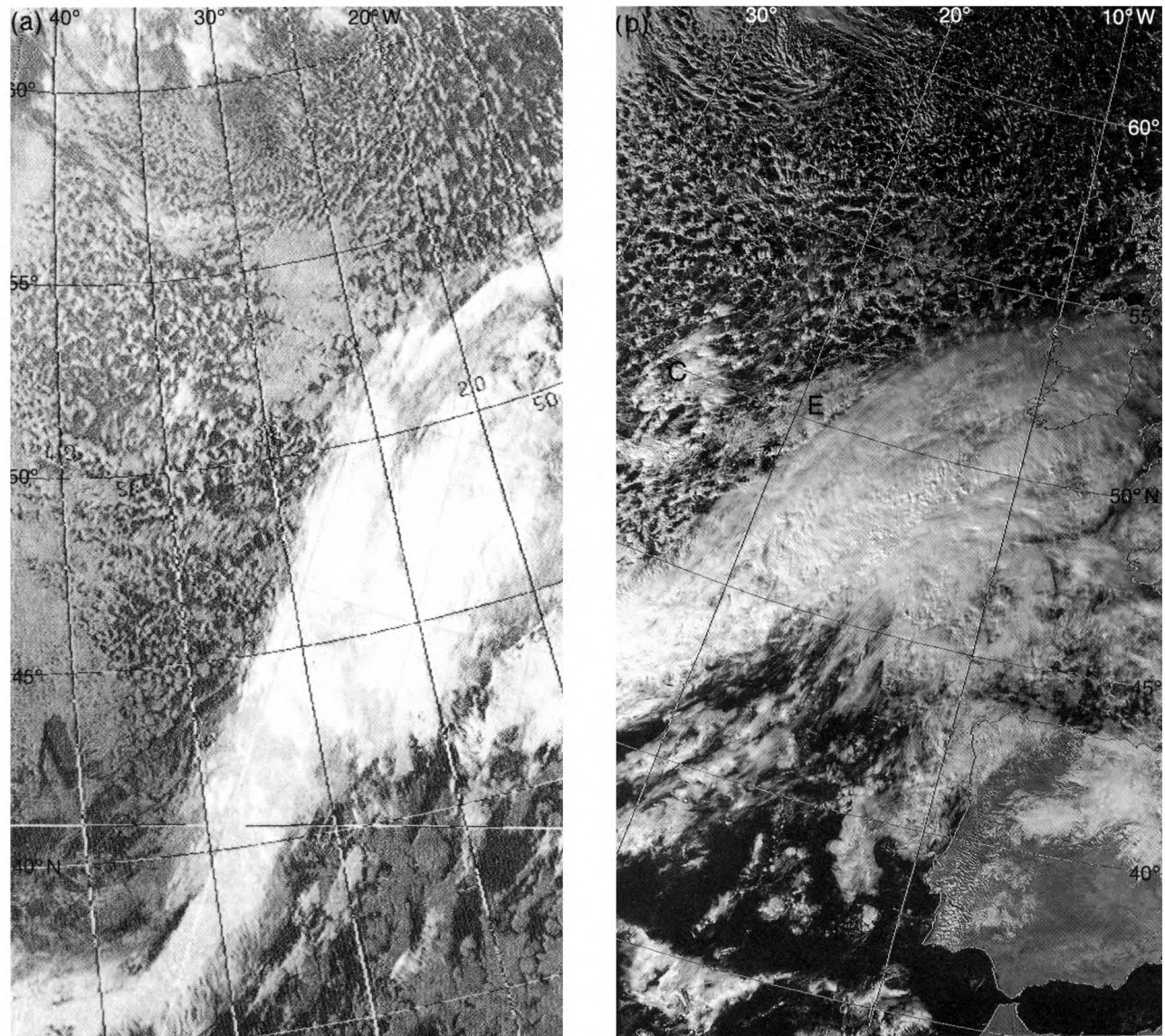


Figure 7. NOAA-11 infra-red images for (a) 0422 UTC and (b) 1359 UTC on 7 November 1989.

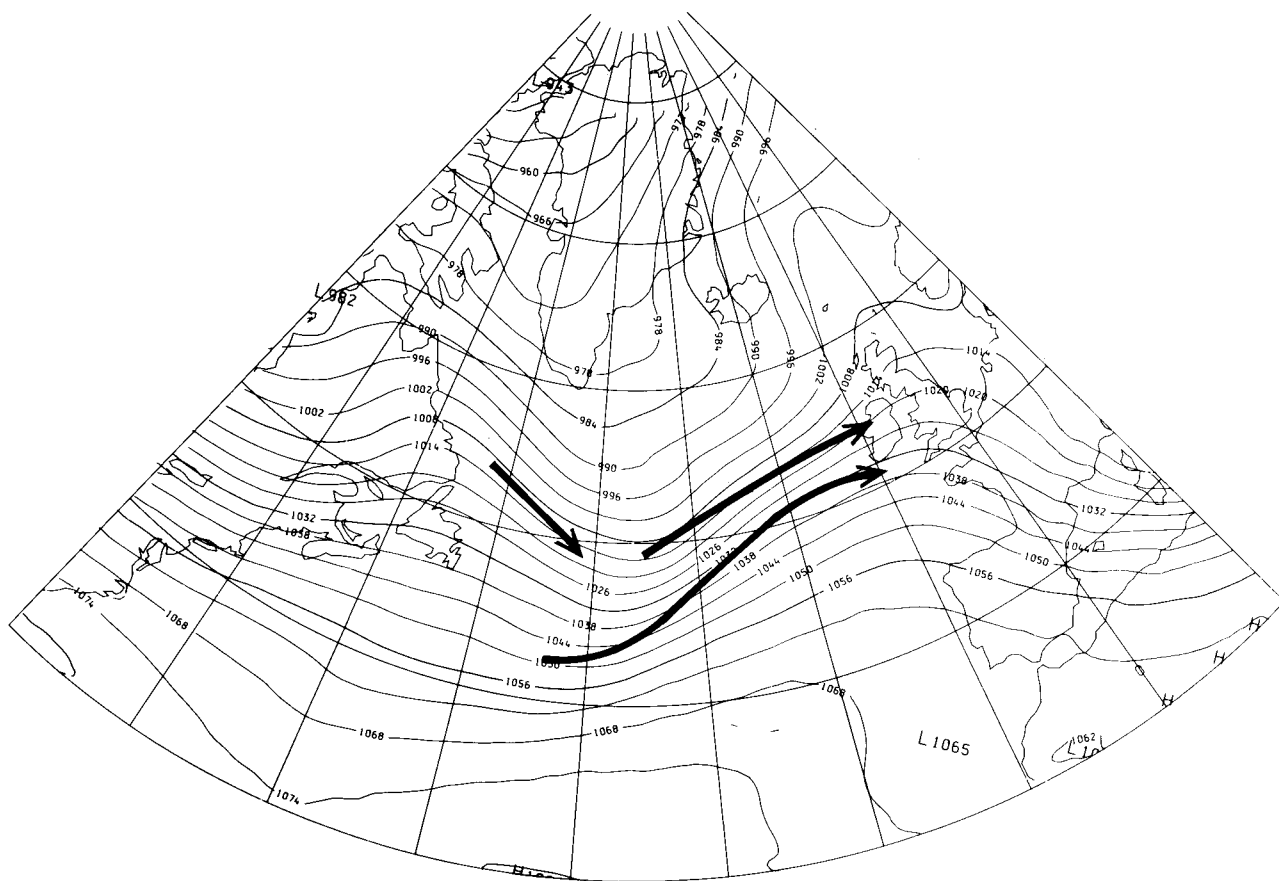


Figure 8. Analysis of the 250 mb surface (heights in dam) for 0000 UTC on 7 November 1989 with solid arrows denoting jet cores.

By that evening, increasing, though still modest, pressure falls over the south-west approaches and reports of gale force winds around the low convinced the CFO forecasters that the anticipated major development was under way. Although the model integrations had started from a good analysis, consideration of the shape and strength of the 1000–500 mb thickness gradients still suggested that the centre would deepen more than indicated and turn on a more northerly track as the thermal pattern became increasingly distorted. The CFO 24-hour MSLP forecast for 1800 UTC on 8 November 1989 (Fig. 9(c)) showed the low about 8 mb deeper than the corresponding fine-mesh product (Fig. 9(b)), whilst tracking the centre across the south-east Midlands to The Wash. Comparison with the analysis in Fig. 9(d) proves that this was excellent guidance, prompting a warning of gales over south-east Britain in the synoptic review issued at 2225 UTC on the 7th, with the possibility of severe gales to the south of the centre as pressure built again behind the confluent upper trough. This theme was followed through the night, specific reference being made in the early morning national radio forecasts of winds up to 60 m.p.h. over southern Britain during the day. Similar early warning was also given of severe gales and later storm-force winds for sea areas in the English Channel and southern North Sea.

5. Fine-mesh forecasts — general aspects

Despite the shortcomings of its MSLP forecasts, the fine-mesh model did give useful general warning of the heavy rain which affected many parts of England and Wales on 8 November. The heaviest rainfall was reported along and to the north of the depression track with totals typically in the range 20–30 mm. However, due to the deficiencies in the forecast depth and track of the depression, the model's rainfall distribution was less satisfactory. For example, the 24-hour forecast in Fig. 9(a) shows the heaviest rain over south-east Britain, whereas the radar display (Fig. 10) indicates that these parts were largely dry at that time, the bulk of the heaviest and most persistent rain being to the north and west of the low centre.

Another feature of the fine-mesh rainfall guidance was that, in general, it spread the rain too quickly north-eastwards across England and Wales. This was particularly noticeable in the run from 0000 UTC on 7 November 1989 which, as discussed earlier, failed to develop a discrete low centre. Despite the deficiencies in the fine-mesh 1000–500 mb thickness analysis referred to in section 4, the initial vertical motion fields (Fig. 11(a)) did show a zone of marked dynamical ascent in the vicinity of the wave. With no significant warm advection diagnosed, this ascent must have been primarily due to positive vorticity advection ahead of the upper-trough

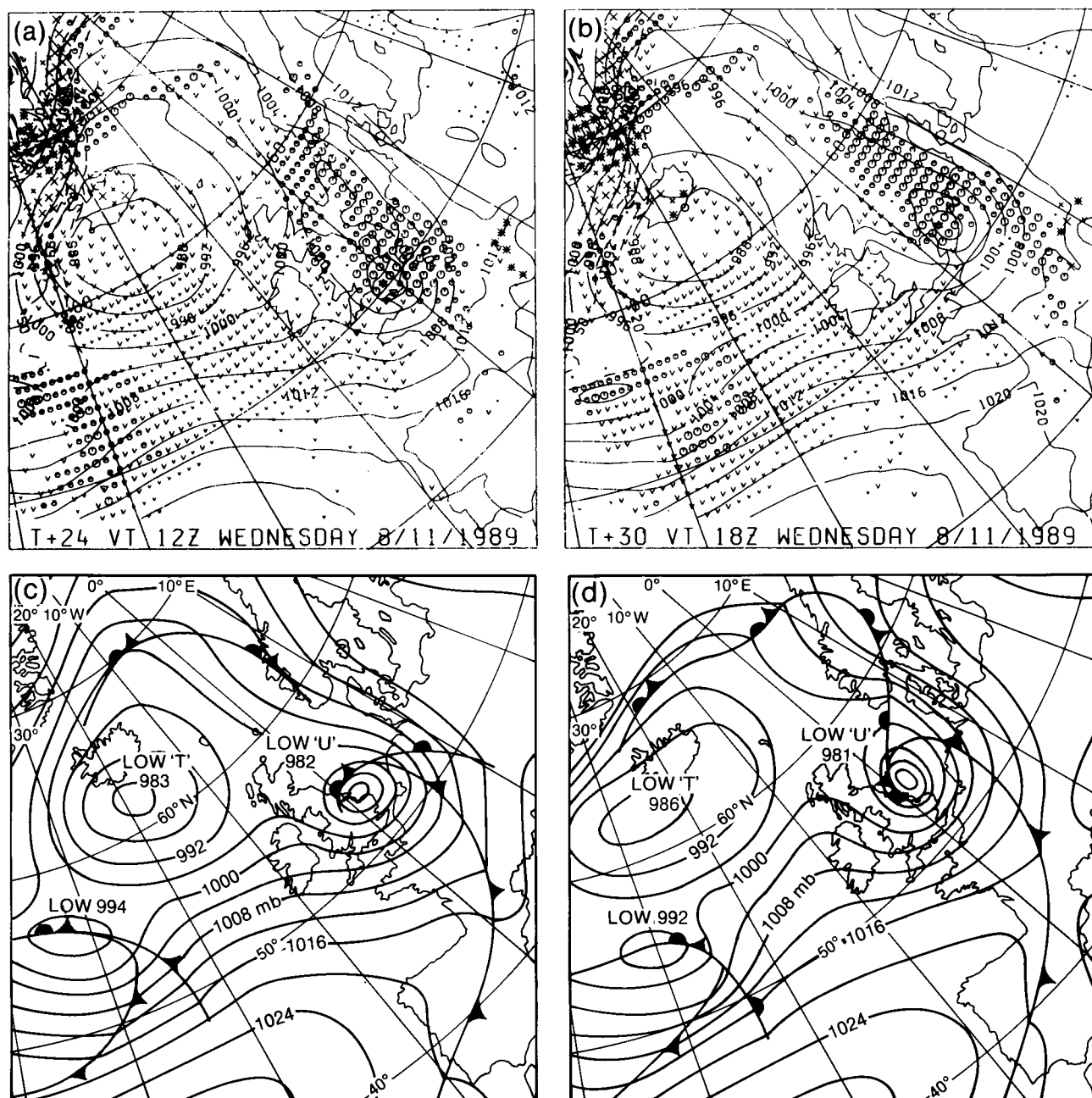


Figure 9. (a) Fine-mesh 24-hour MSL pressure forecast valid for 1200 UTC on 8 November 1989, (b) fine-mesh 30-hour MSL pressure forecast valid for 1800 UTC on 8 November 1989 (the various symbols showing areas of precipitation), (c) CFO 24-hour MSL pressure forecast valid for 1800 UTC on 8 November 1989, and (d) CFO MSL pressure analysis for 1800 UTC on 8 November 1989.

axis. Examination of the thickness and vertical motion fields associated with the 24-hour MSLP forecast in Fig. 5(a) revealed definite signs of a forward shallow wave near St. George's Channel, with a second wave much further back to the north of north-west Spain. Indeed, the forecast vertical motion field (Fig. 11(b)) shows the main area of ascent over and around the United Kingdom at 0000 UTC on 8 November in association with the forward wave and well ahead of the actual position of the low centre at that time. As mentioned earlier, there was some evidence of such a wave to the south of Ireland on the evening of the 7th; however, even if it existed, it was a feeble feature which

was soon swamped by the development of the main centre.

It has been noticed on many occasions previously that the model can appear especially vulnerable in complex situations involving multiple waves. A particular example was the Great Storm where several minor centres are known to have run across the Bay of Biscay before the arrival of the final low which developed into the major storm. In such cases, the potential for development of each individual wave will clearly depend on the precise details of the atmospheric structure. The net effect, as was observed in the case of the Great Storm (Lorenc *et al.* 1988), may be to make the results of the

numerical integrations very sensitive to relatively minor deficiencies in the analysis. In particular, it can be crucial whether the model has properly resolved the details of both the surface and upper-air patterns in the vicinity of the rearward low centre, which is often located in the main cyclonic development area just ahead of the upper-trough axis.

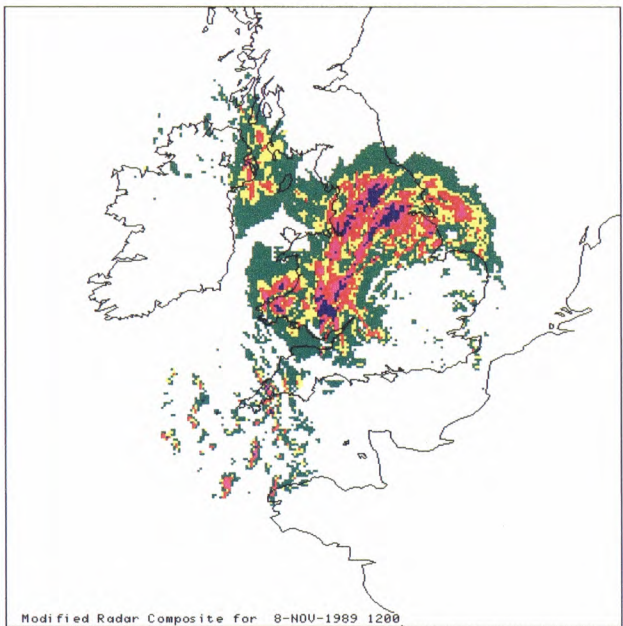


Figure 10. Rainfall radar display at 1200 UTC on 8 November 1989. Colours indicate rainfall rates in ascending order from green, through yellow, red, pink, dark blue and light blue to black.

6. Fine-mesh forecasts — effects of revised analyses

It was noted in section 4 that the poor fine-mesh forecast from 0000 UTC on 7 November 1989 may have been at least partly due to deficiencies in the analysis. This forecast was therefore rerun from the corresponding coarse-mesh analysis which included bogus data designed to improve the MSLP and thickness fields in the vicinity of the wave. However, the net effect on the fine-mesh forecast was minimal, only resulting in very slight deepening of the MSLP trough, with still no hint of a closed low centre.

Further experiments were undertaken in which additional bogus data at the 250 mb height level were included in the assimilation with the aim of optimizing the analysis further. In particular, efforts were directed towards ensuring that the analysis properly reflected the strength of the jets and the sharpness of the upper trough. The best result was obtained by inserting winds alone, and the resultant 36-hour forecast is shown in Fig. 12. It can be seen that in this case the model managed to generate a closed centre of 1003 mb and also produced an improved rainfall forecast. However, the movement of the low was much too slow and its vigour still seriously underestimated.

The results of the reruns carried out to date must be judged disappointing. It has not been possible to demonstrate that the model solution was sensitive to any particular aspect of the initial conditions, unlike the Great Storm where subsequent inclusion of a group of late aircraft reports had a significant impact on the forecast (Lorenc *et al.* 1988).

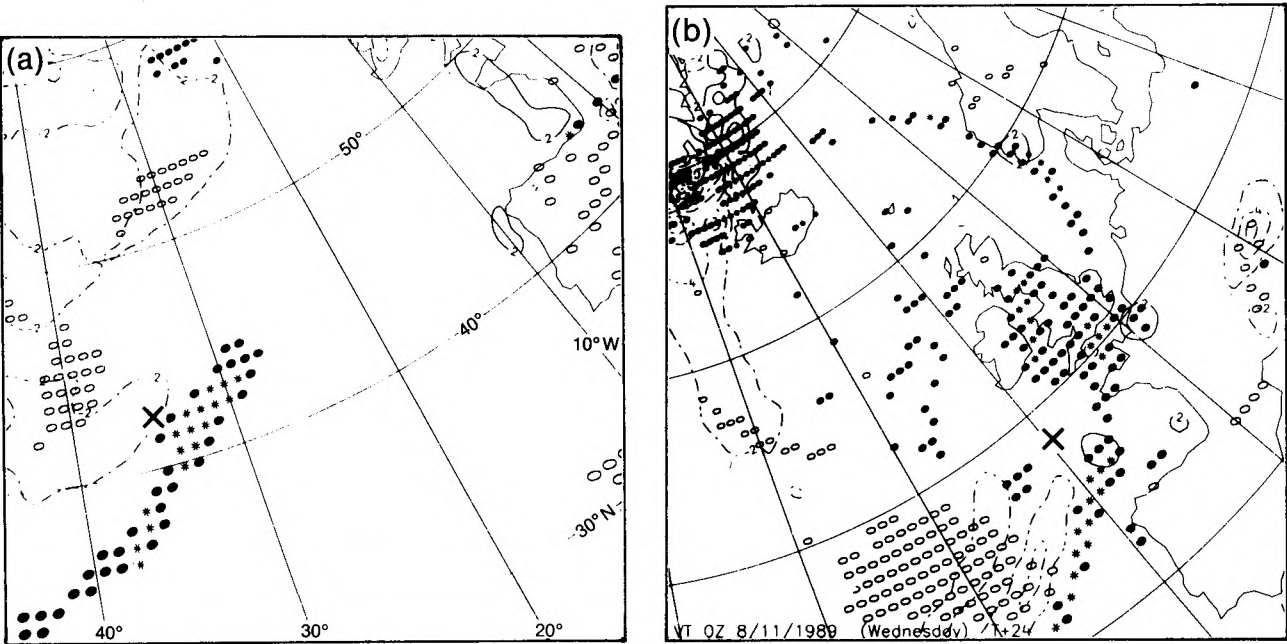


Figure 11. Fine-mesh vertical velocity field (open circles show areas $\geq 6.2 \text{ mb h}^{-1}$ descending, solid circles show areas $6.2\text{--}12.5 \text{ mb h}^{-1}$ ascending and asterisks show areas $\geq 12.5 \text{ mb h}^{-1}$ ascending), and thermal advection field (dash-dot line in $^{\circ}\text{C}$ per 6 hrs). (a) Analysis for 0000 UTC on 7 November 1989, and (b) 24-hour forecast valid for 0000 UTC on 8 November 1989. X marks the position of the low centre.

7. Conclusions

This case-study demonstrates that even in this era of high-quality numerical guidance, the ‘man on the bench’ can still have an important role to play in improving forecasts. There is a danger that, because the model is usually so dependable, forecasters can be lulled into a false sense of security. It is obviously important to recognize those situations where the model may be significantly in error, especially when the deficiencies may result in a failure to predict severe weather.

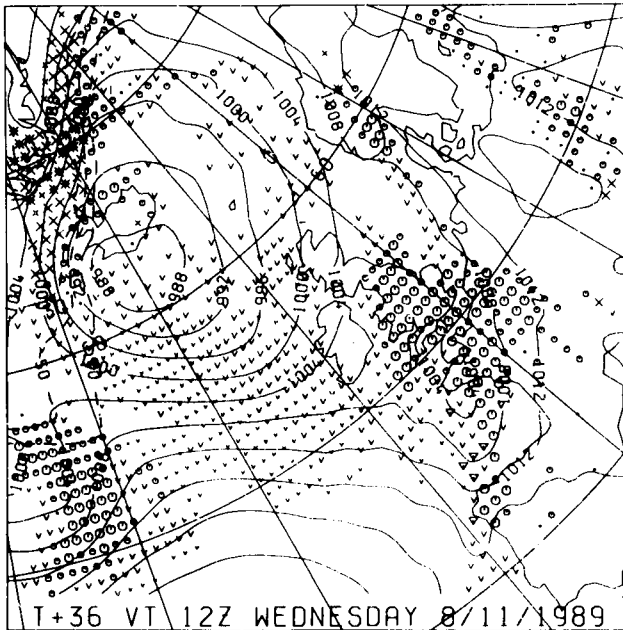
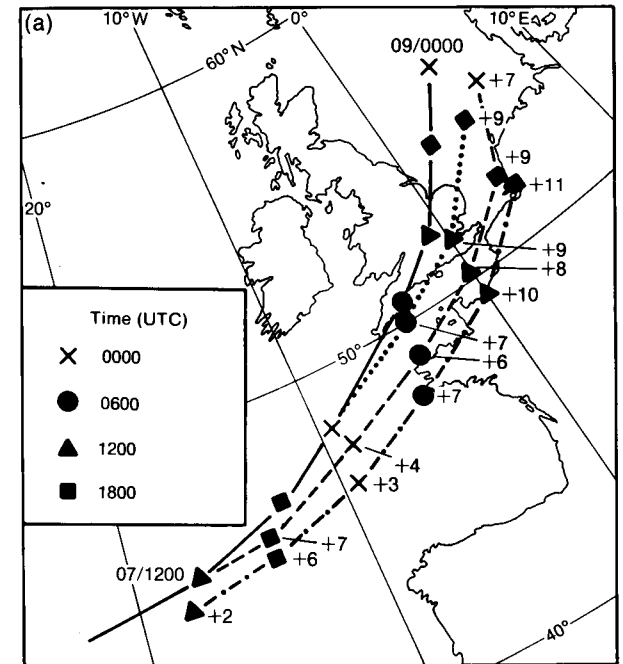


Figure 12. Best rerun fine-mesh forecast valid for 1200 UTC on 8 November 1989 the various symbols showing areas of precipitation.



Particular care is needed in situations involving confluent upper troughs. Rapid pressure rises behind the trough can quickly generate very strong winds to the rear of the associated MSLP low centre, even when pressure falls ahead of the system have been relatively modest. The primary responsibility for identifying such situations rests, of course, with CFO.

Recent experience during the notably stormy winter of 1989/90 (including the Burns’ Day storm of 25 January 1990 (McCallum 1990)) shows that it is not unusual for there to be marked fluctuations in the quality of model guidance from run to run. Despite good earlier indications of major cyclonic development, the model occasionally lapses into a weak or non-developmental mode which can all too easily encourage a downgrading of previous warnings of severe weather. Although limitations in the initial data must play an important part in causing such oscillations, it is noteworthy that reruns of the fine-mesh model from 0000 UTC on 7 November 1989, incorporating additional bogus data to try and improve the analysis, have so far failed to produce a satisfactory forecast. Moreover, Fig. 13(a) shows that, although this run produced by far the worst guidance, the following three runs (based on data times of 0600 and 1200 UTC on 7 November and 0000 UTC on 8 November 1989) all displayed the same systematic error, namely underestimation of the deepening and, as a consequence, the amount of turning to the left. By comparison, errors in the forecast track and depth from successive CFO 24-hour forecasts (Fig. 13(b)) were generally much smaller.

To summarize, one needs to be very wary when the model suddenly reverses earlier indications of vigorous

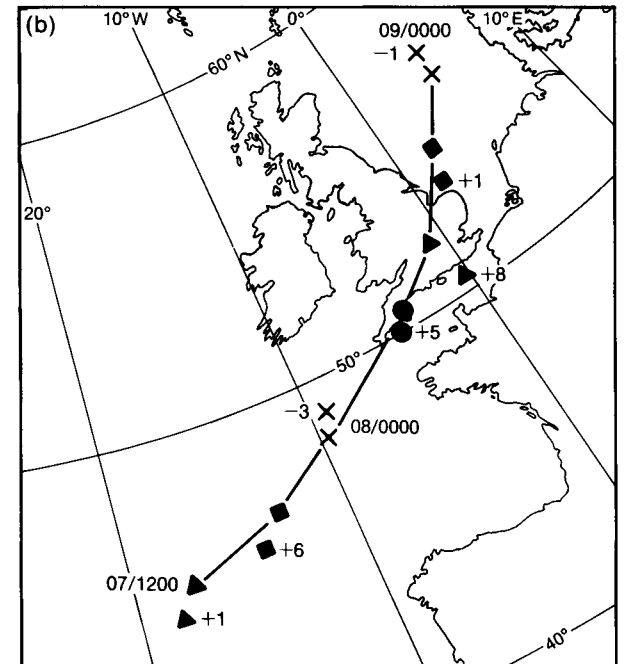


Figure 13. Errors in track and depth (mb) of the low centre from (a) fine-mesh forecasts, and (b) CFO 24-hour forecasts. In (a) the tracks shown are: actual track (continuous line), and fine-mesh runs from 0600 UTC on 7 November (dash-dot line), from 1200 UTC on 7 November (dashed line) and from 0000 UTC on 8 November (dotted line). In (b) the continuous line shows the actual track, and CFO 24-hour forecast with errors in central pressure (mb) alongside (time key as Fig. 13(a)).

cyclonic development. Experience has shown that the latest model guidance may not always be the best, especially when dealing with a complex low-pressure area involving two or more waves. Judgement of the most likely outcome must depend on careful consideration of the satellite imagery in conjunction with the thickness and upper-air patterns.

Acknowledgements

The author would like to thank O.M. Hammon (Forecasting Research Branch) for carrying out the reruns of the fine-mesh model, also M.V. Young (Nowcasting and Satellite Applications Branch) for his useful comments on the interpretation of the satellite imagery.

References

- Gadd, A.J. and Morris, R.M., 1988: Guidance available at Bracknell for the storm of 15/16 October 1987, and the forecasters' conclusions at the time. *Meteorol Mag*, **117**, 110–117.
- Lorenc, A.C., Bell, R.S., Davies, T. and Shutts, G.J., 1988: Numerical forecast studies of the October 1987 storm over southern England. *Meteorol Mag*, **117**, 118–130.
- McCallum, E. 1990: The Burns' Day storm, 25 January 1990. *Weather*, **45**, 166–173.
- Woodroffe, A., 1988: Summary of weather pattern developments of the storm of 15/16 October 1987. *Meteorol Mag*, **117**, 99–103.
- Young, M.V., 1989: Liaison with the Central Forecasting Office regarding imagery interpretation for a cyclogenesis event: 20–21 October 1989. (Unpublished, copy available in National Meteorological Library, Bracknell.)

551.5(09):33:37:06(41–4)

The United Kingdom's contribution to the WMO Voluntary Co-operation Fellowship Programme

F.D. Reece

Meteorological Office College, Shinfield Park

Summary

The history of the World Meteorological Organization (WMO) Voluntary Co-operation Programme Fellowships fund is described, and the operation of the United Kingdom's contribution to it is summarized. The past performance of the fund is reviewed in the light of a recent survey conducted among recipient nations. The current state of the fund is described and plans for its future management are discussed.

1. Introduction

In the 1960s the Voluntary Assistance Programme (VAP) was created by the WMO in order to provide assistance to developing countries for them to fulfil their role in the implementation of the World Weather Watch plan. Under this programme, WMO members provided voluntary contributions of equipment and services in kind, or financial contributions.

Under WMO these resources were distributed to WMO member states who requested assistance. This assistance could take many forms ranging from the supply of equipment for synoptic surface or upper-air observing stations through telecommunications equipment for the Global Telecommunication System to the financial support of students on long- and short-term fellowships for formal or on-the-job training in meteorology abroad. Universities and Regional Meteorological Training Centres (RMTCs) would be the main providers of such formal training while on-the-job training would be achieved through the attachment of

trainees from the Third World countries to more highly developed National Meteorological Services for suitable periods.

In the first year of the VAP the value of the assistance provided through WMO was worth just under US\$1.4 million world-wide and it was the stated aim of the Executive Committee of WMO that ultimately all members of WMO would eventually find it possible to make contributions, however small, to the VAP (World Meteorological Organization 1971). In 1979 the VAP was renamed the Voluntary Co-operation Programme (VCP). By 1986 the value of VCP contributions world-wide had risen to US\$5.4 million.

The Meteorological Office has consistently given support to this programme through two separate funds. The UK/VCP (Equipment and Services) fund administered by the Meteorological Office's International and Planning Branch is the largest of these two funds whilst the UK/VCP (Fellowships) fund is administered by the

Meteorological Office College. It is this latter fund which forms the subject of this article which is based on a presentation given to the Commonwealth Meteorologists Conference in June 1989 (Shaw, personal communication).

2. UK/VCP Fellowships

The UK/VCP Fellowship Programme has now been operating for about 20 years and current expenditure is running at £176 000 per annum. This allows around 15 new Fellowships to be granted in any one financial year. In addition, a flexible approach to the management of the UK/VCP (Equipment and Services) fund makes it possible to provide a few additional Fellowships in the technical training area. To date, all Fellowships have been allocated within the United Kingdom. The Meteorological Office sees its commitment to the VCP Fellowship Programme as a contribution towards the World Weather Watch in particular. More than £1 million has been spent in the last 10 years and clearly such expenditure has to be properly managed. To this end the Meteorological Office carried out a major survey of the VCP Fellowship Programme at the end of 1987 (Mills, personal communication).

3. The 1987 survey

Before the survey there had been little indication as to whether or not any Fellowships granted had proved successful after the return of the Fellows concerned to their home countries. The survey examined 123 Fellowships granted since 1970 and spread among 53 different countries. Questionnaires were sent to the WMO Permanent Representatives of the National Meteorological Services of 110 of the 123 Fellows.

Preparation of the survey led to a better perspective of exactly how the allocation of Fellowships had been made according to the type of training provided. Of the 110 Fellowships considered by the survey, 67 were awarded for places on Meteorological Office College courses. Of these, 43 were for technical training courses and the other 24 were for a variety of meteorological courses. Of the remaining 43 Fellowships, 39 had been awarded for first degree or post-graduate courses at the University of Reading and the other four for a miscellany of other UK-based courses. The degree course Fellowships are more demanding of funds than those for other courses because of their longer duration and so the Fellowships awarded for degree courses are numerically fewer than those awarded for other courses.

The distribution of funds between long- and short-term Fellowships is judged to have been reasonably well balanced to date. It could be argued that a wider distribution of Fellowships among UK training institutions would be desirable, but in practice Fellowships at institutions other than those in the Reading area are not often sought.

The survey questionnaire sought to establish whether the Fellow concerned was still in service and, if so, what post he or she currently held. It also sought information

on any subsequent VCP awards and invited comment from the National Meteorological Service concerned as to the usefulness of the training provided under the Fellowships. Sixty-eight per cent of the questionnaires were returned (76 out of 110). It was gratifying to find that the majority of Fellows who have gained benefit from the training they received under VCP have continued to be employed by their National Meteorological Services.

Leaving aside the unavoidable losses due to retirement or death, only 11 of the 76 Fellows (15%) have been lost to meteorology. This is an encouragingly low wastage rate; it provides the best indication of success which we have for the Fellowship Programme.

The invitation for general comments on the questionnaire yielded no adverse criticisms. However, it should be noted that 18 of the 53 countries who had been granted Fellowships failed to respond to the questionnaire and so the scope of the survey was limited and the results must be treated with caution.

The results of the survey nevertheless indicate that the great majority of Fellows benefit from the Fellowships and return to their National Meteorological Services to give lasting commitments to meteorology. The Meteorological Office has been encouraged by the survey to persevere with its programme of VCP Fellowships.

4. Selection policy

In selecting Fellows for sponsorship the potential for each Fellowship to make a positive contribution to the World Weather Watch remains to the fore. Account must also be taken of the potential value of the training proposed to the National Meteorological Service seeking the Fellowship and the suitability of the candidate.

Management of the VCP fund is tied to the financial year which begins on 1 April. The total monies available, less those committed for ongoing Fellowships, are known some months before this. Early in the calendar year applications for UK/VCP Fellowships received via the WMO Education and Training Department are considered by a Selection Board.

In reaching its decisions the Board seeks the advice of the Head of the International and Planning Branch of the Meteorological Office to ensure that a proper international perspective is maintained and that the programme of Fellowships dovetails with that of the VCP (Equipment and Services) fund. Discussions with the University of Reading (see section 5) may also take place at this stage and there is also some involvement of the Fellowship Division of the WMO Training and Education Department. Soon after the board has completed its deliberations a preliminary proposal for the coming financial year is prepared and a list of recommended fellowships is presented to the Chief Executive of the Meteorological Office for his approval.

This annual review normally commits the bulk of the available funds up to the end of the coming financial

year (i.e. up to 15 months ahead). Later in the calendar year there is limited scope for the reallocation of funds from Fellowships which for various reasons are not taken up, or for considering applications received after the review.

5. Current arrangements

The United Kingdom programme is in a healthy state. Fig. 1 shows the funding levels for the financial years 1985/86 to 1989/90 and the planned levels for the future. The figures are not adjusted for inflation but it is clear that a planned growth of funding in real terms is now taking place.

In spite of the welcome increase in money actually spent over recent years Fig. 1 shows that for each of the first four financial years the monies available have not been fully spent. There are a number of reasons for this. For instance in the financial year 1987/88 the underspend of £40 000 was largely brought about by the late cancellation of our College-based Basic Electronics course due to an insufficient number of students. This in turn was due to a reduction in expected Fellowships

from other funding sources, for example the United Nations Development Programme. In addition, £10 000 had been reserved in recent years as a part contribution to a distance learning project which failed to come to fruition. Another source of underspend has been that some Fellowships offered have not been taken up. If notification of this is not received soon enough it is impossible to allocate the funds released to other fellowships before the start of the academic year.

This failure to fully utilize the available funds has led to a reconsideration of the way in which the fund is managed. In 1989, in addition to the major review of applications early in the calendar year, a second review was taken some weeks before the start of the academic year. This second review has enabled the monies available in financial year 1989/90 to be used to much better effect and it is intended to continue this policy in future years.

The current costs of Fellowships most commonly sought are given in Table I. The first seven courses listed are based at the Meteorological Office College and the last two are based at the University of Reading. The B.Sc. course at the University of Reading is now normally treated as a 4-year Fellowship for overseas students and includes a preparatory year which precedes the formal B.Sc. course. The cost of such a Fellowship (£43 000) is very high, quite apart from the loss of the student to his Meteorological Service for 4 years. This high investment in terms of time and money underlines the need for very careful selection of Fellows for this and all other courses. The courses based at the Meteorological Office College are training, as distinct from educational, courses and are primarily intended for UK Meteorological Office staff. However, if there are vacancies on appropriate courses these are offered to suitable overseas candidates and a proportion of these are VCP Fellows.

On the other hand the Meteorological Engineers course (MEC) and the Instrument Maintenance (non-electronics) course (IMC) are both designed specifically

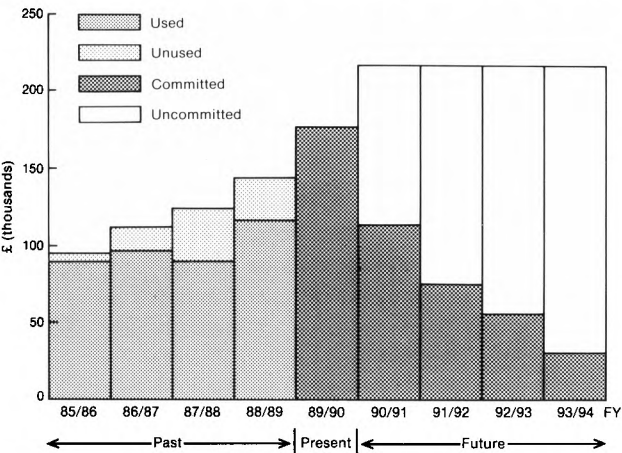


Figure 1. Actual past, expected current and planned future expenditure compared to the total United Kingdom VCP (Fellowship) funds available in each financial year.

Table I. Sample Fellowship costs (pounds sterling) for different Meteorological Office College and University of Reading courses

Course	Duration	Course fees	Fixed* costs	Variable* costs	Total cost
Scientific Officers	21 weeks	7730	919	1278	9927
Applied Meteorology	22 weeks	8302	919	670	9891
Initial Forecasting	18 weeks	6789	919	550	8258
Advanced Forecasting	7 weeks	3138	858	235	4231
Extension Forecasting	4 weeks	1693	858	140	2691
Meteorological Engineers	8 months	14000	919	1155	16074
Instrument Maintenance	16 weeks	4000	1039	1534	6573
B.Sc. (Meteorology)	4 years	22800	1359	18528	42687
M.Sc. (Meteorology)	2 years	11400	1317	9264	21981

* Fixed costs include arrival and departure allowances, books, equipment and clothing allowances plus British Council handling charges. Variable costs include living expenses and health insurance.

for overseas services. Both of these courses attract support not only from VCP but also from other WMO funding agencies, the United Nations Development Programme and the British Council.

The 4-month long IMC provides training in the maintenance, repair and calibration of conventional Meteorological Instruments. It is a well established course having run for several years now.

The MEC lasts 8 months and provides a thorough grounding in the theoretical knowledge and practical skills required to assemble, install, maintain and repair a wide range of operational electrical and electronic equipment (see Fig. 2). The course has replaced the 18-month Basic Electronics course, much of which was based at Reading College of Technology. The MEC is an intensive residential course with evening sessions and on-the-job outstation attachments to consolidate the students practical skills. Successful completion of the MEC will be recognized by the award of a Diploma in Meteorological Engineering (Dip. Met. Eng.). The Business and Technician Education Council (BTEC) believe that the MEC could provide a sound route into higher education and that Dip. Met. Eng. should be considered alongside BTEC National Certificates or Diplomas and General Certificate of Education (GCE) A-level certificates for entry into BTEC Higher National courses in the engineering field.

The first MEC attended by 7 students ended in May 1989; the second began in October 1989 and comprises 9

students. Of these 16 overseas students from 13 different countries, 7 have been funded either wholly or partly through the UK/VCP (Fellowships) fund, 6 through the UK/VCP (Equipment and Services) fund and 3 through other funding agencies.

6. The future

The WMO Panel of Experts on Education and Training in Cairo in 1989 (World Meteorological Organization 1989) highlighted three issues relevant to the Voluntary Co-operation Programme Fellowship scheme.

The first of these issues was the increasing demand for long-term Fellowships (i.e. those longer than one year in duration). In the United Kingdom these Fellowships are nearly always based at universities simply because courses available at the Meteorological Office College are invariably less than a year long. This reflects the training policy of the Meteorological Office for relatively short, intensive training courses. From this parochial viewpoint it is difficult to justify an increased emphasis on long-term VCP Fellowships at the expense of short-term ones, even though the increased demand for long-term Fellowships is real.

The second issue raised by the Panel of Experts concerned the benefits of arranging group, rather than individual, training where possible. This already occurs to some extent in the United Kingdom with the IMC and MEC at the Meteorological Office College. Another



Figure 2. Members of the first Meteorological Engineering course under instruction at the Meteorological Office College, Shinfield Park.

form of group training programme is being developed within the Meteorological Office which involves training in the use and interpretation of Numerical Weather Prediction (NWP) products from the Bracknell Global Forecast Model the output from which is becoming increasingly available for use by forecasters in the developing countries.

Preliminary discussions have taken place on the possible establishment of a programme of Fellowships in which the student would undertake some formal training in NWP appreciation, partly based at the Meteorological Office College. A period of on-the-job training in the Central Forecasting Office would then follow using the Office's NWP products. The aim of these training Fellowships would be to thoroughly familiarize students with these NWP products. On return home they could then use and develop these operationally disseminated products to the special requirements of their own National Meteorological Service.

This type of training is particularly appropriate for those who will be working at the African Centre for Meteorological Applications for Development project and some VCP funds have been set aside to support this undertaking. The logistics of the programme have yet to be decided but it is hoped that training of small groups of Fellows can be arranged. This should be very much in keeping with the Panel's recommendation. It is interesting to note that during 1989 an overseas student successfully completed a 4-month Fellowship of this type. In addition to short-term Fellowships of this sort within the Meteorological Office it may also be appropriate to provide some long-term Fellowships at United Kingdom universities in support of the same programme.

The third recommendation made by the Panel was that consideration should be given to the use of VCP funds in support of Fellowships at the WMO Regional Meteorological Training Centres (RMTCs). There are currently 17 of these RMTCs and the great majority are in the developing countries. Nine of them are in Africa, the Middle East and the Indian Ocean. Of the remaining eight, five are in the Caribbean and Central and South America, with one each in India, the Philippines and Europe.

As a result of the Panel's recommendation a review of UK/VCP Fellowship funding policy was conducted early in 1989 and approval was given for up to 10 per cent of the fund to be spent overseas in support of the RMTCs. The potential benefits of such a policy are numerous. For instance, a course of particular relevance to a WMO Region could be supported at an RMTC in the Region by sponsorship of VCP Fellows for the course in question. Fellowships at the RMTCs promise to be more cost-effective than those taking place in the

United Kingdom because there will be less travel involved and so costs are likely to be lower. In addition, although courses at the RMTCs tend to be long compared to the shorter intensive training courses held at Shinfield Park, the tuition fees and living expenses are much lower in the developing countries. We therefore have the exciting prospect of being able to provide more UK/VCP Fellowships per year than was possible previously.

The practicalities of implementing this policy in a sensible, cost-effective way were addressed in talks at WMO in Geneva in February 1990 when ways and means of achieving this end were explored.

A small portion of the fund for the 1989/90 financial year has already been used for a training project, in support of the Nairobi RMTC early in 1990. This project provided training in the presentation of television weather forecasts for a number of forecasters from several different African countries. The training project was undertaken by one of our television weathermen and a BBC producer in conjunction with the staff of the RMTC. It is hoped that this pilot project will be the standard-bearer of a continuing programme of helping the RMTCs to improve and extend their capability to provide high-quality training for meteorologists within their own Region.

7. Conclusion

The UK/VCP (Fellowship) fund is seen as a significant component of the Voluntary Co-operation Programme world-wide. Results of the 1987 survey confirm that the training provided through the programme has been a sound investment and has contributed to the development of the Meteorological Services of the recipient nations and hence to the World Weather Watch.

The fund is currently being utilized to the full and the size of the fund is being increased in real terms to take account of increased training needs. These needs are commensurate with the spread of modern technology, the improving communication links with the National Meteorological Services of the developing countries and the needs of their staff to acquire new skills.

In order to make best use of the monies available, more cost-effective ways of optimizing the provision of training Fellowships under the fund are being explored. This will require continuing close co-operation with the Education and Training Department of the WMO over the years ahead.

References

- World Meteorological Organization, 1971: WMO helps the developing countries. Geneva, WMO, No.307.
- , 1989: Report of the thirteenth session of the Executive Council Panel of Experts on Education and Training. Geneva, WMO.

The summer of 1989 in the United Kingdom

G.P. Northcott

Meteorological Office, Bracknell

Summary

The summer of 1989 was warm, dry and sunny in most places, with record sunshine in many areas, particularly in the south.

1. The summer as a whole

Mean temperatures over the three months from June to August 1989 were above normal nearly everywhere and ranged from 0.2 °C below normal in a few parts of western Scotland to 2.2 °C above normal in south-west Cornwall. Seasonal rainfall amounts were about average in northern Scotland and above average in western Scotland. Elsewhere the summer was rather dry or in some places very dry, although locally there were large amounts of rainfall, mainly as the result of thundery activity during August. Rainfall amounts ranged from nearly 150% in the Western Isles of Scotland to less than 40% over the Channel Islands and parts of the south coast from Plymouth, Devon to Bognor Regis, West Sussex. The relative lack of rainfall during the summer was reflected in soil moisture deficits of more than 40 mm above average in many parts of central southern and south-west England at the end of June, spreading to eastern areas by the end of July. By the end of August soil moisture deficits were between 30 and 40 mm above average over much of England and Wales, notable exceptions being the Lake District and Snowdonia which were near field capacity. Sunshine amounts were near or slightly above average over Scotland, whilst most of England and Wales had a

sunny summer; amounts exceeded 150% of normal in the Midlands, but were as low as 88% at Benbecula, Western Isles.

Information about temperature, rainfall and sunshine during the period from June to August 1989 is given in Fig. 1 and Table I.

2. The individual months

June. Mean monthly temperatures were generally just above normal in England, Wales and Northern Ireland, but slightly below normal in Scotland, ranging from about 1 °C above normal in places in southern England to nearly 1 °C below normal in the Western Isles. Halesowen, West Midlands had the highest June maximum since 1976 with 29.7 °C on the 20th which was the second warmest June day there since at least 1956; in contrast the 2nd was the coldest June night since 1962, with a minimum temperature of 0.1 °C.

Monthly rainfall amounts were generally below or near normal; however, parts of southern Scotland and northern and eastern England had higher than average values. The most rain fell at Blackpool, Lancashire with nearly twice the normal rainfall, compared with Exeter, Devon where only a third of the normal rain fell.

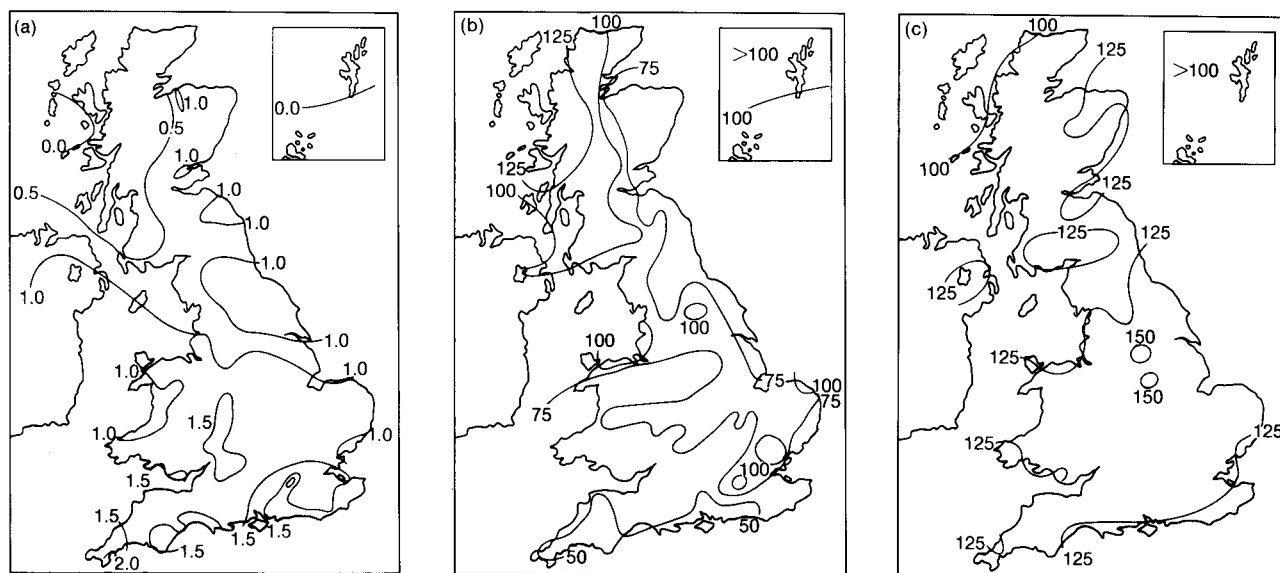


Figure 1. Values of (a) mean temperature difference (°C), (b) rainfall percentage and (c) sunshine percentage for summer, 1989 (June–August) relative to 1951–80 averages.

Table I. District values for the period June–August 1989, relative to 1951–80 averages

District	Mean temperature (°C)	Rain-days	Rainfall	Sunshine
	Difference from average		Percentage of average	
Northern Scotland	+0.4	+1	100	106
Eastern Scotland	+0.9	−3	71	120
Eastern and north-east England	+1.1	−4	75	137
East Anglia	+1.2	−2	84	137
Midland counties	+1.3	−4	73	140
South-east and central southern England	+1.6	−3	59	133
Western Scotland	+0.5	0	103	123
North-west England and North Wales	+0.9	−2	77	131
South-west England and South Wales	+1.4	−4	64	132
Northern Ireland	+1.1	−1	87	125
Scotland	+0.6	−1	95	116
England and Wales	+1.3	−3	71	135

Highest maximum: 34.2 °C in south-east and central southern England in July.
Lowest minimum: −2.4 °C in western Scotland in June.

Monthly sunshine totals were above normal nearly everywhere, although in parts of the Scottish Highlands and the Western Isles it was rather dull, and amounts varied from as much as 139% at Leeming, North Yorkshire to 89% at Stornoway, Western Isles. At Halesowen, June was the sunniest since 1976 with 258 hours of bright sunshine. Wingerworth, Derbyshire reported the sunniest June in 20 years of record at the station, 53 hours higher than the mean for the month.

For the first 8 days of the month the weather was cool and showery in all parts of the United Kingdom, with thundery outbreaks occurring on most days, mainly in southern areas. On the 5th and 6th, thundery showers became widespread and prolonged in some areas, particularly in a belt from Merseyside to south-east England; in the Gillingham area of Kent hailstones lay to a depth of several centimetres, bringing traffic to a halt. The Surrey Fire Brigade were called out to floods, and a mother and her young child were taken to hospital after the roof of their house collapsed when it was struck by lightning. Also on the 6th a tornado was reported near Brightlingsea, Essex. The weather was warmer and predominantly dry from the 9th to the 12th in all areas, while heavy, thundery rain came to much of northern England and north-west Wales on the 13th, with scattered outbreaks of rain in other western areas of England and Wales. All areas again became dry on the 14th. Skies were cloud-free nearly everywhere in Scotland from the 17th to the 20th. Apart from some showers and thunderstorms overnight on the 21st/22nd in parts of East Anglia and Kent, it remained mainly dry until the 24th when rain moved southwards from Scotland replacing dry weather which had in some places lasted 18 days; rain was particularly heavy and prolonged over North Wales and northern England. Elsewhere many places had showers, and some of those in eastern England were accompanied by thunderstorms.

July. Mean monthly temperatures were above normal everywhere, ranging from 0.3 °C above normal in Shetland to more than 3 °C above normal at Plymouth, Devon. Northwood, Greater London reported the 22nd as the hottest day of any month since July 1983. Hampstead, Greater London reported the warmest July since 1983 and its highest minimum of 20.1 °C was second only to that of 1949 (20.4 °C) in a record going back to 1909. The mean maximum of 21.7 °C at Turnhouse (Edinburgh Airport), Lothian Region was the highest since the record began in 1948. The minimum temperature of 3.5 °C at Glasgow Airport, Strathclyde Region was the lowest at the station since 1971.

Monthly rainfall totals were generally below normal apart from some parts of south-east England, Shetland and Northern Ireland, where rainfall amounts were above normal, ranging from 13% at Plymouth, Devon to 162% at Stansted, Essex. The 29th marked the end of a long spell of dry weather in many places. The south coast around Southampton still escaped measurable rainfall, some places having had no measurable rain since the 8th. The monthly total of 9 mm at Edinburgh, Royal Observatory was the lowest ever for July at the station, although there are documented values of 9 mm in July 1868 and 4 mm in July 1825 at other sites in Edinburgh.

Monthly sunshine amounts were above normal everywhere except part of the Western Isles where amounts were just below normal, Benbecula measuring only 94%, whereas the greatest percentage of average sunshine was 192 at Armagh in Northern Ireland. Many places had the sunniest July for many years; Eskdalemuir, Dumfries and Galloway had the sunniest July since records began there in 1910 and Bude, Cornwall the sunniest since records began there in 1913. Wingerworth, Derbyshire had the sunniest July since 1976. Northern Ireland and parts of central and southern Scotland had

the sunniest July since 1955. The 3rd was the sunniest July day this century at Sheffield (Weston Park), South Yorkshire.

After some rain on the 1st it became hot and fine, with northern areas remaining almost completely dry until the onset of rather changeable weather around the 9th and 10th. However, thundery outbreaks in many parts overnight on the 5th/6th, and on the 7th and 8th produced widespread heavy rain. It became mainly dry and hot again between the 12th and the 26th, although thundery outbreaks gave heavy rain in a few places until more widespread rain came to Scotland on the 25th. The rest of the month was rather unsettled in Scotland, and a shorter unsettled spell affected England and Wales (apart from a few south-coastal areas). However, in many places the weather continued mainly dry. There were isolated thunderstorms on the 23rd and 24th. Thunderstorms developed along the Thames Valley and over Northern Ireland and western Scotland on the 25th, spreading later to some parts of eastern Scotland. Further outbreaks occurred over Norfolk on the 29th, and in parts of northern England, the Midlands and East Anglia on the 30th. On the 6th hailstones of 30 mm diameter were reported near Basingstoke, Hampshire and of 15 mm diameter at Sedgely, West Midlands.

August. Mean monthly temperatures were above normal everywhere in the United Kingdom except the far north of Scotland and ranged from just below normal at Lerwick, Shetland to nearly 2 °C above normal at Gatwick, West Sussex.

Monthly rainfall amounts were below normal everywhere except for parts of North Wales, Cumbria and western Scotland and ranged from 264% of normal at Tiree, Strathclyde Region to as little as 16% of normal at Guernsey Airport, Channel Islands. A fall of 21.2 mm of rain was recorded on the 25th at Aldergrove, Co. Antrim between 1430 and 1445; such a fall in 15 minutes has a return period of about 150 years. Some places in the vicinity of Southampton and the Isle of Wight had no measurable rain from 8 July until the end of August.

Monthly sunshine amounts were above normal everywhere except Northern Ireland and western Scotland and ranged from 73% of average at Tiree to 159% of average at Birmingham, West Midlands and Wyton, Cambridgeshire. Sheffield (Weston Park), South Yorkshire had the sunniest August in a record going back to 1898, beating the previous record set in 1947. In the West Midlands, Coventry had the sunniest August since 1947 and Halesowen the sunniest since 1976. Oxford reported another remarkably sunny month, the second sunniest August in 110 years of records. It was generally the third sunniest August in England and Wales this century after 1976 and 1947.

Very little rain fell during the first week except in parts of Scotland. From the 9th to the 17th it was rather unsettled with some rain, heavy in places. On the 14th a tornado struck the Butlins holiday camp at Pwllheli, on

the Lleyn Peninsula in North Wales, removing the roofs of 150 timber chalets and causing considerable damage to other buildings; costs were estimated at more than £2 million. Much of England and Wales remained dry between the 18th and the 23rd inclusive, whilst Scotland and the north of England had further rain. Rain moved southwards across England late on the 24th and the 25th and was persistent in places. Very heavy thundery rain caused flooding at Aldergrove, Co. Antrim on the 25th. Showers were locally heavy in eastern England on the 26th, becoming confined mostly to eastern coasts on the 27th. After a dry day in most places on the 28th, it stayed mainly dry up to the end of the month in the south-east, but became unsettled in the west.

Notes and news

Meteorological Office attains Agency status

As announced in Notes and news in the *Meteorological Magazine*, December 1989, the Meteorological Office has recently become an Executive Agency within the Ministry of Defence. The change in status took place on 1 April 1990 and the occasion was marked by a ceremony at Bracknell on the following day, attended by many representatives of Government, customers, local civic groups and the media. During the ceremony Dr John Houghton, the Chief Executive, was formally handed a copy of the Framework Document, which sets out the rules by which the Agency is to be run, by Mr Michael Neubert MP who is the Government Minister responsible for the Office's affairs.

Dr Houghton spoke of the further opportunities that Agency status would bring to the Office in terms of greater freedom to manage itself in order to bring a better service to its customers.

The structure of the Office has undergone considerable changes for the better use of its resources to meet the challenges of the future. It is to be run by a Management Board lead by the Chief Executive with four further members:

Director of Operations	Dr Peter Ryder
Director of Research	Dr Keith Browning
Director of Commercial Services	Mr Bernard Herdan
Director of Finance and Administration	Mr Michael Bowack

Reporting to the Board are seven Deputy Directors responsible for Central Forecasting, Defence Services, Observations, Communications and Computing, and research into Atmospheric Processes, Short-Range Forecasting, and Extended-Range Forecasting and Climate.

Satellite photograph — 27 May 1990 at 2100 UTC

The infra-red image shown in Fig. 1 was taken by the geostationary satellite, GOES, and was received on facsimile machine at the Meteorological Office at Bracknell via landline from the USA.

In the USA, infra-red images are routinely displayed with enhancement curves. Essentially, grey scales are repeated so as to draw attention to particular ranges of cloud-top temperature. This picture was received with the 'MB' curve, where all cloud colder than -32°C is highlighted. The major cold-cloud regions are labelled M and C, and show a mesoscale convective system just north of the Gulf of Mexico (coldest cloud tops below -70°C) and cloud associated with a mid-latitude depression (Fig. 2) over the Atlantic Ocean.

Elsewhere, a band of convection with less-cold tops (S) extends from western Florida around the Gulf coast probably marking a sea-breeze front, and a large cloud-free zone covers the Great Lakes.

G.A.Monk

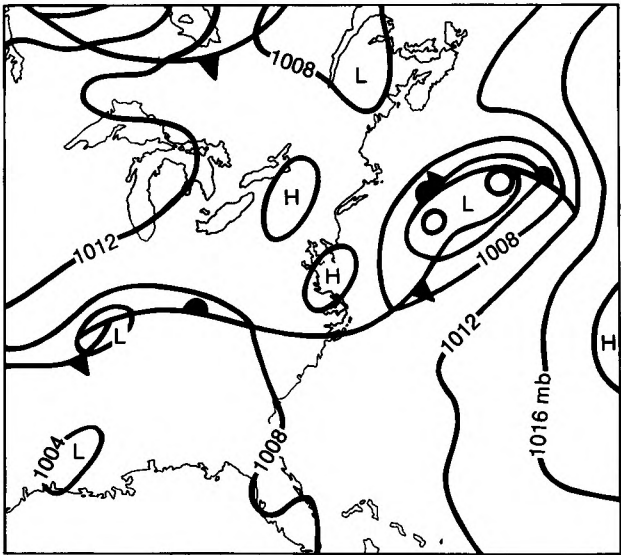


Figure 2. Synoptic analysis at 0000 UTC on 28 May 1990 (polar stereographic projection).

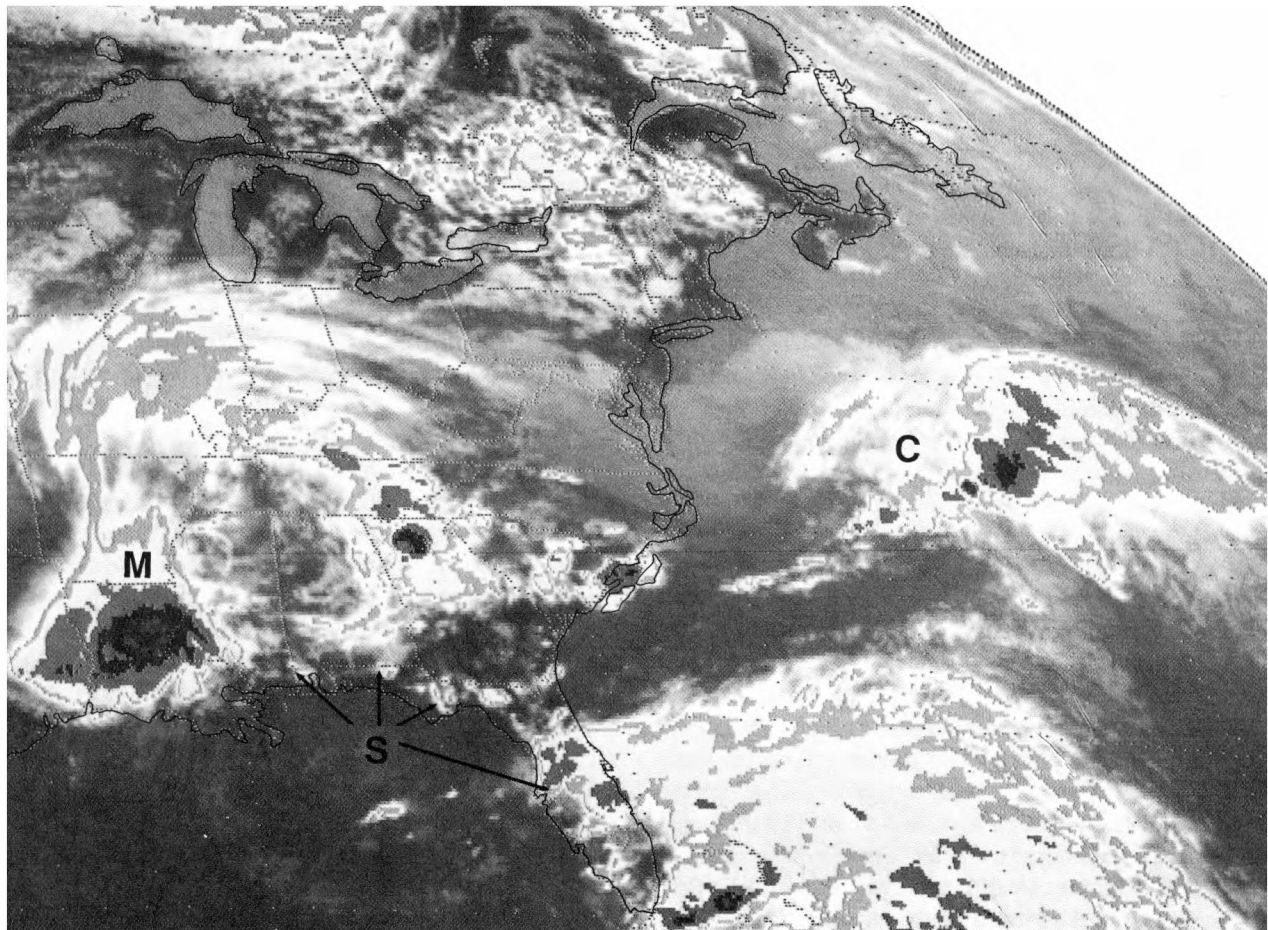


Figure 1. GOES infra-red 'space view' image at 2100 UTC on 27 May 1990 with 'MB' enhancement curve. Repeat grey scales represent the following temperature ranges: medium grey -32 to -41°C , white -41 to -52°C , dark grey -52 to -58°C , black -58 to -62°C , then repeating black to white -62 to -80°C .

GUIDE TO AUTHORS

Content

Articles on all aspects of meteorology are welcomed, particularly those which describe results of research in applied meteorology or the development of practical forecasting techniques.

Preparation and submission of articles

Articles, which must be in English, should be typed, double-spaced with wide margins, on one side only of A4-size paper. Tables, references and figure captions should be typed separately. Spelling should conform to the preferred spelling in the *Concise Oxford Dictionary* (latest edition). Articles prepared on floppy disk (Compucorp or IBM-compatible) can be labour-saving, but only a print-out should be submitted in the first instance.

References should be made using the Harvard system (author/ date) and full details should be given at the end of the text. If a document is unpublished, details must be given of the library where it may be seen. Documents which are not available to enquirers must not be referred to, except by 'personal communication'.

Tables should be numbered consecutively using roman numerals and provided with headings.

Mathematical notation should be written with extreme care. Particular care should be taken to differentiate between Greek letters and Roman letters for which they could be mistaken. Double subscripts and superscripts should be avoided, as they are difficult to typeset and read. Notation should be kept as simple as possible. Guidance is given in BS 1991: Part 1: 1976, and *Quantities, Units and Symbols* published by the Royal Society. SI units, or units approved by the World Meteorological Organization, should be used.

Articles for publication and all other communications for the Editor should be addressed to: The Chief Executive, Meteorological Office, London Road, Bracknell, Berkshire RG12 2SZ and marked 'For Meteorological Magazine'.

Illustrations

Diagrams must be drawn clearly, preferably in ink, and should not contain any unnecessary or irrelevant details. Explanatory text should not appear on the diagram itself but in the caption. Captions should be typed on a separate sheet of paper and should, as far as possible, explain the meanings of the diagrams without the reader having to refer to the text. The sequential numbering should correspond with the sequential referrals in the text.

Sharp monochrome photographs on glossy paper are preferred; colour prints are acceptable but the use of colour is at the Editor's discretion.

Copyright

Authors should identify the holder of the copyright for their work when they first submit contributions.

Free copies

Three free copies of the magazine (one for a book review) are provided for authors of articles published in it. Separate offprints for each article are not provided.

July 1990

Editor: F.E. Underdown
Editorial Board: R.J. Allam, R. Kershaw, W.H. Moores, P.R.S. Salter

Vol. 119
No. 1416

Contents

	Page
Forecasting the storm of 8 November 1989 — a success for the man-machine mix. A. Woodroffe	129
The United Kingdom's contribution to the WMO Voluntary Co-operation Fellowship Programme. F.D. Reece	140
The summer of 1989 in the United Kingdom. G.P. Northcott	145
Notes and news	
Meteorological Office attains Agency status	147
Satellite photograph — 27 May 1990 at 2100 UTC G.A. Monk	148

Contributions: It is requested that all communications to the Editor and books for review be addressed to the Chief Executive, Meteorological Office, London Road, Bracknell, Berkshire RG12 2SZ, and marked 'For *Meteorological Magazine*'. Contributors are asked to comply with the guidelines given in the *Guide to authors* which appears on the inside back cover. The responsibility for facts and opinions expressed in the signed articles and letters published in *Meteorological Magazine* rests with their respective authors.

Subscriptions: Annual subscription £30.00 including postage; individual copies £2.70 including postage. Applications for postal subscriptions should be made to HMSO, PO Box 276, London SW8 5DT; subscription enquiries 071-873 8499.

Back numbers: Full-size reprints of Vols 1-75 (1866-1940) are available from Johnson Reprint Co. Ltd, 24-28 Oval Road, London NW1 7DX. Complete volumes of *Meteorological Magazine* commencing with volume 54 are available on microfilm from University Microfilms International, 18 Bedford Row, London WC1R 4EJ. Information on microfiche issues is available from Kraus Microfiche, Rte 100, Milwood, NY 10546, USA.

ISBN 0 11 728667 2

ISSN 0026-1149

© Crown copyright 1990. First published 1990



The

Meteorological Magazine

August 1990

NWP performance on instant occlusions
Meteorological telecommunication developments
L.G. Groves Awards



DUPLICATE JOURNALS

National Meteorological Library
FitzRoy Road, Exeter, Devon. EX1 3PB

HMSO

Met.O.992 Vol. 119 No. 1417



3 8078 0010 2468 8

Numerical weather prediction model performance on instant occlusion developments

J.B. McGinnigle

Meteorological Office, Bracknell

Summary

The output of numerical weather prediction (NWP) models is recognized as an important component in the forecaster's decision-making process when the possibility of instant occlusion development is being considered. This paper presents three cases of actual or potential instant occlusion development over the North Atlantic and examines the performance of the Meteorological Office fine-mesh NWP model at these times. The cases include two different types of instant occlusion development as identified in previous studies. Manual forecasting guidelines suggested in a earlier paper are also evaluated in each case.

1. Introduction

When a polar vortex or trough approaches a front, the forecaster must consider whether there will be an interaction between these two features such that they will link up to form an instant occlusion, a synoptic feature which resembles a classical occlusion and, in many ways, behaves like one. The decision will of course have important implications for the forecasts of synoptic evolution and associated weather events which will follow. Previous studies (McGinnigle *et al.* 1988) have shown that there are two fundamental types of instant occlusion formation which have significant differences in synoptic development at the time of merging and this will also require consideration. One important source of information in the decision-making process is the advice from numerical weather prediction (NWP) model output. The Meteorological Office currently uses the 15-level fine-mesh NWP model (Gadd 1985) for detailed advice over central and eastern parts of the North Atlantic, an area in which instant occlusion developments often take place. This paper examines the performance of the fine-mesh model in three cases of actual or potential instant occlusion development to assess whether realistic and helpful predictions were

made. In addition, manual forecasting guidelines suggested in a previous paper are examined to see how useful they would have been in each case.

2. A review of instant occlusion processes

Anderson *et al.* (1969) described a merging process between a polar vortex and a front which produced a cloud pattern similar to that of a conventional occlusion. Where observation density was sufficient, it was noted that the rain band of the cold-air trough and the rain area associated with the frontal wave had also merged. The synoptic analysis placed a line of surface discontinuity near the rear edge of the polar vortex/trough cloud area and it is this feature which was referred to as the 'instant occlusion'. This model is similar to that used by Browning and Hill (1985) who proposed the principal airflows of such a system shown in Fig. 1. In both cases, the polar front remained the major baroclinic discontinuity. Fig. 1 also shows the frontal analysis which is normally applied in such situations along with the idealized 850 mb wet-bulb potential temperature (θ_w) field; the strong 850 mb θ_w frontal-zone gradient gives way to a much weaker gradient in the cold air.

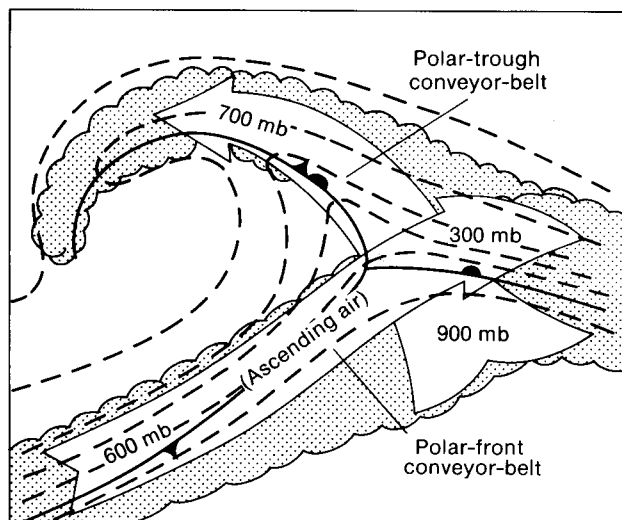


Figure 1. Airflows relative to the motion of the cloud band of the cold-air vortex in the systems described by Browning and Hill (1985). Fronts are shown conventionally. Pecked lines are idealized 850 mb wet-bulb potential temperature (θ_w) isopleths at one degree Celsius intervals. Stippling represents the main cloud areas.

By contrast, the studies of Locatelli *et al.* (1982) suggested a different analysis, where the cold-air trough was identified as a separate baroclinic disturbance. When merging occurred, the transition to cold air became associated with the trough line rather than the polar front. McGinnigle *et al.* (1988) investigated several instant occlusions of this second type and suggested the principal airflows and low-level thermal structure shown in Fig. 2. Fig. 2(a) is the 'conventional' instant occlusion analysis while Fig. 2(b) shows the alternative scheme which was proposed as a more realistic synoptic description.

It will be seen that Fig. 2 indicates a fundamentally different type of development from that described by Browning and Hill in Fig. 1. In the Browning and Hill model (which will be called the 'Type 1' instant occlusion in this paper) a polar-trough (cold) conveyor-belt flows from low levels beneath the polar front conveyor belt and produces the instant occlusion cloud band as it rises towards the forward side of the polar vortex; in Fig. 2 (Type 2 instant occlusion), a warm conveyor belt derived from a low-level shallow moist layer ahead of the polar trough feeds the instant occlusion cloud area. The existence of this shallow, moist layer is a consequence of the northward transportation of modified polar air ahead of the polar trough.

It is also important to observe that the cloud areas associated with the two models shown in Figs 1 and 2 are very different. The Type 1 development has a narrow belt of mainly convective cloud extending at approximately a right angle from the frontal zone and curving towards the cold vortex; infra-red imagery will normally show that this cloud is warmer (lower) towards the front and the edge of the polar-front conveyor-belt (jet stream) will often be clearly visible.

The Type 2 instant occlusion develops a distinctive hook of cloud as it merges; this hook forms by the

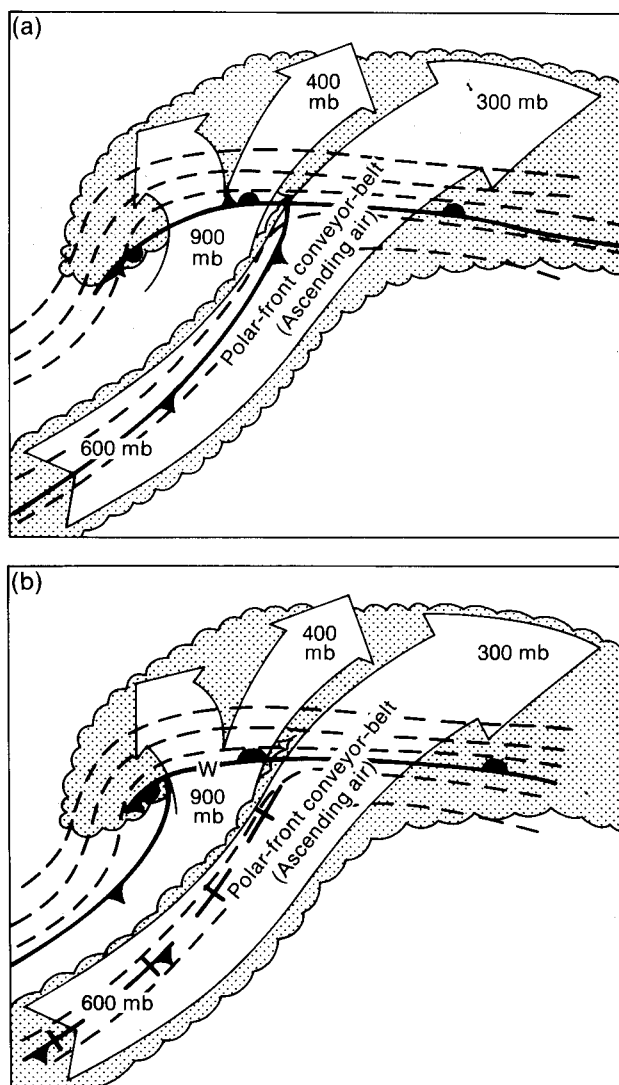


Figure 2. Airflows relative to the motion of the cloud band of the cold-air vortex, (a) 'conventional' and (b) 'alternative' analysis, in the systems described by McGinnigle *et al.* (1988). Fronts shown conventionally (bars indicate weakening). Pecked lines are idealized 850 mb wet-bulb potential temperature (θ_w) isopleths at one degree Celsius intervals. Stippling represents main cloud areas.

apparently rapid rotation of the comma-shaped part of the polar-trough cloud. In fact, this development is due to increasing positive vorticity advection, which results in marked ascent in the merging region, and imposes downward motion at the rear part of the hook, thus creating the illusion of sudden rotation. At the surface, increasing advection of moist, warm, low-level air on the forward side of the polar trough progressively diminishes the thermal contrast across the cold front and so weakens it.

In the Type 2 model, considerable potential instability is generated by the existence of cold dry air at middle and upper levels overlaying warm, moist air at low levels and this is released when merging occurs. By contrast, the Type 1 model generates little potential instability and this marked difference in the models is a significant factor which will assist the forecaster to make the correct type identification.

In comparing both types of instant occlusion events, McGinnigle *et al.* (1988) suggested that, where interaction takes place, polar troughs which have little baroclinicity associated with them are likely to develop into Type 1 instant occlusions, whereas troughs which possess baroclinicity before interaction tend to form Type 2 instant occlusions; it was also observed that, of the two types, the latter appeared to be the more common feature in the North Atlantic.

In data-sparse areas, it will often be difficult to positively establish the degree of baroclinicity possessed by a polar trough. However, Weldon (1979) has suggested that an indication of frontogenesis (and therefore increasing baroclinicity) may be inferred from infra-red satellite imagery. If the cold air feature contained dense, layered cloud (sometimes leaf-shaped), this can be an indicator of associated baroclinicity; by contrast, the comma-shaped cloud consisting mainly of convective cells, characteristic of a positive vorticity advection (PVA) maximum, would suggest that little baroclinicity was present.

This leaf-shaped cloud mass (the 'baroclinic leaf' or 'cloud-head') is a well-accepted precursor of cyclogenesis. It has been observed that some explosive cyclogenesis situations have been preceded by a large 'cloud-head' formation (Böttger *et al.* 1975, Monk and Bader 1988). Reed and Blier (1986) showed that some comma clouds contain large mesoscale convective elements and Young (1988) has observed that the leaf-shaped cloud area associated with Type 2 instant occlusion developments can initially consist of several distinct mesoscale convective elements, before becoming the extensive layered structure seen to precede explosive cyclogenesis.

3. The case-studies

In the case-studies which follow, all the satellite imagery presented is from NOAA polar-orbiting satellites; these images have the best resolution to show the details of the developments. However, much use was also made of Meteosat geostationary imagery and especially of fast movie-loop sequences showing infra-red images (D2 frame) spaced one hour apart. These were used to determine the time at which merging took place and to observe the details of the instant occlusion process at that time.

NWP analysis and forecast fields from the fine-mesh model were available as hard copy from T+0 hours to T+36 hours in 6-hour time-steps but use was also made of output in 3-hour time-steps, available only as soft copy. This was viewed on a high-resolution colour graphics VDU and could be displayed as a movie loop through the time series of the model run; this was useful in establishing the time and details of instant occlusion merging, as predicted by the model.

The following analysis and forecast fields were used to examine and assess the performance of the model runs in each case:

Surface isobars and precipitation (dynamic and convective)

850 mb wet-bulb potential temperature (θ_w)

1000–500 mb thickness and 500 mb contours

250 mb wind speed and direction

Maximum wind isotachs

Vertical motion and thermal advection (850–500 mb layer)

Medium- and high-level convective depth

Medium and low cloud

500–850 mb θ_w difference ($\Delta\theta_w$)

In this paper, the model output charts presented concentrate on the first two items from the list above since this part of the output will normally be routinely available to the forecaster. Surface isobars/precipitation is used as the base chart and the 850 mb θ_w contours are added as appropriate. The vertical motion/thermal advection fields are also shown to explain the model developments. Significant features of the other relevant fields are described in the text. The model runs chosen for detailed examination are those whose Data Time (DT) precedes the instant occlusion event by 12–18 hours; subsequently, two earlier model runs are also briefly appraised.

The paper also intends to test the manual forecasting guidelines proposed by McGinnigle *et al.* (1988) in respect of their usefulness in the pre-merging stage. These guidelines were formulated on the basis of the study of Type 2 instant occlusions only but it is intended to test them against all the cases presented in this paper, which includes a Type 1 development. For this purpose, they will be slightly adapted.

The relevant guidelines were:

'An instant occlusion ...(of Type 2)... may form if all the criteria (i)–(iii) below are satisfied:

- (i) A cold-air cloud cluster, which may be leaf-shaped, contains dense layered cloud.
- (ii) Surface reports or numerical model diagnostics (e.g. 850 mb θ_w) show that a thermal gradient is associated with this cloud.
- (iii) The cloud is embedded in a strong upper flow that will carry it to within 350 n mile of the polar front (Marshall 1982).'

The guidelines will be adapted to apply to potential Type 1 instant occlusion cases as follows:

If examination of a polar trough produces negative answers to (i) and (ii) above, it will be concluded that the trough has formed largely as a response to PVA, and that there is no significant baroclinicity involved. Then, if the answer to question (iii) is affirmative, the formation or otherwise of a Type 1 instant occlusion will test whether this adaptation of the manual forecasting guidelines has any validity. Since Marshall's criterion refers to the critical distance between a 'PVA' and a 'cold front', it is assumed here that the measurement should be from a central point within the 'head' of the comma cloud to the edge of the frontal band where the wave inflection is observed.

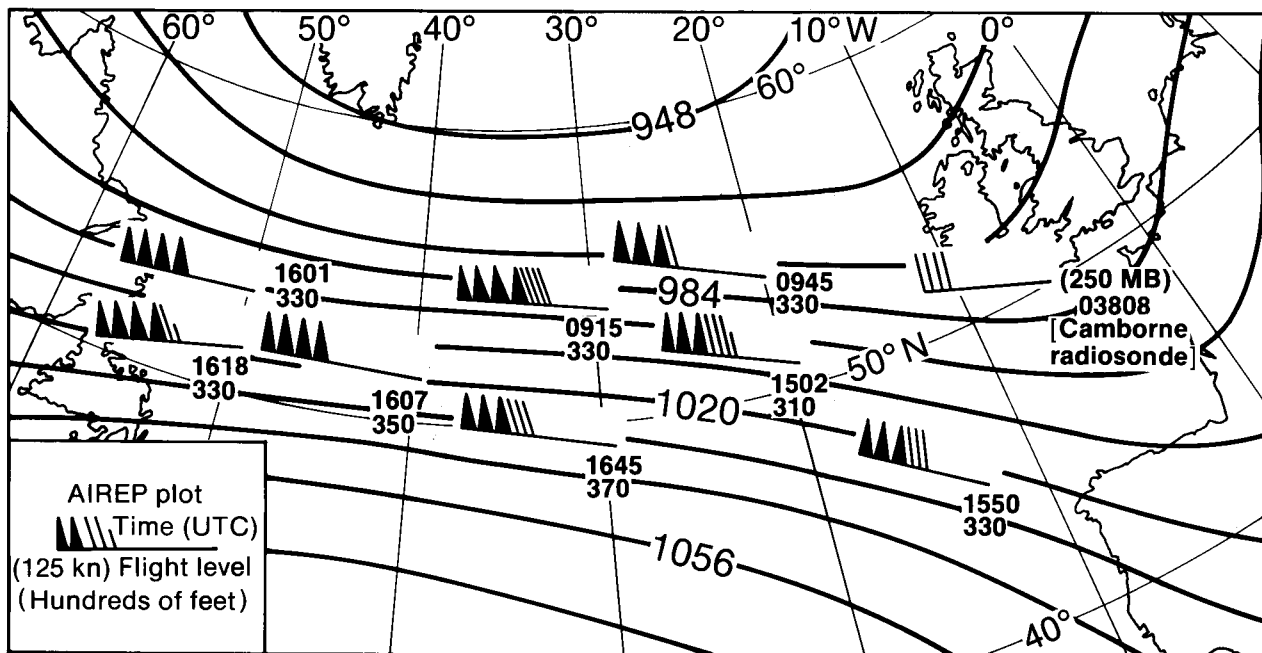


Figure 3. Upper-air pattern (dam) at 250 mb at 1200 UTC on 24 February 1989 with plotted aircraft reports 0915–1645 UTC. Wind arrows are shown traditionally.

3.1 24 February 1989

3.1.1 Synoptic events

The broad-scale situation over the North Atlantic around this date was characterized by an upper jet-stream of exceptional strength. Fig. 3 shows the wind regime which existed at 250 mb at 1200 UTC on 24 February 1989; the strongest reported wind was 240 kn and there were a number of aircraft reports with winds in excess of 200 kn. Infra-red imagery across the North Atlantic showed a very wide band of cloud (at least 5 degrees of latitude) associated with this broad baroclinic zone and surface observations suggested that the main surface frontal discontinuity was located towards the southern boundary of this cloud band (Figs 4(a) and 5(a)).

By 0000 UTC on 24 February, a polar low and trough south of Greenland was observed to be moving quickly east-south-east; in addition, a second weaker low was analysed in the cold air around 55°N, 35°W, on the evidence of ship observations in that area. The satellite imagery around this time clearly marked the main low and trough but, at this stage, there was little cloud evidence for the second low. The NOAA satellite imagery at 0450 UTC on 24 February (Fig. 5(a)) shows the complexity of these features. Near the southern end of the trough cloud, around 37°W, the configuration of the jet-stream cirrus suggested that there were two minor baroclinic waves on the front and these were included in the surface analyses for both 0000 and 0600 UTC on 24 February 1989. The model initialization fields at 0000 UTC agreed with the various elements of the analysis described above. Fig. 6(a) shows the T+0

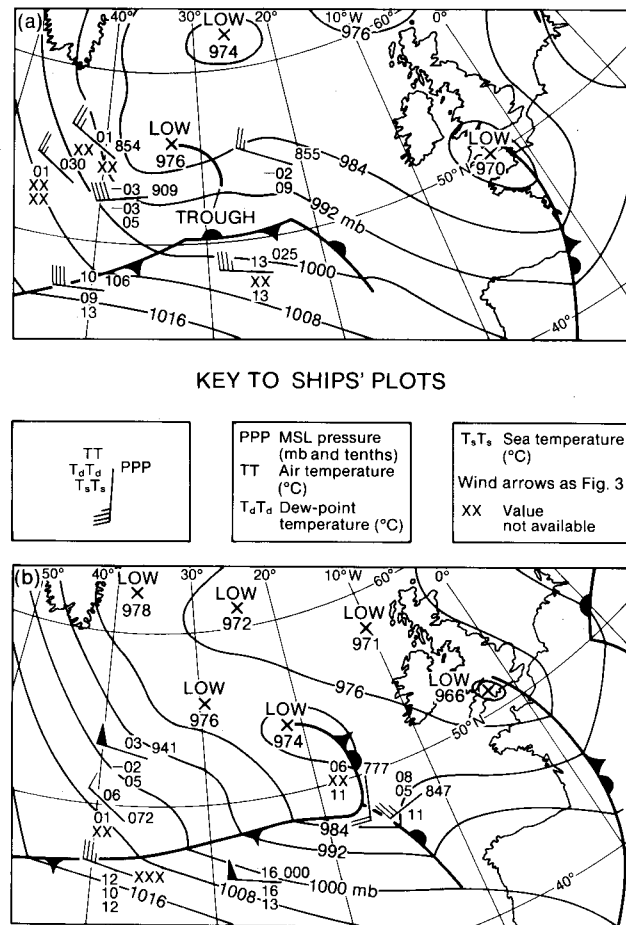


Figure 4. Surface synoptic analyses on 24 February 1989 for (a) 1200 and (b) 1800 UTC. Surface fronts are shown conventionally. Plotted observations are ship reports, with traditional wind arrows.

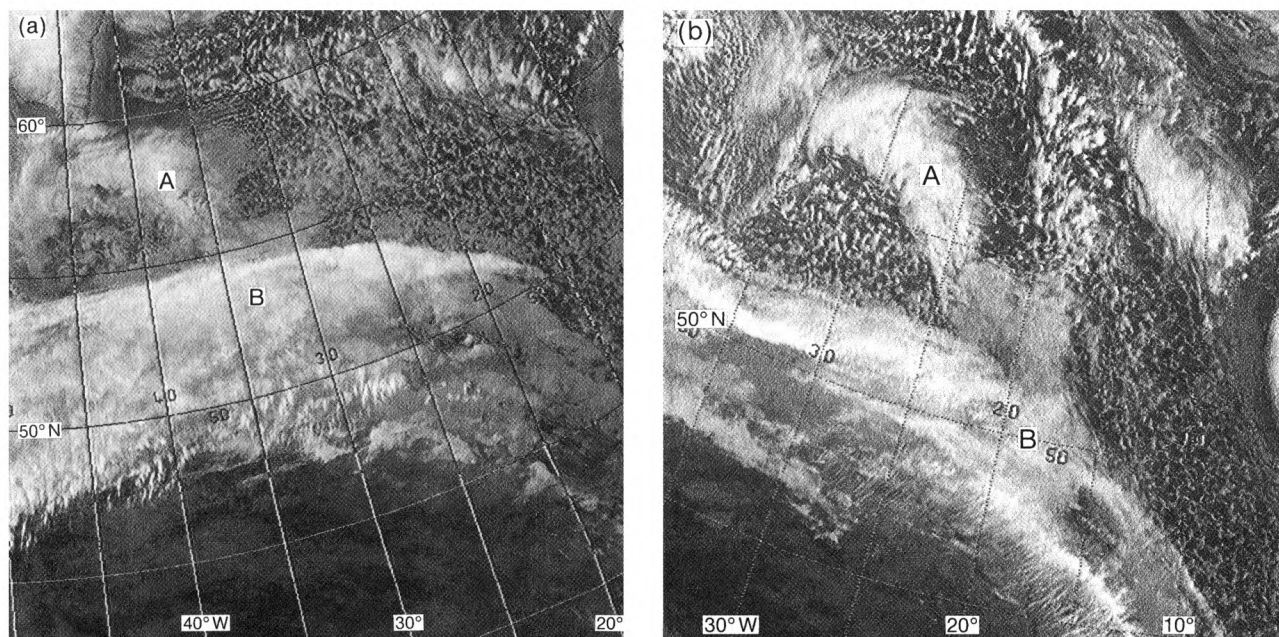


Figure 5. NOAA infra-red satellite imagery for 24 February 1989, (a) 0450 and (b) 1411 UTC. All times are equator crossing times. Cloud area labelled A is the polar trough cloud and B is the frontal band.

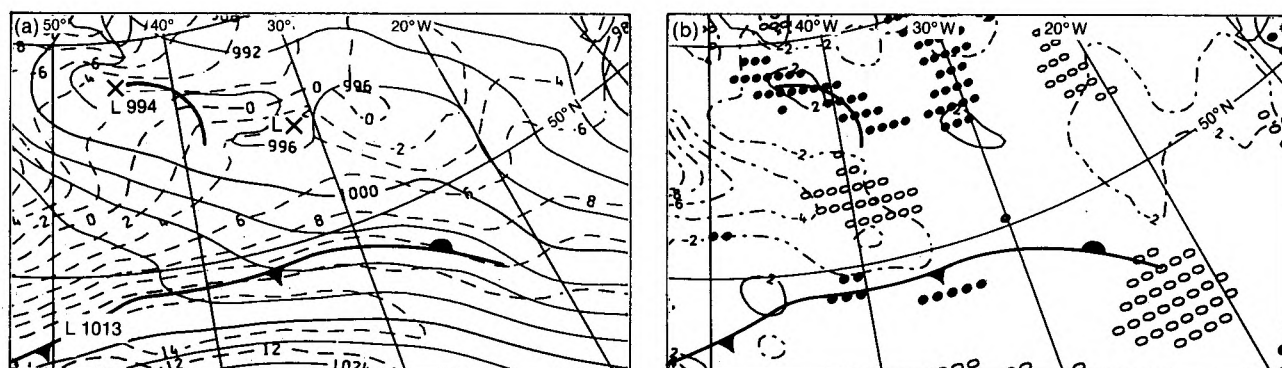


Figure 6. Fine-mesh model analyses for Data Time 0000 UTC on 24 February 1989. (a) Surface pressure pattern (solid contours) and 850 mb θ_w field ($^{\circ}\text{C}$), and (b) diagnostic fields — thermal advection (dashed contours — cooling, full contours — warming, and vertical velocity (open symbols — descending, closed symbols — ascending). Thermal advection/vertical velocity is average of 850, 700 and 500 mb fields, as Fig. 7(b).

surface pressure and 850 mb θ_w fields, with the cold lows and the frontal zone realistically positioned, and the coincident diagnostic chart (Fig. 6(b)) indicated significant uplift associated with the forward side of the surface lows and somewhat lesser values near the front. Both the 850 mb θ_w field and the diagnostic chart suggest a Type 1 model and this was confirmed by the $\Delta\theta_w$ distribution, which showed no potential instability near the waves.

Following very rapid east-south-east movement, cloud developed ahead of the forward cold low, and the associated surface trough and the wave merged into an instant occlusion. The original PVA trough cloud further west became progressively more detached from the forward feature. Fig. 5(b) shows the time at which the forward trough cloud was developing quickly near the frontal cloud band and a study of the Meteosat

imagery movie sequences suggested that merging took place around 1600 UTC. During the following hours, the two areas of trough/instant occlusion cloud continued to become more separate, indicating that two enhanced areas of PVA had developed on the cold side of the very strong jet. After the instant occlusion merging had taken place, the more easterly of the lows moved quickly east-south-east and deepened further near southern England, where the central pressure fell to 950 mb for a time.

Figs 4(a) and 4(b) show the surface analyses for 1200 and 1800 UTC on 24 February. At both times, the polar trough/instant occlusion is placed near the rear boundary of the polar trough cloud. At 1800 UTC, the ship report at 50.3°N, 16.2°W helped to place the recently formed instant occlusion precisely; this ship reported a rapid pressure fall (7.6 mb) over the period

1500–1800 UTC and reflected the movement of the forward cold low as well as the approach of the instant occlusion troughing. The existence of convective cells immediately behind the instant occlusion (partially shielded by upper cloud) coupled with warmer (lower) instant occlusion cloud tops to the north of the wave tip suggested that this case was a Type 1 instant occlusion, as defined earlier in this paper.

3.1.2 Fine-mesh model run DT 0000 on 24 February 1989

Fig. 7 shows output from the above model run, whose initialization fields have already been discussed in the previous section, covering the period around which the instant occlusion formed. Figs 7(a), 7(c) and 7(e) show the surface isobars and precipitation distributions which were predicted by this model run; the 850 mb θ_w fields have been added in the area around the trough. The concurrent thermal advection/vertical velocity diagnostic forecast fields are shown alongside.

In the forecast for 1200 UTC on 24 February (T+12 hours, Fig. 7(a)), the 850 mb θ_w gradients (also the 1000–500 mb thickness gradients, not shown) in the vicinity of the forward trough were relatively slack in comparison with those in the cold-front region towards the western wave. Higher 850 mb θ_w values marked the line of the trough and there was a largely uniform decrease in these values in the following cold air. The precipitation distributions showed an area of dynamic rain associated with the cold low/trough but only a few rain symbols near the wave; at this stage, there was no evidence to suggest instant occlusion formation and this is in accordance with the actual surface analysis at 1200 UTC on 24 February.

The thermal advection/vertical velocity fields (Fig. 7(b)) showed an extensive area of ascent ahead of the polar trough, much of which was not collocated with an area of warm advection between 48 and 55° N. Cold advection was shown behind the trough but there was further significant ascent in the cold air ahead of the polar low and trough further west. Convective-cloud-depth forecasts indicated extensive deep convection in the cold air and around the cold low; however the $\Delta\theta_w$ fields suggested that potential instability would be present only in the immediate vicinity of the cold low ($\Delta\theta_w \approx 0^\circ\text{C}$).

Figs 7(c) and 7(d) show the model predictions 6 hours later at 1800 UTC. Some buckling in the thermal fields (850 mb θ_w and 1000–500 mb thickness) was evident and the area of dynamic rain had extended towards the wave tip; however, no dynamic rain was predicted in the area of the wave; the area of uplift was strengthened and extended south-east with the thermal advection values largely unchanged. At this stage, the model did not suggest that the instant occlusion process had taken place (this actually occurred at 1600 UTC).

The T+24 hour forecast frames (Verification Time (VT) 0000 on 25 February, Figs 7(e) and 7(f)) predicted

that considerable development would take place during the preceding 6-hour period and produced what proved to be a generally realistic low-pressure complex to the west of Ireland. The rain area now extended along the trough to the frontal wave suggesting that an instant occlusion had been formed (this had occurred before 2100 UTC). There was a large area of ascent near the instant occlusion, and the warm advection showed some increase, though still remained below 4°C/6 hours. Convection was forecast to become deeper and more extensive in the cold air; as before, potential instability was forecast only in the area of the cold low. This evidence suggested that the instant occlusion would be a Type 1.

A brief examination of the two immediately previous model runs (DT 0000 and 1200 UTC on 23 February) showed that both had also predicted the formation of a Type 1 instant occlusion. However, there were significant differences in timing and development. The earlier run was far too progressive and the following run developed too much upper trough extension in the cold air, leading to a considerable overdevelopment of the wave, trough and cold low.

3.1.3 Discussion

This chosen model run (DT 0000 UTC on 24 February) presented a realistic sequence of events in many respects. System positioning was good and the development of the low west of Ireland was well handled. The forecast frames gave an indication that the trough and wave would merge and, on the evidence presented by the diagnostic fields and the instability predictions, that this would be a Type 1 instant occlusion. However the timing of the development was in error by several hours; merging did not occur until between 1800 and 2100 UTC (actual event 1600 UTC). Positioning of the instant occlusion was accurate. Dynamic rain was perhaps under-forecast but this cannot be positively established due to the paucity of actual reports in the area. The two previous runs were less successful but still predicted instant occlusion merging.

With regard to the test of the manual forecasting guidelines, at 0000 UTC on 24 February, attention would have been directed towards the major polar low and trough south of Greenland since there was little evidence of any forward development at this time. Applying the guidelines to this area, the appearance and configuration of the trough cloud would not have suggested pre-existing baroclinicity (negative replies to questions (i) and (ii)) and therefore indicated that any instant occlusion formation would be a Type 1. The distance from the centre of the comma head (north of the surface vortex) south-eastwards to the frontal cloud was around 350 n mile and the imagery sequence and upper-wind flow inferred that this spacing would not change much. Thus, strict application of the guidelines would have suggested that Type 1 instant occlusion formation was marginally possible; in fact, this part of

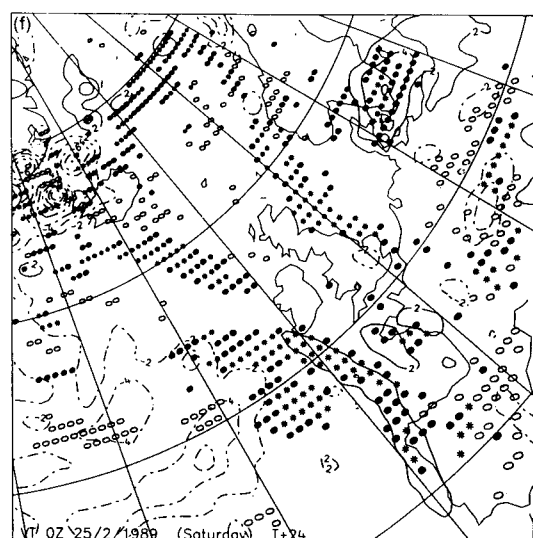
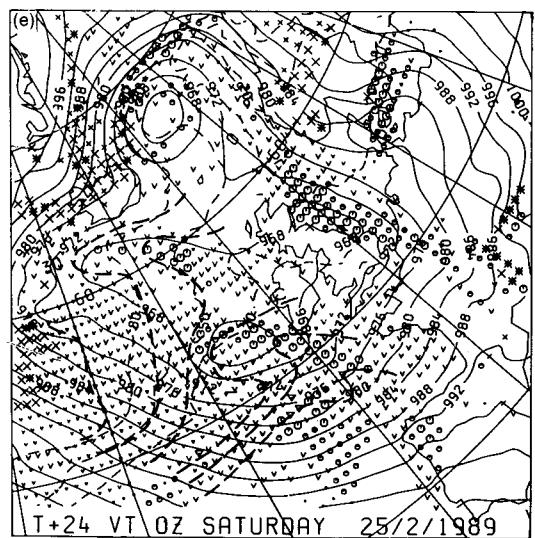
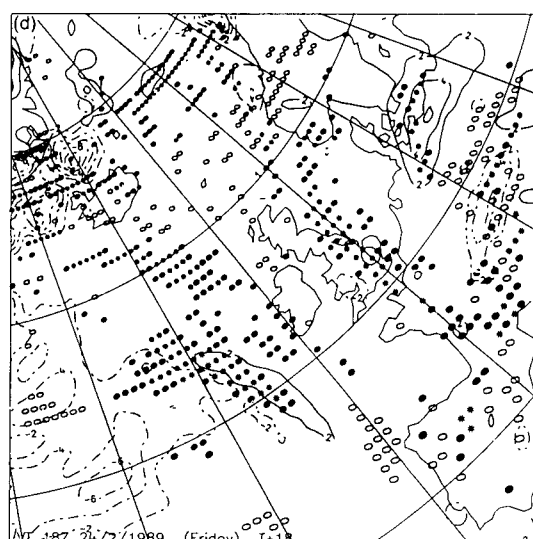
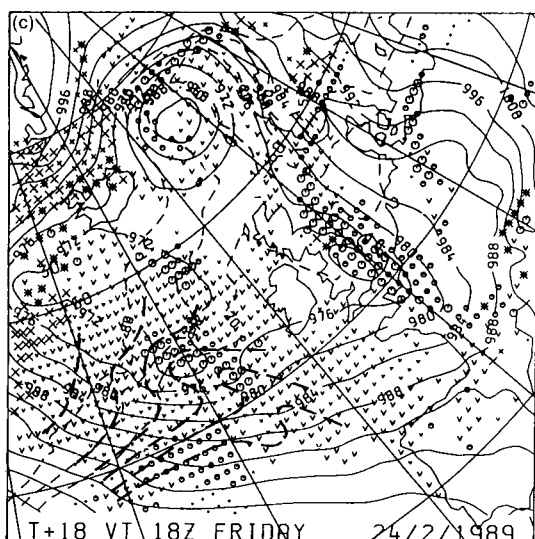
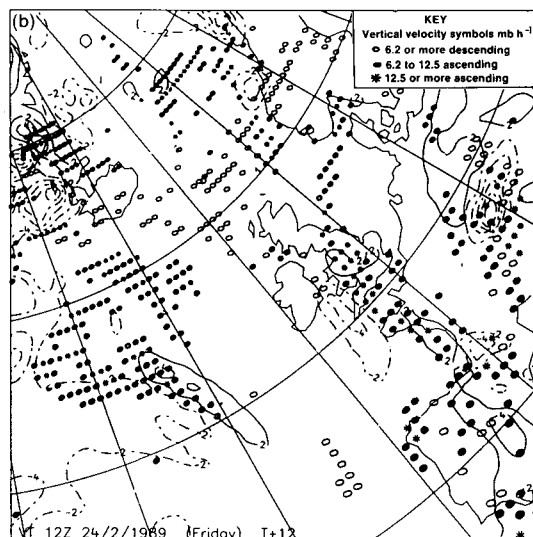
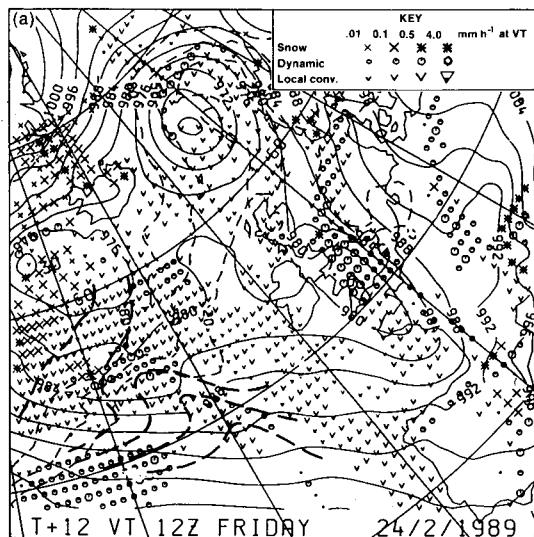


Figure 7. Fine-mesh model predictions Data Time 0000 UTC on 24/25 February 1989. Rainfall rate and m.s.l. pressure: (a) Verification Time (VT) 1200 UTC on 24 February, (c) VT 1800 UTC on 24 February, and (e) VT 0000 UTC on 25 February. Model diagnostics: (b) VT 1200 UTC on 24 February, (d) VT 1800 UTC on 24 February, and (f) VT 0000 UTC on 25 February.

the development did not subsequently form an instant occlusion because of the formation of a new downstream PVA maximum. A later application of the guidelines (e.g. 0600 UTC) to the forward development would have produced a spacing of around 200 n mile, suggesting that the instant occlusion process should already have taken place; however it is reasoned in this case that this instant occlusion formation was a response to *in situ* developmental factors for which the guidelines are not designed.

3.2 15 March 1989

3.2.1 Synoptic events

Fig. 8(a) shows the actual surface analysis at 1200 UTC on 14 March 1989, at which time a well-established polar trough had approached the polar front. A baroclinic wave had been identified on the front as shown and the area containing the polar low/trough and the wave was situated on the forward side of a confluent upper trough. Infra-red imagery at 1445 UTC (Fig. 9(a)) showed that these features were separate at this time; the polar trough was comma-shaped but, in its northern part, there was a large area of layer cloud, with some embedded convection, and this streamed forward in the suggestion of a classic ‘leaf’ shape.

As the upper trough relaxed forward, the frontal wave and the polar trough moved east-north-east and merged to form an instant occlusion around 1200 UTC on 15 March (Fig. 8(b)). This was identified from examination of the movie-loop sequence showing hourly Meteosat images as described previously. Between 1100 and 1200 UTC there was a sudden thickening and increase of cloud in the area north-west of the wave tip and, simultaneously, the ‘tail’ of the comma cloud weakened, giving the illusion that there had been a sudden rotation of the cloud mass. The satellite imagery at 1435 UTC (Fig. 9(b)) shows the post-merged situation; it will be seen that merging took place well ahead of the line of the surface polar trough, which can be seen as a somewhat degenerated comma-shape in the cold air.

It is also noted that there was no convective cloud on the cold side of the front and that there was little change in surface temperature or dew-point reported across the front at this time; this had been a feature of the surface analyses of the previous 24 hours, all of which showed that the really cold air was located behind the polar trough line. Convective cloud in this cold air mass was limited by marked downward vertical motion to the rear of the confluent upper trough.

The T+0 hour model initialization fields, DT 0000 UTC on 15 March, confirm the details of the analysis. The surface analysis (Fig. 10(a)) shows the front and the wave correctly positioned and the 850 mb θ_w field indicates a double thermal structure at the waving front and to the north-west of the cold low while the diagnostic chart (Fig. 10(b)) shows a large area of

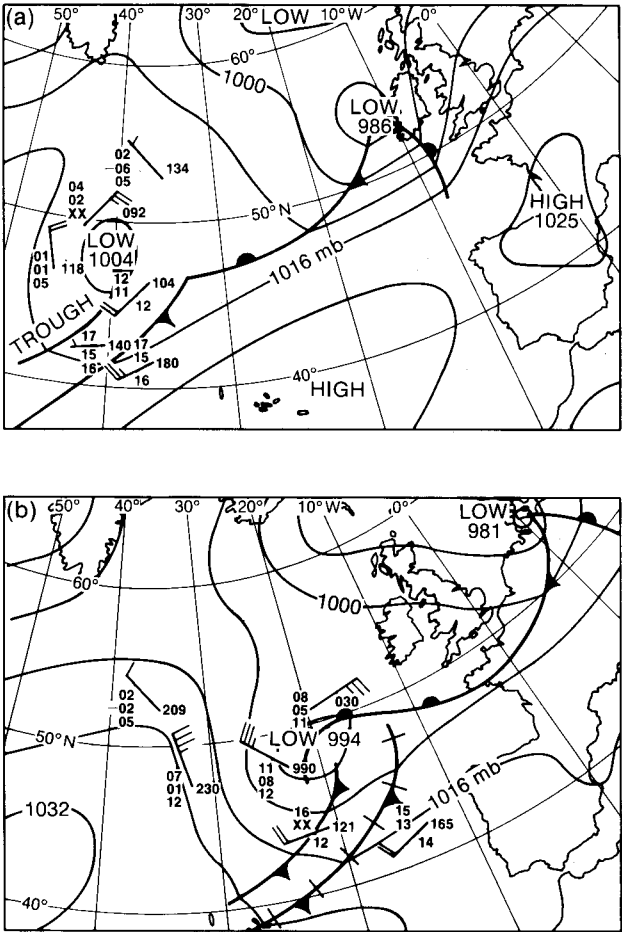


Figure 8. As Fig. 4 but for (a) 1200 UTC on 14 March 1989 and (b) 1200 UTC on 15 March 1989. Bars across forward cold front indicate weakening.

downward motion coupled with some cold advection between front and trough; this is associated with an indication of potential instability in this area from the $\Delta\theta_w$ field ($\Delta\theta_w$ values $<1^\circ\text{C}$).

The evidence above establishes that this was a Type 2 instant occlusion development as defined earlier. During the following 12 hours the surface low elongated eastwards and a new surface low formed on the triple point (wave tip). This new low moved eastwards across southern England and became established as the main low by 1200 UTC on 16 March, at which time it had deepened to 990 mb and was beginning to occlude conventionally; the original polar low became absorbed in its circulation and eventually lost its identity. This sequence of events has been noted to be characteristic of the behaviour of the Type 2 instant occlusion development.

3.2.2 Fine-mesh model run DT 0000 UTC on 15 March 1989

Fig. 11 shows the predictions from the above model run during the period 0600–1800 UTC (T+6 to T+18 hours). The distribution of dynamic rain (and forecast

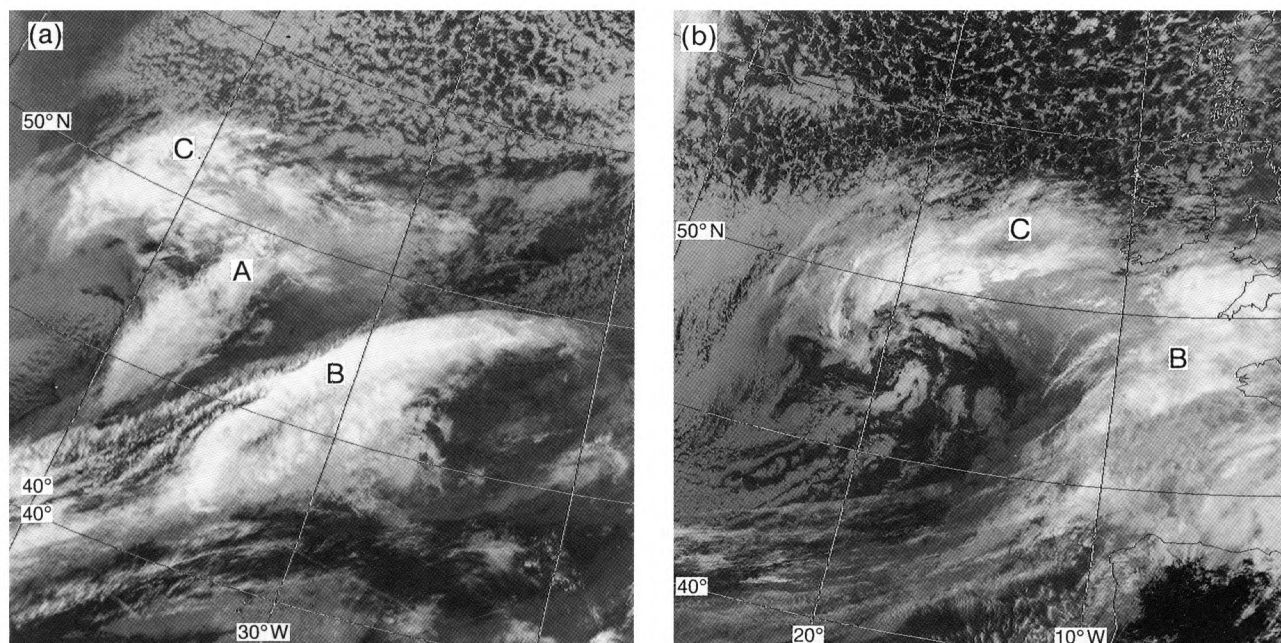


Figure 9. As Fig. 5 but for (a) 1431 UTC on 14 March 1989, and (b) 1421 UTC on 15 March 1989. C is the leaf-shaped cloud referred to in the text.

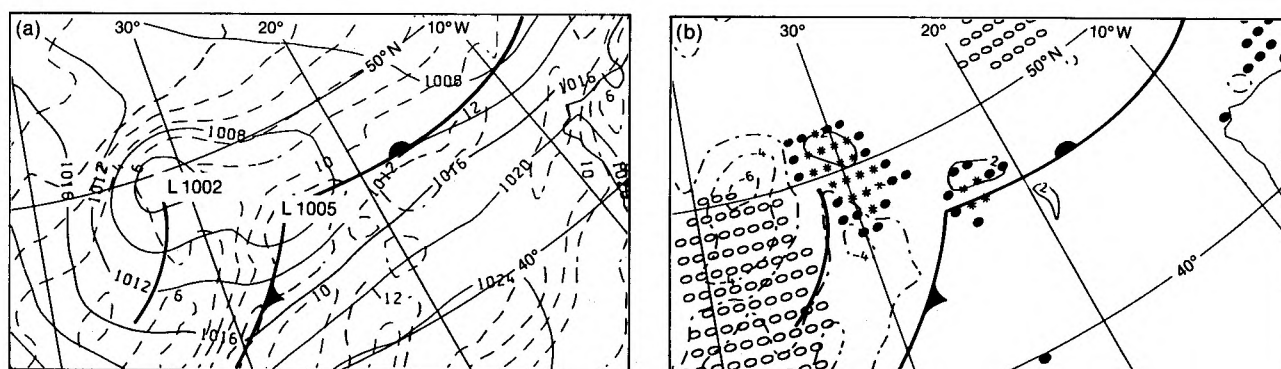


Figure 10. As Fig. 6 but for DT 0000 UTC on 15 March 1989, see key in Fig. 7.

cloud) at 0600 UTC showed the wave and trough as separate features, with some shower activity between. The 850 mb θ_w field indicated that the air behind the cold front was relatively warm (850 mb $\theta_w = 8-10^\circ\text{C}$) and showed significant θ_w gradients on both front and polar trough; the polar trough gradient also extended eastwards near 50°N . Extensive shower activity was forecast in the cold air further north. The diagnostic fields (Fig. 11(b)) indicated that most of the uplift was due to PVA but also with some warm advection shown on the forward side of the frontal wave. The $\Delta\theta_w$ forecast fields continued to show that the area near the wave tip would be highly potentially unstable ($\Delta\theta_w = -1^\circ\text{C}$); potential instability would also be present along the polar trough and in the zone between the polar low and the wave.

Figs 11(c) and 11(d) show the situation 6 hours later, around the time of instant occlusion formation. The areas of dynamic rain have merged and the wave has deepened a little. The separate thermal gradients associated with front and trough have been maintained and there has been a concentration of the gradient along 50°N . However the diagnostic chart (Fig. 11(d)) still shows a gap in the uplift between trough and wave. Considerable potential instability was again shown near the wave, with a tongue of $\Delta\theta_w \leq 1^\circ\text{C}$ values extending west-north-west to the polar-low area.

Finally, the T+18 hour forecast (Figs 11(e) and 11(f)), showed the cold low to be degenerating to a trough, and forecast a line of dynamic rain along the line of the instant occlusion; thermal gradients are maintained as before and a band of strong uplift has been generated

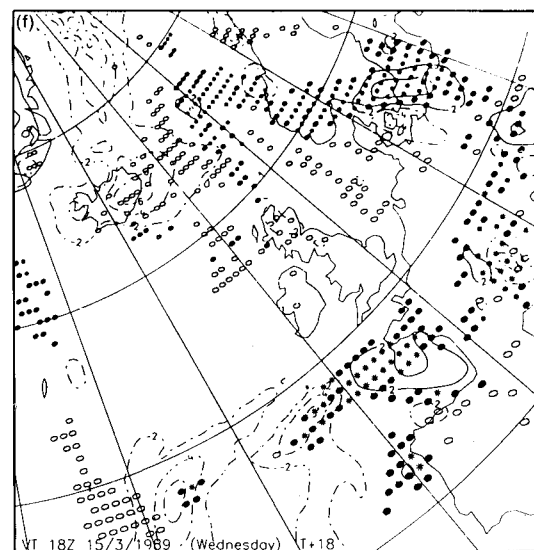
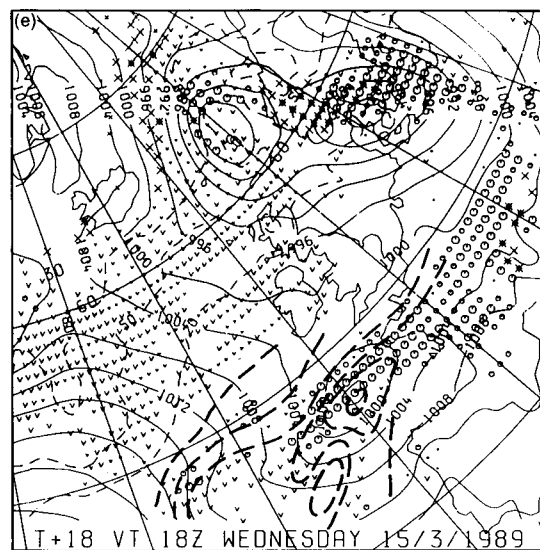
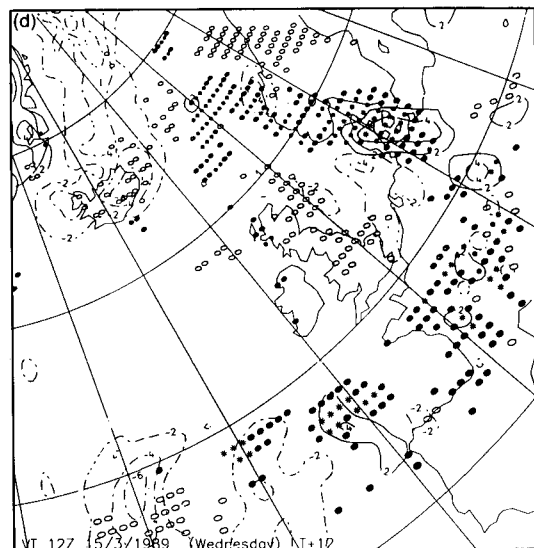
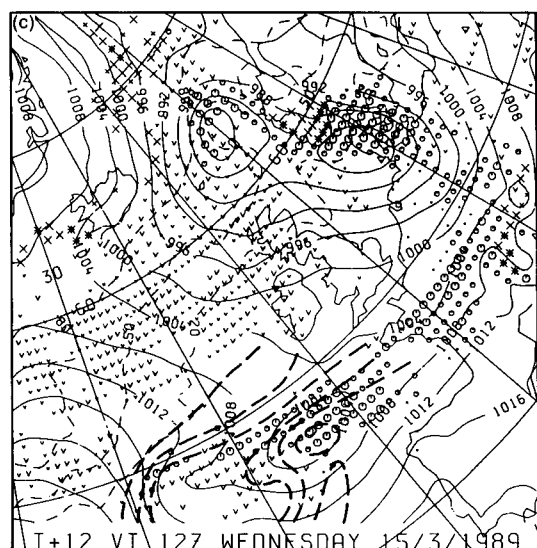
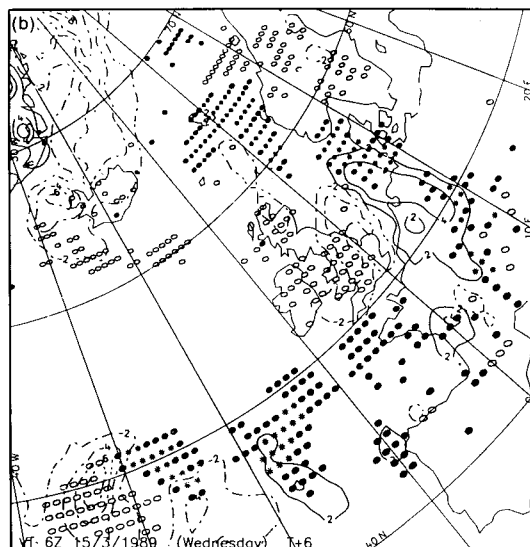
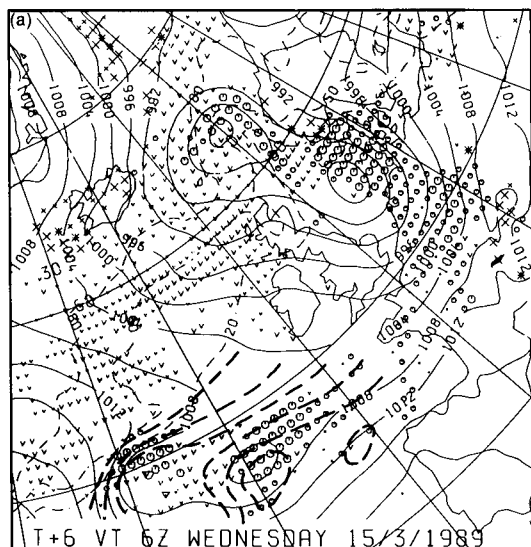


Figure 11. As Fig. 7 but for Data Time 0000 UTC on 15 March 1989. Rainfall rate and m.s.l. pressure: (a) Verification Time (VT) 0600 UTC on 15 March, (c) VT 1200 UTC on 15 March, and (e) VT 1800 on 15 March. Model diagnostics: (b) VT 0600 UTC on 15 March, (d) VT 1200 UTC on 15 March, and (f) VT 1800 UTC on 15 March.

along the instant occlusion and especially near the low. Significant potential instability is again forecast. This model sequences strongly suggested that a Type 2 instant occlusion had formed.

The two previous model runs (DT 0000 and 1200 UTC on 14 March) produced realistic sequences of Type 2 instant occlusion development. However, there were positional errors, especially with the earlier run which was far too progressive.

3.2.3 Discussion

This model run captured the essential details of a Type 2 instant occlusion development; the thermal gradients indicated that there was baroclinicity on the polar trough as well as the front and the existence of a shallow moist zone (SMZ) behind the cold front was well predicted. The forecast of significant potential instability in the merging zone was yet another feature of significance, since the release of potential instability has been recognized as an important mechanism in Type 2 instant occlusion development. Indeed it is noted that this distribution of potential instability is an important precursor of this type of development; this is completely different from the potential instability distribution associated with a Type 1 instant occlusion case, as indicated in the previous case-study.

The merging process was well shown by the vertical motion/thermal advection fields, developing a large area of strong ascent in the appropriate place, though possibly a few hours later than the actual event was observed to take place. However, it is important to note that careful examination of the precipitation forecasts alone would have given a good indication that Type 2 instant occlusion development was forecast to occur and this would be confirmed by consideration of the thermal fields. The model was less successful in predicting the eastward development of the low and with the degeneration of the cold low (both too quick). The previous model runs confirmed Type 2 instant occlusion development but had serious positional errors.

The application of the manual forecasting guidelines should have led to the conclusion that this was a potential Type 2 occlusion case. This would have been suggested by the imagery in the earlier stages and ship reports would have confirmed the development of a SMZ behind the cold front as the polar trough came closer. The upper-wind patterns at 1200 UTC on 14 March and 12 hours later at 0000 UTC (the chosen model DT) would have suggested that PVA and wave cloud should converge, probably reaching the critical spacing during 1200–1800 UTC on 15 March. This would have given a realistic prediction of events. Examination of the imagery sequences revealed that the wave and the polar feature converged very slowly during the period before the instant occlusion had formed. Fig. 9(a) suggests that the ‘baroclinic leaf’ and the wave cloud area were separated by around 550 n mile at that time and Fig. 9(b) shows a spacing of around 350 n mile.

This may suggest that merging had taken place (at 1200 UTC) when the spacing was slightly larger than the specified 350 n mile criterion but, in view of measurement uncertainties, it would be inappropriate to draw any conclusion of positive model error.

3.3 1/2 May 1989

3.3.1 Synoptic events

This was a case where the interaction between a polar trough and the polar front appeared to be at a critical but relatively unchanging stage for a period of 24 hours. Although instant occlusion merging did not occur, the imagery and actual analyses for the period suggested that linkage was almost achieved. As such, this case is an interesting test of instant occlusion merging criteria, for both model performance and manual guidelines.

The polar low/trough was located on the forward side of a sharp upper trough which became more confluent as it moved east across the Atlantic, bringing the surface trough closer to a baroclinic wave which had formed on the front. Positive signs of merging were observed to occur around 1600–1700 UTC, with the polar trough cloud apparently rotating quickly towards the wave tip; however this merging did not occur and the ‘almost merged’ situation proceeded virtually unchanged as the features ran north-east towards the Norwegian Sea. Fig. 12 shows a series of infra-red images, covering a 32-hour period and including the time when merging seemed to be commencing (Fig. 12(b)). At this time, cloud was increasing rapidly to the west of the wave and this appeared to reach a peak around 1600–1700 UTC — this being established by a study of the movie-loop of Meteosat hourly infra-red images.

Imagery during the next 24 hours indicated little change in the cloud pattern as the development ran north-north-east towards the Norwegian Sea. Fig. 12(c) shows the imagery almost at the end of this period. Like the previous case, it is noted that the comma-shaped polar trough cloud has a forward element of mainly layer cloud streaming forward in the south-westerly upper flow (indicating a degree of baroclinicity on the trough) and that deep convective cloud is located only to the rear of the polar trough line. These cloud configurations would suggest that any instant occlusion development would have been a Type 2 and this was confirmed by examination of the T+0 model fields at DT 0000 UTC on 1 May (the chosen model run for this case). The relevant fields (not shown) were similar to the previous Type 2 case; the 850 mb θ_w had a double structure (albeit rather weak near the trough), vertical motion was downwards in the SMZ zone and potential instability was also present in the zone.

Figs 13(a) and 13(b) show the actual surface analyses during the period when it seemed that merging was about to occur. At 1200 UTC on 1 May 1989, the polar vortex and trough had approached the waving cold front. The two features were very clearly separate on all

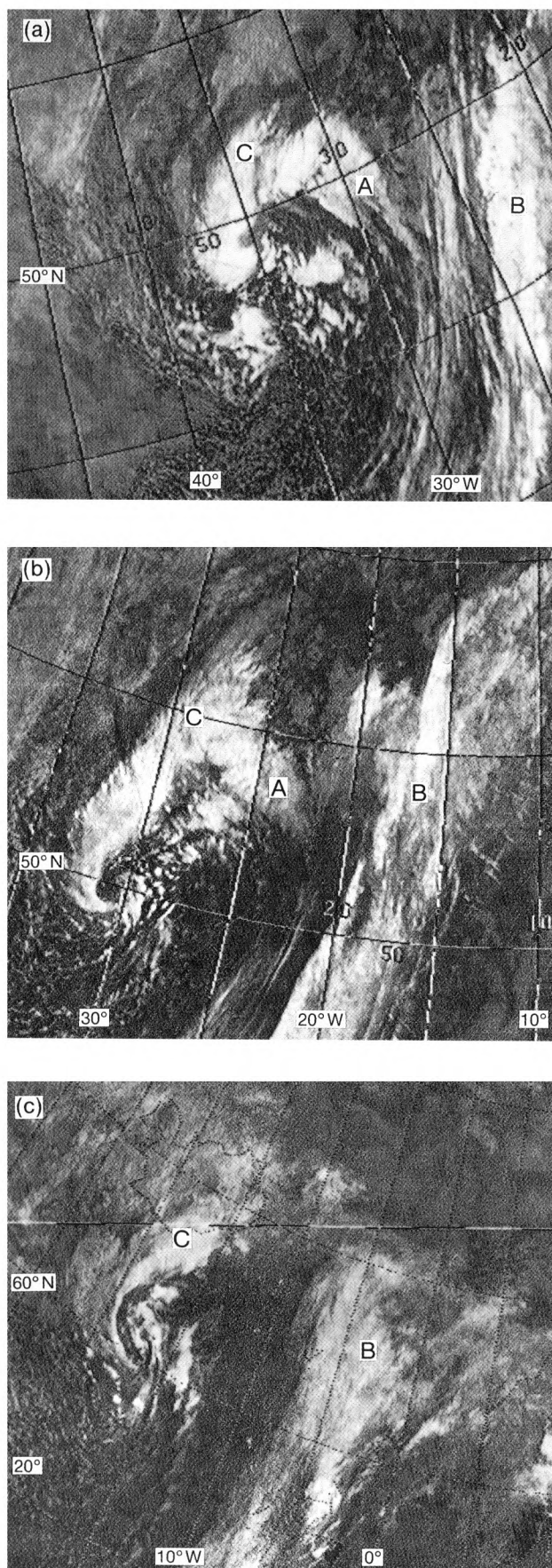


Figure 12. As Figs 5 and 9 but for 1/2 May 1989 at (a) 0522 UTC on 1 May, (b) 1444 UTC on 1 May, and (c) 1251 UTC on 2 May.

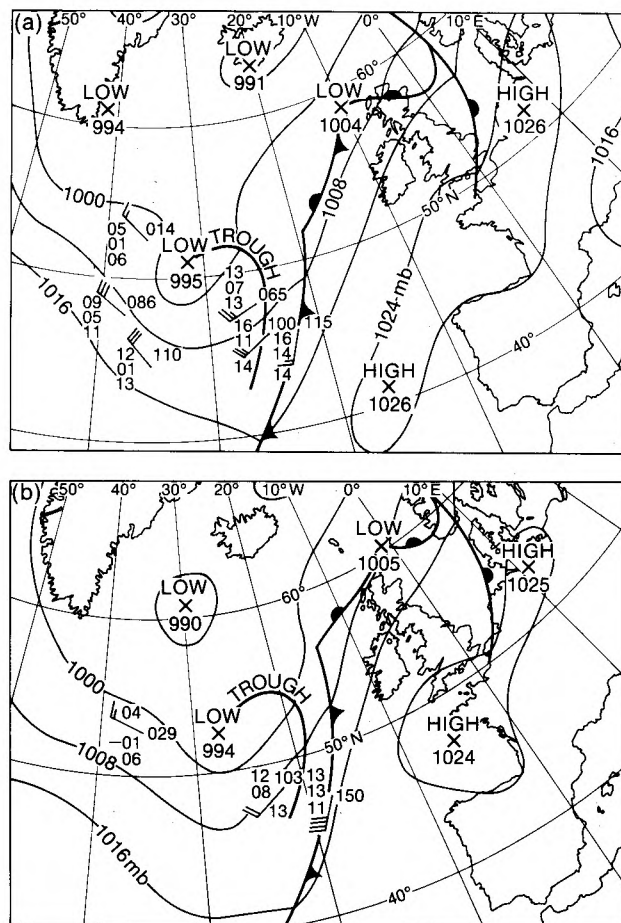


Figure 13. As Fig. 4 but for 1 May 1989 at (a) 1200 UTC and (b) 1800 UTC.

the imagery at that time and ship reports of active showers helped to place the trough line on the surface chart. Examination of all ship reports around this time suggested that dew-points fell from 14 to 11 °C across the cold front and then decreased by another 2 or 3 °C across the trough; further surface troughing was evident south of the polar low as a line of enhanced convection on the imagery, and the air became colder in the north-westerly airstream which followed, with a dew-point of -1 °C reported at Ocean Weather Station 'C'. This identified a SMZ between the front and the polar trough.

The 1800 UTC surface analysis showed the polar low had moved north-east, parallel to the movement of the wave; the trough had been rotated north-east and was placed largely on the evidence of satellite imagery, since surface reports were very sparse. As there was no direct evidence to suggest that frontogenesis was taking place between the SMZ and the colder air to the north of the wave, it was not appropriate to place a line of surface discontinuity there. Such a line would have been placed between polar low and wave tip, along the strong 850 mb θ_w gradient, and would have marked the beginning of a Type 2 instant occlusion development.

As can be seen from Fig. 12(c), the polar trough subsequently degenerated and it became increasingly

difficult to locate the line of the trough on surface analyses. Later surface analyses placed a single trough line rotating around the polar low, well away from the frontal wave.

3.3.2 Fine-mesh model run DT 0000 UTC on 1 May 1989

Figs 14(a) and 14(b) show the model predictions for 1200 UTC on 1 May (T+12 hours), around 3 hours before the first indications of actual merging were observed. The surface isobars and precipitation forecast showed separate areas of dynamic rain associated with the trough and wave with a scattering of showers and dynamic rain symbols between them. The 850 mb θ_w field showed indications of a double thermal gradient structure (weak near the trough) and the diagnostic chart gave some support, with warm advection indicated at both wave and trough (again, weak at the trough). The strong 850 mb θ_w gradient extended from the wave tip south-westwards towards the cold low indicating the northern boundary of a SMZ; however, this gradient decreased markedly before it reached the area of the cold low. The $\Delta\theta_w$ field indicated that potential instability would extend along the line of the incipient link and in the SMZ.

Figs 14(c) and 14(d) show the forecast situation 6 hours later at 1800 UTC on 1 May. There was increased spacing between wave and trough and the dynamic rain between the systems had generally decreased although there was a westward extension of rain around 58°N. The strong 850 mb θ_w gradient was maintained near the wave but had moved further away from the polar trough. Uplift had generally diminished. The $\Delta\theta_w$ field showed that two separate areas of potential instability had developed from the single elongated area shown 6 hours earlier. Examination of the 1500 UTC forecasts revealed that there had been little change in the situation during the period 1200 to 1500 UTC; the degenerations noted at 1800 UTC had occurred between 1500 and 1800 UTC.

The T+24 forecasts (Figs 14(e) and 14(f)) maintained the spacing between trough and wave and indicated some precipitation development north-north-eastwards, with uplift (mainly PVA-generated) extending towards Iceland; there were increased rain/showers in this area. Merging with the wave tip further east was not suggested. Subsequently, the model forecasts to 1200 UTC on 2 May (T+36 hours) showed the polar low/trough and the frontal wave becoming well-separated features as they moved north-east to the Norwegian Sea, with no further signs of positive interaction.

Examination of the two previous runs (DT 0000 and 1200 UTC on 30 April) revealed a divergence of opinion. Both runs suggested a potential Type 2 situation and developed strong 850 mb θ_w gradients from wave to cold low, unlike the subsequent run already examined. The earlier of the two runs indicated a possible merging;

the subsequent run was less enthusiastic. Both runs positioned the features too far east; this appeared to be due to an error in broad-scale development (too little trough extension) which caused too much upper flow to be maintained over the cold low.

3.3.3 Discussion

The chosen model run (DT 0000 UTC on 1 May) successfully indicated that an instant occlusion would not be formed. Neither precipitation or forecast cloud distributions suggested that this would occur, although the T+12 (and T+15) hour frames showed some development in the zone between trough and wave; subsequent frames correctly indicated precipitation/cloud degeneration in the merging zone. The slackening of the 850 mb θ_w gradient towards the cold low is seen as significant; this showed the northern boundary of the SMZ but the gradient was not maintained from the wave tip to the polar low/trough as shown in the previous (Type 2) case-study. Since this strong 850 mb θ_w gradient marks where the instant occlusion (warm front) forms, the lack of a continuous discontinuity suggests that a Type 2 instant occlusion cannot be formed from wave tip to cold low as required. The two earlier runs suggested that instant occlusion merging was more likely (especially the earlier) and both developed strong 850 mb θ_w gradients from wave to cold low.

Application of the manual forecasting guidelines around 0000 UTC on 1 May would have indicated the possibility of a Type 2 situation, using satellite imagery and surface observations. Spacing from trough cloud to wave tip at this time was around 500 n mile and consideration of the upper flow would have implied that this spacing would not decrease much. Thus, instant occlusion formation was not suggested by the guidelines. Measurements from the infra-red imagery indicated that the appropriate part of the trough cloud was at least 400 n mile from the wave cloud at its closest point — during the period 1500–1800 UTC on 1 May.

4. Conclusions

Like all atmospheric processes, the factors which control whether a polar trough and a frontal wave will merge are finely balanced and these three case-studies have illustrated the difficulties of assessing development probabilities with limited information in data-sparse areas. Satellite imagery has been shown to play an essential role in this process, coupled with guidance from NWP models, though both require careful interpretation. The two cases of actual instant occlusion development demonstrated the essential differences between the Type 1 and Type 2 categories and the third case, where an instant occlusion did not form, confirmed the concept of critical system spacing and also revealed the importance of the SMZ boundary structure as a significant indicator in potential Type 2 cases.

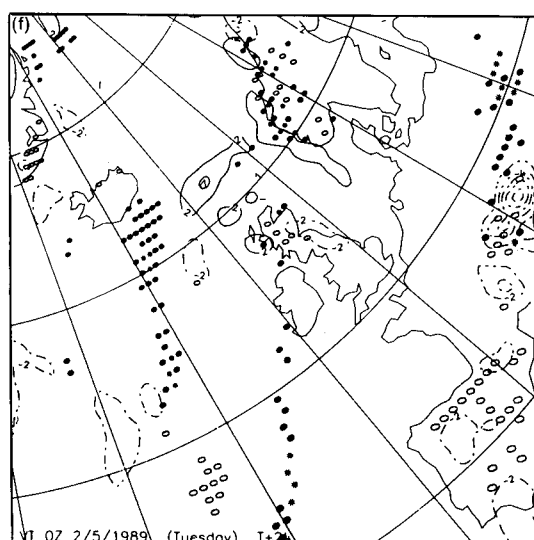
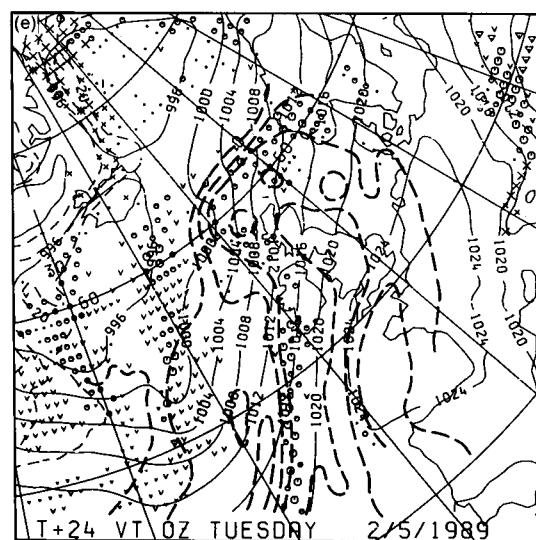
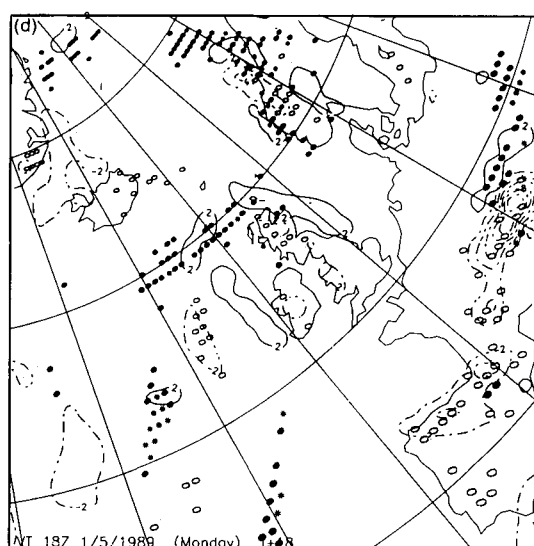
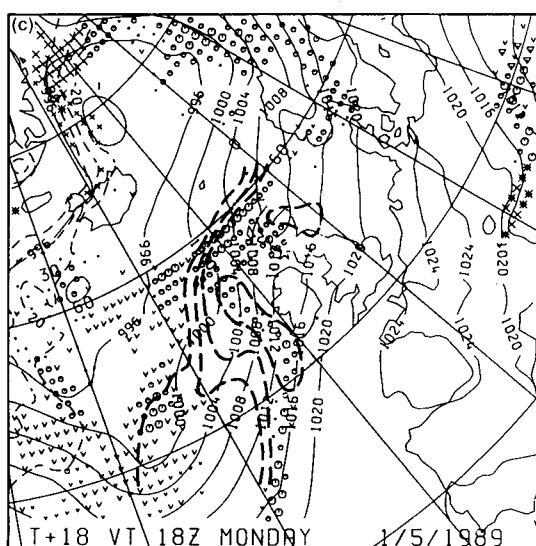
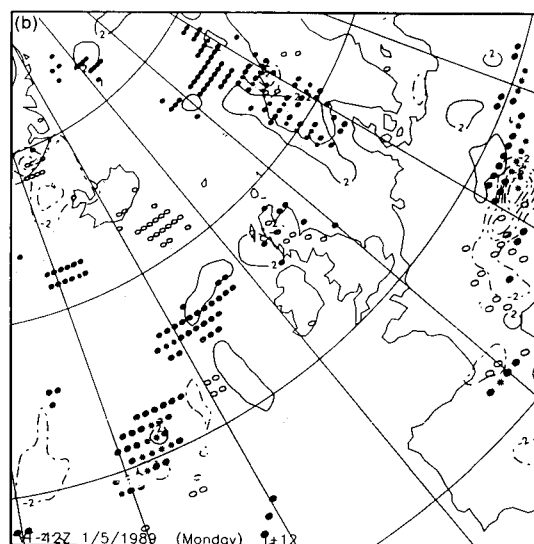
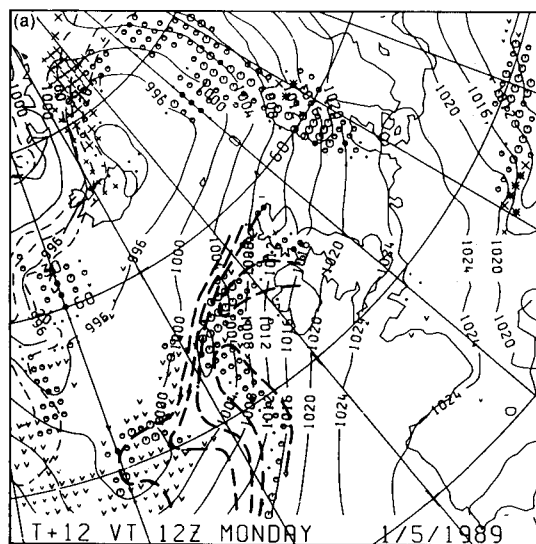


Figure 14. As Fig. 7 but for Data Time 0000 UTC on 1/2 May 1989. Rainfall rate and m.s.l. pressure: (a) Verification Time (VT) 1200 UTC on 1 May, (c) VT 1800 UTC on 1 May, and (e) VT 0000 on 2 May. Model diagnostics: (b) VT 0000 UTC on 1 May, (d) VT 1800 UTC on 1 May, and (f) VT 0000 on 2 May.

The guidance from the chosen fine-mesh model runs was impressive in most respects. In all three cases, instant occlusion development (or not) was correctly indicated and the model clearly and reliably distinguished between Type 1 and Type 2 situations; the resulting weather and cloud patterns were represented satisfactorily. The main fault came with timing errors of up to 5 hours or so within T+18 to T+24 hour forecasts; however, the assessment of actual merging times will also certainly be subject to some degree of error. In the third case-study, when the possibility of instant occlusion development was maintained at a critical stage for an extended period, the model solution correctly indicated the finely balanced nature of the interactions and provided the correct guidance that instant occlusion formation would not occur. It is significant to note that earlier model runs (DTs 12 and 24 hours previously) were generally more unsuccessful in their predictions, especially in timing/positional errors; these were due mostly to the development of synoptic-scale errors. However, instant occlusions of the correct type were predicted in the first two cases and the third case produced differing opinions on whether merging would occur; this generally confirmed the much-discussed interaction spacing concepts. In particular, the importance of the SMZ, as indicated by a correctly located strong gradient of 850 mb θ_w , was demonstrated by the model fields; *inter alia*, such a gradient is an essential requirement for Type 2 instant occlusion development.

It is clear that the fine-mesh model predictions are a valuable source of guidance for the forecaster when there is a possibility of instant occlusion development. In addition to giving advice on placement and timing, the model fields should help to establish whether instant occlusion development is likely and, if so, whether this will be a Type 1 or a Type 2. The interpretation process should include careful examination of the thermal fields, especially the 850 mb θ_w gradients, to establish or confirm which type of instant occlusion is likely. Although the case-studies made use of a whole range of forecast products available from the model, it is suggested that both types of instant occlusion development can be well identified from the first three output fields listed in Section 3 of this paper; these fields will normally be available to the forecaster on a routine basis.

The manual forecasting guidelines (Section 2) appeared to perform successfully in two out of the three cases. The modification made to the original guidelines operated reliably, indicating whether a Type 1 or Type 2 situation was possible. In the first case, the highly developmental nature of the situation, with its extremely rapid eastward movement, defeated the guidelines which can only be applied to existing troughs and waves. In this case, the new PVA development was close enough to the

front to interact immediately and the instant occlusion was formed as the development strengthened. The second and third cases were correctly predicted by the guidelines. The cases here indicated that the critical distance for merging to commence may well be somewhat less than the 350 n mile stated but the evidence is hardly conclusive due to the uncertainties in measurement. It is therefore confirmed that 350 n mile is a reasonable figure to apply.

It is suggested that the main use of the manual forecasting guidelines will be at DTs some 24 to 36 hours before the possible instant occlusion event. At these times, the case-studies presented here have indicated that the fine-mesh model is much less successful in predicting instant occlusion events correctly and the application of the guidelines at these times should provide a useful confirmation (or otherwise) of the model solution. At DTs 12 to 24 hours before the event, the increasing reliability of the model predictions will diminish the importance of the guidelines, although their use may still be regarded as a valuable check on the model.

Acknowledgements

I would like to thank M.J. Bader, R.M. Morris, A. Woodroffe and M.V. Young for their helpful comments and suggestions on the first draft of this paper.

References

- Anderson, R.K., Ashman, J.P., Bittner, F., Farr, G.R., Ferguson, E.W., Oliver, V.J. and Smith, A.H., 1969: Application of meteorological satellite data in analysis and forecasting. Washington DC, Air Weather Service, Technical Report No. 212.
- Böttger, H., Eckardt, M. and Katargiannakis, U., 1975: Forecasting extratropical storms with hurricane intensity using satellite information. *J Appl Meteorol*, **14**, 1259–1265.
- Browning, K.A. and Hill, F.F., 1985: Mesoscale analysis of a polar trough interacting with a polar front. *Q J R Meteorol Soc*, **111**, 445–462.
- Gadd, A.J., 1985: The 15-level weather prediction model. *Meteorol Mag*, **114**, 222–226.
- Locatelli, J.D., Hobbs, P.V. and Werth, J.A., 1982: Mesoscale structures of vortices in polar air streams. *Mon Weather Rev*, **110**, 1417–1433.
- McGinnigle, J.B., Young, M.V. and Bader, M.J., 1988: The development of instant occlusions in the North Atlantic. *Meteorol Mag*, **117**, 325–341.
- Marshall, T.A., 1982: Weather satellite picture interpretation, Vol. 2. London, Ministry of Defence, Directorate of Naval Oceanography and Meteorology.
- Monk, G.A. and Bader, M.J., 1988: Satellite images showing the development of the storm of 15–16 October 1987. *Weather*, **43**, 130–135.
- Reed, R.J. and Blier, W., 1986: A case study of comma cloud development in the Eastern Pacific. *Mon Weather Rev*, **114**, 1681–1695.
- Weldon, R.B., 1979: Cloud patterns and the upper wind field. Satellite training course notes, part IV, pp. 62–79. Scott AFB, Air Weather Service, Report No. WAS/TR-79/003.
- Young, M.V., 1988: Investigation of an instant occlusion event during FRONTS87. (Unpublished, copy available in the National Meteorological Library, Bracknell).

Developments in meteorological telecommunications

S.M. Long

Meteorological Office, Bracknell

Summary

A brief description is given of recent developments in meteorological telecommunications with particular reference to the operation of the Bracknell Meteorological Telecommunication Centre.

1. Introduction

The application of 'new technology' to telecommunications offers many possibilities for the improvement of data exchange between meteorological centres. The functions of the Meteorological Telecommunication Centre (Met TC) at Bracknell are continually expanding as data volumes increase and new types of data are made available for transmission between centres. New methods of transmission using digital techniques and new communications media such as fibre-optic cables can provide higher data rates at lower cost than the existing analogue circuits. Modern technology has also enabled the development of interface units to handle high-speed transmissions for even quite low-cost processing systems.

Allied to the introduction of new types of equipment are the evolving international standards for data handling and data management which enable users to benefit from the capabilities of the new systems without large development costs. These standards aim to provide common interfaces to allow equipment from different manufacturers to work together. The availability from suppliers of software packages, which implement the standards, facilitates rapid integration of new systems and the wide customer-base for such products reduces the cost for individual users.

2. Functions of the Met TC

The Met TC at Bracknell supports the national networks and handles most of the communications between the Meteorological Office and the rest of the world. The principal functions are collection of observational data from UK outstations, distribution of these data and some forecast products to the outstations and exchange of observational data and forecast products with other meteorological centres. These functions are carried out 24 hours per day, every day of the year.

The national observational data are collected from outstations via collecting centres from where bulletins of reports are sent to Bracknell over dedicated circuits. These data together with a selection of forecast products are sent back to the outstations over teleprinter and facsimile circuits. Fig. 1 shows the main links in the

Global Telecommunication System (GTS) of the World Meteorological Organization (WMO).

The international communications use networks — in particular the WMO GTS — which provide medium-speed links and allow exchange of global information between the major data processing centres and facilities for supplying a more limited range of products to less well equipped National Meteorological Centres (NMCs). Bracknell acts as a Regional Telecommunication Hub (RTH) situated on the WMO Main Trunk Network between Washington and Paris with whom large quantities of data are exchanged daily. Bracknell also has connections to Offenbach, to the European Centre for Medium-range Weather Forecasts (ECMWF) and to several other centres in countries which are part of the UK area of responsibility for collection of observations and supply of data to their NMCs.

Fig. 2 shows the steady growth in traffic handled by the Met TC over recent years, amounting to an increase by a factor of 40 from 1972 to 1989. This is due to increased volumes of observational data and more, higher-resolution output products from numerical weather prediction models.

3. Data handling systems at the Met TC

Different types of data are handled by different computer systems within the Met TC. Graphical data are handled by Autofax, a dual Ferranti computer system, and alphanumeric and binary data by the Phase IV, Tandem computers, the main message switching system.

3.1 Autofax

The Autofax system consists of two Ferranti Argus 700GX computers. Normally one of these provides the operational services whilst the other is available as standby in case of failure and can also be used for software development. The system drives all the analogue facsimile services which are received at outstations, such as MOLFAX (Meteorological Office Landline Facsimile), and also provides a digital broadcast of pictorial products for GRAFNET (see section 5). The products for dissemination by the

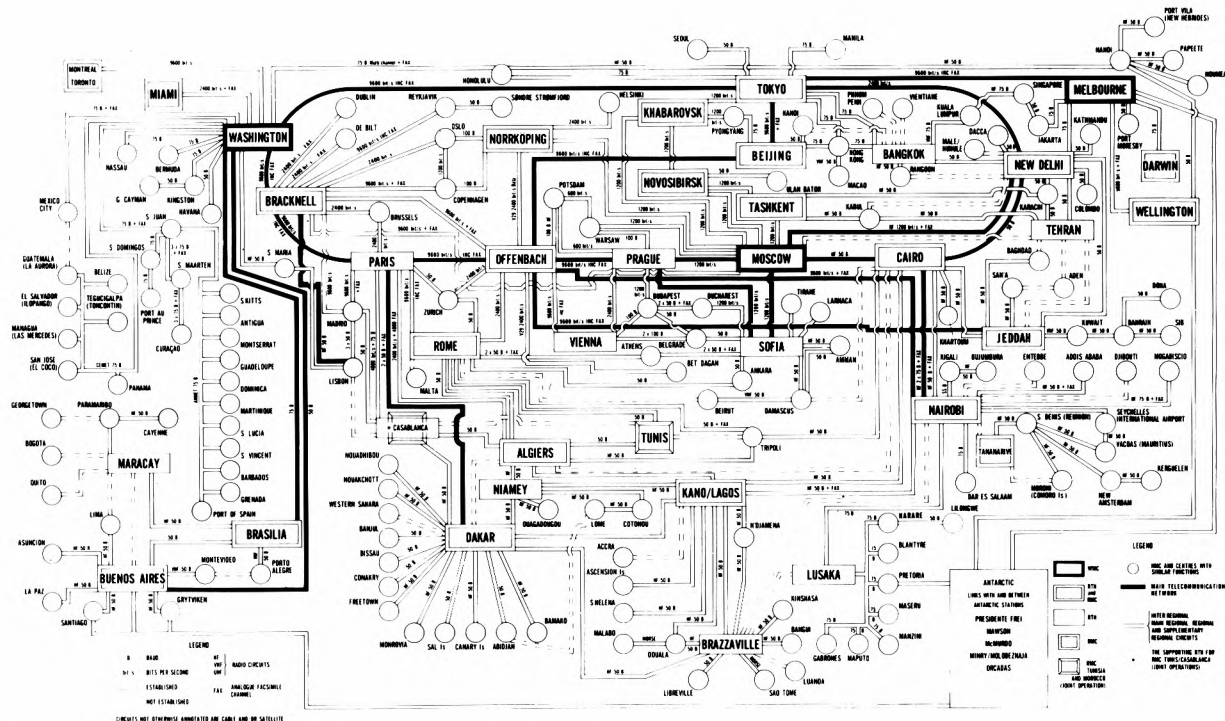


Figure 1. Schematic diagram of the Global Telecommunication System of the World Meteorological Organization.

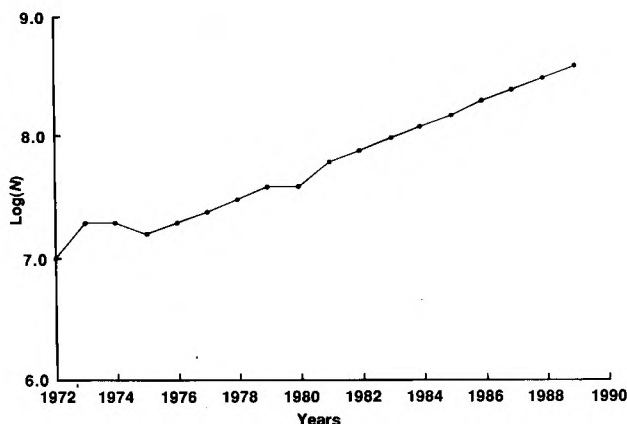


Figure 2. The logarithmic growth of traffic handled by Bracknell Meteorological Telecommunication Centre in recent years. N is the number of characters (including bit-orientated data) exchanged daily.

Meteorological Data Distribution (MDD) mission are also supplied from Autofax (see section 6.2).

3.2 Phase IV

The Phase IV system is a seven processor Tandem TXP Non-Stop II system. It came into operational use in 1986 with five processors and was enhanced by the addition of two more processors in 1987. Owing to the increased volume of message traffic the disk space has been increased to one gigabyte. The disks are run as mirrored pairs and other hardware and connections are duplicated to provide resilience and non-stop capability. Failure of any system component should result in graceful reconfiguration without loss of data or programs.

The Phase IV and Autofax systems were designed as message switches and are not concerned with the content of messages provided that they are correctly formatted and can be routed to their destination. Both are linked at high speed to the main data processing systems, COSMOS, to receive data for transmission.

All the international data links are supported from Phase IV. Also there are links to Meteorological Office outstations, to customers such as airlines and the Civil Aviation Authority (CAA) and to other Government bodies, e.g. the Department of the Environment which receives nuclear monitoring data via the Radiation Incident Monitoring Network. Data that are received are transmitted to COSMOS for analysis and use in the numerical forecast models. Most of the national links to outstations are only used for small amounts (a few kilobytes) of data. This will change with the introduction of the Weather Information Network (WIN) when large amounts (several megabytes) of data will be supplied to the Outstation Display Systems at Meteorological Office locations in the United Kingdom. The WIN will be supported by a Bracknell communications node and there will be a back-up node. Data for distribution will be supplied from Bracknell and also from the Autosat-2 computers at the satellite data receiving station at Lasham operated by a contractor on behalf of the Royal Aerospace Establishment and the Meteorological Office.

The main data flows in Phase IV are, currently, to and from the GTS and these links are gradually moving to higher speed lines and more sophisticated protocols to cope with the increased data rates. There is a need for

error detection and correction during transmission and receipt of forecast products and observational data.

4. Standards in international telecommunications

There are continuing discussions between the major GTS centres about the future development of international meteorological communications. International communications standards are being developed by bodies such as the International Telegraph and Telephone Consultative Committee (CCITT) and the International Standards Organization (ISO). The CCITT has developed the X series of recommendations for communications protocols. Two of these, X.25 and X.400, are discussed below. The ISO has a seven-level reference model (Fig. 3) for the interconnection of open systems which divides the logically homogeneous functions performed by different communicating equipments into a hierarchical structure. It describes the communications functions from the lowest, physical, level to the level 7 application program interface. All these standards are designed to allow equipment from different manufacturers to communicate effectively.

4.1 CCITT recommendation X.25

X.25 is a protocol for the lower levels of the ISO model — up to level 3 in Fig. 3. It splits the data into high-level data-link control frames with headers giving address and control information (Fig. 4). Each level accepts information from a higher level and adds a header and sometimes a trailer before passing the information to the next level down as shown in Fig. 5.

Advantages of X.25 are that the protocol provides for the exchange of data in binary form, error detection and control, and the ability to control data flow to avoid congestion on the link or loss of data when the receiving system is not ready for more data. Sequence checking of received frames is performed and the link can be disconnected, reset and restarted.

It is also possible to use several logical channels on one point-to-point X.25 connection. This can be used to separate different types of data. Each channel can be flow controlled and error checked independently of any other logical channels.

At the Bracknell RTH there are a few international links which still use WMO protocol (a character based protocol) but the links to major centres are being converted to X.25 protocol running at speeds of 2.4 to 9.6 kilobits per second (kbps). All of these X.25 links to Phase IV use permanent virtual circuits (PVCs) on leased lines which are continuously available and ready to transfer data. The alternative to a PVC is a switched virtual circuit (SVC) which only needs to be established when required for data transfer. The transatlantic link to Washington, used for exchange of GTS data and World Area Forecast Centre (WAFC) aviation products, consists of a number of separate physical channels Time

Division Multiplexed (TDM) on to a 16.8 kbps link. One of these channels is further subdivided into two logical channels to aid in separation of different types of data whilst keeping the whole channel running at the highest possible capacity. Each logical channel has independent flow control on the packets and also separate error control.

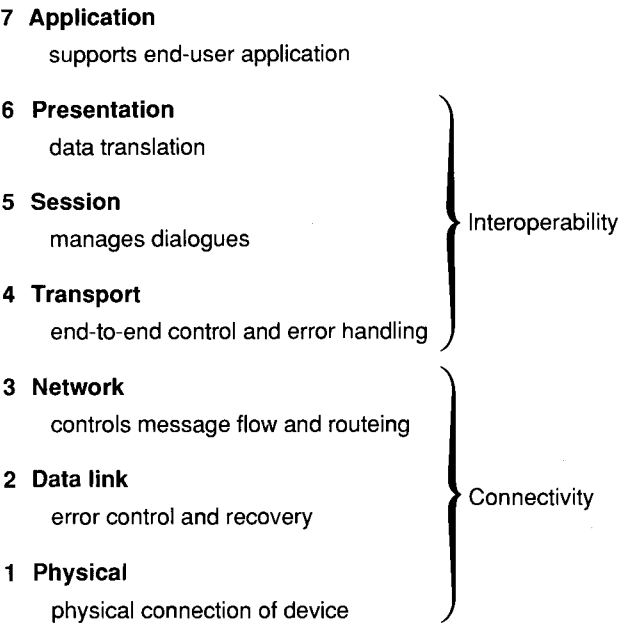


Figure 3. The International Standards Organization seven-level reference model for interconnection of open systems.

The link to the National Weather Service (NWS) at Washington is currently via satellite but is being transferred this year to a new service using a fibre-optic cable across the Atlantic. This new link will operate at the higher speed of 64 kbps and will have separate TDM channels for different data types. As well as GTS data, the circuit will carry digital facsimile products and special satellite data from the National Environmental Satellite Data and Information Service in Washington. This service is cheaper than the corresponding satellite service, provides more security and allows more control.

The implementation of X.25 protocol on links to Phase IV follows the recommendations for the ISO lower layers 1-3. The addition of transport-layer protocol (layer 4) to provide end-to-end confirmation of message delivery was considered by representatives of WMO Members but the software for this is not yet standard for all manufacturers.

In future there will be increased quantities of data and plans are being made for migration of other international circuits, such as those to Paris and Offenbach, to 64 kbps lines which will be subdivided into channels in similar manner to the Washington link. In the longer term only logical separation of data will be used over a single channel thereby providing increased efficiency.

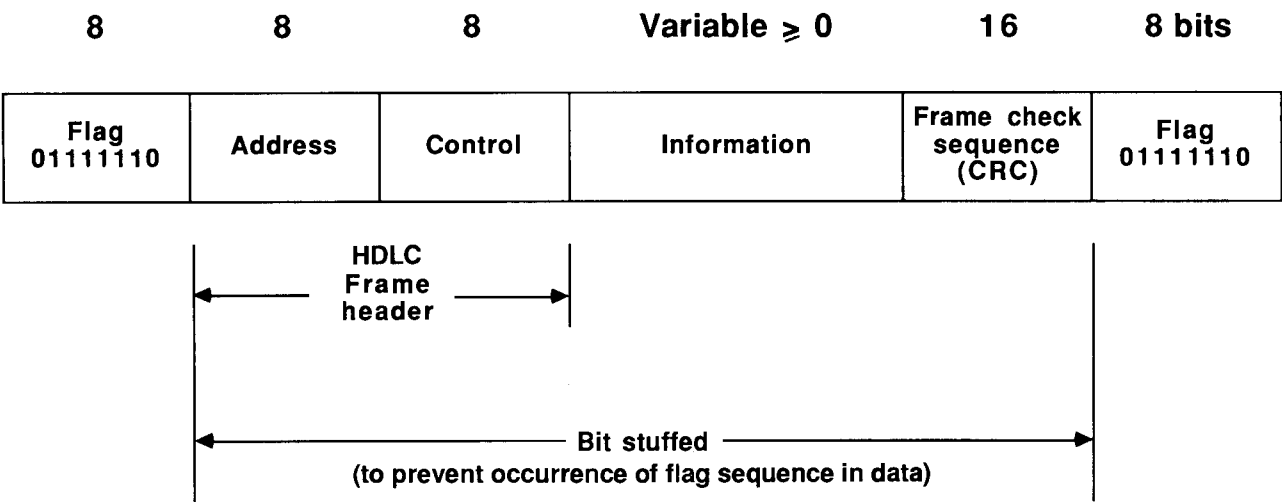


Figure 4. The format of a high-level data link control (HDLC) frame in the X.25 format. CRC is cyclic redundancy check.

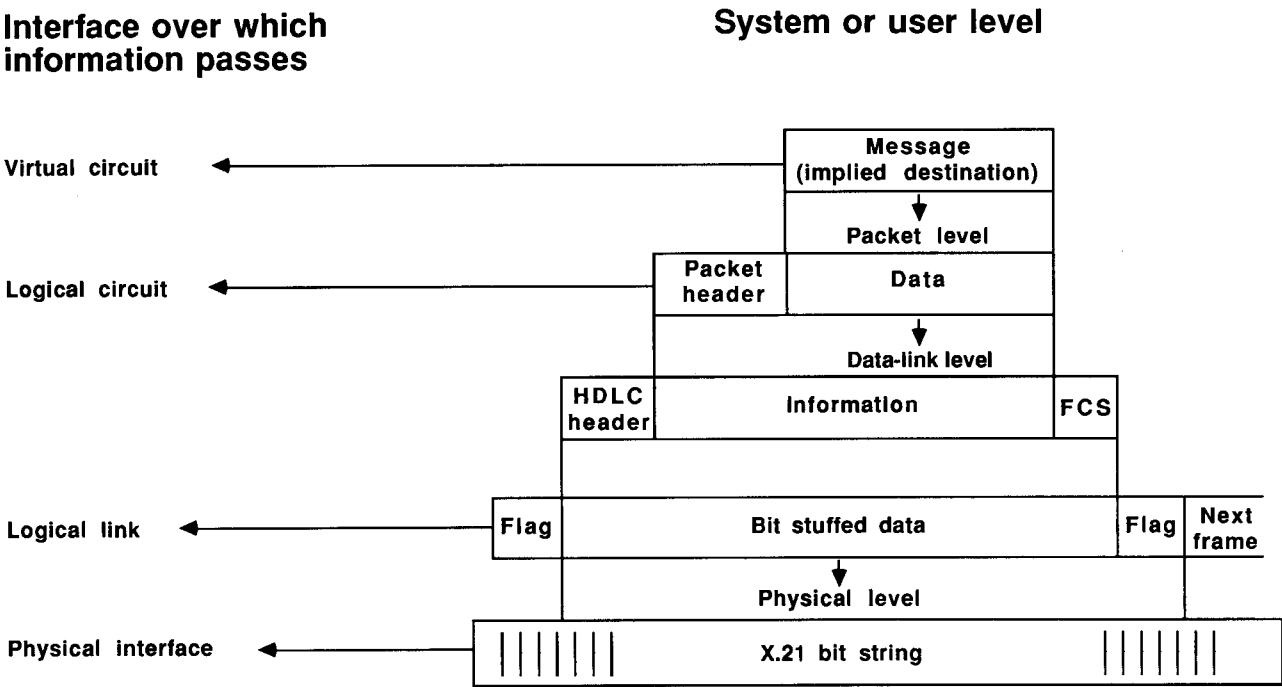


Figure 5. Structure of frame in Fig. 4 showing separate levels. FCS is frame check sequence.

The need for back-up, particularly during an outage of one of the major GTS centres, has to be considered. For this, and to allow flexibility in reconfiguring circuits, the use of packet switches at each centre and SVCs instead of PVCs was recommended. Because the use of SVC includes call set-up, the links can use dial-up connections over public data networks if the leased lines are not available. Large and small messages can be separated by the use of multiple virtual circuits on each connection.

X.25 protocol is used by British Telecom (BT) for its public data network service — Packet Switch Stream (PSS). This provides the ability to transfer data between computers (packet terminals) and other computers or

character terminals. Packet terminals have software to handle incoming X.25 packets and to put data into packets before transmission. Character terminals, which do not have this capability, are connected to PSS via a Packet Assembler/Disassembler which handles the communications protocol for them. PSS has a gateway to similar systems in other countries, e.g. Transpac in France. This service is used by the Meteorological Office to send data to the National Meteorological Services in Singapore and New Zealand and to various commercial customers in the United Kingdom and abroad. Facilities of this type offer a very cost-effective way of providing back-up for GTS leased lines and providing low volumes of data to a number of users.

4.2 CCITT recommendation X.400

X.400 is the CCITT recommendation for message handling systems (MHSs). It is a level 7 (application level) protocol. An MHS consists of a set of interconnected Message Transfer Agents (MTA) which co-operate with User Agents (UAs) to transfer messages between end users as shown in Fig. 6. A message has a content and an envelope which is similar to, but more sophisticated than, the headings added by X.25. There are additional facilities such as message stores to hold data for later examination by a user and access to other services, e.g. physical distribution. Some features of X.400 will be very useful, especially for WIN. These include distribution lists and directories which allow selective distribution of messages and format conversion to, for example, facsimile or graphics. Each user is registered on the system and messages are converted into suitable format for handling by the available equipment.

X.400 will be considered for use on the GTS when centres have gained experience with it for national communications. A number of X.400 services are available from both public and private operators.

The service offered by BT using X.400 is called Gold 400. It provides access from customer terminals or computers, via gateways, to a range of services such as fax, telex and the international network. It also interfaces to the BT mailbox system Telecom Gold.

5. Automation of facsimile product handling at Bracknell

Facsimile products which are produced from charts on the main data processing system, COSMOS, are sent from COSMOS to Autofax in digital form but they can be transmitted from Autofax to either digital or analogue receivers. To reduce transmission times the charts are sent as compressed bit-maps from COSMOS. Originally they were sent in a special code which compresses the bit-map to about one third of its length. Lately the T.4 coding recommendation of CCITT has been adopted. This reduces the bit-map to about one seventh of its original length. The charts are decoded on Autofax before being converted to a special compression code for the Facit printers on GRAFNET or being sent on the analogue broadcasts.

In future there will be a requirement to transmit charts in T.4 code for use by the CAA and also for the MDD mission. This is described later.

Other charts are hand drawn rather than produced on COSMOS. These have to be scanned in a scanner attached to a personal computer (PC) then transferred using X.25 to Autofax before they can be retransmitted. Charts such as significant weather are required in T.4 code for the CAA and MDD and work has been done with an A4 scanner and a PC interface card to produce T.4 coded images directly. This is shown in Fig. 7. An experimental PC system which holds images in store so that they can be retrieved by an authorized caller using

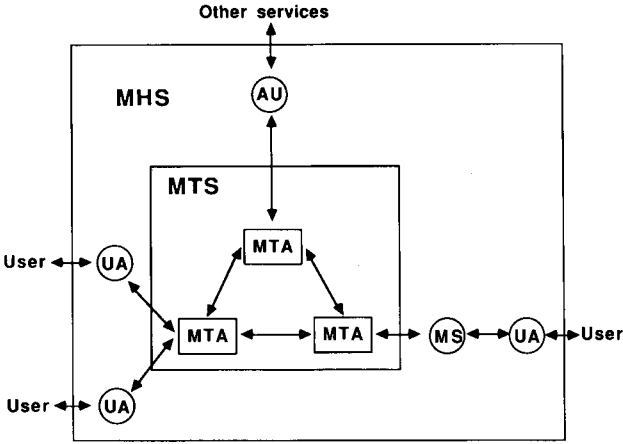


Figure 6. The X.400 message handling protocol. MTS is the Message Transfer System, MS a Message Store, AU an Access Unit. Other abbreviations are explained in the text.

standard Group 3 facsimile equipment has also been demonstrated, and will be developed further to serve commercial customers.

6. Satellite systems

6.1 DCP data collection and OWSE-AF

The Meteosat satellite is used for collection of environmental data from automatic and semi-automatic weather stations located on land (Data Collection Platforms (DCPs)), at sea (Automated Shipboard Aerological Programme (ASAP) and Meteorological Office System for Ships (MOSS)), or in aircraft (Aircraft/Satellite Data Relay (ASDAR)). This Meteosat Data Collection System (DCS) is part of an international DCS using other satellites. The DCP transmits its data

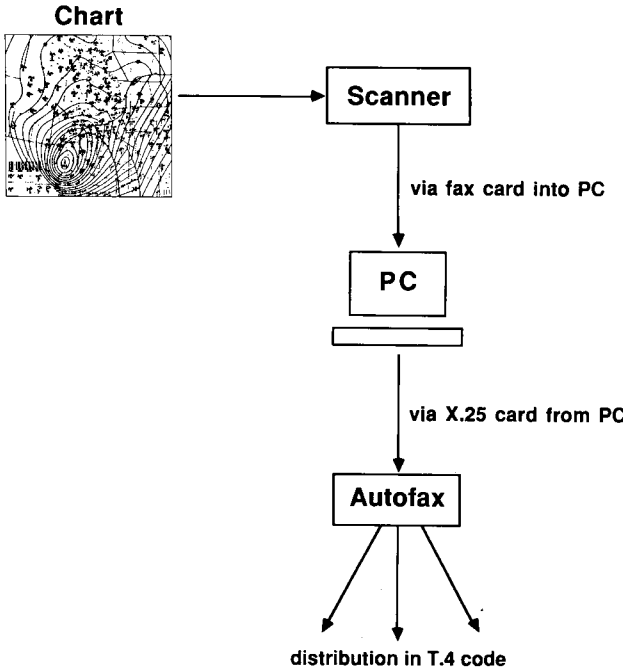


Figure 7. Conversion of image data into T.4 code and its distribution.

to the satellite at predetermined times and all the data are sent to the European Space Operations Centre's Data Acquisition Telecommand and Tracking Station (DATTS) as in Fig. 8. From there the data are sent to Darmstadt for distribution by land-based communication systems (e.g. GTS) and a selection of the data is sent back to the satellite via the Data Relay System (DRS) for broadcast to user stations in the gaps between the Wefax (image) frames.

The Meteorological Office has automatic weather stations (AWSs) using DCPs to report in a national code from buoys and also similar AWSs are replacing

manual reports from Light-vessels. These observations are received from Darmstadt and are code converted to SYNOPs in Phase IV before to distribution.

Plans are under way for a study of the meteorological data exchange requirements in Africa — this is the Operational World Weather Watch Systems Evaluation Africa (OWSE-AF). The aim is to improve the collection and distribution of data in the WMO Regional Association I area (Africa). Initially the suitability of DCP/DRS systems for use in Africa will be evaluated and later the effectiveness of a satellite based dissemination service will be studied (see Fig. 9).

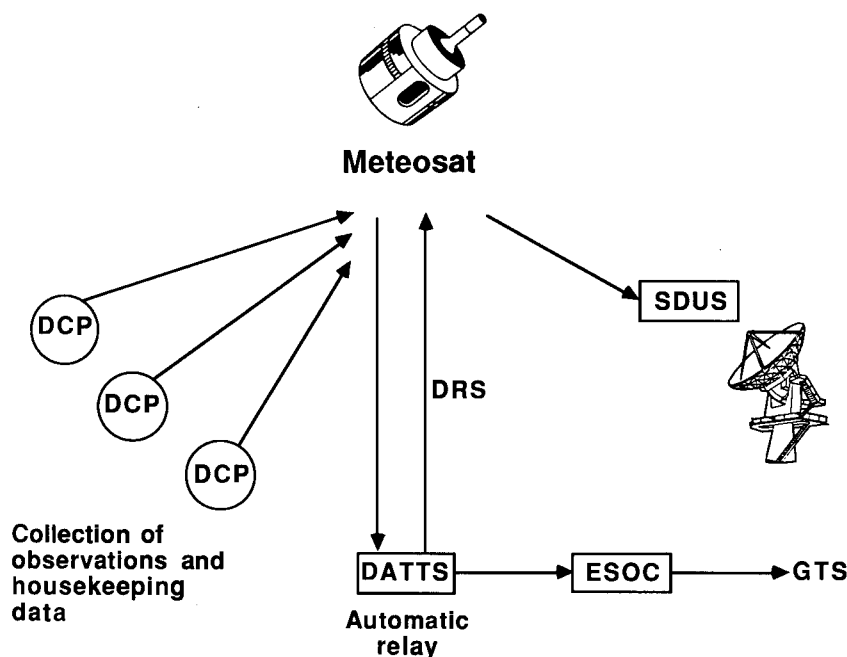


Figure 8. Meteosat Data Collection Platform System. SDUS is a secondary data users' station. Other abbreviations are explained in the text.

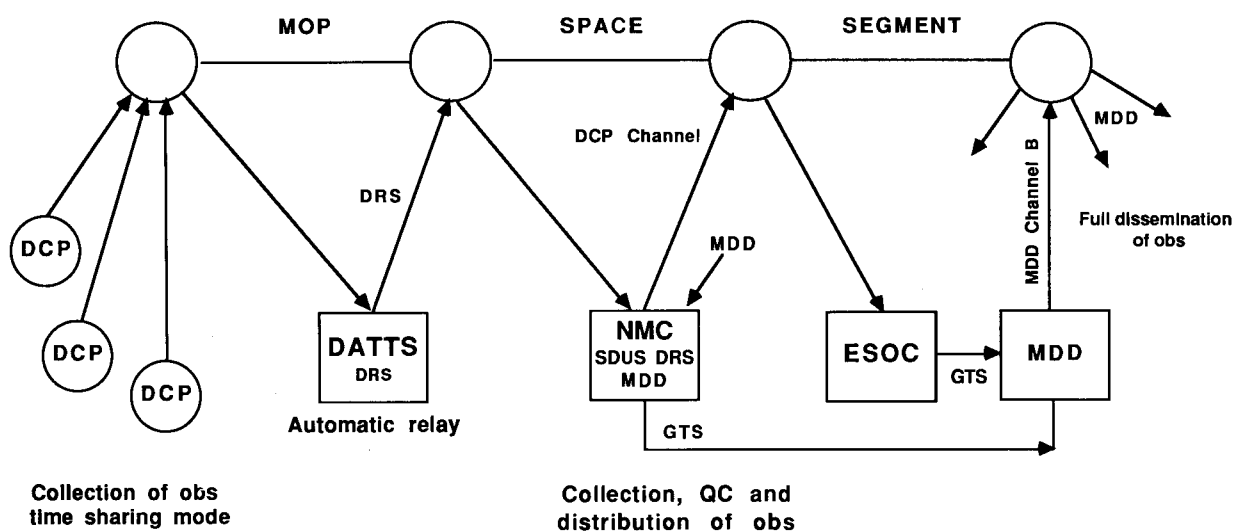


Figure 9. The Operational World Weather Watch System Evaluation Africa (OWSE-AF); a possible use of DCP, DRS and MDD missions for observation collection and distribution.

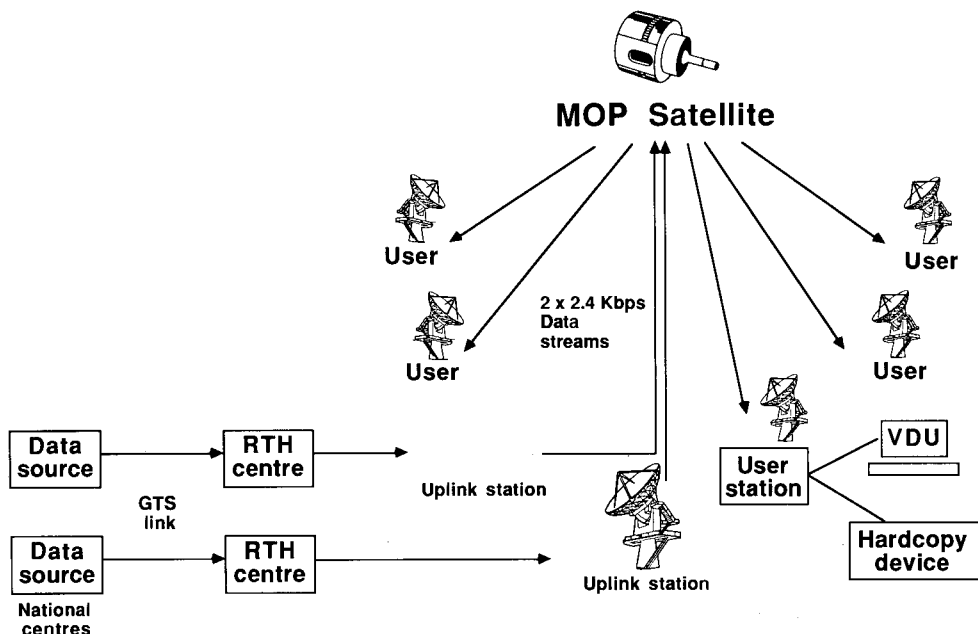


Figure 10. The Meteorological Data Distribution mission concept. Abbreviations are explained in the text.

6.2 Meteorological Data Distribution

The MDD mission has been set up primarily to provide meteorological data to national meteorological services in Africa and the Near East. It will use the new Meteosat Operational Programme satellites, the first of which was launched last year. Four satellite communication channels have been reserved for MDD although only two will be used to start with. A ground station at Bracknell will use one channel to transmit coded facsimile data and a similar station in Rome will send alphanumeric data on a different channel. Both these data streams will be 2.4 kbps (Fig. 10). There are plans to encrypt the data to restrict its use to authorized receivers though this would reduce the effective data rate and a study on encryption is being carried out for the European Space Agency.

Receiver stations will be equipped with a user station, micro-processor, data store, visual display unit and hard copy device. Although orientated towards African users the broadcast will be able to be received by similar systems in Europe, the Caribbean and parts of South America.

6.3 Commercial satellite systems

As well as communication via Meteosat there are also commercial companies offering a variety of satellite data distribution systems. These usually have a central transmitting station to which customers send their data by conventional means and these data can then be broadcast to reception equipment at customer sites. Two-way communication is possible via the satellite, provided that the customer sites are equipped with a suitable transmitter (Fig. 11). The data can be protected from unauthorized use by encryption. Several WMO members use such systems for their national networks.

The political, financial and organizational aspects of the use of such systems internationally needs consideration at all levels in WMO.

The INMARSAT service for collection of SHIP observations is proving most valuable although there are areas, particularly the Indian Ocean, where no WMO Member has offered to accept reports via an appropriate Coast Earth Station (CES). At Bracknell about 130 reports are accepted each day using a special short dialling code. This represents about 40% of the

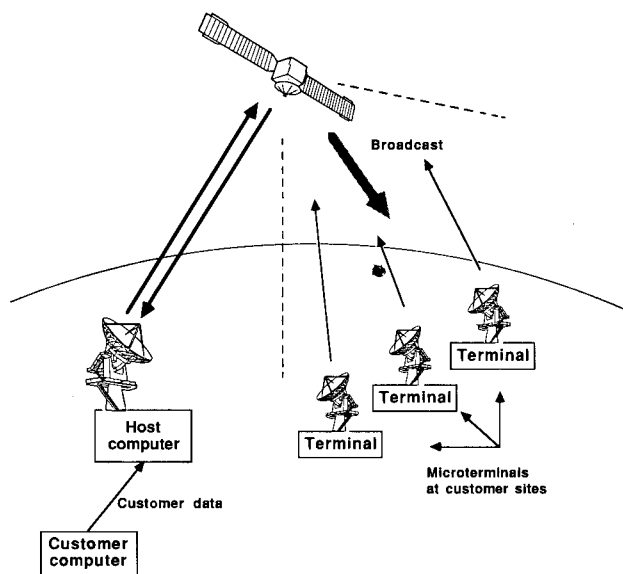


Figure 11. Commercial satellite broadcasting.

reports collected. Bracknell has also participated in the Enhanced Group Call system which is to be used for the INMARSAT SAFETYNET service which will form part of the Global Maritime Distress and Safety Communications system organized by the International Maritime Organization (IMO). Input of meteorological warnings and forecasts for the oceanic areas to the system is through direct communication with the CES, very much on the lines of information provided to Coast Radio Stations under NAVTEX.

7. Conclusion

Continuing increases in the volume of data to be handled on both national and international links in

the Met TC are anticipated as more observational data such as that from satellites becomes available, higher-resolution model products are generated at major centres and more specialized products are made available for customers. These will require the development of the existing systems and also investment in new technology as it becomes widely available. Various systems for providing effective communications links have been described above. The availability of satellite-based systems for point to multipoint transmissions is growing rapidly and the use of such systems can be very valuable to the meteorological community. The use of these communication methods will be examined as the need arises.

Awards

L.G. Groves Memorial Prizes and Awards for 1988

These awards were instituted in 1946 by Major and Mrs Keith Groves in memory of their son, Sergeant Louis Grimble Groves RAFVR, who lost his life while flying on a meteorological sortie with 517 Squadron on 10 September 1945. The 1988 awards were presented by Mr Andrew Douglas-Bate (a relative of the Groves family) on 8 December 1989 at RAF Brampton, HQ RAF Support Command, and the citations were read by the Inspector of Flight Safety, Air Commodore G.R. Profit, OBE, AFC, RAF.

Meteorology Prize — Dr B.W. Golding

The citation for this award was:

'Local-scale forecasts for periods of 12 hours or so ahead are important for many weather-sensitive activities. This is particularly true for aviation; civil aircraft need to know details of the wind, temperature, visibility and cloud base near the ground both for flight safety during take-off and landing and for effective management of airline operations; military aircraft are also sensitive to small-scale weather features, especially during low-level flying when factors such as precipitation, wind shear and icing are particularly important. The Meteorological Office's mesoscale model, which has a horizontal resolution of 15 km and a detailed representation of the structure of the atmosphere at low levels, has been designed to provide improved guidance to forecasters in the outfield on such local weather conditions. Over the past 7 years Dr Golding has successfully transformed the model from a research tool into a potentially important practical component of the Office's operational numerical weather prediction system. The model's wind and temperature forecasts are recognized as already being very accurate; modifications to improve the predictions of more difficult quantities such as cloud, rainfall and visibility will be introduced prior to the



operational implementation of the model on the Office's new Cray supercomputer. The model's forecasts are much appreciated by those forecasters who have already received them on a trial basis.

'The provision of sufficiently detailed input data for the model has posed special problems because the model's 15 km resolution is much finer than the distribution of observing stations. Also, some of the model's variables, such as the liquid water content of clouds, are not observed by the routine meteorological observing system. Dr Golding has conceived, designed and implemented a system which displays radar rainfall and satellite cloud pictures on a screen together with computer analyses of conventional observations. Forecasters are then able to interactively adjust and merge data from different sources to obtain the best possible initial conditions for the model. Both the model itself and the interactive initialization system provide the Meteorological Office with a facility that is unique in the world of meteorology.'

Award for Meteorological Observations — Mrs J. Harmer

The citation for this award was:

'Since Mrs Harmer joined the Meteorological Research Flight in 1983 she has made important contributions to the collection of airborne meteorological observations. She has flown many times as Flight Leader, co-ordinating the collection and verification of data from the aircraft instruments. This task demands persistent concentration and awareness in uncomfortable conditions. During the July 1988 detachment to Dakar, Senegal, she was Flight Leader on every mission, requiring intensive flying for long hours, and her consistently good performance was a large factor in the eventual success of the experiment. Mrs Harmer has also been responsible for the meticulous but essential task of maintaining the high quality of the measured data. This has culminated in the implementation of a new on-board system for displaying observations as they are taken, a project of considerable complexity which she developed herself using her knowledge and understanding of the aircraft



instruments and their operation. The main phase of the project was completed in 1988 and now provides a powerful tool for making and monitoring observations during flight.'

Reviews

Earth's changing climate and **Our drowning world** (second edition), by A. Milne. 142 mm × 223 mm and 134 mm × 215 mm, pp. 167 and 176, *illus.* Bridport, Dorset, Prism Press, 1989. Prices £12.95, \$17.95 and £5.95, \$10.95.

Environmental scientist Antony Milne's book *Earth's changing climate – the cosmic connection* is published simultaneously with the second edition of his earlier work *Our drowning world*. Both books are intended for a general readership.

Earth's changing climate aims to demonstrate the major effects of 'extra-terrestrial forces' and the role of both uniformitarian and catastrophic influences on earth's climate and history. The book is divided into three, somewhat blurred, sections which together cover magnetic influences, the Jupiter effect, the evolution of the sun, sunspots, the Milankovitch theory, volcanic forcing and impact extinction theories. There is no general introduction to climatic history or processes and it is hard for the general reader to distinguish between the different time-scales under discussion. The author himself seems somewhat confused about earth's history and what we do and don't know about different events. No distinction is made between, for example, the Pleistocene Ice Ages (which can be adequately explained by the Milankovitch theory) and those of the Pre-Cambrian.

Only in the Epilogue does the author admit that many of these 'entertaining and plausible' theories are speculative. Yet, on the same page, he claims they all

have a '50-50 chance of being correct'! The real problem with this book is that it is impossible for the reader to distinguish between theories which are (a) widely accepted, e.g. the Milankovitch theory, (b) controversial, e.g. the sunspot-climate link, and (c) wild flights of fancy, e.g. the effect of planetary alignments on human personality.

Similar problems beset *Our drowning world*, the sleeve-notes of which talk of an apocalyptic thesis. The first section of this book attempts to describe the environmental impacts of population and urban growth, atmospheric pollution (including ozone and CFCs), deforestation and the greenhouse effect. The concept of the greenhouse effect and the ability of scientists to predict its impacts are not particularly well described. The second section opens with a catalogue of recent extreme events and a brief discussion of two potential climate change mechanisms (orbital forcing and sunspots) before going on to consider the impacts of greenhouse-gas-induced warming on sea level. The societal impacts of large rises in sea level are then discussed at some length, while ecosystem impacts are given more cursory attention. This latter chapter closes with a description of future UK summers when, drawing a parallel with 1976, 'fewer British men will be growing beards or wearing ties'!

It could be argued that, in a popular text like this, the specialist should be prepared to accept some simplification and exaggeration and maybe even to tolerate some factual errors, but only up to a certain point. That point is overstepped many times in *Our drowning world*. In

chapter 9, for example, the author claims that there is a general consensus that sea level will rise by about 20 feet by 2100. Of which group this represents a general consensus I am not sure. Worse still, the same chapter includes two maps, not mentioned in the text, which show the extent of European and eastern USA flooding with sea level rises of 200 and 250 feet respectively! The factual errors become too numerous to ignore: the Laurentide ice sheet does not include the Fenno-Scandinavian (page 118), 1645–1715 is the date of the Maunder Minimum and not the Little Ice Age (page 98) ... and so on.

The general public are becoming more and more concerned about potential climate change and other environmental issues. In order to make fully informed decisions about energy policy and sensitive issues such as the defence or abandonment of coastal areas we need accessible, well written and researched, responsible books. Unfortunately *Our drowning world* is not one of these. This is perhaps not surprising given the list of references: this relies too heavily on newspaper and popular magazine articles and not on the best of the new scientific literature. Sea level rise is presented as an inevitable catastrophe about which we can do nothing. There seems little hope of early or successful international government action on environmental problems if this fatalistic view becomes widely held.

If I had to give one of these two books to a friend to read I'd pick *Earth's changing climate* and a large pinch of salt. It does at least give something of the feel of the complexities of the earth's climatic history and its future.

C. Goodess

Weather radar and the water industry, by the British Hydrological Society. 208 mm × 295 mm, pp. ii+91, *illus.* Wallingford, Oxfordshire, Institute of Hydrology, 1989. Price £12.00.

This Occasional Paper of the British Hydrological Society summarizes the proceedings of a meeting at which the state of the art of weather radar in the United Kingdom and its current and future use in the water industry were discussed. The meeting was organized by the Natural Environment Research Council (NERC) Steering Committee on Hydrological Applications of Weather Radar. Eight papers were presented by experts in rainfall data provision and application. They review investments and achievements to date and provide revised and new assessments of potential uses and benefits of radar data to the water industry in the 1990s.

In the first paper Collinge examines investment in the radar network by the water industry. Contrary to previous cost-benefit analyses Collinge includes both costs of research and development and of deferring benefit until adequate research is completed. Additional benefits such as reduced traffic dislocation and better flood warning are also included. From his study

Collinge suggests a new benefit/cost ratio of the radar network to the water industry of 3.0–3.5.

It is unusual in many radar texts to find a simple technical description of the radar system. However an excellent description of the principles, aims and limitations of the UK radar system is given by Lawler.

In the following two papers the uses of radar as a tool to measure and to assist in the forecast of precipitation are discussed. In an interesting and well written paper Moore considers measurement of precipitation by radar. He places particular emphasis on perceived problems with the existing radar measurements. He reviews recent investigations of local recalibration of radar, by telemetry gauge networks, prompted by the suggested accuracy requirements of the precipitation measurements used by the hydrological community.

The use of radar as a tool for short-period weather forecasting is examined by Collier. The most commonly employed short-period extrapolation techniques and associated problems are identified. Suggested future developments include using meteorological forecast model products such as storm-steering-level wind to improve storm extrapolation techniques. Assimilation of radar data into forecast models is also envisaged.

Many of the topics of the preceding two papers are considered within the context of flood warning by Haggett. He presents a brief outline of progress in this field from the Dee Weather Radar project in the 1960s to the establishment of the existing radar network. The recent trend towards quantitative requirements such as subcatchment totals is explored and expected growth areas of local calibration, short-period forecasting, snow measurements and distributed flow forecasting models are discussed.

In the following paper, Cluckie and Tyson explore further the potential for use of quantitative radar data in urban systems. A brief overview is given of three international projects associated with storm recognition and drainage management. Detailed summaries of progress in British research are provided. Particular attention is given to the use of *Wallingford Storm Sewer Package* (WASSP) and other drainage models and to the impact of intensity resolution of the input rainfall data to such models.

A complementary paper by Reed and Stewart considers rural storm hazard assessment. Good statistical analysis of storm hazard is required for engineering and environmental hazard assessment. After briefly describing the technique for return-period assessment commonly used, based on the *Flood Studies Report*, the authors highlight the problem of insufficient regional variation that can occur with this technique. An alternative method aimed at reducing the problem of spatial dependence in hydrological extremes is proposed. The role of radar is seen primarily as one of providing sub-daily rainfall at a higher resolution than is possible with the existing gauge network. The use of geostatistics in conjunction with radar is advocated.

In the final paper Walsh considers research needs and commercial opportunities for radar in the water industry. The NERC Radar Steering Committee has identified radar calibration, flow forecasting, urban applications and archiving as areas requiring research. The projects being undertaken under the first three topics are listed. The problem of establishing funding and instigating fundamental research in the United Kingdom within the next 5–10 years is highlighted. The paper ends with a series of challenging and important questions as to how investigations can be best organized to meet the research requirements and commercial opportunities of the next decade.

Published soon after the meeting, this document provides a valuable statement on the current state of development of radar and its use to the water industry. There is only slight overlap on basic points between papers. The content is primarily review material and speculation of future advances. It is well written with ample reference material. It provides useful information presented in a fairly simple way for anyone interested in the hydrological application of weather radar. The reader is given up-to-date information about successes and problems of radar use in the water industry. The challenge to use quantitative rainfall estimates in a wide range of applications must be met if the full benefit of radar is to be exploited. This document enhances appreciation of the scale of this challenge and of the resources required to face it.

M.F.Mylne

Noctilucent clouds, by M. Gadsden and W. Schröder. 157 mm × 240 mm, pp. ix+165, *illus.* Berlin, Heidelberg, New York, London, Paris, Tokyo, Hong Kong, Springer-Verlag, 1989. Price Dm. 138.00.

Noctilucent clouds — a new volume in the 'Physics and Chemistry in Space' series — is an excellent distillation of the history and science of this beautiful upper-atmospheric phenomenon by two internationally recognized scientists whose expertise and enthusiasm shine through the pages they have written. Their declared aim of bringing together in one volume a summary of present knowledge of noctilucent clouds has been successfully accomplished in an account that is both comprehensive and concise.

The introduction gives a good thumbnail sketch of the appearance and general properties of the clouds which should prove helpful to readers who are not familiar with the phenomenon. The different structural forms are classified and beautifully illustrated in a few well-chosen photographs. The clouds themselves are water-cluster-ions that condense out in a narrow range of heights at the temperature inversion close to the mesopause. 'Night luminosity' occurs when they are critically illuminated by sunlight from below the horizon during nautical twilight.

For the historian, there is a well illustrated section which considers possible sightings going back to the eighteenth century. Interesting though these are, they do not challenge the traditional view that Jesse (1885) was probably the first to recognize the true nature of the clouds and measure their height at 82 km. The classical optical methods used in later observing programmes elucidated the general conditions required for cloud formation, fixed their heights, established their velocities and thus gave much insight into atmospheric dynamics at these heights. They also elucidated the geometry of cloud illumination and showed that the screening height (the lowest height at which grazing sunlight can pass through the atmosphere) is sometimes as low as 7 km. While the above studies have defined most of the physical properties of noctilucent cloud, the authors stress that there is still no agreement about the size of cloud particles. Most spectrophotometric and polarimetric studies suggest a particle size of 0.13 μm or less, whereas some spectrophotometric and direct (rocket-borne) sampling studies indicate a particle size of 0.7–0.9 μm or more. The nature of the particle nucleus is also in doubt, there being no clear evidence whether these are solar ions, terrestrial dust or simply hydrated protons. Despite these difficulties, the authors have presented the evidence impartially with helpful summaries of current views at the end of appropriate chapters.

Having considered the physics and chemistry of noctilucent cloud as an entity, the authors turn their attention in the latter part of their account to other interacting environmental conditions and phenomena. Possible relationships with solar and lunar cycles, airglow, temperature, volcanoes, the underlying tropospheric weather and other phenomena are all considered in detail. These other phenomena include: the aurora, with which there may be an inverse relationship due to dissipation of noctilucent cloud as a consequence of mesopausal heating; internal gravity waves, which may play a major role in generating the wave-like structures in noctilucent cloud; and polar mesospheric clouds, which may be a precursor of noctilucent clouds. The possible role of noctilucent cloud as a sensitive indicator of long-term climatic changes, such as the greenhouse effect, is also noted. With the above exciting new developments in upper-atmospheric research, the appearance of this review is most timely for all with an interest in noctilucent cloud or related phenomena.

The book is well written and nicely produced. Its literary style is simple and lucid; its reading, easy and compelling. The bibliography is exhaustive, the index more than adequate and the text almost free from typographical error. The book is highly commended to all 'dedicated research workers, the interested scientist and the enthusiastic amateur' as a most readable and informative account of noctilucent cloud. It looks set to be a standard text on the subject for some years to come.

D.A.R. Simmons

Global climate change, edited by S.F. Singer. 155 mm × 235 mm, pp. vii+424, *illus.* New York, Paragon House, 1989. Price \$34.95.

When I started doing research on the 'greenhouse' effect, people's response to being told my job was often 'Yes, isn't acid rain awful?'. After a few years this became 'Yes, isn't the ozone hole awful?'. Now even the layman often seems to know the difference, so that I was rather surprised to find a Professor of Environmental Sciences using the title 'Global Climate Change' for a collection covering these and other disparate topics. There are even two chapters on 'nuclear winter' (remember that?), perhaps the most obviously dated — though in fact most of the contributions seem four or five years old. The piece I found most fresh was Rowland's on the ozone hole, first published in 1988, and written just as the current synthesis was becoming established. The contrast is marked with the editor's brief chapter following, which argues for the importance of solar cycles rather than CFC levels and predicts global ozone increases for 1987–90.

Professor Singer has chosen to have several of the contributions followed by 'commentaries'. This could be a useful way of exploring the uncertainties of current science, especially where strongly differing views are held by people who genuinely know a field, but it does require a reasonable knowledge of the area and the ability to commission pieces that will complement one another well. I found the results here inconsistent and unsatisfactory, especially where the book does discuss climate change. The mainstream view is represented by a chapter by Covey on the basics of climate modelling and one by Kellogg on the possible impacts of, and human response to, the predicted climate change due to increased CO₂. The latter does not discuss the physics involved, which makes the next contribution, a lengthy attack on the greenhouse consensus, seem a little out of place as a 'response to Kellogg's paper'. In this, Elsasser mixes statements about the uncertainties in climate modelling and the dangers of bandwagon science, which I trust most scientists in the field would sympathize with, and attacks on the science, or what he believes it to be. Printing this with a detailed refutation could have been an inter-esting didactic exercise complementing a straight presentation of the consensus, but the brief reply-to-the-response just makes some general statements about the complexity and reliability of modern models. An even briefer 'coda' re-emphasizes the uncertainties.

The other commentaries are all short, but have little else in common. One totally ignores the paper it is supposed to be about. Norton's response to Park's detailed description of ocean pollution does not disagree about facts, but shows more optimism about the current situation and the likelihood of action to improve it. Lal's chapter asserting the importance of volcanic and meteoritic dust to climate gets two commentaries, one

emphasizing the need for detailed and discriminating study but accepting the reality of such effects, and one arguing that there is no real evidence for their existence at all.

Elsewhere Cicerone provides a good review of atmospheric methane. Stanhill's overview of water management is very clearly written, and if his meteorology seemed perhaps vague at points, this is easily forgiven a man who cites the *Journal of Irreproducible Results*. Mellanby's brief review of acid rain is also very clear, despite emphasizing the complexities, as does Everett's description of surface-water acidification. Two chapters deal with the possibility of artificially mixing the Eastern Mediterranean sea surface to make it warmer in winter and increase rainfall downwind — not an idea I felt had been thought through very thoroughly.

Though I found some contributions well worth reading, and the book is well produced, I hesitate to recommend the collection as a whole. The environmental science student I assume it is aimed at could be harmed as much as helped, unless his reading was carefully directed by a good teacher — who could presumably garner a consistently good reading list at rather less expense. An established scientist wanting a review of an unfamiliar field could benefit from some chapters, but I imagine similar work is available elsewhere.

W.J. Ingram

Books received

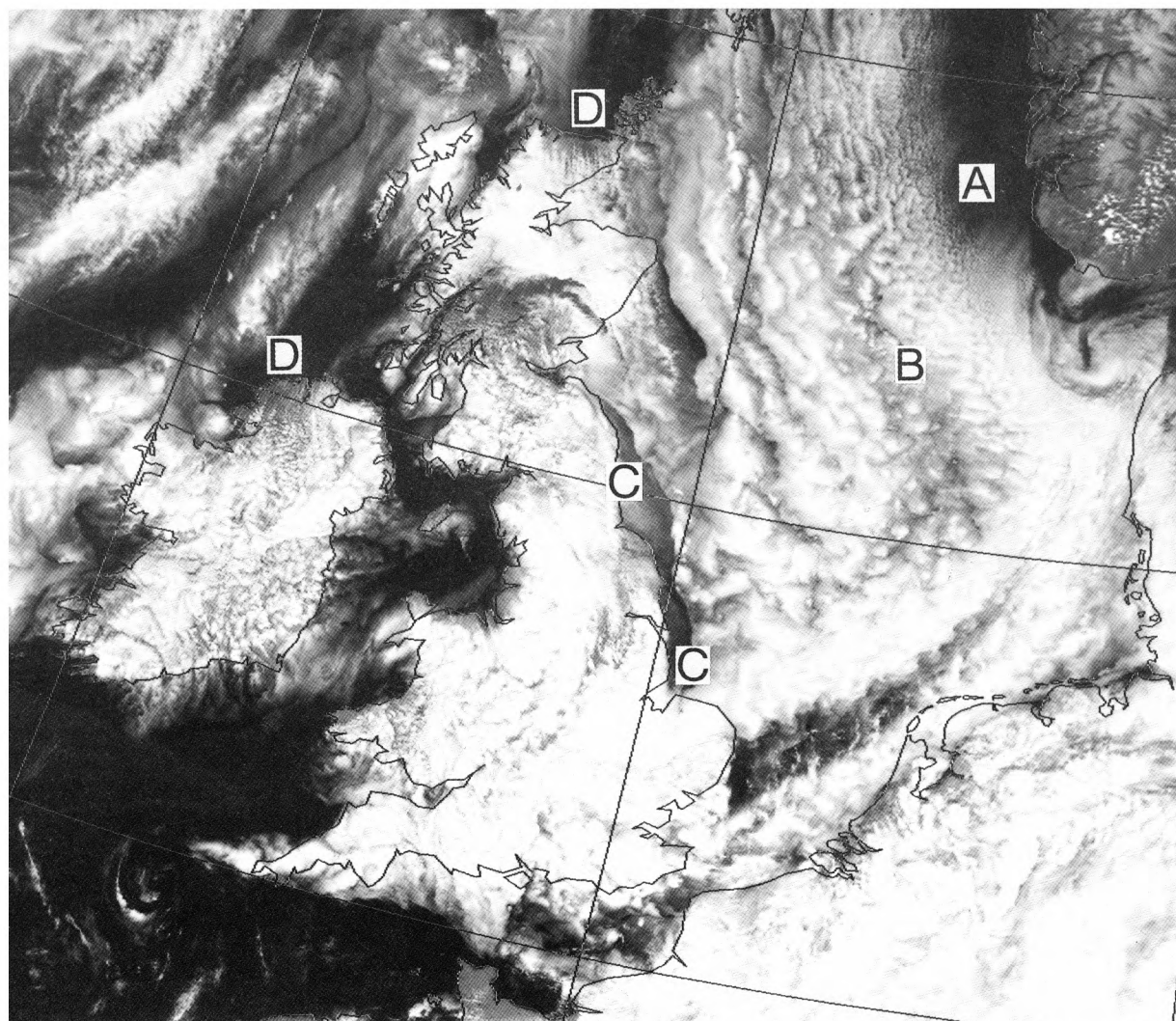
The listing of books under this heading does not preclude a review in the Meteorological Magazine at a later date.

Elementary fluid dynamics, by D.J. Acheson (Oxford University Press, 1990) presents the basic physics and mathematics of fluid motion in a form for newcomers to the subject. Topics covered include viscous and inviscid flow, vorticity, waves, aerofoil theory and boundary layers.

Applied environmental meteorological tables, by T. Beer (Balwyn, Melbourne, Applied Environmetrics, 1990) contains a variety of tables for meteorological use (on an accompanying disk). The 5.25-inch disk will run on IBM compatible computers which has DOS 2.10 or later and at least 256K of RAM.

Climatic atlas of the Indian Ocean. Part III: Upper-ocean structure, by S. Hastenrath and L.L. Greischar (The University of Wisconsin Press, 1990) contains calendar monthly maps of various oceanic parameters at standard depth levels. This third volume is intended as a further contribution to the exploration of ocean climate.

Satellite photograph — 13 June 1990 at 1330 UTC



Photograph by courtesy of University of Dundee.

Figure 1. NOAA-11 visible image on 13 June 1990 at 1330 UTC. The labelling A–D is referenced in the text.

The NOAA-11 AVHRR visible image shown here (Fig. 1) was taken during a period of cool northerly winds and generally persistent cloud cover over the British Isles and North Sea (Fig. 2).

Convection was limited by a marked subsidence inversion near 850 hPa with the cloud a combination of shallow cumulus and more extensive sheets of strato-cumulus. Considerable detail can be seen in the scale of cellular convection. Note the increase in cell size from A to B over the North Sea. Marked variations in cloud thickness can also be clearly discerned. The band of much thinner and less textured cloud near the east coast at C may be due to low-level divergence and sinking motion induced by the land–sea temperature contrast.

Overland, narrow cumulus streets can be seen at D aligned with the low-level northerly flow.

A.J. Waters

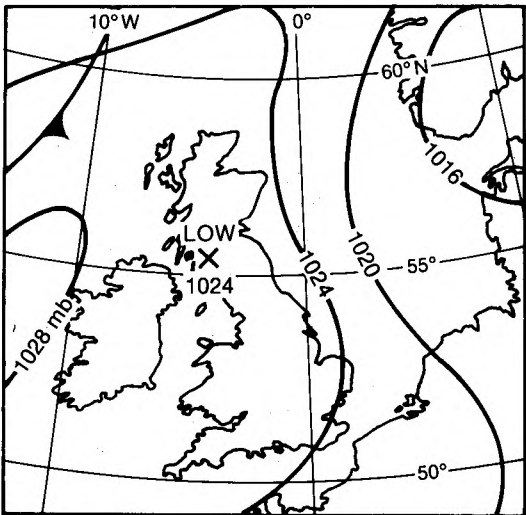


Figure 2. Surface analysis on 13 June 1990 at 1200 UTC.

GUIDE TO AUTHORS

Content

Articles on all aspects of meteorology are welcomed, particularly those which describe results of research in applied meteorology or the development of practical forecasting techniques.

Preparation and submission of articles

Articles, which must be in English, should be typed, double-spaced with wide margins, on one side only of A4-size paper. Tables, references and figure captions should be typed separately. Spelling should conform to the preferred spelling in the *Concise Oxford Dictionary* (latest edition). Articles prepared on floppy disk (Compucorp or IBM-compatible) can be labour-saving, but only a print-out should be submitted in the first instance.

References should be made using the Harvard system (author/date) and full details should be given at the end of the text. If a document is unpublished, details must be given of the library where it may be seen. Documents which are not available to enquirers must not be referred to, except by 'personal communication'.

Tables should be numbered consecutively using roman numerals and provided with headings.

Mathematical notation should be written with extreme care. Particular care should be taken to differentiate between Greek letters and Roman letters for which they could be mistaken. Double subscripts and superscripts should be avoided, as they are difficult to typeset and read. Notation should be kept as simple as possible. Guidance is given in BS 1991: Part 1: 1976, and *Quantities, Units and Symbols* published by the Royal Society. SI units, or units approved by the World Meteorological Organization, should be used.

Articles for publication and all other communications for the Editor should be addressed to: The Chief Executive, Meteorological Office, London Road, Bracknell, Berkshire RG12 2SZ and marked 'For Meteorological Magazine'.

Illustrations

Diagrams must be drawn clearly, preferably in ink, and should not contain any unnecessary or irrelevant details. Explanatory text should not appear on the diagram itself but in the caption. Captions should be typed on a separate sheet of paper and should, as far as possible, explain the meanings of the diagrams without the reader having to refer to the text. The sequential numbering should correspond with the sequential referrals in the text.

Sharp monochrome photographs on glossy paper are preferred; colour prints are acceptable but the use of colour is at the Editor's discretion.

Copyright

Authors should identify the holder of the copyright for their work when they first submit contributions.

Free copies

Three free copies of the magazine (one for a book review) are provided for authors of articles published in it. Separate offprints for each article are not provided.

August 1990

Editor: F.E. Underdown

Editorial Board: R.J. Allam, R. Kershaw, W.H. Moores, P.R.S. Salter

Vol. 119

No. 1417

Contents

	Page
Numerical weather prediction model performance on instant occlusion developments. J.B. McGinnigle	149
Developments in meteorological telecommunications. S.M. Long	164
Awards	
L.G. Groves Memorial Prizes and Awards for 1988	171
Reviews	
Earth's changing climate and Our drowning world. A. Milne. C. Goodess	172
Weather radar and the water industry. British Hydrological Society. M.F. Mylne	173
Noctilucent clouds. M. Gadsden and W. Schröder. D.A.R. Simmons	174
Global climate change. S.F. Singer (editor). W.J. Ingram	175
Books received	175
Satellite photograph — 13 June 1990 at 1330 UTC A.J. Waters	176

Contributions: It is requested that all communications to the Editor and books for review be addressed to the Chief Executive, Meteorological Office, London Road, Bracknell, Berkshire RG12 2SZ, and marked 'For *Meteorological Magazine*'. Contributors are asked to comply with the guidelines given in the *Guide to authors* which appears on the inside back cover. The responsibility for facts and opinions expressed in the signed articles and letters published in *Meteorological Magazine* rests with their respective authors.

Subscriptions: Annual subscription £30.00 including postage; individual copies £2.70 including postage. Applications for postal subscriptions should be made to HMSO, PO Box 276, London SW8 5DT; subscription enquiries 071-873 8499.

Back numbers: Full-size reprints of Vols 1-75 (1866-1940) are available from Johnson Reprint Co. Ltd, 24-28 Oval Road, London NW1 7DX. Complete volumes of *Meteorological Magazine* commencing with volume 54 are available on microfilm from University Microfilms International, 18 Bedford Row, London WC1R 4EJ. Information on microfiche issues is available from Kraus Microfiche, Rte 100, Milwood, NY 10546, USA.

ISSN 0026-1149

© Crown copyright 1990. First published 1990

ISBN 0-11-728668-0



The Meteorological Magazine

September 1990

The Great Storm: passive microwave evaluations
Heavy mesoscale snowfall in northern Germany



DUPLICATE JOURNALS

National Meteorological Library
FitzRoy Road, Exeter, Devon. EX1 3PB

HMSO

Met.O.992 Vol. 119 No. 1418



3 8078 0010 2464 7

The Meteorological Magazine

September 1990
Vol. 119 No. 1418

551.501.795:551.515.12:551.553.8(261.2+261.26+41): 551.577.37:551.465.75

The Great Storm of 15/16 October 1987: passive microwave evaluations of associated rainfall and marine wind speeds

E.C. Barrett, C. Kidd, and J.O. Bailey

Remote Sensing Unit, Department of Geography, University of Bristol

C.G. Collier

Meteorological Office, Bracknell

Summary

The Special Sensor Microwave Imager (SSM/I) carried by current US military meteorological satellites has proven capabilities for the evaluation of several weather and weather-related parameters, including instantaneous rain areas and rain rates, and marine wind speeds. Analyses of SSM/I data for the British Isles and surrounding waters from 15–16 October 1987 throw new light upon the Great Storm at its peak intensity, and raise the possibility of improved forecasting of such events in the future.

1. Introduction

Much has already been written on the Great Storm which struck southern Britain on the night of 15/16 October 1987 (see Fig. 1 for synoptic charts). At least 18 people lost their lives as a direct result of the gale, hundreds of millions of pounds worth of damage resulted, and millions of trees were blown down in what the Home Secretary described as ‘...the worst, most widespread night of disaster in the south-east of England since 1945’. In one sense the extreme events of January/February 1990 have since at least partially diverted attention from the Great Storm of 1987, but in another sense these subsequent events have only heightened interest in, and concern for, severe events of this nature. It is therefore even more important than before that such events should be studied in as much detail as possible, and using all the facilities at our disposal. Clearly meteorological satellites have an important part to play in helping to evaluate and

forecast potentially dangerous weather systems approaching the British Isles from the North Atlantic. The use of NOAA, and more particularly Meteosat, satellite data in these respects is by now well established and widely appreciated. Fortunately, the technology of meteorological satellites is not standing still, and recent advances in satellite instrumentation are opening up new possibilities of monitoring features of North Atlantic depressions which were previously not amenable, or easily amenable, to elucidation using satellite data. This paper seeks to present some new information concerning the Great Storm of 15/16 October 1987, as seen by the newest member of the US Military Defense Meteorological Satellite Program (DMSP) satellite family, through the eyes of its Special Sensor Microwave Imager (SSM/I), the newest and most promising passive microwave imaging radiometer (see Barrett *et al.* 1988).

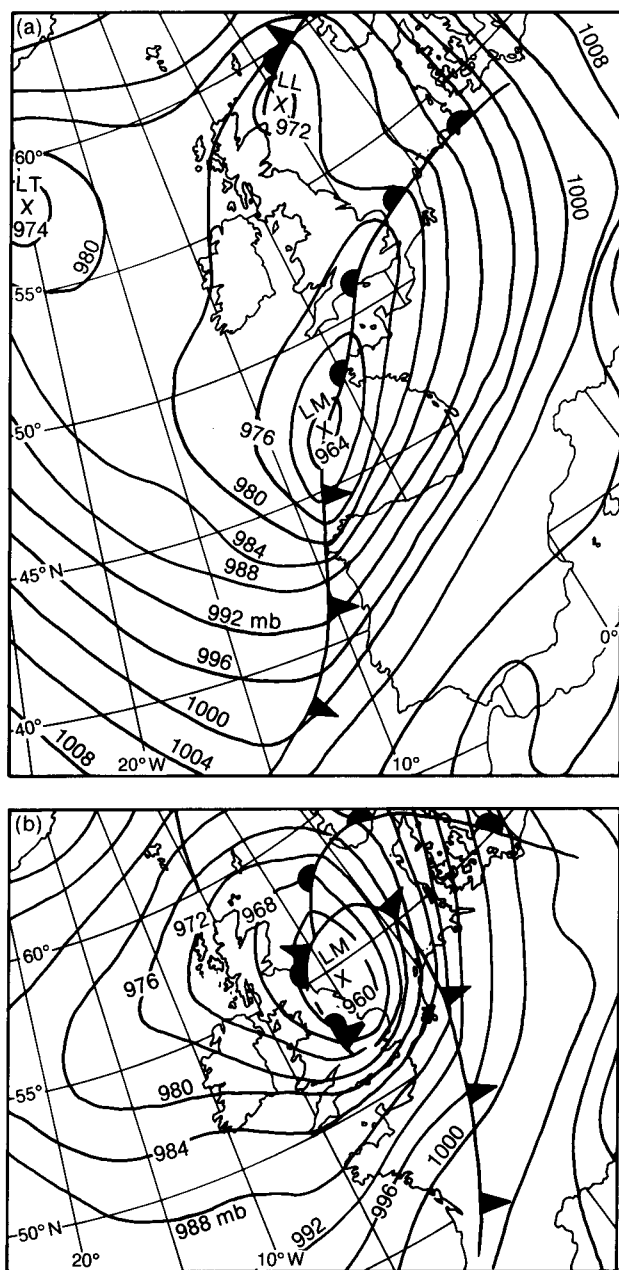


Figure 1. Synoptic weather maps for (a) 1800 UTC on 15 October 1987, and (b) 0600 UTC on 16 October 1987.

2. Satellite passive microwave radiometers

Table I gives details of those satellite microwave imaging instruments which have flown on meteorological satellites since the early 1970s, and have provided data to which the general scientific community has had at least some access. Of these, the first three (ESMR-5, ESMR-6 and SMMR) all flew on Nimbus satellites, and all are now defunct. However the fourth (the SSM/I), part of the payload of the current DMSP Block 5D-2 spacecraft F8, is both currently functional, and a significant advance over previous passive microwave imaging instruments. Launched on 19 June 1987, this DMSP satellite occupies a circular, sun-synchronous near-polar orbit at an altitude of 833 km, with an inclination of 98.8° to the equator, and an orbital period

of 102.0 min. The satellite has an ascending node equatorial crossing time of 06.12 hrs, and provides an observation swath width of 1394 km. The SSM/I instrument, as detailed in Table I, is a standardized channel, 4-frequency, linearly polarized, passive microwave radiometric system (Hollinger *et al.* 1987). Built by the Hughes Aircraft Company under the direction of the US Naval Space Systems Activity and the US Air Force Space Division, the SSM/I was designed primarily to support operational environmental products prepared by the US Fleet Numerical Oceanography Command and the US Air Force Weather Center. Fortunately, despite the military origin of SSM/I, its data are being archived by the Satellite Data Services Division of NOAA/NESDIS (National Environmental Satellite and Data Information System), from whence they will soon be available to the general scientific community for research and algorithm development. In the meantime, quantities of SSM/I data have been made available to the Remote Sensing Unit in the University of Bristol (RSUUB) under a co-operative agreement between them and NOAA/NESDIS (Satellite Applications Laboratory), and under the auspices of the NASA-led WetNet project, in which the RSUUB is involved.

The SSM/I represents an advance over previous instruments in that it is the first sensor equipped to monitor in the 85.5 GHz region, it has a much broader swath width than previous instruments, it is in continuous operation, its data have been more directly calibrated, its feed horn antenna are in synchronous rotation (eliminating the need for polarization rotation corrections), its noise levels are lower, and the footprints from all its channels enjoy co-aligned sampling.

It will be seen from Table I that the SSM/I is intended for use in respect of a variety of meteorological and geophysical parameters, including ocean wind speed and intensity of precipitation. Whilst the earliest studies based upon the SSM/I in the RSUUB have focused primarily upon rainfall (e.g. Kidd *et al.* 1989), this paper seeks to explore the value of the instrument for both wind speed and rainfall estimation in the vicinity of the British Isles for extreme weather conditions using the Great Storm of October 1987 as an interesting test case. Fig. 2 presents false-colour images of the Great Storm using yellow, green and blue to represent vertical polarization data (V), horizontal polarization data (H), and the vertical minus horizontal polarization difference, respectively, all at 85.5 GHz.

3. Application of an SSM/I wind-speed algorithm

Extraction of the wind-speed parameter from passive microwave radiometer data was discussed in Munn (1978) and Swift (1977) where it is demonstrated that wind speeds near the ocean surface can be remotely sensed by both scatterometers and microwave radiometers, in the first case by measuring the component of transmitted power that is back-scattered from the ocean

Table I. Satellite passive microwave imaging instruments (from Bailey *et al.* 1986)

Instrument	ESMR-5	ESMR-6	SMMR	SSM/I
Spacecraft launch date	Nimbus-5 December 1972	Nimbus-6 June 1975	Nimbus-7/Seasat October/June 1978	DMSP 5D-2/SX June 1987
Frequencies/ footprint sizes				
6.6 GHz	—	—	VH 121 × 79 km	—
10.7 GHz	—	—	VH 74 × 49 km	—
18.0 GHz	—	—	VH 44 × 29 km	—
19.35 GHz	X 25 × 25 km	—	—	VH 69 × 43 km
21.0 GHz	—	—	VH 38 × 25 km	—
22.235 GHz	—	—	—	V 50 × 40 km
37.0 GHz	—	VH 25 × 45 km	VH 21 × 14 km	VH 37 × 28 km
85.5 GHz	—	—	—	VH 15 × 13 km
Primary aims of mission	Liquid water contents of clouds, sea ice and open sea coverage. Surface composition and soil type, with surface features and surface moisture.		Sea surface temperature, near sea surface winds. Water vapour, liquid water content and cloud droplet size. Rainfall rate.	Ocean wind speed and ice coverage, age, and extent. Intensity of precipitation, cloud water content and land surface moisture.

Key: ESMR = Electrically Scanning Microwave Radiometer, SMMR = Scanning Multi-channel Microwave Radiometer, SSM/I = Microwave Imager, V = vertical polarization, H = Horizontal polarization, and X = non-polarized.

surface, and in the second by measuring radiation naturally emitted from the ocean surface. Both the back-scattered radiation and emitted radiation are affected directly by ocean surface roughness, which is, in turn, related to the near-surface wind speed.

Detailed empirical work has been reported by Wentz *et al.* (1986) in which wind speed results were obtained from a Seasat scatterometer algorithm and compared with wind speed measurements from US National Data Buoy Office buoy observations. A total of 1623 buoy wind speed/Seasat results were compared, and the agreement was such that an r.m.s. discrepancy of only 1.6 m s^{-1} was found. The correlation coefficient of 0.89 suggested a high level of association between the two variables despite such factors as temporal and spatial sampling problems. These results were then used to assess the performance of a brightness temperature (T_b) model based on Nimbus-7 Scanning Multi-channel Microwave Radiometer (SMMR) data. Wentz cites the results of 123 000 wind-speed comparisons between the two methods for T_b algorithms using different channel combinations, for which he found generally good agreements. For the most favourable channel combinations, this agreement was broadly within 1.3 m s^{-1} . Taking into account the improvements in design that were to be incorporated in the SSM/I microwave radiometer, Wentz confidently predicted that, using appropriate channel combinations, near-surface wind speeds should be determinable usually to within 2 m s^{-1} with the new instrument.

The SSM/I wind-speed extraction algorithm of Hollinger *et al.* (1987) (portrayed in Fig. 3), which includes different weights for different latitudes and seasons of the year, fulfils Wentz's expectations. Based on the 19H, 22V, 37V and 37H channel data (19H, 22V, etc. are channel reference numbers) with a spatial resolution of 25 km and a range of values from $3\text{--}25 \text{ m s}^{-1}$, the Hollinger algorithm yields wind-speed products with a claimed accuracy of $\pm 2 \text{ m s}^{-1}$. Early analyses of SSM/I wind speed algorithm outputs by Wentz (personal communication) using this algorithm confirm that results obtained have indeed been to this general level of accuracy.

There are, however, reasons to believe that because of a number of physical conditions, properties and associated processes, care must be taken in the application of the SSM/I algorithm for wind speed. As early as 1971 Nordberg, using data from the SMMR on a Nimbus-7, indicated that even over open water the T_b value is affected by a number of factors, especially the ocean surface emissivity E , and that changes in E were non-linear with respect to wind speed because the T_b value measured by the satellite is affected by both the wind-induced surface roughness, and the presence of foam at the surface (Nordberg *et al.* 1971). Nordberg's results suggested that the T_b increased linearly with wind speeds above 7 m s^{-1} , mainly due to the presence of foam, whilst below 7 m s^{-1} no foam forms. The relationship of wind speed to T_b observed by Hollinger using SSM/I data is shown in Fig. 3. Since ship-borne

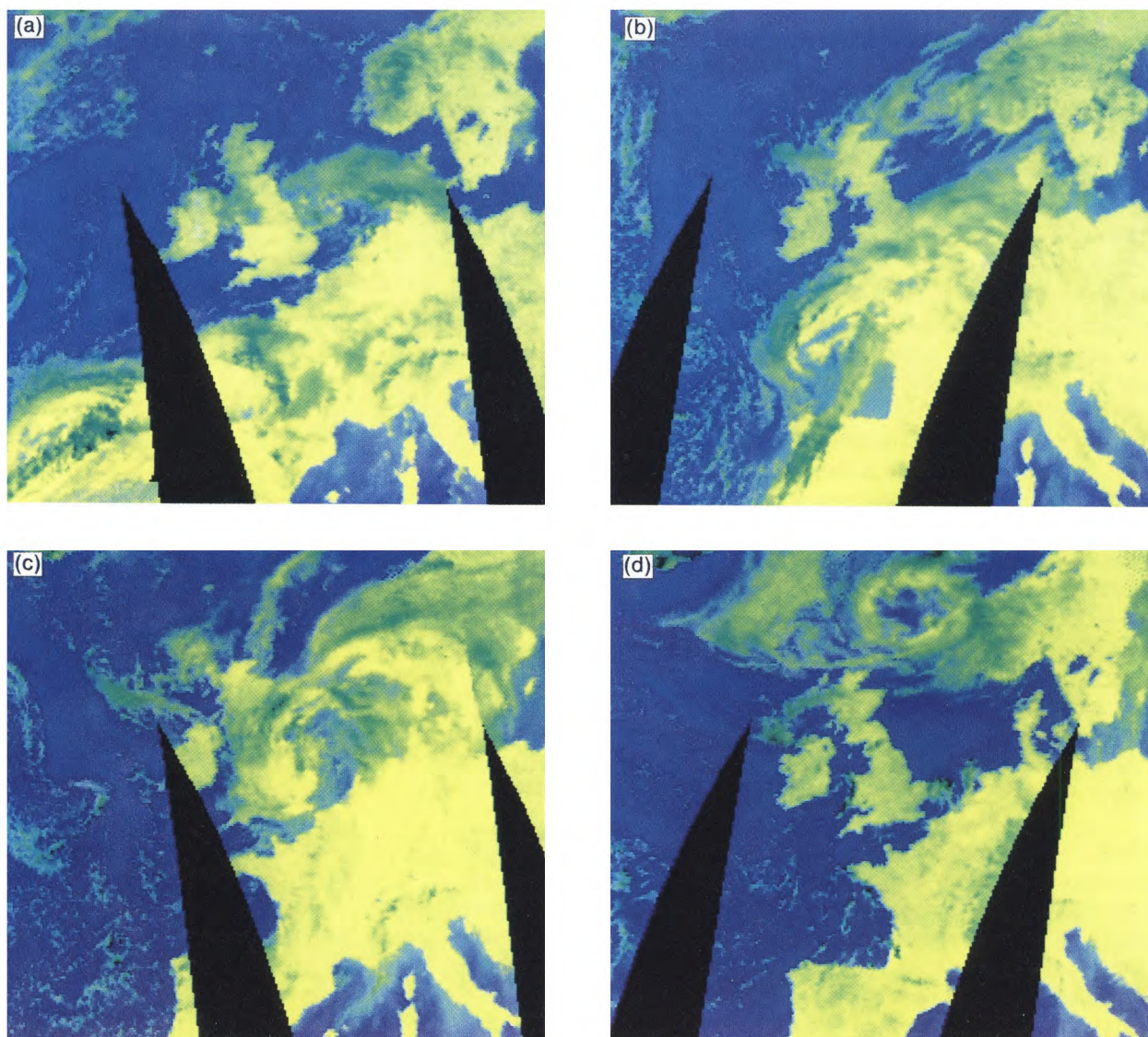


Figure 2. False-colour images of SSM/I swaths for (a) the evening of 15 October, (b) the morning of 16 October, (c) the evening of 16 October, and (d) the morning of 17 October, showing stages in the development and dissipation of the Great Storm as it moved north-east from the Bay of Biscay, across the British Isles, to the north-east of Scotland. Green areas are mainly hydrometeors and the most likely to be precipitating; cloud cover on all four occasions was much broader than the areas of hydrometeors.

wind measurements are standardized to a height of 20 m above the ocean surface, whereas the microwave observation is for the ocean-air interface, Hollinger *et al.* (1987) sought to extrapolate from the surface measurement of the SSM/I to a height of 20 m using a relationship developed by Cardone (1969).

Further complications are likely where radiometer cell values are contaminated by the presence of land or sea-ice; indeed, at present it seems prudent not to attempt wind-speed estimation in cells containing either of these features. Further, it has been suggested that when rain occurs wind speed estimates may be in error (Wentz 1988), although the degree to which the wind speed estimate is degraded by rain is still uncertain. In view of the physical principles underpinning the algorithm in question, it seems likely that useful wind-speed estimates should be obtainable, at least providing rain is light.

Notwithstanding the above problems, all of which call for detailed future examination, wind-speed products have been prepared using the image processing system in the RSUUB for the evening of 15 October 1987, and the morning of 16 October 1987. The mid-latitude spring/autumn relationships in the Hollinger algorithm have been used, the winds being contoured in knots to facilitate intercomparisons with numerical weather analyses, as presented and discussed below. The results are shown in Fig. 4. In Fig. 4(a) the highest values appear in the Bay of Biscay, reaching over 61 kn in places. High wind speeds are evident in some windward coastal regions, including the west coast of France, the Strait of Dover, and even parts of the west coast of Norway. The lowest wind speeds (below 20 kn) are found to the south-west of Ireland, corresponding with the location of the weak col in that position at that time. In Fig. 4(b), by which time the Great Storm vortex

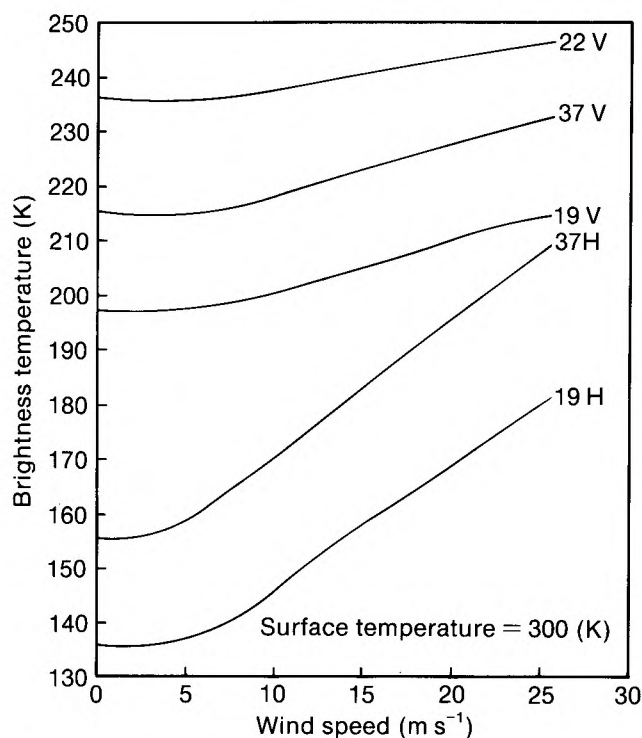


Figure 3. The relationship between wind speed and the SSM/I-derived brightness temperatures, for various channels, as found by Hollinger *et al.* (1987).

centre was over the north-eastern Midlands, wind speeds had increased along the North Sea coasts of England and Scotland, very locally seeming to exceed 61 kn in The Wash and off the Forth Estuary. The maps in Fig. 5 are constructed in the RSUUB from the Meteorological Office fine-mesh model wind analyses for 18 UTC on 15 October (Fig. 5(a)), and 06 UTC on 16 October (Fig. 5(b)) for times approximately one hour before the evening SSM/I overpass, and one hour after the morning SSM/I overpass respectively.

Allowing for the time differences between the model and satellite products, an intercomparison of Figs 4 and 5 reveals the following:

(a) The ranges of wind speeds from the analytical model and the satellite image analyses are similar, the model maxima being in excess of 50 kn compared with the satellite maxima in excess of 60 kn; the satellite minima are also generally higher (sometimes considerably higher) than the model minima especially near centres of positive vorticity.

(b) The model and satellite patterns of wind speeds for the evening of 15 October show many general similarities, including maxima in the Bay of Biscay, the southern North Sea, and in the region of Orkney and Shetland, and minima to the west of Ireland and the east of Scotland and north-east England. However, relative differences occur over some large areas, e.g. the southern North Sea versus the region of Orkney and Shetland (the model evaluating the

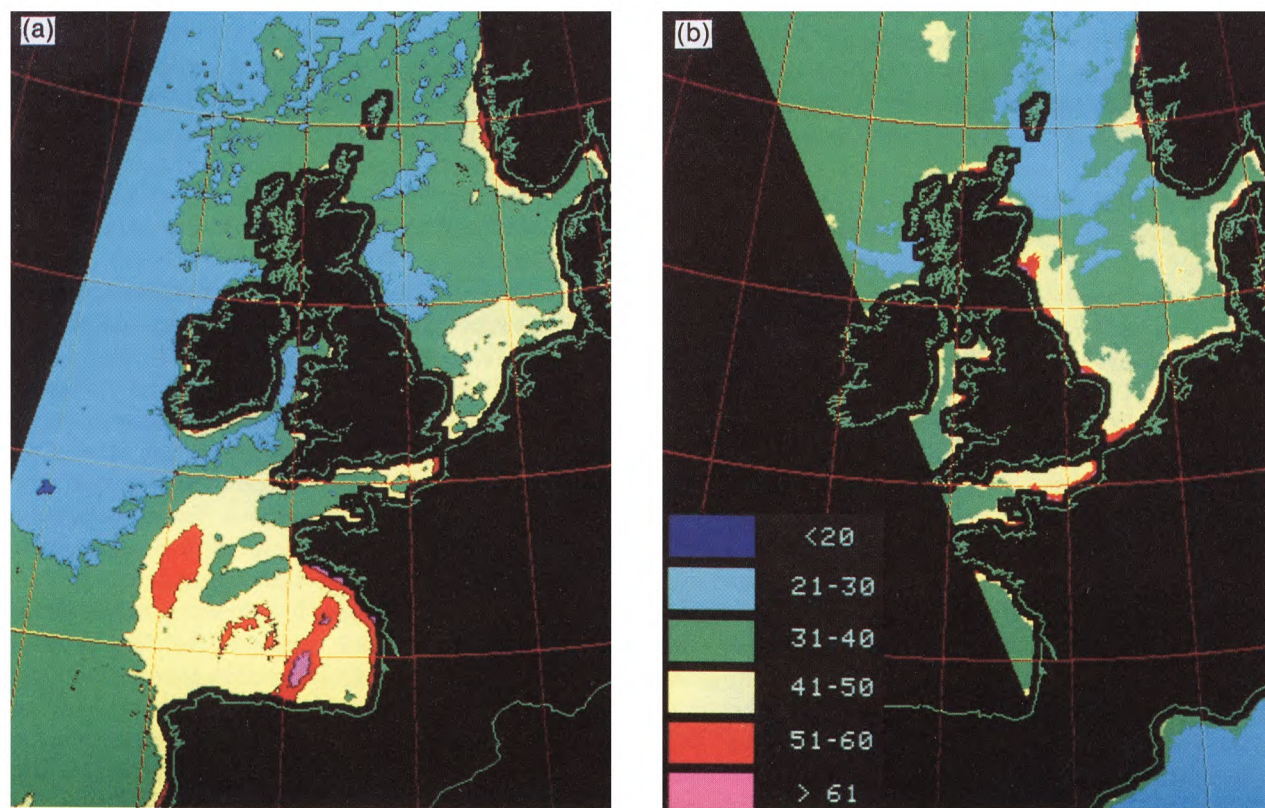


Figure 4. SSM/I-derived wind speeds (kn) for the seas surrounding the British Isles on (a) 15 October at approximately 1900 UTC, and (b) 16 October at approximately 0500 UTC, using the Hollinger *et al.* (1987) algorithm for mid-latitude in spring/autumn.

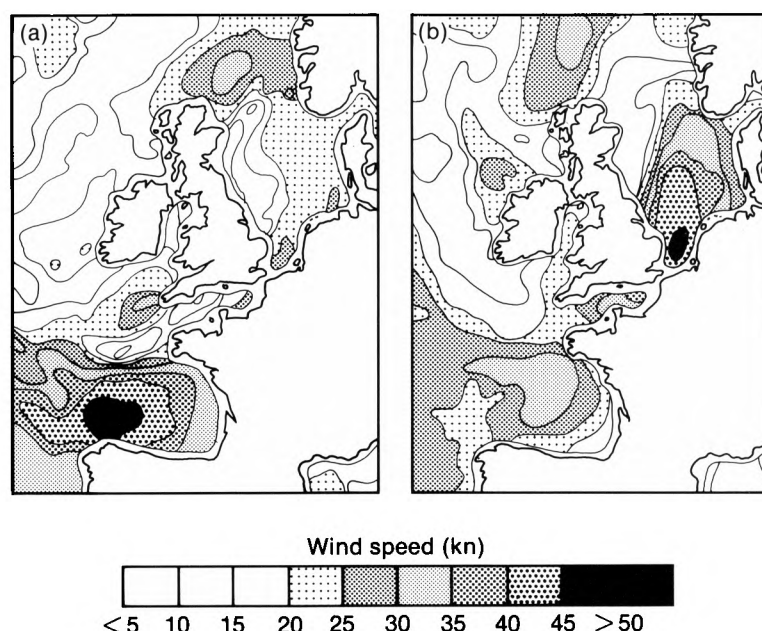


Figure 5. Wind speeds (kn) for (a) 18 UTC on 15 October, and (b) 06 UTC on 16 October 1987, compiled from the Meteorological Office fine-mesh model.

former as the windier of the two, whilst the satellite suggests the reverse relationship). Further, quite strong detail differences occur in a few areas, e.g. the Strait of Dover and the exposed coasts of western France, where the satellite estimates are more than double the model estimates.

(c) The model and satellite patterns of wind speeds for the morning of 16 October show more differences than (b), the satellite estimates again tending to be generally higher, although the model gives higher wind speeds in the southern North Sea. Otherwise the most notable difference perhaps is in the Forth Estuary region, where the model suggests light onshore winds and the satellite strong winds. It seems likely that the one-hour lag between the satellite image and the model outputs has been more obviously important in this case, for within that hour the area of maximum wind speed seems to have moved from the land into the southern North Sea.

4. Application of an SSM/I rainfall algorithm

It is now well known that, at certain frequencies, passive microwave radiation from the earth-atmosphere system relates to hydrometeors in the atmosphere, permitting estimation of instantaneous rain-rates (see Barrett and Martin 1981). Because the physical relationships between the radiation observed by the satellite and the precipitation process are more direct in the case of passive microwave than visible and/or infra-red radiation observed from satellite altitudes, it is expected that passive microwave sensors such as SSM/I will prove much better for rainfall monitoring than any visible and/or infra-red sensors, which are only able to observe radiation reflected or emitted from cloud tops.

Early work based upon SMMR imagery was undertaken by Wilheit *et al.* (1977) who calculated radiative properties of hydrometeors in the atmosphere, and Savage (1978) who computed the radiative properties of hydrometeors at microwave frequencies from 20 to 183 GHz. As a result of these works, and others which have added further detail, it is now recognized that rain areas can be detected by passive microwave imagery within the region from about 6 to 90 GHz. This is the result of absorption and emission from raindrops below about 22 GHz, by the scattering from larger particles, raindrops and/or ice crystals above about 60 GHz, and by either or both processes between 22 and 60 GHz as determined by the actual occurrence, nature and quantity of both liquid droplets and ice particles (Bailey *et al.* 1986).

Investigations into rainfall monitoring using passive microwave image data were first concentrated over the oceans. Here the water surface provides a low background temperature which is essentially uniform, for the emissivity and absolute temperature of ocean surfaces are inversely proportional to each other. Over such areas, at low frequencies, the presence of precipitation causes an increase in the T_b because of emission from water droplets in the atmosphere, producing 'warm' islands seen against 'cold' ocean surfaces. Indeed, it has been found that, for a wide range of over-water rain-rates, there is an almost linear relationship between rain-rates and observed T_b values. Therefore, it has proved possible to develop simple algorithms for rainfall retrieval over oceans using data at frequencies less than 22 GHz. The most extensive work of this nature was undertaken by Rao (1984), who had produced a global atlas of oceanic precipitation (Rao *et al.* 1976) based on data from the Nimbus-5

Electrically Scanning Microwave Radiometer, which operated at 19.35 GHz. The spatial resolution of the atlas maps is 1° lat \times long. Despite the limitations of the SMMR instrument Rao felt able to conclude even at that early stage that '...in spite of various drawbacks, the microwave radiometer is at present indeed the best available means for estimating oceanic rainfall on a world-wide scale'.

Since then, the physical understanding of the relationships between hydrometeors in the atmosphere and microwave radiation measured by satellites has been further advanced particularly by Wu and Weinman (1984), through their studies of the effects of hydrometeor types, including aspherical ice, combined phase and liquid hydrometeors, and by Grody (1984), Spencer *et al.* (1983), and Spencer (1984) who pioneered the development of algorithms for passive microwave evaluation of rainfall over land as well as water, using higher-frequency data from the SMMR sensor on Nimbus-7.

The retrieval of rain over land, including land/sea mixed pixels, has proven more problematic than the retrieval of rain over water, primarily because the emissivity is generally high (and similar to that of precipitation), and very variable. However, despite many difficulties, even single passive microwave channel brightness temperatures may be used for rainfall identification over land, especially in the scattering region, if precipitation is relatively heavy. In these cases, especially at higher frequencies, some of the upwelling radiation stream from the surface is scattered by the precipitation, and a decrease in brightness temperature is observed by the satellite in the presence of rainfall. Spencer *et al.* (1983) suggested that, at 37 GHz, the scattering due to precipitation may be sufficient to lower the brightness temperatures to an asymptotic level of 230 K at 20 mm h^{-1} . Brightness temperatures as low as 163 K have been reported in extreme cases. However, perhaps the most useful approach so far to rainfall monitoring in the passive microwave over land has involved frequency differencing. The frequency algorithm of Grody (1984) uses two frequencies but like polarizations for rainfall-area delineation through the subtraction of the higher frequency brightness temperature from the lower frequency brightness temperature. Unfortunately, in general, such an approach can only be applied over land, although it is sometimes useful over water where heavy and very heavy rainfall is involved.

A second approach to rainfall monitoring over land involves the exploitation of polarization principles, through which radiation of a single frequency can be exploited, taking account of its horizontal and vertical polarization. It has been shown by Grody (1984) that, by using a proportion of each polarization, background characteristics can be subdued, even where these are complex, leaving attenuation by the atmosphere as the major influence on the signal. The polarization approach has been tested over both land and water. However, the

consensus of opinion based on SMMR data analyses was that, over land, the use of polarization algorithms was less successful than that of frequency algorithms. Further, in the case of the polarization algorithms, the choice of rain/no-rain threshold was always subjective.

Recently, research in the RSUUB, supported by NOAA, the Meteorological Office, and the US Universities Space Research Association, has involved a combination of frequency and polarization approaches so that rain/no-rain boundaries might be established objectively for both frequency and polarization approaches, and so that radar might be used for rain/rain-rate calibration, and verification of results. In the RSUUB approach, a frequency algorithm and a polarization technique have been applied simultaneously over land. The purpose for this is two-fold: to generate rain areas and rain-rates for overland areas from the frequency algorithm, because SMMR-based research showed that 37–18 GHz frequency algorithms generally out-performed 37 GHz polarization algorithms over land; and second, to use the outputs from the frequency algorithm to help set objective rain/no-rain boundaries for the polarization technique, so that this technique could be used to produce realistic rain areas and rain-rates over neighbouring sea areas where the frequency approach is unrealistic.

Fig. 6 demonstrates the identified relationship between the brightness temperature difference of a frequency algorithm, and the polarization-corrected temperatures of a polarization algorithm for a test period in 1987. By projecting a line upwards from the zero point on the ordinate (line a) and calculating the best-fit regression through the distribution of points (line b), the rain/no-rain boundary of the polarization algorithm can be identified by the horizontal line c which passes through the point at which lines a and b intersect. Using this approach in relation to a large number of case-studies, verification statistics for satellite passive microwave versus radar rain/no-rain pixel classification have generally revealed a correspondence of about 95% (Barrett and Kidd 1989).

Figs 7(a) and 7(b) were produced for the evening of 15 October 1987 and the morning of 16 October 1987, respectively, using the combined frequency/polarization approach described above. Fig. 7(a) indicates heavy rain south-west of Cornwall with instantaneous rain rates as high as 64 to 128 mm h^{-1} on the eastern fringes, whilst over Spain even higher rainfall rates are indicated. By the morning of 16 October 1987 as shown by Fig. 7(b), when the centre of the Great Storm low-pressure system had crossed the United Kingdom to lie just off the Humber Estuary, the satellite detects an area of rain curving in an anticlockwise arc from the Scottish lowlands, across the Irish Sea and the Bristol Channel and into the Thames Valley. Another area of heavy rain is indicated off the east coast of Scotland with associated rainfall rates of up to 64 mm h^{-1} . In the centre of the North Sea, rain rates of up to 32 mm h^{-1} are observed.

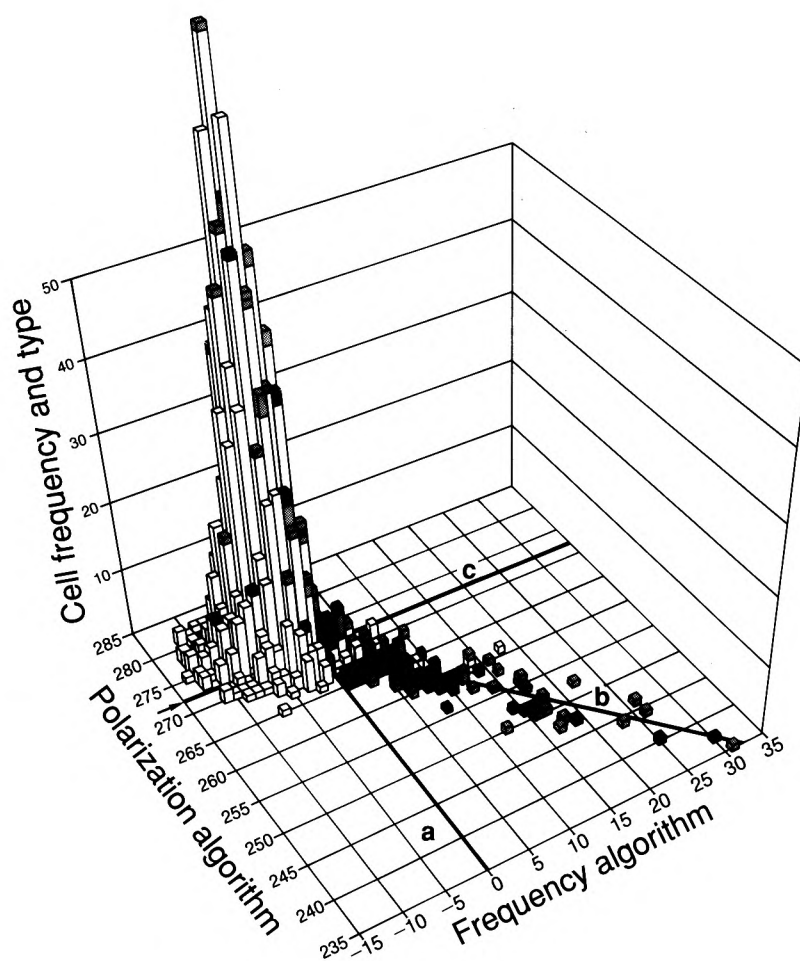


Figure 6. The basis of the Barrett and Kidd (1989) SSM/I rainfall algorithm — a plot of 85 GHz polarization versus 37–85 GHz frequency algorithm outputs to establish rain/no-rain boundaries objectively for both. Rainfall-rate data have been obtained from comparisons with FRONTIERS radar data. For further details see text.

Figs 7(c) and 7(d) show ground-based radar data from radars in the United Kingdom, Ireland, France and The Netherlands combined with Meteosat infra-red data at times corresponding to Figs 7(a) and (b). The success of the SSM/I algorithm in depicting the rain over France and elsewhere and especially beyond the limits of the radar coverage is evident.

Table II presents comparisons between FRONTIERS radar and microwave rain/no-rain pixels for this event in contingency table form. Since it has been demonstrated by Collier (1986) and many others, and confirmed for the present work by Barrett and Kidd (1989), that quantitative use of radar data is reasonably dependable up to a range of 100 km, and may be useful up to a range of about 140 km, but that beyond that limit only qualitative assessments of rainfall from the weather radar should be made, the data in Table II relate to a maximum range of 140 km from each radar location. Table II(a) shows results for the evening of 15 October 1987, when the R:R plus NR:NR (R=rain, NR=no rain) classifications were the same for 75% of all pixels within the areas of radar coverage. Table II(b) shows that, on the morning of 16 October 1987, the comparable result was lower, at 59% of all such pixels. Table II(c)

shows that results for the entire period from 13 to 19 October 1987 yielded R:R and NR:NR correspondences on 80% of all occasions. It is interesting to note that the percentage correspondences on the morning of 16 October 1987 are the lowest yet obtained in any of the RSUUB SSM/I versus FRONTIERS radar studies. It is thought that the most likely reasons for this include the following.

- (a) Temporal differences: Although the radar and satellite images have been obtained as close together in time as possible, small differences remain.
- (b) Physical differences. The satellite, in observing a column of rain, does not, strictly speaking, yield an instantaneous rain rate but a rain rate related to circumstances prevailing over a period as long as 20 minutes in duration, dependent upon the depth of cloud and rate of fall of the hydrometeors.
- (c) Disparities between the satellite and radar viewing geometry, i.e. the satellite receives radiation vertically, whereas the radar views rainfall more or less horizontally. The effect of this factor may have been particularly strong in the case of the Great Storm because of the influence of the exceptionally strong winds on the falling hydrometeors.

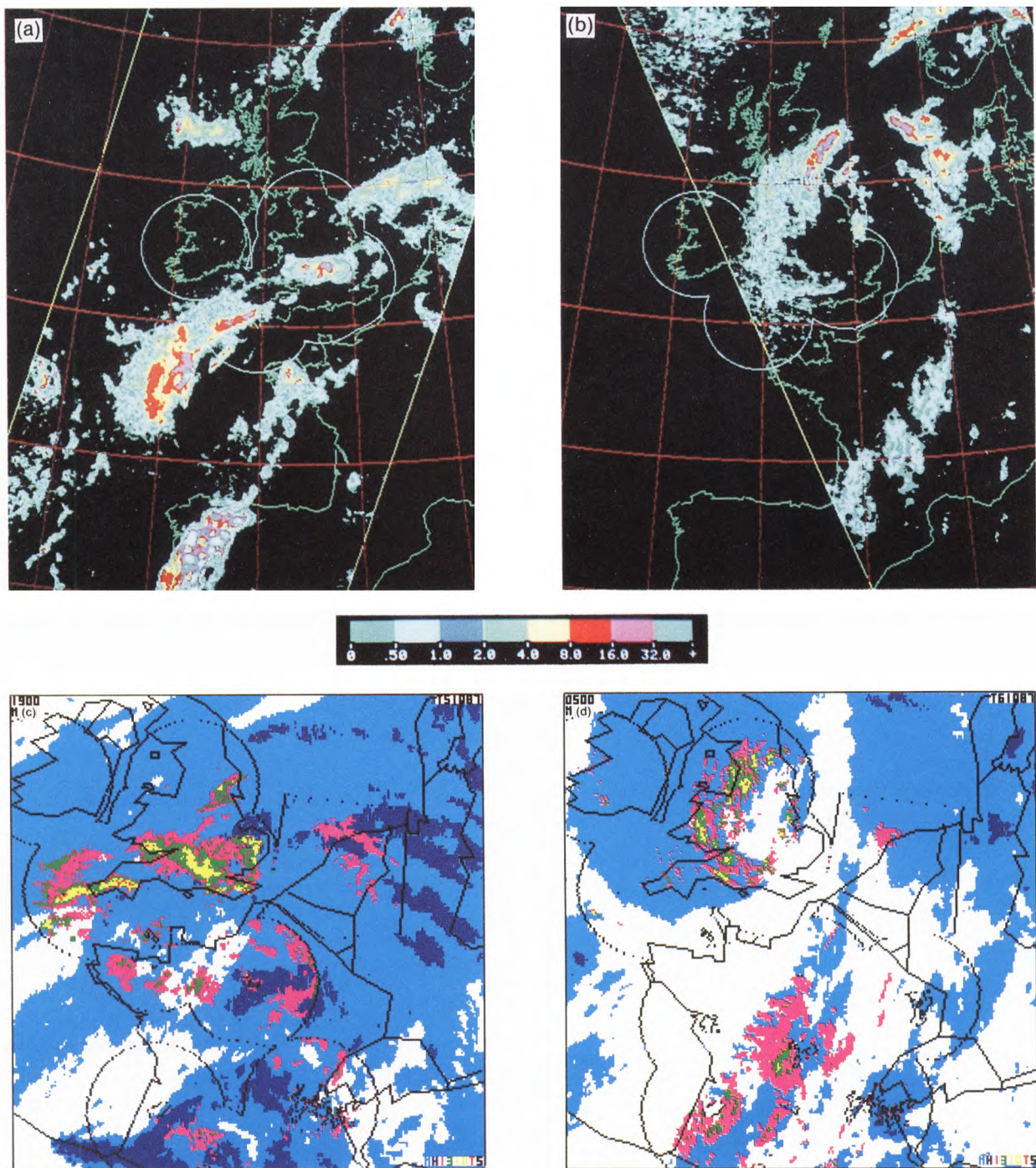


Figure 7. SSM/I-derived rainfall distribution on (a) 15 October at approximately 1900 UTC, and (b) 16 October at approximately 0500 UTC using the Barrett and Kidd (1989) algorithm. Rainfall rates (mm h^{-1}) are shown by the adjacent scale. Circles over southern Britain are drawn at 210 km radii from FRONTIERS radars. The combined Meteosat infra-red and ground-based radar image derived as part of the COST-73 Project (Collier *et al.* 1988) at (c) 1900 UTC on 15 October, and (d) 0500 UTC on 16 October. Radar data from the United Kingdom, Irish Republic, France and The Netherlands are used. Colours indicate — cloud temperatures; cyan -15°C to -45°C and blue $< -45^{\circ}\text{C}$; and rainfall intensities; magenta 0.3 to 1 mm h^{-1} , green 1 to 3 mm h^{-1} , yellow 3 to 10 mm h^{-1} , red 10 to 30 mm h^{-1} and black $>30 \text{ mm h}^{-1}$. Coastlines and country boundaries are shown black. Also shown is the limit of the radar coverage (circles and rectangular frames). The projection of (c) and (d) is polar stereographic and each pixel is approximately $5 \times 5 \text{ km}$.

5. Conclusions and recommendations

The satellite rainfall analyses presented in this paper follow earlier studies in the British Isles region using FRONTIERS radar data to calibrate the SSM/I rainfall algorithm, but the satellite wind-speed analyses have been prepared using a general model which, to our

knowledge, has not yet been verified or calibrated in such northerly mid-latitudes. However, both the rain and wind-speed results reported above seem to confirm that the SSM/I instrument has clear potential for the monitoring of both rainfall and surface wind speeds in the British Isles region, especially over water, and,

Table II. Contingency tables (Rain (R), No Rain (NR)) for FRONTIERS radar/satellite SSM/I intercomparisons for the polarization algorithms over water plus coasts (left-hand side), and the frequency algorithm over land (right-hand side) within 100 km of each radar site for (a) the evening of 15 October, (b) the morning of 16 October, and (c) the period 13–19 October 1987 (from Barrett and Kidd 1989).

		Microwave		
Radar		R	NR	Total
	R	274	263	537
	NR	208	1681	1889
	Total	482	1944	2426

		Microwave		
Radar		R	NR	Total
	R	207	68	275
	NR	634	869	1503
	Total	841	937	1778

		Microwave		
Radar		R	NR	Total
	R	2595	1417	4012
	NR	3281	17478	20759
	Total	5876	18895	24771

		Microwave		
Radar		R	NR	Total
	R	59	342	401
	NR	17	551	568
	Total	76	893	969

		Microwave		
Radar		R	NR	Total
	R	49	389	438
	NR	25	488	513
	Total	74	877	951

		Microwave		
Radar		R	NR	Total
	R	312	2256	2568
	NR	105	7791	7896
	Total	417	10047	10464

therefore, for improving weather forecasts not least in times of extremes.

We hope the future will see a continuation of the SSM/I north-west European rainfall monitoring programme currently centred in the RSUUB through our participation in the NASA WetNet project, and with support from NOAA and the Meteorological Office, and that a British Isles region-specific wind-speed evaluation and calibration programme will be commenced as soon as possible. SSM/I and SSM/I-type data are expected to become available for near-real-time forecasting purposes in the United Kingdom within 3 years. It is important to refine the more useful algorithms based on such data before then, so that they will be able to play their parts in improving forecasts, and investigating the impacts, of severe rain and wind storms as early as possible.

Acknowledgements

The authors wish to thank all their colleagues in the United Kingdom and USA who have helped in the preparation of this paper either through discussions or provision of data. Special thanks for one or both of such types of help are due to Drs D.B. Miller, P.K. Rao, J. Alishouse, R. Scofield and J. Wilkerson of NOAA/NESDIS, Washington DC; Drs R. Spencer and M. Goodman of NASA's Marshall Space Flight Center, Huntsville, Alabama; Dr R.C. Savage of Hughes Aircraft Company, F. Wentz of Remote Sensing Systems, Santa Barbara, California, and R. Brown and G. Shutts of the Meteorological Office.

References

- Bailey, J.O., Barrett, E.C. and Kidd, C., 1986: Satellite passive microwave imagery and its potential for rainfall estimation over land. *J Br Interplanet Soc*, **39**, 527–534.
- Barrett, E.C. and Kidd, C., 1989: Rainfall monitoring by the SSM/I with special reference to light rain over parts of north-west Europe. Final report (Stage I) to the Universities Space Research Association, Columbia, Maryland. University of Bristol, Remote Sensing Unit.
- Barrett, E.C., Kidd, C. and Bailey, J.O., 1988: The Special Sensor Microwave Imager: a new instrument with rainfall monitoring potential. *Int J Remote Sensing*, **9**, 1943–1950.
- Barrett, E.C. and Martin, D.W., 1981: The use of satellite data in rainfall monitoring. London, Academic Press.
- Cardone, U.J., 1969: Specification of the wind field distribution in the marine boundary layer for wave forecasting. New York University, Geophysical Science Laboratory, Report No. 69-1.
- Collier, C.G., 1986: Accuracy of rainfall estimates by radar. Part I: Calibration by telemetering raingauges. *J Hydrol*, **83**, 207–223.
- Collier, C.G., Fair, C.A. and Newsome, D.H., 1988: International weather-radar networking in western Europe. *Bull Am Meteorol Soc*, **69**, 16–21.
- Grody, N.G., 1984: Precipitation monitoring over land from satellite using microwave radiometry. In *Proceedings of the International Geoscience and Remote Sensing Symposium (IGARSS 1984)*, Strasbourg 27–30 August 1984. Strasbourg, European Space Agency, No. ESA SP-215.
- Hollinger, J., Lo, R., Poe, G., Savage, R. and Pearce, J., 1987: Special sensor microwave/imager user's guide. Washington DC, Naval Research Laboratory.
- Kidd, C., Barrett, E.C., Bailey, J.O. and Palmer, H., 1989: The use of SSM/I imagery for rainfall monitoring, with special reference to the UK and surrounding seas. In *Remote sensing for operational applications. Proceedings of the 15th Annual conference of the Remote Sensing Society, Bristol, 13–15 September 1989*. University of Bristol, Remote Sensing Unit.
- Munn, R.E. (ed), 1978: IUCRM colloquium on radio oceanography. *Boundary Layer Meteorol*, **13**, 1–429.
- Nordberg, W., Conway, J., Ross, D. and Wilheit, T., 1971: Measurement of microwave emissions from a foam-covered wind-driven sea. *J Atmos Sci*, **28**, 429–435.

- Rao, M.S.V., 1984: Retrieval of worldwide precipitation and allied parameters from satellite microwave observations. *Adv Geophys*, **26**, 237–336.
- Rao, M.S.V., Abbott, W.V. and Theon, J.S., 1976: Satellite-derived global oceanic rainfall atlas (1973 and 1974). Washington DC, NASA, No. NASA SP-410.
- Savage, R.C., 1978: The radiative properties of hydrometeors at microwave frequencies. *J Appl Meteorol*, **17**, 904–911.
- Spencer, R.W., 1984: Satellite passive microwave rain rate measurement over croplands during spring, summer and fall. *J Clim Appl Meteorol*, **23**, 1553–1562.
- Spencer, R.W., Olsen, W.S., Martin, D.W., Weinman, J.A. and Sartek, D.A., 1983: Heavy thunderstorms observed over land by the Nimbus-7 scanning multichannel microwave radiometer. *J Clim Appl Meteorol*, **22**, 1041–1046.
- Swift, C.T. (ed), 1977: Special joint issue on radio oceanography. *IEEE J Oceanic Eng*, **OE2**, 1–159.
- Wentz, F.J., 1988: User's manual, SSM/I Ocean products tapes. RSS Technical Report 033088. Santa Barbara, Remote Sensing Systems.
- Wentz, F.J., Mattox, L.A. and Peteherych, S., 1986: New algorithms for microwave measurement of ocean winds: Applications to SEASAT and the Special Sensor Microwave Imager. *J Geophys Res*, **91**, 2289–2307.
- Wilheit, T.T., Chang, A.T.C., Rao, M.S.V., Rodgers, E.B. and Theon, J.S., 1977: A satellite technique for quantitatively mapping rainfall rates over the oceans. *J Appl Meteorol*, **16**, 551–559.
- Wu, R. and Weinman, J.A., 1984: Microwave radiances from precipitating clouds containing aspherical ice, combining phase and liquid hydrometeors. *J Geophys Res*, **89**, 7170–7178.

551.578.45(430.1):551.578.46:551.515

A heavy mesoscale snowfall event in northern Germany

W.S. Pike

19 Inholmes Common, Woodlands St. Mary, Newbury, Berkshire RG16 7SX

Summary

The geographical extent and particular causes of localized heavy snowfalls which occurred near south-west Baltic Sea coasts on the night of 11/12 January 1987 are investigated. The roles of convergence lines, coastal fronts, stationary 'warm cyclones' and eddy vortices are discussed.

1. Introduction

While heavy coastal snowfall was occurring in south-east England (Pike 1990a), a similar mesoscale event affected a narrow belt of Mecklenburg and Schleswig-Holstein in northern Germany. By 0600 UTC on 12 January 1987 a maximum 24-hour accumulation of 70 cm was reported from the Nusse area, some 30 km east-north-east of Hamburg.

2. The synoptic situation

Fig. 1 shows an extremely cold east to north-easterly airstream at 1200 UTC on 11 January 1987 over the Baltic Sea and surrounding land areas, between a strong anticyclone centred over Norway and a major low pressure complex centred well to the south between Corsica and Italy. A shallow thermal depression had formed over the Oder Bight, probably a similar development to that described in Pike (1990a) as occurring over the southern North Sea.

Tiesel (1984) identifies stationary depressions over sea areas adjacent to eastern Germany as 'Baltic heat cyclones'. Their formation occurs over the relatively warm water of the Mecklenburg and/or Oder Bights, whose coastlines these depressions tend to model themselves on. Tiesel explains their cyclogenesis as taking place during the calming phase after cold air penetration has occurred, which itself causes the weakness by means of stronger night-time cooling.

While the greatest weather activity may be expected when maximum thermal contrast exists between land and sea surfaces during hours of darkness, the depression can exist in a shallow and less-active form throughout the day, only completely losing identity when overwhelmed by synoptic-scale events, such as cloud spreading over or a stronger gradient/wind-field prevailing.

3. Satellite picture analysis

Fig. 2 is an AVHRR infra-red satellite image of the Baltic Sea area taken at 1236 UTC on 11 January by the NOAA-9 satellite. It gives a good general picture of the cloud patterns associated with the synoptic situation in Fig. 1, with any influence of major upper-cloud shields excluded to the south, we can form a very good impression of the wind direction prevailing in the lower troposphere. Here, given favourable conditions, streets of convective cloud (identified by Miura (1986) as requiring a certain wind increase with height*) parallel to the wind are forming almost immediately as the extremely cold arctic continental air advects from over land or ice surfaces out over the relatively warm Baltic

* Longitudinal rolls are realized when vertical wind shear (based on the wind difference between 1000 mb and the inversion base) is between 10^{-3} and 10^{-2} s^{-1} , and open cells are realized when it is smaller.

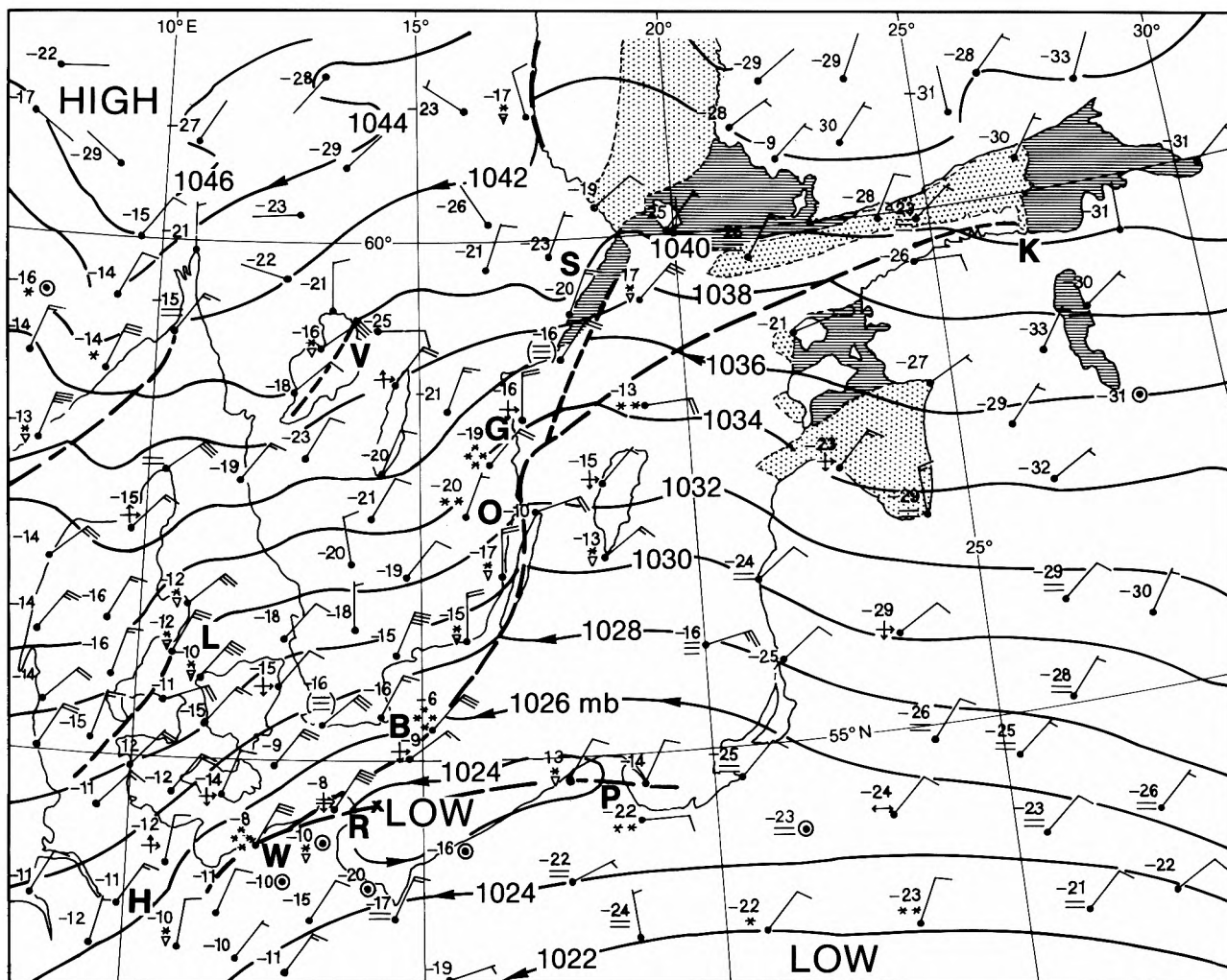


Figure 1. Surface synoptic chart for the southern Baltic and surrounding land areas at 1200 UTC on 11 January 1987. Heavy dashed lines indicate low-level convergence lines or coastal fronts, and letters indicate locations mentioned in the text. Shaded areas denote older ice areas and stippled areas denote young ice.

Sea and other areas of water. At first shallow and low, these cumuliform clouds eventually develop tops to 10 000–15 000 ft (see also Scorer (1986) chapter 6).

At this time, a pool of extremely cold air (temperatures at or below -20°C at 850 mb, and -30°C at 700 mb) was centred over southern Sweden and moving south-westwards (see chart in Kresling 1987a). The southern Baltic had surface temperatures of between 0°C and 4°C , hence great instability at low levels. Close inspection of Fig. 2 reveals cloud streets beginning to form over areas of young ice to the west and south of Finland.

Evidence of convergence can soon be seen, characterized by more prominent long plumes of cloud, such as that originating from near the older ice edge in the Gulf of Finland, just north-east of Kunda (K in Figs 1 and 2) in Estonia and running south-westwards, indicative of a major convergence line between the north-easterly airstream over Finland and the general east-north-easterly flow prevailing over most of the Baltic Sea further south. This persistent plume (it was in evidence in much the same location throughout the 12th) merges

with another shorter one originating at the ice edge just east of Stockholm (S), and the two combine to produce much snow on the Swedish coast in the Gladhammar-Västervik region (G).

The convergence continues down the Swedish coast where the over-water flow meets a northerly land breeze, but some cells do travel 20–30 km inland in the Oskarshamn (O) area where the coastline is more nearly at right angles with the onshore wind, and the sheltering effect of Gotland causes a change in pattern. Further south the convergence plume curves south-westwards over Bornholm (B) towards Warnemünde (W) on the north German coast. Here again there are clear signs of merging convergence plumes, with another well marked line of cloud forming between near gale force east-north-easterlies over the Baltic and near-calm, clear conditions to the south, running from northern Poland (P) over Rügen (R) and then merging towards Warnemünde. Showing up more clearly in Fig. 3 (the AVHRR visible picture which covers the western section of Fig. 2) is the cloud formation resembling a ship's wake in the lee of Rügen Island. Here, the steep



Photograph by courtesy of University of Dundee

Figure 2. NOAA-9 AVHRR infra-red satellite picture at 1236 UTC on 11 January 1987. See text for locations indicated by letters.

cliffs rise to 100–150 m AMSL in the Stubbenkammer–Königsstuhl area of the north-east coast.

Fig. 3 also shows close proximity of the cirrus shield in the extreme south, as well as giving an enlarged view of a genuine lake convergence effect of cloud streets over Lake Vänern (V) which remains unfrozen. Convective cells moving inland near Oskarshamn (O) appear to converge into two brightly illuminated streets, suggesting uplift produced by land-breeze near the coast. A similar effect occurs at the eastern Danish coast around $55\frac{1}{2}^{\circ}\text{N}$, 10°E . Medium-level wave-cloud is just visible in the top right corner of this picture over central Sweden, forming at right angles to the wind direction.

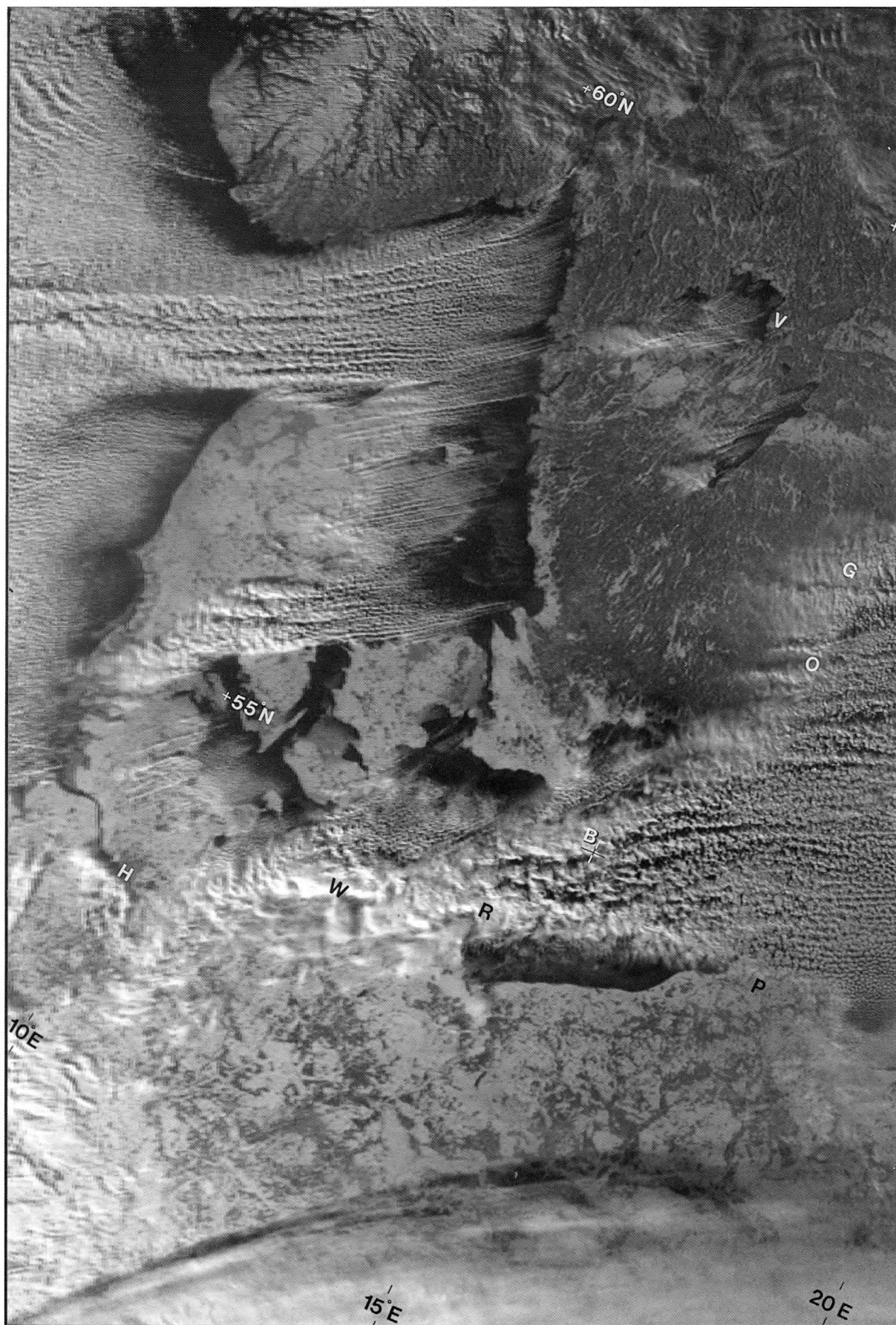
The shield of upper cloud moved north-north-eastwards to cover areas south-east of a line from Oskarshamn to Rügen by 0230 UTC on the 12th (in NOAA-9 composite from *Das Europäische Wetterbild* — not shown), and Fig. 4 shows that the upper cirrus had, by 1224 UTC, moved further westwards, to lie from central Denmark to the Dutch border. This picture marks the temporary end of significant coastal-front activity in the south where upper-cloud and synoptic-scale features overwhelm radiation effects. However, further north, the Kunda to Gladhammar convergence line is still in evidence, although the strong east-north-

easterlies have swept inland over south-eastern Sweden behind an active, warm coastal front.

Nevertheless, the 'lumpy' nature of the cloud tops over East Germany in Fig. 4 does indicate that Baltic warming of the strong north-easterly airstream was producing much activity from embedded cumulus and cumulonimbus which were being swept southwards inland, within the general background of thick upper and medium frontal cloud layers.

4. Discussion of the snowfalls

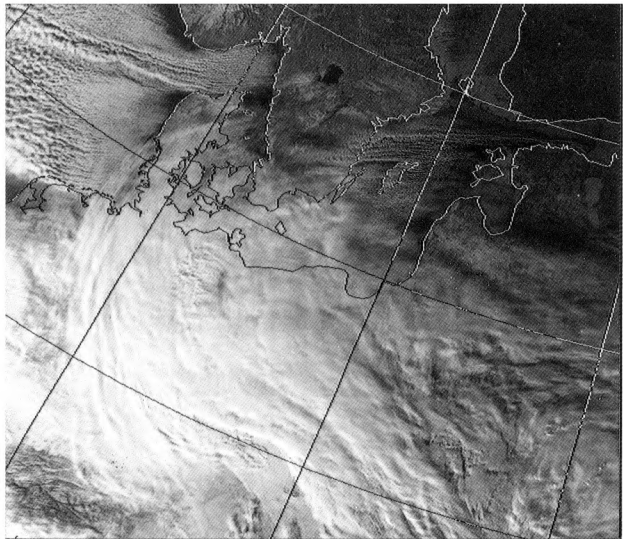
With 40–50 cm of snow already lying in south-east Sweden, coastal accumulations over the period 9–14 January 1987 during the cold outbreak tended to increase gradually by 5–15 cm per day until some stations reported approximately 90 cm (nearly 3 ft) lying, e.g. at Oskarshamn and Krokshult by 0600 UTC on the 12th, then at Gladhammar-Västervik and Herrvik by 0600 UTC on the 14th, when Oskarshamn measured a maximum reported value of 105 cm, an increment of 50 cm since the north-easterlies began on the 9th. Gladhammar registered a maximum 24-hour fall of 23 cm up to 0600 UTC on the 12th, and this was the period when spectacular snowfalls occurred further south in Germany.



Photograph by courtesy of University of Dundee

Figure 3. NOAA-9 AVHRR visible imagery satellite picture at 1236 UTC on 11 January 1987, corresponding to Fig. 2.

Fig. 5 gives the distribution of new snowfall recorded in the 24-hours up to 0600 UTC on 12 January 1987 in northern Germany. The heaviest accumulations occurred in a long, narrow belt stretching from Warnemünde to near south-east Hamburg. A secondary wedge-shaped area stretches from just north of Greifswald towards Teterow, with a thin division where negligible snow fell between these two areas. In extreme south-east Schleswig-Holstein, several locations to the north-east of Hamburg (e.g. Trittau and Ratzeburg) recorded 40–50 cm, with a maximum fall of 70 cm reported from the Nusse area.



Photograph by courtesy of University of Dundee

Figure 4. NOAA-9 AVHRR visible imagery satellite picture at 1224 UTC on 12 January 1987.

At Bergedorf (a south-east suburb of Hamburg) reliable observations of the snowfall indicate that, with only few interruptions, it continued from 1500 UTC on the 11th until about 0630 UTC next morning. The most intense snowfall, accumulating at a rate of 7 cm h^{-1} , occurred on the evening of the 11th between 1900 and 2115 UTC as the cold pool centre was, by extrapolation, passing overhead (see Kresling 1987a).

This 16-hour period of snow produced a total of 30–50 cm in the Bergedorf area. One station measured a water equivalent of 23.4 mm from 37 cm of fresh snow, which gives a ratio near 1:15 in the very cold conditions, temperatures during the snowfall rising from around -12 to -10°C in that time-span. Given similar water equivalents to those recorded in the United Kingdom, the higher rainfall to snow depth ratios (than the 1:11 or 1:12 experienced in England) may explain why maximum snow depths in colder German conditions yielded 10–20 cm more snow on the ground (temperatures were nearer -5 to -8°C in south-east England, see Pike 1990a).

Wright (1987) mentions similar problems occurring on the local German suburban railway lines (conductor rail) to those experienced in north-west Kent, also due to heavy snow that Sunday evening (11th). Fig. 6 gives a visual indication of snow depths that affected Rhinebeck, 2–3 miles north-east of Bergedorf. Some cars were still almost buried by snow a week later, although the German legal requirement that domestic front paths are to be kept clear of fresh snow accumulations resulted in much activity during the 11th and 12th for local townspeople.

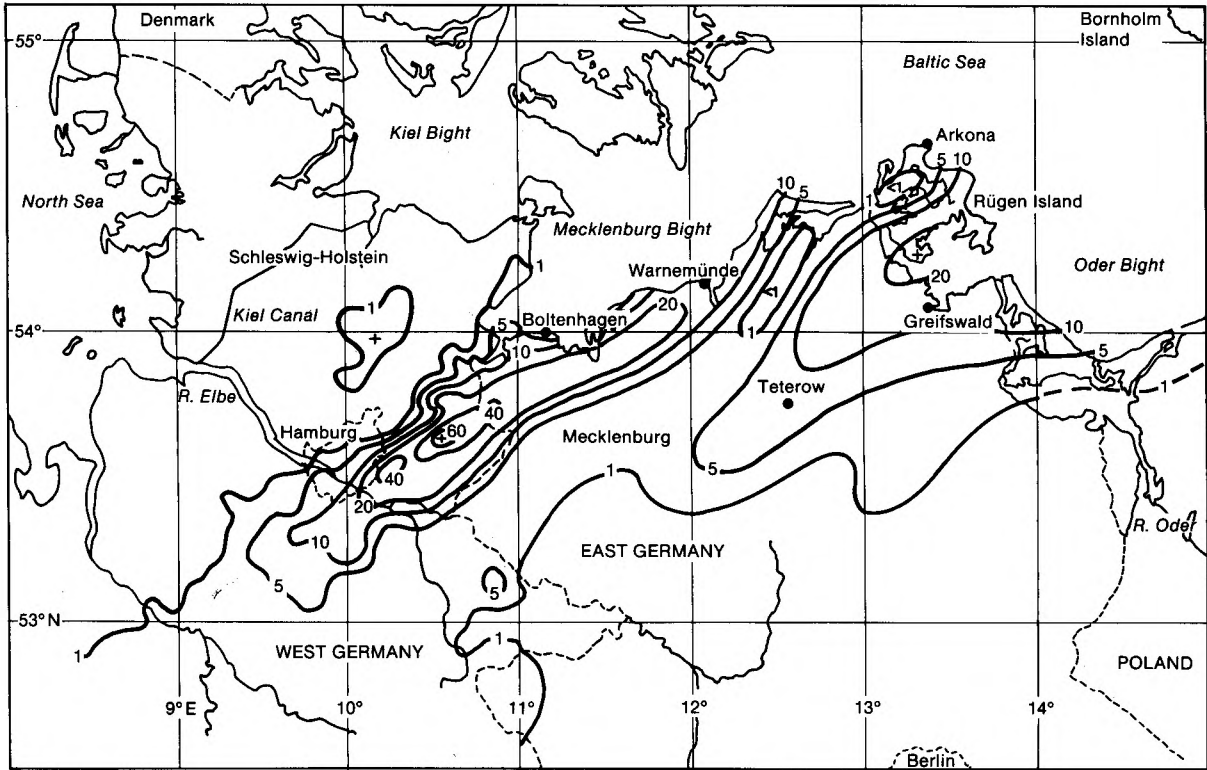


Figure 5. New snowfall (cm) in northern Germany in the 24 hours up to 0600 UTC on 12 January 1987.



Photograph by courtesy of P.B. Wright

Figure 6. A suburb of Hamburg after the snowfall of 11/12 January 1987.

5. Mesoscale analysis

The general synoptic situation over northern Germany, as described in section 2, appears similar to that of 9 February 1956, outlined in Tiesel (1984). In both cases a stationary warm cyclone lay over the Oder Bight. An unstable boundary line was formed between streams of air moving at very different speeds, characterized by a Beaufort Force 8–9 north-easterly wind at Arkona Lighthouse (on the northern tip of Rügen Island) and a near-calm at Greifswald, some 66 km to the south.

From 0000 UTC on the 11th to 0000 UTC on 12 January 1987, radiosonde ascents from Greifswald showed the air to be extremely cold, moist and unstable to sea temperatures up to about 650 mb (12 000 ft). They featured a north-easterly wind which was increasing with time and height in this layer, and such conditions of wind shear are thought to be very conducive to the formation of streets of cumuliform cloud, as seen in Fig. 2 (Miura 1986, Scorer 1986).

By 2100 UTC on the 11th (Fig. 7), a pronounced coastal front had developed along the Mecklenburg Bight coast, primarily due to the coldest air passing overhead at that time and also radiation cooling over snow covered ground providing a near -20°C thermal contrast across the boundary (convergence) line, with Baltic Sea-surface temperatures remaining in the range 0 to 4°C .

Marked by convergence and convection forming a procession of heavy snow-showers (as shown by radar study in Pike (1990b), and in Kresling (1987b)), the unstable boundary line/coastal front produced many

small lateral oscillations. A few of these developed into eddy vortices which either became detached from the stationary warm cyclones over the sea, or else were shed downwind of an island or promontory (see the detailed study in Walter 1989). One suspects that areas of water just downwind from Bornholm or Rügen are two such preferred sites for formation of eddy vortices off north-east Germany in cold north-easterly airstreams. Although spacing of synoptic stations does not permit mesoscale analysis, one small eddy vortex appears to have produced heavy snow in passing close to Arkona soon after 1400 UTC on the 11th, and this affected Warnemünde between 1600 and 1700 UTC. Tiesel (1984, pp. 360/1) describes detached eddy vortices being shed south-westwards from the stationary Oder Bight warm cyclone on 9 February 1956. Generally speaking, one may expect them to travel downstream along the boundary line at a speed intermediate between low-level airflows on either side of the discontinuity (after Tricker 1964, pp. 179–180). The German term for eddy vortex is *randwirbel*, which is used by Tiesel to describe the 1956 case.

Formation of a small, marine, warm cyclone was noted further east at 2100 UTC on 10th January, some 40 km north-west of Gdynia, off the Polish coast (personal correspondence with Dr R. Tiesel), with timing of development (and that of subsequent similar warm cyclones) strongly suggesting that they are likely to appear just as the pool of coldest upper air is approaching.

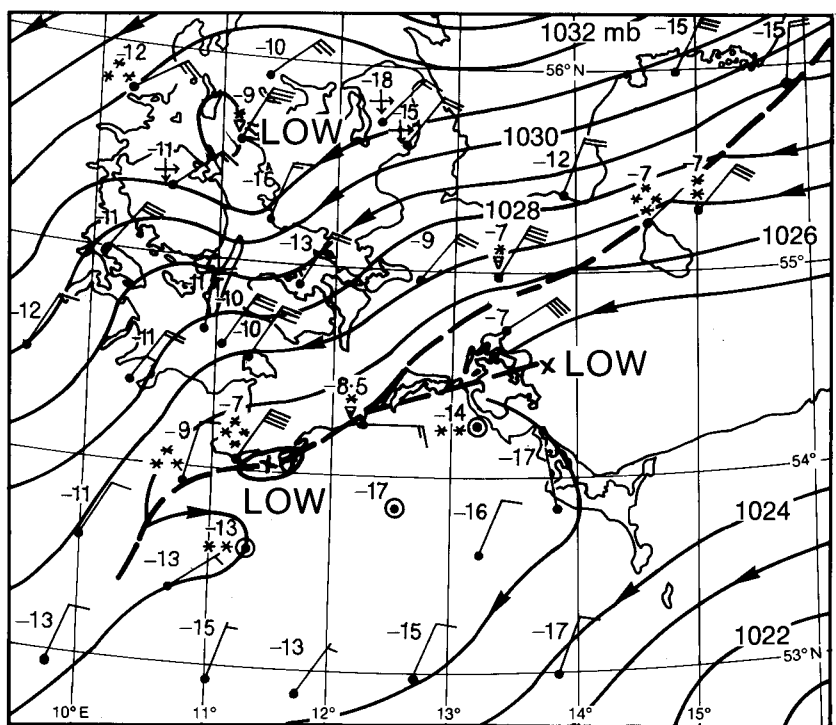


Figure 7. Surface synoptic chart for northern Germany at 2100 UTC on 11 January 1987, with isobars drawn at 1 mb intervals. Heavy dashed lines indicate position of low-level convergence lines/coastal fronts.

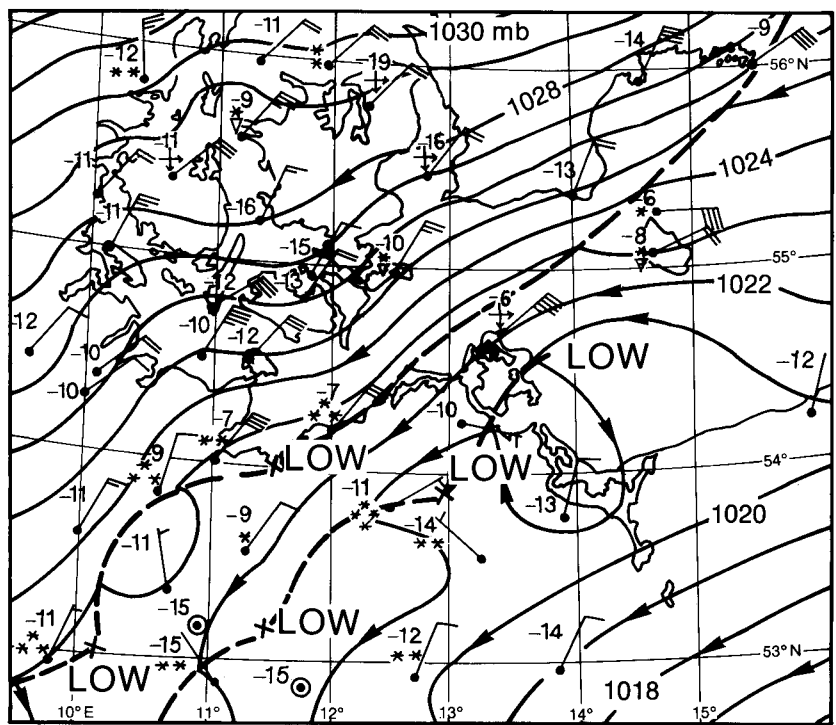


Figure 8. As Fig. 7 but for 0600 UTC on 12 January 1987.

However, on 11 January 1987 a small stationary mesoscale heat-low appears to have developed intermittently *in situ* on the marked coastal front over the Mecklenburg Bight between Warnemünde and Boltenhagen from just before 1400 UTC, with this showing up well in Fig. 7 when weather activity was intense. Fig. 8 suggests a meso-low is still in evidence at

0600 UTC the next morning, although it is fading fast beneath increasing cloud and strengthening gradient wind. It appears to be a stationary eddy-vortex type of development, forming near the coast at the edge of the very strong north-easterly airflow over the sea, and plays an important part in maintaining heavy precipitation along a narrow belt downwind.

Such *in situ* developments of small vortices, particularly when they happen to occur in a favoured area nearby and just downstream of a particular coastal station, would explain the surface wind veering rather than backing there as the land-breeze sets in (see Weybourne and Wainfleet AWS observations in Pike (1990a)). Two similar events which are believed to have occurred in association with the intermittent development over the southern Mecklenburg Bight are in evidence from the Warnemünde anemograph trace (not shown); the first occurring between 1400 and 1600 UTC, and the second is demonstrated by reproduced surface observations (Fig. 9) during the night of the 11th/12th. This shows what may be interpreted as a temporary oscillation of the coastal front out to sea, with a distinct land-breeze regime lowering temperatures by an average of 1°C h^{-1} during a 4-hour period, during which the surface wind was southerly or calm between 2230 and 0010 UTC, then being immediately replaced again by the strong north-easterly wind with rapid recovery of temperature by 0100 UTC on the 12th.

It appears that several mesoscale eddy vortices moved inland from the Mecklenburg Bight towards south-east Hamburg, occasionally intensifying the overnight snow along a narrow belt where the coastal front extended over part of Schleswig-Holstein. These developments appear to have had a similar effect to the small eddy-vortex over Lincolnshire, described in Pike (1990a), which also gave heavy snow over a small area. The features behave as mesoscale, shallow polar-lows in (a) forming over the sea, (b) continuing over the coast then (c) decelerating and filling up over land.

The distribution of snow in Fig. 5 appears to have been due to a series of small eddy disturbances passing south-westwards from the stationary Oder Bight warm cyclone, this process beginning towards midnight, with Greifswald reporting continuous moderate snow throughout the night from 2300 UTC on the 11th.

This process extended a second coastal front south-westwards from the Rügen area, as indicated in Fig. 8, during the latter part of the night, and this analysis in part explains the distinct gap between the two snow areas in Fig. 5. The satellite pictures suggest a second factor was involved, associated with the ship's-wake cloud pattern in the lee of Rügen Island, from which one suspects that subsidence would have earlier been affecting a short length of the coastal front along the north German coastline, damping its shower activity there (see Scorer 1986, chapter 9).

6. Conclusions

The east-north-east to west-south-west orientation of the coastline along the Mecklenburg Bight (south side) presented a shallow angle to the onshore wind which was an extremely favourable situation to permit continuing coastal convergence and uplift between (a) a strong, moist, showery north-easterly airflow over the sea, with the air temperatures typically -6 to -10°C , and

(b) stagnating, colder overland air near -20°C . A well marked coastal front formed between the two airflows.

During the hours of darkness overnight 11/12 January 1987, while thermal contrast between the airflows was greatest, a heavy snowfall of between 20 and 70 cm occurred in a 16-hour period along a narrow, sharply defined belt which was, geographically speaking, an extension of the southern Mecklenburg Bight coastline downwind to the west-south-west towards south-eastern Hamburg.

The formation of small Baltic Sea warm cyclones forming first over the Oder Bight and later over the Mecklenburg Bight in the extreme south, intensified the snowfall from time to time in association with smaller eddy-vortices which were shed south-westwards, extending eventually two coastal fronts; one from Warnemünde to south-east Hamburg and another from Rügen towards Teterow.

The steep cliffs of Rügen Island also provide a natural topographic division of a cold north-easterly airstream, downwind of which the coastal convergence line (or often a more developed coastal front) is likely to form along a marked boundary between fast- and slow-flowing airstreams at low levels.

The case of 11/12 January 1987 was similar to that producing 20–50 cm of fresh snow at a similar local time in coastal areas of south-east England and East Anglia (Pike 1990a). However, accumulations 10–20 cm deeper in northern Germany were most probably the result of 'water-equivalent to snow-depth ratios' nearer 1:15 in the colder conditions, as opposed to the 1:11 or 1:12 experienced simultaneously in England. Water yields from snowfalls were comparable (generally between 22 and 32 mm) in both countries.

While the formation of a marine warm cyclone is occurring *in situ* nearby, and especially when this occurs immediately downstream of a particular coastal station, a temporary veering of the surface wind is likely to occur as the land-breeze sets in. Heavy and prolonged showers tend to accompany these changes of wind direction, but often affect only a limited and narrow belt (25–30 km wide) near the coast.

Both Figs 7 and 8 confirm that analysis of surface synoptic charts with isobars drawn at 4 or 5 mb intervals is too coarse to depict the small mesoscale heat cyclones and eddy vortices which are more readily observed with isobars spaced at 1 or 2 mb intervals.

Acknowledgements

At Bracknell, to Meteorological Office staff: G.A. Monk of the Nowcasting and Satellite Applications Branch for discussions and extra satellite data. Also to L. Rowley for accessing the data bank's surface- and upper-air information to allow Figs 1, 7 and 8 to be drawn and conclusions made. Baltic Sea ship observations were kindly sent by R. Whyman of the Marine Advisory and Consultancy Service. Further data was obtained courtesy of helpful staff in the Library and Archives.

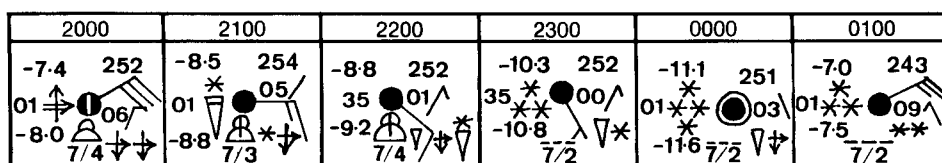


Figure 9. Sequential synoptic observations for Warnemünde from 2000 UTC on 11 January to 0100 UTC on 12 January 1987.

Much useful co-operation came from A. Kresling in the Deutschen Wetterdienst Seewetteramt at Hamburg, including early morning satellite data for Eastern Europe*, snowfall information over West Germany (upon which half of Fig. 5 is based), some extra synoptic observations from German shipping in the Baltic Sea, and water equivalents of snowfall at Hamburg-Bergedorf. The other half of Fig. 5 is based on information supplied by the Met. Dienst der DDR: from Dr Kolbig in the Climatological Headquarters (Hauptamt für Klimatologie), Potsdam and Drs Holz and Tiesel at the Rostock-Warnemünde Meteorological Office.

The paper by Tiesel (1984) was sent by Prof. Dr Manfred Geb of the Meteorological Institute, Free University of Berlin (and further information was sent by Dr Tiesel later). Photographs (of which Fig. 6 is one) and helpful correspondence came from Dr Peter Wright, who was then at the Max-Planck Institute for Meteorology in Hamburg during the 1987 snowfall.

Snowfall data from stations in south-east Sweden came from S. Larsson-McCann at the SMHI Climat Division, Norrköping.

References

- Kresling, A., 1987a: Die starken schneefälle östlich Hamburgs vom 11 auf den 12 Januar 1987. *Wetterkarte des Deutschen Wetterdienstes*. Nr. 11, Freitag, den 16 Januar 1987.
- , 1987b: *Wetterkarte des Deutschen Wetterdienstes*. Nr. 13, Dienstag, den 20 Januar 1987.
- Miura, Y., 1986: Aspect ratios of longitudinal rolls and convection cells observed during cold air outbreaks. *J Atmos Sci*, **43**, 26–39.
- Pike, W.S., 1990a: Persistent coastal convergence in a heavy snowfall event on the south-east coast of England. *Meteorol Mag*, **119**, 21–32.
- , 1990b: Radar study of the snowfall in south-west Cornwall on 12 January 1987. *Meteorol Mag*, **119**, 97–102.
- Scorer, R.S., 1986: *Cloud investigation by satellite*. Chichester, Ellis Horwood.
- Tiesel, R., 1984: Die Wärmezyklonen der westlichen und mittleren Ostsee. *Z Meteorol*, **34**, 354–365.
- Tricker, R.A.R., 1964: *Bores, breakers, waves and wakes*. London, Mills and Boon.
- Walter, B.A., 1989: A study of the planetary boundary layer over the polynya downwind of St. Lawrence Island in the Bering Sea using aircraft data. *Boundary Layer Meteorol*, **48**, 255–282.
- Wright, P.B., 1987: German Weather Conditions. *Climatol Obs Link*, No. 201. p. 20.

* *Das Europäische Wetterbild* — satellite composites (NOAA-9 AVHRR) issued by the Institute of Meteorology at the Free University of Berlin.

Reviews

Carbon dioxide and global change: earth in transition, by S.B. Idso. 150 mm × 220 mm, pp. viii+292, *illus.* Tempe, Arizona, IBR Press, 1989. Price \$19.95.

Over the last decade, a general scientific consensus has developed that rising concentrations of the greenhouse gases in the atmosphere will lead to fundamental climatic changes, with severe impacts on our way of life. This consensus has received widespread publicity. But throughout this time Sherwood Idso, a research physicist with the Water Conservation Laboratory in Phoenix, Arizona, has maintained that we should welcome increases in atmospheric CO₂, since the results will be entirely beneficial for life on Earth. His articles on the subject have appeared in a wide range of journals. Now, the sum of his ideas is gathered between the covers of this book.

Idso takes as his starting point the variations in atmospheric CO₂ concentrations over the totality of the Earth's existence. As the luminosity of the Sun has increased, so atmospheric CO₂ concentrations have decreased, thus maintaining an approximate balance which has produced climatic conditions suitable for the development and sustenance of life. Present-day CO₂ concentrations are dangerously low for the maintenance of plant life, and therefore any process which augments their levels is to be welcomed. Idso then argues that the temperature increases predicted by general circulation models (GCMs) for an equivalent doubling of atmospheric CO₂ are gross exaggerations. He proposes, by comparison with conditions on Mars, Venus and the early Earth, an equivalent CO₂ doubling temperature increase of only 0.4 °C. Therefore, on the one hand increasing CO₂ concentrations will bring valuable direct effects to the biosphere whereas on the other hand the dramatic climatic changes suggested by modelling studies will simply not occur.

The book is divided into two main parts. The first is devoted to the climatic aspects of the greenhouse effect, and contains five sections. The first of these defines the problem in the context of the long-term history of the Earth. The second reviews the GCM modelling results for doubled CO₂ concentrations. Both sections are quite brief, taking together only 15 pages. We then move into the real 'meat' of the book. The third section is devoted to a strong criticism of GCMs. It should be noted, however, that these criticisms add nothing more to what is already openly admitted and debated by the modellers themselves. In the fourth section Idso then proceeds to present his empirical approach to the problem, outlined above, which yields a 0.4 °C warming for doubled CO₂. He further proposes that there may be a maximum limit to the greenhouse warming of the Earth of 38.5 °C (4.5 °C above the current figure) provided all else

(planetary albedo, atmospheric pressure, etc.) remains constant. The first part of the book closes with a critical review of attempts to pin-point the signal of greenhouse warming through, for example, analysis of regionally averaged temperature series.

The second part of the book discusses the beneficial direct effects of increasing CO₂ concentrations on the biosphere. There are four sections dealing respectively with plant responses, the beneficial effects of high levels of atmospheric CO₂ on plants experiencing environmental stress, a review of studies which suggest that there are already signs of a CO₂-induced 'greening of the Earth', and the beneficial affects for animals. The book closes with a general review of the evidence that has been presented in the context of other environmental problems.

There is a clear change of pace between the first and second parts of the book, and Idso is clearly more at ease discussing the direct effects of CO₂ on the biosphere than he is with the indirect effects. Notwithstanding this point, the writing is clear and intelligible to the non-specialist reader. The production is camera-ready with few, but adequate, explanatory diagrams. One hundred of the 292 pages are devoted to the list of references, some 2700 in all. Idso is uncritical of those authors whose work supports his views. However, he devotes many pages of argument to undermine, for example, the Jones *et al.* temperature series which suggests a 0.5 °C global warming this century.

This is a biased book, devoted to the explanation and support of one man's ideas. Anyone buying it should be aware of this fact, and I would only recommend it either to those who wish to learn more about Idso's ideas, or to politicians seeking justification for their unwillingness to take action to limit emissions of the greenhouse gases. We must still await the much-needed publication of an objective and well-informed discussion of all the scientific points-of-view in the greenhouse debate.

J.P. Palutikof

Climatic atlas of the Indian Ocean. Part III: Upper-ocean structure, by S. Hastenrath and L.L. Greischar. 345 mm × 230 mm, pp. xxvi + 247 charts, *illus.* University of Wisconsin Press, 1989. Price \$40.00.

For more than a decade the first two parts of this atlas series by Hastenrath and Lamb (1979) have been a useful reference on the surface climate and heat budget of the Indian Ocean. This third part, documenting the annual cycle of subsurface structure and the upper-ocean heat budget, is a welcome addition. It covers the same area on the same scale and in the same format at the first two volumes. However, the relative sparseness of subsurface observations makes some loss of resolution inevitable. In this volume the data are presented on a

2° latitude × longitude grid. Most of the material comes from the Master Oceanographic Observation Data Set (MOODS) compiled by the Fleet Numerical Oceanography Center, Monterey, California. In the area under consideration (The Indian Ocean to 30°S, 120°E) this comprised nearly 320 000 temperature soundings and 18 000 for salinity at the time when the atlas was made. The authors found it necessary to screen out more than one third of the temperature soundings, reducing the number used to less than 200 000. Of these, 88% were collected during 1963–84. In contrast, about 4.5 million sets of surface ship observations were used in compiling the first two volumes — from the TDF-11 data set for the years 1911–70.

About one third of this volume is devoted to monthly charts of temperature at seven levels: surface, 50, 100, 150, 200, 300, 400 m below sea level, contoured at 2 °C intervals. One can see fairly well the annual cycle of major features like the subtropical gyre and the zonal band of low temperature separating it from the equatorial counter-current, and their vertical structure. At the surface though, the extra resolution in the charts of Part I of the series allows smaller-scale phenomena such as the upwelling regions off Arabia and Somalia to be seen more clearly than here. Subsurface there are some intriguing features, for example at 100 m to the west of Sumatra. They could have some bearing on the development of the Indonesian warm pool and its relationship to the twice-yearly equatorial jet in the Indian Ocean. But are they real? One would like to look more closely at them.

Other thermal products include monthly charts of mixed-layer depth, base depth of the thermocline, thermocline intensity, heat storage (to 400 m) and oceanic heat export. The monthly and annual charts of 'net oceanic heat gain' in Part II of the series are reproduced here, reanalysed at 2° spatial resolution for convenient comparison. All the products shown in the atlas are clearly defined and briefly discussed in the 26 pages of introductory notes.

With so few observations available, salinities have been averaged into two 6-monthly periods (November–April and May–October) corresponding to the north-east and south-west monsoon seasons, and charts show the distributions at the surface, 100 m and 300 m. Despite the shortage of salinities, the authors offer monthly charts of geopotential anomaly at the sea surface relative to 400 decibars. They justify this by showing that, in five selected areas, the temperature–salinity relationship is sufficiently well defined to allow anomalies to be calculated directly from temperature profiles — with sufficient accuracy for the contour interval (10 dyn cm) adopted here. Monthly charts of surface currents and their divergences (regrettably not extending east of 100°E) are based on the archive of the Meteorological Office. Again, whilst the evolution of the major currents can be followed clearly, the scarcity of observations, particularly south of the Equator,

makes one doubtful of the reality of some of the smaller features.

The atlas concludes with a set of selected vertical sections and temperature profiles. Very few errors were noticed — a few wrongly directed arrows in some of the charts of geopotential anomalies. What has been done is clearly defined. The limitations are on the sparseness of the data and their uneven distribution rather than in the treatment.

It is timely. Many more data have gone into this atlas than any previous one dealing with thermal properties in this region. It should be in any library with an interest in marine climate.

J.C. Swallow

Applications of weather radar systems — a guide to uses of radar data in meteorology and hydrology, by C.G. Collier. 170 mm × 246 mm, pp. 294, *illus.* Chichester, Ellis Horwood, 1989. Price £44.50.

Applications of radar technology in meteorology have been under development for over 40 years, and weather radars are now used in many countries for operational and research purposes. Chris Collier has been closely involved in the developments in the United Kingdom for many years, and this book reflects his wide experience of the subject. He currently leads a Branch of the Meteorological Office responsible for 'nowcasting' and satellite applications. This book, one of a series on remote sensing, is directed towards the practical applications of weather radars that can be used operationally, and provides information on techniques and an assessment of their success in a wide range of applications.

Following an account of the basic theory, which includes Doppler and multi-parameter radars, chapter 3 deals with precipitation measurement; later chapters discuss the role of satellites in this very important application and extend the subject into precipitation forecasting. Here we find some strange imbalances. For example, the choice of wavelength is dealt with in one paragraph, whilst the real-time calibration system developed by the author occupies over ten pages when this (excellent) work is fully covered in numerous published papers. The use of X-band radars for urban storm warning purposes, which featured prominently at the 1989 conference on Hydrological Applications of Weather Radar at the University of Salford, is also neglected. The chapter on satellite sensors for precipitation measurement (estimation would be a more suitable word) is succinct and well written, and is coupled with five colour plates illustrating the potential of using combined satellite and radar images for precipitation forecasting. Appropriately, short-period forecasting (chapter 6) receives extensive treatment,

covering methods of describing and tracking precipitation echoes, and the forecasting of severe storms, also looking forward to the possibilities for combining radar data with numerical forecasting models.

The logical development is flood forecasting using radar data; chapter 7 starts with some data on flood damage costs and potential savings in England and Wales, but contains little information of direct use on hydrological forecasting methods. It concludes that 'only if ways can be found for dealing with errors in radar estimates of precipitation, will radar attain its potential in hydrological forecasting'. Amen to that!

Weather radar networks now exist in quite a few countries and regions, so it is appropriate for this book to include a chapter on this topic, concentrating on the factors influencing network design. The section giving examples of networks is disappointing. The description of radar networking in the United Kingdom and the USA has a curious emphasis on the history of the developments, with no technical information on equipment, data, format, transmission speeds, etc. Japan, with perhaps the densest network in the world, receives scant mention.

Further applications dealt with in later chapters include the use of radar data to improve our knowledge of the frequency of extreme amounts of precipitation, depth-area-duration analysis for use in storm drainage design, and probable maximum precipitation estimation. These are undoubtedly areas where the full potential of radar data has still to be explored. The role of radar in studies of airborne pollutants is an important application, and its inclusion illustrates the breadth of coverage of this book. Illustrations of the rainfall over the United Kingdom during the passage of the Chernobyl plume and a map of the deposition of caesium-137 underline the contribution radar has to make in this field, which has grown rapidly in importance in the last few years. The concluding chapter outlines a number of uses of weather radars in furthering research into meteorological phenomena such as severe convective storms and hurricanes, and discusses some of the recent developments in radar technology including Doppler radars.

Overall, this book is notable for its breadth of coverage and the huge volume of scientific literature it has drawn on. There are no less than 780 references cited. The author's experience has enabled him to draw heavily on information from many parts of the world, which will give the book a strong international appeal. Typographical errors are relatively few for a book of this size and character. Its cost is not too excessive in these days and I have no doubt it will find a place on the shelves of some who work in this specialized field either in research or in an operational role, as well as being an important addition to the shelves of university libraries and research institutes as a major reference work.

V.K. Collinge

Books received

The listing of books under this heading does not preclude a review in the Meteorological Magazine at a later date.

The dynamics of the coupled atmosphere and ocean, edited by H. Charnock and S.G.H. Philander (London, The Royal Society, 1989) comprises papers presented at a Discussion Meeting in December 1988. They describe work being carried out on both regional and global models.

Compact data for navigation and astronomy for the years 1991–1995, by B.D. Yallop and C.Y. Hohenkerk (Cambridge University Press, 1990) aims to provide navigators and astronomers with simple, efficient methods for calculating the positions of heavenly bodies. It has been prepared by HM Nautical Almanac Office at the Royal Greenwich Observatory, Herstmonceux Castle.

Rainbows, halos, and glories, by R. Greenler (Cambridge University Press, 1989) is a paperback edition of the book which was originally published in 1980. It contains many illustrations of the various phenomena with explanations in non-technical language and ways of finding them.

Global environmental issues, by D.D. Kemp (London, New York, Routledge, 1990) analyses the role in global environmental issues of the greenhouse effect, acid rain, ozone depletion, drought and nuclear winter by way of the common thread of climatology. The author has sought the middle ground in discussing the complexity of the problems.

The earth's climate and variability of the sun over recent millenia, edited by J.-C. Pecker and S.K. Runcorn (London, The Royal Society, 1990) contains the contributions to the Discussion Meeting held at The Royal Society in February 1989. It was the first joint meeting with the Académie des Sciences in over 300 years of both their functionings.

Theoretical geophysical fluid dynamics, by A.S. Monin (Dordrecht, Boston, London, Kluwer, 1990) deals with the modern foundation of the theoretical description of natural currents in rotating stratified fluids and gases. Included is a discussion of the general circulation of planetary mantles.

The hurricane, by R.A. Pielke (London, New York, Routledge, 1990) aims to give a detailed descriptive discussion in a non-mathematical framework. Also included is an illustrated assessment of the climatology, forecasting and physical processes involved.

Satellite and radar photographs — 26 June 1990 at 1800 UTC and 27 June 1990 at 0000 UTC

The COST-73 (Co-operation in Science and Technology) pictures covering much of western Europe show radar rainfall data from several countries superimposed on infra-red cloud imagery from Meteosat. The pictures illustrate the evolution of thunderstorms on a variety of scales, some with very distinctive signatures.

At 1800 UTC (Fig. 1) a large, nearly circular, mesoscale convective system (MCS) covers much of the Massif Central in France. There are areas of heavy rainfall within the larger cloud-shield. The distinctive shape results from a merging of high-level anvil outflows from the active cells within a region of weak vertical wind-shear. The satellite image also clearly shows at

least three further MCSs tied to the Alps (radar data were not available for this area). Over northern France there is a broader band of cloud and heavy (thunderstorm) rainfall associated with a convergence zone marking the northern boundary of a tongue of air with very high wet-bulb potential temperature at low levels (Fig. 2).

By 0000 UTC (Fig. 3) the MCS previously over the Massif Central has moved north-east ahead of a weak short-wave upper-level trough (Fig. 4) and merged with an intensifying system on its south-east flank. Meanwhile the band of precipitation further north has edged south and also intensified. Violent storms within this band caused serious flooding on the Paris Metro.

A.J. Waters

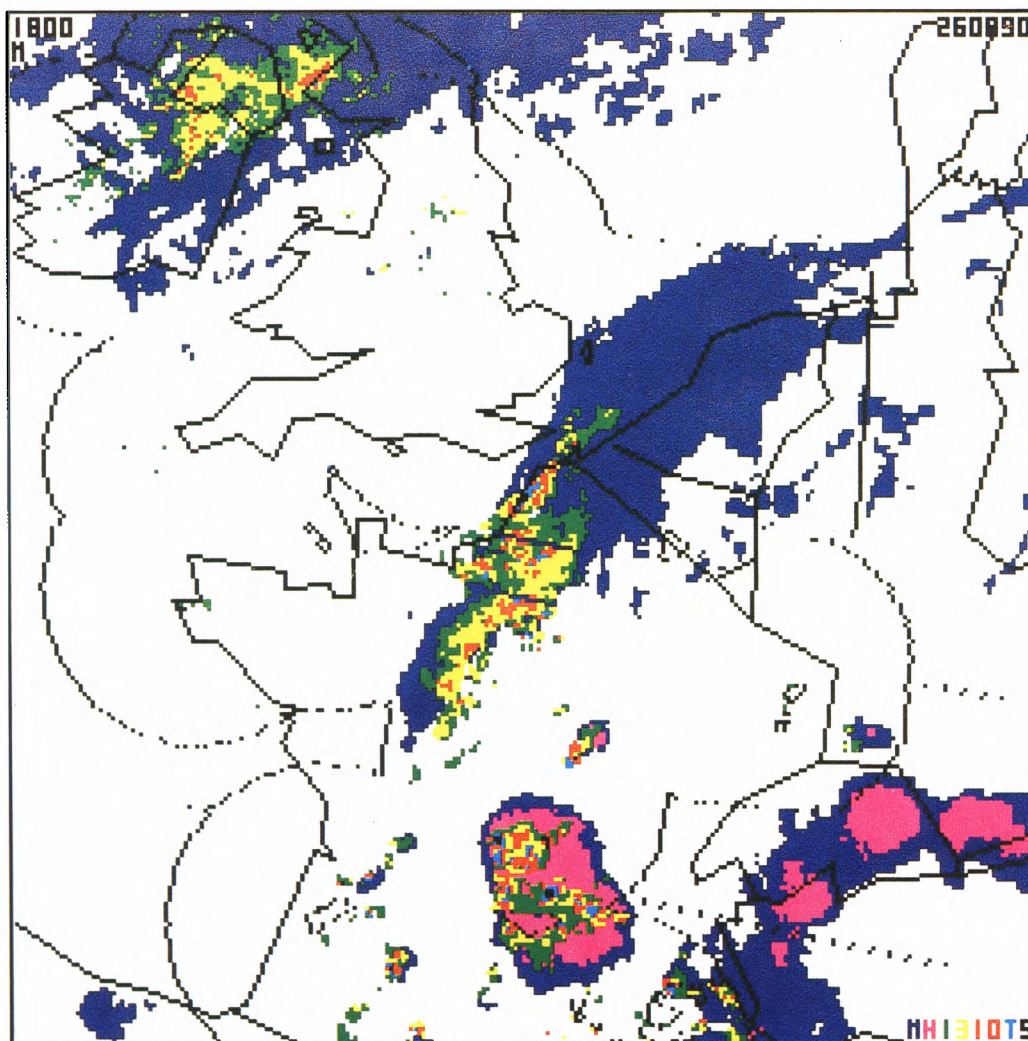


Figure 1. COST-73 satellite and radar image for 1800 UTC on 26 June 1990. Dark blue represents cloud tops with temperatures between -15 and -45 °C, and pink < -45 °C. Rainfall intensities (mm h^{-1}) are shown as follows: green < 1 , yellow 1–3, red 3–10, light blue 10–30 and black > 30 . Coastlines, national boundaries and the limits of radar coverage are shown in black.

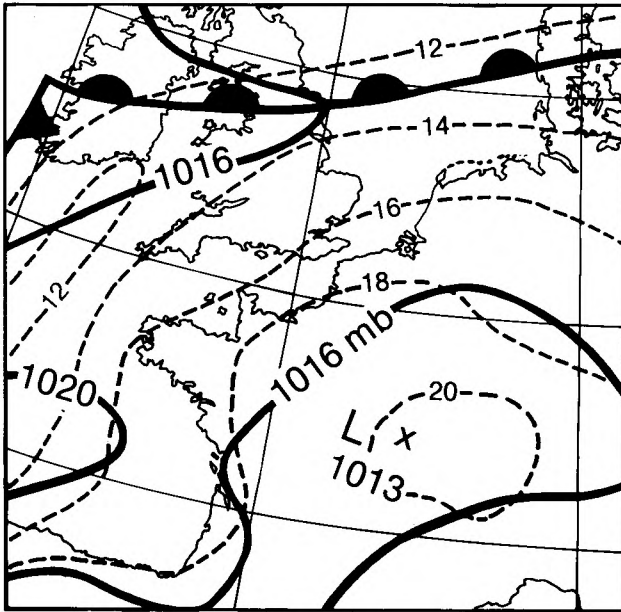


Figure 2. Surface analysis for 1800 UTC on 26 June 1990 with 850 mb wet-bulb potential temperature isotherms (°C) shown as dashed lines.

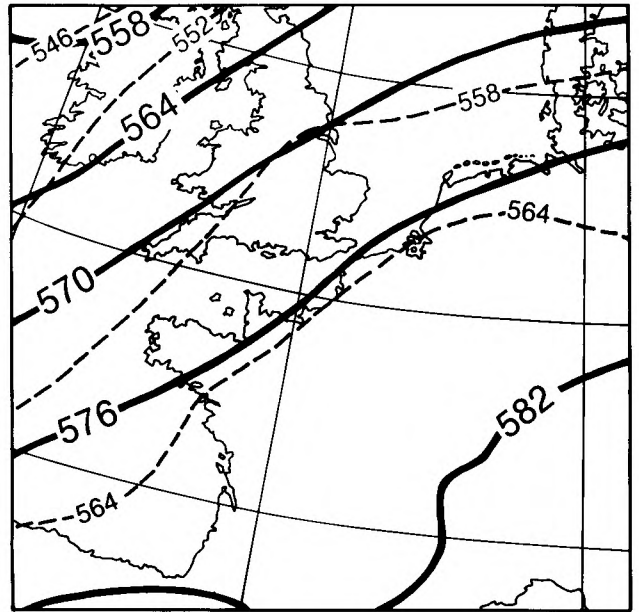


Figure 4. Upper-air analysis for 0000 UTC on 27 June 1990. Solid lines depict 500 mb contours and dashed lines the 1000-500 mb thickness (both in decametres).

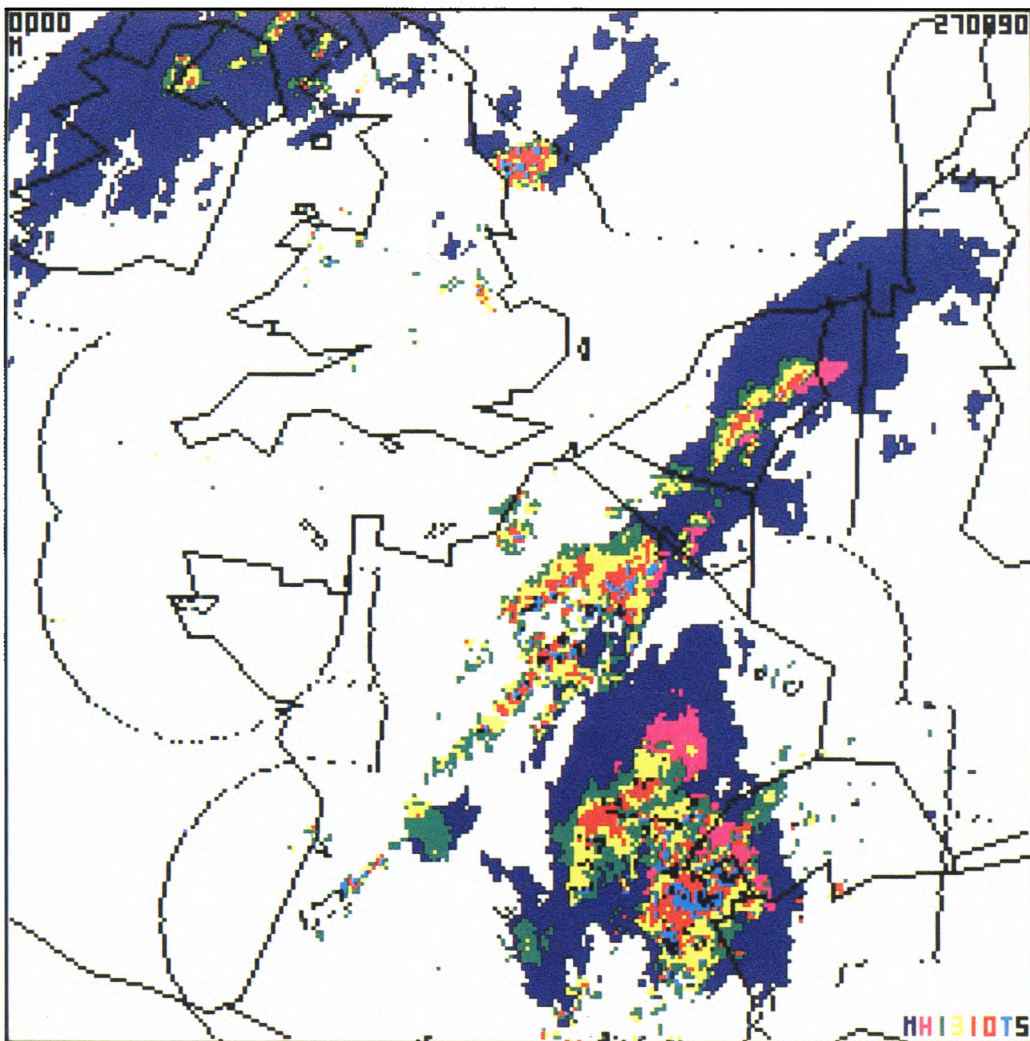


Figure 3. As Fig. 1 but for 0000 UTC on 27 June 1990.

GUIDE TO AUTHORS

Content

Articles on all aspects of meteorology are welcomed, particularly those which describe results of research in applied meteorology or the development of practical forecasting techniques.

Preparation and submission of articles

Articles, which must be in English, should be typed, double-spaced with wide margins, on one side only of A4-size paper. Tables, references and figure captions should be typed separately. Spelling should conform to the preferred spelling in the *Concise Oxford Dictionary* (latest edition). Articles prepared on floppy disk (Compucorp or IBM-compatible) can be labour-saving, but only a print-out should be submitted in the first instance.

References should be made using the Harvard system (author/date) and full details should be given at the end of the text. If a document is unpublished, details must be given of the library where it may be seen. Documents which are not available to enquirers must not be referred to, except by 'personal communication'.

Tables should be numbered consecutively using roman numerals and provided with headings.

Mathematical notation should be written with extreme care. Particular care should be taken to differentiate between Greek letters and Roman letters for which they could be mistaken. Double subscripts and superscripts should be avoided, as they are difficult to typeset and read. Notation should be kept as simple as possible. Guidance is given in BS 1991: Part 1: 1976, and *Quantities, Units and Symbols* published by the Royal Society. SI units, or units approved by the World Meteorological Organization, should be used.

Articles for publication and all other communications for the Editor should be addressed to: The Chief Executive, Meteorological Office, London Road, Bracknell, Berkshire RG12 2SZ and marked 'For Meteorological Magazine'.

Illustrations

Diagrams must be drawn clearly, preferably in ink, and should not contain any unnecessary of irrelevant details. Explanatory text should not appear on the diagram itself but in the caption. Captions should be typed on a separate sheet of paper and should, as far as possible, explain the meanings of the diagrams without the reader having to refer to the text. The sequential numbering should correspond with the sequential referrals in the text.

Sharp monochrome photographs on glossy paper are preferred; colour prints are acceptable but the use of colour is at the Editor's discretion.

Copyright

Authors should identify the holder of the copyright for their work when they first submit contributions.

Free copies

Three free copies of the magazine (one for a book review) are provided for authors of articles published in it. Separate offprints for each article are not provided.

September 1990

Editor: F.E. Underdown

Vol. 119

Editorial Board: R.J. Allam, R. Kershaw, W.H. Moores, P.R.S. Salter

No. 1418

Contents

	Page
The Great Storm of 15/16 October 1987: passive microwave evaluations of associated rainfall and marine wind speeds.	
E.C. Barrett, C. Kidd, J.O. Bailey and C.G. Collier	177
A heavy mesoscale snowfall event in northern Germany. W.S. Pike	187
Reviews	
Carbon dioxide and global change: earth in transition. S.B. Idso.	
J.P. Palutikof	196
Climatic atlas of the Indian Ocean. Part III: Upper-ocean structure.	
S. Hastenrath and L.L. Greischar. J.C. Swallow	196
Applications of weather radar systems — a guide to uses of radar data in meteorology and hydrology. C.G. Collier. V.K. Collinge	197
Books received	198
Satellite and radar photographs — 26 June 1990 at 1800 UTC and 27 June 1990 at 0000 UTC. A.J. Waters	199

Contributions: It is requested that all communications to the Editor and books for review be addressed to the Chief Executive, Meteorological Office, London Road, Bracknell, Berkshire RG12 2SZ, and marked 'For *Meteorological Magazine*'. Contributors are asked to comply with the guidelines given in the *Guide to authors* which appears on the inside back cover. The responsibility for facts and opinions expressed in the signed articles and letters published in *Meteorological Magazine* rests with their respective authors.

Subscriptions: Annual subscription £30.00 including postage; individual copies £2.70 including postage. Applications for postal subscriptions should be made to HMSO, PO Box 276, London SW8 5DT; subscription enquiries 071-873 8499.

Back numbers: Full-size reprints of Vols 1-75 (1866-1940) are available from Johnson Reprint Co. Ltd, 24-28 Oval Road, London NW1 7DX. Complete volumes of *Meteorological Magazine* commencing with volume 54 are available on microfilm from University Microfilms International, 18 Bedford Row, London WC1R 4EJ. Information on microfiche issues is available from Kraus Microfiche, Rte 100, Milwood, NY 10546, USA.

ISBN 0 11 728669 9 ISSN 0026-1149

© Crown copyright 1990. First published 1990

ISBN 0-11-728669-9



9 780117 286696

DUPLICATE

The Meteorological Magazine

October 1990

The storms of January–February 1990



DUPLICATE JOURNALS

National Meteorological Library

FitzRoy Road, Exeter, Devon. EX1 3PB

HMSO

Met.O.992 Vol. 119 No. 1419



National Meteorological Library & Archive
London Road, Bracknell, Berkshire, RG12 2SZ U.K.
TEL: 01344 85 4838 GTN: 1443 4838
fax : 01344 85 4840 EMAIL: metlib@meto.gov.uk
<http://www.meto.gov.uk/sec1/sec1pg7.html>

This publication must be returned or renewed by the last date shown below.
Renewal depends on reservations. Extended loans must be authorised by
the Librarian. Publications must NOT be passed to other readers.

2 NOV 1998		
12 DEC 2011		



3 8078 0004 5732 7

The

Meteorological Magazine

October 1990
Vol. 119 No. 1419

551.553.8:551.515.1(4)

The storms of January and February 1990

E. McCallum and W.J.T. Norris
Meteorological Office, Bracknell

Summary

A synoptic review is undertaken of the windy period that affected the United Kingdom and much of northern Europe from late January to the end of February 1990 and an attempt made at classification of the cyclogenesis events.

1. Introduction

The 1990 winter period of intense storminess over the United Kingdom and north-west Europe began with the Burns' Day storm on 25 January (McCallum 1990) and ended soon after the major low of 26 February. In this article the general characteristics of the separate storm events will be assessed and a tentative classification proposed. A rather more detailed study will be made of the 26 February event and some comparisons drawn with the Burns' Day storm. An attempt will be made to put the period in some perspective in terms of the broad-scale atmospheric anomalies and a review will be made of some of the numerical guidance available during the period. The role of the forecasters in their interpretation and tuning of this guidance will be stressed.

2. Setting the scene — early winter in the North Atlantic

In the early part of the winter (Nov./Dec. 1989) much of northern Europe had already experienced stormy interludes and some exceptionally deep lows had developed over the Atlantic. The Atlantic jet stream was unusually strong and had become displaced further south than normal during December with an area of exceptional cold (large negative) 1000–500 mb thickness anomaly (hereafter referred to as thickness anomaly) extending across north-eastern USA, eastern Canada and Newfoundland. Early January saw a transition to a more zonal regime and a recovery of thickness values over much of the USA but it remained anomalously cold

over Labrador and to the north-east of Newfoundland, maintaining the exceptionally strong baroclinic zone well to the south of its normal latitude. Whether through atmospheric coupling or some other mechanism, sea surface temperatures (SSTs) were abnormally cold to the east of Newfoundland while further to the south values were actually a little above normal. Thus the SST gradient between the Gulf Stream and Newfoundland was even stronger than usual (Fig. 1).

Past studies have indicated that the distribution of SST may have a significant influence on the development of depressions. For example Sanders and Gyakum (1980) noted a significant association between rapid

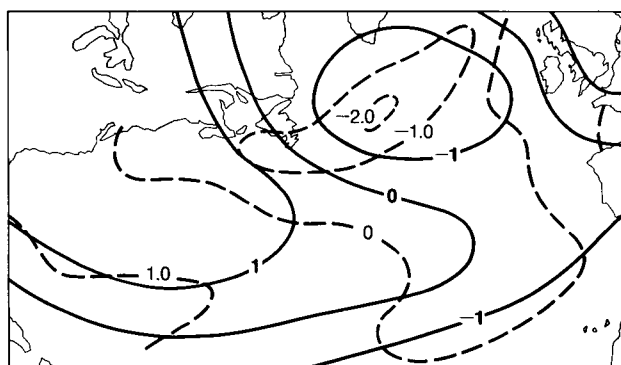


Figure 1. Anomalies of normalized 1000–500 mb thickness (standard deviations, January 1990) (solid lines) and sea surface temperatures (°C, 1–25 January) (dashed lines) for the period preceding the stormy period.

deepening and SST gradient, with a preference for the initiation of explosive deepening over or just to north of the mean winter position of the Gulf Stream. They suggested that the exchange of sensible and latent heat between cold continental air and a relatively warm sea surface is an important contributor to cyclogenesis and should be most marked where cold air moves rapidly across a strong SST gradient towards warmer water. The importance of latent heat in intense cyclogenesis has been demonstrated in a number of numerical model studies; Hoskins (1980), for instance, described a case in which latent heat processes accounted for more than 60% of the forecast deepening of a Pacific low.

Namias (1987, 1989) has also drawn attention to the concurrence of warm SST anomalies south of Newfoundland with negative geopotential anomalies further north in the periods preceding both the record Atlantic low of December 1986 (Burt 1987) and the October 1987 'Great storm' and suggests that such combinations are always likely to foreshadow extreme cyclogenesis during the following weeks. Fig. 1 emphasizes that anomalously strong gradients of both SST and thickness existed in the first few weeks of 1990; the antecedents for a stormy interlude had been established.

It is of interest to note that the continued cyclogenesis during February served to amplify the pre-existing temperature anomalies. Indeed, in mid Atlantic the negative thickness anomaly for the month exceeded 15 dam (3 standard deviations from normal) and the pressure of the mean Iceland low was more than 30 mb (3.5 standard deviations) below normal; both figures the largest recorded anomaly since records began in 1873.

3. The cyclogenesis events of the period

3.1 Some characteristics of the lows

The period from 24 January to 28 February 1990 was notable for the succession of storms that battered the United Kingdom and north-west Europe, attracting a high level of media attention. The period opened with the Burns' Day storm on 25 January when winds were of a magnitude comparable with those of the Great Storm of October 1987. It ended with the deep low and following wave depression on 26–28 February. The significance of the windiness of the period in a historical context is discussed elsewhere (Hammond 1990), though it is worth noting that many sites in southern England recorded their highest ever maximum wind speeds for the months of January and February. For example London (Heathrow) Airport recorded a gust of 76 kn on 25 January (compared with 66 kn in October 1987) and its highest ever maximum wind in February with a gust to 61 kn on the 7th. It was extreme gusts such as these that were largely responsible for the extensive damage and loss of some 80 lives.

The high frequency of the stormy spells was memorable; despite a week of anticyclonic regime in the middle of February, 15 major lows passed close to or over the British Isles during the 5-week period.

The separate tracks of the 15 lows are shown at Fig. 2. They are labelled in order of their occurrence from A to O and their positions marked at 6-hourly intervals. The position of each of the lows at the start of the period of maximum 24-hour deepening is indicated by a bold dot. Each low was steered quickly east-north-east across the

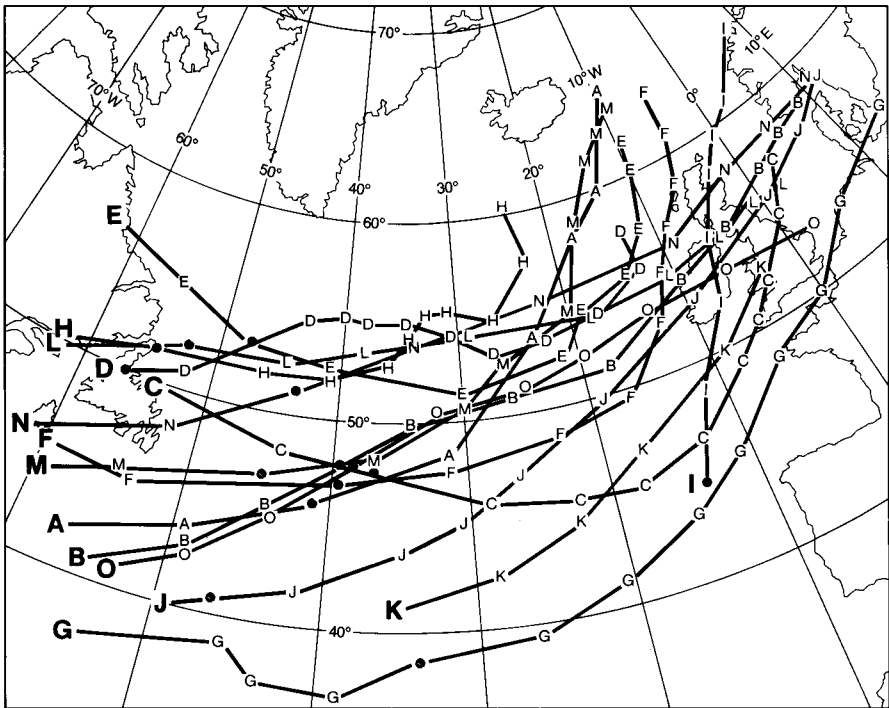


Figure 2. Tracks of the 15 lows. Positions of centres shown at 6-hour intervals, marked by identifying letter. Bold dots mark the start of period of maximum 24-hour deepening.

Atlantic and most deepened rapidly as they approached Europe. All were the result of baroclinic instability.

No two lows behaved in quite the same way; each had unique characteristics dictated by subtle differences in the dynamic forcing. It is beyond the scope of this article to examine each one in detail but it is possible to identify certain recurring patterns of behaviour which suggest a tentative classification into archetypes. A more detailed analysis is reserved for the two major lows of the period on 25 January and 26 February (described in section 4).

Table I provides details of the individual lows and their relationship with the 250 mb long-wave pattern. Sanders and Gyakum coined the term ‘bomb’ for lows in which the 24-hour fall in central pressure equalled or exceeded a latitude-dependent critical value, which ranges between 18 mb at latitude 40°N and 24 mb at 60°N. It will be seen that 11 of the depressions considered here can be classified as explosive deepeners or ‘bombs’. Perhaps significantly, each of the bombs developed over or to north of the Grand Banks of Newfoundland: the other four developed south of 45°N.

The table also emphasizes the strong winds at jet levels above each centre — an indication of the marked baroclinicity and the reason for the rapid movement of each system. The ‘standard textbook’ idea that many baroclinic disturbances begin life (relative to the jet) as right entrance features or embedded in the jet axis itself and end their deepening phase in the left exit region is borne out by 13 of the 15 depressions. This simplistic idea belies the complexity of the dynamics and feedback mechanisms involved as developing surface low

and propagating jet evolve, but is nonetheless a useful forecasters’ rule of thumb.

3.2 A classification into archetypes

In Fig. 3 a tentative classification of the lows is suggested in which five basic archetypes are identified according to their relationship to the major 250 mb trough. This is similar to the scheme adopted in the new *Forecasters’ imagery interpretation manual* (currently being co-ordinated by the Meteorological Office — due for publication 1991) and resembles a classification proposed by McClennan and Neil (1988) for identifying cyclogenesis in the Pacific Ocean. In the period considered here, there are examples of all five archetypes.

3.2.1 Type I — Mobile, flat, confluent trough

Many of these lows were associated with a short-wave trigger or jet streak which moved around the flat, confluent, upper trough although in each case they remained in close association with the long-wave pattern. This was a typical pattern for rapid cyclogenesis found by Young (1989) and was the most common configuration here with eight examples, including five ‘bombs’ moving east-north-east from the Grand Banks area (A,B,F,O,M), a modest deepener that approached from the Azores (G) and the non-deepening couplet that formed near 40°N (J,K). Three of the lows (A,F,M) turned to the left to pass to the north-west of Scotland bringing gales to the far north-west of the British Isles. Low G passed through the English Channel bringing widespread storm damage to northern France and the

Table I. Relationship of surface low centres to certain features of flow patterns at 250 mb. (a) at start of period of maximum 24-hour deepening, and (b) 24 hours later.

Low designator (see text)		A	B	C	D	E	F	G	H	I	J	K	L	M	N	O	
		January						February									
Date/time (UTC)		(a)	22/00	24/06	26/06	27/12	29/12	31/12	02/00	02/12	05/18	06/00	06/00	10/06	18/00	25/06	27/06
Position	Lat. (°N)	(a)	46	47.5	47.5	50	53	46.5	38.5	51	44	41	41	51.5	46.5	51	47.5
	Long. (°W)	(a)	41	39	37	56	47	39	34	55	14	35	47	52.5	45	43	39
24-hour pressure fall (mb)			62	46	29	46	27	36	17	38	15	−5	10	26	34	27	23
24-hour average speed (kn)			55	48	41	29	47	46	47	32	42	50	42	52	45	60	42
250 mb																	
Distance from trough (n mile)	(a)	720	600	−1200	360	250	350	240	150	420	950	540	860	880	950	600	
	(b)	540	460	0	0	250	300	240	0	250	960	420	>1200	920	>1200	540	
Trough character	(a)	C	C	C	C	D	C	C	D	C	C	C	C	C	C	C	
	(b)	C	C	D	C	D	C	C	S	C	C	C	C	C	C	C	
24-hour maximum jet speed (kn)			210	170	210	170	210	140	140	140	165	165	180	180	180	210	
Overhead maximum wind speed (kn)	(a)	140	120	100	140	90	120	100	65	60	100	125	90	120	150	130	
	(b)	70	100	50	20	35	50	110	35	100	100	125	100	70	120	140	
Jet-stream sector	(a)	R O	R E	L X	R E	J X	J O	J E	L X	R E	R X	R O	J X	J X	R O	R E	
	(b)	L X	L X	L X	L X	L X	L X	R E	L X	J E	J X	L O	L X	L X	L X	R O	
Low archetype			I	I	V	III	IV	I	I	IV	III	I	I	II	I	II	I

Key: R,L,J = to right of, to left of, and at, jet axis. E = entrance, X = exit, O = mid jet, C = confluent, D = diffluent, S = symmetrical

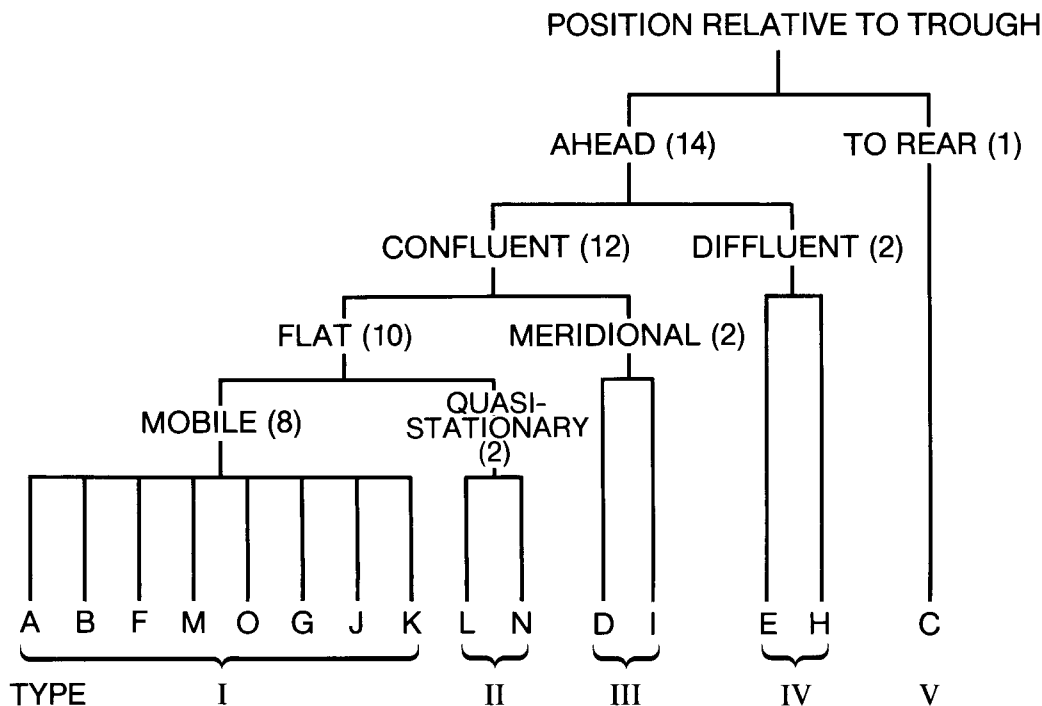


Figure 3. Tentative classification of lows into archetypes, based upon their relation to major troughs at 250 mb.

other four (B,K,J,O) crossed some part of the United Kingdom bringing gusts to at least 80 kn. The Burns' Day Storm (B) was one of these, bringing the highest gust of 93 kn (see section 4). A general schematic of this type is shown in Fig. 4; in particular the position of the jet stream relative to the low centre early in its life cycle (Fig. 4(a)) and as a mature system (Fig. 4(b)), with superimposed typical significant cloud distribution shown shaded.

A characteristic feature of those type I lows was the surge of pressure that followed in the wake of the centre (due to marked subsidence, which typically occurs immediately behind the confluent upper trough), leading to very strong winds on their western and southern flanks. Low G which brought storms to northern France was a particularly striking example of this marked anticyclogenesis with pressure rises of over 20 mb per 3 h to the rear of the centre although it was not an explosive deepener itself (see Young 1990).

Except for the warm front wave (K) all of this group exhibited characteristic cyclogenetic signatures on satellite imagery; notably the baroclinic leaf and dry slot (Weldon 1979, Monk and Bader 1988). However, although some showed these characteristics before the rapid deepening phase, others did not develop a good cloud head until the explosive deepening was well under way.

3.2.2 Type II — Quasi-stationary, flat, confluent trough

Lows L and N developed ahead of a slow-moving 250 mb trough. Each progressed very rapidly east-north-east with little curvature of track, moving well to poleward of the main baroclinic zone and driven by a

shallow, fast-moving, short-wave perturbation near the left exit region of a propagating polar-jet streak. The developing centres were associated with an area of local diffluence and moved away from the slower moving long-wave, confluent, upper trough. In neither case was there marked anticyclogenesis following the passage of the centre due to the diffluent nature of the associated short-wave upper trough. One of this pair, the 26 February low N gave a highest gust of 87 kn over the United Kingdom and is discussed in more detail in section 4 below.

Satellite imagery showed some degree of the classical dry-slot and baroclinic-leaf signatures but these were generally less organized than in type I storms.

3.2.3 Type III — Meridional confluent trough

Two lows (D,I) developed on the forward side of large-amplitude, 250 mb troughs (i.e. trough amplitude \approx half the wavelength). Low D deepened as it moved seaward from Newfoundland in association with a disrupting upper trough. Its subsequent movement was dictated by progression of the closed upper circulation. Low I ran quickly north-east across Britain in the entrance region of a jet ahead of a relaxing 500 mb trough.

3.2.4 Type IV — Diffluent trough

Two lows (E,H) deepened ahead of a diffluent, long-wave, upper trough. Both were well to poleward of the main jet and already under a closed 500 mb contour pattern on moving east from Labrador. As with the type III low mentioned above, subsequent progress was controlled by the upper vortex. Both lows passed to the north-west of Scotland as mature systems with no exceptional wind speeds.

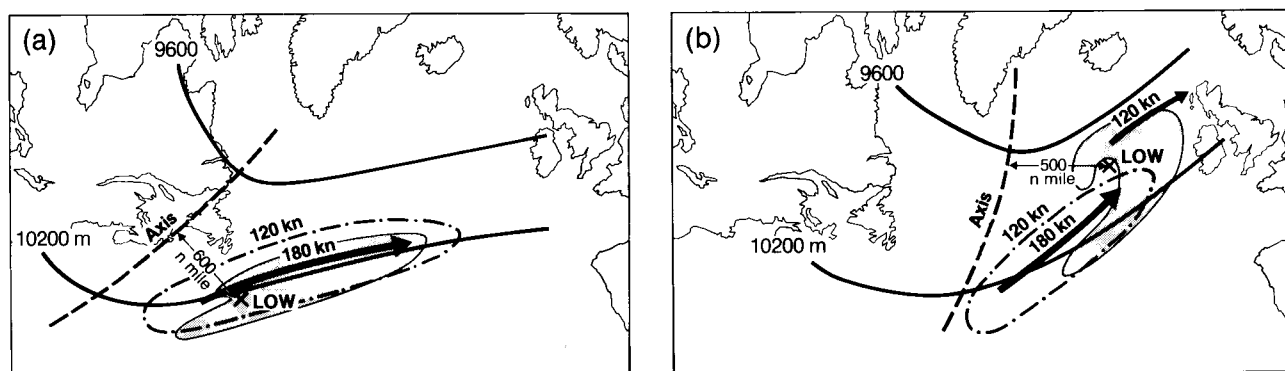


Figure 4. Schematic of low development ahead of a broad, mobile, confluent 250 mb trough. Disposition of surface centre relative to 250 mb pattern (a) at time of onset of rapid deepening, and (b) 24 hours later. Main cloud bands are stippled.

3.2.5 Type V — Development to rear of trough

Low C was the only low to develop in the north-westerly flow to the rear of a long-wave upper trough. It developed in the left exit of a propagating and veering polar jet with a developing short-wave feature in close association. Cyclogenesis occurred in conjunction with this short-wave perturbation although the classical cloud head and dry-slot signatures were not apparent on imagery until the development was well under way.

3.3 Summary of types

The following general conclusions emerge from this study:

- Marked anticyclogenesis to rear of the surface centre is a potent generator of strong winds and appears to be a characteristic of lows developing in, or advancing to, a position ahead of a mobile, flat, confluent 250 mb trough.
- Such a surge of pressure is not a feature of lows ahead of a diffluent trough, nor of the important type II lows which run rapidly ahead of, and away from, a quasi-stationary, long-wave, upper trough.
- There is no simple correlation between severity of surface wind gusts and amount of deepening. Low G was one of the most damaging but was a comparatively modest deepener. The warm front wave (K) did not deepen at all yet produced gusts of 80 kn.
- Satellite imagery is often invaluable in drawing attention to the onset of major deepening but it is not always useful as a predictor of such events. Cyclogenetic signatures evident on imagery are helpful in determining the conceptual type. However, the waxing and waning of cloud features and changing cloud-top temperatures as witnessed on satellite movie-loops give a more useful insight into development.

4. Dynamical evolution on 26 February — comparison 25 January 1990

To understand a little more of some of the dynamics involved with two major storms during the period, the depression of 26 February is compared here with the

Burns' Day storm of 25-January. It was the severe gales from these two lows that attracted most media attention and heralded the commencement and end of the windy period.

The embryonic storm of 26 February, as did the other, formed as a minor perturbation on the main baroclinic zone over the eastern USA. A closed isobaric circulation first developed over New England around midnight on 24 February. Embedded in a powerful westerly jet (maximum speed 180 kn), it moved rapidly east-north-east in association with a minor, short-wave, upper trough developing on the western flank of the main baroclinic zone.

The low began to deepen soon after moving east of Newfoundland early on 25 February. Satellite pictures at this time indicated the typical signature seen on many of the cyclogenesis events during this period with the appearance of a double baroclinic zone, emphasized by two parallel cloud bands. Deepening was to continue for more than 48 hours, by which time the centre had reached the Gulf of Bothnia and the central pressure fallen by 42 mb.

At midnight on the 26th, the low was centred in sea area Malin and the dynamics of the system are well represented by diagnostic output from the Meteorological Office fine-mesh regional model for that time (Fig. 5). Marked vertical motion well ahead of the low was mainly due to the substantial maximum in the warm advection field, with rapid ascent over the centre itself due to differential vorticity advection ahead of the fast moving, slightly diffluent, short-wave, upper trough. Behind the upper trough axis, marked subsidence resulted from a combination of cold advection and negative vorticity advection. This symmetrical pattern of warm and cold advection emphasized the translatory nature of the system while the ascent over the centre of the low explains the continuing fall in central pressure, features identified in the study of the October 1987 storm by Morris (1988). The pressure rises behind the system were of a similar order to the falls ahead and were modest by comparison with the Burns' Day storm which exhibited rises of more than 20 mb in 3 hours. This

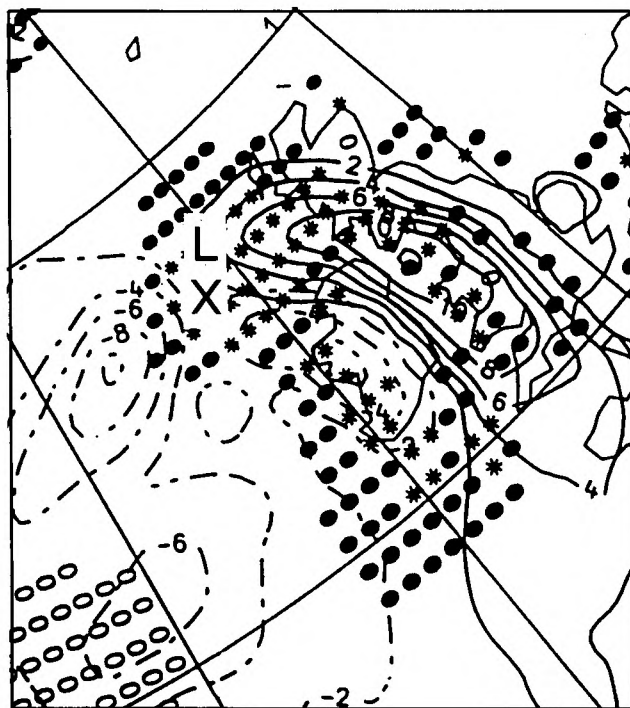


Figure 5. Diagnostic output from the Meteorological Office fine-mesh model for 0001 UTC on 26 February 1990.

reflected the slightly diffluent shape to the associated upper trough, as opposed to the confluent nature of the Burns' Day storm, where marked anticyclogenesis behind the centre contributed to the greater pressure surge.

Satellite pictures during the early deepening phase (Fig. 6) showed some signs of the baroclinic leaf structure and dry slot; features normally associated with rapid cyclogenesis, but the signature was less pronounced than in the Burns' Day storm which exhibited a larger cloud head (compare with Fig. 7).

Tightest gradients were on the western and southern flanks of the low, and by 0600 UTC on the 26th covered a large part of the United Kingdom (Fig. 8) with some of the strongest winds associated with the surface cold front. This distribution of wind and the rapid movement of the system were important features identified in the Burns' Day storm (McCallum 1990). Highest mean speeds were again at western and southern coastal sites with 40–50 kn fairly common. However, it was the powerful gusts that were important factors in the widespread damage and loss of life; factors which, along with the severe flooding in North Wales, attracted much media attention. It was a very windy day nation-wide

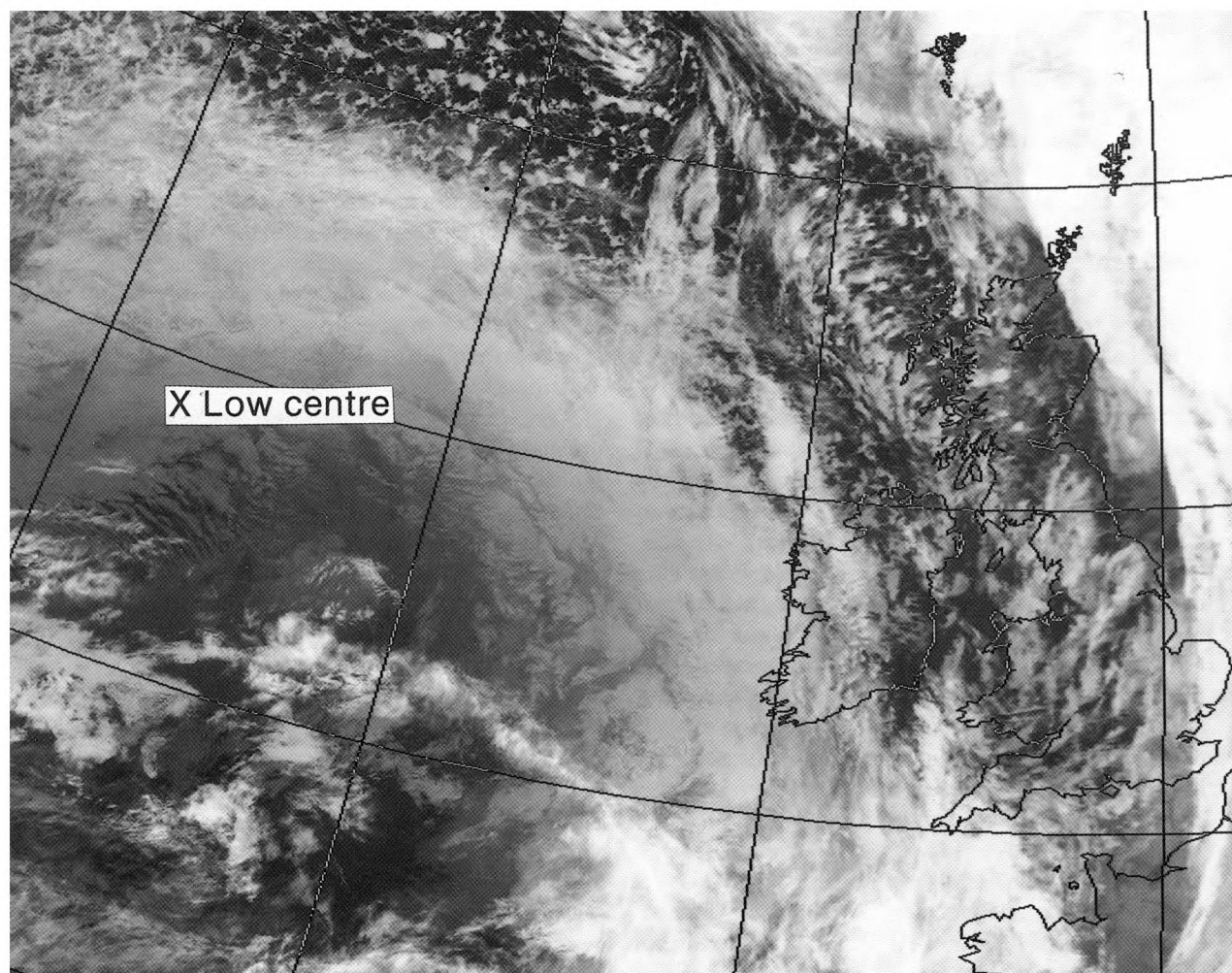


Figure 6. NOAA-11 infra-red image for 1435 UTC on 25 February 1990.

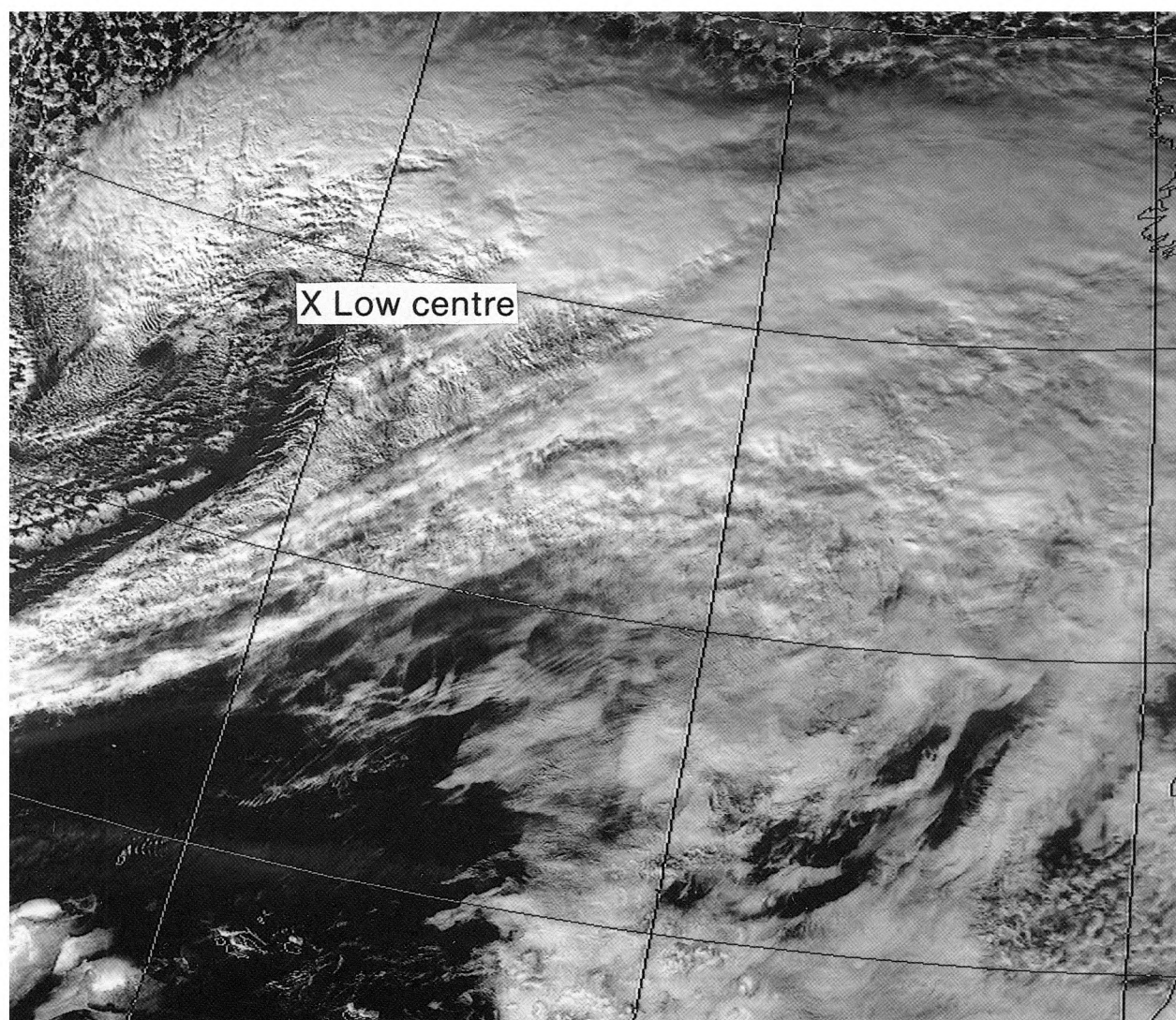


Figure 7. NOAA-11 visible image for 1518 UTC on 24 January 1990.

but the maximum gusts were generally less than those observed on the Burns' Day storm, except for the north of England which had its windiest day of the winter.

5. How well were the cyclogenesis events forecast?

The current generation of operational NWP models shows considerable skill in handling major cyclogenesis events, and the Meteorological Office's 15-level model is widely regarded as a leader in this field. The global (coarse-mesh) version of this model was useful in giving advance warning of potential storms up to 6 days ahead. Accurate notice of the (Thursday) Burns' Day storm was first given in the television farming forecast on the previous Sunday. For the finer detail that was necessary for the framing of warnings for the media the regional (fine-mesh) version was useful in giving detailed guidance up to 36 hours ahead. Gadd *et al.* (1990) have shown that the regional model is capable of realistic representation of explosive deepening. A similar study

by Hall (personal communication) for this present period is presented at Fig. 9. Cases included are those in which a pressure fall of at least 24 mb was forecast by the regional model or was observed to occur in a period of 24 hours commencing at 0000 or 1200 UTC. There appears to be a slight bias towards larger falls than forecast, which was not apparent in the longer analysis of Gadd *et al.* Of particular note, though, is that the two poorest forecasts relate to the major storms of the period, those of 25 January and 26 February.

Handling of these two lows highlighted the crucial role of the forecaster in overcoming the occasional major deficiencies in numerical guidance that occur from time to time.

The deficiency in the Burns' Day case is an example of the 'rogue run' where the model lapses into a weak or non-developmental mode after a consistent and clear signal for marked cyclogenesis. Such lapses have been noted by Woodroffe (1990) and by Reed *et al.* (1988) and if followed may prompt a downgrading of a previous

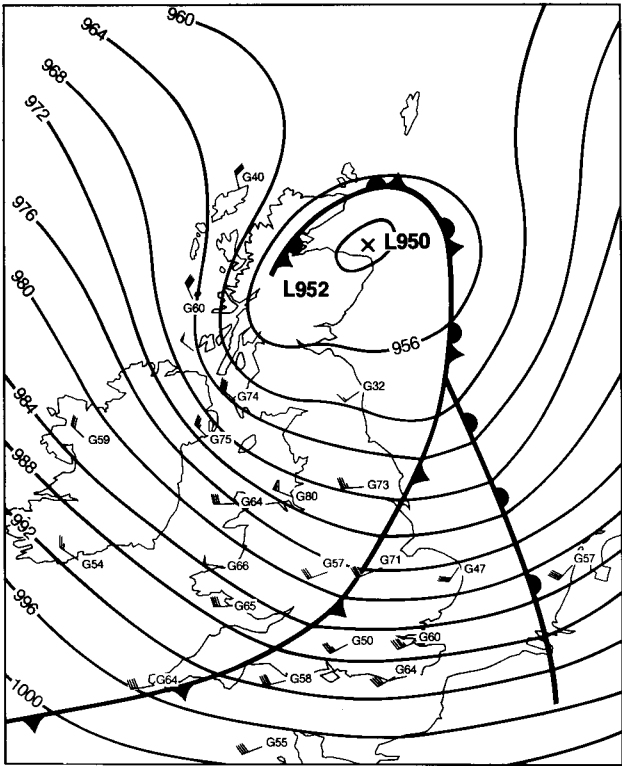


Figure 8. Mean-sea-level pressure pattern and fronts at 0600 UTC on 26 February 1990, with winds and gusts shown conventionally at selected stations.

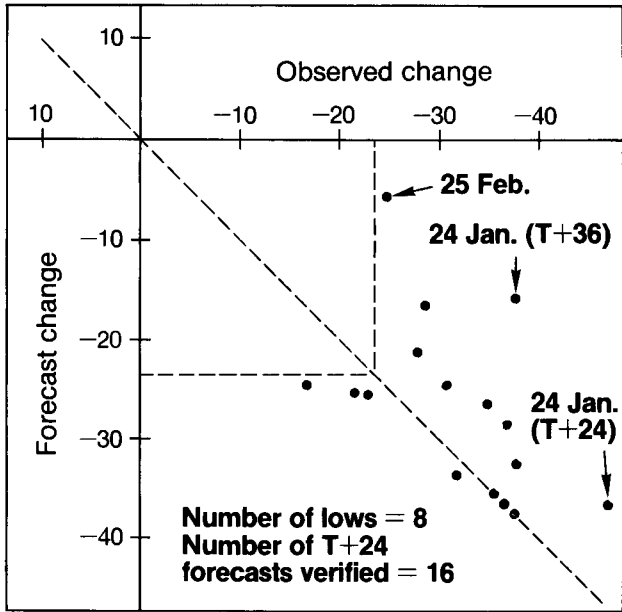


Figure 9. Observed 24-hour change in central pressure (mb) of rapidly deepening lows in the North Atlantic compared with values forecast by the fine-mesh model during period 22 January–28 February 1990. Only cases where observed or forecast change exceeded 24 mb are shown.

warning of severe weather. Fig. 10 shows forecasts from two consecutive runs for verifying time of 1200 UTC on the 25th. The 36-hour forecast (T+36) shown in Fig. 10(a) typifies the non-developmental mode and can be contrasted with the much better 24-hour forecast shown at Fig. 10(b). Fortunately, forecasters were alert to the problem and warnings were issued on the strength of the overall signal from an ensemble of solutions. Clearly, confidence was also increased by the marked cyclogenesis of the latest run although it should be emphasized that this is not always the case and indeed this particular forecast was greatly improved by the

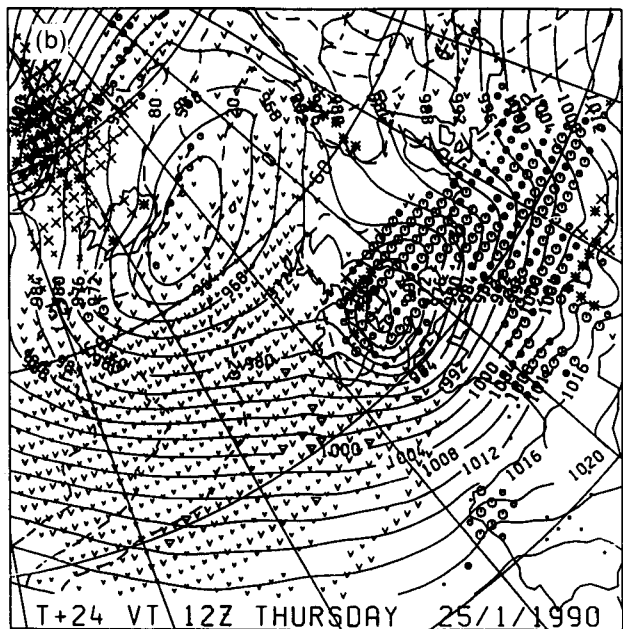
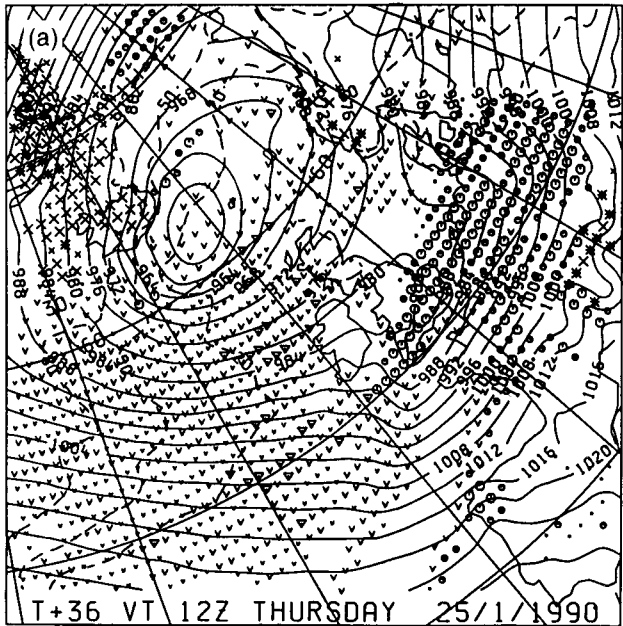


Figure 10. Fine-mesh model output from consecutive runs, both verifying at 1200 UTC on 25 January 1990. (a) T+36 forecast from data time 0001 UTC on 24 January 1990 and (b) T+24 forecast from data time 1200 UTC on 24 January 1990.

observations from two ships near the low centre (Heming 1990).

The second problem identified during the period was the tendency to 'nudge' towards the correct solution (of intense development) from run to run rather than a sudden change to explosive cyclogenesis. This again was highlighted by Woodroffe (1990) and was particularly manifest in the 26 February storm. Fig. 11 shows a set of tracks from a succession of 6-hourly fine-mesh runs for this event; note the trend to more development and a more northerly track for each forecast. This trend is symptomatic of greater distortion of the steering flow (hence change of track) caused by feedback effects from the more intense circulation. How well the forecaster pre-empted this trend is shown by the 24-hour forecast for 26 February at 0600 UTC (Fig. 12). In reality this extrapolation erred on the conservative side as the depression took an even more northerly track through the Great Glen in northern Scotland, a deviation that was covered by a subsequent amendment.

These examples emphasize that, although the overall numerical guidance was good, there were some very important occasions when the forecaster added significantly to the accuracy of the warnings issued to the media and population at large.

6. Conclusions and forecaster guidelines

The period from 25 January to 28 February 1990 was unusually windy over the United Kingdom and much of northern Europe and was associated with the lowest pressure anomaly since records began. This stormy spell was preceded by a protracted spell of abnormal cold over Canada and the northern North Atlantic and by anomalously high SST south of Newfoundland. These are the very antecedent conditions which Namias (1987, 1989) considers to predispose the atmosphere to the occurrence of one or more extreme cyclogenetic events in the North Atlantic.

Many of the 15 baroclinic disturbances identified were explosive deepeners or 'bombs' with latent-heat processes an important contributory factor in the intensity of the development. Eight of the lows were associated with a highly mobile, flat, slightly confluent, upper trough and exhibited baroclinic leaf and dry-slot characteristics on satellite imagery and marked pressure rise behind the centre.

Numerical guidance was useful in predicting overall developments on the majority of occasions but the lows of 25 January and 26 February low are a reminder that the forecaster must not have blind, unquestioning, dependence upon numerical weather prediction (NWP)

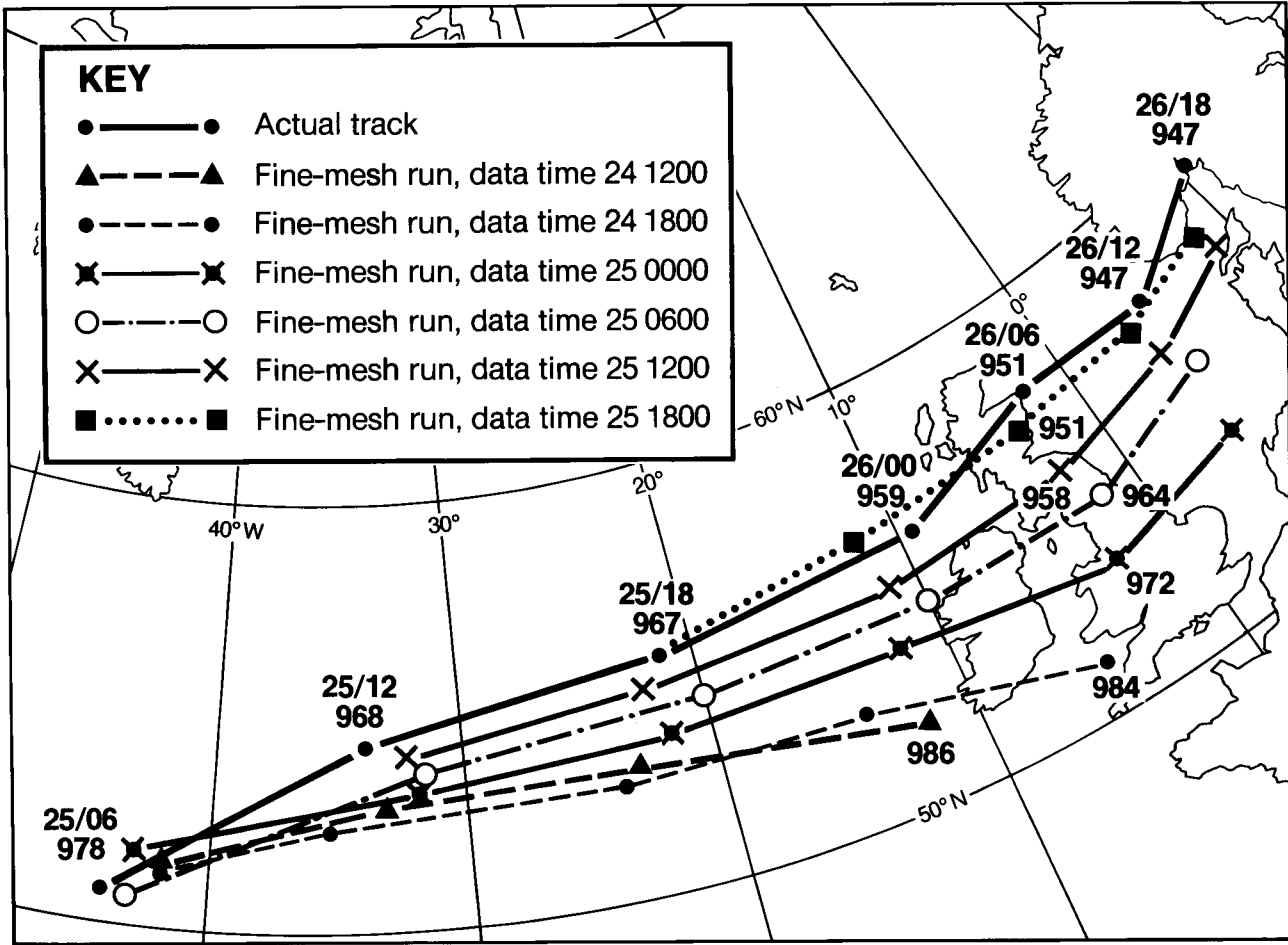


Figure 11. Tracks of low of 26 February 1990. A comparison between its actual track and successive forecast tracks is distinguished in the key) from the fine-mesh model. Central pressure (mb) is shown where feasible.

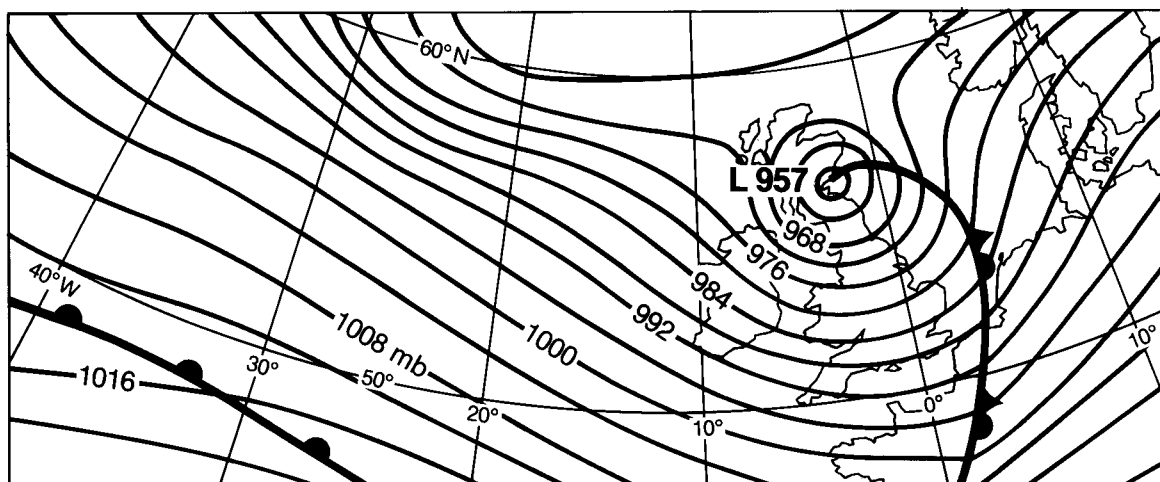


Figure 12. Meteorological Office 24-hour forecast for 0600 UTC on 26 February 1990.

products. In consideration of this, and other cases from the period, the following guidelines emerge for forecasters when interpreting NWP products on occasions of possible cyclogenesis.

1. Do not accept model guidance at face value without first trying to understand (qualitatively at least) the dynamical logic behind the model predictions.
2. Consider a sequence of runs for the same verifying time. The most recent run is not always the best — it may be a 'rogue'. The degree of consistency from run to run will determine the confidence with which a solution can be reached. Also when successive forecast runs show a continuing and consistent trend, be prepared to anticipate the likely outcome by extrapolation.

Although not specifically highlighted in the cases discussed above the following points are also important when utilizing numerical products.

3. Look at an ensemble of solutions from different models. Some may have a particular sensitivity to certain initial conditions.
4. The broad-scale upper pattern will reveal the potential for cyclogenesis but its precise timing and location will usually (perhaps always) depend upon the timely intervention of a 'trigger', some small-scale perturbation or jet streak. This is most likely to be picked up from close scrutiny of satellite imagery. A single frame 'snapshot' may, fortuitously, capture the crucial moment of initiation, but a movie-loop is likely to be more revealing.

Acknowledgements

The authors would like to thank Dr R.W. Riddaway for his typically constructive and incisive comments, and A. Woodroffe and M.V. Young for helpful remarks on an early draft of the paper.

References

- Burt, S.D., 1987: A new North Atlantic low pressure record. *Weather*, **42**, 53–56.
- Gadd, A.J., Hall, C.D. and Kruze, R.E., 1990: Operational numerical prediction of rapid cyclogenesis over the North Atlantic. *Tellus*, **42A**, 116–121.
- Hammond, J.M., 1990: The strong winds experienced during the late winter of 1989/90 over the United Kingdom: Historical perspectives. *Meteorol Mag*, **119**, 21?–21?
- Heming, J.T., (1990): The impact of radiosonde observations from two Atlantic ships on a forecast for the storm of 25 January 1990. (To be published in *Meteorol Mag*.)
- Hoskins, B.J., 1980: Effect of diabatic processes on transient mid-latitude waves. Workshop on Diagnostics of Diabatic Processes. 85–99. (Available from ECMWF, Shinfield Park, Reading, Berkshire RG2 9AX, England.)
- McCallum, E., 1990: The Burns' Day storm, 25 January 1990. *Weather*, **45**, 166–173.
- McClennan, N. and Neil, L., 1988: Marine Bombs Programme — Final Report Pacific Region internal document. AES Canada. (Unpublished, copy available in National Meteorological Library, Bracknell.)
- Monk, G.A. and Bader, M.J., 1988: Satellite images showing the development of the storm of 15–16 October 1987. *Weather*, **43**, 130–135.
- Morris, R.M., 1988: The synoptic-dynamical evolution of the storm of 15/16 October 1987. *Meteorol Mag*, **117**, 293–306.
- Namias, J., 1987: Factors relating to the explosive North Atlantic cyclone of December 1986. *Weather*, **42**, 322–325.
- , 1989: Anomalous climatological background of the storm of 15/16 October 1987. *Weather*, **44**, 98–105.
- Reed, R.J. and Albright, M.D., 1986: A case study of explosive cyclogenesis in the eastern Pacific. *Mon Weather Rev*, **114**, 2297–2319.
- Reed, R.J., Simmons, A.J., Albright, M.D. and Uden, P., 1988: The role of latent heat release in explosive cyclogenesis: three examples based on ECMWF operational forecasts. *Weather and Forecasting*, **3**, 217–229.
- Sanders, F. and Gyakum, J.R., 1980: Synoptic-dynamic climatology of the 'bomb'. *Mon Weather Rev*, **108**, 1589–1606.
- Weldon, R.K., 1979: Cloud patterns and the upper air wind field, Part IV National Weather Service Satellite training notes. (Unpublished manuscript available from Applications Division, National Earth Satellite Service, NOAA, US Dept of Commerce.)
- Woodroffe, A., 1990: Forecasting the storm of 8 November 1989 — a success for the man-machine mix. *Meteorol Mag*, **119**, 129–140.
- Young, M.V., 1989: Liaison with the Central Forecasting Office regarding imagery interpretation for a cyclogenesis event: 20–21 October 1989. (Unpublished, copy available in National Meteorological Library, Bracknell.)
- , 1990: Satellite and radar images, 0900 GMT 3 February 1990. *Weather*, **45**, 268–270.

The strong winds experienced during the late winter of 1989/90 over the United Kingdom: Historical perspectives

J.M. Hammond

Meteorological Office, Bracknell

Summary

The persistently windy period of late January and February 1990 included three widespread and damaging gales. Using a variety of statistical and graphical techniques, this period is assessed in a long-term context to judge how unusual it was. The question arises as to whether changes in the wind-climate mean that this type of weather is recurring more often.

1. Background

A period of particularly sustained windiness affected the United Kingdom during the late winter of 1989/90. The period was punctuated by three especially stormy events.

The first and most damaging event, on 25 January, was confined largely to southern and eastern parts of the United Kingdom. Gusts of 70–90 kn in this region were comparable with those of the 'Great Storm' of October 1987. However, because the strongest winds occurred

during the day, and over a wider area, the more recent event caused a greater loss of life (McCallum 1990). Damage to buildings and trees occurred widely, with dislocation of power and transport causing major inconvenience. Many places reported their highest gust on record. Boscombe Down (near Salisbury), for example, recorded 79 kn, the strongest wind since the station opened in 1933. Fig. 1 shows the return periods of the maximum gusts recorded at a selection of

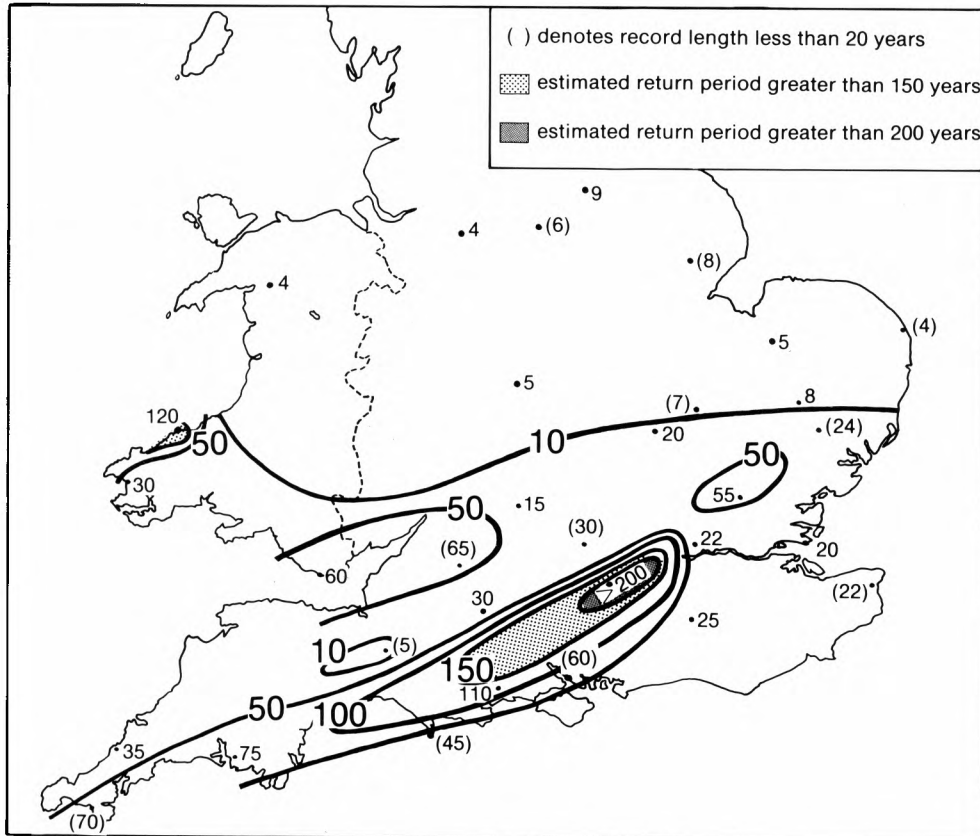


Figure 1. Return periods (years) for maximum gusts recorded on 25 January 1990.

anemograph stations in southern parts of the United Kingdom. The most exceptional gusts were concentrated in a densely populated band from Dorset north-eastwards to London.

The second bout of especially strong winds occurred during 7 and 8 February, and the most exceptional gusts were again in southern parts of the United Kingdom. Gusts of 50–70 kn were reported widely in this area, London (Heathrow) Airport having its highest February gust on record with 61 kn.

In contrast, the strong winds between 26 and 28 February were spread throughout the United Kingdom. Mean speeds in excess of 40 kn were common, with gusts above 80 kn in northern England.

Indeed, although the gusts of February did not reach the damaging levels of 25 January in the south, February 1990 over the whole of the United Kingdom was persistently windy, all the more unusual because it is often the least windy month of the winter.

2. Is it getting windier?

The evolving wind climate affects a diversity of activities. Each has its own sensitivity to change on different temporal and spatial scales, which the climate is constantly undergoing. Where incidents of unusually high wind speed are isolated occurrences within an essentially stationary long-term distribution, the impact may be restricted to personal inconvenience, temporary disruption to industrial activity, or sporadic building damage. More serious difficulties arise where such variations are associated with prolonged trends in the mean wind regime; or alternatively, where a change in variability produces a greater frequency of extreme events. For example, Palutikof *et al.* (1987) have sought to show that long-term variability in the wind field is sufficient to be a matter of concern to the wind energy industry. Building design is another sector which should be wary of relying on existing long-term averages, which may not reflect adequately the wind climate's inherent potential to change.

To help answer the question 'Is it getting windier?' a long-term view of the windy period of the winter of 1989/90 needs to be taken. To do this satisfactorily requires different scales of analysis. Injudicious selection of the wrong scale of analysis could bias unfairly the prominence of one spell compared with another; a combination of techniques will best reveal how the windy period of last winter appears in the long-term context.

3. Data sources

3.1 Anemograph data

Hourly mean and gust speeds are recorded routinely at over 100 anemograph stations around the United Kingdom. These records are archived on computer for 1970 onwards (Collingbourne 1978). Manuscript records exist further back for a number of stations; but due to

site, exposure or instrument changes, there are only a handful of stations for which long-period hourly wind speed data can be analysed as an homogeneous time-series. Six stations currently operating have records extending back to before the First World War.

3.2 Spot-wind data

A further network of about 50 synoptic sites record routinely the 'spot' wind each hour. This is the mean wind over the 10 minutes before the hour, and is archived on computer typically from the mid-to-late 1950s onwards. It is therefore a longer, computer-based archive, but is less representative of the entire hour than anemograph data.

Both anemograph and spot-wind data, when averaged monthly, seasonally or annually, can be used for assessing long-term trends in the mean wind climate.

3.3 Windiness indices

Smith (1982) used homogeneous anemograph records for the period 1965–80 to devise an index based on monthly mean winds, and so assess the relative windiness of a particular month compared to the same month through the rest of the record. These indices can be averaged into seasonal or annual values, regionally or nationally. Also, using surface pressure gradients between six grid-points around the British Isles, Smith obtained national estimates of the monthly windiness index from 1881 onwards. Using a synthesis of the two techniques, monthly indices can be produced from January 1881 onwards.

3.4 Spell analysis

Series based on monthly means can often disguise individual windy periods of varying length, and the especially stormy events within them. Anemograph or spot-wind data held on computer can be processed easily, this allows flexible analysis of monthly or annual averages and, in particular, enables individual spells of any chosen time period to be studied and compared.

3.5 Storm analysis

3.5.1 Maximum gusts

As it is maximum gusts that usually cause the most damage within any one storm event, they are often more appropriate to use in assessing the changing frequency of extreme winds (for example, in terms of return periods), and in comparing the severity of individual storm events.

3.5.2 Subjective assessment

Another, and more subjective, analysis of the changing frequency of individual windy events is to identify qualitatively the 'notable incidences of widespread gales'. A selection of gales was made by Harris (1970) from the period 1920–70. However, not only do different gales exhibit differing characteristics in terms

of duration, mean wind speed, and strength and frequency of gusts, but they vary crucially in terms of timing and areal extent. Selection can therefore often be a haphazard procedure, based partly on personal memory or inconsistent media exposure. Complicating conditions such as high tides, prolonged rainfall and heavy snowfall, make comparison of different gales still more difficult.

4. February 1990 — how unusual?

4.1 Comparison with previous Februarys

4.1.1 Monthly mean winds

Fig. 2 shows how February 1990 compares nationally with other Februarys since 1970. These national averages have been calculated using data from 17 anemograph stations, divided into three regions as follows:

- North: Leuchars, Kinloss, Kirkwall, Fort Augustus, Benbecula, Prestwick,
- Central: Aldergrove, Valley, South Shields, Waddington, Leeming, Fleetwood, and
- South: Boscombe Down, Plymouth, Honington, Aberporth, Avonmouth.

Nationally, monthly mean speeds in February have fluctuated generally between 8 and 13 kn up until 1988.

However, 1989 was windier, with an average of 13.7 kn, while February 1990 was by far the windiest, with an average hourly wind speed of 17.2 kn. The pattern is somewhat confused when the data are broken down into the three regions, but in each case the last three Februarys have shown increasing windiness, with February 1990 having the maximum monthly wind speed by a clear margin, especially in the South region, where the average speed was 18.8 kn.

4.1.2 Monthly windiness index

The use of the Smith (1982) windiness index allows the difference between the mean speed for an individual month and the 1970–89 averages for that month to be determined and expressed as a proportion of the standard deviation. So for each month a standardized anomaly is obtained.

For 15 of the 17 stations listed in section 4.1.1, the February 1990 index values are shown in Fig. 3. Fleetwood and Fort Augustus indices could not be calculated because data were missing or incomplete for February 1990. The index values shown are the highest (most unusually windy) since 1970 at all of the stations in the South and Central regions, with the exception of South Shields. In the North region, all stations except Kirkwall recorded their highest index.

To put February 1990 in the longer context of Smith’s 1881–1980 windiness index record, the nationally averaged January 1970–February 1990 index values

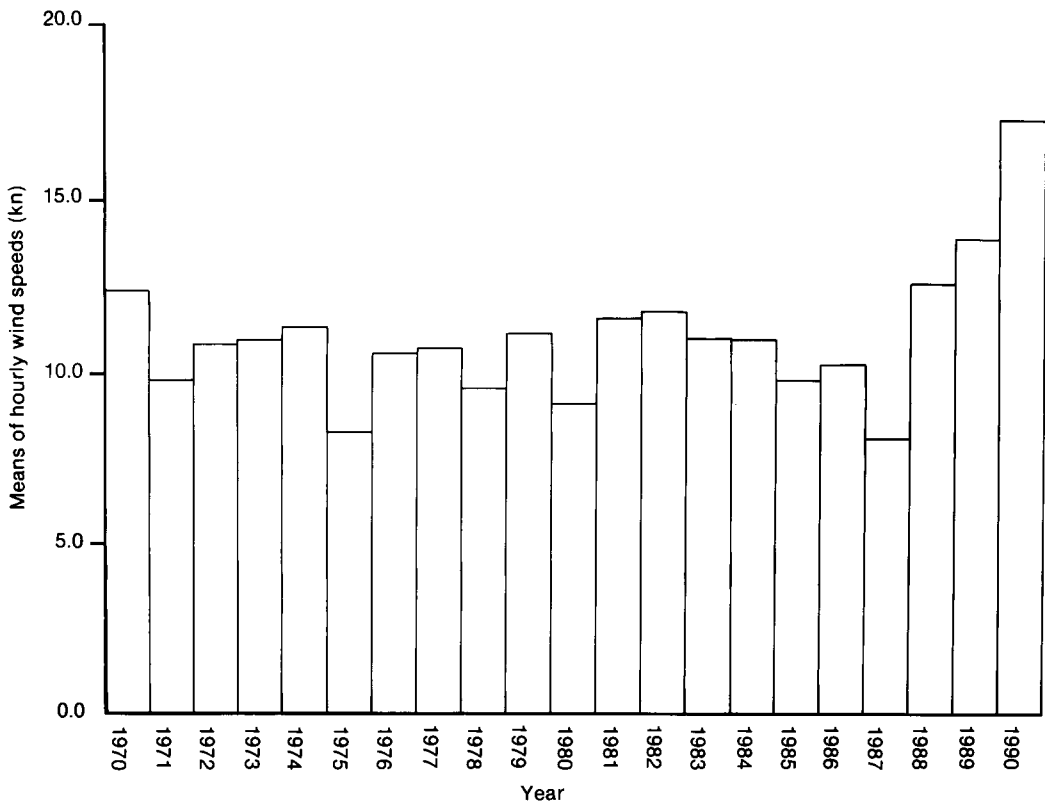


Figure 2. Mean wind speed (kn) for Februarys, averaged from 17 anemograph stations for the period 1970–90.

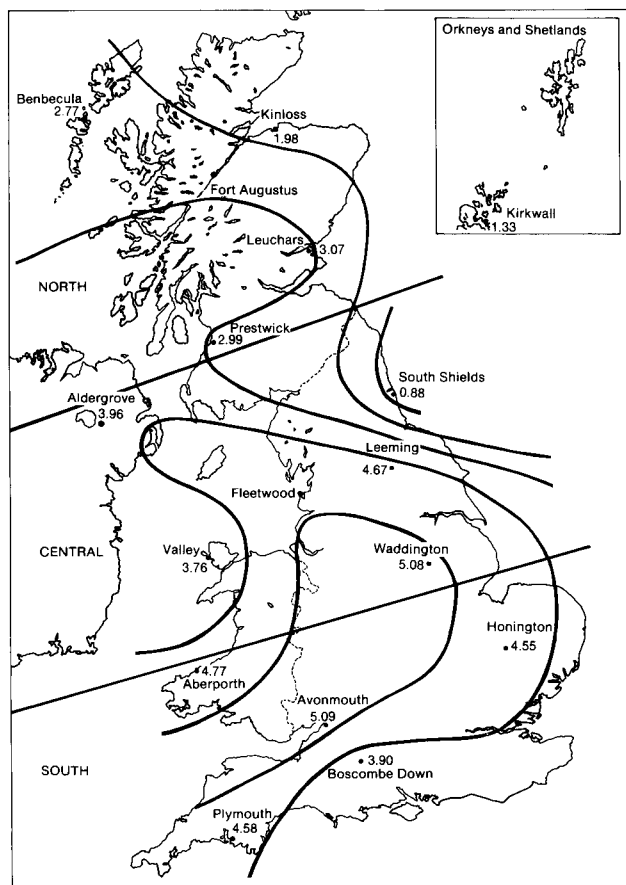


Figure 3. Windiness index for February 1990, see text for derivation.

were calculated and corrected to compensate for differing averaging periods and stations used, after Crummay (1987), (see Table I).

Fig. 4 shows the entire series from 1881–1990. February 1990 does appear to have been the most windy since before 1881, the index of 3.6 exceeding marginally the February 1903 value of 3.5. The time series as a whole is very ‘noisy’ with no obvious trends in the raw data. The smoothed graph, however, reveals a steady decline in indices from around 1960 until the 1980s. Indeed the February index fell as low as –1.4 in 1987, prior to the increasingly windy last 3 years.

When looked at in the long-term context then, the last 3 years cannot be interpreted as a clear signal of a sustained tendency towards windier Februarys; indeed February 1990 was an anomalous month compared with the long-term trend of previous Februarys.

4.2 Comparison with all months of the year

4.2.1 Monthly mean winds

The anomalous windiness of February 1990 is confirmed when monthly mean winds are compared for all months of the year. Fig. 5 shows nationally averaged monthly mean wind speeds since January 1970, for the same 17 anemograph stations. February 1990 had the highest mean (17.2 kn) of any month, with December 1974 and January 1983 the next two highest with 15.8 kn and 16.3 kn respectively. February 1990 stands out particularly because there had not been any notably high means since January 1983.

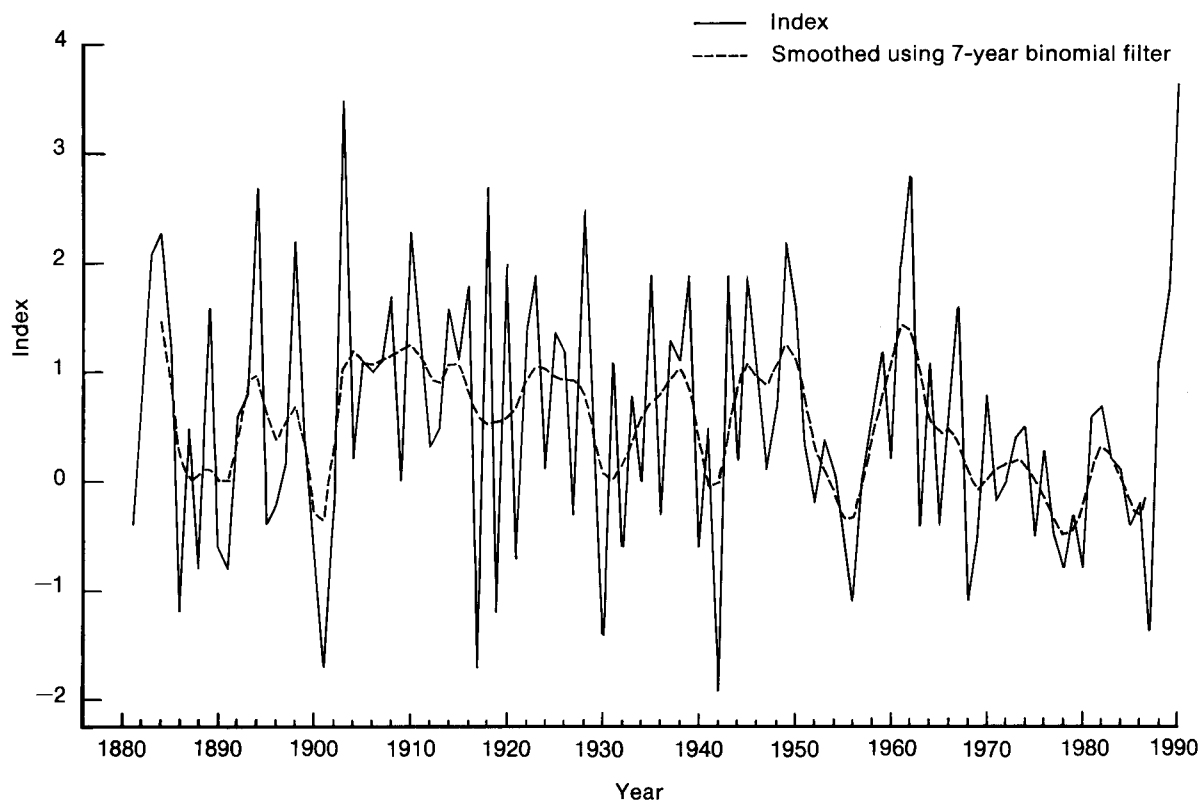


Figure 4. Windiness index for Februarys for the period 1881–1990.

Table I. Monthly indices averaged over the three regions for January 1980–February 1990 (values for 1881–1980 can be found in Smith (1982))

Year	Jan.	Feb.	Mar.	Apr.	May	June	July	Aug.	Sept.	Oct.	Nov.	Dec.
1980	−1.2	−0.8	−0.3	−0.3	−0.3	0.7	0.7	0.9	0.7	0.9	0.6	0.9
1981	0.1	0.6	0.6	−0.6	0.3	1.2	0.4	−0.7	0.2	0.7	0.5	−0.6
1982	−0.3	0.7	0.4	−0.8	−0.4	−0.9	−0.8	1.6	0.2	0.4	0.6	−0.1
1983	1.9	0.2	0.1	−0.9	−0.6	−0.4	−1.8	−1.1	1.0	1.4	−1.6	0.1
1984	1.0	0.1	−1.5	−1.3	−1.7	−0.5	−1.1	−1.2	−0.2	0.5	−0.4	−0.8
1985	−1.4	−0.4	−0.9	0.2	−1.1	−0.8	−0.2	1.9	−0.5	−1.3	−0.9	0.1
1986	0.6	−0.2	0.5	−0.4	1.5	−0.1	−0.1	0.0	−0.9	0.3	0.6	0.6
1987	−1.3	−1.4	−0.1	−1.3	−0.2	−1.1	−0.4	−0.2	−0.3	−0.9	−1.1	−1.1
1988	−0.2	1.1	−0.4	−1.5	−0.8	−1.6	0.6	0.5	−0.5	−0.3	−1.7	−0.2
1989	0.0	1.7	0.2	−1.2	−0.9	−0.8	−0.7	0.9	−0.6	0.2	−1.4	−1.4
1990	0.8	3.6	—	—	—	—	—	—	—	—	—	—

4.2.2 Monthly windiness index

As well as being windy in absolute terms, the unusual occurrence of high mean wind speeds in February is emphasized by the fact that apart from South Shields, Kirkwall, Leuchars and Kinloss, all the other stations (with February 1990 data) recorded their highest Smith’s windiness index value of all months since before January 1970.

5. Analysis of 35-day spells

5.1 24 January–27 February 1990 — unusually persistent windiness?

To see just how unusual the entire windy spell of late January and February 1990 was, requires greater flexibility of analysis. The strong winds of that period were not conveniently contained within one month, but lasted some 35 days. While February was arguably unprecedented, what of the windy period as a whole?

Again, using the same anemograph stations, the average hourly mean wind speeds through all 35-day periods from January 1970 to March 1990 were

compared. As Table II shows, 24 January–27 February had an average hourly mean wind speed higher than any other 35-day period at all stations in the Central and South regions — with the exception of Fleetwood (no data available), Valley and South Shields.

For stations which make synoptic reports this analysis can be extended back to include earlier spells, typically from the late 1950s, using spot-wind data. Fort Augustus, Fleetwood, South Shields and Avonmouth are not synoptic stations. Of the remainder, the 35-day period from 24 January to 27 February again figures prominently. As Table II shows, this was the windiest 35-day period on the synoptic record at Aberporth, Plymouth and Waddington.

5.2 Other windy spells

Other comparable windy spells have occurred in recent decades. Table III ranks periods according to the position of their most windy 35-day spell. So here we are not considering just one 35-day spell (as with 24 January–27 February 1990), but any within the three periods noted.

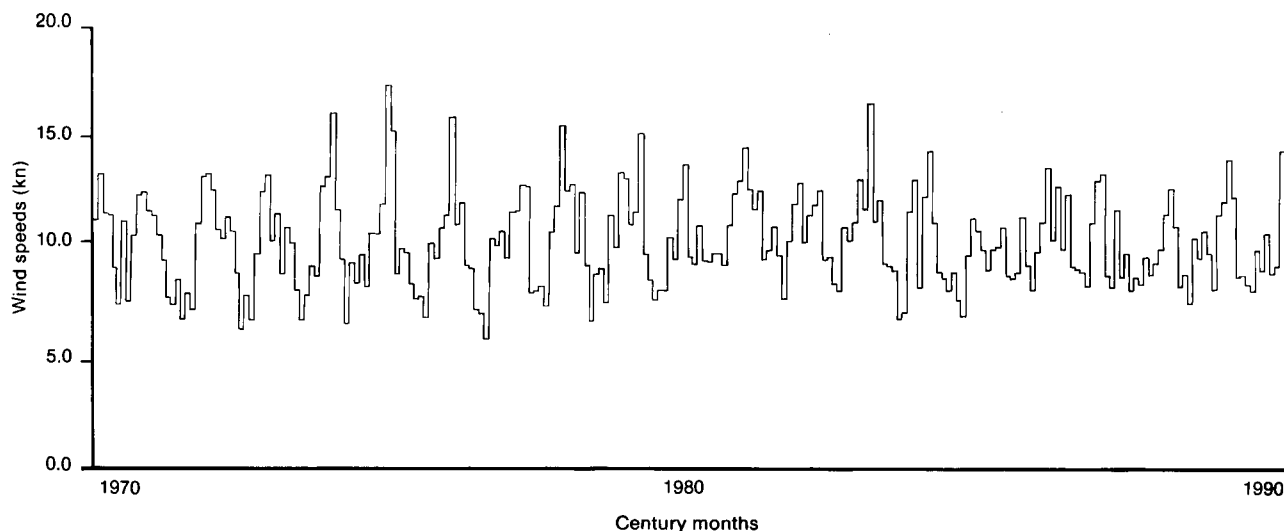


Figure 5. Monthly mean wind speeds averaged from 17 anemograph stations for the period January 1970–February 1990.

Table II Stations where the 35-day period 24 January–27 February had the highest mean speed (kn) on record using either anemograph (A) or spot wind (S) data

Station	Data used	Mean wind speed during period	Previous highest 35-day	
			Mean speed	Dates
South Region				
Avonmouth	A	18.9	16.8	25.11.74–29.12.74
Honington	A	15.4	14.8	25.11.74–29.12.74
Boscombe Down	A	16.7	15.9	8.1.74–11.2.74
Plymouth	A,S	20.2	19.6	8.1.74–11.2.74
Aberporth	S	25.4	21.1	3.1.84–6.2.84
Central Region				
Waddington	A,S	16.4	14.9	24.11.54–28.12.54
Aldergrove	A	15.2	14.8	29.12.73–1.2.74
Leeming	A	15.2	14.7	2.12.80–5.1.81

5.2.1 The late winter/spring of 1967

Several spells during February, March and April 1967 were as windy as, or in some cases windier than, those during the 1989/90 winter.

As Table III shows, at Benbecula, Prestwick, Aldergrove, Valley, Waddington, Honington and Boscombe Down, at least one 35-day spell during the late winter and early spring of 1967 has a mean within the top four on record; while at Leuchars, Kinloss, Kirkwall and Leeming, 35-day mean speeds are the highest on record.

Reference to synoptic charts reveals that the end of February and beginning of March 1967, in particular, were characterized by a series of intense depressions passing, in general, but not entirely, just to the north of the United Kingdom. Hence the rankings of 35-day mean speeds show greatest prominence at the more northern stations. The weather from mid February until early April was particularly disturbed, usually with a strong zonal pressure gradient.

5.2.2 The winter of 1974/75

Although the winter of 1974/75 was on the whole windy, the mid to latter parts of December and January featured some especially strong zonal gradients, within which deep depressions formed. Honington recorded its highest 35-day mean wind on record between 25 November and 29 December.

5.2.3 The winter of 1982/83

Thirty-five-day spells during the winter of 1982/83 rank prominently in the analysis, especially over Scotland, where at Benbecula and Prestwick the highest average 35-day wind speeds on record occurred. Unlike 1967, this period was not as continuously windy throughout, but did include a number of deep depressions passing over, or just to the north of the United Kingdom, in a mobile west or north-westerly airstream. This pattern was especially prevalent in early

December, early January, and again in late January and early February.

Apart from the above examples, very few 35-day spells compare with the period from 24 January to 27 February 1990 in terms of (hourly or spot) mean wind speed. Indeed, only the late winter of 1967, arguably, contains spells of comparable or greater mean windiness over a wide area, in recent decades.

6. Annual trends — increasingly windy?

6.1 Annual mean winds

Fluctuations in the windiness of individual months and spells can be compared to broader trends using long-term records of annual mean winds.

Palutikof *et al.* (1987) studied annual mean winds at Southport from 1895 to 1955. They observed that annual mean wind speeds were about 5.7 m s^{-1} at the end of the nineteenth century increasing rapidly (to over 6.5 m s^{-1}) in the 1910s, and subsequently falling back (to under 6.0 m s^{-1}) in the late 1920s; remaining at about that level to the end of the record. Using a dense network of stations for the period 1956–82, they detected a rapid decrease in wind speeds around 1970, after a trend of increasing windiness through the 1960s.

6.2 Annual windiness indices

Fig. 6 shows the 1881–1989 annually averaged national indices. The smoothed graph shows a decline from the early 1950s until the mid 1980s, with minor increases in the early 1960s and around 1980.

It should be emphasized that this series does not simply reflect the monthly average wind speeds recorded over each station each year, but is also a function of how *unusually* windy the mean speeds in any particular month were, averaged over the year.

Table III Rank of other notable periods containing high 35-day mean speeds. The ranking is according to the position of each period's highest 35-day mean speed.

Station	Data used	Late winter/ spring 1967	Winter 1974/75	Winter 1982/83
North Region				
Leuchars	S	1	5	2
	A	*	3	1
Kinloss	S	1	5	3
	A	*	4	2
Kirkwall	S	1	4	2
	A	*	4	1
Benbecula	S	2	2	1
	A	*	3	1
Fort Augustus	S	*	*	*
	A	*	*	*
Prestwick	S	3	2	1
	A	*	2	1
Central Region				
Leeming	S	1	3	5
	(1) A	*	4	3
Valley	S	3	—	—
	A	*	—	4
Aldergrove	S	2	4	5
	(1) A	*	3	4
Waddington	(1) S	4	5	3
	(1) A	*	4	3
Fleetwood	S	*	*	*
	A	*	*	*
South Shields	S	*	*	*
	A	*	3	1
South Region				
Plymouth	(1) S	—	—	—
	(1) A	*	—	—
Boscombe Down	S	2	3	4
	(1) A	*	3	4
Aberporth	(1) S	—	—	3
	A	*	—	2
Honington	S	3	1	*
	(1) A	*	2	3
Avonmouth	S	*	*	*
	(1) A	*	2	4

Key: S = Spot (10-minute) mean; A = Anemograph (hourly) mean; — denotes rank > 5; * denotes no available data; (1) shows where 24 January–27 February 1990 mean was highest.

However, the background of a general decline of index values in recent decades suggests that February 1990 is not symptomatic of a long-term trend in overall monthly mean wind strength, but is, at this stage, to be treated as a ‘random’ fluctuation.

7. Incidence of severe winds

To look simply at winds averaged over months, spells or years conceals other facets that determine the impact

of the wind. What made the recent winds seem so unusual were the severity of gusts and the close succession of three widespread gales.

7.1 Gusts

We have already seen how unusual the gusts of 25 January were in terms of return periods (see Fig. 1). To emphasize this point Fig. 7 shows the annual maximum gust recorded at one station, Boscombe Down, since records began in 1933. Whereas the 1990 gust (79 kn on 25 January) was the highest on record, gusts recorded in the persistently windy spells during 1967, 1974/75 and 1982/83 were not nearly so exceptional. In other words, these windy spells did not contain extreme gust conditions, and so, arguably, had less of a damaging impact at the time.

The graph should show a similar peak in early 1990 for other central and southern locations, but for some stations, especially the more northern ones, recent peak gusts were not so unusual. Certainly, overall there is no indication of a sustained trend towards higher peak gusts over the years.

7.2 Recurrence of gales

The type of analysis shown in Fig. 7 does not, however, show the distribution of high gusts within any one year, a close succession of damaging gust events being more likely to have greater impact (perhaps because repairs to damaged structures have not been completed before further damage is caused by the next storm). How unusual this scenario is can be gauged by comparing historically the frequency of notable windy events.

Fig. 8 shows notable incidents of widespread gales, updated to include the storms up to January and February 1990, after Harris (1970), who produced the series from 1920 to 1970. Although far from an objective representation of the length, severity or spatial extent of windy events, it does give an indication of their distribution through time.

The three stormy events of 25 January, 7/8 February and 26/27 February 1990 do indeed seem to be unusual in terms of their closeness of occurrence. Note again that the windy periods of 1967, 1974/75 and 1982/83 do not appear to have had widespread gusts or mean speeds, of exceptional strength — the criteria by which the gales are selected. While these spells contained widespread and persistently strong winds, the windy period of the winter of 1989/90 had far greater impact because, additionally, it featured a successive recurrence of storms with damaging gusts.

8. Conclusions

In trying to answer the question ‘Is the weather getting windier?’, a number of different techniques have been used in placing a single windy spell in a long-term context.

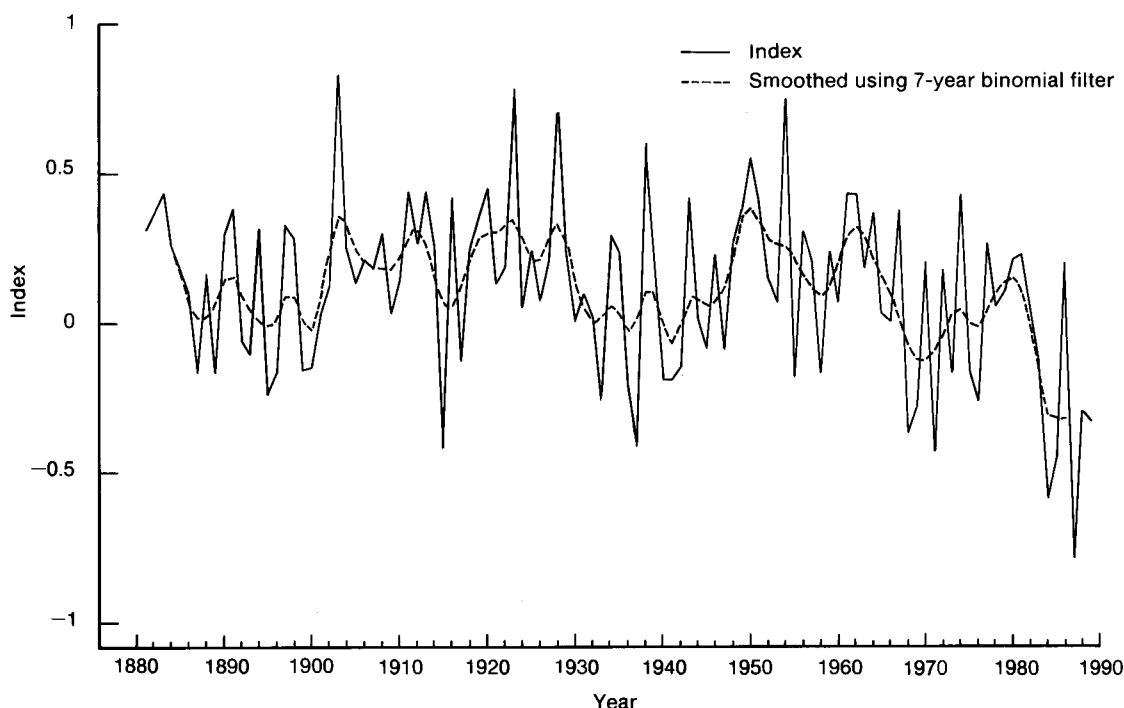


Figure 6. Annual windiness index 1881-1989.

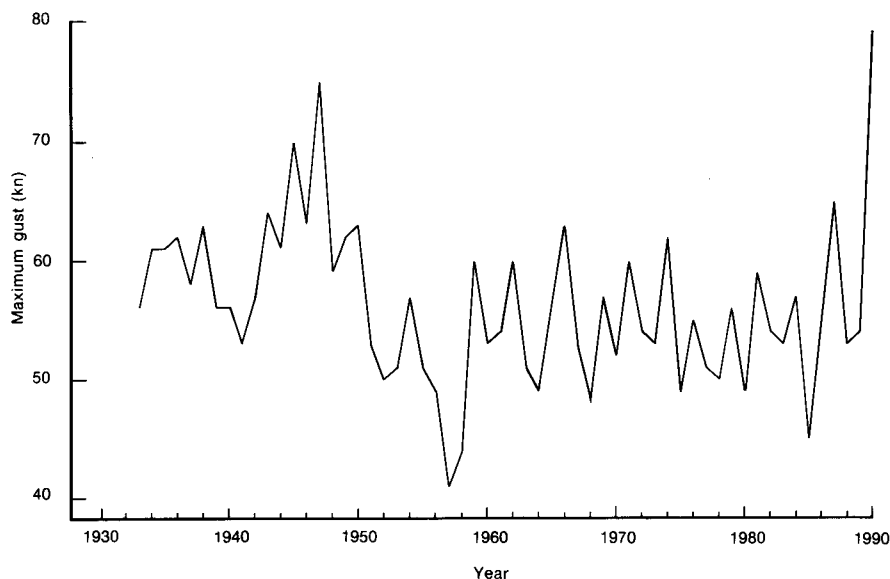


Figure 7. Annual maximum gusts at Boscombe Down for the period January 1933-June 1990.

Was the period from late January to the end of February 1990 a symptom of a more variable wind climate in which peak gusts become more extreme? Return-period analysis has demonstrated that the winds of 25 January in particular were exceptionally strong over parts of southern England. However, they did not in general exceed those of 16 October 1987, and long-term analysis of annual maximum gusts shows no sign of a sustained upward trend.

Does the closeness of those individual storm events over the United Kingdom indicate more frequent

recurrence, nowadays, of periods of damaging gales? Although their grouping was indeed rare, the incidence of the three storms in close succession during late January and February 1990 is not proven to be part of a longer-term tendency for a more frequent recurrence or clustering of storm events.

As a sustained period of strong winds, how uncommon was the recent spell and is it indicative of increasing levels of mean winds either during February or over the year as a whole? The 35-day mean wind speeds between 24 January and 27 February 1990 were almost unpreced-

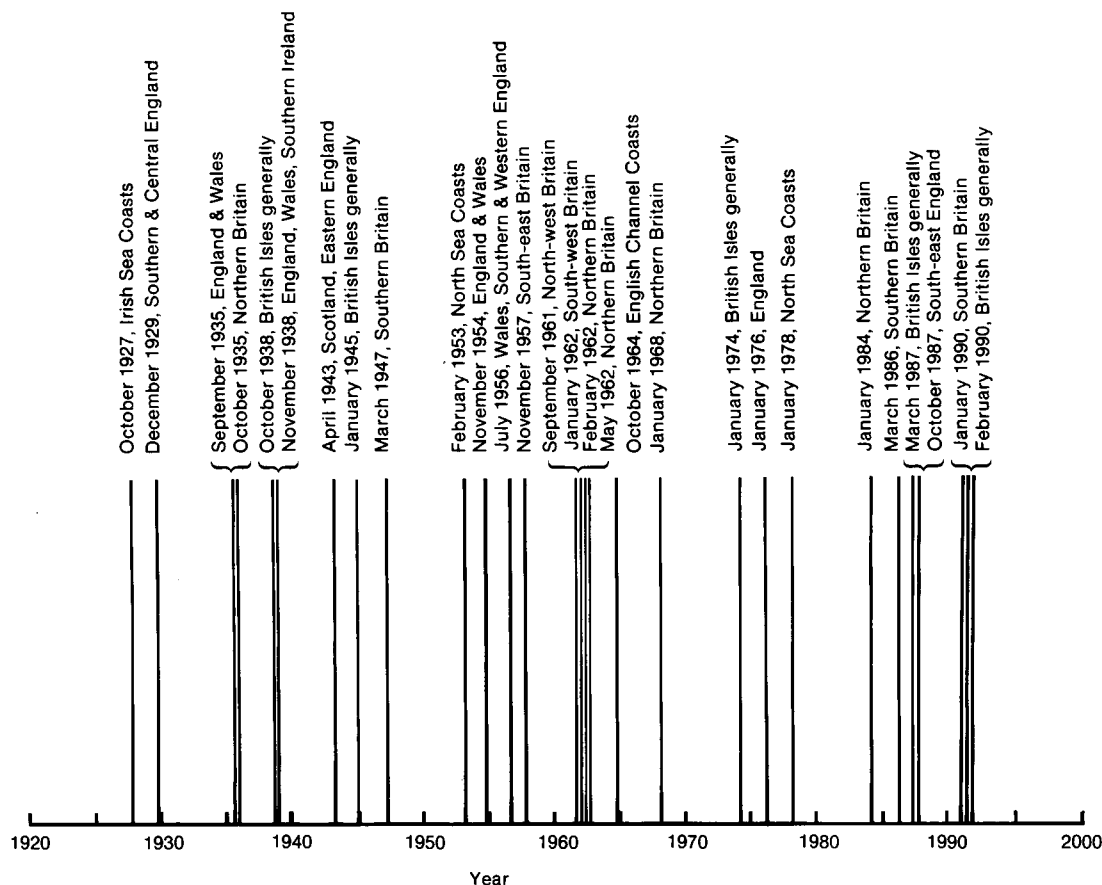


Figure 8. Notable gales affecting at least part of the United Kingdom for the period 1920–90, after Harris (1970).

ented in recent decades especially over central and southern districts, although a number of comparable windy spells have occurred during that time over the British Isles.

When February alone is analysed, the last 3 years have shown an increasing tendency towards higher mean winds, Smith's windiness index indicating that February 1990 was the most windy nationally, since before 1881; yet the recent February winds would not, arguably, appear so unusual had not the 1970s and much of the 1980s, in particular, been so anomalously quiet.

Using windiness indices averaged over the year, the general trend in recent decades is for wind anomalies to decline since the early 1950s.

Returning to the original question posed, it depends on the scale being considered, but as yet any changes in the wind climate of the United Kingdom which can be detected are 'wanderings' in the long-term mean speed, and these do not support the hypothesis of an increasingly windy United Kingdom. The exceptional features of the last windy spell do not show significantly an increasing frequency of persistent windy periods, or more frequent or extreme storm events, but are part of the 'random' fluctuations to be expected in the long-term wind climate of the United Kingdom.

Yet we should be vigilant, because if rises either in long-term mean winds or in the frequency of short-term extreme events should start to accelerate, the resilience of modern social and industrial activities to a non-stationary climate will be tested. Prudent advance measures will help ameliorate the impacts of future wind conditions.

Acknowledgements

I am grateful to J. Prior for his helpful advice throughout the preparation of this article, to Dr W.H. Moores and C.K. Ormonde for assistance in some of the data-processing, and to J.C. Dixon, M.R. Woodley and J.M. Nicholls for their constructive comments.

References

- Collingbourne, R.H., 1978: Wind data available in the Meteorological Office. *J Ind Aerodyn*, **3**, 145–155.
- Crummay, F.A., 1987: Wind and the summer of 1985. *Meteorol Mag*, **116**, 50–56.
- Harris, R.O., 1970: Notable British gales of the past fifty years. *Weather*, **25**, 57–68.
- McCallum, E., 1990: The Burns' Day storm. *Weather*, **45**, 166–173.
- Palutikof, J.P., Kelly, P.M., Davies, T.D. and Halliday, J.A., 1987: Impacts of spatial and temporal windspeed variability on wind energy output. *J Clim and Appl Meteorol*, **26**, 1124–1133.
- Smith, S.G., 1982: An index of windiness for the United Kingdom. *Meteorol Mag*, **111**, 232–247.

Satellite photograph — 30 June 1990 at 1347 UTC

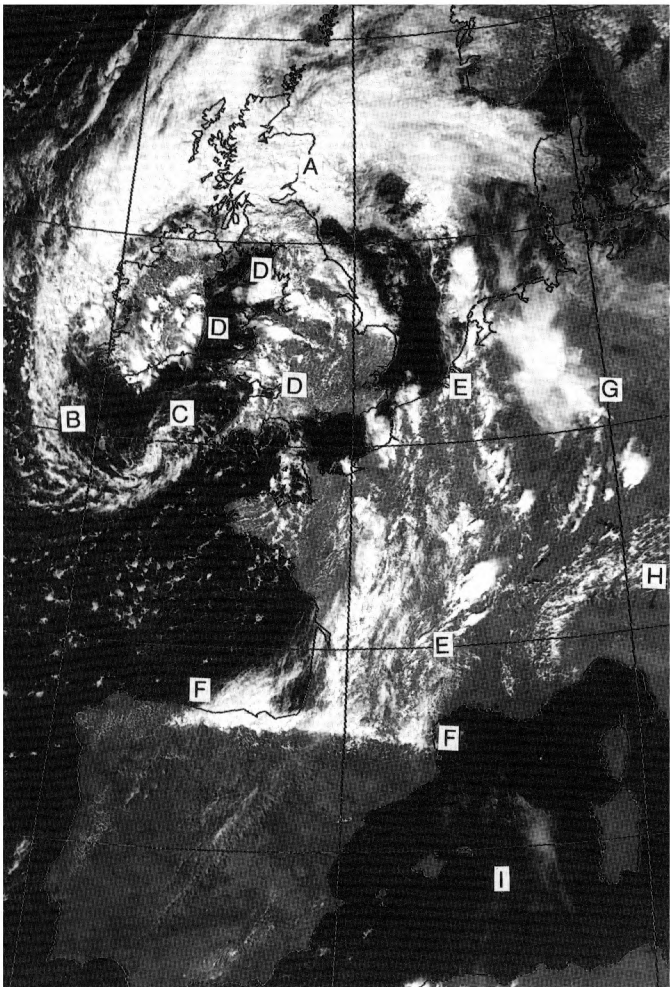


Figure 1. NOAA-11 AVHRR visible image on 30 June 1990 at 1347 UTC, the labelling A-I is referenced in the text.

The NOAA-11 visible image in Fig. 1, covering part of western Europe, shows cloud features associated with the fronts and circulation of an Atlantic depression. The synoptic situation is shown in Fig. 2. Corresponding upper-air charts (not shown) reveal an upper low over Ireland, a trough extending to north-west Spain and a south-westerly jet over France.

The occlusion over the northern United Kingdom can be clearly identified on the image. Embedded convective elements are evident, especially over central Scotland (A). A tail of mostly shallow convective cloud (B) curls round towards south-west England. Some deeper convective elements can be seen near (C). Deep convective cloud can also be identified at several locations (D) where heavy showers and thunderstorms occurred.

The cold front fragmented and weakened as it moved over the near continent, becoming difficult to locate on the synoptic chart. On the image it is marked by a

broken line of convective cloud extending from The Netherlands to southern France (E-E).

An interesting feature on the image is the cloud that appears to be streaming away from the mountains of northern Spain and the Pyrenees (F). Relevant upper-air ascents (not shown) and surface observations suggest that most of this cloud is cumulus and stratocumulus with tops around 6000 ft. Some of this may be the remnants of cloud associated with the weak cold front trapped against the mountains. The marked surface ridge in this area (see Fig. 2) was a shallow boundary-layer feature, with cloud above this level advecting north-eastwards in the upper flow.

Other features shown include a convective complex (G) over Germany, shallow convective cloud (H) outlining the Alps and an area of fog and/or low stratus (I) to the west of Sardinia.

D. Ratcliff

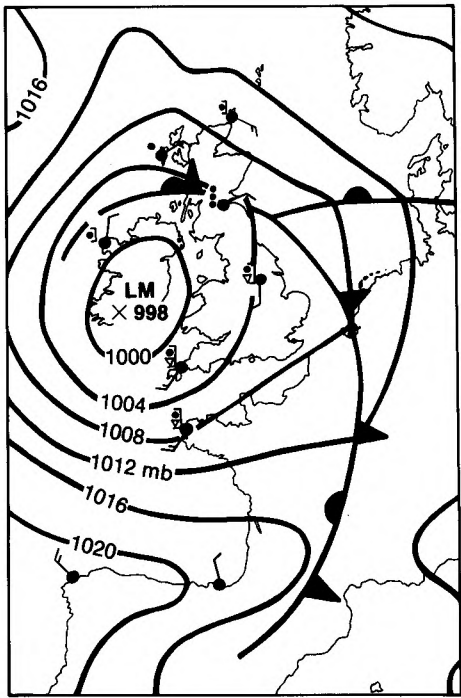


Figure 2. Surface analysis on 30 June 1990 at 1200 UTC. Present weather symbols are shown conventionally.

GUIDE TO AUTHORS

Content

Articles on all aspects of meteorology are welcomed, particularly those which describe results of research in applied meteorology or the development of practical forecasting techniques.

Preparation and submission of articles

Articles, which must be in English, should be typed, double-spaced with wide margins, on one side only of A4-size paper. Tables, references and figure captions should be typed separately. Spelling should conform to the preferred spelling in the *Concise Oxford Dictionary* (latest edition). Articles prepared on floppy disk (Compucorp or IBM-compatible) can be labour-saving, but only a print-out should be submitted in the first instance.

References should be made using the Harvard system (author/date) and full details should be given at the end of the text. If a document is unpublished, details must be given of the library where it may be seen. Documents which are not available to enquirers must not be referred to, except by 'personal communication'.

Tables should be numbered consecutively using roman numerals and provided with headings.

Mathematical notation should be written with extreme care. Particular care should be taken to differentiate between Greek letters and Roman letters for which they could be mistaken. Double subscripts and superscripts should be avoided, as they are difficult to typeset and read. Notation should be kept as simple as possible. Guidance is given in BS 1991: Part 1: 1976, and *Quantities, Units and Symbols* published by the Royal Society. SI units, or units approved by the World Meteorological Organization, should be used.

Articles for publication and all other communications for the Editor should be addressed to: The Chief Executive, Meteorological Office, London Road, Bracknell, Berkshire RG12 2SZ and marked 'For Meteorological Magazine'.

Illustrations

Diagrams must be drawn clearly, preferably in ink, and should not contain any unnecessary or irrelevant details. Explanatory text should not appear on the diagram itself but in the caption. Captions should be typed on a separate sheet of paper and should, as far as possible, explain the meanings of the diagrams without the reader having to refer to the text. The sequential numbering should correspond with the sequential referrals in the text.

Sharp monochrome photographs on glossy paper are preferred; colour prints are acceptable but the use of colour is at the Editor's discretion.

Copyright

Authors should identify the holder of the copyright for their work when they first submit contributions.

Free copies

Three free copies of the magazine (one for a book review) are provided for authors of articles published in it. Separate offprints for each article are not provided.

Contributions: It is requested that all communications to the Editor and books for review be addressed to the Chief Executive, Meteorological Office, London Road, Bracknell, Berkshire RG12 2SZ, and marked 'For *Meteorological Magazine*'. Contributors are asked to comply with the guidelines given in the *Guide to authors* which appears on the inside back cover. The responsibility for facts and opinions expressed in the signed articles and letters published in *Meteorological Magazine* rests with their respective authors.

Subscriptions: Annual subscription £30.00 including postage; individual copies £2.70 including postage. Applications for postal subscriptions should be made to HMSO, PO Box 276, London SW8 5DT; subscription enquiries 071-873 8499.

Back numbers: Full-size reprints of Vols 1-75 (1866-1940) are available from Johnson Reprint Co. Ltd, 24-28 Oval Road, London NW1 7DX. Complete volumes of *Meteorological Magazine* commencing with volume 54 are available on microfilm from University Microfilms International, 18 Bedford Row, London WC1R 4EJ. Information on microfiche issues is available from Kraus Microfiche, Rte 100, Milwood, NY 10546, USA.

October 1990

Editor: F.E. Underdown
Editorial Board: R.J. Allam, R. Kershaw, W.H. Moores, P.R.S. Salter

Vol. 119
No. 1419

Contents

	<i>Page</i>
The storms of January and February 1990. E. McCallum and W.J.T. Norris	201
The strong winds experienced during the late winter of 1989/90 over the United Kingdom: Historical perspectives. J.M. Hammond	211
Satellite photograph — 30 June 1990 at 1347 UTC. D. Ratcliff	220

ISSN 0026-1149



The Meteorological Magazine

November 1990

Extended-range forecasting
The Interactive Mesoscale Initialization
The autumn of 1989



DUPLICATE JOURNALS

National Meteorological Library
FitzRoy Road, Exeter, Devon. EX1 3PB

HMSO

Met.O.992 Vol. 119 No. 1420

© Crown copyright 1990.

First published 1990



HMSO publications are available from:

HMSO Publications Centre
(Mail and telephone only)
PO Box 276, London, SW8 5DT
Telephone orders 071-873 9090
General enquiries 071-873 0011
(queuing system in operation for both numbers)

HMSO Bookshops
49 High Holborn, London, WC1V 6HB 071-873 0011 (counter service only)
258 Broad Street, Birmingham, B1 2HE 021-643 3740
Southey House, 33 Wine Street, Bristol, BS1 2BQ (0272) 264306
9-21 Princess Street, Manchester, M60 8AS 061-834 7201
80 Chichester Street, Belfast, BT1 4JY (0232) 238451
71 Lothian Road, Edinburgh, EH3 9AZ 031-228 4181

HMSO's Accredited Agents
(see Yellow Pages)

and through good booksellers



3 8078 0010 2460 5

The Meteorological Magazine

November 1990
Vol. 119 No. 1420

551.509.333

Practical extended-range forecasting using dynamical models

S.F. Milton

Meteorological Office, Bracknell

Summary

Real-time ensembles of dynamical model forecasts are now a regular component of the long-range forecasts of temperature and rainfall for the United Kingdom issued on a twice-monthly basis by the Meteorological Office. Results are presented showing the impact of the ensemble technique on predictability, and comparisons are drawn between the skill of this dynamical technique and the current statistical technique. Also discussed is the ability of the ensemble to provide an a priori estimate of forecast skill.

1. Introduction

Since December 1963, twice-monthly forecasts of temperature and rainfall for the month ahead have been produced for the United Kingdom by the Meteorological Office. Until recently, the long-range forecast (LRF) has relied heavily upon statistical techniques to forecast for the period beyond 10 days, commonly referred to as the extended range. The latest of these is the multi-variate analysis (MVA) forecasting technique introduced in 1982 and described in detail by Maryon and Storey (1985), Folland and Woodcock (1986) and Gilchrist (1986). However, the improvements in medium-range skill of numerical weather prediction (NWP) models in the late 1970s and 1980s have led to renewed interest in the dynamical model as a tool for extended-range forecasting, with research into the problem being carried out at most of the major weather-forecasting and climate centres throughout the world.

Since December 1988, real-time, dynamical model forecasts have been made using the ensemble forecast technique, and these have been considered as part of the input to the twice-monthly conferences at which the LRF is decided. The introduction of dynamical model techniques coincided with the forecasts of rainfall and temperature being issued to selected companies in a commercial trial which began in June 1989. This article discusses the practical impact of the dynamical forecasts,

and reviews the current status of dynamical extended-range forecasting at the Meteorological Office.

2. The role of dynamical models

2.1 The ensemble technique

Much of the research into applying dynamical models to the problem of extended-range forecasting has concentrated on the ensemble forecast method proposed by Leith (1974). Detailed accounts of the technique are given by Murphy (1988), but it is worthwhile giving a summary of the major points. Such an ensemble comprises several dynamical model forecasts run from slightly different initial conditions. The rationale of basing extended-range forecasts on ensembles arises from two facts, namely:

- (a) the initial state of the atmosphere can never be measured perfectly, and
- (b) the dynamical equations of motion are non-linear and unstable to small perturbations.

Under condition (a) an ensemble of equally likely initial states can be realized, where each state is consistent with the errors inherent in current observational networks and NWP analyses. Under condition (b) the differences between the initial states grow as the

model forecasts progress until any two states are as different as random states drawn from model climatology and all predictability is lost. Lorenz (1982) estimated this theoretical limit of deterministic predictability to be around 14 days for prediction of instantaneous weather states from a NWP model. The practical limit determined by verifying forecasts against their corresponding analyses was found to be 8–10 days. However, numerous studies have shown cases which remain predictable beyond this limit.

NWP is, therefore, a probabilistic process. The ensemble forms a probability distribution and, providing it is assumed that the states in a large well-sampled ensemble are distributed normally, the ensemble mean represents the ‘best-estimate’ forecast, and the variance of the probability distribution, or spread of the ensemble members, an estimate of the uncertainty associated with the ensemble mean. When all ensemble members agree (disagree) there is confidence (no confidence) in the prediction. In theory the ensemble should provide a means of identifying those cases which exhibit predictability beyond the deterministic limit. In practice the technique is made less effective by external sources of error due to imperfect model formulation; these force the model to drift towards its own climate, and away from that of the atmosphere, as the forecasts progress. This is discussed in section 4.

If the atmosphere possesses non-Gaussian properties, as is suggested by recent research showing the bimodality in the amplitude of large-scale planetary waves (Sutera 1986), then it may be possible that ensembles will form clusters of states (Murphy and Palmer 1986). In this event, a more probabilistic approach is appropriate, with the ensemble offering a number of possible alternatives to the ensemble mean, each with its own probability of occurrence (Brankovic *et al.* 1990, Déqué 1988, Murphy 1990).

2.2 Real-time ensemble forecasts

Several methods exist for generating the initial states for ensemble forecasts, most involving the addition of suitably chosen perturbations to some reference state, usually the latest operational analysis from a NWP model. Indeed the optimal choice of such perturbations is itself an active research area.

The lagged average forecast (LAF) approach of Hoffman and Kalnay (1983) was adopted for the Meteorological Office ensemble forecasts as it represented the only practical approach to running regular ensemble forecasts given the computational constraints. Each LAF ensemble consists of nine forecasts run from consecutive 6-hourly analyses up to and including the latest operational analysis available. Therefore at the initialization time of the ensemble (corresponding to the latest analysis time or day 0), the first member is a 48-hour forecast, the second a 42-hour forecast, and so on up to the ninth member which is the latest analysis. This distribution of initial states at day 0 is taken to be

representative of the uncertainty in the analysis. The forecast integrated from the latest analysis time (hereafter referred to as the operational dynamical forecast (ODF)) is run for 30 days and the earliest ensemble member for 32 days, so that each member covers the 30 days comprising the forecast period.

The model used is a reduced horizontal-resolution (2° latitude by 2.8° longitude) version of the 15-level, global operational NWP model (Bell and Dickinson 1987). This is in contrast to the real-time ensemble of Murphy and Palmer (1986) where the 11-level general circulation model was used.

In addition to the real-time ensembles a number of hindcast LAF ensembles have been run, and a continuous time-series of forecast ensembles, each separated by 14 days, exists from September 1987 to August 1989. Ensembles for the winters of 1985/86 and 1986/87 have also been run bringing the total number to 65, or 578 individual forecasts. A number of ensembles have less than 9 members owing to operational problems. This is a much larger and more extensive database than used in previous studies, such as the dynamic extended-range forecasts experiments carried out at the National Meteorological Centre (NMC) (Tracton *et al.* 1989).

2.3 Methodology for the LRF

The methods used to produce long-range forecasts of temperature and rainfall in the Meteorological Office are discussed by Folland and Woodcock (1986). Indeed much of their procedure is still pertinent to the issued forecast today, and is outlined below. The MVA method forecasts on a half-monthly basis using linear discriminant equations, whose input is a set of recent atmospheric and sea surface temperature (SST) predictors, to assign probabilities to six pre-determined half-monthly mean-sea-level pressure (MSLP) patterns (‘clusters’). These MSLP forecasts are considered along with the dynamical model forecasts to produce a final MSLP forecast for the 3 periods, days 1–5, days 6–15 and days 16–30. In the first period the operational dynamical forecasts from the Meteorological Office and the European Centre for Medium-range Weather Forecasts (ECMWF) figure heavily in the decision-making process. In the second period the forecaster uses the guidance from the days 6–10 of the ECMWF forecast, the nine-member ensemble forecast, and MVA. At days 16–30 the latter two are used exclusively.

Once the MSLP forecasts are decided upon, the temperature and rainfall are derived from ‘objective specification equations’. These are multiple regression equations relating temperature anomalies and rainfall (as a percentage of normal) to the predictor variable MSLP, from which the predictors vorticity and the northerly and easterly wind components are derived. Temperature regressions also include the SST anomalies and 1000–500 mb thickness (for days 1–5 only) as additional predictors. The relationships between the

predictor variables and the temperature and rainfall are derived using data from 1951–80. No direct model output is currently used.

The remaining sections describe the extent to which ensemble forecasts are able to provide an accurate prediction of MSLP, as well as provide additional information on the likely skill of a given forecast based upon the ensemble spread.

3. Skill of the dynamical models

3.1 Practical impact of ensemble averaging

For the purposes of this article the anomaly correlation coefficient (ACC) (Miyakoda *et al.* 1972) is the main measure of skill used. Essentially it measures the agreement between forecast and analysis in terms of the phase of the anomaly patterns. A score of +1 represents a skilful forecast (e.g. forecasting and observing positive anomalies in the same location), and a score of –1 an unskilful forecast (e.g. forecasting

positive anomalies when negative anomalies are observed). The scores quoted in the following sections are measured over an area covering the North Atlantic and Europe 30°N–60°N, 60°W–40°E), corresponding to the area considered in the LRF. The anomalies are formed with respect to a 1951–80 climatology.

The skill of the dynamical model is shown on a seasonal basis in Fig. 1. This gives the ACC for MSLP measured over consecutive pentad periods of the forecast (days 1–5, 6–10 ... 26–30), for the unweighted ensemble mean, ODF, and the average skill of the individual ensemble members. Pentads are used in preference to the forecast periods to avoid the complication of using different averaging periods. Considering the ODF, all seasons display a steady decrease in skill with ACC falling from values in excess of 0.8 at days 1–5 to near constant values ranging from +0.2 to –0.2 by around days 11–15. Winter appears most skilful with a slower decay in ACC than the other seasons. Autumn is least skilful with ACC becoming

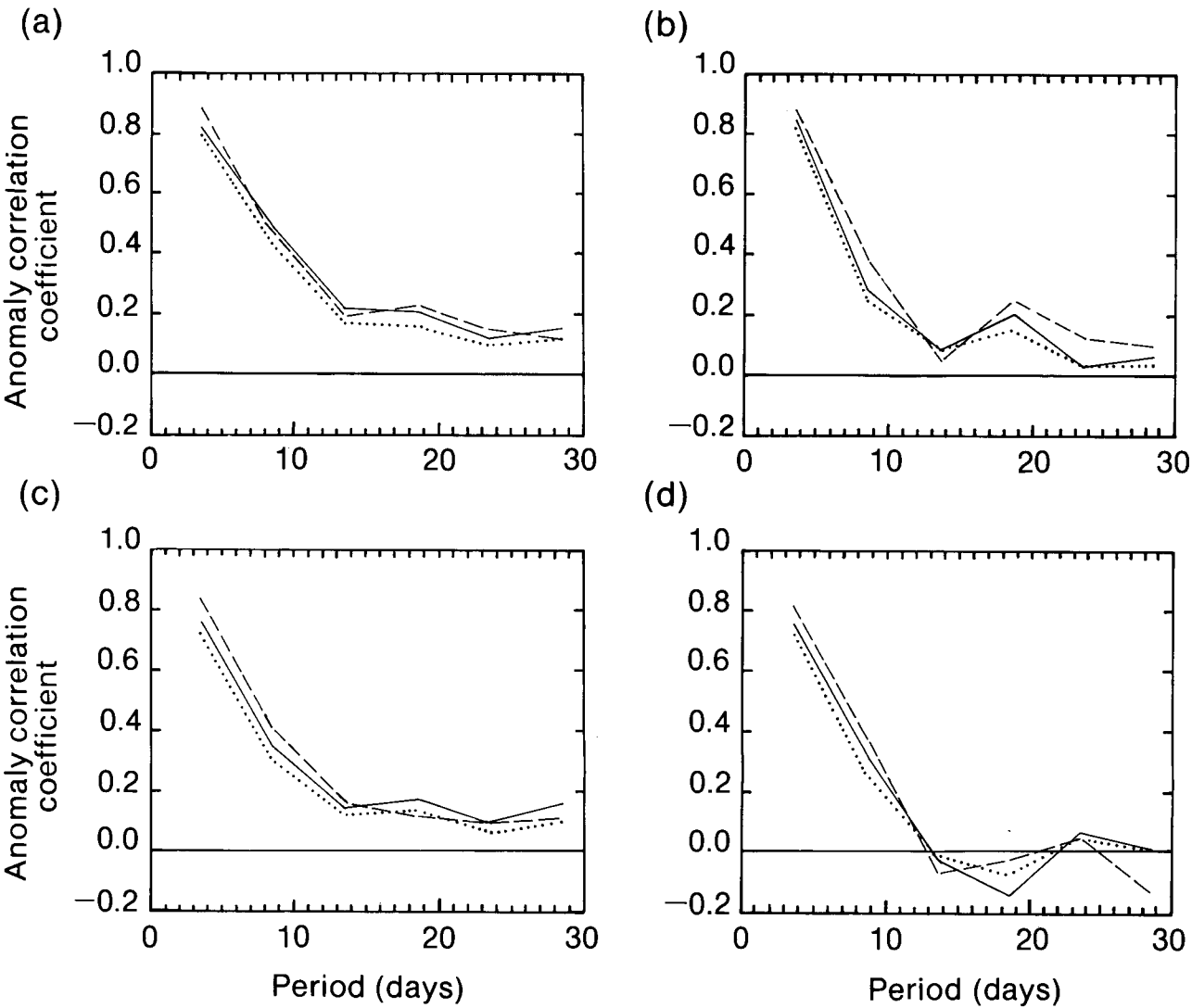


Figure 1. Average MSLP anomaly correlation coefficient for the North Atlantic and Europe for 5-day mean forecast periods plotted at the mid-point of the 5-day means for (a) winter (December–February), (b) spring (March–May), (c) summer (June–August), and (d) autumn (September–November). Continuous lines represent the ensemble mean, dotted lines the average of individual ensemble members and dashed lines the operational dynamical forecast.

negative at days 11–15. These results are typical of the modest levels of skill obtained in extended-range predictions from dynamical models at other centres such as ECMWF and NMC.

In comparison with the ODF the improvement due to ensemble averaging appears rather disappointing with the ensemble mean rarely an improvement over the ODF. As expected from theory (Brankovic *et al.* 1990) the ensemble mean is more skilful than the average skill of the individual members in most periods. However, this improvement is much less than the potential demonstrated by Murphy (1988) using the perfect model approach, where the ensemble is verified against an additional integration of the model taken to represent the real atmosphere. This measures the impact of the ensemble under the assumption that the model possesses no systematic biases.

If we composite the average skill into predictable and unpredictable cases as in Murphy (1990) then the impact of the ensemble averaging is more clearly seen. Fig. 2(a) shows the average ACC for MSLP of the ensemble mean, ODF, and average of the individual members, where ensembles have been assigned to various skill categories according to the average ACC of the individual ensemble members. This clearly shows that when the ensemble possesses above-average skill

(categories B1 and B2) then the ensemble-mean shows a greater improvement over the average ACC of the individual members than is suggested by Fig. 1. In fact in these two top categories the ensemble mean is also, on average, more skilful than the ODF. Fig. 2(b) shows that approximately 55% of the ensembles have ACC above 0.2 at days 6–15, and 15% ACC in excess of 0.6.

3.2 Variability in ensemble skill

Seasonal variations in skill are clearly evident from Fig. 1. However, there is also considerable variation on a case-by-case basis, seasonally, and interannually. It is the case-by-case variations in skill one is attempting to predict using the ensemble spread. To demonstrate this variability the ensemble-mean skill at days 6–15 is plotted as a pseudo time-series as in Fig. 3(a), beginning with the ensemble from 25 November 1985 and ending with that on 14 August 1989. There are considerable fluctuations in skill with ACC ranging from -0.6 to $+0.9$. The average ACC over all 65 cases is 0.24. The earlier impression of winter as most skilful can clearly be seen, although there are large interannual fluctuations, with the winter of 1988/89 being particularly skilful, compared with the winters of 1985/86 and 1986/87. On average autumn has low skill in this period with three of the worst forecasts appearing in this season. However,

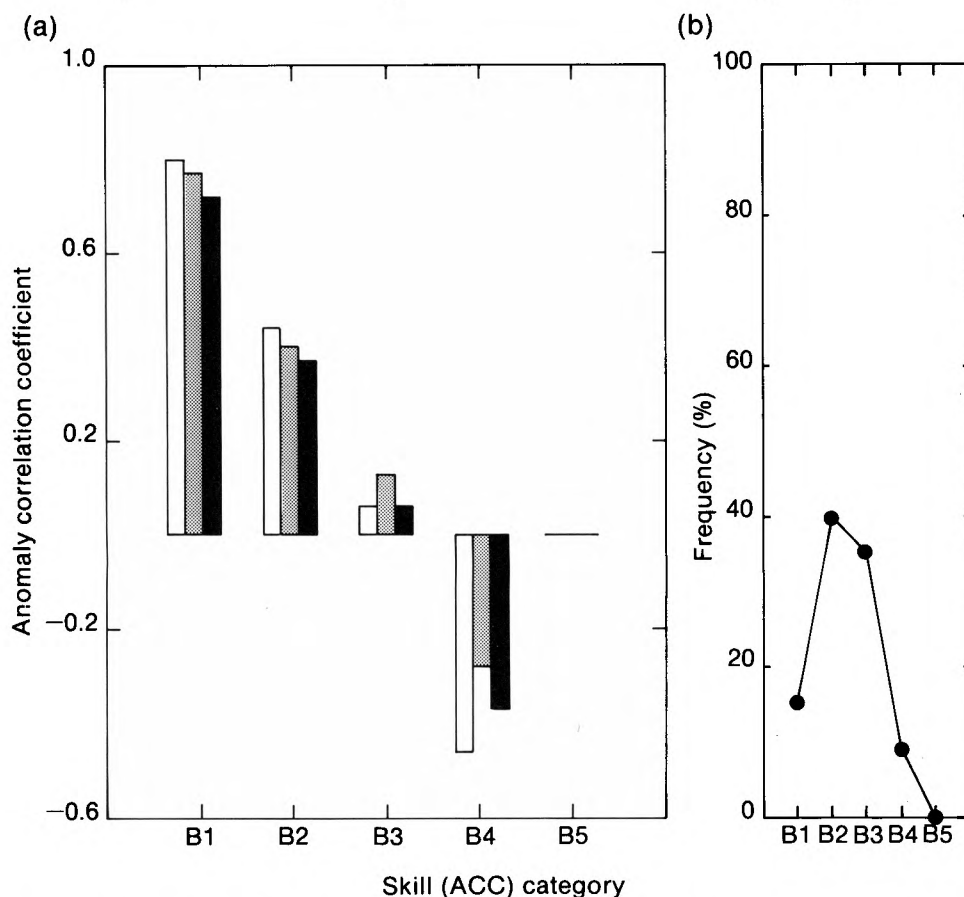


Figure 2. (a) Average MSLP anomaly correlation coefficients (ACC) of the operational dynamical forecast (stippled columns), ensemble mean (unshaded columns), and average of individual ensemble members (solid columns) at days 6–15 over the North Atlantic and Europe, assigned to skill categories (B1–B5) according to the ACC of the individual ensemble members. B1 = $1.0 > \text{ACC} > 0.6$, B2 = $0.6 > \text{ACC} > 0.2$, B3 = $0.2 > \text{ACC} > -0.2$, B4 = $-0.2 > \text{ACC} > -0.6$ and B5 = $-0.6 > \text{ACC} > -1.0$. (b) Frequency of ensembles falling into each skill category.

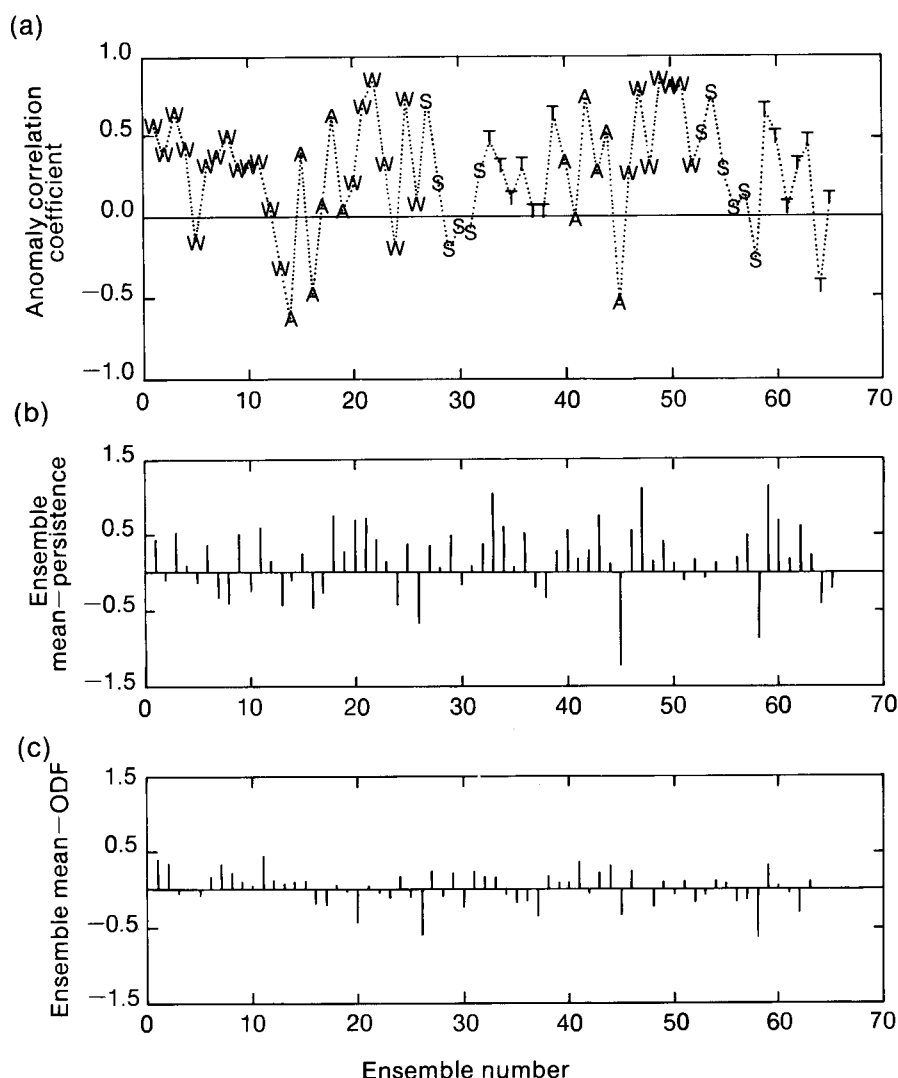


Figure 3. (a) Time series of anomaly correlation coefficients (ACC) for the ensemble mean for MSLP over the North Atlantic and Europe at days 6–15. W = winter, S = spring, T = summer, and A = autumn, for the 65 ensembles 1985–89. (b) As (a) but for the difference in ACC between the ensemble mean and persistence. (c) As (a) but for the difference in ACC between the ensemble mean and the operational dynamical forecast (ODF).

large case-by-case fluctuations are again evident. In contrast, both spring 1988 and 1989 follow similar patterns with the skill dropping rapidly as the season advances, not returning to higher levels until early summer (late May and June).

Figs 3(b) and 3(c) show the differences in ACC between the ensemble mean and persistence/ODF respectively. When this index is positive the ensemble mean is most skilful. Persistence represents a ‘zero-cost’ forecast, and is formed by persisting the anomaly from the 10 days before the analysis time. The ensemble mean is more skilful than persistence on 68% (54%) of occasions at days 6–15 (16–30), and more skilful than the ODF on 57% (43%).

The model performs particularly well during certain persistent episodes in the real atmosphere, such as the winter of 1988/89. However, there are numerous cases where the model skill is very high and persistence is low, such as cases 21, 22, 25 and 47. Fig. 4 shows a 3-point running mean of the ACC for the 52 cases forming a

continuous time-series (cases 14–65). Also plotted is the running mean of persistence. Both of these plots show the large-scale trends in skill, and it can be seen that the ACC of the ensemble forecasts is in some sense modulated by the observed persistence (the overall correlation between the two curves is 0.54, compared with 0.24 for the unsmoothed curves). This is most obvious in winter when persistence and ensemble-mean ACC are maxima, and spring where the decrease in persistence is matched by a decay in ACC of the ensembles; it is most likely a reflection of the model’s inability to undergo low-frequency transitions. Exceptions to the above are summers 1988 (cases 33–39) and 1989 (cases 59–65), where the ensemble–mean ACC, though lower than other seasons, was a significant improvement over persistence.

Finally, it is interesting to consider the degree of variation in skill amongst the individual members of any one ensemble. Fig. 5 presents the ACC for MSLP at days 6–15 for each of the 27 ensembles which make up

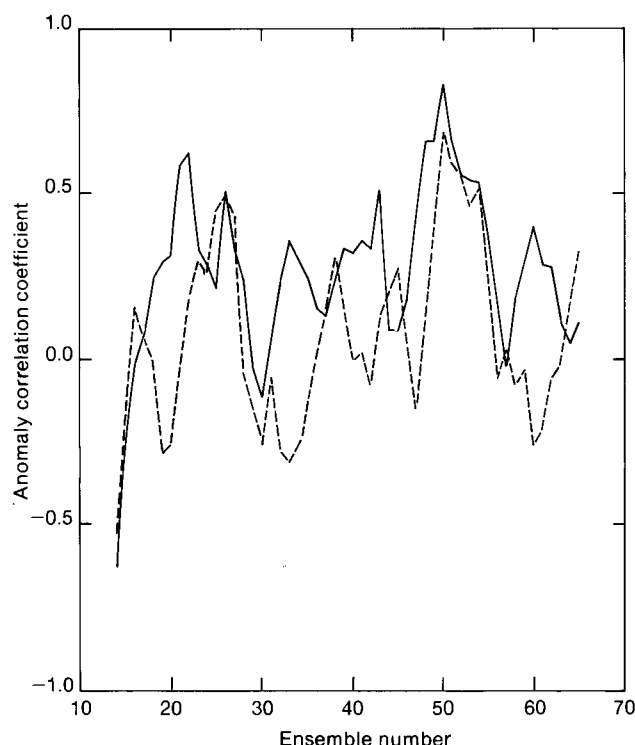


Figure 4. Smoothed anomaly correlation coefficients (ACC) for the 52 ensembles (continuous line) beginning 31 August 1987, and the corresponding persistence ACC scores (dashed line). Smoothing is applied using a 3-point running mean.

the winter set. The histograms show the marked variations in skill for some of the ensembles (e.g. 3 February 1986 and 5 January 1987). In this period it is evident that the ODF is not the most skilful forecast, with 17 out of 27 cases showing the ensemble mean with higher ACC. At days 1–5 the ODF is consistently the best dynamical forecast. This is a consequence of the LAF technique. The perturbations to the initial state represented by the time-lagged ensemble arise from forecast error growth, and such perturbations are generally larger for the earlier ensemble members. Thus, at days 1–5 and 6–10 the members are not a priori

equally likely. Hoffman and Kalnay (1983) found that by weighting the individual ensemble members they could make their ensemble mean more skilful than the ODF in these time ranges, and a similar procedure could be applied to the LAF ensembles in an attempt to maximize their usefulness. Beyond the medium range, at days 11–15, the ensemble members are a priori equally likely, and no weighting of the members is necessary.

The winter of 1988/89 stands out with high skill and good agreement between ensemble members for four forecasts; a reflection of the persistent, stable, and predictable nature of the pattern which led to a very mild, dry winter (Northcott 1989) leaving many areas of England under drought conditions in the warm summer that followed.

3.3 Dynamical versus statistical forecasts

With the MVA predicting on a half-monthly basis it is difficult to make a direct comparison between the dynamical and statistical inputs to the issued forecasts. However, Table I is an attempt to do this, and compares the scores for MSLP for the two forecasting techniques. The MVA scores are based on the top cluster-pattern (i.e. that with the highest probability) for forecasts covering the half-months from 1986–89. The ACCs for the ensemble mean are based upon a sub-sample of the 65 forecasts covering those ensembles with verification times closest to the MVA half-months. Note that the ensemble forecast for days 6–15 is compared with the MVA forecast for days 1–15, as it is felt that the inclusion of the very skilful days 1–5 from the dynamical forecasts is an unfair comparison. Also the seasons are defined slightly differently from those used in previous sections to agree with the MVA forecasts.

The ensemble-mean predictions averaged over all seasons provide the highest skill out to day 15. This holds for individual seasons except summer where the skill of the ensemble mean is marginally less than MVA, and autumn, where both techniques are poor. For days 16–30 both the ensemble mean and MVA perform

Table I. Anomaly correlations of the top cluster from statistical (MVA) forecasts January 1986 to August 1989 versus the ensemble-mean forecasts available over the same period, measured over a 30-point grid around the United Kingdom (30° W–20° E, 45° N–65° N). The first half-month MVA forecasts are compared with days 6–15 of the ensemble forecasts and the second half-month with days 16–30. Each season is composed of four half-months (e.g. winter is Jan1, Jan2, Feb1 and Feb2).

Season	First half-month		Second half-month	
	MVA	Ensemble mean	MVA	Ensemble mean
Winter	0.10	0.34	0.03	0.08
Spring	0.03	0.30	–0.09	–0.13
Pre-summer	0.06	0.25	0.13	0.29
Summer	0.21	0.17	0.04	0.01
Autumn	0.00	–0.02	0.12	–0.29
Pre-winter	0.25	0.43	–0.02	0.27
All seasons	0.11	0.24	0.04	0.04

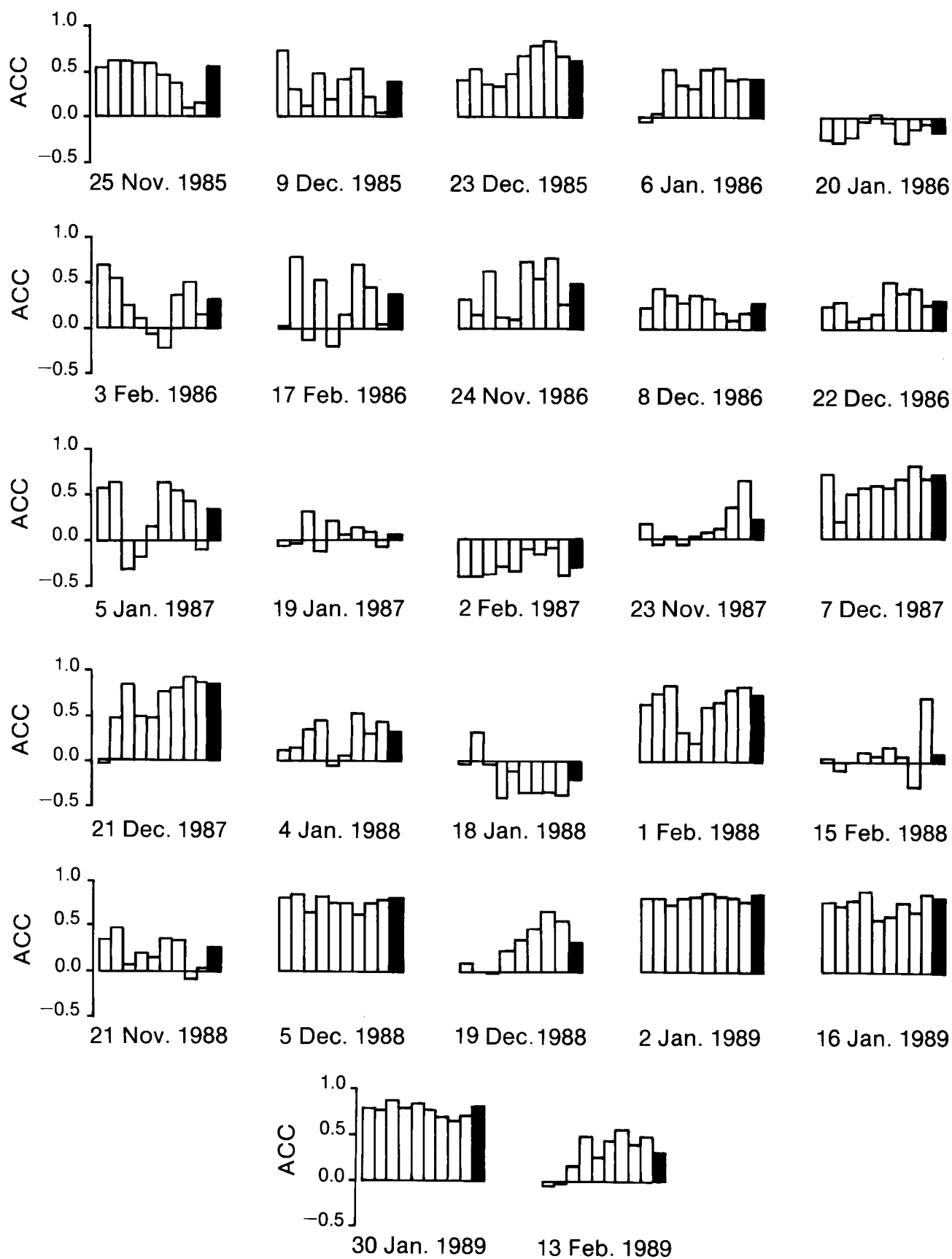


Figure 5. Histograms of anomaly correlation coefficients (ACC) across the individual ensemble members for the 27 winter ensembles at days 6–15 for MSLP over the North Atlantic and Europe. The solid bar is the ensemble mean and the individual members are plotted in order of increasing analysis time from left to right.

poorly, with no difference in skill between the two when averaged over all seasons. On a seasonal basis the ensemble mean is an improvement over MVA in pre-summer (May/June) and more notably in pre-winter (November/December). However, given the small number of samples in any one season and ACC close to their saturation values (noise level) these differences cannot be considered statistically significant.

One question not addressed is whether the additional skill in the ensemble MSLP fields at days 6–15 is actually communicated to the forecasts of temperature and rainfall via the regression equations. The 1-year running-mean skill for the issued temperature forecasts using the Folland–Painting score (Folland *et al.* 1986) from December 1963 to December 1989 is shown in Fig. 6. The skill score is calculated by classifying the forecast and observed temperatures/rainfall into equiprobable quintiles/terciles derived from the climate distribution for 1951–80, and then scoring according to how close the forecast and observed quintiles/terciles are to one another. A score of 100% represents a perfect forecast, 0% a random forecast and –100% a mirror image forecast of the observed state (e.g. forecasting extreme warm conditions when extreme cold ones occurred). The time-series may be tentative evidence of the influence of the dynamical forecasts, with the skill of the recently issued forecasts at an all-time high of 40%.

Although the skill of persistence is almost as high it is noticeable that in past persistent periods issued forecasts have not been as skilful.

4. Prediction of forecast skill

The second and perhaps more important objective of the ensemble forecast is to provide an estimate of the forecast skill at the time the forecast is issued. This opinion is voiced most strongly by Tennekes *et al.* (1986), who state that ‘forecast skill ought to be treated as one of the major forecast variables’. In theory this is provided by the ensemble spread. As with skill, a number of spread measures can be calculated. The one used is analogous to anomaly correlation, and is formed as the average anomaly correlation between the individual ensemble members and the ensemble mean. This measure is termed forecast agreement (Kistler *et al.* 1988), and has a value close to one when the agreement is good.

Table II gives the correlation coefficients between ensemble-mean anomaly correlation and ensemble forecast agreement for the three forecast periods and for each season. At days 1–5 for the North Atlantic and Europe the correlation is generally high, the exception being the summer forecasts. However, by days 6–15 the correlation between spread and skill has dropped dramatically, becoming negative for summer and

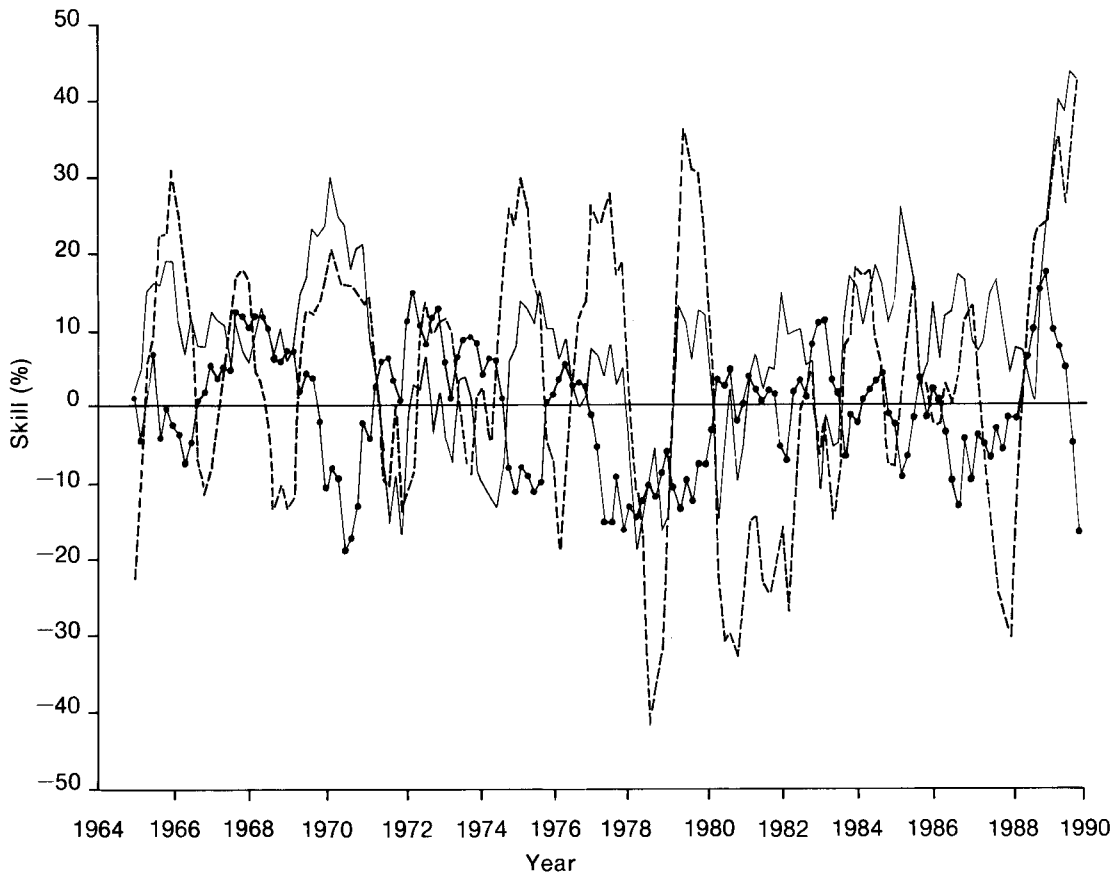


Figure 6. One-year running-mean skill for temperature quintiles, based on the Folland–Painting score, plotted every 2 months from December 1963 to December 1989. The continuous line represents the issued forecast, the dashed line the persistence and the continuous line with dots the climatology.

autumn, and just above zero for the winter ensembles. For the spring ensembles the correlation remains remarkably high. The correlations are improved at days 6–15 if one considers the northern hemisphere, with all seasons displaying positive correlations and spring once again producing a high correlation coefficient. However, even this fairly large database still suffers from considerable sampling fluctuations.

The scatter diagram between ACC and forecast agreement for the winter ensembles is presented in Fig. 7. The linear relationship between the two is clear at days 1–5, but the scatter is much larger at days 6–15. Closer inspection reveals that there is some variation in the spread–skill relationship between years. For 1985/86 there is a clear linear relationship for six of the seven forecasts, with one forecast for 20 January 1986 (marked A) showing good agreement when the skill was poor. Similarly 1988/89 has five out of seven forecasts in which the forecast agreement gave the correct indication as to the nature of the skill. However, by the same token the relationships for the other two winters are very poor

with 1987/88 showing little variation in its values of forecast agreement, but large variations in the skill of the ensemble forecasts.

The cases where the skill is poor but all the ensemble members are in agreement are characterized by low frequency transitions which occurred in the real atmosphere but were missed by all the ensemble members. The case of 20 January 1986 was a transition from a zonal flow in January 1986 to a blocked flow in February 1986, which none of the members forecast. Use of the alternative measures of root-mean-square (r.m.s.) error and r.m.s. spread (ensemble standard deviation) in general produce even worse spread–skill correlations. However because the r.m.s. error is not bounded, cases such as 20 January 1986 have a much larger impact on the correlation. In this case the r.m.s. error was almost five times the size of the r.m.s. spread.

It is interesting that the four cases with the lowest agreement or highest spread all began from initial conditions which were blocked in the Atlantic sector, and three of the same four cases also produced the

Table II. Correlations between ensemble-mean anomaly correlation and ensemble forecast agreement for the mean-sea-level pressure field over the North Atlantic and Europe (NA) and the northern hemisphere (NH) for three forecast periods; days 1–5, 6–15 and 16–30.

Season	Number of ensembles	Forecast period Days 1–5		Forecast period Days 6–15		Forecast period Days 16–30	
		NA	NH	NA	NH	NA	NH
Winter	27	0.83	0.25	0.11	0.28	0.16	0.16
Spring	12	0.81	0.71	0.67	0.73	0.08	0.02
Summer	14	0.20	0.71	–0.52	0.02	–0.35	0.52
Autumn	12	0.58	0.72	–0.16	0.35	0.32	–0.60

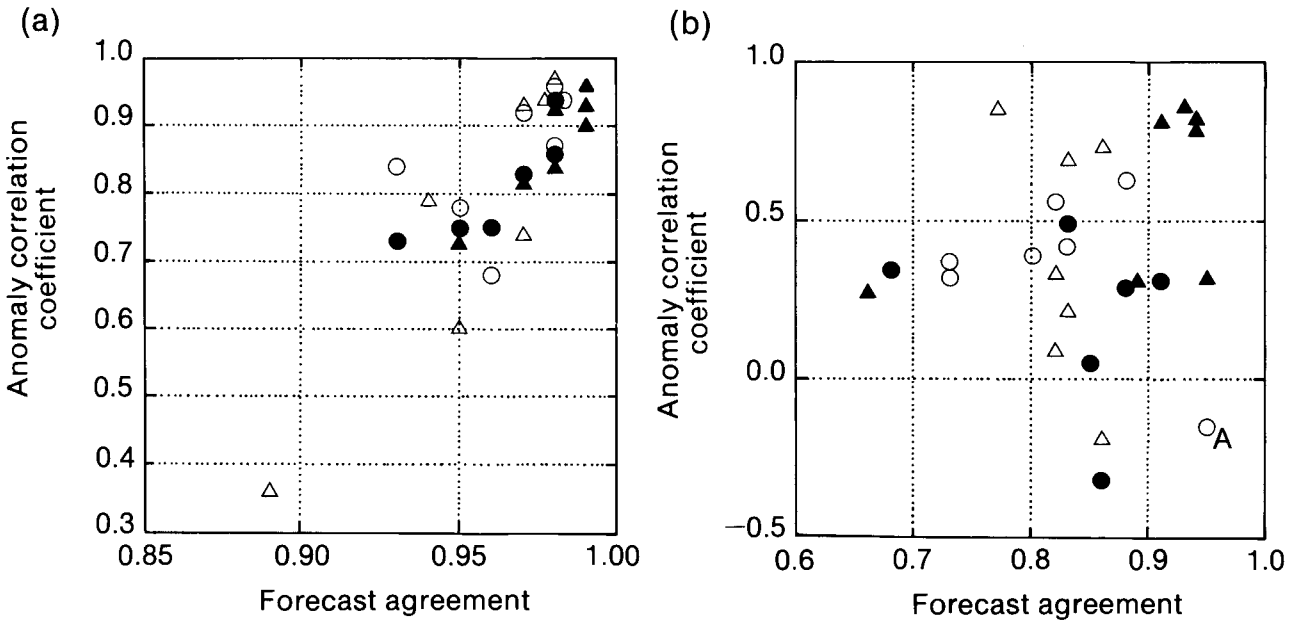


Figure 7. (a) Scatter plot of ensemble-mean anomaly correlation coefficients versus forecast agreement for 27 winter ensembles for MSLP over the North Atlantic and Europe at days 1–5. (b) As (a) but for days 6–15. The winters represented are 1985/86 (open circle), 1986/87 (solid circle), 1987/88 (open triangle) and 1988/89 (solid triangle). For explanation of the plot marked A see text.

highest r.m.s. spreads in the sample. More fruitful results may be gained from considering the dispersion of ensembles in terms of more advanced diagnostics such as the phase-space trajectories used by Brankovic *et al.* (1990), which are able to give information on the temporal evolution of the ensemble probability distribution. This is particularly true if the ensembles exhibit clustering, in which case conventional spread measures may have little meaning.

5. A case-study

The block which formed in February 1986 was the subject of a detailed diagnostic investigation by Hoskins and Sardeshmukh (1987). They concluded that important ingredients for the changes between January and February were the differences in fluxes of heat and momentum due to synoptic weather systems, but that a possible catalyst for the block could have been the anomalous diabatic forcing in the Caribbean region, which may in its turn have been a response to changes in SSTs in this region, or a planetary-scale response to a 30–60 day event which occurred in the tropical west Pacific. This block was also discussed by Folland and Woodcock (1986) in the context of the MVA forecast, as they were able to correctly forecast the persistence of the block for the whole of February, and by Brankovic *et al.* (1990), whose LAF ensemble initialized on 19 January 1986 also failed to capture the transition from zonal to blocked flow. In subsequent experiments Brankovic *et al.* were able to produce a slightly improved forecast by removing the influence of the tropical systematic errors in their model.

As mentioned above, the ensemble initialized on 20 January 1986 failed to capture the transition from zonal to blocked flow. Fig. 8 shows the MSLP fields for the ensemble over the period 31 January–4 February, corresponding to days 11–15 of the forecast. Clearly none of the members has reproduced the blocking signature present in the analysis. The ensemble run from 14 days previously and initialized on 6 January 1986 is shown in Fig. 9, over the verifying period of 1–5 February, corresponding to days 26–30 of the ensemble forecast. At least two of the members from this ensemble have produced a blocking signature. The ODF from 00 UTC on 6 January 1986 has a blocking anticyclone over Denmark, and something of the easterly flow which is present in the verifying analysis that made this February one of the coldest on record. Even more remarkable is the member from 00 UTC on 5 January 1986; this has captured all of the major features, including the cut-off low and large block east of Scandinavia. Although it cannot be ruled out that the similarity is a random event, it must be remembered that such a pattern represents a large departure from the model's own climatology. Indeed the temporal evolution over the previous two pentads shows that the transition was accurately forecast (Fig. 10)

Whilst the forecast from 00 UTC on 5 January 1986 is not typical it does raise a number of important points. Firstly the model is able to produce dynamical structures which resemble blocks in the real atmosphere, as well as the processes which can initiate such low frequency transitions. However, it does so infrequently, and in common with other dynamical models usually produces blocks which have insufficient amplitude and are too short-lived (Tibaldi and Molteni 1990). The ability of dynamical models to capture such low-frequency transitions is the key to successful dynamical extended-range forecasting, and this failing is the major drawback to realizing the potential of the ensemble forecast technique. More studies such as those of Hoskins and Sardeshmukh (1987) into the relevant mechanisms in such cases are necessary if improvements to dynamical models and ultimately progress in dynamical extended-range forecasting are to be made.

Hope for the future is that improvements in model formulation will lead to a more realistic representation of low-frequency variability, at least to the extent that when a block occurs in the real atmosphere a certain proportion of the ensemble members capture it. This would lead to the more probabilistic framework discussed in section 2.1.

6. Conclusions

Real-time, lagged-average forecast ensembles are now a regular feature of the long-range forecasts at the Meteorological Office, and are the dominant component at least out to 15 days. The superiority of the dynamical forecasts in this time range over the statistical techniques has been clearly demonstrated, and the ensemble mean proves to be the best dynamical forecast beyond days 1–5 when the individual ensemble members themselves possess some predictability. At days 16–30 the levels of skill are on average low and very variable, and the product provided by the ensemble forecasts is in this sense a marginal one.

There is, on average, a small positive correlation between the skill and the spread, and this may prove only marginally useful in a practical sense. The theoretical relationship between the spread and skill is undoubtedly destroyed by the growth of systematic deficiencies in the model's climate at medium and extended range. This manifests itself most clearly as an inability of the model to undergo major regime transitions with sufficient frequency beyond days 1–5, an example of which was the ensemble from 20 January 1986. The ensemble member from 00 UTC on 5 January 1986 was one of the rare occasions when the model was able to forecast a major transition from zonal to blocked flow. Such variations in predictability, and their sensitivity to initial conditions and model formulation, must be understood if progress is to be made in forecasting for the extended range. These questions will be addressed with the future generation of dynamical models.

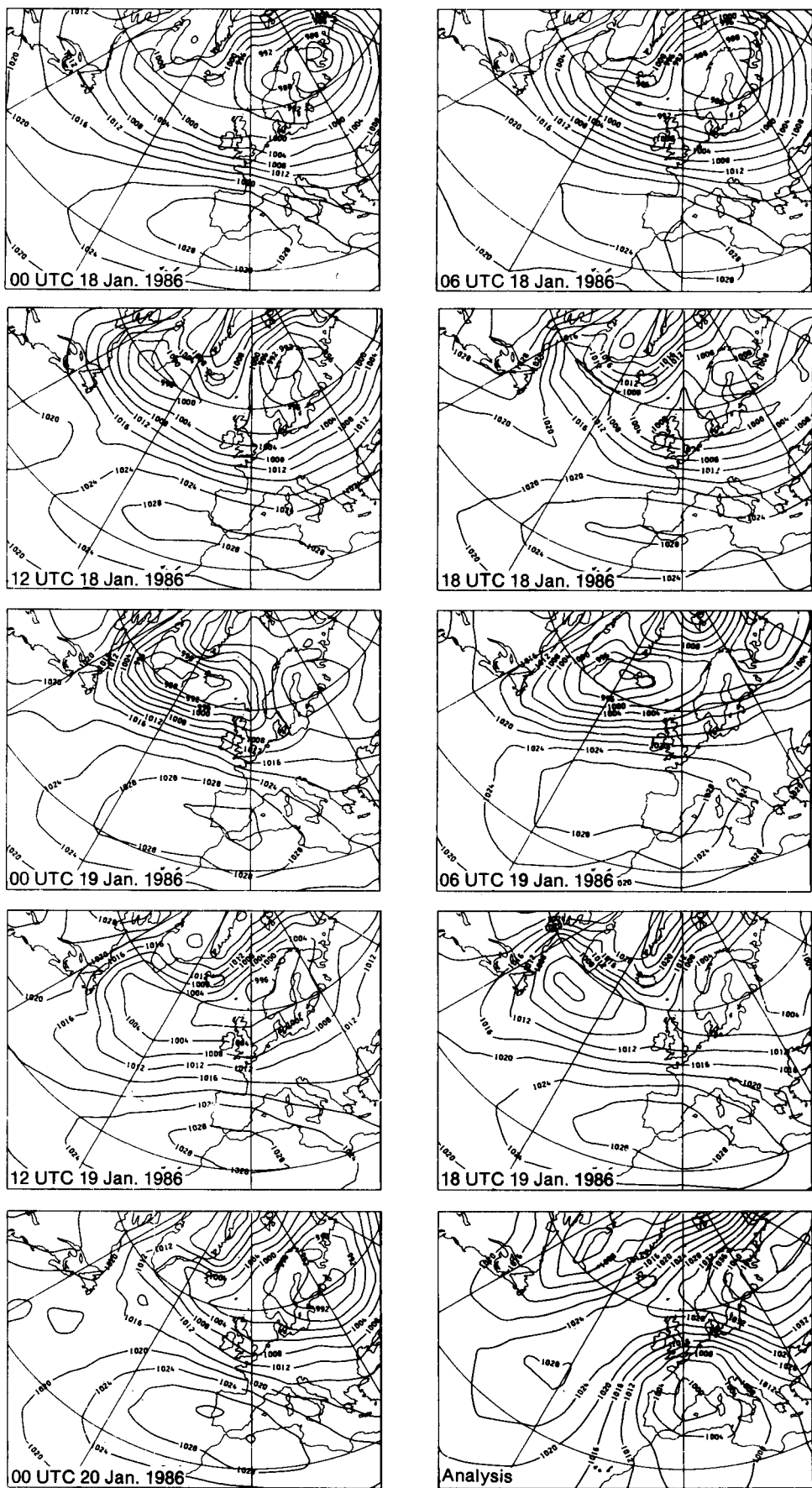


Figure 8. MSLP fields for the individual members of the ensemble initialized on 20 January 1986 and the verifying analysis, for the period 31 January to 4 February, which corresponds to days 11–15 of the ensemble forecast.

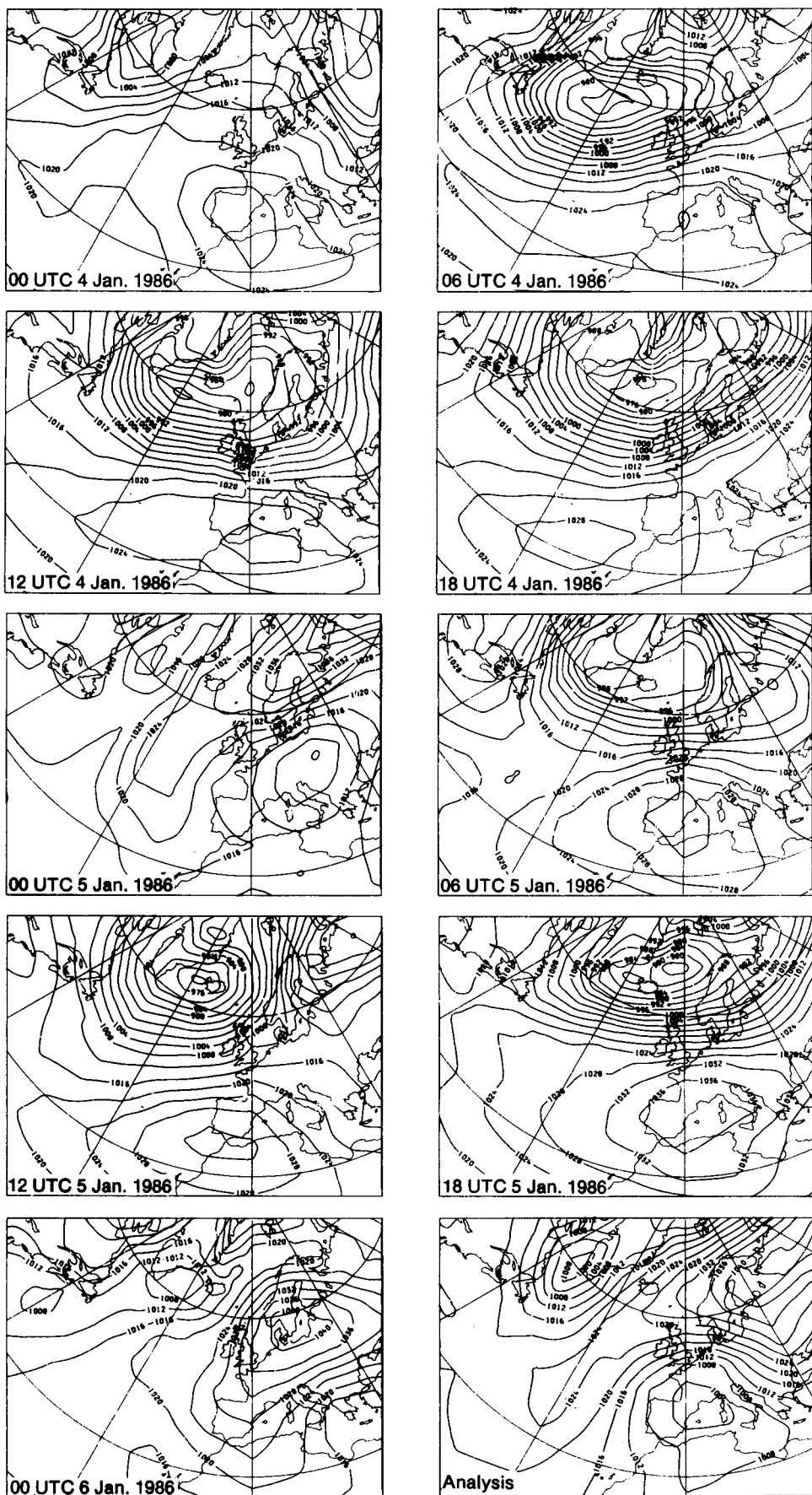


Figure 9. As Fig. 8 but for the ensemble initialized on 6 January 1986. The verification period (1–5 February) corresponds to days 26–30 of the ensemble forecast.

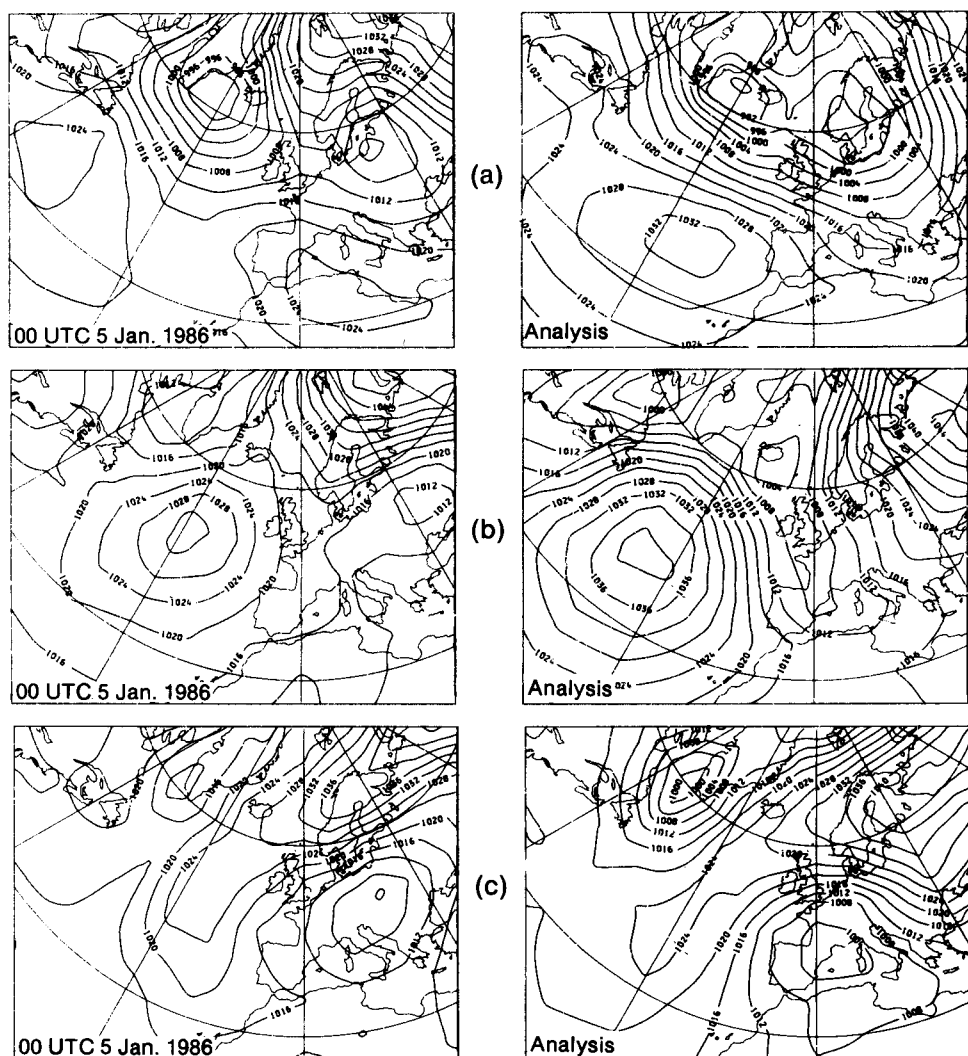


Figure 10. Evolution of the MSLP for the ensemble member initialized at 00 UTC on 5 January 1986 and verifying analysis for (a) days 16–20, (b) days 21–25 and (c) days 26–30 of the ensemble forecast period.

References

- Bell, R.S. and Dickinson, A., 1987: The Meteorological Office operational numerical weather prediction system. *Sci Pap, Meteorol Off*, No.41.
- Brankovic, C., Palmer, T.N., Molteni, F., Tibaldi, S. and Cubasch, U., (1990): Extended-range predictions with ECMWF models. III. Time lagged ensemble forecasting. To appear in *Q J R Meteorol Soc*.
- Déqué, M., 1988: The probabilistic formulation: A way to deal with ensemble forecasts. *Ann Geophys*, **6**, 217–223.
- Folland, C.K. and Woodcock, A., 1986: Experimental monthly long-range forecasts for the United Kingdom. Part I. Description of the forecasting system. *Meteorol Mag*, **115**, 301–318.
- Folland, C.K., Woodcock, A. and Varah, L.D., 1986: Experimental monthly long-range forecasts for the United Kingdom. Part III. Skill of the monthly forecasts. *Meteorol Mag*, **115**, 377–395.
- Gilchrist, A., 1986: Long-range forecasting. *Q J R Meteorol Soc*, **112**, 567–592.
- Hoffman, R.N. and Kalnay, E., 1983: Lagged average forecasting, an alternative to Monte Carlo forecasting. *Tellus*, **35A**, 100–118.
- Hoskins, B.J. and Sardeshmukh, P.D., 1987: A diagnostic study of the dynamics of the northern hemisphere winter of 1985–86. *Q J R Meteorol Soc*, **113**, 759–778.
- Kistler, R., Kalnay, E. and Tracton, M.S., 1988: Forecast agreement, persistence and skill. In Eighth Conference on Numerical Weather Prediction, Baltimore, Maryland, 22–26 February 1988. Boston, American Meteorological Society.
- Leith, C.E., 1974: Theoretical skill of Monte Carlo forecasts. *Mon Weather Rev*, **102**, 409–418.
- Lorenz, E.N., 1982: Atmospheric predictability experiments with a large numerical model. *Tellus*, **34A**, 505–513.
- Maryon, R.H. and Storey, A.M., 1985: A multivariate statistical model for forecasting anomalies of half-monthly mean surface pressure. *J Climatol*, **5**, 561–578.
- Miyakoda, K., Hembree, G.D., Strickler, R.F. and Shulman, I., 1972: Cumulative results of extended forecast experiments. I: Model performance for winter cases. *Mon Weather Rev*, **100**, 836–855.
- Murphy, J.M., 1988: The impact of ensemble forecasts on predictability. *Q J R Meteorol Soc*, **114**, 463–493.
- , 1990: Assessment of the practical utility of extended-range ensemble forecasts. *Q J R Meteorol Soc*, **116**, 89–125.
- Murphy, J.M. and Palmer, T.N., 1986: Experimental monthly long-range forecasts for the United Kingdom. Part II. A real-time long-range forecast by an ensemble of numerical integrations. *Meteorol Mag*, **115**, 337–349.
- Northcott, G.P., 1989: The winter of 1988/89 in the United Kingdom. *Meteorol Mag*, **118**, 265–267.
- Sutera, A., 1986: Probability density distribution of large-scale atmospheric flow. *Adv Geophys*, **29**, 227–249.
- Tennekes, H., Baede, A.P.M. and Opsteegh, J.D., 1986: Forecasting forecast skill. Proceedings of ECMWF seminar on predictability in the medium and extended range, 17–19 March 1986. Reading, ECMWF. (Copy available in ECMWF, Reading.)
- Tibaldi, S. and Molteni, F., 1990: On the operational predictability of blocking. *Tellus*, **42A**, 343–365.
- Tracton, M.S., Mo, K., Chen, W., Kalnay, E., Kistler, R. and White, G., 1989: Dynamical extended range forecasting (DERF) at the National Meteorological Center. *Mon Weather Rev*, **117**, 1604–1635.

The Interactive Mesoscale Initialization

B.J. Wright and B.W. Golding

Meteorological Office, Bracknell

Summary

The Interactive Mesoscale Initialization (IMI) has been developed to prepare the initial fields for the Meteorological Office mesoscale model. In addition to surface observations, use is made of satellite and radar imagery. Human analysts monitor the initialization procedure, and can incorporate their own knowledge of the situation. Subjective assessment of several cases demonstrates that use of the IMI can lead to improved forecasts.

1. Introduction

The Meteorological Office mesoscale model is used routinely to predict the weather over the British Isles on a 15 km grid. Synoptic-scale development is largely controlled by the time-dependent boundary conditions. However, the mesoscale evolution is sensitive to the initial conditions within the domain, and especially to the humidity distribution. One of the main problems in attempting to specify these initial conditions is the lack of data. The surface observing network has at best a resolution of 50 km, with upper-air observing stations being spaced more than 300 km apart. Over the sea areas the problem becomes greater still with only a few ships and oil rigs providing regular observations.

In an attempt to solve this problem, the Interactive Mesoscale Initialization (IMI) has been developed. This provides an environment within which to make the best possible use of all the available data. A broad range of surface observations is incorporated, including cloud reports, visibility and snow depth, with satellite and radar imagery acting as additional data, providing much needed information over sea areas. These data, together with the most recent forecast fields, are used to produce a set of key analyses of surface variables and cloud distribution. The whole system is under the control of human analysts who, in addition to having control over the use of the data, are able to modify the analyses in order to incorporate their extra knowledge of the situation. Conceptual models are used to relate the other model variables to the analysed quantities.

An assessment programme has been carried out, with subjective comparisons being made between the forecasts run from the current objective initialization (OI) and those run from the IMI. Particular attention has been given to cases where the routine forecast (initialized using the OI) was deficient in some way.

After describing the initialization procedures in some detail (section 3), a summary of the results of this assessment is presented in section 4, with a more detailed look at two of the cases of particular interest.

2. Model formulation

The Meteorological Office mesoscale model (Golding 1987, 1990) uses a non-hydrostatic, compressible

formulation of the primitive equations with a semi-implicit finite difference scheme, allowing a forecast time-step of one minute. An Arakawa C grid of 89×91 points covers the British Isles, with a resolution of 15 km, giving good representation of orography (Fig. 1). A model domain of 63×79 points was used for all the case studies except one, which used an enlarged domain of 120×133 points. The vertical coordinate is height above orography, with 16 levels in the vertical, the lowest at 10 m, the highest at 12 010 m, with the level spacing increasing linearly with height from 110 m to 1510 m.

The model has a detailed boundary-layer mixing formulation with turbulent kinetic energy carried as a variable. Cloud water and humidity are predicted separately to give a good representation of cloud, and both grid-scale and convective precipitation processes are modelled. The radiation scheme is also particularly detailed with respect to cloud.

A continuous 3-hour assimilation cycle is run. The observations are analysed using a combination of a 3-hour mesoscale model forecast and fields interpolated from the most recent forecast from the fine-mesh model (the Meteorological Office regional model) as a first guess. This 'hybrid' first guess takes the synoptic-scale component of the upper-air fields from the fine-mesh model, with the short-wave component derived from the mesoscale model forecast. The cloud and surface fields are also taken from the mesoscale model forecast. The analyses are used to modify the other model variables to obtain a consistent set of model fields. The IMI can be used in the place of this objective initialization.

Two 18-hour forecasts are run each day, from midnight and midday. Hourly predictions are obtained of pressure, wind, grid-scale and convective precipitation, cloud cover and base, visibility, temperature and humidity.

Three-hourly boundary conditions are taken from the fine-mesh model — a 15-level sigma coordinate model, with a resolution of about 75 km in the area of interest. Cloud water mixing ratio is not carried as a variable in the fine-mesh model, and so has to be diagnosed from the relative humidity. This, and the interpolation

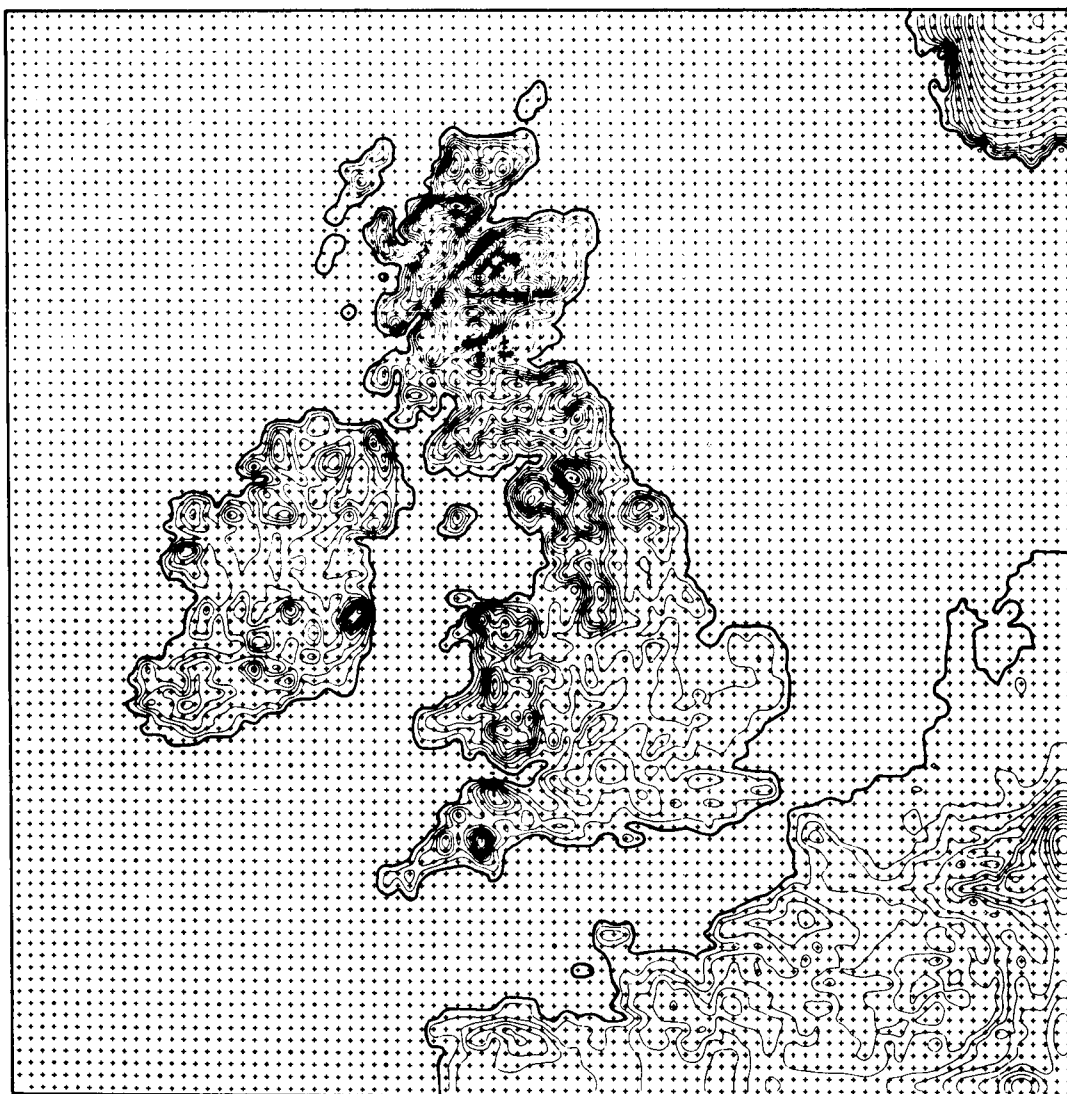


Figure 1. Model domain and orography. The grid points have a 15 km spacing and the contour interval is 50 m. The bold contour is at zero height and indicates the model coastline.

required, can cause undesirable effects close to the boundaries. Because the edges of the model domain are so close to the forecast area the forecast is generally driven by the boundary conditions in the latter stages, although it can develop topographically driven meso-scale features well. But in the first 6–9 hours, and longer in static situations, the initial conditions are very important.

3. Description of initialization schemes

3.1 Interactive Mesoscale Initialization

The IMI is a menu-driven system, controlled by 'mouse' input (and keyboard where required), which is operated by a human analyst on an interactive graphics workstation (Fig. 2). It allows the analyst to monitor the use of surface observations, and satellite and radar imagery, in the production of a set of key analyses of surface variables and the cloud distribution. The analysts are able to modify the data which are used in the analyses and modify the analyses themselves, thus

incorporating their own knowledge of the situation into the final result. Conceptual models are used to make remaining model fields consistent with these analyses.

The analysts have a choice of using the hybrid (see section 2) or a set of fields interpolated from the most recent fine-mesh model forecast as a first guess. The latter is normally selected only if a serious timing error is present in the forecast from the mesoscale model. The first guess is then used as a background field to carry out all the analyses, which are displayed with the observations, for them to check. If they are not satisfied with an analysis, then they have the option of either modifying the observations and reanalysing or modifying the analysis.

The analysts are able to delete, correct or add observations which are then reanalysed using either the first guess or the original analysis as the background field. The use of the original analysis allows the observations to be repeatedly analysed, if necessary, to fit them better. Corrections to the analysis itself can be applied in a broad variety of ways. Areas, lines and

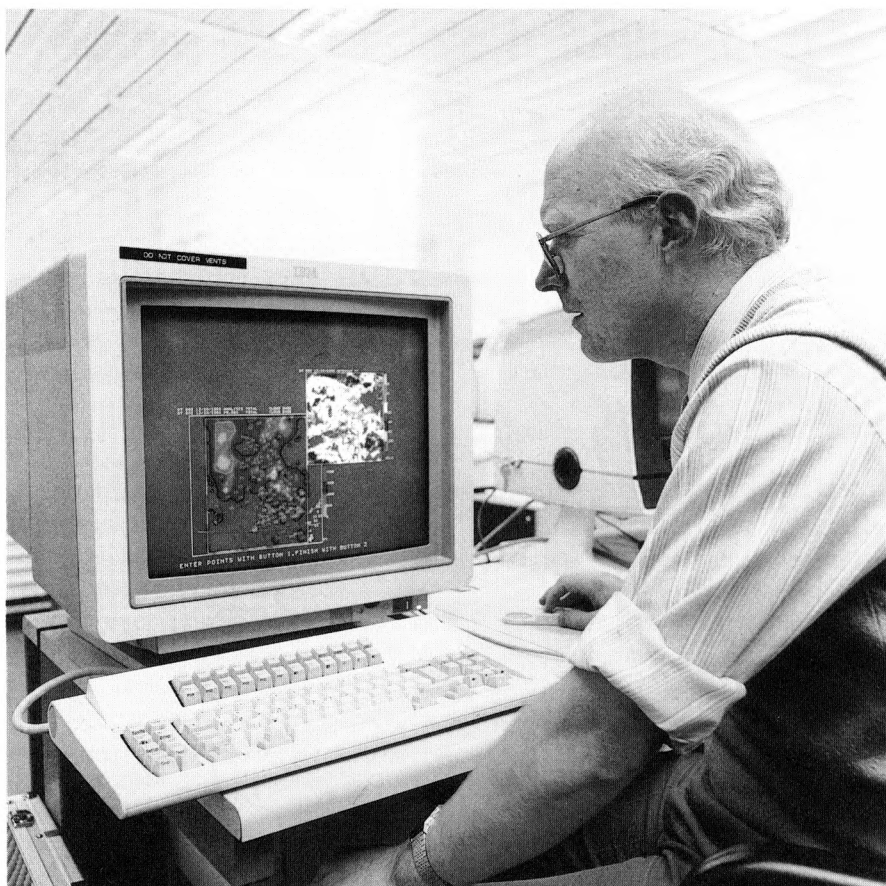


Figure 2. A forecaster in the Central Forecasting Office performing the Interactive Mesoscale Initialization.

points to be altered can be selected on the screen or from a range of values in any of the fields available. In the area selected it is possible to set a value, apply a correction, multiply by a factor, copy values from another field, or smooth the current values with a user-selected smoothing radius. Finally, if the analysts are not satisfied with the result, they have the option of restarting the analysis.

The mean-sea-level (MSL) pressure is analysed first, followed by the 10 m wind components. Before the wind analysis, corrections are made to the first guess to reflect the changes to the geostrophic wind in the pressure analysis. Corrections to the upper-level pressure, potential temperature and wind fields are computed from the pressure and wind analyses. The pressure corrections are calculated from the change in MSL pressure, assuming a slope of one in a hundred normal to the mean MSL pressure gradient, with a linear decrease in magnitude to zero at 8 km. Potential-temperature increments are computed hydrostatically from the pressure corrections at each level. Above 1 km, adjustments to the wind fields are obtained geostrophically from the pressure corrections. Below 1 km a height-dependent, linear combination of the geostrophic correction and the surface correction is used.

A surface precipitation rate analysis is carried out using a FRONTIERS (Brown 1987) radar image as the first guess within the radar coverage area, if an image is available for the correct time. Present weather reports

and hourly accumulations are used to estimate the precipitation rate at the observing stations. These rates are then analysed assuming a small area of influence within the radar domain, but a broader influence outside it. The Meteosat cloud-top-temperature image and sferics reports are usually available to aid the forecaster in verifying the analysis. The distinction between water and ice precipitation is made within the analysis, but is not as yet made use of in the initialization procedure.

The Meteosat cloud-top-temperature image is used to derive an improved first-guess total cloud cover, by assuming that cloud is present whenever the satellite temperature is 10 °C or more colder than the first-guess surface temperature. Because the satellite image is retrieved with a resolution of 7 km, counting the 'cloudy' pixels gives a good estimate of the total cloud cover. The surface reports are then analysed using this improved first guess.

The satellite image is adjusted for surface radiation effects in partially cloudy areas, using the cloud-cover analysis. A cloud-top height field is then derived by using first-guess temperature profiles to assign heights to the satellite cloud-top temperatures. If a satellite image is not available, then the first-guess cloud distribution is used to define the cloud top.

The first-guess cloud base is adjusted to ensure that it is at least 200 m below the cloud top, before it is used as

the background field to analyse the surface observations. If cloud top and cloud base conflict after the cloud-base analysis, then one or the other is modified. Below 8000 ft the cloud base is assumed to be more accurate, so adjustments are made to the cloud top. But, above 8000 ft more faith is placed in the satellite-derived cloud top, so the base is adjusted.

The 8-group cloud reports are analysed using the first-guess cloud distribution, with the cloud-top, base and total-cover analyses acting as constraints. This is carried out by interpolating the first-guess cloud-cover values to the observation points and using them to interpret the 8-groups to give a profile of cloud-cover values at model levels. The values are then analysed level by level.

The cloud and temperature structures may be examined in more detail by selecting up to 20 locations within the model area for which profiles of cloud cover and potential temperature are displayed. Either or both of these profiles may be adjusted if desired, with the temperature corrections and the adjusted cloud-cover values being imposed over an area selected on the screen. To assist the analyst, if a radiosonde ascent is available at the selected location it will also be displayed.

The final four analyses are visibility, lying water (snow depth), screen temperature and dew-point. For the lying-water analysis, state of ground reports of dry, damp, flooded and frost are interpreted quantitatively, and snow depth reports are used directly. The screen-temperature analysis is used to modify the soil, surface and first-level temperatures assuming either a logarithmic or a linear profile depending on the first-guess temperature profile.

The low-level relative humidity, cloud water and the boundary-layer cloud condensation nucleus (CCN) concentration are initialized using the temperature, dew-point and visibility analyses. The humidity mixing ratio is calculated at screen level, and the relative humidity at the lowest level is computed from this by assuming that the humidity mixing ratio remains constant up to 20 m. Where the relative humidity is greater than 99%, or the visibility is less than 1.5 km, cloud water is assumed to be present in the atmosphere and is initialized using an empirical relationship relating it to visibility and CCN concentration (derived from Kunkel 1984):

$$M = \frac{0.03058}{[\text{visibility} \times \{\log_{10}(C_0) + 0.25\}]^{3/2}}$$

where M is the cloud water mixing ratio and C_0 is the first-guess CCN concentration. The relative humidity is also increased to 100% and 8 oktas cloud is set. Elsewhere, the visibility is assumed to depend only on the humidity and the aerosol content. The analysed visibility and relative humidity are used to diagnose the boundary-layer CCN concentration, using an empirical relationship derived from Hänel (1987) and Kunkel (1984):

$$C = \frac{-109732 \times \log_e(0.01 \times RH)}{[\text{visibility} \times \{\log_{10}(C_0) + 0.25\}]^{3/2}}$$

where C is the diagnosed CCN concentration, C_0 is the first-guess CCN concentration, and RH is the relative humidity. The cloud-water mixing ratio and the cloud cover are set to zero. The resulting field of C is inherently rough, so it is constrained to be between 20 and 500 cm^{-3} and smoothed.

The upper-level humidity distribution is adjusted to be consistent with the analysed cloud cover, using a simplified form of the equations which are used in the forecast model. Empirical relationships are used to initialize the cloud water/ice profiles consistent with the analysed cloud and precipitation. A single-column version of the model precipitation scheme is used to adjust the cloud water/ice profile iteratively and so produce the analysed precipitation rate at the surface for each grid point.

After the surface temperature has been initialized, it is possible for the analyst to modify the field either by hand or by copying in a sea surface temperature field which has been generated using successive infra-red Meteosat images over the period of a week.

Temperature profiles are adjusted from the lowest level upwards to spread the influence of the surface observations and to enforce stability where no cloud is present. The temperature is adjusted to be stable, using the modified temperature from the level below, and assuming a cloud-fraction dependent, linear combination of the saturated adiabatic lapse rate and the dry adiabatic lapse rate. Immediately above the cloud top, the temperature is adjusted to be stable to air parcels following a saturated adiabat from anywhere within the cloud deck. This allows convective instability within the cloud itself, in a way that is consistent with the forecast-model turbulence scheme, but does not allow instability in the clear air. If necessary, where excess stability is present, it may be eroded in order to minimize deviations from the mean temperature in the first guess. The temperature stability adjustment has been added in an attempt to limit excessive convection which often occurs in the early stages of the forecast.

The divergence profile is adjusted to give zero vertical velocity at the upper boundary. A single-column version of the model precipitation scheme is also used to calculate the height-dependent precipitation rate using the initialized cloud-water profile. Where precipitation is being produced, the vertical velocity is reset so as to lift enough saturated air to replace the precipitation falling out of the layer. The cloud top is reinforced by a small negative vertical velocity. Within the lowest kilometre, the vertical velocity is set equal to a height-dependent, exponentially weighted combination of the vertical velocity recalculated from the horizontal winds and the initialized vertical velocity. A heavy smoothing is applied and values are limited, in order to eliminate sudden changes and unreasonably high values. The

divergence structure is adjusted again to be in balance with this final vertical velocity. Finally, the analyst has to make a 'Yes' or 'No' response, either to use the initial fields which have been created by the IMI, or to fall back on the initial fields generated by the OI.

3.2 Objective initialization (OI)

The main differences between the OI and the IMI are the use of radar and satellite imagery and interactive control given to the analyst. In the OI a similar set of key analyses is carried out and a more limited set of conceptual models is used to make the other model variables consistent. Overall a less thorough knowledge of the situation is incorporated into the initial fields.

The hybrid (see section 2) is taken as a first guess, and thus is used as a background for the analyses of MSL pressure, wind, precipitation rate, cloud cover, visibility, snow depth, screen temperature and dew-point. The soil, surface and first-level temperatures are adjusted to be consistent with the analysed screen temperature, preserving the the initial-model lapse rate. The temperature, relative humidity and winds within the boundary layer (whose depth is diagnosed from the first-guess temperature profile) are adjusted to be consistent with the analysis values. Super adiabatic lapse rates are removed at all levels. No geostrophic adjustment is made to the winds, but the upper-level pressures are recalculated hydrostatically, starting from the analysed MSL pressure.

The first-level relative humidity and cloud-water mixing ratio are diagnosed from the analysed visibility. The surface observations of cloud are used in conjunction with the cloud-cover analysis to generate a three-dimensional cloud analysis, which in turn is used to initialize relative humidity and to obtain a first-guess cloud-water mixing ratio distribution. A single-column version of the model precipitation scheme is used iteratively to adjust the cloud-water mixing ratio until it produces the analysed precipitation rate. The divergence profile is recalculated to give zero vertical velocity at the upper boundary, but no account is taken of precipitation within the vertical-velocity initialization.

4. Case studies

4.1 Summary of results

Forecasts were run for eight cases using initial conditions generated by both the OI and the IMI. Each case was chosen because the routine forecast (initialized using the OI) was deficient in some way. The comparison between the two forecast runs was, in each case, a subjective one, with the type of comparison being dictated by the particular details of the weather which were of interest to the forecaster on that day.

A summary of the cases is given below, with the impact to the forecast of using the IMI referred to as either none (no major differences from the OI forecast), some (some significant improvements to the forecast)

and good (some very marked improvements to the forecast). It is worth noting that in none of the cases investigated did the use of the IMI have a negative impact on the forecast.

Case 1. Stratocumulus cloud and fog. Analysis time 1200 UTC on 5 November 1988. Impact – good.

See section 4.2.

Case 2. Rain and snow. Analysis time 1200 UTC on 26 February 1989. Impact – none.

A complex low-pressure system covered the British Isles. Within the north-westerly flow a small low centre formed and swung south-eastwards across Ireland, Wales and southern England, bringing rain across the south of the country, with snow on the northern edge, and triggering some thunderstorms along the south coast. Both of the forecasts failed to maintain the area of precipitation for more than a few hours into the forecast, leaving most of southern England with a dry afternoon.

Case 3. Frontal precipitation. Analysis time 0600 UTC on 15 February 1989. Impact – some.

See section 4.3.

Case 4. Stratocumulus cloud. Analysis time 0000 UTC on 12 December 1988. Impact – good.

An anticyclone was centred over Ireland, with a weak cold front moving south-westwards across England. There was much low cloud associated with the front and the general area of warm, moist air circulating around the high centre. The OI forecast maintained too much cloud over southern England, whereas the IMI forecast developed the observed breaks and so gave much better guidance.

Case 5. Winds. Analysis time 0000 UTC on 5 May 1989. Impact – some.

A generally slack, anticyclonic pressure gradient covered the British Isles. The OI forecast developed unrealistically strong southerly winds in the North Sea, resulting in a spurious trough which propagated slowly eastwards. The winds were much lighter in the IMI forecast, leading to a more realistic evolution.

Case 6. Convection. Analysis time 0000 UTC on 23 May 1989. Impact – none.

Under the influence of anticyclonic conditions, with very warm, moist air feeding northward across the country, a mesoscale convective system (MCS) moved north from France and redeveloped over Hampshire. Both the forecasts totally failed to develop this feature.

Case 7. Convection. Analysis time 0000 UTC on 24 May 1989. Impact – some.

The situation was the same as case 6 except that the MCS developed slightly later in the night. Despite

initially having quite a good representation of the feature the OI forecast failed to maintain it beyond 06 UTC. The IMI forecast did not have the feature particularly well represented at the beginning of the forecast, but did manage to develop and maintain the feature, correctly moving it north-westwards, albeit rather slower than reality.

Case 8 (carried out on the large model area). Depression. Analysis time 0000 UTC on 11 April 1989. Impact – some.

A deep depression was centred to the north-west of Scotland, with a strong south-westerly flow covering the British Isles. A small low ran to the south of the main centre, developing as it moved into Ireland. The OI forecast did not develop the small low properly, instead concentrating on another centre further north, which meant the frontal rain bands were not well predicted. The IMI forecast developed the small low more successfully, resulting in a more realistic rain-band structure. It also correctly had stronger winds in the following westerly flow.

The following two sections take a more detailed look at cases 1 and 3.

4.2 Anticyclonic stratocumulus (5 November 1988)

The use of satellite imagery and manual intervention within the IMI should lead to a better cloud analysis, and thus a better cloud forecast. This is especially true for static situations involving persistent layer-cloud, such as anticyclonic stratocumulus, where the boundary conditions become less crucial. The case investigated here is such a cloud forecast.

On the evening of 5 November 1988, under the influence of anticyclonic conditions (see Fig. 3), fog formed over much of southern England and remained for several days in some parts. The thickness of the fog

experienced in many places may have been a consequence of the large amount of smoke ejected into the air by bonfires on that evening, but the actual distribution of the fog was very much dependent on the low-cloud distribution, as Fig. 4 shows. A good forecast of the movement and development of the stratocumulus cloud present in the high cell circulation was crucial for the prediction of the onset and the distribution of the fog that night. The midday run of the mesoscale model did not produce a very good 18-hour cloud forecast and failed to develop the observed fog, instead keeping

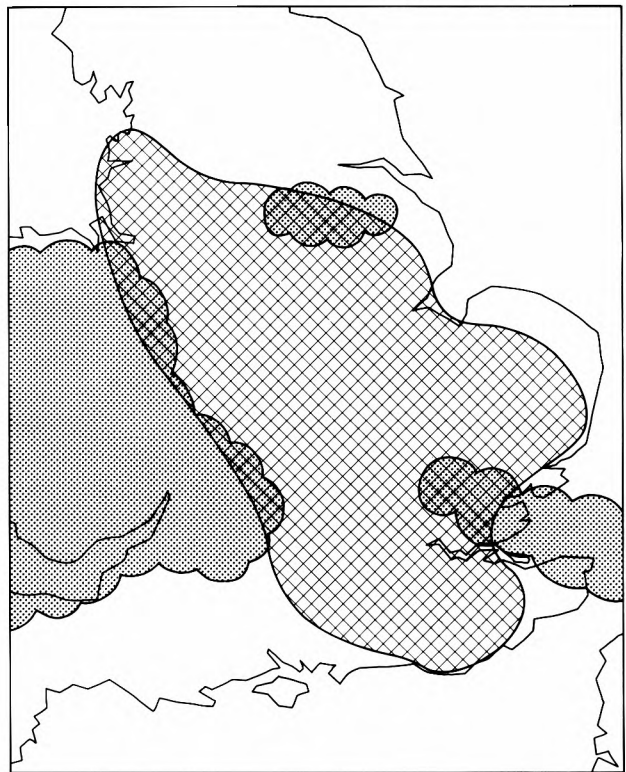


Figure 4. Observed low-cloud areas and fog distribution for 06 UTC on 6 November 1988. Stippling denotes areas with more than 5 oktas low-cloud cover, and hatching denotes areas of less than 100 m visibility.

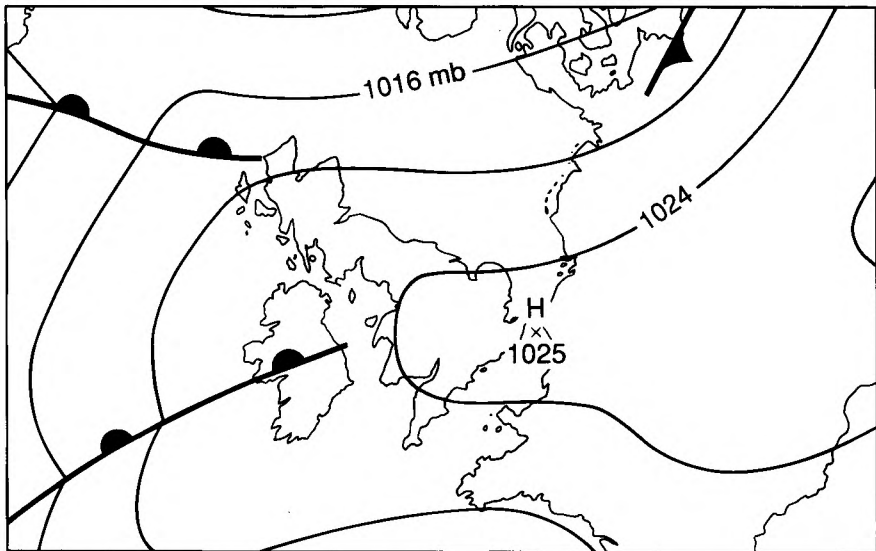


Figure 3. Mean-sea-level pressure analysis and fronts at 06 UTC on 6 November 1988.

visibilities in excess of 20 km. The forecast run from the IMI had a better cloud distribution which was reflected in the lower visibilities produced.

Within the IMI, the Meteosat image was used in both the cloud-cover and the cloud-top analyses. After incorporating the observations, the cloud cover appeared slightly deficient to the north of East Anglia, so 7 oktas cloud was set where the satellite image showed cloud temperatures colder than 0 °C. With very little data present to influence the analysed cloud bases over the sea areas, they appeared to be too high over the North Sea and to the west of Scotland. So, in these areas, the bases were adjusted to agree with the few observations that were available. The resultant cloud analysis produced by the IMI (Fig. 5(a)) has much more low cloud over the sea areas than the objective analysis (Fig. 5(b)), which illustrates the importance of the satellite image over data-sparse areas. Otherwise the two analyses are generally similar over much of the British Isles, except over Wales and the Irish Sea, where the cloud is more broken in the IMI analysis. There is also less high cloud in the IMI analysis and cloud tops over Ireland are higher.

The 18-hour forecast run from the IMI has a cloud sheet covering Wales and just beginning to extend into England, but with the majority of southern England cloud free (Fig. 6(a)), which compares favourably with the observed low-cloud distribution at 06 UTC (Fig. 4). By contrast, the forecast run from the OI has much of southern England under a veil of low cloud, with the only significant breaks being on the south coast and in

Humberside (Fig. 6(b)), this being a very poor reflection of reality. So the incorporation of satellite imagery has had a marked impact on the 18-hour low-cloud forecast.

The forecast visibilities were not as impressive, with the IMI forecast failing to develop the observed fog. But its visibilities were of the order of 4 km over most of southern England, which is a marked improvement on the OI forecast which kept visibilities at over 20 km. The improvement in the visibility forecast is a result of the improved cloud forecast and the higher aerosol concentrations initialized in the visibility analysis. Possible reasons for the failure to forecast the fog are the non-representation of the increase in aerosol concentration which occurred during the evening as a result of the bonfires across the country, and the omission of any interaction between the cloud condensation nucleus concentration (which acts only as a tracer in the forecast) and other model variables.

The use of the satellite imagery within the IMI was reflected in the overall improvement in the forecast. The failure to produce the observed fog is disappointing, but the cloud forecast in itself would have been good guidance to the forecaster trying to predict the fog distribution on the morning of the 6th.

4.3 Frontal precipitation (15 February 1989)

Radar imagery is currently the only available source of data that captures the mesoscale detail present within frontal rain bands. Thus the incorporation of these data within the IMI should lead to a better precipitation analysis, which, when used in conjunction with the

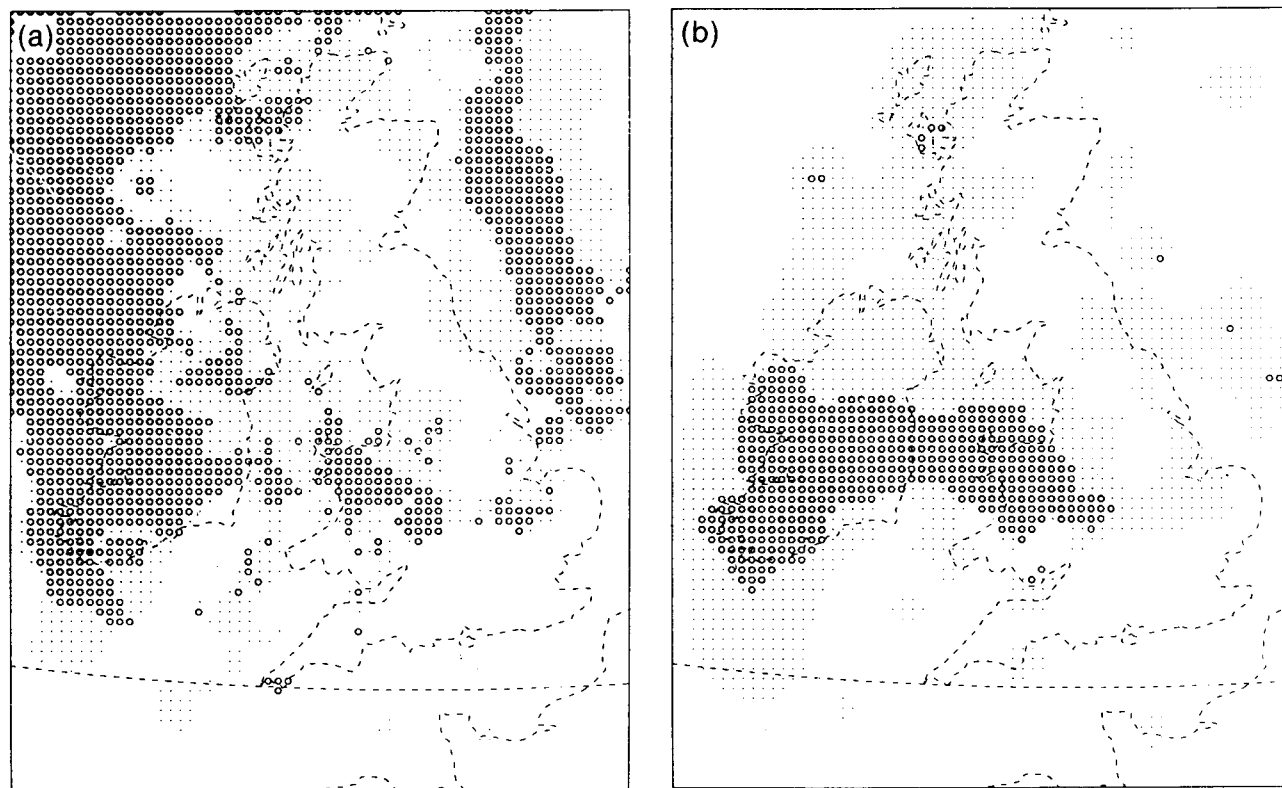


Figure 5. Model analyses of low-cloud cover for 12 UTC on 5 November 1988 for (a) the IMI analysis, and (b) the objective analysis. Cloud amounts are shown as dots, > 4 oktas, or circles, > 7.5 oktas.

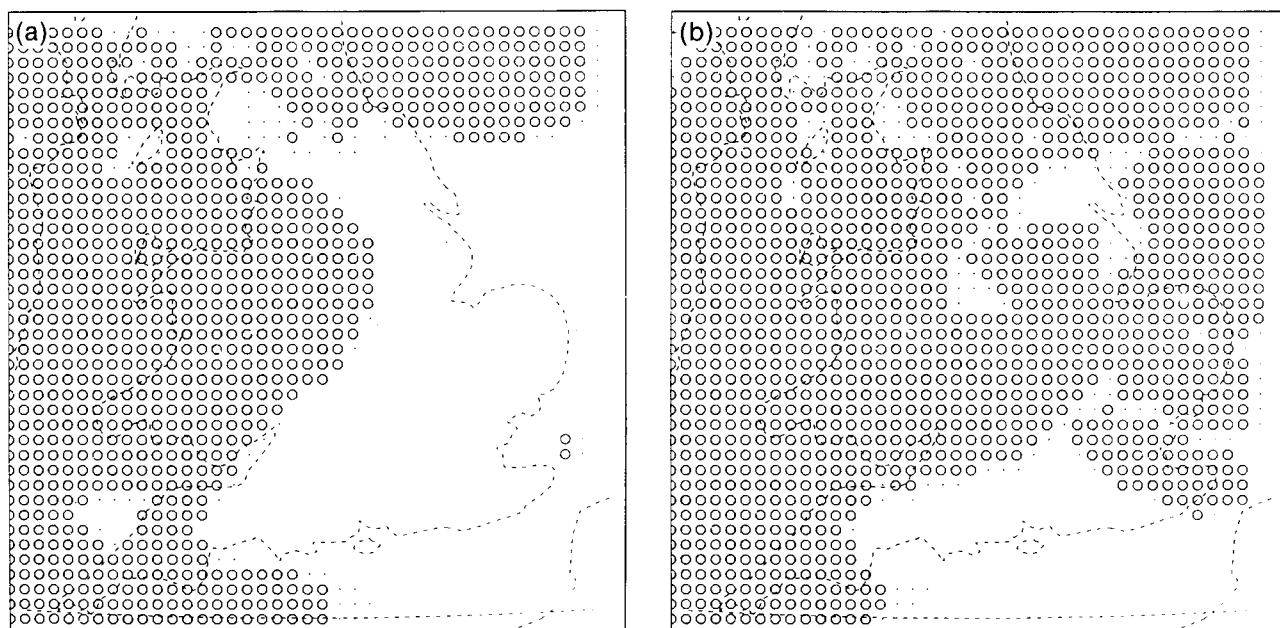


Figure 6. Eighteen-hour forecast low-cloud cover for 06 UTC on 6 November 1988 for (a) the IMI forecast, and (b) the objective forecast. Cloud amounts are shown as dots, > 4 oktas, or circles, > 7.5 oktas.

satellite-derived, three-dimensional cloud analysis in the initialization of the cloud water and the vertical velocity, should generate and maintain a realistic frontal structure. This case investigates the impact of the IMI in the forecasting of a cold front.

On 15 February 1989 an active cold front passed south-eastwards across the British Isles (Fig. 7). Associated with it was an area of heavy rain and a well marked band of line convection (see Fig. 9). Both the midnight and midday runs of the mesoscale model moved the front on too fast, tending to lose the rain to the rear of the front, developing instead a spurious area of rain in the English Channel, well ahead of the front. It was decided to run the mesoscale model, using initial fields generated by both the IMI and the OI at 06 UTC, which was the time when the front first entered the radar domain.

Within the IMI the radar data were incorporated into the precipitation analysis, and produced a good representation of the front over Ireland and northern England. Over the North Sea, where there was no radar coverage and observations were sparse, the front was badly represented. So, within that area, the precipitation was replaced by a rate of 0.4 mm h^{-1} where the Meteosat image showed cloud tops colder than -20°C . The satellite image was also used in generation of the cloud-cover and cloud-top analyses. The front was badly represented in the pressure pattern, so a trough was inserted before the observations were analysed, and was maintained in the analysis. Some spurious fog over northern France was removed. The resultant precipitation analysis produced by the IMI (Fig. 8(a)) had a more continuous band of precipitation than the objective analysis (Fig. 8(b)), with the main area of rain further

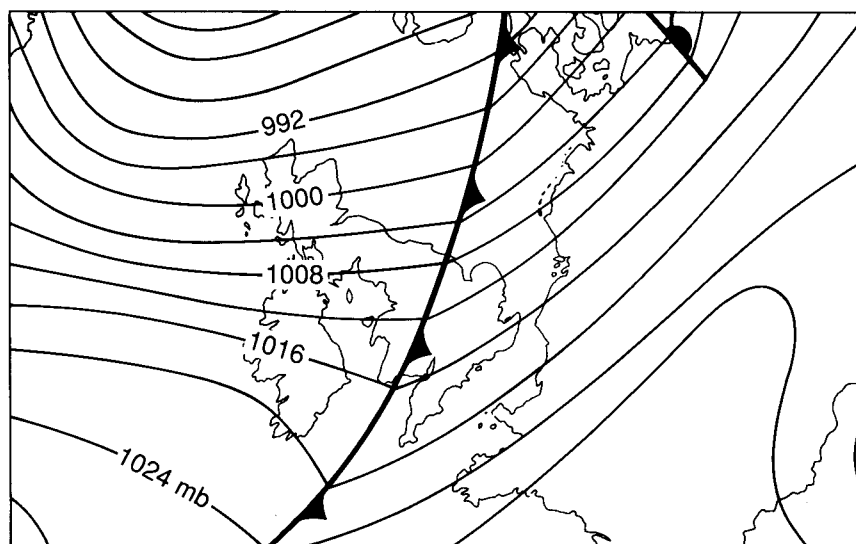


Figure 7. Mean-sea-level pressure analysis and fronts at 12 UTC on 15 February 1989.

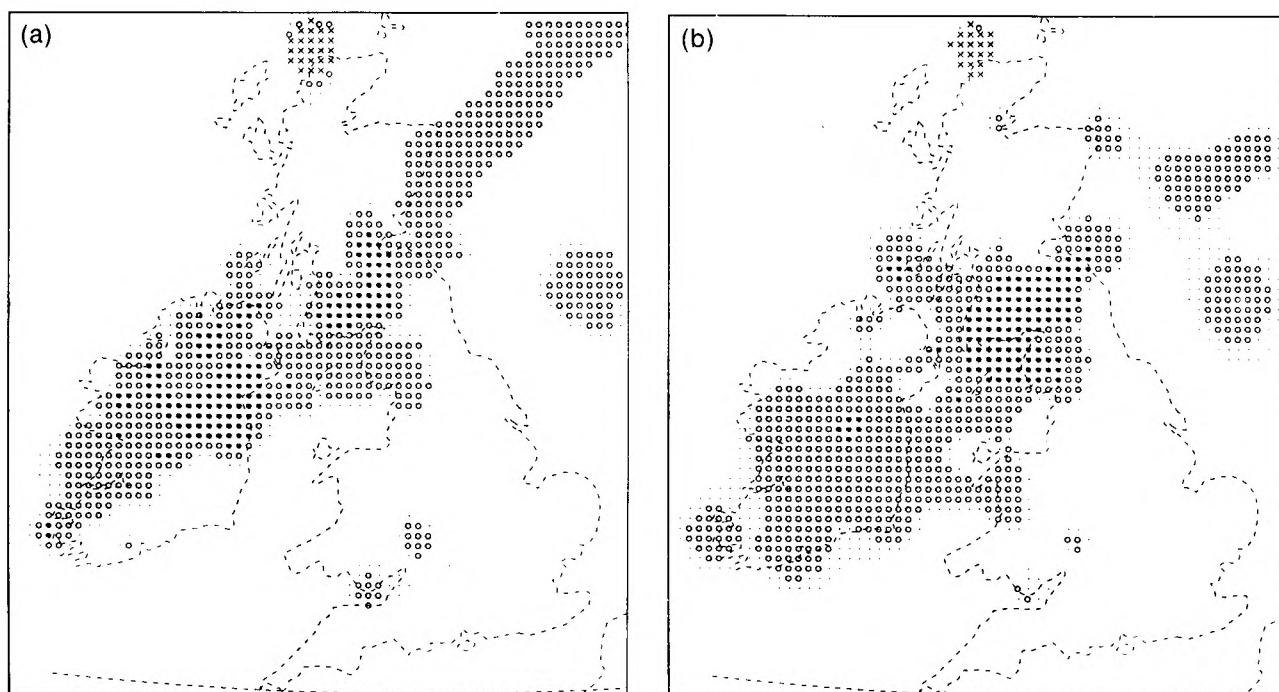


Figure 8. Model analyses of precipitation for 06 UTC on 15 February 1989 for (a) the IMI analysis, and (b) the objective analysis. Dynamic rainfall rates are shown by dots, $> 0.05 \text{ mm h}^{-1}$; open circles, $> 0.1 \text{ mm h}^{-1}$; solid circles, $> 0.5 \text{ mm h}^{-1}$, plus snowfall (rainfall equivalent) by crosses, $> 0.05 \text{ mm h}^{-1}$ or asterisks, $> 0.5 \text{ mm h}^{-1}$.

north over Ireland, leaving southern Ireland and Wales dry at 06 UTC.

The radar image for 12 UTC (Fig. 9) shows a large area of moderate rain over Wales, with a narrow band of line convection stretching from The Wash through to the Bristol Channel. There are some smaller areas of rain apparent over Cornwall, and there is an area of light rain over south-west and central southern England which does not show up on the radar, but was observed, the area at 12 UTC being shown in Fig. 10.

The 6-hour forecast run from the OI (Fig. 11(b)) has a band of rain which is roughly coincidental with the line convection, but far too wide, with too much rain over East Anglia. It has the main area of rain too far south, over south-west England, where there was only light rain in reality, and much of Wales is completely dry. It has also developed a large area of precipitation over the English Channel, giving southern England and the north coast of France some rain. This area of rain was not supported by observations or radar and appears to be totally spurious.

The forecast run from the IMI (Fig. 11(a)) has a sharper band of quite heavy rain which agrees well with the actual position of the line convection. Like the OI forecast, it has the main area of moderate rain too far south, but does have slightly more rain over Wales. South-east England has been left completely dry which is in accordance with reality, and although there is evidence of the area of spurious rain in the English Channel, it has not been developed to the same extent as in the OI forecast.

Further into the forecast period, both the OI and the IMI forecasts continued to have the rain too far south,

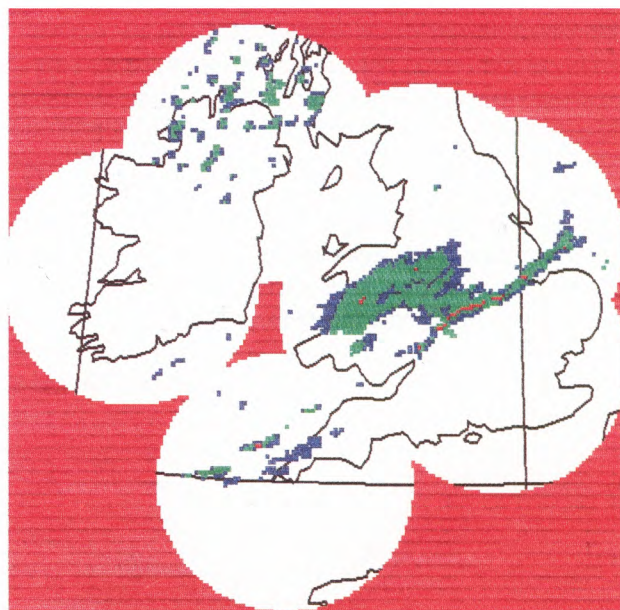


Figure 9. Composite radar image showing areas of precipitation for 12 UTC on 15 February 1989. Within the area of radar coverage the colours blue, green and red denote increasing rates of rainfall.

and developed the spurious rain area over the English Channel. However, the spurious rain was not developed so soon or to the same extent within the IMI forecast as it was within the OI forecast. The IMI forecast also had the convective band slightly further north towards the end of the forecast, giving a better indication of the real distribution of the rain.

Although the use of the satellite and radar data within the framework of the IMI did not totally remove the

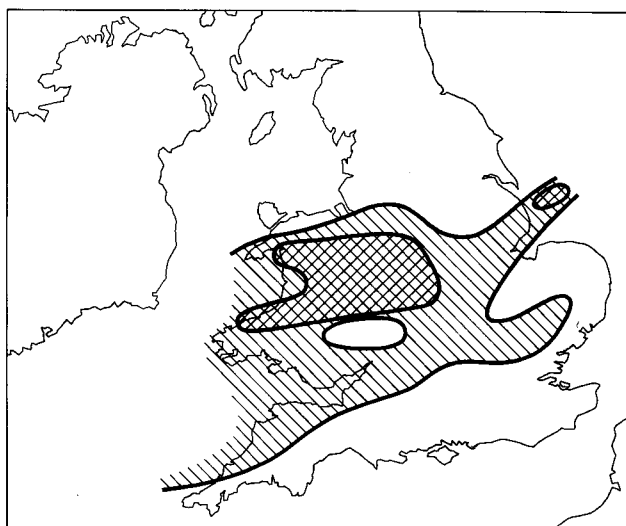


Figure 10. Areas of rain from surface observations for 12 UTC on 15 February 1989. Hatching denotes areas of light rain and cross-hatching areas of moderate or heavy rain.

forecast errors, it did provide some improvements on the OI forecast, especially in the early stages, and would have acted as better guidance to the forecaster attempting to predict the rain areas. The incorrect development of rain in the English Channel may have been a result of erroneous boundary conditions.

5. Conclusions and further work

The eight cases investigated here illustrate that the use of the IMI scheme, incorporating satellite and radar imagery, can have a positive impact on the mesoscale model forecasts.

The most significant improvements occurred in the predicted low-cloud distribution, in static situations such as cases 1 and 4. These cases illustrate that the impact of an improved cloud analysis can last throughout the forecast period. The impact was generally not so long-lived in more mobile situations, such as case 3, with significant improvements tending to last only for the first 6–9 hours. The prolonged impact experienced in case 8 when using a larger domain supports the idea that this limit is due to the influence of the boundary conditions. In cases 2 and 6 the use of the IMI appeared to have no effect on the forecasts, which in both cases, failed to develop a small-scale feature which had a significant effect on the weather. One possible explanation is that the observed feature was not initialized properly, due either to lack of information or shortcomings in the methods used to initialize the upper-air fields.

Future improvements which may reduce the problems are likely to come from increasing the model domain, the use of more conceptual models and the utilization of other sources of data as they become available. Further comparisons between the OI and the IMI could usefully be carried out in several ways.

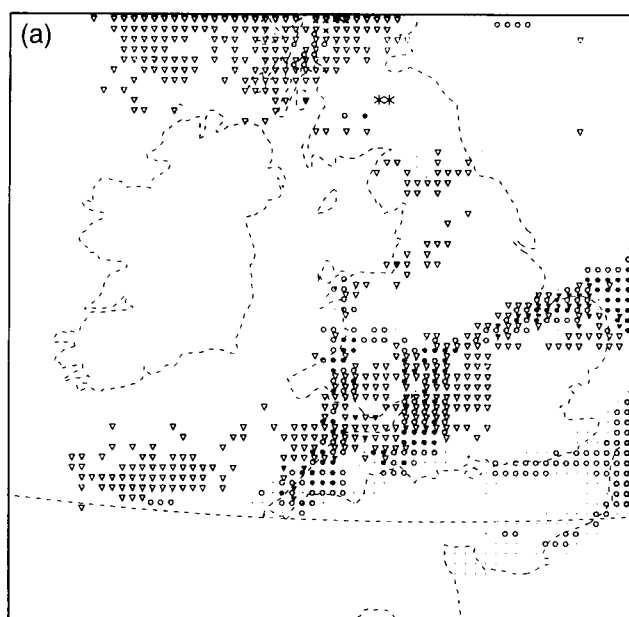


Figure 11. Six-hour forecast precipitation for 12 UTC on 15 February 1989 for (a) the IMI forecast, and (b) the objective forecast. Dynamic rainfall rates are as in Fig. 8 with the addition of convective rainfall denoted by open triangles, $> 0.4 \text{ mm h}^{-1}$ or solid triangles, $> 2 \text{ mm h}^{-1}$.

In all the cases investigated here, the routine forecast (initialized using the OI) has been deficient in some way, thus leaving plenty of room for improvement. To obtain a more balanced view of the effect that the use of the IMI has on the forecast, it would be beneficial to run some comparisons on cases where the use of the OI has resulted in a good forecast, to see if the IMI provides further improvements to the forecast, has no impact or possibly degrades it.

Another factor in this assessment is that the cases shown here have all been carried out in a research environment, away from the pressures and time constraints experienced by a forecaster in the Central

Forecasting Office (CFO). The next logical stage in the assessment of the IMI, would be to compare forecasts initialized by forecasters in CFO using the IMI with those initialized using the OI. This would provide a much better insight into the improvements that could be obtained by using the IMI operationally.

Since the mesoscale model has a continuous assimilation cycle, it would also be useful to compare forecasts when the OI and the IMI had been used on more than one assimilation cycle.

References

- Brown, R., 1987: The use of imagery in the FRONTIERS precipitation nowcasting system. *In* Proceedings of the workshop on satellite and radar imagery interpretation, Reading, England, 24 July 1987.
- Golding, B.W., 1987: Short-range forecasting over the United Kingdom using a mesoscale forecasting system. *In* Matsuno T. (Ed.), Short and medium-range numerical weather prediction. Tokyo, Meteorological Society of Japan.
- , 1990: The Meteorological Office mesoscale model. *Meteorol Mag*, **119**, 81–96.
- Hänel, G., 1987: The role of the aerosol properties during the condensational stage of cloud: A reinvestigation of the numerics and microphysics. *Contrib to Atmos Phys*, **60**, 321–339.
- Kunkel, B.A., 1984: Parameterization of droplet terminal velocity and extinction coefficient in fog models. *J Clim Appl Meteorol*, **23**, 34–41.

551.506.1(41-4)

The autumn of 1989 in the United Kingdom

G.P. Northcott

Meteorological Office, Bracknell

Summary

The mild, dry and mainly sunny weather of the summer continued well into the autumn, but with localized thundery outbreaks in September, some windy days in October and widespread fog for a while in November.

1. The autumn as a whole

Over the autumn season mean temperatures were above normal in all areas of the United Kingdom except parts of western Scotland and ranged from 1.4 °C above normal in the area north of London to 0.4 °C below normal on the Isle of Rhum. Rainfall amounts were below normal nearly everywhere with as little as 40% in parts of East Anglia, north-east England and south-east Scotland. However, in parts of South Wales and the west of England amounts were above normal, with about 120% in Hereford and Worcester and north Cornwall. Autumn sunshine totals were high in many inland areas, but rather low in the west, ranging from more than 120% of normal in the north of Scotland to less than 80% of normal in the Isle of Man.

Information about the temperature, rainfall and sunshine during the period from September to November 1989 is given in Fig. 1 and Table I.

2. The individual months

September. Mean monthly temperatures were above normal in England and Wales but near normal in Scotland and Northern Ireland, ranging from 0.5 °C below normal at Abbotsinch, Strathclyde Region to 2.1 °C above normal at Gatwick, West Sussex. The mean temperature over England and Wales was the highest since 1961, not because daytime temperatures were particularly notable, but rather that night-time temperatures were unusually high. Hampstead, Greater London reported the highest mean maximum since 1964

(19.9 °C), the highest mean minimum since 1961 (12.5 °C), and the highest mean temperature since 1961. Oxford reported the warmest September since 1949 (mean maximum 20.1 °C, mean 15.6 °C, mean minimum 11.9 °C). Northwood reported the highest monthly mean since 1959 and 1961. The temperature of 26.1 °C on the 7th gave Northwood its warmest September day since 1972. Broom's Barn, Suffolk had the highest mean air temperature for 40 years (14.2 °C). Monthly rainfall amounts were below normal nearly everywhere, apart from Kinloss, Grampian Region and northern parts of Devon and Cornwall, where rainfall was just above average, ranging from 101% at St Mawgan, Cornwall to only 11% at Leeming, North Yorkshire. Generally it was the driest September only since 1986. However, many places in eastern England had the driest September since 1969, including Hampstead and Northwood, both in Greater London, and Broom's Barn, Suffolk; Durham and Tynemouth in the north-east had the driest September since 1898. Monthly sunshine totals were above normal in northern and eastern Scotland and north-eastern and central areas of England, and near or below normal elsewhere, ranging from 137% at Lerwick, Shetland to 78% at Marham, Norfolk.

The weather was generally fairly settled, warm and dry, but less sunny in many areas than over the previous months. The period from the 10th to 19th was unsettled, and localized severe thunderstorms between the 10th and 13th caused lightning damage and flooding in the

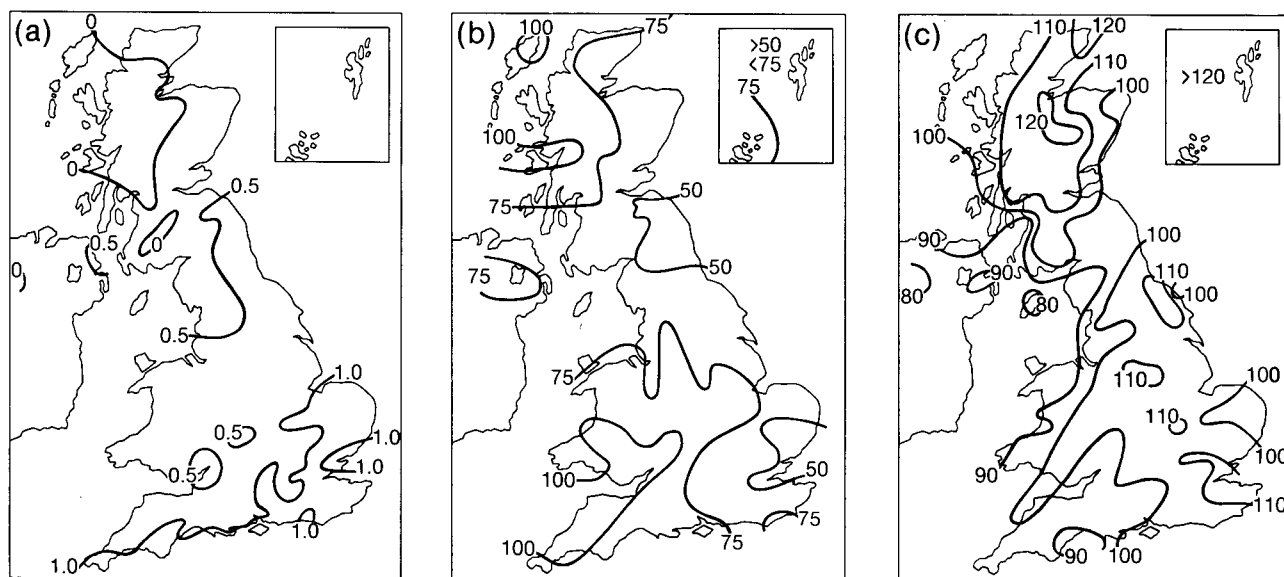


Figure 1. Values of (a) mean temperature difference ($^{\circ}\text{C}$), (b) rainfall percentage and (c) sunshine percentage for autumn, 1989 (September–November) relative to 1951–80 averages.

Table I. District values for the period September–November 1989, relative to 1951–80 averages

District	Mean temperature ($^{\circ}\text{C}$)	Rain-days	Rainfall	Sunshine
	Difference from average		Percentage of average	
Northern Scotland	+0.1	–2	87	118
Eastern Scotland	+0.4	–2	67	112
Eastern and north-east England	+0.8	–3	62	108
East Anglia	+1.0	–2	58	114
Midland counties	+0.8	–3	84	108
South-east and central southern England	+1.1	–3	69	119
Western Scotland	+0.2	–2	80	104
North-west England and North Wales	+0.5	–1	75	100
South-west England and South Wales	+0.8	–2	96	98
Northern Ireland	+0.4	–1	80	88
Scotland	+0.2	–2	81	111
England and Wales	+0.8	–2	77	108

Highest maximum: 27.1°C in Midland counties in September.

Lowest minimum: -8.4°C in western Scotland in November.

south. Areas affected included Kent early on the 10th, Devon and Dorset on the 11th, south Devon and many parts of south-east England on the 12th. Late on the 12th lightning struck and badly damaged houses near Wokingham, Berkshire and at nearby Bracknell. Lightning disrupted ambulance communications at Wokingham for a time. In south and east London flood-water was up to half a metre deep in places. In Kent lightning left thousands of homes in Faversham and some other places without power; near Herne Bay a man was killed by lightning. Among the buildings struck was the Guildhall Museum at Rochester. Many rail services in Kent were disrupted, while rain caused a landslide on the railway at Ruscombe, Berkshire adding to problems caused by signals failures.

October. Mean monthly temperatures were above normal everywhere except northernmost parts of Scotland, ranging from just below normal at Wick,

Highland Region to about 2°C above normal in the London area. Monthly rainfall totals were above normal nearly everywhere apart from parts of eastern and southern Scotland and parts of eastern England and East Anglia, ranging from more than 180% in the south-west Midlands and South Wales to as little as 56% at Lowestoft, Suffolk. Monthly sunshine amounts were about or below normal nearly everywhere. Parts of the east Midlands had between 100% and 123% of normal, while western Wales had only just half the normal.

The weather was relatively quiet at the beginning of the month, then became unsettled with some windy spells; but, between the 14th and 18th it was mainly dry in southern areas of Great Britain. From the 19th it was generally unsettled, with some very wet weather at times. Over Wales the 20th was probably the wettest day since 23 January 1990. Late on the 20th and on the 21st England and Wales became very windy with gusts of more than 50 kn over southern counties of England and

Wales including 63 kn at Sheerness, Kent and 69 kn at Portland Bill, Dorset; two people were killed and several had narrow escapes as gale-force winds and heavy rain disrupted traffic in western areas, brought down trees and caused widespread flooding. Many parts had a period of very heavy rain and strong winds on the 28th, when a very vigorous depression brought gales to many exposed parts of southern England and Wales, with widespread gusts of more than 60 kn in the south-west and a peak of 88 kn at Portland Bill. Further heavy rain affected southern counties overnight on the 30th/31st.

November. Mean monthly temperatures were generally near normal, although some regional differences were evident: values were slightly above average in eastern Scotland, north-east England, Wales and south-west England, while in many central and south-eastern areas of England it was rather cool. Averages ranged from 1.2 °C above normal at Aberdeen, Grampian Region and Falmouth, Cornwall to 0.7 °C below normal at Alice Holt, Hampshire. Monthly rainfall totals were below normal everywhere in the United Kingdom, ranging from as little as 21% at Edinburgh, Lothian Region to 93% in North Wales. Some parts of the Moray Firth area received less than 3 mm of rain during the first 14 days of November, and a few widely scattered locations had no measurable rainfall through-

out the month. Monthly sunshine amounts were above normal nearly everywhere in the United Kingdom except for one or two places in north-west England, the Isle of Man, eastern Scotland and south Devon, and much of Northern Ireland, where it was a little below normal, and ranged from 202% at Folkestone, Kent to about 60% of normal at Omagh, Co. Tyrone. Over much of southern England it was the sunniest November on record. The highest monthly sunshine amount was 147 hours at Folkestone, Kent, the highest November total anywhere in the United Kingdom since sunshine records began. Scotland also had a sunny month, and Edinburgh Royal Observatory recorded 94 hours of sunshine, this value having been exceeded only once (99 hours in 1947) in a record going back to 1901.

The unsettled weather of the last 2 weeks of October continued into the first 10 days or so of November, with some further heavy rain, especially in hilly western areas of Wales and England, although eastern Scotland and coastal areas of north-east England often escaped significant rainfall. Towards mid month settled weather gradually became established over the whole United Kingdom although bringing with it periods of widespread fog, persistent from the 13th to 14th. From the 15th it was mostly dry; most of any rain fell in northern Scotland, or in eastern coastal areas and, until the 22nd, the far south-west of England and Wales.

Notes and news

Water-resource assessment experts meet to develop a strategy for the 1990s

A group of experts met in the Headquarters of the World Meteorological Organization (WMO) from 17 to 19 July to take the first steps towards the preparation of a water-resource assessment strategy for the 1990s. The meeting was sponsored by WMO, the United Nations Educational, Scientific and Cultural Organization (UNESCO), the United Nations Department of Technical Co-operation for Development (UNTCO) and the UN Department of International Economic and Social Affairs (UNDIESA).

In preparation for the meeting, experts/consultants visited countries in different regions of the world. The meeting identified the following problem areas:

- (a) Inability of many nations to assess and manage their water resources wisely, because legislation and/or institutions to carry out the work are lacking.
- (b) Reduction of hydrological networks, as well as the analyses of data from them, by countries suffering from economic difficulties.
- (c) Lack of measurements of ground water and water quality in many regions of the world.
- (d) Inadequate facilities to train and educate technicians and professionals in water-resource assessment in many parts of the world.

The outcome of the meeting and its proposals for future action on national, regional and global scales will be incorporated in an overall assessment report to be prepared by WMO and UNESCO. This report will be submitted to the UN Committee on Natural Resources. It will guide the preparation of plans and projects for water-resource assessments into the next millennium.

European nations check ozone monitoring equipment

More than 40 scientists spent four weeks checking the measuring equipment which provides the world with vital information on the state of the ozone layer. The Ozone Instrument Intercomparison began on 15 July and was scheduled to finish on 10 August. During this period 18 Dobson ozone spectrophotometers, the commonly used ground-based ozone measuring instrument, located in different countries in Europe, were compared. Arrangements were also made for a 2-day seminar on the operation and maintenance of the Brewer ozone spectrophotometer, a newer model first introduced a few years ago.

The current intercomparison, organized by the World Meteorological Organization (WMO), is the third held in Arosa, Switzerland, at the kind invitation of the Swiss Meteorological Institute. Intercomparisons are organized in different regions of the world at three- to four-yearly intervals.

Measurements of the ozone layer began more than 35 years ago. Observations taken with the Dobson equipment are the mainstay of the WMO's Global Ozone Observing System. Today, more than 140 ground-based ozone stations, supplemented by satellites, constitute the backbone of the system. Some 60 WMO Members operate these stations and hundreds of scientists are involved in manning them.

Books received

The listing of books under this heading does not preclude a review in the Meteorological Magazine at a later date.

Principles of air pollution meteorology, by T.J. Lyons and W.D. Scott (London, Belhaven Press, 1990) has an emphasis on industrial emissions but the methods described can be applied generally. The pollutant effects of the principal chemical compounds are also discussed.

The dawn of massively parallel processing in meteorology, edited by G.-R. Hoffman and D.K. Mareis (Berlin, Heidelberg, New York, London, Paris, Tokyo, Hong Kong, Springer-Verlag, 1990) contains the proceedings of the third workshop on this topic held at the European Centre for Medium-range Weather Forecasts (ECMWF). It includes documentation of the advent of such systems and experience in their operational use.

Organic chemistry of the earth's atmosphere, by V.A. Isidorov (Berlin, Heidelberg, New York, London, Paris, Tokyo, Hong Kong, Springer-Verlag, 1990) summarizes the multidisciplinary data on sources and transformations of organic components in the atmosphere. Methods of atmospheric microimpurity analysis and models of time-dimensional distribution are included.

Asymptotic modelling of atmospheric flows, by R. Zeytounian (Berlin, Heidelberg, New York, London, Paris, Tokyo, Hong Kong, Springer-Verlag, 1990) aims to obtain asymptotic models using singular perturbation techniques from fluid mechanics. For meteorological applications filtering to eliminate local interference phenomena is introduced.

Satellite photographs — 13 September 1990 at 1130 UTC

Images from the $6.7\text{ }\mu\text{m}$ water-vapour channel on Meteosat often show distinctive moist (white therefore cold) and dry (black therefore warm) bands that can be related to surface analyses and upper-tropospheric flow patterns. The images are essentially portraying the integrated water-vapour content of a deep layer from 300 mb to near 800 mb, but with a peak contribution from around 400 mb. A real impression of fluid flow can be gained especially when images are viewed on movie-loops. Forecasters can use the images to fine-tune upper-air analyses, with water-vapour images having an important advantage over the $10\text{--}12\text{ }\mu\text{m}$ infra-red channels since zones of high or low moisture have spatial continuity that may not be apparent on the concurrent infra-red image if cloud is not present.

In the water-vapour panorama covering the Atlantic and western Europe in Fig. 1 the boundary between moist and dry air at A is clearly related to the position of the 300 mb jet axis (bold arrowed line). This relation still holds at B although not as clearly defined. The marked dry tongue C south of Iceland is associated with a strong south-westerly jet. The low in this region (the surface analysis is superimposed on the infra-red image in Fig. 2) deepened rapidly during the following 24 hours. The band of moisture associated with the frontal system connected to this low can be traced well south into the subtropics, appearing to be linked with the spiralling outflow from hurricane 'Isidore' (I). Areas of deep convection that have transported moisture up into an otherwise dry upper atmosphere can be seen at D.

A.J. Waters

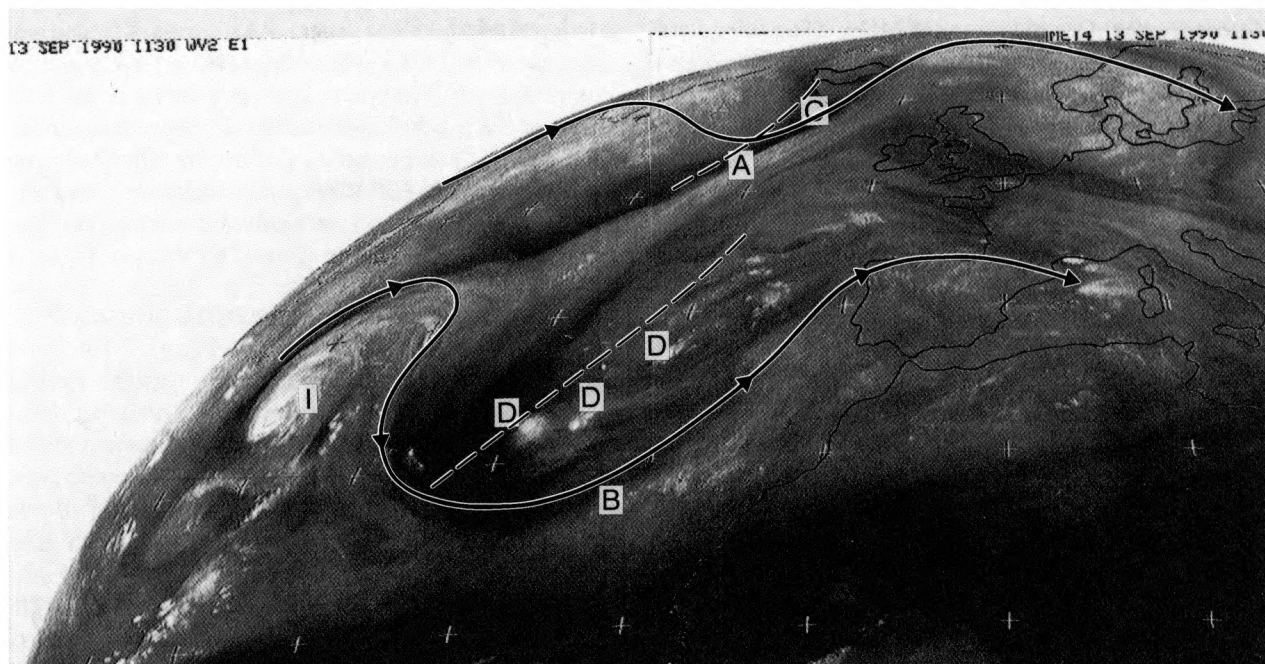


Figure 1. Meteosat water-vapour image at 1130 UTC on 13 September 1990 with the 300 mb jet axis (bold arrowed line) and the 300 mb trough axes (dashed lines) superimposed. Other areas marked are A, the moist-dry boundary layer in the Atlantic; B, as A but near the Azores; C, the dry tongue near Iceland; D, an area of mid-Atlantic deep convection; I, hurricane 'Isidore'.

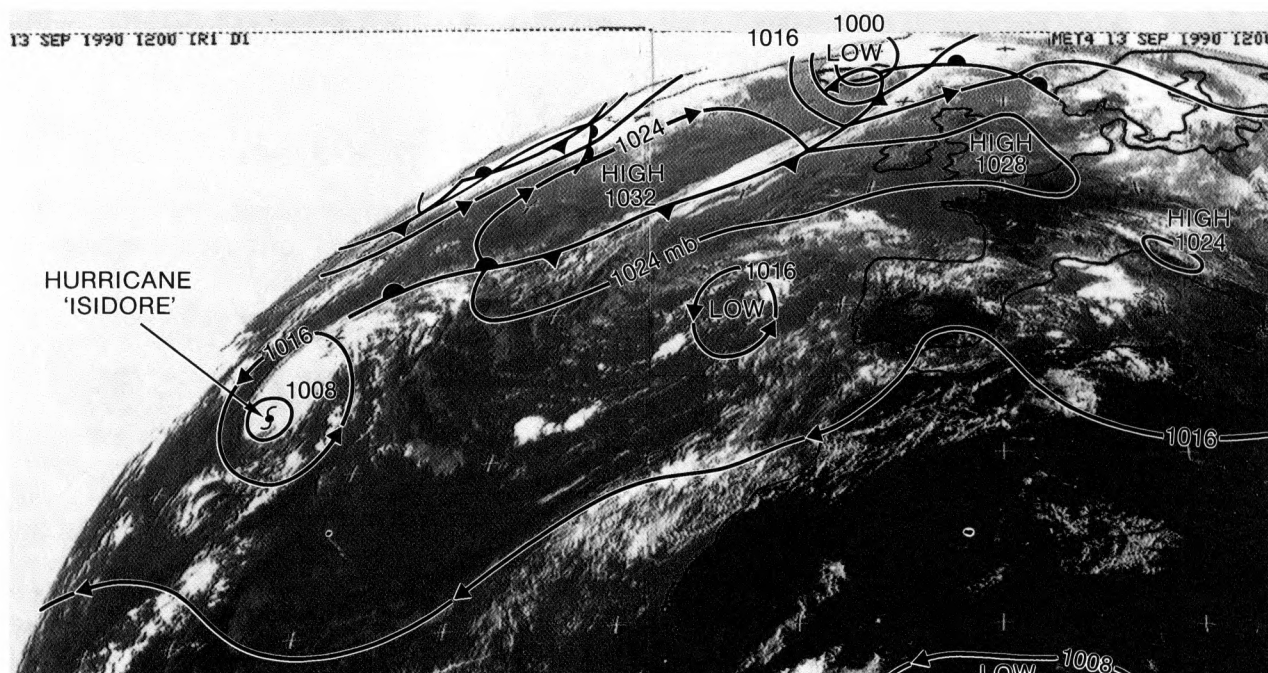


Figure 2. Meteosat infra-red image at 1200 UTC on 13 September 1990 with surface analysis superimposed.

GUIDE TO AUTHORS

Content

Articles on all aspects of meteorology are welcomed, particularly those which describe results of research in applied meteorology or the development of practical forecasting techniques.

Preparation and submission of articles

Articles, which must be in English, should be typed, double-spaced with wide margins, on one side only of A4-size paper. Tables, references and figure captions should be typed separately. Spelling should conform to the preferred spelling in the *Concise Oxford Dictionary* (latest edition). Articles prepared on floppy disk (Compucorp or IBM-compatible) can be labour-saving, but only a print-out should be submitted in the first instance.

References should be made using the Harvard system (author/date) and full details should be given at the end of the text. If a document is unpublished, details must be given of the library where it may be seen. Documents which are not available to enquirers must not be referred to, except by 'personal communication'.

Tables should be numbered consecutively using roman numerals and provided with headings.

Mathematical notation should be written with extreme care. Particular care should be taken to differentiate between Greek letters and Roman letters for which they could be mistaken. Double subscripts and superscripts should be avoided, as they are difficult to typeset and read. Notation should be kept as simple as possible. Guidance is given in BS 1991: Part 1: 1976, and *Quantities, Units and Symbols* published by the Royal Society. SI units, or units approved by the World Meteorological Organization, should be used.

Articles for publication and all other communications for the Editor should be addressed to: The Chief Executive, Meteorological Office, London Road, Bracknell, Berkshire RG12 2SZ and marked 'For Meteorological Magazine'.

Illustrations

Diagrams must be drawn clearly, preferably in ink, and should not contain any unnecessary or irrelevant details. Explanatory text should not appear on the diagram itself but in the caption. Captions should be typed on a separate sheet of paper and should, as far as possible, explain the meanings of the diagrams without the reader having to refer to the text. The sequential numbering should correspond with the sequential referrals in the text.

Sharp monochrome photographs on glossy paper are preferred; colour prints are acceptable but the use of colour is at the Editor's discretion.

Copyright

Authors should identify the holder of the copyright for their work when they first submit contributions.

Free copies

Three free copies of the magazine (one for a book review) are provided for authors of articles published in it. Separate offprints for each article are not provided.

Contributions: It is requested that all communications to the Editor and books for review be addressed to the Chief Executive, Meteorological Office, London Road, Bracknell, Berkshire RG12 2SZ, and marked 'For *Meteorological Magazine*'. Contributors are asked to comply with the guidelines given in the *Guide to authors* which appears on the inside back cover. The responsibility for facts and opinions expressed in the signed articles and letters published in *Meteorological Magazine* rests with their respective authors.

Subscriptions: Annual subscription £30.00 including postage; individual copies £2.70 including postage. Applications for postal subscriptions should be made to HMSO, PO Box 276, London SW8 5DT; subscription enquiries 071-873 8499.

Back numbers: Full-size reprints of Vols 1-75 (1866-1940) are available from Johnson Reprint Co. Ltd, 24-28 Oval Road, London NW1 7DX. Complete volumes of *Meteorological Magazine* commencing with volume 54 are available on microfilm from University Microfilms International, 18 Bedford Row, London WC1R 4EJ. Information on microfiche issues is available from Kraus Microfiche, Rte 100, Milwood, NY 10546, USA.

November 1990

Editor: F.E. Underdown
Editorial Board: R.J. Allam, R. Kershaw, W.H. Moores, P.R.S. Salter

Vol. 119
No. 1420

Contents

	Page
Practical extended-range forecasting using dynamical models.	
S.F. Milton	221
The Interactive Mesoscale Initialization. B.J. Wright and B.W. Golding	234
The autumn of 1989 in the United Kingdom. G.P. Northcott	244
Notes and news	
Water-resource assessment experts meet to develop a strategy for the 1990s	246
European nations check ozone monitoring equipment	246
Books received	247
Satellite photographs — 13 September 1990 at 1130 UTC.	
A.J. Waters	247

ISSN 0026-1149



The

Meteorological Magazine

December 1990

Impact of two observations on a model forecast
Battle of Britain weather
Road slipperiness

DUPLICATE JOURNALS

National Meteorological Library

FitzRoy Road, Exeter, Devon. EX1 3PB



HMSO

Met.O.992 Vol. 119 No. 1421

© Crown copyright 1990.

First published 1990



HMSO publications are available from:

HMSO Publications Centre
(Mail and telephone only)
PO Box 276, London, SW8 5DT
Telephone orders 071-873 9090
General enquiries 071-873 0011
(queuing system in operation for both numbers)

HMSO Bookshops
49 High Holborn, London, WC1V 6HB 071-873 0011 (counter service only)
258 Broad Street, Birmingham, B1 2HE 021-643 3740
Southey House, 33 Wine Street, Bristol, BS1 2BQ (0272) 264306
9-21 Princess Street, Manchester, M60 8AS 061-834 7201
80 Chichester Street, Belfast, BT1 4JY (0232) 238451
71 Lothian Road, Edinburgh, EH3 9AZ 031-228 4181

HMSO's Accredited Agents
(see Yellow Pages)

and through good booksellers



3 8078 0010 2456 3

Met.O.992

THE METEOROLOGICAL MAGAZINE

1990

Volume 119

The responsibility for facts and opinions expressed in the signed articles and letters published in this magazine rests with their respective authors.

Published for the Meteorological Office by HMSO
© *Crown copyright 1990*

INDEX

	<i>Pages</i>
January	1-20
February	21-40
March	41-60
April	61-80
May	81-104
June	105-128

	<i>Pages</i>
July	129-148
August	149-176
September	177-200
October	201-220
November	221-248
December	249-272

American Society for Testing and Materials (ASTM) symposium on Mapping and Geographic Information Systems, San Francisco, California, 21-22 June 1990, 37
Autumn of 1989 in the United Kingdom; G.P. Northcott, 244
Awards

The Rank Prize Fund Award for Opto-electronics, 1989, 18

Bader, M.J., see Sanderson, Golding and Bader

Bailey, J.O., see Barrett, Kidd, Bailey and Collier

Barrett, E.C., Kidd, C., Bailey, J.O. and Collier, C.G.; The Great Storm of 15/16 October 1987: passive microwave evaluations of associated rainfall and marine wind speeds, 177

Blackall, R.M., Brown, R. and Collier, C.G.; Real-time analysis of surface wind gusts using radar data: 25th January 1990, 121

Bogren, J., see Gustavsson and Bogren

Books received, 39, 103, 127, 175, 198, 247, 271

Bradbury, T.A.M.; Links between convection and waves, 112

British Hydrological Society, 59

Brown, R., see Blackall, Brown and Collier

Collier, C.G., see Barrett, Kidd, Bailey and Collier

Collier, C.G., see Blackall, Brown and Collier

Collinge, V.K., see Reviews, 197

Developments in meteorological telecommunications; S.M. Long, 164

European nations check ozone monitoring equipment, 246

Exeter temperatures: monthly means from 1782 to 1839, and from 1985 to 1988; R.F.M. Hay, 33

Extending the reach — the Defence Oceanology International 91 conference and exhibition, 271

First All Africa International Symposium on Lightning, Harare, Zimbabwe, 30 April-4 May 1990, 59

Forecasting the storm of 8 November 1989 — a success for the man-machine mix; A. Woodroffe, 129

Golding, B.W.; The Meteorological Office mesoscale model, 81

Golding, B.W., see Sanderson, Golding and Bader

Golding, B.W., see Wright and Golding

Goodess, C., see Reviews, 172

Great Storm of 15/16 October 1987: passive microwave evaluations of associated rainfall and marine wind speeds; E.C. Barrett, C. Kidd, J.O. Bailey and C.G. Collier, 177

Gustavsson, T. and Bogren, J.; Road slipperiness during warm-air advections, 267

Hammond, J.M.; The strong winds experienced during the late winter of 1989/90 over the United Kingdom: Historical perspectives, 211

Hay, R.F.M.; Exeter temperatures: monthly means from 1782 to 1839, and from 1985 to 1988, 33

Heavy mesoscale snowfall event in northern Germany; W.S. Pike, 187

Heavy snowfall within a mesoscale convergence zone; R.M. Sanderson, B.W. Golding and M.J. Bader, 41

Heming, J.T.; The impact of surface and radiosonde observations from two Atlantic ships on a numerical weather prediction model forecast for the storm of 25 January 1990, 249

Hundredth meeting of the Meteorological Committee, 57

Hydrologists meet to study precipitation measurement problems, 102

Impact of surface and radiosonde observations from two Atlantic ships on a numerical weather prediction model forecast for the storm of 25 January 1990; J.T. Heming, 249

Ingram, W.J., see Reviews, 175

Interactive Mesoscale Initialization; B.J. Wright and B.W. Golding, 234

Jonas, P.R., see Reviews, 38

Kidd, C., see Barrett, Kidd, Bailey and Collier

L.G. Groves Memorial Prizes and Awards for 1988, 171

Links between convection and waves; T.A.M. Bradbury, 112

Lloyd, B.K., see Workshop reports, 19

Lloyd, L.M.; The sea-breeze at Darwin: a climatology, 105
Long, S.M.; Developments in meteorological telecommunications, 164

Lumb, F.E.; Comments on 'A heavy mesoscale snowfall event in northern Germany' by W.S. Pike, *letter*, 271

Lunnon, R.W., see Satellite and/or radar photographs, 60

McCallum, E. and Norris, W.J.T.; The storms of January and February 1990, 201

McGinnigle, J.B.; Numerical weather prediction model performance on instant occlusion developments, 149

Meteorological Office attains Agency status, 147

Meteorological Office mesoscale model; B.W. Golding, 81

Milton, S.F.; Practical extended-range forecasting using dynamical models; 221

Modelling long-term rainfall patterns in north-east England; D. Wheeler, 68

Monk, G.A., see Satellite and/or radar photographs, 20, 40, 78, 104, 128, 148

Mylne, M.F., see Reviews, 77, 173

Naidu, C.V., see Subbaramayya, Vivekananda Babu and Naidu

New Meteorological Office buildings at Bracknell, 102

Norris, W.J.T., see McCallum and Norris

Northcott, G.P.; The autumn of 1989 in the United Kingdom, 244

The Meteorological Magazine

December 1990
Vol. 119 No. 1421

551.509.52:551.507.2:551.508.822

The impact of surface and radiosonde observations from two Atlantic ships on a numerical weather prediction model forecast for the storm of 25 January 1990

J.T. Heming

Meteorological Office, Bracknell

Summary

At 1200 UTC on 24 January two Atlantic ships, positioned near the centre of a developing depression, reported surface and upper-air observations. In the next 24 hours the depression deepened explosively and caused much damage as it crossed the United Kingdom. The impact of these ships' data on a forecast from a numerical weather prediction model is examined with particular reference to the storm's development.

1. Introduction

The storm of 25 January 1990 tracked across the United Kingdom causing extensive damage and loss of life throughout a wide area (McCallum 1990). The depression reached its greatest intensity during the late afternoon, having earlier crossed southern Scotland. As a result, most of England and Wales experienced severe gale-force winds at times throughout the day and in some coastal areas winds reached storm force.

During the late afternoon and early evening of 24 January the Meteorological Office issued warnings to the military and civilian population of the severity of the impending storm and of possible structural damage. Numerical weather prediction (NWP) models are a vital source of guidance to forecasters and on this occasion they had products from the 1200 UTC run of the limited-area (fine-mesh) model, which covers Europe and the North Atlantic, and the 1200 UTC run of the global model.

The UK operational global and fine-mesh models each have 15 levels and a grid spacing of approximately 150 km and 75 km respectively. The principles of the

15-level model are described by Gadd (1985). The global model produces a 5-day forecast every 12 hours from 0000 and 1200 UTC starting analyses, whereas the fine-mesh model produces operational forecasts for the period up to 36 hours ahead and is run on a 12-hour cycle as follows:

0000/1200 UTC Global analysis interpolated onto the fine-mesh grid
0300/1500 UTC Assimilation
0600/1800 UTC Intermediate assimilation and 36-hour forecast
0600/1800 UTC Update assimilation including data received after the intermediate assimilation
0900/2100 UTC Assimilation
1200/0000 UTC Assimilation and 36-hour forecast.

Each fine-mesh assimilation accepts data within a time window of ± 90 minutes from the nominal analysis time. The assimilation method, known as the 'Analysis

Correction Scheme', gives each observation its maximum weight in the assimilation at its validity time. It is described in more detail by Lorenc *et al.* (1991).

The facility exists for forecasters to reject or correct observations before each run of the global and fine-mesh models. It is also possible for them to create 'bogus' observations for use in data-sparse areas or as support for existing observations. Such manual action is known as Intervention and is part of the continual monitoring of data in the Central Forecasting Office (CFO) at Bracknell.

This article assesses the impact of the surface and upper-air observations from two Atlantic ships on the fine-mesh forecast from data time 1200 UTC on 24 January. Both ships were positioned close to the developing depression, one just to the north and the other just to the south, at the time of the 1200 UTC analysis.

2. Summary of the life of the storm

On Tuesday 23 January the depression was part of a complex shallow area of low pressure moving slowly eastwards off the eastern seaboard of North America. Late in the day, the associated baroclinic wave engaged a short-wave upper trough and the depression began to deepen. During Wednesday 24 January the depression centre deepened by 37 mb in 24 hours and moved rapidly east in a powerful westerly jet, nearing the west coast of Ireland by the end of the day. On 25 January the storm tracked across Ireland and southern Scotland reaching its greatest intensity over the North Sea of 949 mb at approximately 1600 UTC. Most of England and Wales experienced severe gales. Mean wind speeds were in excess of 50 kn in many coastal areas and gusts in excess of 90 kn were reported. Fig. 1 is an analysis of the observed mean-sea-level pressure valid at 1200 UTC on 25 January. During 26 January the storm continued

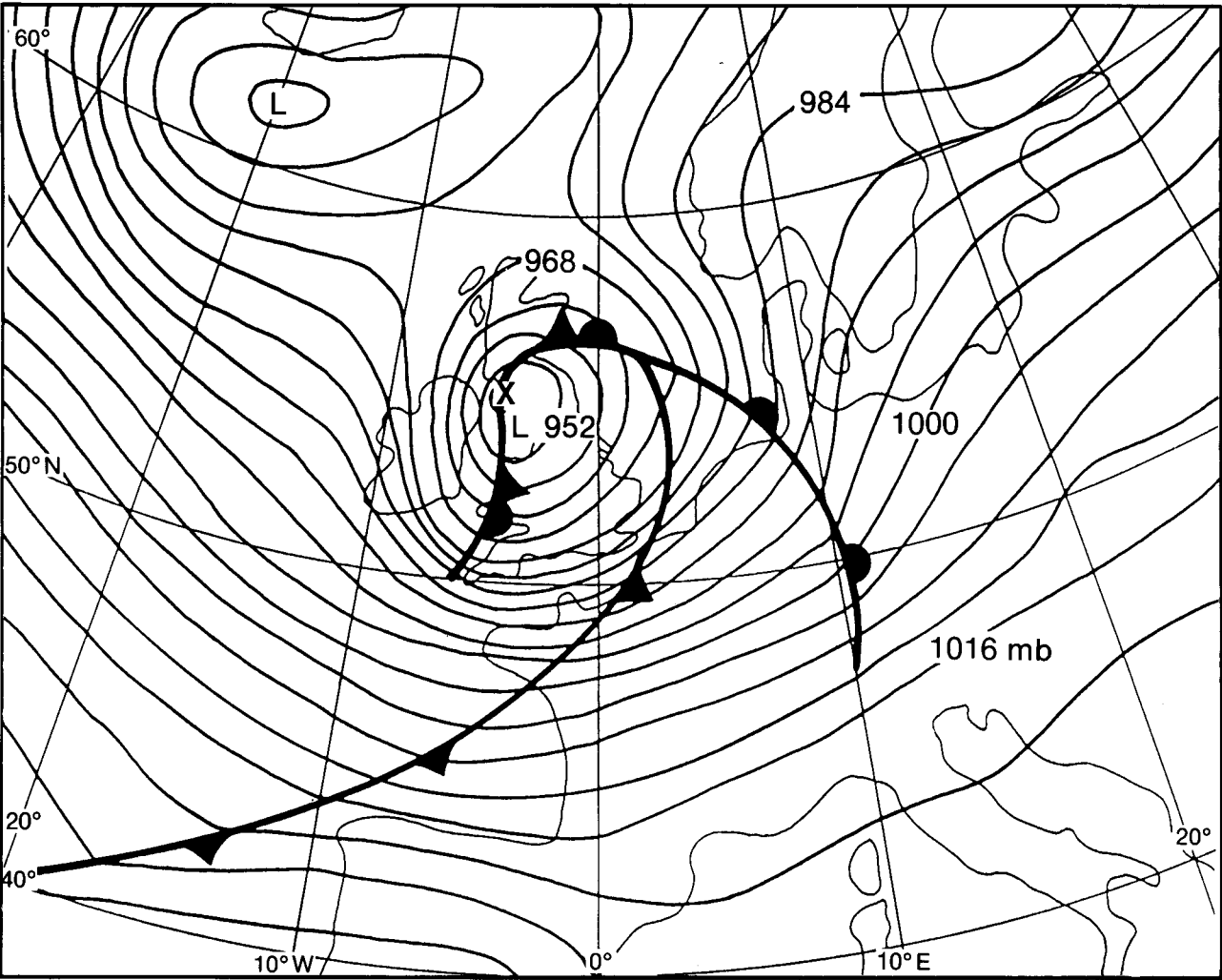


Figure 1. Analysis of observed mean-sea-level pressure for 1200 UTC on 25 January 1990.

its rapid eastward movement towards Denmark, then filled as it moved across southern Scandinavia.

3. Numerical model guidance for the storm

3.1 Forecasts before 1200 UTC on 24 January

The UK operational global model provided good guidance beyond 4 days ahead as to the development of the Great Storm of October 1987 (Gadd and Morris 1988). On this occasion the global model gave guidance during the 5 days preceding the storm which indicated that a depression would cross the United Kingdom on 25 January. Of particular interest is the 108-hour forecast from the 0000 UTC global analysis on the 21st verifying at 1200 UTC on the 25th (Fig. 2) which was used to warn of stormy conditions on Thursday the 25th in the farming forecast on television presented on the previous Sunday (21st). Mean surface winds of up to 50 kn were forecast in the approaches to south-west Ireland by this particular run.

The earliest operational fine-mesh forecast valid for 1200 UTC on the 25th, when the storm was expected at its greatest intensity, was the 36-hour forecast from data time 0000 UTC on the 24th (Fig. 3). This forecast runs the depression across the south of England as a relatively shallow wave, and both the depth of the depression and the strength of the surface winds are greatly underpredicted. Indeed, this forecast is considerably inferior to the global-model forecast 3 days earlier.

Operational fine-mesh forecasts from intermediate analyses at 0600 and 1800 UTC are available for guidance in the CFO. On this occasion the 30-hour forecast from the 0600 UTC analysis on the 24th showed a marked improvement on the previous forecast as can be seen in Fig. 4. The depression has a distinct centre and is some 8 mb deeper than in the previous forecast. This improvement was found to be due to a wide range of observational data valid between 0130 and 0730 UTC, and also the use of the 0000 UTC global analysis as a start field for the subsequent 12-hour fine-mesh assimilation cycle (Heming 1990). However, this forecast is still poor when compared with the verifying analysis for 1200 UTC on the 25th (Fig. 1).

3.2 Data in the North Atlantic

At 1200 UTC on the 24th there were many merchant ships in the North Atlantic reporting surface observations. There were three Ocean Weather Ships (OWSs) operating at the time, reporting surface and upper-air observations. Two of these, situated at stations Charlie and Lima (hereafter referred to as OWS C and OWS L), were positioned to the west of the United Kingdom. Upper-air reports were also received from some merchant ships which are part of the Automated Shipborne Aerological Program. These are commonly known as ASAPs. Fig. 5 shows the distribution of marine surface and upper-air observations at 1200 UTC

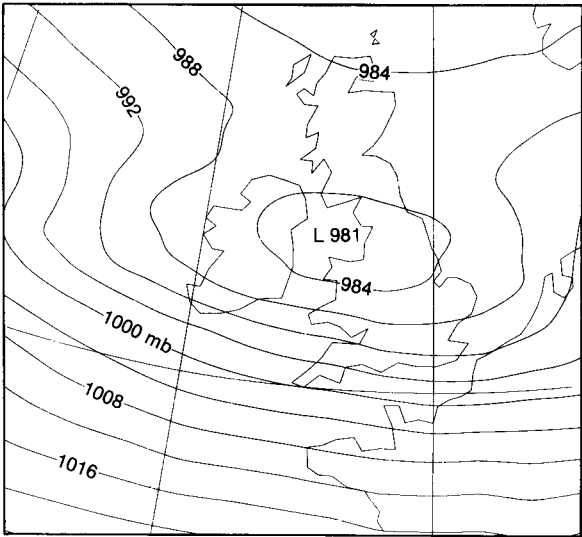


Figure 2. T+108 global model forecast of mean-sea-level pressure. Data time 0000 UTC on 21 January 1990.

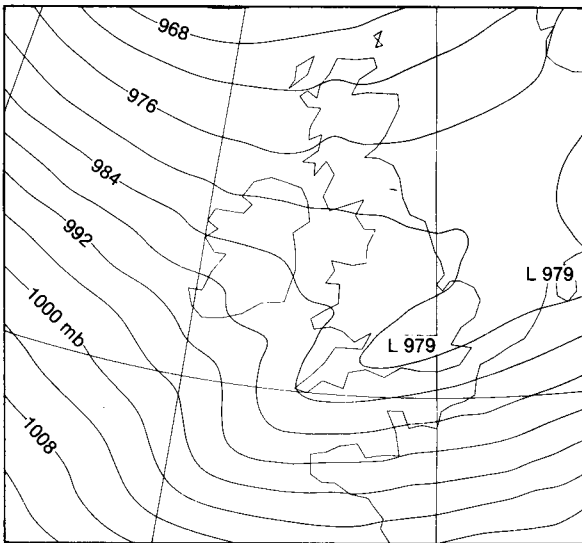


Figure 3. T+36 operational fine-mesh forecast of mean-sea-level pressure. Data time 0000 UTC on 24 January 1990.

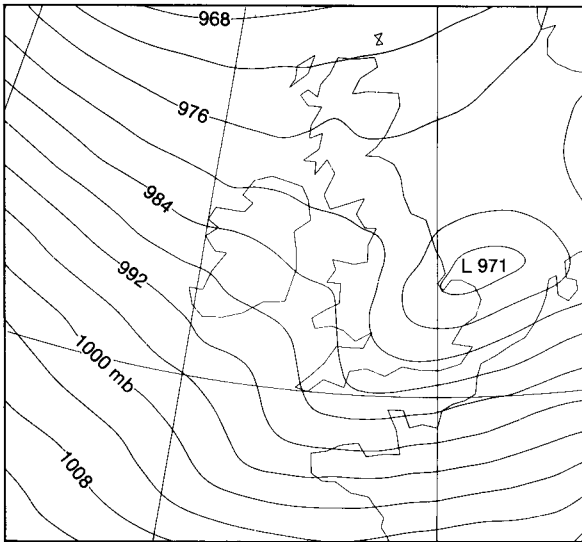


Figure 4. T+30 operational fine-mesh forecast of mean-sea-level pressure. Data time 0600 UTC on 24 January 1990.

on the 24th. Upper-air data in the North Atlantic were fairly sparse and just two ships were reporting upper-air observations in the vicinity of the developing storm. These were OWS C positioned just to the north of the depression and the ASAP with call-sign ONDA positioned just to the south. In addition to surface and upper-air data from ships, data was also available from aircraft, drifting buoys and land stations within the

fine-mesh area at 1200 UTC. No satellite sounding data were received by the 1355 UTC fine-mesh data cut-off.

For use in NWP models, radiosonde observations, at standard as well as special levels, are used to calculate mean values about each of the model levels as described by Atkins and Woodage (1985). The layer-mean values for the two ships' reports are shown in Tables I and II together with the background field values. The back-

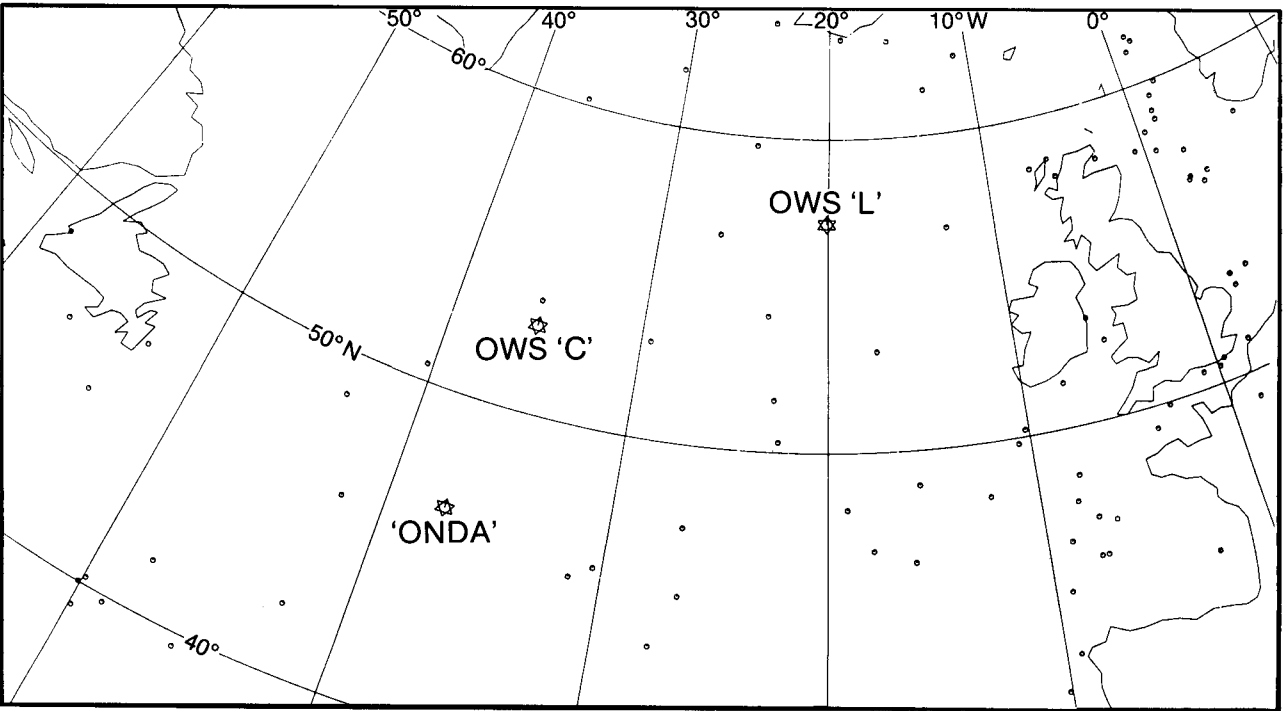


Figure 5. Distribution of surface and upper-air marine observations at 1200 UTC on 24 January 1990 marked by circles and stars respectively.

Table I. SYNOP (1200 UTC) and TEMP (1100 UTC) observations (Obs) from OWS C (52.7°N, 35.5°W) on 24 January 1990 as used by the model, with values of the background (Back) given alongside. Vertical averaging has been performed on the full observed profile to give values at each model level.

	Level (mb)	MSLP Back	Temperature (°C)		Wind (° / kn)	
			Obs	Back	Obs	Back
SYNOP	1001.3	1003.4	1.3	3.0	300/ 17	292/ 17
TEMP	1000.0	1003.6	1.2	2.9	295/ 14	292/ 17
	997.0		1.0	2.7	294/ 14	292/ 17
	974.9		-0.8	1.0	293/ 14	292/ 17
	934.8		-4.2	-2.3	292/ 15	294/ 18
	869.8		-10.0	-6.9	287/ 16	306/ 15
	789.9		-16.2	-12.6	271/ 20	299/ 14
	690.1		-18.3	-19.8	255/ 31	277/ 22
	590.1		-24.1	-24.0	249/ 49	263/ 36
	490.1		-33.9	-33.4	245/ 75	255/ 50
	390.0		-43.5	-44.1	238/ 117	247/ 66
	309.9		-54.0	-53.4	240/ 122	246/ 82
	249.8		-58.7	-55.7	244/ 114	247/ 93
	189.7		-59.6	-55.0	246/ 99	250/ 100
	124.8		-66.6	-62.0	250/ 92	255/ 106
	66.0		—	—	/	/
	25.0		—	—	/	/

Table II. As Table 1, but observations from ONDA (46.5° N, 37.4° W) on 24 January 1990

	Level (mb)	MSLP Back	Temperature (°C)		Wind (° /kn)	
			Obs	Back	Obs	Back
SYNOP	997.1	1006.2	14.1	11.7	230/ 50	261/ 33
TEMP	996.0	1006.7	13.2	11.1	230/ 51	265/ 34
	993.0		13.0	10.9	230/ 51	265/ 35
	971.0		11.7	9.1	234/ 53	266/ 38
	931.1		9.3	6.1	240/ 57	267/ 44
	866.3		5.3	2.1	247/ 66	267/ 49
	786.8		2.3	-1.9	247/ 75	264/ 55
	687.4		-1.8	-8.3	245/ 85	258/ 65
	587.8		-9.9	-12.2	245/ 95	253/ 85
	488.1		—	—	245/ 106	249/ 102
	388.4		—	—	/	/
	308.8		—	—	/	/
	249.0		—	—	/	/
	189.2		—	—	/	/
	124.5		—	—	/	/
	65.7		—	—	/	/
	24.9		—	—	/	/

ground field is the fine-mesh model's 3-hour forecast from the 0900 UTC analysis. Large differences between observations and background (increments) indicate large errors in the short-term forecasts at these locations and the data assimilation has to make large adjustments to the numerical field to accommodate the observation. In this case the surface pressure observation from both the SYNOP (surface observation) and TEMP (upper-air observation) from ONDA were flagged by the model's quality control and consequently not used in the fine-mesh model's data assimilation stage. The observations were flagged because these observations were substantially different from the background values and there were no nearby observations which supported such large increments. The 'Intervention' forecaster on duty at the time perceived these model rejections to be incorrect, since the depression was deepening more rapidly than the background field suggested, and so provided 'bogus' surface and upper-air data in the vicinity of ONDA to support the ship's observation and prevent it being rejected in the 1200 UTC run of the global model that followed. The principles of model data quality control and use of 'bogus' data are described by Atkins and Woodage (1985). It must also be noted that the ascent from OWS C reached the 100 mb level whereas that from ONDA only reached the 400 mb level.

3.3 Fine-mesh analyses with and without OWS C and ONDA

Figs 6(a) and 6(b) show the operational fine-mesh analyses at 1200 UTC on the 24th with the positions of OWS C and ONDA marked. A rerun of the model analysis without the TEMP and SYNOP reports from OWS C and ONDA show some small differences from

the operational versions of the mean-sea-level pressure, 500 mb height and 1000–500 mb thickness fields (Figs 7(a) to 7(c)).

Despite the surface pressure observations from ONDA being rejected by the model, Fig. 7(a) shows that the effect of the remaining unflagged part of the TEMP report, together with OWS C's report, was to reinforce the western centre of the low pressure complex, although by not nearly as much as the surface observations indicated.

Fig. 7(b) shows differences between the two 500 mb height fields. The positive values to the south of the depression and negative to the north clearly indicate a tightening of the contour gradient in this region as a direct result of the inclusion of the two ships' data. Fig. 7(c) shows the differences between the two 1000–500 mb thickness fields. The negative values to the north and the positive values of even greater magnitude to the south indicate both a tightening of the thermal gradient and an amplification of the thermal ridge associated with the depression. The analysis differences for both these fields are consistent with the temperature and wind-speed increments for the observations from both OWS C and ONDA. Tables I and II show that the temperature increments from OWS C's ascent are nearly all negative and those from ONDA are all positive. The ascent from OWS C also shows a strong jet around 300 mb — absent in the background values — and positive wind-speed increments of up to 51 kn between the 700 and 250 mb levels.

3.4 Fine-mesh forecasts with and without OWS C and ONDA

Fig. 8(a) shows the operational fine-mesh 24-hour mean-sea-level pressure forecast verifying at 1200 UTC

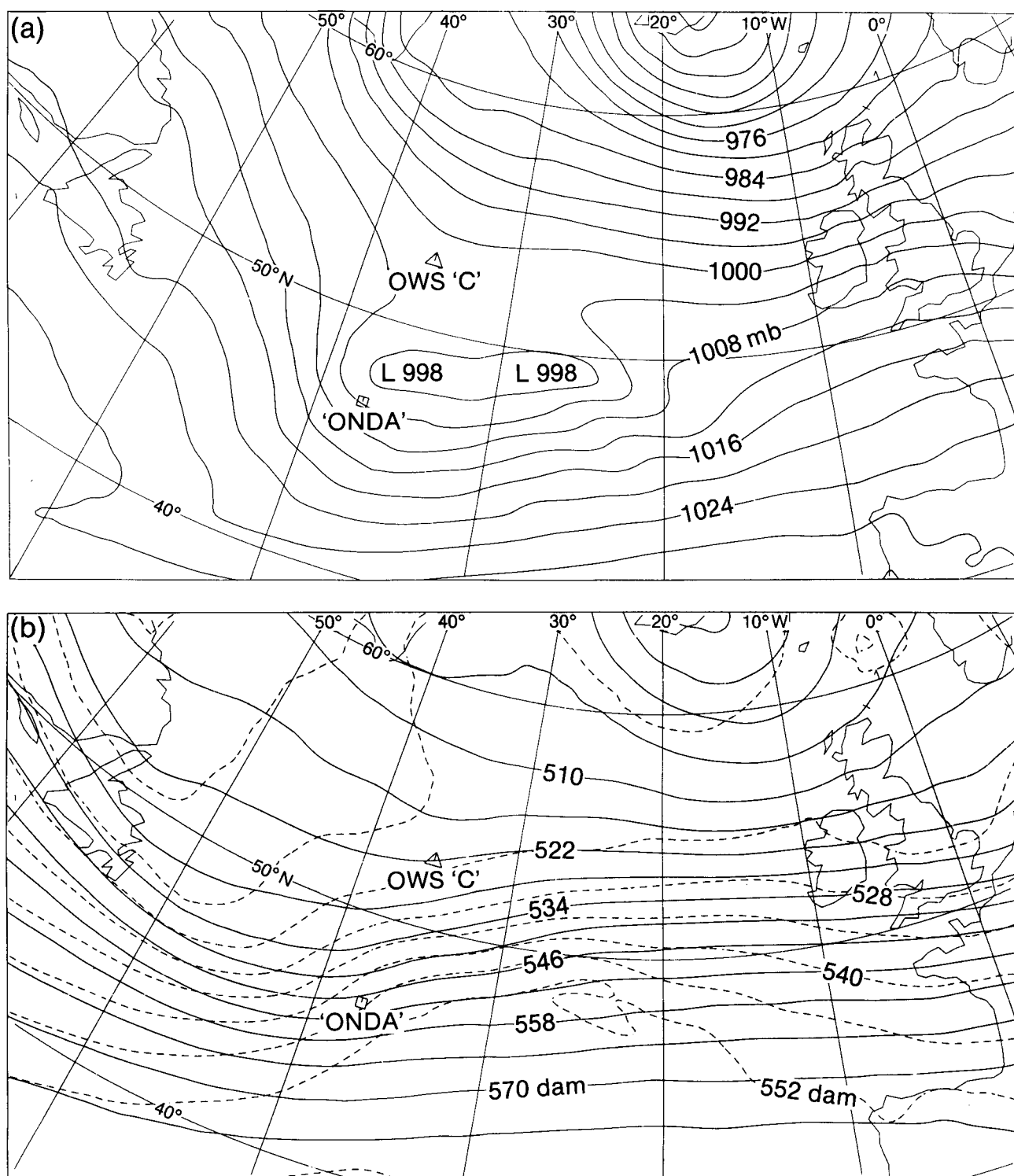


Figure 6. T+00 operational fine-mesh analysis for 1200 UTC on 24 January 1990, (a) mean-sea-level pressure, and (b) 500 mb height (full lines) and 1000–500 mb thickness (dashed lines).

on the 25th. Fig. 8(b) is the corresponding forecast from the analysis without observations from OWS C and ONDA. Whilst the operational forecast was still some 9 mb too shallow and too far south in its forecast of the low centre when compared with the verifying analysis (Fig. 1), it is clear that the inclusion of the two ships has had a beneficial impact. The forecast run from the analysis without OWS C and ONDA features a low

centre which is much broader and 8 mb shallower than the operational forecast.

Figs 9(a) and 9(b) show the 24-hour forecasts from the operational and rerun analyses respectively for the 500 mb height and 1000–500 mb thickness fields. The operational forecast features a significant amplification of the thermal ridge and the upper trough when compared with the forecast from the analysis without

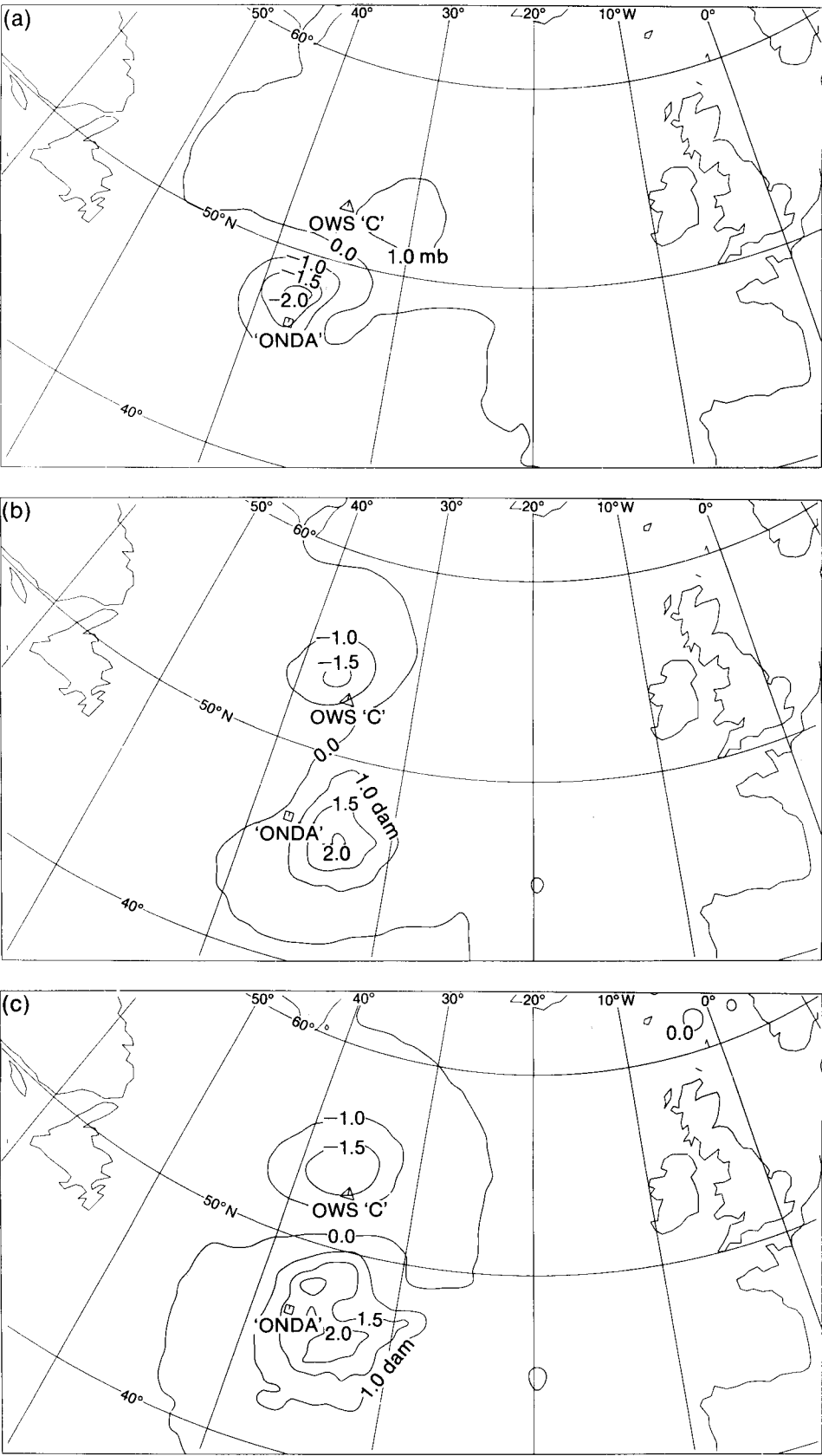


Figure 7. Difference between fine-mesh operational analysis and analysis without OWS C and ONDA for 1200 UTC on 24 January 1990, (a) mean-sea-level pressure, (b) 500 mb height, and (c) 1000–500 mb thickness. Positions of the two ships marked.

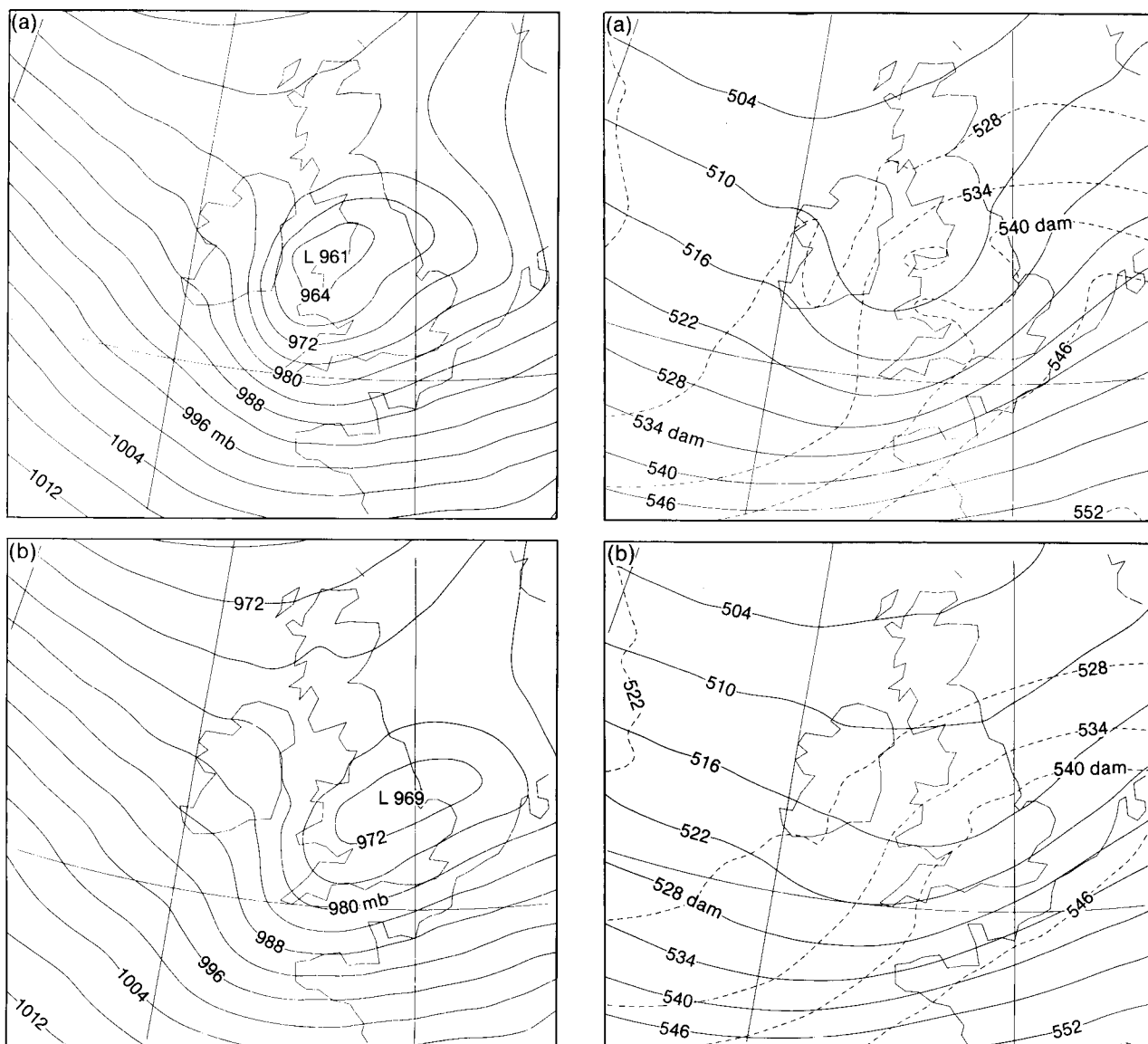


Figure 8. T+24 fine-mesh forecast of mean-sea-level pressure. Data time 1200 UTC on 24 January 1990, (a) operational run, and (b) rerun without OWS C and ONDA.

OWS C and ONDA. This is clearly a much better forecast on inspection of the verifying model analysis (Fig. 9(c)).

To determine the impact of each ship separately, forecasts were run from an analysis without OWS C (Fig. 10(a)) and an analysis without ONDA (Fig. 10(b)). It appears that in both cases there is a similar impact on the depth of the low, although the observation from ONDA has the effect of correctly placing the centre about 200 km further west in the forecast. It is interesting to note that the sum of the individual impacts of OWS C (5 mb deepening) and ONDA (3 mb deepening and a 200 km movement of the centre) is equal to their combined impact (8 mb deepening and 200 km movement of the centre).

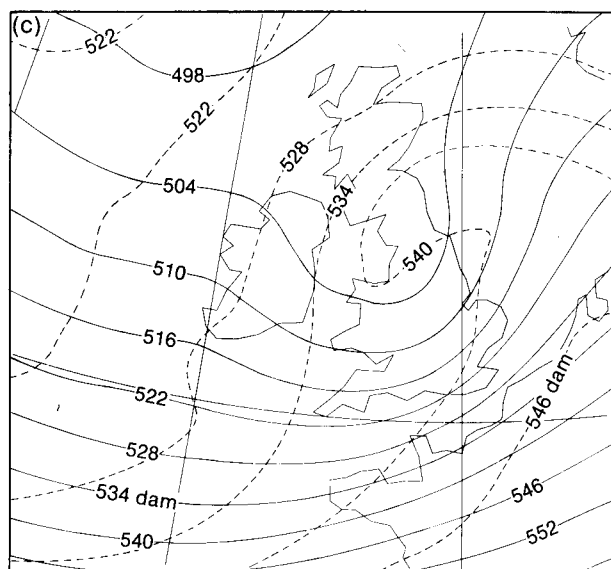


Figure 9. T+24 fine-mesh forecast of 500 mb height (full lines) and 1000-500 mb thickness (dashed lines). Data time 1200 UTC on 24 January 1990, (a) operational run, (b) rerun without OWS C and ONDA, and (c) verifying analysis for 1200 UTC on 25 January 1990.

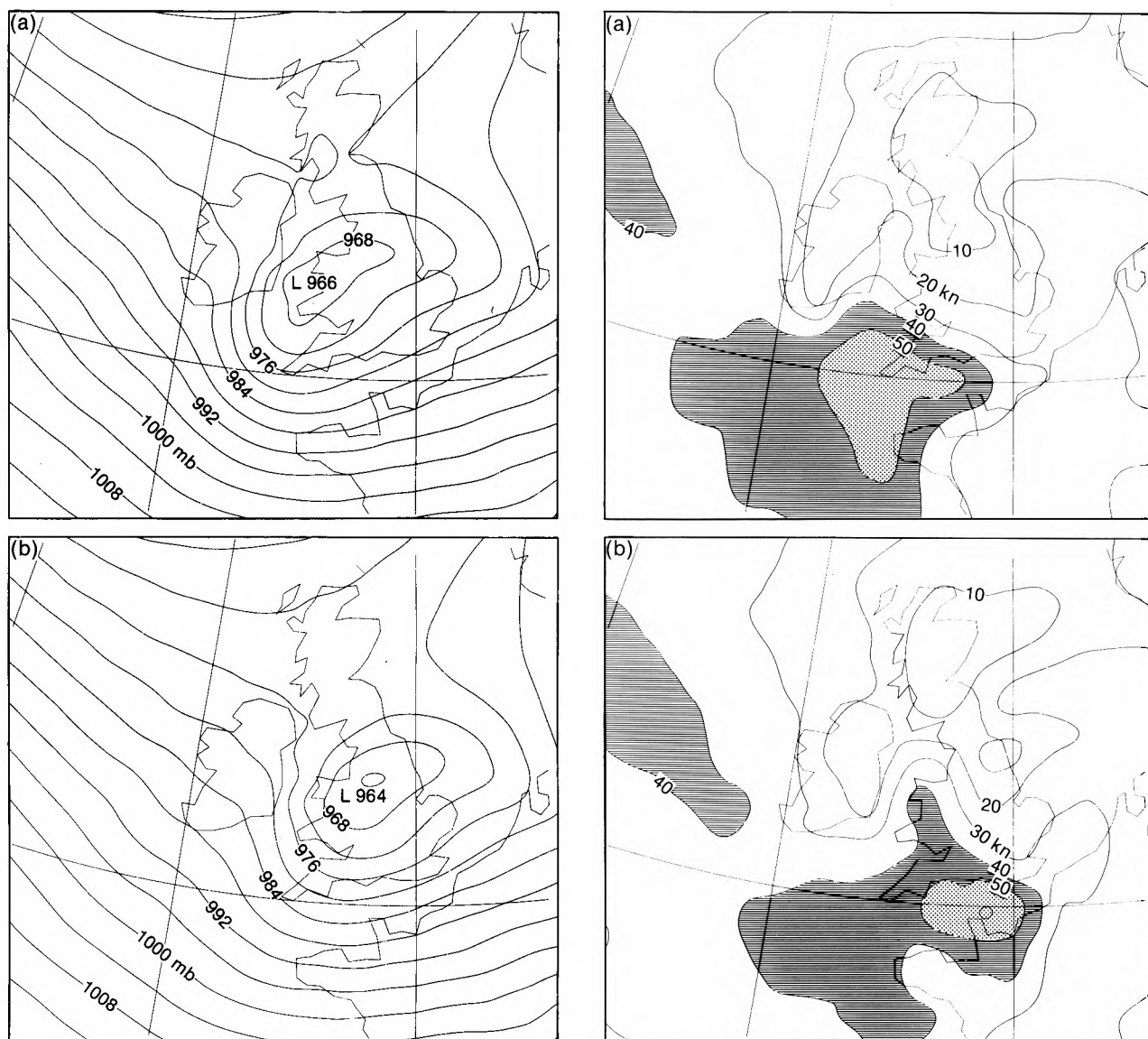


Figure 10. T+24 fine-mesh forecast of mean-sea-level pressure. Data time 1200 UTC on 24 January 1990, (a) rerun without OWS C only, and (b) rerun without ONDA only.

4. Surface winds over the United Kingdom

Of greatest importance to the civilian population was the surface wind which was at its most severe between 0900 and 1800 UTC on the 25th. Figs 11(a) to 11(c) show the operational forecasts of surface (10 m) wind speed verifying at 1200, 1500 and 1800 UTC on the 25th. These forecasts indicate mean wind speeds in excess of 40 kn over a wide area initially across the south-west of the United Kingdom, and later extending east and north along the English Channel and into Wales, eventually into the North Sea and the Low Countries by 1800 UTC. The forecast area of winds in excess of 50 kn moves up the Channel and just extends into south coast areas of England.

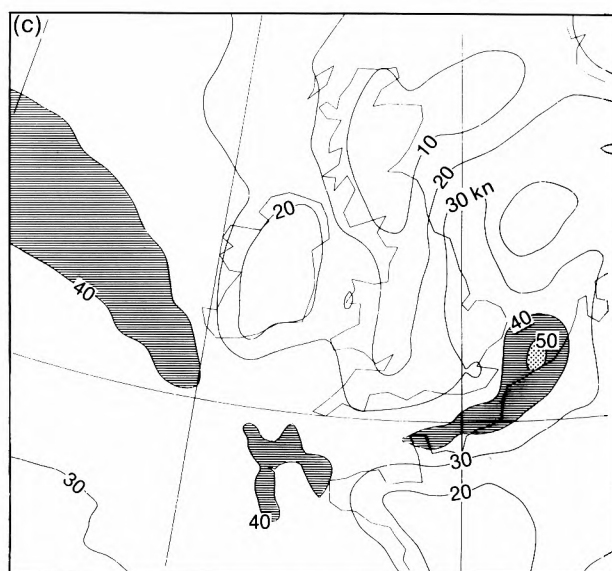


Figure 11. Operational fine-mesh forecast of surface (10 m) wind speed. Data time 1200 UTC on 24 January 1990, (a) T+24, (b) T+27, and (c) T+30. Hatched areas highlight the progression of the maximum winds.

At 1200 UTC the operational 24-hour forecast verifies well with observations of mean wind speed in Wales and the south and west of England. These range from 20 kn in North Wales to 60 kn along the south coast. Further east the observations are up to 15 kn stronger than the forecast. At 1500 UTC the operational forecast predicts the position of the strongest winds with a high degree of accuracy. In the English Channel a maximum wind strength of 59 kn was forecast and winds of up to 65 kn were reported. The forecast wind speeds are generally less than 15 kn different from the observations, with a few observations up to 25 kn different. Fig. 12 shows the reports of mean wind speeds and maximum gusts reported at 1500 UTC. At 1800 UTC the wind speeds forecast across the south and east of the United Kingdom verify well against the observations. However, the forecast for the north of England was not so good; several observations were more than 25 kn stronger than the forecast values.

The forecasts from the analysis without OWS C and ONDA (Figs 13(a)–13(c)) show a much smaller area of winds in excess of 40 kn than obtained from the operational forecast; the maxima of 50 kn at some fine-mesh grid points in the English Channel at 1500 UTC compare with 59 kn operationally. These are clearly

inferior to the operational forecasts (Figs 11(a)–11(c)).

Some of the strongest winds experienced in the United Kingdom on 25 January 1990 were at Aberporth in south-west Wales between 1400 and 1500 UTC where a mean speed of 65 kn and a maximum gust of 93 kn were reported. The operational 27-hour forecast verifying at 1500 UTC (Fig. 11(b)) indicates mean wind speeds of up to 45 kn at fine-mesh grid points nearest and to the north and east of Aberporth. The forecast wind speeds at these grid points from the analysis without the two ships are up to 25 kn less. Even the forecast from the analysis just without ONDA predicts winds some 20 kn less than the operational forecast in places.

5. Conclusions

It has been found that the improvement between the fine-mesh forecast from 0000 UTC on the 24 January 1990, which featured a shallow complex depression of 979 mb positioned in the area of East Anglia (Fig. 3), and the forecast from 1200 UTC on the 24th, which predicted a much deeper low of 961 mb positioned over North Wales (Fig. 8(a)), was due to the combined effects of many observation types in the area of development in the North Atlantic over the intervening 12 hours

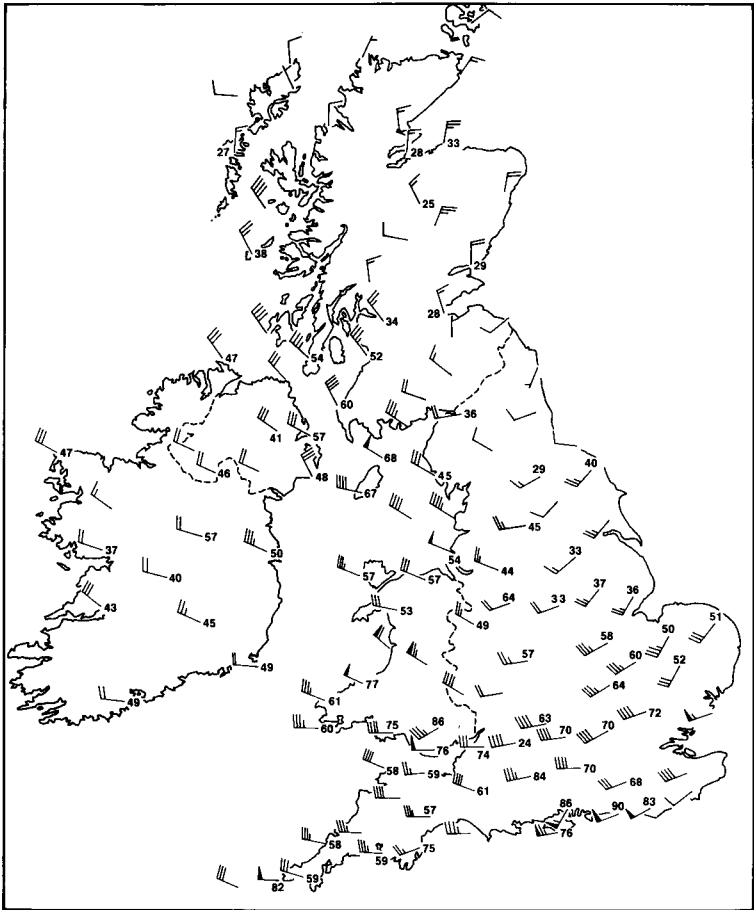


Figure 12. Observed 10-minute mean wind speeds (traditional wind arrows) and maximum gusts (if over 25 kn) within the previous hour at 1500 UTC on 25 January 1990.

(Heming 1990). The impact of two particular observations at 1200 UTC, the reports of OWS C and ONDA, has been studied in detail and it is shown that they make the largest single contribution to the improvement of the forecast. This clearly shows the value of upper-air data in the North Atlantic. Another important point to be made is that, on this occasion, small differences produced in the analysis, as a result of the inclusion of these two ships' observations, amplified to produce considerably larger differences in the 24-hour forecast.

Operationally, the forecaster was supplied with very good guidance from the fine-mesh model during the afternoon of 24 January with regard to the impending wind strengths, and warnings were issued to the military and civilian population in good time. The fine-mesh model is widely acclaimed in its ability to handle intense low-pressure systems owing to its high horizontal resolution. However, a limiting factor on forecast accuracy is the sparsity of observations in the North Atlantic, where most of the UK's weather systems originate. The problem is made worse in the fine-mesh model by its early data cut-off, mentioned earlier. It was found that the lack of observations in an area of explosive cyclogenesis was a contributory cause of the poor fine-mesh forecast of the Great Storm of October 1987. The inclusion of aircraft observations valid just outside the fine-mesh data time window made a vast improvement to the forecast (Lorenc *et al.* 1988). On 24 January 1990, two ships were positioned near one such area of low pressure in the North Atlantic that was set to deepen explosively. Their observations, received before the fine-mesh data cut-off, made a significant contribution to the quality of model guidance by providing vertical profiles of the atmosphere at a critical stage in the development of the severe storm which crossed the United Kingdom the following day.

Acknowledgements

The author would like to thank C.D. Hall for his assistance during this investigation and the preparation of this article, and E. McCallum for comments on a rough draft of the paper.

References

Atkins, M.J. and Woodage, M.J., 1985: Observations and data assimilation. *Meteorol Mag*, 114, 227-233.
 Gadd, A.J., 1985: The 15-level weather prediction model. *Meteorol Mag*, 114, 222-226.
 Gadd, A.J. and Morris, R.M., 1988: Guidance available at Bracknell for the storm of 15/16 October 1987, and the forecasters' conclusion at the time. *Meteorol Mag*, 117, 110-117.
 Heming, J.T., 1990: The impact of data on fine-mesh forecasts for the storm of January 25th 1990. (Unpublished, copy available in the National Meteorological Library, Bracknell.)
 Lorenc, A.C., Bell, R.S., Davies, T. and Shutts, G.J., 1988: Numerical forecast studies of the October 1987 storm over southern England. *Meteorol Mag*, 117, 118-130.
 Lorenc, A.C., Bell, R.S. and MacPherson, B., (1991): The new Meteorological Office data assimilation scheme. (To be published in *QJR Meteorol Soc.*)
 McCallum, E., 1990: The Burns' Day storm, 25 January 1990. *Weather*, 45, 166-173.

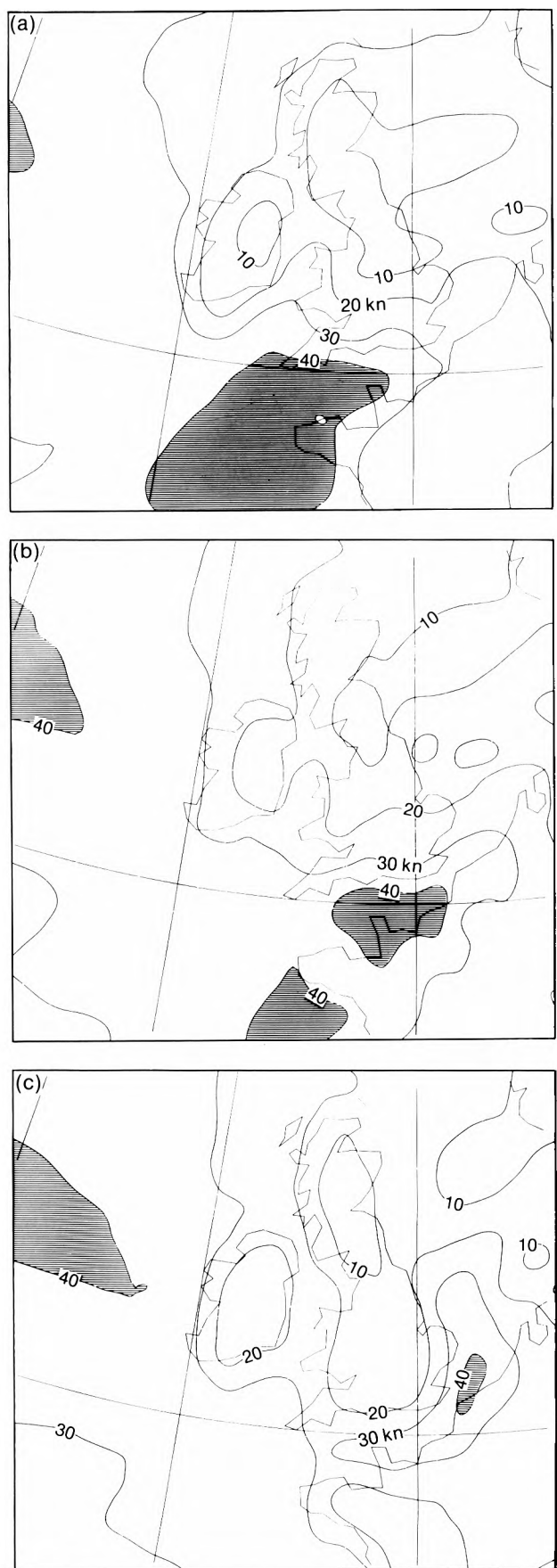


Figure 13. Fine-mesh forecast of surface (10 m) wind speed from analysis without OWSC and ONDA. Data time 1200 UTC on 24 January 1990, (a) T+24, (b) T+27, and (c) T+30.

The Battle of Britain — a meteorological retrospect

R.J. Ogden
Camberley, Surrey

Summary

To mark the 50th anniversary of the Battle of Britain, the meteorological services in RAF Fighter Command at that time are described, and reference is made to some of the difficulties faced and overcome. The weather during the core of the Battle is also analysed and is related to the pattern of air attacks.

1. The organizational background

In the tactical planning developed during the late 1930s under Air Chief Marshal Dowding, the first Air Officer Commanding-in-Chief of the newly formed RAF Fighter Command, it was envisaged that day-to-day control of fighter operations would rest at Group rather than Command level (Wright 1969). It was therefore decided that in the event of war, independent forecasting offices should be established at each Group Headquarters (HQ). The limited range of pre-war fighter aircraft such as the Gloster Gladiator originally suggested that airfield meteorological offices were unnecessary, but by the spring of 1939, with the emergence of the Hurricane and Spitfire that would be controlled in the air from Sector Operations rooms, it was recognized that small meteorological units should also be located at the key airfields designated as Sector HQ. These policies were implemented at the beginning of September 1939 or as soon as practicable thereafter; for information purposes a small office was also set up at HQ Fighter Command, but forecasting facilities were not introduced there until after the Battle of Britain when tactical considerations had changed (Air Ministry 1954).

Independent forecast offices were thus established at HQ 11 Group (Uxbridge), HQ 12 Group (Hucknall, later Watnall) and HQ 13 Group (Newcastle) at the outbreak of war, and at HQ 10 Group (Rudloe Manor, Wiltshire) shortly after that new Group was introduced in July 1940 to take over responsibility for south-west England and South Wales, leaving 11 Group to concentrate on the major task of covering London and the south-east. These four offices were all manned 24 hours a day by teams of civilian forecasters and civilian assistants. The forecasters provided meteorological advice for the air staff and controllers, and also originated all the forecasts needed by the Sector and other fighter airfields in the Group area; 11 Group additionally looked after HQ Fighter Command at Bentley Priory, Stanmore. Another important function was to prepare upper-wind and temperature forecasts for Army anti-aircraft (AA) batteries; for obvious

reasons, the activities of AA Command had to be very closely co-ordinated with those of RAF Fighter Command, and to ensure this an Army AA liaison officer was always on duty with the Group controllers. The Group meteorological offices were also, to an extent, involved with RAF Balloon Command; although at this stage of the war small meteorological units were attached to most of the main balloon barrages (Air Ministry 1954), their resources were limited and Group forecasters provided advisory and back-up support. The assistants at the Group offices did all the chart and tephigram plotting and also the tedious 6-hourly ballistic wind computations for the AA batteries. In addition to many minor tasks including decoding observations for display in the operations room, they also operated the meteorological teleprinter switchboard, assembling the hourly Group collectives, passing these to Dunstable and sending routine area forecasts to all the outstations.

The Sector airfields in 11 Group were at Kenley, Biggin Hill, Hornchurch, Debden, North Weald, Northolt and Tangmere; each of these had its own subsidiary meteorological office as did RAF Hendon, RAF Manston (where there were also at first some dependent forecasters) and the pre-war civil airfields of Croydon, Heston, Lympne and Shoreham that had been taken over as RAF stations. Just outside the 11 Group area there were Sector meteorological offices at Middle Wallop (10 Group) and at Duxford and Coltishall (12 Group) (see Fig. 1). The staff complement at the outstation offices varied between three and five so that there was always at least one person on duty throughout the 24 hours. In most cases, the Officer-in-charge was a member of the pre-war Observer grade, his staff being a mixture of Observers, A IIIs, Royal Air Force Volunteer Reserve (RAFVR) (Met) airmen and a few Meteorological Assistants; although there were many Women's Auxiliary Air Force (WAAF) plotters in the Group and Sector operations rooms, the trade of meteorologist was not introduced in the WAAF until September 1941, so that there were no meteorological

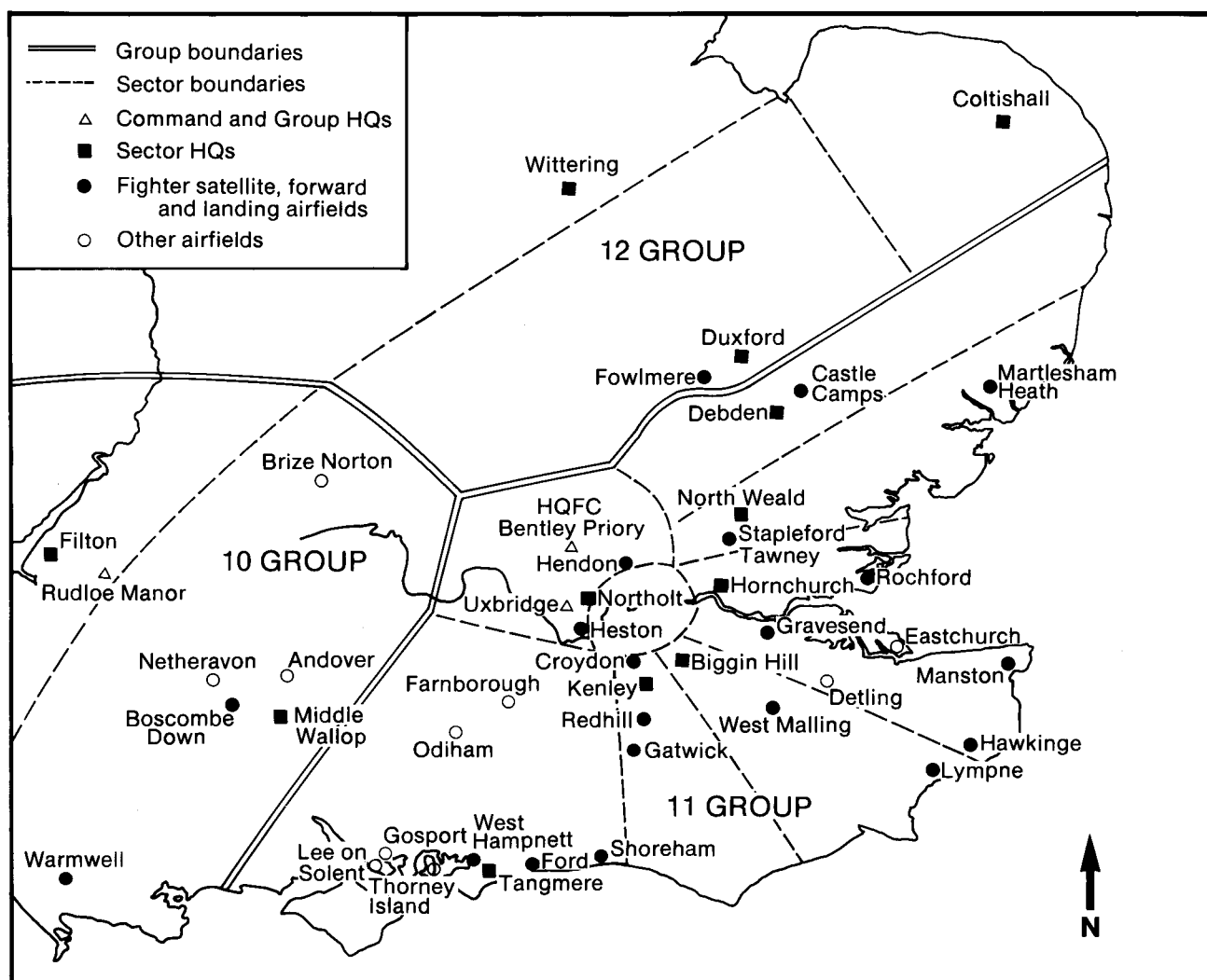


Figure 1. Group and Sector boundaries, Headquarters and airfields at the time of the Battle of Britain.

‘WAAFs’ during the Battle of Britain (Ogden 1986). The primary function of the outstation assistants was to observe the weather continuously, paying particular attention to surface wind, cloud and visibility; nephoscope observations also had to be made whenever suitable medium or high cloud was visible at those stations issued with this equipment. An important supplementary task was that of pilot-balloon work. In 11 Group, each outstation was allocated several specified times during the 24 hours at which ascents had to be made, cloud permitting, unless some overriding operational requirement turned up. In this way the Group forecasters were normally assured of a regular supply of upper-wind information to help with their aviation and AA forecasts. Secondly, the assistants maintained an up-to-date supply of decoded actual weather reports in the Sector operations rooms. Thirdly, the controllers and the Squadrons were provided with whatever forecasts they needed, these being obtained from the Group office. It was made clear to all concerned that the staff at the Sector offices were not themselves forecasters but that within this well understood constraint were always willing to help with

advice and interpretation, and a good local rapport was normally established on that basis.

2. The Battle period and the relevant meteorological factors

Although the precise dates of the Battle of Britain are not clear cut, there is a general consensus that it started on 10 July 1940 and ran until around the end of October, by which time the large-scale daylight operations by bombers and fighters ceased, leaving for the most part just the night blitz. Within this 16-week period there were four distinct phases. At first the attacks were directed primarily at coastal convoys in the English Channel and the North Sea, with some raids also on south coast ports from Falmouth to Dover. The second phase, launched on 13 August, concentrated on the fighter airfields, both on the coast and well inland, and on the radar stations. On 7 September, in a switch of tactics, London and the Thames Estuary became the primary target by day, with heavy night raids as well. This phase continued until 30 September, with some attacks on Bristol, Plymouth and Southampton and at night on Merseyside. The final phase of fighter-bomber

incursions in smaller formations, often at quite high levels, lasted through the month of October (Wright 1969). It was the second and third phases, i.e. from 13 August to 30 September, that formed the core of the Battle and which had the maximum impact on the meteorological services.

Hazy blue skies with many condensation trails are enduring folk memories of the Battle of Britain, but the records show a very mixed bag of weather; there were certainly some fine warm days, but equally others that were dull, cool, wet and much more typical of mid-autumn. Weather factors played a part on the operations of both sides, but in several ways the *Luftwaffe* (German Air Force) was affected more than the RAF.

The *Luftwaffe* bombers then operating had neither airborne radar nor radio-beam position-fixing techniques such as the *Knickerbein* system which only became operational in their night bombing raids in late October (Saward 1985). Navigation was, therefore, a matter of dead reckoning (for which a knowledge of upper winds is vital) plus map reading. Moreover, as during the attacks on airfields and radar stations, the *Luftwaffe* orders specifically forbade indiscriminate bombing (Price 1988); success was contingent on visual identification of specific targets. For low-level daylight operations this was not too difficult given a reasonable cloud base and adequate visibility, though summer haze was sometimes a problem. However, after the heavy losses of Ju87 (*Stuka*) dive bombers in some of the early airfield attacks, that type of aircraft was largely withdrawn following the raids on 18 August (Saward 1985); admittedly, some low-level raids were also made by other aircraft, notably at Croydon, Kenley, Manston and Biggin Hill, but these were only a small minority of the total. The more general altitude for the *Luftwaffe* bombers was well above 10 000 feet, and for them the amount of cloud below that level was crucial, both for navigation and target identification; many attacks were broken up, misdirected or aborted because of cloud. The height and thickness of medium-cloud layers over northern France and the English Channel must also have had an effect on the practicability of assembling large formations of bombers and fighters. The forecasting of stratocumulus and cumulus cloud is notoriously difficult even today, but the British meteorologists had a significant advantage in that throughout almost the whole Battle period, the flow was predominantly from the quadrant between west and north, so that the fairly close network of hourly reporting stations over the British Isles gave them a much clearer picture of what was going on. The *Luftwaffe* had to rely on what their meteorologists could infer from the general weather situation, amplified by reports from their high-level weather and photographic reconnaissance aircraft that were regularly sent to England, and the Fw200 aircraft that operated long-range weather reconnaissance flights west of Ireland. Another problem was that the

endurance of fighters at high level could be reduced by strong northerly winds.

By comparison, the meteorological requirements of the RAF fighter pilots and their controllers were modest. Acceptable weather was needed for take-off and landing, and all concerned required a general picture of the height, thickness and amount of the various cloud layers, together with warning of cumulonimbus cloud with severe up- or downdraughts. The upper airflow was also relevant, and if strong especially so for controllers when vectoring aircraft onto targets. Given that the weather was good enough for the *Luftwaffe* to mount a daylight raid during most of the Battle, the RAF fighters could almost certainly operate without serious meteorological problems, but difficulties did arise in October due to fog and low cloud at airfields.

Clearly neither side in the conflict wished to advertise their location by producing contrails, and during the Bomber Command offensive later in the war the prediction of contrails became a matter of considerable operational significance. But it was probably the introduction and widespread use of aircraft like the Hurricane, Spitfire and Messerschmitt with service ceilings above 30 000 feet that first alerted meteorologists to the problem; predictive techniques did not emerge until after the Battle (Parker 1942).

3. The fighter airfields under attack, 13 August to 6 September 1940

The German *Adlerangriff* (Eagle attack), designed to destroy the RAF as a prerequisite for invasion, was originally scheduled to start on 10 August, but the previous night it was postponed pending the arrival of better weather. By 12 August there was an anticyclone near the Isles of Scilly and the German meteorologists predicted good clear weather on the following day, which was then confirmed as *Adler Tag* (Eagle Day). With no more than small patches of stratocumulus over south-east England on 12 August, the *Luftwaffe* had no meteorological problems in sending preliminary raids to Lympne (twice), Manston, Hawkinge and six radar stations as well as maintaining pressure on ports and convoys. Cloud cleared that night, but by the morning of 13 August a weak warm front moving round the flank of the anticyclone had already reached Bristol, bringing thickening layers of cloud as the day wore on. The opening of the assault was disorganized by this cloud and some aircraft returned to base. Targets, including Odiham and Farnborough, could not be found and the bombers attacking Middle Wallop were so disoriented by cloud and harried by fighters that they dropped their bombs over three counties. Attacks were pressed home at Eastchurch and Detling and at Southampton but, thanks to the weather, it was a poor start to the campaign. During 14 August the anticyclone receded further and a weak cold front moved south-east across the country, followed by a more active one with rain, so that *Luftwaffe* activity was much reduced; Manston was

hit again, also Middle Wallop, although the latter was attacked in the belief that it was Netheravon. The second cold front moved right across Britain during the night, leaving behind it a light north-westerly flow with generally clear weather in all eastern districts. This set the stage for the major onslaught of 15 August, the most wide-ranging series of attacks during the entire Battle.

The opening raids on Lympne, Hawkinge and the nearby radar stations were mounted in the late morning, that at Lympne being particularly severe. A pencilled note inside the cover of their *Observations Register* reads 'The enclosure was hit by a few bombs and everything destroyed except the rain-gauges and a minimum thermometer! Also, three 500 lb bombs landed just in front of the office making it unusable. During this period, which was the heaviest in the blitz, observations were only missed on occasions when bombs, AA or machine-gun fire made it very unsafe to venture in the open'. This dedicated approach seems to have been characteristic of the fighter airfield outstations. In surviving Registers, there are several examples of complete entries throughout periods when severe attack is known to have been taking place.

After the attack at Lympne, the meteorological office was re-established in the private house of the Observer, not far away. The Air Ministry agreed to pay rental for a room, the RAF installed a tie-line to Hawkinge to restore communication with 11 Group, replacement instruments were sent and when the airfield again became fully operational less than 48 hours after the raid, hourly reports recommenced (Meteorological Office 1941). Within an hour of this opening sally, bombers came from Norway to attack targets in north-east England; the formations were broken up by RAF fighters and failed to reach targets at Usworth, Linton and Dishforth, but did bomb Driffield. Shortly after this, the third attack was again in south-east England; among other airfields Manston was hit once more. Some three hours later the fourth raid came towards Portland and Portsmouth and yet again to Middle Wallop, but the meteorological office there appears to have been undamaged in all the raids.

The final raid of the day, in the early evening, appears to have been aimed at Biggin Hill and Kenley, but the force was split up by RAF fighters and had to seek alternative targets, one of these being West Malling which was bombed from high altitude. The other was Croydon which received a low-level attack by Me110s that caused many casualties and considerable damage, especially to a large and very busy aircraft maintenance hangar, a radio component works and the Bourjois perfume factory which were all on the industrial estate bordering the apron. The terminal building was also hit, but the meteorological office, just beneath the famous control tower, received only minor damage. However, in a second raid three days later, by stragglers from one of the Kenley attacks, the terminal was again hit, this time more seriously and the following morning the RAF

decided the building was structurally unsafe and must be evacuated. Fortunately during July the RAF had requisitioned several private houses to the south of the airfield and one of these was allocated to the meteorological office. That afternoon and evening (19 August) all the records and instruments were moved and reinstalled and full observations recommenced the following morning (Meteorological Office 1941 and Cluett *et al.* 1984).

During 16 August there was a ridge across England with no more than broken cumulus and stratocumulus at 3000 feet. Manston and West Malling were again hit and there were heavy attacks on Brize Norton (then a training and maintenance airfield) and Tangmere. At Brize Norton, the office had to be evacuated because of delayed-action bombs outside, and was located for a time in a wooden hut pending repairs. At Tangmere there were broken windows, a hole in the roof and damage to instruments in the enclosure. Thereafter, the staff worked in the Watch Office after dark, but continued in their own office by day (Meteorological Office 1941). August 17 was a perfect summer day, but there was little *Luftwaffe* activity, no doubt while they prepared for the series of raids being planned for the morrow.

August 18 dawned fine and clear and the *Luftwaffe* opened the proceedings with both high- and low-level attacks at Kenley and Biggin Hill. First to arrive at Kenley was a formation of Do17s at very low level which caused many casualties, a great deal of damage and also fires, whose smoke was slow to clear in the stable light westerly flow, making the visibility so poor that the high-level force of Ju88s could not identify the airfield and diverted to an alternative target at West Malling instead. Some of the Do17s at high level did bomb the airfield, but others moved on to bomb Croydon instead (Price 1988). One of the many buildings destroyed at Kenley was Station Headquarters where the meteorological office had been located earlier in the year, but presumably it had been moved by this time to Sector Operations which were not hit though most of their communications were cut. The Kenley *Observation Registers* for this period have unfortunately not survived. By contrast, surprisingly little damage was caused at Biggin Hill on this occasion.

The second series of attacks on 18 August, also in good weather, were at Thorney Island, Ford and Gosport. Ford in particular was severely damaged and was abandoned by the Fleet Air Arm, being subsequently taken over by the RAF as another satellite field for the Tangmere Sector. Meteorologically, it was the third attack of the day that was the most interesting. During the morning a warm front had moved east across Scotland, followed by a cold front which moved steadily south-east as the ridge ahead of it gave way. By early afternoon, cloud and rain had spread as far south as North Wales and Lincolnshire, and three hours later, as the bombers were crossing the Essex and Kent coasts *en*

route for Hornchurch and North Weald, both medium and low cloud layers were spreading into south-east England from the west; indeed it was raining in London by early evening. The raiders realized that there was no chance of being able to identify their primary targets from a high level and both attacks were aborted. The aircraft then returned to base, some of them bombing secondary targets in Shoeburyness and at Manston *en route* (Price 1988).

The cold front had moved down into the English Channel by the following morning, leaving behind a cloudy, showery airstream as a fairly deep depression moved south-east from Shetland to southern Sweden, introducing a strong north-northwesterly flow. A local teenager visiting Croydon Airport for some aircraft spotting recorded in his diary that 22 August was 'a very grey, dull typical autumn day and hardly weather to suite the *Luftwaffe*' (Cluett *et al.* 1984). This was a very fair assessment as, apart from a few minor raids at airfields, there was very little *Luftwaffe* activity for the five days from 19 to 23 August inclusive. However, the rise of pressure behind a cold front which cleared the south coast during the afternoon of 23 August soon damped out showers and next morning it was clear.

Manston was raided twice on 24 August, making a total of 9 raids in 13 days. After the second attack, hardly any buildings remained intact, all communications were cut and delayed-action bombs littered the airfield. Fighter Command decided that Manston should, for the time being, be evacuated and reduced to an emergency only airfield. Bombs had fallen within 20 yards of the meteorological office from which, in view of the RAF change of status, the dependent forecasters were withdrawn; alternative premises for an observing office were found on the other side of the airfield. There were also raids that afternoon at both North Weald and Hornchurch, but apart from the interruption of power supplies the meteorological offices appear to have been unaffected (Meteorological Office 1941).

August 25 also started clear over south-east England, but during the day medium and low cloud spread in as a weak cold front approached from the north, reaching Norfolk by evening. Warmwell was attacked but *Luftwaffe* activity was curtailed. However, the front became quasi-stationary and then returned northwards for a time, leaving southern England in a westerly on 26 August with little more than patchy cloud at 3000 feet. Raids were directed to Kenley, Biggin Hill, Hornchurch, North Weald and Debden, but the first four of these were broken up by RAF fighters before the targets were reached. Debden was hit, causing both damage and casualties, though not in the meteorological office. After this interlude, the front again moved south, bringing showers right down to the English Channel coast by the evening of 27 August. The same front appears to have restricted *Luftwaffe* activity for two more days, because it remained stationary over the English Channel on 28 August, then returned north on

29 August linked to a warm front over Scotland, and brought stratocumulus at 2000 feet back into south-east England. Although the weather on 28 August was ideal for bombing, *Luftwaffe* flights must have been hampered by cloud to the south, and on 29 August they were no more than fighter sweeps.

On 30 August, however, it was a very different story. The front had at last cleared through into Europe, the cloud dispersing as the pressure rose behind it, and the anticyclone, which since 12 August had been near or well to the south-west of the British Isles, moved east to dominate the English Channel and northern France, later settling over Germany. This introduced the longest spell of fine summer weather during the entire Battle, lasting for 9 days from 30 August to 7 September.

The primary target during this period was Biggin Hill which received 9 attacks in 7 days, the evening raids on both 30 and 31 August being particularly severe. The former wrecked workshops, equipment section, hangars, motor transport section, barracks, dining halls and camp roads. Electricity, gas, water, sewerage and telephone services were all cut and three air raid shelters received direct hits (Ogley 1990). Among those killed were the observer-in-charge, N.A. Roberts, and two RAFVR (Met) Leading Aircraftmen, Buttfeld and Brunning, i.e. three of the four meteorological staff on the strength at the time. The RAF decided that with swift remedial action to restore services, the airfield could remain fully operational, but that all personnel whose presence there was not essential should move away. Three new meteorological staff were immediately posted in as replacements for those killed, and although for a short time they had no office, observations were maintained from a point near the Sector Operations building. But on the evening of 31 August this received a direct hit and an Emergency Operations room was at once set up in an empty shop in Biggin Hill village. The meteorological office was allocated a house on the northern edge of the airfield (Meteorological Office 1941 and Ogley 1990). On 31 August Croydon, Detling, Debden and Hornchurch were also attacked, but the meteorological offices do not seem to have been directly affected on this occasion.

During the first 6 days of September the airfield attacks continued in glorious weather. On 3 September North Weald was severely damaged and the meteorological office was reduced to a total wreck. It was moved to a new position near Sector Operations, and, as the meteorological teleprinter had been badly damaged, RAF Signals staff had to send the observations to Uxbridge (this second location was also wrecked in October and the office then had to move again). On 6 September, three large attacks were directed at the five Sector airfields round London, but all of these were broken up and few of the bombs reached their targets. On the following morning, however, the meteorological staff at Hornchurch had to move their screen to a new location.

4. The location of Fighter Command meteorological offices

At Group HQ, the forecasting offices were established in the Operations blocks which were purpose-built concrete bunkers, well underground; these became known to all who worked in them as 'The Hole'. The original Command policy for the Sector meteorological offices was that they should be housed in the Sector Operations buildings (Air Ministry 1954), but this was not implemented for some time and a more usual location was near the watch office, from which there was a good view across the airfield. Perhaps surprisingly, when the Battle of Britain started, the Sector Operations blocks were usually above ground at one side of the airfield, protected only by blast walls and camouflage netting. Air Chief Marshall Dowding commented that 'it would have been admirable if fine underground installations could have been built, but there simply was not time for that. The system had to be brought into being as quickly as possible, and the best was done in the time available' (Wright 1969). Emergency arrangements were, however, made in case the above-ground locations on the airfields became untenable.

As noted above, when Biggin Hill Operations was hit on 31 August, an immediate move was made to a shop in the village, and when communications to the Operations block at Kenley were cut on 18 August, a similar move was made to a butcher's shop in Caterham High Street, chosen because it was immediately over the main Post Office telephone cable in the area (Price 1988). In these very cramped emergency conditions there was certainly no room for the meteorological offices which normally remained for a time on or alongside the airfields. However, steps were taken as soon as possible to prepare more suitable alternative operations rooms well away from the airfields. In many cases, large buildings were requisitioned and converted; Biggin Hill for example took over a large mansion in Keston Mark (Ogley 1990), Kenley chose the Vicarage in Old Coulsdon, Duxford moved to Sawston Hall and Hornchurch to a building in Romford. In other cases, temporary buildings were erected as at Debden which went to the outskirts of Saffron Walden, and at North Weald which moved to Ongar.

Once these alternative Operations rooms were fully established, in almost all cases the meteorological offices moved to them, and having done so remained there until 1944 when they moved back to the airfields. These relocations of the Sector meteorological offices no doubt brought a feeling of some relief at being less adjacent to primary target areas, but were sometimes rather cramped (Kenley for example was in the butler's pantry). The moves did however bring about the intended close contact and integration of the meteorological work into the activity of the Operations rooms. As a further precaution against any more disasters, emergency alternatives to the alternative Operations rooms were earmarked and the meteorological offices

were invited to make contingency planning for a sudden move if this ever became necessary; in the event it is believed that this never happened. One minor problem that arose from the relocation of the meteorological office well away from the airfield, is that the observations are supposed to refer to the latter. When the two sites were at similar heights within a mile or so of each other (as at Kenley), the differences were not normally significant, but when the sites were several miles apart and at quite different altitudes (as at Debden), the observer had to telephone the Duty Pilot in the Watch Office and accept his values for cloud and visibility whenever there was a chance that these were significantly different.

5. London becomes the major target, 7–30 September 1940

On 7 September the weather was still clear in the south-east and heavy attacks were made throughout that day and the following night. But this was the end of the 9-day spell of summer weather, as by next morning a cold front had brought rain as far south as East Anglia; some morning raids were sent to fighter airfields, but to little effect. With the switch of objectives from specific targets like airfields and radar stations to a very large area such as London, the need for precision in navigation and target identification diminished, so that cloud amounts below the aircraft were from here on of less account. On the following day, 9 September, a very showery northerly airstream at first restricted *Luftwaffe* activity; but convection quickly died down as the ridge collapsed ahead of the next frontal system, and afternoon raids were sent to London. The fronts crossed the country during 10 September bringing thick cloud, rain and a largely peaceful day. It was mainly clear in the north-northwesterly behind the cold front on 11 September, allowing raids to London, Southampton and Portsmouth, and that night to London and Merseyside. But then the weather intervened once more, another warm front brought rain across the country on 12 September, with cloud bases down to 500 feet in the warm sector, and the cold-frontal clearance the next day was only partial. Interestingly, around midday on 13 September, radio monitoring of *Luftwaffe* transmissions reported that an enemy aircraft over Kent was sending messages that cloud was only 7/10 at 1500 metres and that attack was possible. Some raids were indeed mounted that afternoon, but the reconnaissance was over-optimistic and they achieved little. The cloud and showers persisted through the next day as well, and the true clearance did not develop until the early hours of 15 September, when a more active cold front with rain had moved through to the continent.

September 15 has come to be known as Battle of Britain Day, largely because of heavy *Luftwaffe* losses in a series of raids on London on a similar scale to those of 7 September. The weather was by no means clear, but with only half cover or less of cumulus cloud it proved to

be the best day for over a week. Next morning an active warm front was sweeping rain across the country, and when the cold front cleared around midday on 17 September, it left behind a very strong westerly circulation round the parent low near Shetland which had a central pressure as low as 970 mb. The gradient had eased by 18 September and with broken cloud some raids were mounted both day and night, but by then upper cloud ahead of yet another frontal system was spreading in to give a wet day on 19 September, the rain intensifying that night as a wave developed on the cold front near the Isles of Scilly and moved up the English Channel. Despite these most unfavourable conditions, some *Luftwaffe* bombers did penetrate to London shortly before the wave arrived in south-east England, and a parachute mine descended on Heston, then the home of the Photographic Reconnaissance Unit, which damaged the roof and windows of the first floor meteorological office there. A few days earlier, an AA shell had fallen through the roof and floor of this office before exploding in the room underneath. All this damage was repaired in due course, but the offices at Heston, Hendon and Northolt, being on the fringe of the London area, were all damaged further during October and November, though fortunately without serious effects on the meteorological work.

The next 3 days, 20–22 September, were dominated by a second wave on the cold front moving up the English Channel, followed by an active frontal system associated with the next depression in the family which tracked from west of Ireland to north Scotland; *Luftwaffe* activity on these days was confined to reconnaissance and a few fighter sweeps. However, the cold frontal clearance during the late evening of 22 September was sharp, and by midnight, in the words of Lord Alanbrooke 'London was like Dante's Inferno', as indeed it was on the following night as well. No doubt because of the commitment to these two very heavy night raids, the *Luftwaffe* mounted no more than fighter sweeps during daylight hours on 23 September, despite only well broken cumulus at 3000 feet. Around this time a large anticyclone became established north-west of Ireland, and for the rest of the month the flow over Britain was predominantly from the north, with troughs bringing cloudy spells and showers, especially on 28 and 29 September. During this period, cloud was more broken in the west, and for the most part raids were

concentrated on Portsmouth, Southampton, Bristol and Plymouth. Some bombers did reach London on 27, 28 and again on 30 September, but this last occasion proved to be the final large-scale engagement of the daylight Battle.

6. Conclusions

Two facts emerge clearly from this meteorological look back at the Battle of Britain. Firstly, there is no doubt that the pattern of German air attacks was considerably affected by the weather. Secondly, the civilian meteorological staff played a full part alongside their RAF colleagues at Groups, Sectors and other airfields, and despite very exacting working conditions the service was maintained.

Acknowledgements

My thanks are due to Maurice Crewe, Meteorological Office Librarian, who drew my attention to the invaluable M O 7 damage report of 1941 which is in his care; also to Michael Wood, Meteorological Office Archivist, who gave me free access to the 6-hourly synoptic charts of the Battle period, also to the station histories and all the surviving *Observation Registers* of the Fighter Command Stations.

Except where otherwise specified, all the day-to-day operational details of the Battle are drawn from *A summer for heroes* by Wood and Dempster, which is based on a 1961 book by the same authors called *The narrow margin*.

References

- Air Ministry (Air Historical Branch), 1954: The Second World War 1939–1945: Meteorology. (Unpublished, copy available in National Meteorological Library, Bracknell.)
- Cluett, D., Bogle, J. and Learmonth, B., 1984: Croydon Airport and the battle for Britain 1939–1940. London Borough of Sutton, Libraries and Arts Services.
- Meteorological Office, 1941: Damage by enemy action to M O 7 outstations. (Unpublished, copy available in National Meteorological Library, Bracknell.)
- Ogden, R.J., 1986: Meteorological Office training of assistant staff: 1939–51. *Meteorol Mag*, **115**, 200–213.
- Ogley, B., 1990: Biggin on the bump. Westerham, Froglets Publications.
- Parker, A.E., 1942: On the formation of condensation trails. London, Air Ministry, Meteorological Office, Synoptic Division Technical Memorandum No. 42.
- Price, A., 1988: The hardest day. Arms and Armour Press.
- Saward, D., 1985: Victory denied. Buchan and Enright.
- Wood, D. and Dempster, D., 1990: A summer for heroes. Shrewsbury, Airline Publications.
- Wright, R., 1969: Dowding and the Battle of Britain. MacDonald.

Road slipperiness during warm-air advections

T. Gustavsson and J. Bogren

University of Gothenburg

Summary

This article deals with two cases of road slipperiness in Sweden caused by sublimation during warm-air advections. The weather preceding frontal movements causes differences in local climate to occur which affect the geographical distribution of the occurrence of slipperiness.

1. Introduction

Formulae for forecasting road surface temperatures and the risk of road slipperiness have traditionally been developed for conditions with falling temperatures during evenings and nights when there could be a possibility of road icing (e.g. Parmenter and Thornes 1986, Rayer 1987). However, analyses of recordings from field stations in the Swedish Road Weather Information System (VVIS) have shown that road slipperiness, caused by sublimation, also occurs during rapid weather changes, chiefly during warm-air advections (Gustavsson 1985, Bogren and Gustavsson 1986 and 1989, Gustavsson 1990). (This type of road slipperiness could be dangerous for road users as it appears very unexpectedly.) The variation in warming between the air and the road surface, in addition to the advection of warm, humid air, leads to an intense deposit of rime on the road surface. Great local variations in sublimation risk occur in complex terrain as a result of varying local topography and other factors. The effects of local climatological factors on the risk of road slipperiness have earlier been documented by Lindqvist (1975, 1982).

This study is part of a project concerned with the analysis of temperature variations in complex terrain and their association with the occurrence of local slipperiness. In this paper the topographical factors which control the local risk of slipperiness during warm-air advections are identified and the variations in sublimation due to the weather situation preceding the warming illustrated.

2. Data

The climatological data used in this study are recordings from 48 field stations in the VVIS in the counties of Bohuslän, Älvsborg and Jönköping in the south-western part of Sweden (see Fig. 1) with additional information from synoptic maps to determine the prevailing weather conditions. Each station is equipped with sensors for the measurement of air temperature and humidity at a level of 2 m, and a probe at the surface for the measurement of the road surface temperature. Additional sensors at some selected stations measure wind speed, wind direction, precipitation and residual salinity on the road surface. The measured variables are

recorded every half hour during the winter season and stored on a computer. Thus it is possible to analyse the interaction between such factors as temperature development and prevailing weather.

The most important parameter giving information about the variation between field stations when there is a risk of slipperiness due to sublimation is the actual time when the dew-point temperature is higher than the road surface temperature. This parameter has therefore been analysed in relation to such factors as local topography, distance between field stations, and the temperature development during the warm-air advection. However, this parameter is only of interest when the road surface temperature is below 0 °C.

3. Results

To illustrate the effects of local topography on temperature development during warm-air advections, two types of weather situations have been studied. The first situation is characterized by clear, calm conditions preceding the warm-front movement, and the second situation is marked by cloudy, windy weather preceding the rise in temperature.

3.1 Case-study of 18 January 1986

The weather events of 18 January 1986 were characterized by clear, calm conditions preceding a warm front.

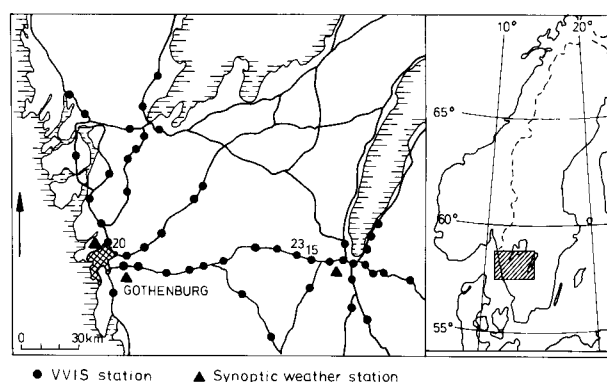


Figure 1. Map of the study area.

Recordings of temperature, cloudiness and wind from synoptic weather stations in the area show that this was a stable situation with minimum air temperature ranging from -11°C to -24°C within the region, a cloud cover not exceeding 2 oktas and almost no wind. During the early morning of the 18th, however, a warm front moving north-eastwards from the British Isles reached the south-western parts of Sweden (Fig. 2) and the weather changed rapidly. Owing to the warm-air advection, the temperature rose markedly while the degree of cloudiness changed from clear to completely overcast and the wind increased from 0 m s^{-1} to 7 m s^{-1} in a primarily south-westerly direction.

The effect of the weather change on the distribution of the time at which the risk of slipperiness occurred in the study area is illustrated by three VVIS stations, numbers 15, 20 and 23. These represent three different types of location. Station 20 is located close to the coast in a flat, open, wind-exposed area and station 15 is sited 115 km inland in a small, shallow valley, with gentle slopes admitting pooling of cold air yet surrounded by a forest which provides wind shelter. Station 23 is located 110 km inland in a large valley surrounded by open areas where cold air could pool during stable weather conditions, but the openness also creates great wind exposure.

The temperature development and the time of the risk of sublimation for stations 15, 20 and 23 are shown in Fig. 3. The shaded area indicates risk of slipperiness, i.e. the dew-point temperature is higher than the road surface temperature and a flux of humid air develops towards the surface.

As a result of the variation in the ability of cold air to pool around the stations, the night minimum temperature differs between the sites. The lowest temperature

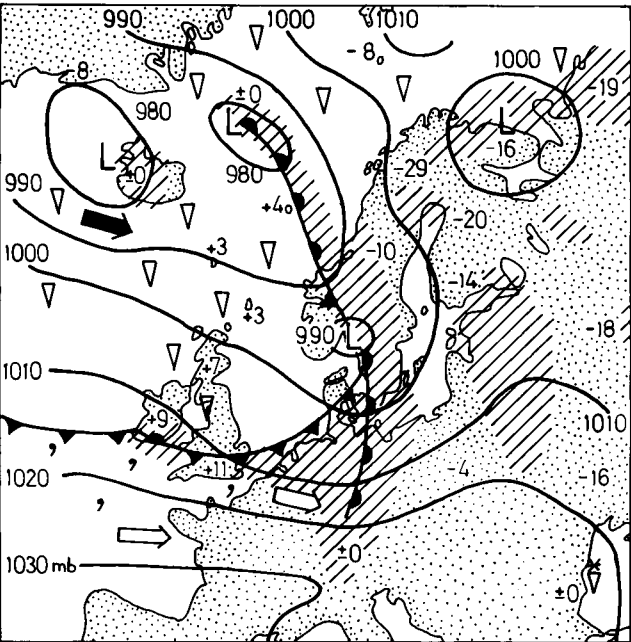


Figure 2. Surface analysis for 1200 UTC on 18 January 1986. Stylized symbols show precipitation areas.

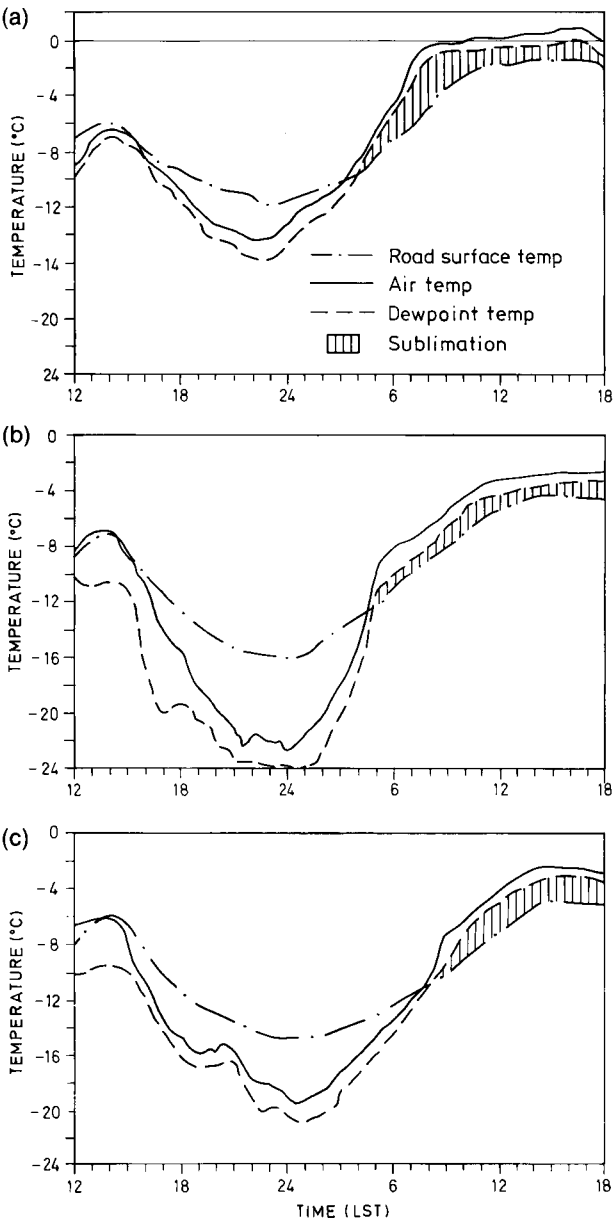


Figure 3. Temperature curves at three VVIS stations during 17 and 18 January 1986, (a) station 20, (b) station 23, and (c) station 15.

occurred at station 23, where the minimum air temperature was -23°C . Station 15 had a minimum temperature of -19°C and station 20 -13°C , i.e. 10°C warmer than station 23. Recordings from the synoptic stations in Fig. 1 have been used to confirm that there were no differences in the regional weather in the area studied.

Station 20 was first reached by the warm air at 2300 Local standard time (LST) on 17 January and the air temperature rose from -13°C to 0°C by 0800 LST the following day, showing a warming rate of $1.4^{\circ}\text{C h}^{-1}$. The warm air reached the two inland stations 1.5 hours later, at 0030 LST. The reaction to the warm air at station 23 was immediate. The air temperature started to rise at a rate of $3.0^{\circ}\text{C h}^{-1}$ during the first 5 hours of the warming trend, until 0500 LST, and continued

thereafter at a more modest rate. At station 15 the rise in air temperature was slower, $1.5^{\circ}\text{C h}^{-1}$, due to the surrounding forest which provided a wind shelter for the pooled cold air.

The variation in the onset of the risk of slipperiness is associated with the rapid rise of both the air and dew-point temperature in relation to the less responsive road surface temperature. As a result of the rapid rise of the air temperature, the risk of slipperiness occurred almost simultaneously at stations 20 and 23, at 0400 LST and 0430 LST, respectively, in spite of the large regional distance between the sites. But not until 0830 LST was station 15, in the sheltered valley, exposed to risk of slipperiness, i.e. a difference of 4 hours between the valley stations (numbers 15 and 23) although they are sited less than 10 km apart from each other.

3.2 Case-study of 20 January 1986

Weather conditions on 20 January were characterized by low air temperatures, an overcast sky and a strong prevailing wind chiefly from the north-east. In the course of the afternoon, a rise in temperature and a change in the wind direction from north-east to south-west took place when the area under study was reached by a warm front moving from the west towards Scandinavia (Fig. 4).

The conditions on the 20th were quite different from those of the 18th owing to the cloudiness and prevailing winds which effectively prevented the development of large local temperature variations. The temperature recordings in Fig. 5 show how the three sites were reached by the warm air during the day resulting in a risk of slipperiness in the afternoon. Because of its westerly position, station 20 was reached first by the warm air, resulting in a warming rate of $1.6^{\circ}\text{C h}^{-1}$, and at 1530 LST there was a risk of slipperiness. The two inland

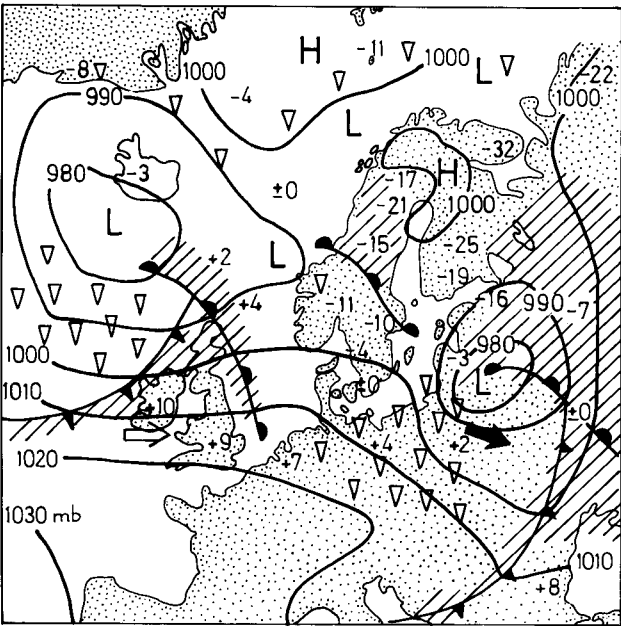


Figure 4. As Fig. 2, but for 20 January 1986.

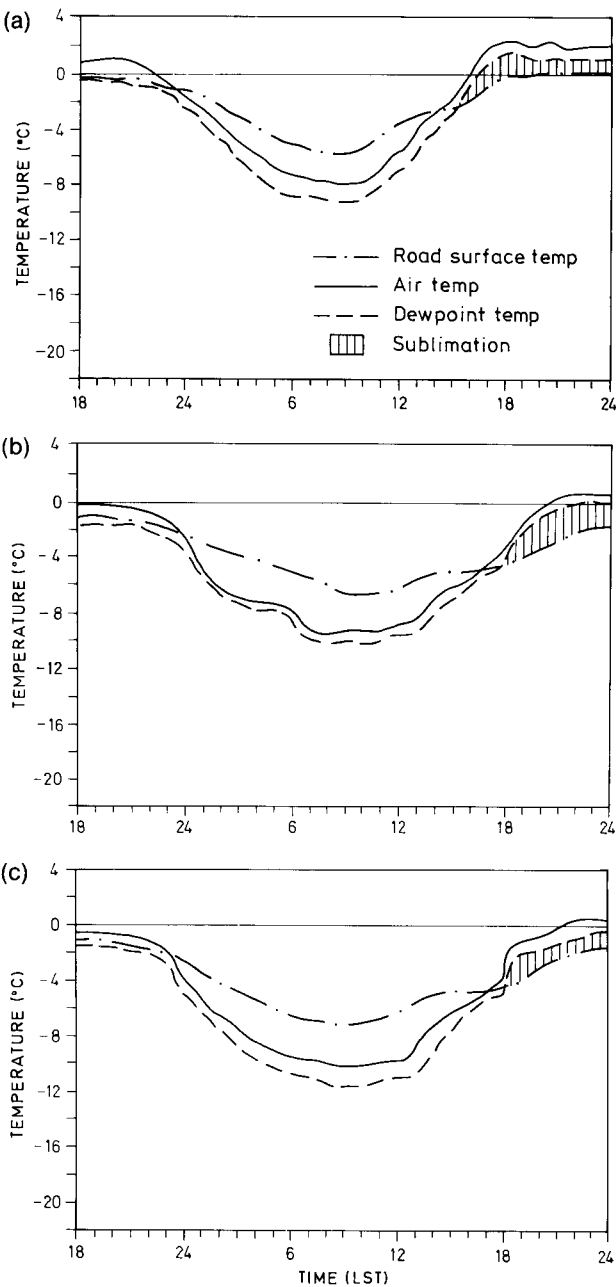


Figure 5. Temperature curves at three VVIS stations during 19 and 20 January 1986, (a) station 20, (b) station 23, and (c) station 15.

stations were not affected by the warming until 1230 LST; with a warming rate close to $1.0^{\circ}\text{C h}^{-1}$, they were not exposed to a risk of sublimation until 1800 LST, i.e. 2.5 hours later than at the coastal site. The maximum temperature at station 20 was approximately $1.5\text{--}2^{\circ}\text{C}$ higher than at the other two stations, which could partly explain the variation in the warming rate between the two inland stations. The higher maximum temperature at station 20 was a result of the variation in altitude between the three stations, which is approximately 250 m. The difference in time of commencement of risk of slipperiness under these conditions of these sites was a result of the relation of the region positions versus the frontal movement direction.

4. Discussion

The frontal movements on both the 18 and 20 January were from the south-west to the north-east, which means that they reached the study area in the coastal zone first and then moved inland. The difference in the reactions of the sites within the study area to the warm air advections is illustrated by Figs 6 and 7. The relative difference in time for the start of slipperiness is calculated in relation to the station which was first exposed to slipperiness. This time difference is plotted against the position of the station expressed as distance from the coast. The scatter in the figures is a reflection of the different weather conditions preceding the frontal movements. During 18 January, the time at which a site was affected by a risk of slipperiness was a result of the local 'climate' which developed at each site, and hence

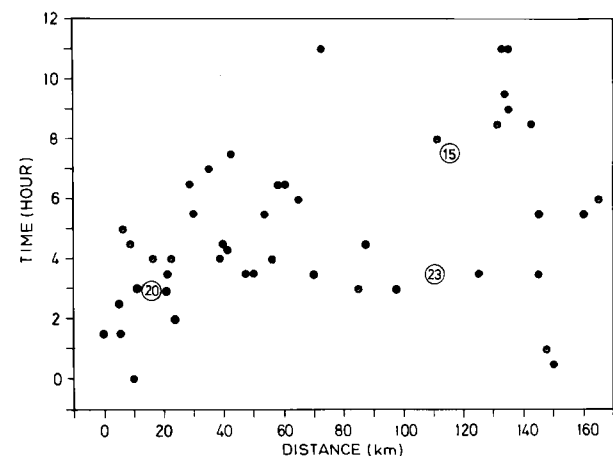


Figure 6. Relative time difference between the 48 field stations in the VVIS for start of sublimation versus distance from the coast on 18 January 1986.

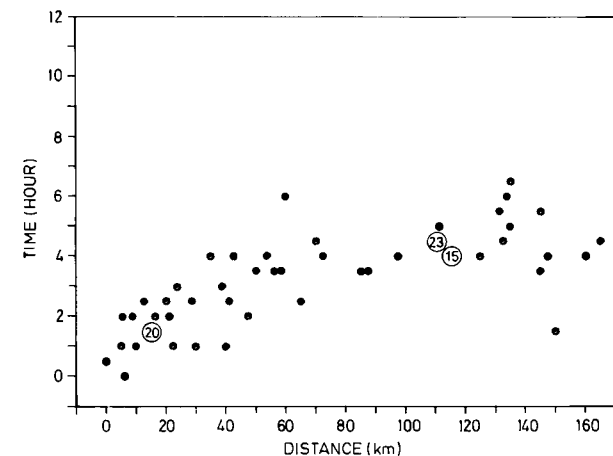


Figure 7. As in Fig 6, but for 20 January 1986.

great time differences between sites which were located quite near to one another occurred. During 20 January, the time at which the risk of slipperiness began is closely correlated to the position of the site in relation to the frontal movement.

5. Conclusions

The two cases show that the spatial distribution of slipperiness is controlled by the weather situation preceding the warm-air advection. If the preceding weather is characterized by clear, calm conditions, it is possible for local temperature differences to develop at the sites, according to their topographical environments. Due to the individual variations in local climate between the sites there are great differences in how rapidly they react to the warming and there thus lies a different pattern of when a risk of slipperiness will occur. This implies that there can be considerable time differences between adjacent sites as regards their exposure to the risk of slipperiness. On the other hand, the effect of local topography is not as important when the warm front is preceded by cloudy, windy conditions, making the warming and the risk of slipperiness at each site more dependent upon the progressing frontal movement.

Acknowledgements

This project is financially sponsored by the Swedish Transport Research Board and the Swedish National Road Administration. Adviser for the project is Professor S. Lindqvist. Linguistic revision was done by B. Kroeber and J. Vesterlund. S. Svensson drew the figures.

References

Bogren, J. and Gustavsson, T., 1986: A method for the development of a local climatological model for prediction of slipperiness on roads. GUNI rapport 20, Department of Physical Geography, Gothenburg.

—, 1989: Modelling of local climate for prediction of road slipperiness. *Phys Geogr*, **10**, 147–164.

Gustavsson, T., 1985: Tillämpad väglämplighet — förstudie. M. Sc. Thesis. Department of Physical Geography, Gothenburg.

—, 1990: Analyses of local climatological factors controlling risk of slipperiness during warm-air advections. Accepted for publication in *Int J Climatol*.

Lindqvist, S., 1975: Vaghalkans beroende av mikro-och lokal-klimatiska faktorer. GUNI rapport 8, Department of Physical Geography, Gothenburg, (summary in English).

—, 1982: Neue Methoden der Glatteisüberwachung in Schweden. GUNI rapport 16, Department of Physical Geography, Gothenburg, (summary in English).

Parmenter, B. and Thornes, J.E., 1986: The use of a computer model to predict the formation of ice on road surfaces. Crowthorne, Berkshire, TRRL Research Report RR71.

Rayer, P.J., 1987: The Meteorological Office forecast road surface temperature model. *Meteorol Mag*, **116**, 180–191.

Correspondence

551.578.45(430.1)551.578.46:551.515

Comments on 'A heavy mesoscale snowfall event in northern Germany'

Pike (*Meteorol Mag*, 119, 187–195) draws attention to the convergence line during 11–12 January 1987 near the coast of north Germany (see Figs 1, 7 and 8 of his article). However, this feature does not explain why the heaviest snowfall, as shown in Fig. 5, occurred 40–80 km inland, downwind from the Lübeck Bight. The width of the associated snow belt was about the same as the width of the Bight itself. Kresling (referenced in Pike) states that weather radar showed that new shower cells were being continually generated in the Bight during the 24 hours up to 1200 UTC on the 12th. It is therefore probable that convergence of land-breeze components (not necessarily actual land-breezes) over the Bight, within the flow of unstable air from the Baltic, played an important part in producing the heavy snowfall east and north-east of Hamburg. Many of the shower cells, on crossing the southern shore of the Bight, would still be in the developing stage, with upcurrents predominating. Consequently, given the fairly strong wind speed in the unstable layer (about 50 km h^{-1}) they deposited most of their snow content well inland.

41 York Road
Camberley
Surrey GU15 4HS

F.E. Lumb

Reply by W.S. Pike

Unfortunately, in 1987, the Hamburg Offices were not archiving their radar data which could have verified this 'continued-snow-shower-generation' over the Lübeck Bight (southern waters of the Mecklenburg Bight) referred to by Anders Kresling. Nevertheless, I have no reason to doubt his first-hand observations.

At risk of offending mariners, there is no really satisfactory way of confirming the snowfall maxima which radar tells us are occurring at sea! Andersson and Nilsson (*Weather and forecasting*, 5, 299–312) summarize that, in the majority of cases 'heavy snowfall does not extend far inland' and 'all available radar evidence indicates that the maximum snowfall occurs over the sea'. However, over northern Germany during 11–12 January 1987 we find that, in conditions of strong onshore windflow at cloud levels, a mesoscale 'coastal' snowfall maximum has been swept some 50–60 km inland.

Such extreme events may be defined as 'the currently known limits to general rules', and I welcome Frank Lumb's erudite comments which form a well-considered and logical postscript to this particular investigation.

W.S. Pike

19 Inholmes Common
Woodlands St. Mary
Newbury RG16 7SX

Notes and news

Extending the reach — the Defence Oceanology International 91 conference and exhibition.

The theme of the Admiralty Research Establishment (ARE) sponsored Defence Oceanology International 91 conference and exhibition, being held on 6–8 March 1991 at the Brighton Metropole, reflects the defence requirements that represent the new order of the 1990s.

In choosing the theme 'Extending the Reach', the increasing importance to navies throughout the world of flexibility, both in out-of-area operations and in response to the changing nature of the threat, is recognized, as is the importance of new technology and new operational concepts and operational costs.

A call for papers has now been published. Papers are invited on surface and sub-surface issues under the following headings: sonar and acoustics; communications, command, control and information; signature measurement; environment monitoring and control; power, propulsion and manoeuvrability; oceanography and climatology; vulnerability/durability/survivability; new concepts and systems; and defence technology transfer. Copies of the Call for Papers and full details on all aspects of DOI 91 are available from:

The Spearhead Group
Rowe House
55/59 Fife Road
Kingston upon Thames
Surrey KT1 1TA
United Kingdom
Tel: 081-549 5831 Fax: 081-541 5657
Telex: 928042 SPEARS G.

Books received

The listing of books under this heading does not preclude a review in the Meteorological Magazine at a later date.

Weather watch, by R.F. File (London, Fourth Estate Ltd, 1990) is a multi-faceted investigation of British weather, but in the context of the world's weather. Weather lore is tested and descriptions of a multitude of phenomena are included.

Television weathercasting; a history, by R. Henson (London, McFarland and Company, 1990) describes the progress of weather presentation on American television, including all the variety of personalities involved.

Radar image — 19 October 1990 at 0600 UTC

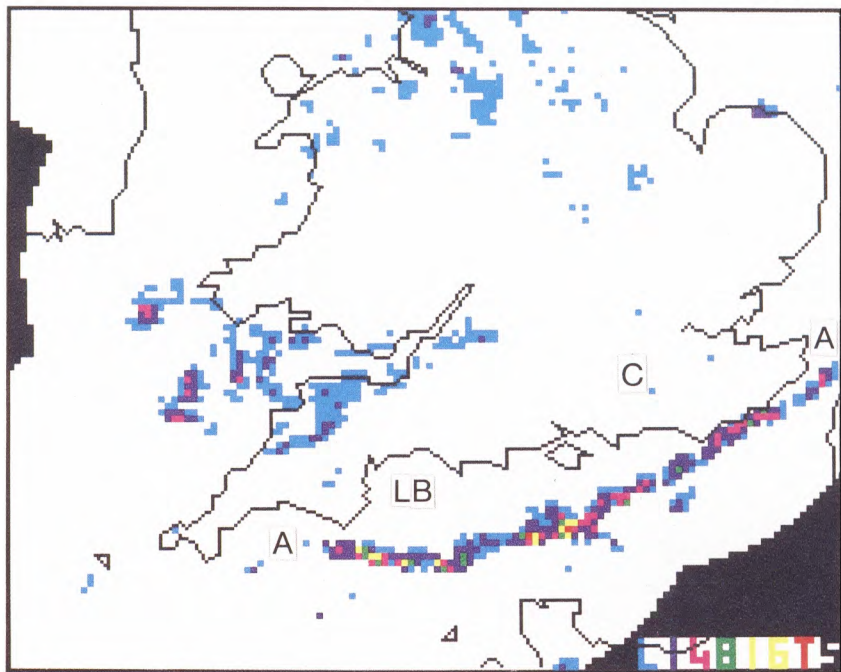


Figure 1. Rainfall intensity (mm h^{-1}) from the UK weather radar network for 0600 UTC on 19 October 1990. Blue < 1 , purple > 1 , pink > 4 , green > 8 , yellow > 16 , and red > 32 . Black areas are outside radar coverage. See text for explanation of lettering.

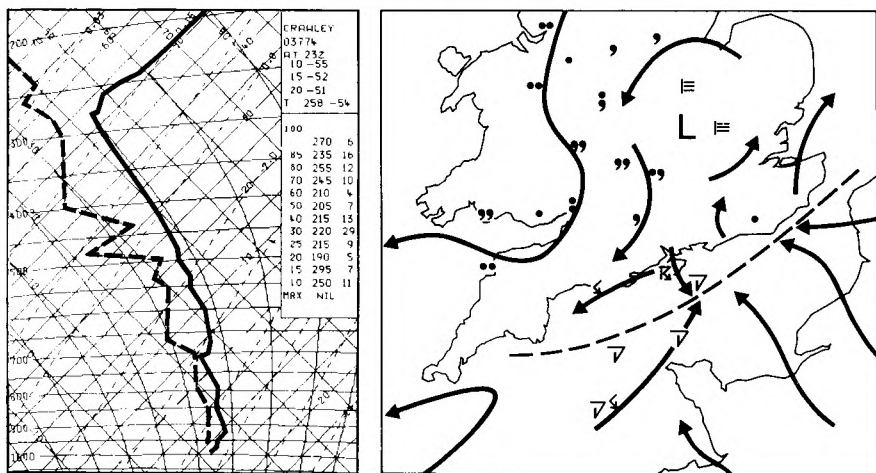


Figure 2. Surface wind streamlines (arrowed) and present weather including spheric location reports (conventional symbols) for 0600 UTC on 19 October 1990. The dashed line shows the position of the convergence zone. The radiosonde sounding for Crawley for 0000 UTC on 19 October 1990 is incorporated on the left.

The main feature on this image from the UK weather radar network (Fig. 1) is the narrow band of precipitation extending almost the entire length of the English Channel (A — A). Embedded cells of heavy rain are evident, particularly towards the west of the band, and some were associated with thunderstorms.

The band developed along a low-level convergence zone in the circulation of a shallow slow-moving low pressure area centred over south-east England (L in Fig. 2). The convergence zone acted as a focus for preferential shower development to sea surface temperatures of the order of 15°C . The upper-air sounding

from Crawley (C in Fig. 1 and insert to Fig. 2) implied deep convection was possible to around 300 mb.

The first main cells formed in the central part of Lyme Bay (LB in Fig. 1) as early as 2300 UTC the previous evening with convergence possibly being locally enhanced by the focusing of offshore land-breeze circulations. The band subsequently extended towards the east, persisting as a marked feature until mid morning, but then tending to fragment. However over extreme south-east England the band reformed in the afternoon when surface temperatures had risen sufficiently for deep land-based convection to develop.

A.J. Waters

- Northcott, G.P.; The spring of 1989 in the United Kingdom, 75
- Northcott, G.P.; The summer of 1989 in the United Kingdom, 145
- Numerical weather prediction model performance on instant occlusion developments; J.B. McGinnigle, 149
- Ogden, R.J.; The Battle of Britain — a meteorological retrospect, 260
- Old views on climate change, 126
- Palutikof, J.P., see Reviews, 127, 196
- Persistent coastal convergence in a heavy snowfall event on the south-east coast of England; W.S. Pike, 21
- Pike, W.S.; A heavy mesoscale snowfall event in northern Germany, 187
- Pike, W.S.; Persistent coastal convergence in a heavy snowfall event on the south-east coast of England, 21
- Pike, W.S.; Radar study of the snowfall in south-west Cornwall on 12 January 1987, 97
- Pike, W.S.; Reply to comments by Lumb on 'A heavy mesoscale snowfall event in northern Germany', *letter*, 271
- Pilsbury, R.K., see Reviews, 39
- Practical extended-range forecasting using dynamical models; S.F. Milton, 221
- Radar study of the snowfall in south-west Cornwall on 12 January 1987; W.S. Pike, 97
- Ratcliff, D., see Satellite and/or radar photographs, 220
- Real-time analysis of surface wind gusts using radar data: 25th January 1990; R.M. Blackall, R. Brown and C.G. Collier, 121
- Reece, F.D.; The United Kingdom's contribution to the WMO Voluntary Co-operation Fellowship Programme, 140
- Remotely sensed data for wave forecasting; R.A. Stratton, 9
- Reviews
- Applications of weather radar systems — a guide to uses of radar data in meteorology and hydrology*, C.G. Collier (V.K. Collinge), 197
- Carbon dioxide and global change: earth in transition*, S.B. Idso (J.P. Palutikof), 196
- Climatic atlas of the Indian Ocean. Part III: Upper-ocean structure*, S. Hastenrath and L.L. Greischar (J.C. Swallow), 196
- Earth's changing climate and Our drowning world*, A. Milne (C. Goodess), 172
- Global climate change*, ed. S.F. Singer (W.J. Ingram), 175
- Noctilucent clouds*, M. Gadsden and W. Schröder (D.A.R. Simmons), 174
- A short course in cloud physics* (third edition), R.R. Rogers and M.K. Yau (P.R. Jonas), 38
- Spacious skies*, R. Scorer and A. Verkaik (R.K. Pilsbury), 39
- The human impact of climate uncertainty*, W.J. Maunder (M.F. Mylne), 77
- Turning up the heat*, F. Pearce (J.P. Palutikof), 127
- Weather radar and the water industry*; British Hydrological Society (M.F. Mylne), 173
- Weather sensitivity and services in Scotland*, eds S.J. Harrison and K. Smith (K.J. Weston), 37
- Road slipperiness during warm-air advections; T. Gustavsson and J. Bogren, 267
- Sanderson, R.M., Golding, B.W. and Bader, M.J.; A heavy snowfall within a mesoscale convergence zone, 41
- Satellite and/or radar photographs
- 8 November 1989 at 0600 and 1200 UTC; G.A. Monk, 20
- 23 November 1989 at 0824 UTC; G.A. Monk, 40
- 16 January 1990 at 1200 UTC; R.W. Lunnon, 60
- 24 January 1990 at 1515 UTC and 25 January 1990 at 0330 and 1325 UTC; G.A. Monk, 78
- 25 March 1990 at 0900 and 1500 UTC; G.A. Monk, 104
- 21 April 1990 at 1445 UTC; G.A. Monk, 128
- 27 May 1990 at 2100 UTC; G.A. Monk, 148
- 13 June 1990 at 1330 UTC; A.J. Waters, 176
- 26 June 1990 at 1800 UTC and 27 June 1990 at 0000 UTC; A.J. Waters, 199
- 30 June 1990 at 1347 UTC; D. Ratcliff, 220
- 13 September 1990 at 1130 UTC; A.J. Waters, 247
- 19 October 1990 at 0600 UTC; A.J. Waters, 272
- Sea-breeze at Darwin: a climatology; L.M. Lloyd, 105
- Simmons, D.A.R., see Reviews, 174
- Simmons, E.L.; Sixty-four years of regular ozone measurements, 53
- Sixty-four years of regular ozone measurements; E.L. Simmons, 53
- Spring of 1989 in the United Kingdom; G.P. Northcott, 75
- Steady states in a turbulent atmosphere; A.A. White, 1
- Storms of January and February 1990; E. McCallum and W.J.T. Norris, 201
- Stratton, R.A.; Remotely sensed data for wave forecasting, 9
- Strong winds experienced during the late winter of 1989/90 over the United Kingdom: Historical perspectives, J.M. Hammond, 211
- Subbaramayya, I., Vivekananda Babu, S. and Naidu, C.V.; Variations in the onset of the Indian south-west monsoon and summer circulation anomalies, 61
- Summer of 1989 in the United Kingdom; G.P. Northcott, 145
- Swallow, J.C., see Reviews, 196
- The Battle of Britain — a meteorological retrospect; R.J. Ogden, 260
- United Kingdom's contribution to the WMO Voluntary Co-operation Fellowship Programme; F.D. Reece, 140
- Variations in the onset of the Indian south-west monsoon and summer circulation anomalies; I. Subbaramayya, S. Vivekananda Babu and C.V. Naidu, 61
- Vivekananda Babu, S., see Subbaramayya, Vivekananda Babu and Naidu
- Water-resource assessment experts meet to develop a strategy for the 1990s, 246
- Waters, A.J., see Satellite and/or radar photographs, 176, 199, 247, 272
- Weston, K.J., see Reviews, 37
- Wheeler, D.; Modelling long-term rainfall patterns in north-east England, 68
- White, A.A.; Steady states in a turbulent atmosphere, 1
- Woodroffe, A.; Forecasting the storm of 8 November 1989 — a success for the man-machine mix, 129
- Workshop reports
- Workshop on Numerical Products from Bracknell, Meteorological Office College, Shinfield Park, Reading, 26–28 June 1989; B.K. Lloyd, 19
- Wright, B.J. and Golding, B.W.; The Interactive Mesoscale Initialization, 234

GUIDE TO AUTHORS

Content

Articles on all aspects of meteorology are welcomed, particularly those which describe results of research in applied meteorology or the development of practical forecasting techniques.

Preparation and submission of articles

Articles, which must be in English, should be typed, double-spaced with wide margins, on one side only of A4-size paper. Tables, references and figure captions should be typed separately. Spelling should conform to the preferred spelling in the *Concise Oxford Dictionary* (latest edition). Articles prepared on floppy disk (Compucorp or IBM-compatible) can be labour-saving, but only a print-out should be submitted in the first instance.

References should be made using the Harvard system (author/date) and full details should be given at the end of the text. If a document is unpublished, details must be given of the library where it may be seen. Documents which are not available to enquirers must not be referred to, except by 'personal communication'.

Tables should be numbered consecutively using roman numerals and provided with headings.

Mathematical notation should be written with extreme care. Particular care should be taken to differentiate between Greek letters and Roman letters for which they could be mistaken. Double subscripts and superscripts should be avoided, as they are difficult to typeset and read. Notation should be kept as simple as possible. Guidance is given in BS 1991: Part 1: 1976, and *Quantities, Units and Symbols* published by the Royal Society. SI units, or units approved by the World Meteorological Organization, should be used.

Articles for publication and all other communications for the Editor should be addressed to: The Chief Executive, Meteorological Office, London Road, Bracknell, Berkshire RG12 2SZ and marked 'For Meteorological Magazine'.

Illustrations

Diagrams must be drawn clearly, preferably in ink, and should not contain any unnecessary or irrelevant details. Explanatory text should not appear on the diagram itself but in the caption. Captions should be typed on a separate sheet of paper and should, as far as possible, explain the meanings of the diagrams without the reader having to refer to the text. The sequential numbering should correspond with the sequential referrals in the text.

Sharp monochrome photographs on glossy paper are preferred; colour prints are acceptable but the use of colour is at the Editor's discretion.

Copyright

Authors should identify the holder of the copyright for their work when they first submit contributions.

Free copies

Three free copies of the magazine (one for a book review) are provided for authors of articles published in it. Separate offprints for each article are not provided.

Contributions: It is requested that all communications to the Editor and books for review be addressed to the Chief Executive, Meteorological Office, London Road, Bracknell, Berkshire RG12 2SZ, and marked 'For *Meteorological Magazine*'. Contributors are asked to comply with the guidelines given in the *Guide to authors* which appears on the inside back cover. The responsibility for facts and opinions expressed in the signed articles and letters published in *Meteorological Magazine* rests with their respective authors.

Subscriptions: Annual subscription £30.00 including postage; individual copies £2.70 including postage. Applications for postal subscriptions should be made to HMSO, PO Box 276, London SW8 5DT; subscription enquiries 071-873 8499.

Back numbers: Full-size reprints of Vols 1-75 (1866-1940) are available from Johnson Reprint Co. Ltd, 24-28 Oval Road, London NW1 7DX. Complete volumes of *Meteorological Magazine* commencing with volume 54 are available on microfilm from University Microfilms International, 18 Bedford Row, London WC1R 4EJ. Information on microfiche issues is available from Kraus Microfiche, Rte 100, Milwood, NY 10546, USA.

December 1990

Editor: F.E. Underdown
Editorial Board: R.J. Allam, R. Kershaw, W.H. Moores, P.R.S. Salter

Vol. 119
No. 1421

Contents

	Page
The impact of surface and radiosonde observations from two Atlantic ships on a numerical weather prediction model forecast for the storm of 25 January 1990. J.T. Heming	249
The Battle of Britain — a meteorological retrospect. R.J. Ogden	260
Road slipperiness during warm-air advections. T. Gustavsson and J. Bogren	267
Correspondence	
Comments on 'A heavy mesoscale snowfall event in northern Germany' (by W.S. Pike, 119, 1990, 187–195). F.E. Lumb	271
Reply by W.S. Pike	271
Notes and news	
Extending the reach — the Defence Oceanology International 91 conference and exhibition	271
Books received	271
Radar photograph — 19 October 1990 at 0600 UTC. A.J. Waters	272

ISSN 0026–1149

